2010-10-26

Drosophila piRNA Function in Genome Maintenance, Telomere Protection and Genome Evolution: A Dissertation

Jaspreet S. Khurana
University of Massachusetts Medical School

Drosophila piRNA function in genome maintenance, telomere protection and genome evolution

A Dissertation Presented

By

Jaspreet Singh Khurana

Submitted to the Faculty of the

University of Massachusetts Graduate School of Biomedical Sciences, Worcester

In partial fulfillment of the requirements for the degree of

DOCTOR OF PHILOSOPHY

MOLECULAR MEDICINE

26th October, 2010

DROSOPHILA piRNA PATHWAY FUNCTION IN GENOME MAINTENANCE, TELOMERE PROTECTION AND GENOME EVOLUTION

A Dissertation Presented By

Jaspreet S. Khurana

The signatures of the Dissertation Defense Committee signifies completion and approval as to style and content of the Dissertation

William Theurkauf, Ph.D., Thesis Advisor

Kirsten Hagstrom, Ph.D., Member of Committee

Nelson Lau, Ph.D., Member of Committee

Craig Peterson, Ph.D., Member of Committee

Zhiping Weng, Ph.D., Member of Committee

The signature of the Chair of the Committee signifies that the written dissertation meets the requirements of the Dissertation Committee

Phillip Zamore, Ph.D., Chair of Committee

The signature of the Dean of the Graduate School of Biomedical Sciences signifies that the student has met all graduation requirements of the School

Anthony Carruthers, Ph.D.
Dean of the Graduate School of Biomedical Sciences

Interdisciplinary Graduate Program
October 26, 2010

To my parents, my sister and my wife

Acknowledgements

It has been a true pleasure working under the guidance of my thesis advisor, Dr William Theurkauf. He has been very supportive throughout the course of my PhD in his lab. When I started working in his lab back in 2005, things were not really coming my way. As a young and naïve graduate student, I wasn't even sure what to do when the project was going nowhere. Rather than troubleshoot my way out of those situations, I decided, instead, to flee the problems. Bill helped me realize my true potential and pushed me into facing the problems head-on. If it weren't for him, I wouldn't be here today, writing this thesis. His constant encouragements and support helped me through the most difficult times in my academic career. I really enjoyed the brain-storming sessions with him in his office discussing the truly amazing questions in developmental biology. I will miss that the most. It is because of his mentorship that I can say, with some confidence, that I am ready to take the next step in my academic career- that I can become a better scientist.

I am very thankful to my thesis research advisory committee members- Drs. Phillip D. Zamore, Craig L. Peterson and Kirsten Hagstrom for their constant support, constructive criticism and encouragement.

I would like to thank all the members of the Theurkauf lab for their wholehearted support and helpful discussions. I had a great time with everyone, thanks to the vibrant atmosphere in the lab. I am thankful to Nadine Schultz and Birgit Koppetsch for making my life so much easier. They taught me a lot of different techniques from fly husbandry to confocal microscopy. It wouldn't have been possible without their help.

I had a very fruitful collaboration with many people here at UMass. Jie Wang and Jia Xu from Dr. Zhiping Weng's lab and Chengjian Li from Dr. Phillip Zamore's lab were critical to many experiments and analyses presented in my thesis. I especially am thankful to Dr Zhiping Weng and her group for helpful discussions towards many projects.

I am indebted to my parents in India, for without their constant support, blessings and sacrifice, I wouldn't be here today. My sister always helped boost my morale, telling me always to give it my best shot, a 110%. I hope I made her proud. Lastly, I want to thank my wife, Parneet for she was supportive and understanding when I spent long nights and weekends in the lab. Her love and affection made it possible to survive those stressful times during my work.

ABSTRACT

Upon fertilization, the early embryo sustains most of the cellular processes using the maternally deposited reserves in the egg itself until the zygotic gene expression takes charge. Among the plethora of essential components provided by the mother are small non-coding RNAs called PIWI-interacting RNAs (piRNAs), which provide immunity to the zygote against transposon challenge. In this thesis, I have presented three different functions of piRNAs in *Drosophila melanogaster*- in maintenance of genomic integrity, telomere protection and their role as an adaptive immune system against genomic parasites.

In Chapter 2, I have described the phenotypic effects of the loss of piRNA function in early embryos. The mutations affecting the piRNA pathway are known to cause embryonic lethality. To describe this lethality in detail, I have shown that all the characterized piRNA mutants show compromised zygotic genomic integrity during early embryogenesis. In addition, two piRNA pathway components, Aubergine (Aub) and Armitage (Armi) are also required for telomere resolution during early embryogenesis. Aub and Armi recruit telomeric protection complex proteins, HOAP and HP1, to the telomeric ends and thus avoid activation of the Non-homologous end joining (NHEJ) DNA repair pathway at the telomeres.

There are about 120 transposon families in *Drosophila melanogaster* and piRNA pathway mutations cause activation of many of the resident transposons in the genome. In Chapter 3, I have described the effects of infection by a single transposon, *P-element*, in naïve strains by introduction through the zygote. Activation of the *P-element* leads to desilencing of unrelated transposons, causing accumulation of germline DNA damage which is linked to severely reduced fertility in the hybrid females. However, there is partial restoration of fertility as the hybrid progeny age, which correlates with *P-element* piRNA production and thus *P-element* silencing.

Additionally, a number of transposons mobilize into piRNA generating heterochromatic clusters in the genome, and these insertions are stably inherited in the progeny. Collectively our data shows that piRNA production can be triggered in the adults in an absence of maternal contribution and that piRNAs serve as an adaptive immune system which helps resolve an internal genetic conflict between the host and the parasite.

In an effort to understand the phenotypic effects of piRNA dysfunction in *Drosophila*, we have uncovered new exciting roles for piRNAs in development and presented evidence how transposons can act as architects in restructuring the host genome.

Copyright notice

List of figures

List of Tables

List of contributions

Data from Figure 2.10A and 2.12 was analyzed by Jia Xu.

Figure 2.10B and C were prepared by William Theurkauf.

Data from Table 2.3 was analyzed by Jia Xu.

Figure 3.2 D and E was prepared by Jia Xu. Small RNA sequencing was performed by Chengjian Li.

Figure 3.3 A and B and Figure 3.4 were prepared by Jie Wang. Tiling array hybridization was carried out by Phyllis Spatrick from the Genomics Core facility at UMass. Raw data was analyzed by Jie Wang.

Illumina paired-end genomic sequencing was performed in the Deep Sequencing Core facility by Ellen Kittler and Maria Zapp. Raw data was analyzed by Jie Wang.

Figure 3.6 was plotted by Jie Wang

Data in Figure 3.7 was analyzed by Jie Wang.

Table of contents

Chapter I

piRNAs, transposon silencing and *Drosophila* germline development

Introduction

Transposons are major structural elements of essentially all eukaryotic genomes, and mobilization of these elements can lead to genetic instability and cause deleterious mutations (McClintock, 1953). Mobile genetic elements also carry transcriptional enhancers and insulators, thus transposition can alter expression of nearby genes and potentially large chromatin domains, triggering coordinated changes in gene transcription that could disrupt development or drive evolution (Feschotte, 2008). Transposon silencing is particularly important in the germline, which maintains the genetic information that will be inherited by future generations. Recent studies indicate that transposon silencing during germline development is imposed by piRNAs, which guide a small RNA-based immune response related to RNA interference (RNAi) (Malone and Hannon, 2009). Here we review piRNA biogenesis and function during *Drosophila* female germline development, where recent molecular and biochemical observations have provided significant insight into the mechanism of piRNA production and transposon silencing, and where the developmental defects associated with piRNA mutations can be evaluated within a well established genetic, cellular and developmental framework (Spradling, 1993).

Gene silencing by microRNAs (miRNAs) and small interfering RNAs (siRNAs) is well established (Filipowicz et al., 2005; Ghildiyal and Zamore, 2009), and studies on these small regulatory RNAs have guided work on the more recently identified piRNAs. The 21 to 22 nt siRNAs and miRNAs are generated from double stranded precursors by the RNase III enzyme

Dicer and bind to Argonaute proteins (Ghildiyal and Zamore, 2009). The Argonaute-miRNA complexes direct sequence-specific translational silencing or target destruction. Small interfering RNAs (siRNAs) in animals, by contrast, appear to primarily induce target destruction. However, endogenous siRNAs (endo-siRNAs) direct chromatin assembly and transcriptional silencing in the fission yeast *S. pombe,* and endo-siRNAs have been implicated in repressing transposons and other repetitive sequences during somatic development in flies (Czech et al., 2008; Ghildiyal et al., 2008; Hartig et al., 2009; Kawamura et al., 2008; Okamura et al., 2008; Verdel et al., 2004; Volpe et al., 2002). miRNAs and siRNAs, in complexes with Argonautes, can therefore silence transcription, trigger target destruction, or inhibit translation. The piRNAs are less well understood, but may be equally versatile.

piRNA identification and genomic origins

piRNAs were first identified through studies on the *Drosophila Stellate* locus, which is composed of repeated copies of a gene encoding a casein kinase II beta subunit homolog (Livak, 1990). The *Drosophila Stellate* protein has no known biological function, but mutations in the *suppressor of stellate [su(ste)]* locus lead to Stellate protein over-expression during spermatogenesis, which leads to Stellate crystal formation and reduced fertility (Livak, 1990). It is now clear that *su(ste)* encodes piRNAs that are homologous to *ste* and silence this locus in *trans* (Aravin et al., 2001). Small RNA cloning and sequencing studies subsequently showed that related 22 to 30-nt long RNAs, derived largely from retrotransposons and other repetitive sequence elements, are abundant in the male and female germline (Aravin et al., 2003). These novel small RNAs were therefore initially named repeat-associated siRNAs (rasiRNAs) (Aravin et al., 2003). In some other systems, however, the majority of small RNAs in this class are not enriched in transposon sequences. In addition, these RNAs bind germline-enriched PIWI clade of

Argonaute proteins that are distinct from the Argonautes that bind miRNAs and siRNAs (Aravin et al., 2006; Girard et al., 2006a; Grivna et al., 2006a; Lau et al., 2006). As a result, this new small RNA family was subsequently renamed PIWI interacting RNAs (piRNAs) (Brennecke et al., 2007; Yin and Lin, 2007).

Many of the piRNAs expressed in *Drosophila* ovaries are derived from transposons and other repeats, and thus cannot be assigned to specific chromosomal loci (Brennecke et al., 2007; Gunawardane et al., 2007; Yin and Lin, 2007). piRNAs that map to unique sites, however, are clustered in large pericentromeric or subtelomeric domains of up to 240 kb that are rich in transposon fragments (Brennecke et al., 2007). Most of these clusters produce piRNAs from both genomic strands, but a subset of clusters produces unique piRNAs almost exclusively from one strand (Aravin et al., 2006; Brennecke et al., 2007; Girard et al., 2006a; Gunawardane et al., 2007; Houwing et al., 2007). The *Drosophila flamenco* locus falls into this second class, and genetic and molecular studies on *flamenco* have provided important insights into piRNA function (Brennecke et al., 2007; Malone et al., 2009). Single P-element insertion mutations in the telomere-proximal side of *flamenco* disrupt piRNA production and downregulate expression of longer transcripts from across the entire 60 kb locus, suggesting that transposition has disrupted a transcriptional promoter for this cluster (Brennecke et al., 2007). *flamenco* contains fragments of active transposons located throughout the genome, and mutations in this locus lead to over-expression of these dispersed elements (Brennecke et al., 2007; Mével-Ninio et al., 2007). These observations strongly suggest that piRNAs derived from *flamenco* silence transposon expression in *trans*.

The *flamenco* locus appears to function primarily in ovarian somatic cells, while the major dual-strand cluster at cytological position 42AB appears to be germline specific. Mutations in

42AB and other dual strand clusters have not been reported, but mutations in the *rhino* (*rhi*) locus lead to both dramatic reductions in piRNAs from these clusters and to 10 to 150 fold over-expression of approximately 20% of transposon families (Klattenhoff et al., 2009b). piRNAs derived from dual strand clusters thus appear to act in the germline to silence target transposons in *trans*.

piRNA clusters represent approximately 1% of the *Drosophila* genome, and it is unclear how these limited chromatin domains are specified. Most clusters are located in heterochromatin and contain complex arrays of transposon fragments, but only a subset of transposon-rich heterochromatic regions produce piRNAs. These observations suggest that piRNA clusters are epigenetically defined. However, single P element insertions disrupt *flamenco* locus function, suggesting that, at a minimum, cluster promoters are hard-wired. The *rhi* locus is required for accumulation of putative piRNA precursor RNAs from the 42AB cluster, and the Heterochromatin Protein 1 (HP1) homolog encoded by this locus binds to this cluster (Klattenhoff et al., 2009b; Vermaak et al., 2005). HP1a, the founding member of the HP1 family, binds to methylated lysine 9 on Histone H3 (Bannister et al., 2001; Lachner et al., 2001; Nakayama et al., 2001). HP1 then recruits Histone methyltransferase, which methylates neighboring H3 to extend an epigenetic structure that is generally associated with transcriptional silencing (Nakayama et al., 2001). Rhi binding may therefore promote histone modifications that differentiate piRNA clusters from surrounding chromatin.

Transposons and other repetitive elements are among the most divergent components in the genome. This calls for a selection for advantageous changes in host genes involved in transposon targeting. Thus, the host and parasite are in a constant genetic conflict inside the cell and co-evolve with each other. Intriguingly, *rhi* is rapidly evolving and appears to be under strong

positive selection, which is a hallmark of genes involved in host-pathogen interactions. This led Vermaak et al. to speculate that *rhi* evolution is driven by a germline specific genomic conflict (Vermaak et al., 2005). The role for Rhino in piRNA biogenesis strongly suggests that the conflict between transposons and the host genome drives *rhi* evolution (Klattenhoff et al., 2009a). Brennecke et al. (2007) speculated that piRNA clusters actively attract transposons, which would presumably lead to production of homologous piRNAs capable of trans-silencing active elements throughout the genome (Brennecke et al., 2007). Within this appealing model, Rhino protein could interact directly with transposon-encoded integration proteins, and thus drive adaptive silencing by promoting transposition into clusters.

piRNA biogenesis

Deep sequencing and genetic studies suggest that two spatially and mechanistically distinct processes drive piRNA biogenesis (reviewed in (Siomi et al., 2010)). As noted above, the majority of unique piRNAs are derived from transposon rich heterochromatic clusters (Brennecke et al., 2007; Yin and Lin, 2007). The most abundant piRNAs are anti-sense to mRNAs from active transposons, and these antisense RNAs preferentially associate with Piwi and Aubergine (Aub), two PIWI clade Argonautes (Brennecke et al., 2007; Gunawardane et al., 2007; Yin and Lin, 2007). Sense strand piRNAs, by contrast, preferentially associate with Argonaute 3 (Ago3) (Brennecke et al., 2007; Gunawardane et al., 2007). *In vitro,* all three *Drosophila* PIWI proteins, when programmed with piRNAs, cleave target RNAs between positions 10 and 11 of the guide strand (Gunawardane et al., 2007; Nishida et al., 2007; Saito et al., 2006). Significantly, *Drosophila* piRNAs from opposite strands tend to have a 10 nt 5' end overlap, and antisense piRNAs bound to Piwi and Aub show a strong bias toward a Uracil (U) at the 5'end, while sense strand piRNAs bound to Ago3 tend to have an Adenine (A) at position 10

(Brennecke et al., 2007; Gunawardane et al., 2007). These findings suggest that antisense piRNAs derived from piRNA clusters bind to Aub and Piwi and direct cleavage of sense strand transcripts from active transposons, generating RNA fragments with an A 10 nt from the 5' terminus (Figure 1.1C). These sense strand cleavage products are proposed to associate with Ago3, following 3' trimming by an undefined mechanism producing mature sense strand piRNAs. The resulting piRNA-Ago3 complexes then cleave anti-sense piRNA precursors from clusters to produce RNA fragments that associate with Aub and Piwi (Figure 1.1C). Trimming generates mature anti-sense piRNAs, completing the cycle. In this model, reciprocal cycles of PIWI-mediated cleavage thus amplify the pool of sense and antisense piRNAs. This "ping-pong" amplification cycle thus obviates the need for an RNA dependent RNA polymerase (RdRp), which is needed to amplify siRNA triggers in plants, nematodes and yeast (Verdel et al., 2009). The ping-pong model was developed from observations in *Drosophila*, but a similar mechanism appears to function in other animal groups (Aravin et al., 2007; Grimson et al., 2008; Houwing et al., 2007; Lau et al., 2009a; Palakodeti et al., 2008).

Figure 1.1. piRNA biogenesis and transposon silencing in the germline and soma. The mechanisms that drive piRNA biogenesis and transposon silencing are not well understood. Here we summarize speculative models based on the available data.

A. Primary piRNA biogenesis in the germline. Long sense (blue) and anti-sense (red) precursor transcripts from piRNA clusters are cleaved by sequence-independent nucleases, which could include Zucchini (Zuc) and/or Squash (Squ), producing intermediates that bind Ago3 and Aub. Processing and modification of the 3'ends generates mature piRNA complexes that drive that ping-pong amplification loop.

B. Primary piRNA biogenesis in the soma. Anti-sense precursor transcripts (red) from *flam* and other uni-strand clusters are cleaved by Zuc to produce intermediate species that bind to Piwi. 3' processing generates mature anti-sense piRNAs.

C. Ping-pong amplification in the germline. Transcripts from functional transposons (blue) and piRNA clusters (blue and red) are exported from the nucleus. Aub, pre-programmed with piRNAs generated through the primary biogenesis pathway, cleaves complementary transposon and cluster transcripts (blue), yielding randomly sized RNA fragments that bind Ago3. 3' end trimming produces mature Ago3-sense strand piRNA complexes, which cleave anti-sense cluster transcripts (red). The resulting fragments bind to Aub and 3' end processing generates anti-sense piRNAs, completing the amplification cycle.

D. Potential modes of piRNA mediated transposon silencing. 1. Transcriptional silencing of target transposons. piRNAs bound to Piwi, which accumulates in the nucleus, direct heterochromatin assembly at target elements. 2. Post-transcriptional target destruction. Transposon transcripts are recognized by Aub-piRNA complexes in the nuage, which catalyze homology-dependent cleavage. 3. Aub-piRNA complexes bind transposon transcripts and repress translation.

Figure 1.1

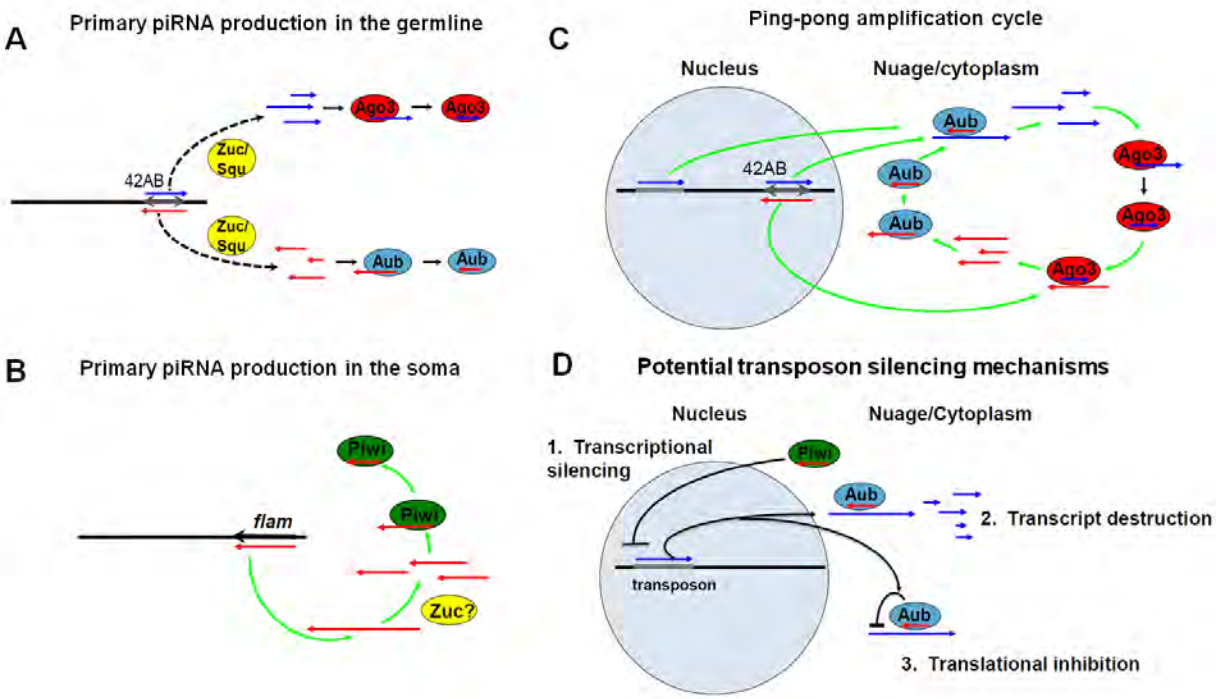
A
Primary piRNA production in the germline
Ago3
Ago3
Zuc/
Squ
42AB
Zuc/
Squ
Aub
Aub
B
Primary piRNA production in the soma
Piwi
Piwi
flam
Zuc?
C
Ping-pong amplification cycle
Nucleus
Nuage/cytoplasm
Aub
42AB
Aub
Aub
Ago3
Ago3
Ago3
D
Potential transposon silencing mechanisms
Nucleus
Nuage/Cytoplasm
1. Transcriptional
silencing
Piwi
Aub
2. Transcript destruction
transposon
Aub
3. Translational inhibition

The ping-pong model requires pre-existing "primary" piRNAs, presumably derived from clusters, to initiate the amplification cycle. How these primary piRNAs are produced remains to be determined, but piRNA production from the *flamenco* cluster has been proposed as a model for this process. piRNAs from this locus appear to be expressed primarily in the somatic follicle cells, which express only one PIWI Argonaute, Piwi. In addition, this locus produces unique piRNAs from only one genomic strand and complementary piRNAs drive biogenesis in the ping-pong model (Brennecke et al., 2007). Somatic piRNA production by *flamenco* may provide a model for primary piRNA biogenesis. However, somatic follicle cells surround the germline cells in the ovary, and the mixture of germline and somatic tissue complicates interpretation of studies on intact tissue. Recently, homogenous cell lines derived from the ovarian somatic sheets (OSSs) and ovarian somatic cells (OSCs) have been used to circumvent this limitation (Lau et al., 2009b; Niki et al., 2006; Robine et al., 2009; Saito et al., 2009). These cells express Piwi but do not express Ago3 or Aub, and produce piRNAs from one strand of the *flamenco* cluster (Lau et al., 2009b; Saito et al., 2009). Piwi thus appears to drive ping-pong independent piRNA production in somatic cells. The putative nuclease encoded by the *zucchini* locus is also required for piRNA production in the soma (Malone et al., 2009; Robine et al., 2009; Saito et al., 2009). Transcripts encoded by *flamenco* could be cleaved by Zucchini, producing RNA fragments that bind to Piwi (Figure 1.1B). Each of the PIWI-clade proteins binds piRNAs with a unique length distribution, suggesting that processing take place after binding (Brennecke et al., 2007). Precursor RNA fragments bound by Piwi could be trimmed to produce mature primary piRNAs (Figure 1.1B).

However, the available data on primary piRNA production are very limited and the proposed model is therefore highly speculative. In addition, several observations suggest that primary

piRNA production in the germline may be independent of Piwi. For example, mutations that disrupt piRNA production in the germline lead to severe defects in axis specification and oocyte nuclear organization (Chen et al., 2007; Klattenhoff et al., 2007; Klattenhoff et al., 2009a; Pane et al., 2007), but germline depletion of Piwi does not disrupt egg chamber development or axial patterning(Cox et al., 2000). In addition, *piwi* mutations reduce, but do not eliminate piRNAs mapping to the major germline-specific 42AB cluster (Malone et al., 2009). Since a loss of primary piRNAs should lead to a collapse of the entire piRNA biogenesis cycle, these findings suggest that primary piRNA production in the germline does not require Piwi. The mechanism of primary piRNA production in the germline thus remains to be explored, and could be distinct from piRNA production in ovarian somatic tissue.

The majority of germline piRNAs appear to be produced by the ping-pong amplification cycle, and a simple modification of this cycle could explain primary piRNA biogenesis during germline development (Figure 1.1A). During ping-pong amplification, primary piRNAs are generated by Ago3 or Piwi-mediated cleavage of piRNA precursor transcripts derived from clusters, which produces longer fragments that bind to Aub and are subsequently trimmed to final length (Figure 1.1A). During primary piRNA biogenesis, piRNA cluster transcripts could be cleaved by sequence-independent endonuclease producing long RNA fragments that enter the biogenesis cycle by binding to Aub or Ago3. Subsequent processing by the same mechanisms employed using the ping-pong cycle could then generate the mature primary piRNAs that initiate the amplification loop (Figure 1.1C).

Mutations that eliminate primary piRNAs are predicted to lead to a collapse of the ping-pong cycle. However, mutations that only reduce primary piRNA production should allow reduced piRNA production by the ping-pong cycle. Intriguingly, mutations in *squash* and *zucchini*, which

encode putative nucleases that localize to the perinuclear nuage, reduce piRNA levels without blocking ping-pong bias (Malone et al., 2009). As noted above, Zucchini has been implicated in ping-pong independent piRNA biogenesis in somatic cells (Robine et al., 2009; Saito et al., 2009). Zucchini and/or Squash could therefore cleave cluster transcripts to produce RNAs that bind to PIWI clade proteins and generate the primary piRNAs that initiate the germline amplification loop (Figure 1.1A and B).

Modification of piRNAs and Piwi proteins

Like siRNAs, the 3' ends of most mature piRNAs are 2'-O-methylated, while the 5' end carries a phosphate group (Girard et al., 2006a; Grivna et al., 2006a; Horwich et al., 2007; Houwing et al., 2007; Saito et al., 2007; Vagin et al., 2006). The 2' O-methylation is carried out by DmPimet (piRNA methyltransferase)/DmHEN1, the *Drosophila* homolog of *Arabidopsis* HEN1 (Horwich et al., 2007; Saito et al., 2007). *Dmhen1* mutants eliminate 2'-O-methylation and reduce average piRNA size and abundance, suggesting that this modification protects mature piRNA from degradation (Horwich et al., 2007; Saito et al., 2007). These mutations also lead to a modest loss of transposon silencing, although mutants are viable and fertile (Horwich et al., 2007; Saito et al., 2007). These findings suggest that 3' end modification is not essential to piRNA function, but existing *Dmhen1* alleles may not be null.

The Piwi proteins Aub and Ago3 have recently been shown to be modified by the methyltransferase PRMT5, which generates symmetrical Dimethyl Arginines (sDMAs), which creates a binding site for Tudor domains (Kirino et al., 2009). There are 23 Tudor domain proteins in *Drosophila*, including the founding member of the family, Tudor (Tud), which is required for assembly of germ plasm and Aub localization in the germline (Boswell and

Mahowald, 1985; Nishida et al., 2009). In addition, the Tudor domain proteins Krimper, Spindle-E and Tejas have been implicated in PIWI localization, piRNA production, and transposon silencing (Lim and Kai, 2007; Malone et al., 2009; Patil and Kai, 2010; Vagin et al., 2004; Vagin et al., 2006). These findings suggest that Piwi family protein dimethylation leads to assembly of higher order complexes that promote piRNA biogenesis and transposon silencing.

Transposon silencing

The majority of *Drosophila* piRNAs map to transposons and other repetitive elements, and piRNA mutations lead to massive transposon over-expression. piRNA-PIWI complexes are therefore assumed to directly control transposon activity. piRNAs bound to PIWI proteins direct homology dependent target cleavage *in vitro*, suggesting that transposons are silenced through post-transcriptional transcript destruction (Gunawardane et al., 2007; Nishida et al., 2007; Saito et al., 2006). Intriguingly, a number of the piRNA pathway components, including Aub and Ago3, localize to Nuage, an evolutionarily conserved perinuclear structure associated with germline RNA processing (Brennecke et al., 2007; Eddy, 1974; Gunawardane et al., 2007; Ikenishi, 1998; Nishida et al., 2007; Saito et al., 2006). In addition, protein coding genes with transposon insertions within introns escape silencing by the piRNA pathway. These observations suggest that piRNAs bound to Aub and Ago3 direct homology dependent cleavage of mature transposon transcripts following export from the nucleus (Figure 1.1D). In this model, protein coding genes containing intronic transposon insertions are not silenced because piRNA homology is removed by splicing.

However, several lines of evidence raise the possibility that piRNAs act at several levels. Piwi, the founding member of the PIWI clade, localizes to the nucleus, binds HP1a and has been

implicated in heterochromatin assembly in the soma (Brower-Toland et al., 2007b; Pal-Bhadra et al., 2004b). In addition, mutations in *spn-E,* which encodes a putative helicase required for piRNA production, reduce HP1a binding to the telomere specific transposon *TART* (Klenov et al., 2007). These findings suggest that piRNA bound to Piwi guide heterochromatin assembly, and thus impose transcriptional silencing. Consistent with this speculation, piRNA mutations reduce DNA methylation in mouse testes. However, piRNAs have also been found in polysome fractions (Grivna et al., 2006b) and the mouse Piwi protein Mili associates with translation initiation factors and may positively regulate translation (Unhavaithaya et al., 2009). These finding raise the possibility that piRNAs also control translation (Figure 1.1D).

piRNA control of gene expression

In many organisms, including poriferans, cnidarians, *C.elegans* and mouse, the majority of piRNAs map to the unannotated regions of the genome and only a limited set match transposons and other repeats (Aravin et al., 2006; Batista et al., 2008; Girard et al., 2006a; Grimson et al., 2008; Ruby et al., 2006). *Drosophila* also express piRNAs derived from the 3'-UTRs of a subset of mRNAs (Aravin et al., 2006; Robine et al., 2009; Saito et al., 2009). These observations suggest that piRNAs control gene expression. Recent studies support this hypothesis. The most abundant genic piRNAs in *Drosophila* somatic cells are linked to the 3'-UTR of a transcription factor, *traffic jam* (*tj*) (Robine et al., 2009; Saito et al., 2009). In cultured somatic cells, *tj* piRNAs co-immunoprecipitate with Piwi protein, and in ovaries their levels are reduced in *zucchini* mutants, but not in ovaries mutant for several other genes implicated in secondary piRNA amplification (Saito et al., 2009). Mutations in *tj* appear to reduce Piwi protein levels in somatic follicle cells, suggesting that this locus controls Piwi expression and is the source of piRNAs that bind to it. Mutations in *tj* and *piwi* produce similar defects in oogenesis and lead to

2 to 4 fold over-expression of *FasIII*, a cell adhesion molecule necessary for oogenesis. These changes are modest compared to the 100 to 200 fold increases in transposon expression observed in several piRNA pathway mutants. Nonetheless, these findings suggest that piRNAs from the *tj* locus downregulate *fasIII* in the somatic follicle cells (Saito et al., 2009). In fly testes, the *vasa* and *stellate* (*ste*) genes also appear to be targeted by the piRNA pathway (Aravin et al., 2001; Nishida et al., 2007; Vagin et al., 2006). *vasa* encodes a germline specific DEAD box protein required for piRNA production (Malone et al., 2009; Schupbach and Wieschaus, 1991), piRNAs derived from the AT-chX-1 and AT-chX-2 loci are homologous to the *vasa* gene, and mutations in *aub* and *ago3* that disrupt production of these piRNAs lead to Vasa over-expression (Li et al., 2009; Nishida et al., 2007). Recently, it has been reported that the piRNA pathway has a role in maternal mRNA decay and translational repression in early *Drosophila* embryo (Rouget et al., 2010). During early embryogenesis in *Drosophila*, a number of maternally deposited mRNAs are deadenylated to program their decay before zygotic transcription begins. A number of piRNA pathway genes were shown to affect this maternal mRNA degradation and deadenylation during maternal-zygotic transition (Rouget et al., 2010).

However, tiling array analyses show that mutations in the piRNA pathway genes *aub, ago3, rhi* and *armi* do not significantly alter expression of protein coding genes during oogenesis (Klattenhoff et al., 2009b; Li et al., 2009). However, piRNAs may have a more prominent role in gene expression in ovarian somatic cells and the male germline.

piRNAs and speciation

Owing to their sequence complementarity to transposable elements, piRNAs have been implicated in transposon silencing and germline development in a variety of organisms. The

presence of piRNAs and a complement of proteins involved in piRNA metabolism (inferred by electronic annotation) in early animal phyla like cnidaria or porifera suggest a conserved piRNA function in protecting the host genome throughout the evolution of animal phyla (Grimson et al., 2008). Although there is no direct evidence that the piRNA pathway is involved in species divergence, there is data suggestive that the pathway, in competition with the transposons, has helped diverge organisms enough to cause reproductive isolation. The best examples of this come from *Drosophila*, where it has been reported that the progeny of inter-strain or inter-specific crosses are sterile. In 1970's, a number of labs reported that the crosses between geographically isolated populations of *D.melanogaster* resulted in sterile progeny (Bucheton, 1973; Bucheton, 1979; Hiraizumi, 1971; Kidwell and Kidwell, 1976; Kidwell et al., 1977; Picard et al., 1972). The F1 progeny from such crosses showed hypermutability, male recombination, chromosome rearrangements and thus sterility. This phenomenon, known as hybrid dysgenesis, was assigned to chromosomal factors specific to freshly obtained wild-type stocks (Kidwell and Kidwell, 1975). These genetic factors were later identified as transposable elements which were absent in the lab stocks, suggesting that the sterility in hybrid progeny was due to mobilization of the transposon in question (Picard, 1976; Rubin et al., 1982). In addition, these observations were further complicated by the fact that the phenotypes displayed by the progeny were non-reciprocal. So, when the transposon was transmitted in the zygote through females, the resulting progeny were fertile. These females thus transmit cytoplasmic factors which provide the zygote with the necessary immunity against the transposon. These cytoplasmic factors are now recognized as piRNAs mapping against the particular transposon (Blumenstiel et al., 2008; Brennecke et al., 2008; Chambeyron et al., 2008). Thus, there is a correlation between absence of maternally inherited piRNAs against a single transposon and the resulting dysgenic effects. This

system of uni-directional hybrid incompatibility between two different strains shows the consequences of a competition between the host and the parasite. By virtue of their mobilization potential, a new transposon invasion can cause major restructuring of the host genome. In its response, the host must rapidly evolve strategies to target those changes. piRNA clusters, with their potential to silence transposons in *trans*, have shown a rapid expansion pattern with signs of positive selection in mammals (Assis and Kondrashov, 2009; Lau et al., 2006). In addition, proteins involved in piRNA pathway show signs of positive selection, consistent with the suggested role of this pathway in species divergence (Vermaak et al., 2005).

In contrast to the proposed role of maternally inherited piRNAs in suppressing hybrid dysgenesis, *Penelope* elements in *D.virilis* hybrid dysgenesis crosses are predominantly targeted by the endo-siRNAs (Rozhkov et al., 2010). While it is unclear why piRNAs don't target *Penelope* elements, this likely reflects the plasticity in different small RNA silencing pathways in targeting particular transposons.

Germ cell maintenance in Zebrafish

The zebrafish genome encodes two Piwi homologs, Ziwi and Zili. Based on sequence similarity, Ziwi appears to be the ortholog of mouse MIWI, and Zili is the ortholog of MILI (Houwing et al., 2007). Ziwi localizes to the perinuclear nuage, which appears to represent germ granules and specifies the primordial germ cells during early embryogenesis (Tan et al., 2002). piRNAs are found in both testes and ovaries, and their localization and temporal pattern of expression are coincident with Ziwi. A significant fraction of these piRNAs derive from transposable elements, suggesting that this pathway also silences transposons in zebrafish. Ziwi-bound piRNAs have a similar 5' end modification and length as their cousins in *Drosophila* and

mammals (Houwing, Kamminga et al. 2007). As observed in mouse Piwi mutants, *ziwi* mutants show a progressive decline in the germ cells due to apoptosis. Another striking feature of loss of Ziwi is that the mutants are all phenotypically males. This defect, however, seems to be a secondary consequence of loss of primordial germ cells (PGCs) which are required during early embryogenesis for female development (Slanchev et al., 2005).

piRNAs and mouse spermatogenesis

The mouse genome encodes three Piwi homologs, MIWI (PIWIL1), MILI (PIWIL2) and MIWI2 (PIWIL4). All three of these proteins have distinct spatial and temporal expression patterns in the male germline. Knockout animals in any of the mouse *piwi* genes disrupt male germline development (Carmell et al., 2007; Deng and Lin, 2002; Kuramochi-Miyagawa et al., 2004). Mouse spermatogenesis initiates at day 3 after birth (de Rooij and Grootegoed, 1998). The primordial germ cells, after reaching the gonad, form spermatogonia, subsets of which are stem cells capable of self-renewal. The stem cells then differentiate to produce primary spermatocytes up to day 6. At day 10, the primary spermatocytes enter meiosis I and yield a pair of secondary spermatocytes, which complete the second meiotic division. The haploid cells from the meiotic process are called spermatids, which undergo the process of sperm maturation or spermiogenesis, to yield mature sperm. While *Mili* and *Miwi2* null mice show meiotic arrest, *Miwi* null mice show defects in spermiogenesis (Carmell et al., 2007; Deng and Lin, 2002; Kuramochi-Miyagawa et al., 2004). These knockout phenotypes correlate well with the expression pattern of the Piwi proteins. Mutation in any of the *piwi* genes causes loss of germ cells due to increased apoptosis. *Miwi2* mutant spermatocytes show an increased accumulation of γ-H2AX during zygotene, which indicates the presence of unrepaired meiotic double-strand breaks and/or DNA damage due to other reasons (Fig. 3C) (Carmell, Girard et al. 2007). For

example, increased γ-H2AX staining has been observed in mutants defective in synapsis. A peculiar feature of mammalian male meiosis is the formation of a dense sex body by the XY bivalent that undergoes transcriptional silencing. The sex body is positive for γ-H2AX and other DNA repair proteins, including BRCA1, RAD51 and RPA. However, *Miwi2* mice fail to stain for γ-H2AX during pachytene, suggesting that sex body formation is disrupted. Interestingly, some piRNAs or their precursors have been localized to regions on the sex body (Marcon et al., 2008). These findings suggest that the piRNA pathway may be involved in the transcriptional silencing of the XY bivalent.

Many components of the mouse piRNA pathway are conserved across different species. For example, mouse Vasa homolog (MVH), an evolutionarily conserved RNA helicase essential for germ cell development, is required for piRNA biogenesis and transposon silencing during mouse spermatogenesis, just as the *Drosophila* homolog is crucial to fly oogenesis (Kuramochi-Miyagawa et al., 2010; Malone et al., 2009). Similarly, mutations in putative DExD-box helicase, *MOV10L1,* lead to defects in piRNA biogenesis and activation of LTR and LINE-1 retrotransposons (Frost et al., 2010; Zheng et al., 2010). *Drosophila* homolog of MOV10L1, Armitage, is required for piRNA biogenesis and germline development in *Drosophila*.

Although mammalian piRNAs are depleted of repetitive sequences, a detailed analysis of developmentally expressed MILI-bound piRNAs revealed two distinct populations and a significant number of piRNA clusters correspond to repeats (Aravin et al., 2007). In addition, some transposons are demethylated in the *Mili* and *Miwi2* mice, suggesting that they are transcriptionally active (Aravin et al., 2007; Carmell et al., 2007). These findings suggest that the mammalian Piwi-piRNA pathway, like the *Drosophila* piRNAs, may be required for transposon

silencing. However, majority of piRNAs expressed in the male germline have targets other than the transposable elements.

MIWI and its piRNAs are found in the polysome fractions (Grivna et al., 2006b). Additionally, MIWI is found in ribonuclear protein fractions along with a testis-expressed kinesin, KIF17b, and binds the mRNAs of ACT and CREM target genes, which are the master regulators of spermiogenesis (Kotaja et al., 2006). Consistent with this, *Drosophila* Aub has been implicated in translational regulation of some targets like Oskar. The presence of MIWI piRNAs against the target mRNAs would give a much more direct evidence for the role of this pathway in translational control.

In contrast to flies and zebrafish, the mouse piRNA pathway mutations do not disrupt the female germline. This is because retrotransposon silencing in the mouse oocytes seems to be largely dependent on the endogenous RNAi pathway. Endogenous siRNAs, with sequence homology to retroelements, have been cloned from growing mouse oocytes. Consistent with this observation is the disruption of transposon silencing in the conditional Dicer or Ago2 mutants. Therefore, piRNAs primarily silence transposons in the male germline, and a distinct class of endogenous siRNAs silence transposons during oogenesis (Watanabe et al., 2006).

piRNA function and *Drosophila* germline development

In every system studied to date, mutations in piRNA pathway genes disrupt germline development, often producing complex and poorly understood phenotypes that are difficult to directly associate with transposon targets of the pathway. Analyses of the ovarian phenotypes in *Drosophila* piRNA mutants, however, have helped link transposon mobilization to germline

development and may provide a paradigm for phenotypic analysis of piRNA mutants in other systems.

Drosophila oogenesis is initiated by the division of a germline stem cell within a somatic cell niche at the tip of the germarium (Spradling, 1993) (Figure 1.2). Signaling between the niche and the stem cell controls stem cell division and is likely to orient division plane (Deng and Lin, 1997; Lin and Spradling, 1997). The latter process is critical to asymmetric cleavage, which regenerates the stem cell and produces the cystoblast precursor of the oocyte and nurse cells (Deng and Lin, 1997). Mutations in *piwi*, which encodes a founding member of the PIWI clade of Argonaute proteins, lead to a near complete loss of germline stem cells (Cox et al., 1998). Genetic mosaic studies indicate that Piwi protein is required in both the somatic cells of the niche and in the germline (Cox et al., 1998; Cox et al., 2000). Eliminating *piwi* from the soma disrupts stem cell maintenance, but does not alter the viability of the eggs that are produced (Cox et al., 2000). By contrast, germline clones of *piwi* mutations slow stem cell division and the eggs that are produced do not hatch (Cox et al., 2000). Unlike mutations in many other piRNA pathway genes, however, *piwi* germline clones do not disrupt oocyte patterning, which appears to be a downstream consequence of transposon over-expression (see below). The function for Piwi and piRNAs in stem cell maintenance and divisions are not well understood, and may be distinct from latter functions in transposon control.

Figure 1.2. **Microtubule polarity and axis specification in wild type (A) and piRNA mutant (B) oocytes**. A pair of germline stem cells (red) in region 1 of the germarium divide to produce cystoblasts (light green), which divide with incomplete cytokinesis to produce inter-connected 16-cell cysts. Meiotic recombination initiates in region 2a (green) and DSBs are formed. Meiosis is restricted to a single pro-oocyte in the center of the cyst in region 2b (dark green). DSBs are repaired by region3/stage 2 (blue) of oogenesis. Microtubule-organizing center (MTOC) forms in the oocyte where microtubules direct *osk* mRNA (yellow) to the posterior pole. In piRNA mutants, meiosis is initiated normally in region 2a (B). However, transposon overexpression and increased DSB accumulation occurs in region 2b. DSBs persist in region 3, activating Chk2 signaling which blocks MTOC formation and affects *grk* mRNA localization. Lower panel shows early and late stage 8 oocytes in wt (A) and piRNA mutants (B). The oocyte cortex nucleates microtubules (green, arrow heads indicate plus end). Kinesin moves osk mRNA (red) to the interior. Later, posterior follicle cells (yellow) signal to the oocyte (blue arrow), triggering depolymerization of cortical microtubules. Osk mRNA moves to the posterior by Kinesin-dependent random walk. In piRNA mutants (B, lower panel), *osk* mRNA moves to the interior. Posterior follicle cell signaling fails and posterior microtubules persist. *osk* mRNA gets trapped in the interior.

Figure 1.2

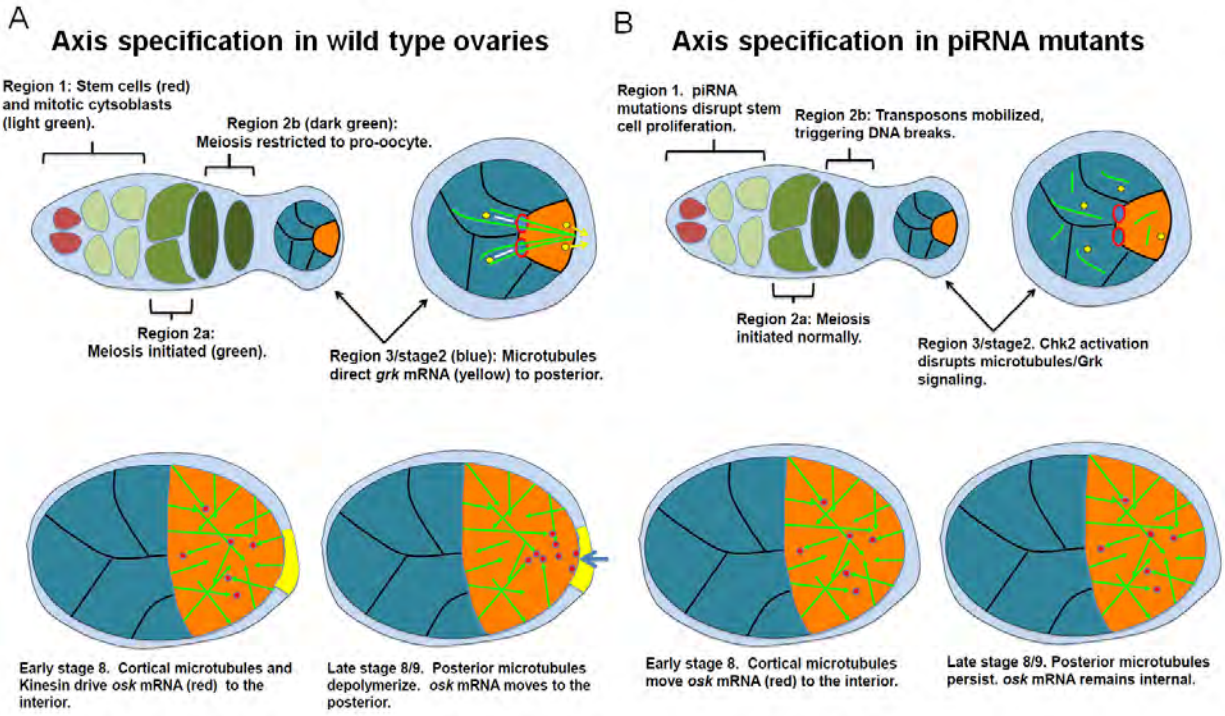
A
Axis specification in wild type ovaries
Region 1: Stem cells (red) and mitotic cytsoblasts (light green).
Region 2b (dark green): Meiosis restricted to pro-oocyte.
Region 2a: Meiosis initiated (green).
Region 3/stage2 (blue): Microtubules direct grk mRNA (yellow) to posterior.
B
Axis specification in piRNA mutants
Region 1. piRNA mutations disrupt stem cell proliferation.
Region 2b: Transposons mobilized, triggering DNA breaks.
Region 2a: Meiosis initiated normally.
Region 3/stage2. Chk2 activation disrupts microtubules/Grk signaling.
Early stage 8. Cortical microtubules and Kinesin drive osk mRNA (red) to the interior.
Late stage 8/9. Posterior microtubules depolymerize. osk mRNA moves to the posterior.
Early stage 8. Cortical microtubules move osk mRNA (red) to the interior.
Late stage 8/9. Posterior microtubules persist. osk mRNA remains internal.

In the majority of piRNA pathway mutations, the earliest phenotype is an increase in DNA damage in germline cells of the germarium (Klattenhoff et al., 2007; Klattenhoff et al., 2009b). Following the stem cell division, the cystoblast proceeds through four incomplete divisions to produce a cysts of 16 interconnected cells that will differentiate into a single oocyte and the nurse cells (Spradling, 1993). Region 2a of the germarium contains early 16 cell cysts, and all 16 cells begin to accumulate double strand breaks and initiate synaptonemal complex (SC) assembly (Carpenter, 1975; Carpenter, 1979). The SC is progressively restricted to a single oocyte, located at the posterior pole, as cysts progress to region 3, where they are surrounded by a monolayer of somatic follicle cells and bud from the germarium to form stage 2 egg chambers (Spradling et al., 1997). During the progression, meiotic DNA breaks are first restricted to the pro-oocyte and then repaired in the oocyte (Jang et al., 2003). Reorganization of the microtubule cytoskeleton is coordinated with these nuclear changes. In early region 2a cysts, the microtubule network shows no clear polarity. However, a single microtubule-organizing center (MTOC), focused on the pro-oocyte, begins to dominate as cysts progress through region 2b and into region 3. This polarized microtubule scaffold is required for asymmetric localization of a TGF-β homolog encoded by the *grk* gene, which signals to posterior follicle cells that are in contact with the pro-oocyte. This initiates a reciprocal germline to soma signaling cascade that patterns the oocyte and the surrounding egg shell (Neuman-Silberberg and Schupbach, 1993; Schupbach, 1987). In piRNA mutants, double strand breaks form normally in region 2a cysts, but the breaks persist and appear to increase as egg chambers mature (Klattenhoff et al., 2007). In addition, the microtubule network is not polarized, which disrupts Grk signaling and initiation of oocyte patterning (Chen et al., 2007; Klattenhoff et al., 2007; Klattenhoff et al., 2009a; Pane et al., 2007).

The first clear oocyte patterning defects associated with piRNA mutations are observed in late stage 8 and early stage 9 (Chen et al., 2007; Klattenhoff et al., 2007; Pane et al., 2007). By early stage 8, most of the oocyte cortex appears to nucleate microtubules, and the microtubule network shows no clear polarity. At this stage, *osk* mRNA, which specifies the posterior pole, is localized to the anterior and lateral cortex (Kim-Ha et al., 1991). By stage 9, however, *osk* mRNA is tightly localized to the posterior cortex. Both fluorescence *in situ* hybridization and time lapse studies using molecular beacons show that *osk* mRNA transiently accumulates in the center of the oocyte before moving to the posterior pole (Bratu et al., 2003; Cha et al., 2002). The second step in *osk* mRNA localization temporally correlates with loss of cortical microtubules specifically at the posterior pole, and mutations in *grk, pka,* and *par1* trap *osk* mRNA in the interior of the oocyte and block depolymerization of microtubules at the posterior cortex (Benton et al., 2002; Cox et al., 2001; Lane and Kalderon, 1993; Roth et al., 1995). In addition, *osk* mRNA remains uniformly at the cortex in oocytes mutant for *khc*, which encodes the plus end directed microtubule motor Kinesin-I (Brendza et al., 2000; Cha et al., 2002). These findings support a two-step model in which microtubules nucleated at the cortex and randomly projecting into the oocyte support Kinesin-dependent movement of *osk* mRNA toward the interior. Depolymerization of posterior microtubules, induced by a signal from the posterior follicle cells and mediated by par-1 and cAMP-dependent protein kinase in the oocyte, eliminates the cortical exclusion force specifically at the posterior pole (Figure 1.2). The remaining oocyte microtubules then support a biased random walk toward the posterior (Serbus et al., 2005; Zimyanin et al., 2008). Assembly of a single MTOC in the oocyte during early oogenesis thus leads to polarized Grk signaling to follicle cells (Figure 1.2, lower panel), which differentiate and signal back to the oocyte during mid-oogenesis, inducing a second microtubule

reorganization that allows *osk* mRNA movement to the posterior cortex (Figure 1.2A). At the same time, *grk* mRNA localizes to the anterior-dorsal cortex of the oocyte, leading to Grk/TGFb signaling to the dorsal follicle cells. It is unclear how *grk* mRNA moves to the dorsal cortex, but this process requires microtubules and the minus end motor Dynein. Mutations that disrupt *osk* mRNA localization generally disrupt *grk* mRNA localization, suggesting that both processes may be initiated by Grk signaling from the oocyte to the follicle cells during early oogenesis.

In piRNA pathway mutants, *osk* mRNA fails to localize to the posterior pole and *grk* mRNA fails to localize to the dorsal cortex during late stage 9 and early stage 10, and this correlates with persistence of cortical microtubules at the posterior pole (Chen et al., 2007; Cook et al., 2004; Klattenhoff et al., 2007; Pane et al., 2007) (Figure 1.2B). These patterning defects during mid-oogenesis lead to production of elongated eggs with reduced or missing dorsal appendages, which are egg shell structures induced by Grk signaling. These findings suggest that piRNA mutations disrupt assembly of the MTOC early in oogenesis, disrupting an early step in oocyte patterning that ultimately leads to production of spindle shaped eggs.

Insight into the link between piRNA function in transposon silencing and these polarity defects came from studies by Schüpbach and colleagues, who showed that a subset of spindle class genes encodes meiotic DNA break repair enzymes, and that these mutations lead to persistent DNA breaks during early oogenesis (Ghabrial et al., 1998). They speculated that these breaks activate damage signaling, which in turn disrupts oocyte patterning. Supporting this hypothesis, they showed that mutations in *mei-41* and *mnk*, which encode ATR and Chk2 kinases that function in DNA damage signaling, suppress the axis specification defects associated with meiotic DNA repair mutations (Abdu et al., 2002; Ghabrial and Schupbach, 1999). Transposon mobilization, and particularly the excision of DNA elements, can lead to DNA breaks

(Belgnaoui et al., 2006; Gasior et al., 2006), and piRNA mutations lead to persistent DNA damage during early oogenesis. Significantly, mutations in *mnk* and *mei-41* dramatically suppress the patterning defects associated with these mutations (Chen et al., 2007; Klattenhoff et al., 2007; Klattenhoff et al., 2009b; Pane et al., 2007) (Figure 1.3B). These observations support a model in which loss of silencing leads to transposon mobilization and DNA break accumulation, which in turn trigger Chk2-dependent defects in axis specification (Klattenhoff and Theurkauf, 2007).

As noted above, posterior patterning of the oocyte appears to require assembly of a single microtubule organizing center in the pro-oocyte during oogenesis. This leads to oocyte-specific localization of *grk* mRNA and Grk/TGFb signaling to the posterior follicle cells.

Figure 1.3. piRNA mutations trigger Chk2-dependent defects in microtubule polarity. A. During early oogenesis in wild type females (wt), a prominent microtubule-organizing center (MTOC) forms in the pro-oocyte. The resulting microtubule scaffold mediates asymmetric *grk* mRNA localization and Grk signaling to the follicle cells, initiating axis specification. The MTOC fails to form in *armi* mutants (*armi*). By contrast, a prominent MTOC forms in females mutant for both *armi* and *mnk,* which encodes the DNA damage signaling kinase Chk2 (*mnk;armi*). B. Osk protein (green) localizes to the posterior of wild type stage 9 oocytes (wt), but is dispersed in *armi* mutants (*armi*). Posterior localization of Osk protein is restored in oocytes mutant for both *armi* and *mnk.* F-actin is shown in red. Adapted from Klattenhoff et al., 2007.

Figure 1.3

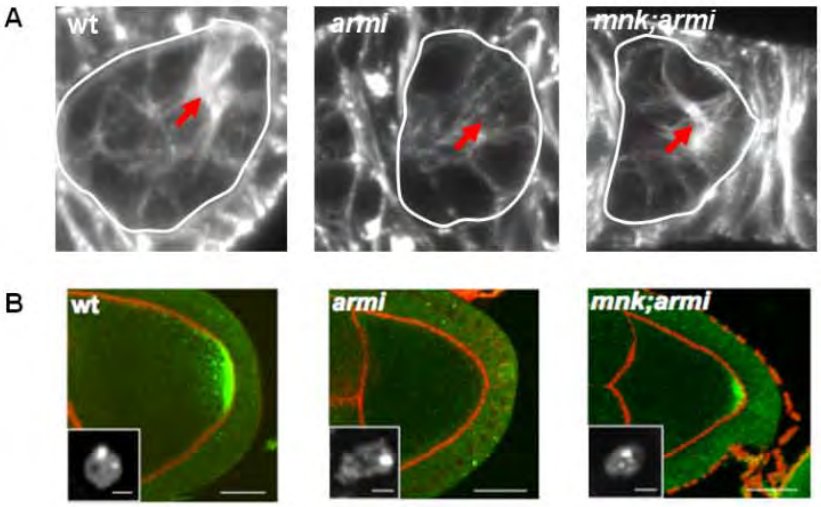

Mutations in the piRNA genes *armi* and *aub* disrupt this MTOC, and the subsequent depolymerization of microtubules at the posterior cortex of stage 9 oocytes (Cook et al., 2004). Significantly, the mutations in *mnk* and *mei-41* that suppress defects in patterning also restore MTOC formation during early oogenesis (Klattenhoff et al., 2007) (Figure 1.3A). In early *Drosophila* embryos, Chk2 activation triggers γ-Tubulin ring complex dissociation from centrosomes, disrupting mitotic MTOC formation (Takada et al., 2003). Taken together, these finding suggest that piRNA pathway mutations lead to transposon over-expression and mobilization, which triggers Chk2-dependent defects in MTOC formation early in oogenesis, thus preventing an early step in the oocyte patterning cascade (Figure 1.3A and B).

While this model is appealing, DNA damage in the piRNA pathway mutations has not been directly linked to transposon mobilization, and the mechanism of Chk2 dependent disruption of the oocyte MTOC remains to be determined. In addition, mutations in *mnk* and *mei-41* do not suppress the maternal-effect embryonic lethality associated with piRNA pathway mutation, and the essential embryonic functions for this pathway remain to be explored. Nonetheless, the available data suggest that the axis specification defects produced by many *Drosophila* piRNA mutations are an indirect consequence of transposon over-expression and DNA damage signaling.

Conclusions

Mutations that disrupt the piRNA pathway in mouse and fish lead to germline specific cell death and sterility, and are also associated with increased transposon expression (Aravin et al., 2007; Carmell et al., 2007; Houwing et al., 2007). Studies in *Drosophila* suggest that transposon mobilization represent the primary biological trigger for these phenotypes, and that mobile

elements are the primary targets for the piRNA pathway. However, the vast majority of piRNAs in the mouse germline map to unique sequences in unannotated regions of the genome, a subset of *Drosophila* piRNAs are derived from protein coding genes, and piRNAs appear to control at least one gene target in *Drosophila* ovarian somatic cells (Aravin et al., 2006; Girard et al., 2006a). This observation merits further investigation to understand the biological relevance of these genic piRNAs. Piwi, in complex with some miRNA pathway components, has also been suggested to be involved in pole-plasm maintenance and germline determination (Megosh et al., 2006). There is also intriguing data implicating the piRNA pathway in learning and memory and chromatin assembly in the soma (Ashraf et al., 2006; Brower-Toland et al., 2007a; Pal-Bhadra et al., 2004a). The biological function for this novel class of small RNAs may therefore extend well beyond transposons and germline development.

CHAPTER 2

Distinct functions for the *Drosophila* piRNA pathway in genome maintenance and telomere protection

Summary

Transposons and other selfish genetic elements make up a significant fraction of all eukaryotic genomes, and the piRNA pathway appears to have a conserved function in transposon silencing and genome maintenance. However, other functions for this pathway have not been fully explored. Telomeres must be protected from recognition as DNA breaks by the repair machinery, which can covalently ligate unprotected chromosome ends and thus disrupt meiotic and mitotic chromosome segregation. I show that mutations in a subset of piRNA pathway genes disrupt meiotic and mitotic chromosome separation, and that these segregation defects are suppressed by a mutation that blocks ligation of non-homologous DNA ends. These mutations also disrupt assembly of the telomere protection complex and reduce expression of a subpopulation of 19 to 22 nt telomere specific RNA. We therefore propose that a subpopulation of short piRNAs direct assembly of the telomere protection complex.

Introduction

Drosophila piRNAs have been implicated in transposon silencing and maintenance of genome integrity during female germline development, but piRNA pathway mutations lead to complex developmental phenotypes (Chen et al., 2007; Cook et al., 2004; Klattenhoff et al., 2007; Li et al., 2009; Malone et al., 2009; Pane et al., 2007; Vagin et al., 2004). In addition, recent studies

suggest that piRNAs can regulate gene expression in different systems (Aravin et al., 2001; Nishida et al., 2007; Saito et al., 2009; Vagin et al., 2006), and the majority of piRNAs in other systems, including mouse testes, are not derived from repeated elements (Aravin et al., 2006; Batista et al., 2008; Girard et al., 2006b; Grimson et al., 2008; Grivna et al., 2006a). The full extent of piRNA functions thus remains to be explored.

Mutations in the majority of *Drosophila* piRNA pathway genes disrupt asymmetric localization of RNAs along the axes of the oocyte, and lead to maternal effect embryonic lethality (Chen et al., 2007; Cook et al., 2004; Klattenhoff et al., 2007; Pane et al., 2007). The axis specification defects linked to several of piRNA pathway mutations are dramatically suppressed by a null mutation in *mnk,* which encodes a Checkpoint kinase 2 (Chk2) homolog required for DNA damage signaling, indicating that the loss of asymmetric RNA localization is downstream of DNA damage (Chen et al., 2007; Klattenhoff et al., 2007). Oocyte patterning defects generally lead to embryonic lethality, but the *mnk* allele that suppresses the axis specification defects associated with piRNA mutations does not suppress embryonic lethality (Chen et al., 2007; Klattenhoff et al., 2007; Pane et al., 2007). piRNAs thus have an essential function during embryogenesis that is independent of Chk2 activation and DNA damage signaling. To gain insight into potential new functions for the piRNA pathway, we have characterized the embryonic lethality associated with four piRNA pathway mutations. These studies reveal a novel function for a subset of piRNA genes in assembly of the telomere protection complex, and suggest that this process is directed by a subpopulation of 19-22 nt piRNAs.

Results and Discussion

The *armi* and *aub* genes encode a putative RNA helicase and a piRNA binding PIWI Argonaute protein, and recent studies suggest that they have distinct functions in piRNA biogenesis (Klattenhoff et al., 2007; Klattenhoff et al., 2009b; Malone et al., 2009; Vagin et al., 2006) Mutations in *aub* dramatically reduce piRNA species that overlap by 10 nt, which is characteristic of ping-pong amplification, while *armi* mutations reduce total piRNA production but enhance the ping-pong signature (Li et al., 2009; Malone et al., 2009). Mutations in *aub* and *armi* lead to maternal-effect embryonic lethality, however, suggesting that these genes share an essential function. To gain insight into the lethality associated with these mutations, we first analyzed DNA break accumulation during oogenesis. Germline-specific DNA breaks normally form during early oogenesis, as meiosis is initiated (McKim et al., 2002). In several piRNA mutants, however, DNA breaks persist, which could compromise the female pronucleus and thus lead to genetic instability in the early zygote (Klattenhoff et al., 2007; Klattenhoff et al., 2009b). DNA breaks trigger phosphorylation of histone H2Av, producing γ-H2Av foci near the break sites (Madigan et al., 2002). In wild-type ovaries, γ-H2Av foci begin to accumulate in region 2 of the germarium, as meiotic breaks are formed (McKim et al., 2002). These foci are significantly reduced in stage 2 egg chambers, which have completed meiotic repair and budded from the germarium. Later in oogenesis, γ-H2Av foci accumulate in the nurse cell nuclei, which undergo endo-reduplication. However, these foci remain undetectable in the oocyte (McKim et al., 2002). In ovaries mutant for *aub* or *armi,* γ-H2Av foci appear in germarium region 2, but persist

in nurse cells and oocyte through stage 4. By stage 5, however, γ-H2Av foci are undetectable in 50% of *armi* and *aub* mutant oocytes, and are significantly reduced in the remaining oocytes (Figure 2.1). Both *armi* and *aub* mutations thus increase DNA damage during early oogenesis, but damage in the oocyte appears to be repaired as oogenesis proceeds.

As wild type oocytes mature and initiate meiotic spindle assembly, the major chromosomes form a single mass at the spindle equator and the non-exchange 4^{th} chromosomes move toward the poles (Gilliland et al., 2009; Theurkauf and Hawley, 1992). In *OregonR*, we observed distinct 4^{th} chromosomes in 79% of stage 13 oocytes. In stage 13 *aub* and *armi* mutants, by contrast, distinct 4th chromosomes were observed in only 11% and 18% of stage 13 oocytes, respectively (Figure 2.2, Table 2.1). However, a single primary mass of chromatin was always observed.

Figure 2.1: DNA breaks in the piRNA mutants disappear by the end of oogenesis

Immunostaining of ovaries from *OregonR* control, *aub* and *armi* mutants for γ-H2Av (green) and DNA (blue) during stage 3, 5 and 8/9 of oogenesis showing the disappearance of the γ-H2Av signal by late stages. The arrow points to the karyosome. F-actin is displayed in red.

Figure 2.1

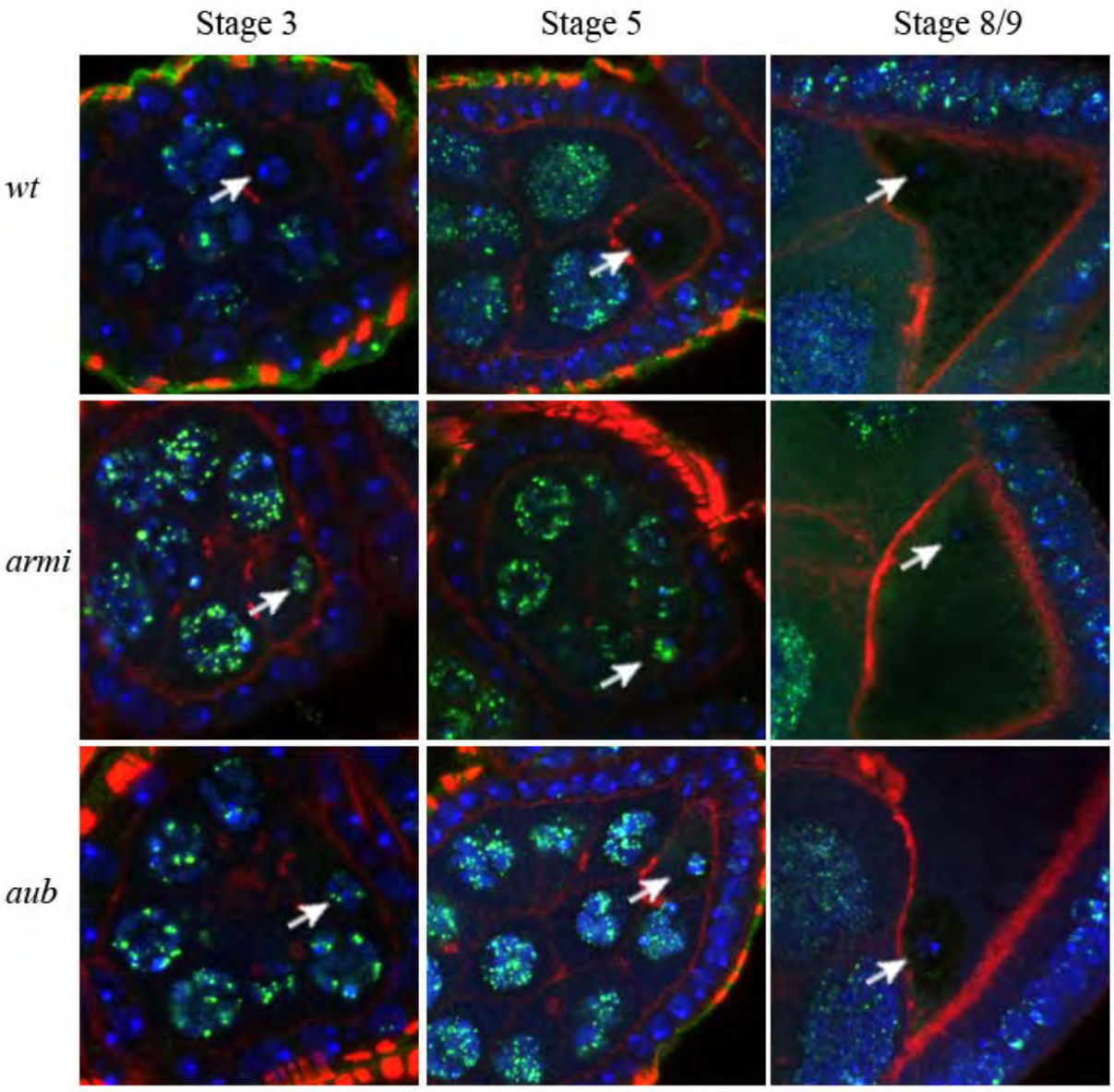

Figure 2.2: Mature oocytes in piRNA mutants show compact chromatin mass

Overview of stage 13 oocytes in *OregonR*, *armi* and *aub* females stained for DNA, showing lack of compromised genome integrity in the mutants. Inset at the bottom right shows the magnified view of the oocyte nucleus.

Figure 2.2

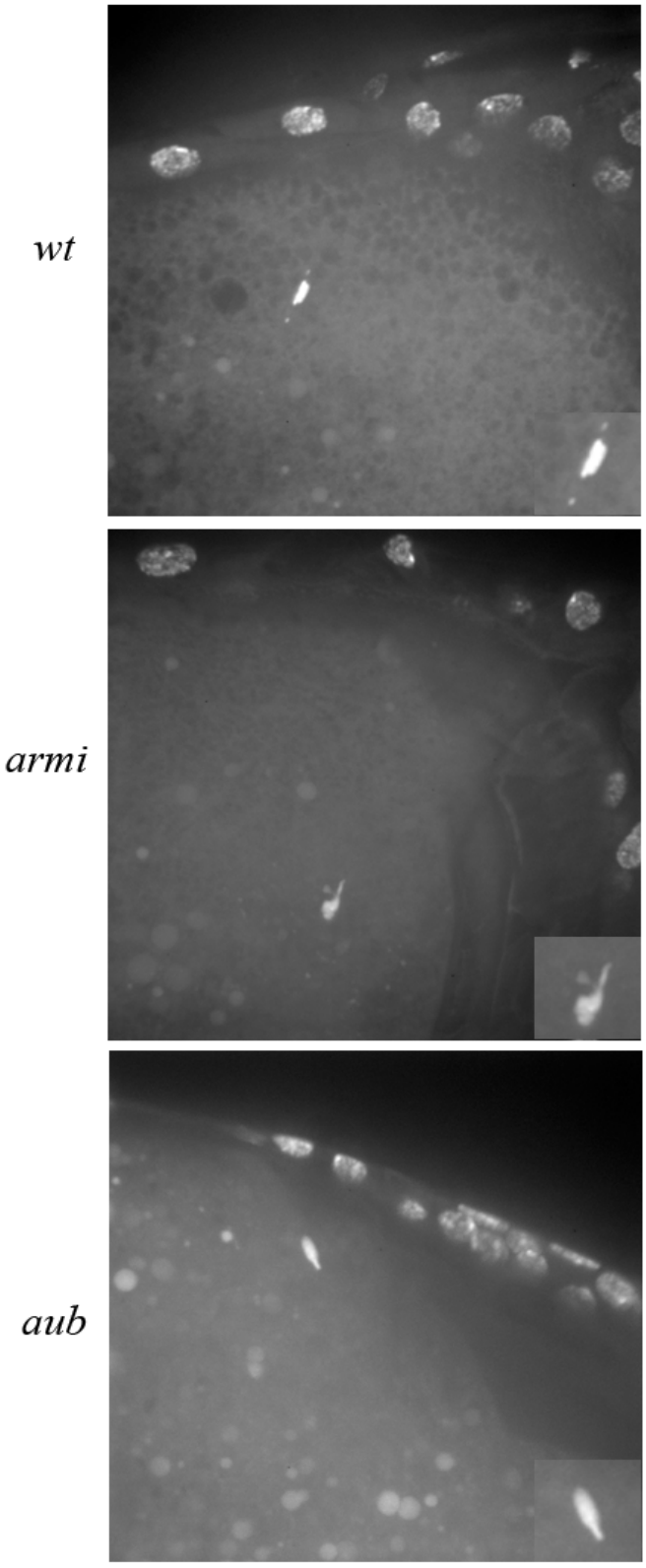

Table 2.1: 4th chromosome morphology in stage 13 oocytes

Genotype	Percentage of Stage 13 oocytes showing separate 4th chromosomes	Number of oocytes scored
OregonR	78.57	28
$armi^{1/72.1}$	17.65	17
$aub^{HN/QC}$	11.11	18

These observations are consistent with the conclusion that DNA breaks formed during early oogenesis are often repaired as the oocyte matures. In addition, both *aub* and *armi* mutations appear to inhibit separation of the small 4th chromosomes, although it is also possible that this small chromosome is fragmented and thus difficult to detect cytologically.

Drosophila oocytes are activated as they pass through the oviduct, which triggers completion of the meiotic divisions. The first meiotic division is completed in the oviduct, but meiosis II can be observed in freshly laid eggs and is characterized by four well-separated meiotic products on tandem spindles (Figure 2.3A). In *aub* and *armi* mutant embryos, the meiotic chromatin was either stretched across the paired meiotic spindles, or fragmented and spread over both spindles (Figure 2.3A). No wild type meiotic figures were observed. Breaks thus appear to persist in some stage 14 oocytes, although this does not disrupt the karyosome organization during earlier stages. However, other oocytes appear to have intact chromosomes that fail to resolve during the meiotic divisions.

Compromised zygotic genomic integrity in piRNA mutants

Fertilization and pronuclear fusion then initiate 13 rapid cleavage stage mitotic divisions (McKim et al., 2002). These divisions are syncytial, but membranes surround the cortical nuclei to form cells following mitosis 13 (Foe, 1993). 0 to 3-hr old cleavage stage *aub* and *armi* mutant embryos showed two distinct phenotypes. 60% of *aub* mutant embryos and 90% of *armi* mutant embryos contained dispersed chromatin fragments that were often associated with small spindle-like microtubule bundles (Figure 2.3B, Table 2.2).

Figure 2.3: Chromatin defects in piRNA mutants

A. Immunostaining for α-tubulin (green) and DNA (blue) in 0-30-min-old embryos showing chromatin fragmentation and chromatin fusions in *aub* and *armi* mutant embryos during meiosis II. Scale bar is 15μM.

B. Cross-section of 0-3-hr-old embryos during syncytial mitotic divisions showing DNA fragmentation and chromatin bridges during segregation in *aub* and *armi* mutants. Scale bar is 10μM.

C, D. Dual-label FISH for two Y-chromosome-specific satellites, (AATAC)n in green and (AATAAAC)n in red, with DNA in blue showing mis-segregation of these repeats in *aub* and *armi* embryos (C). In contrast, embryos undergoing cleavage mitotic divisions show both the labels in most of the segregating chromatids in *aub* (D).

Figure 2.3

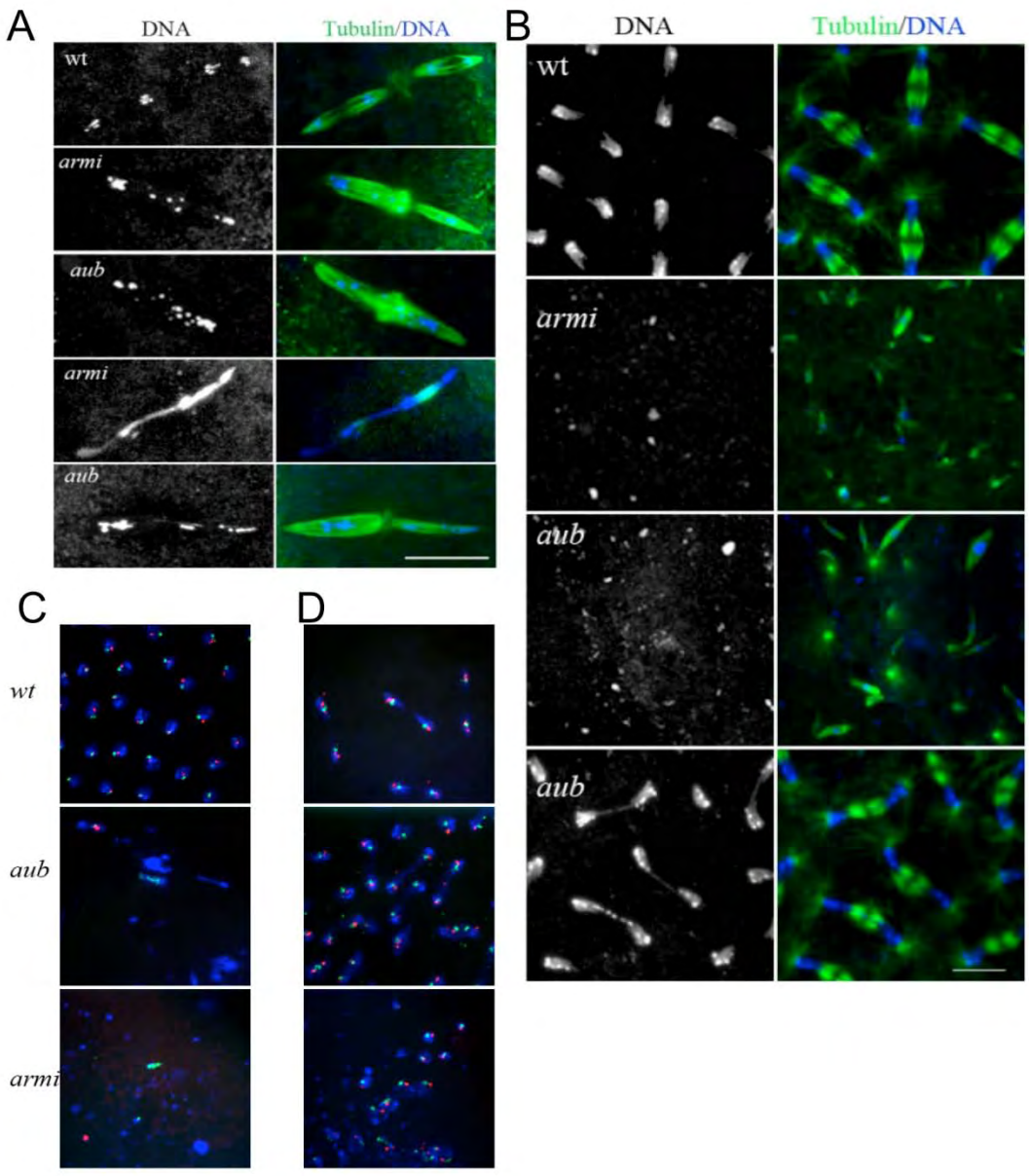
A
DNA
Tubulin/DNA
wt
armi
aub
armi
aub
B
DNA
Tubulin/DNA
wt
armi
aub
aub
C
D
wt
aub
armi

Table 2.2: Percentage of embryos from different genotypes showing chromatin fragmentation

Genotype	Fragmented	Cycling	Mixed
$aub^{HN2/QC42}$	60	38	2
mnk^{p6},aub^{HN2}/mnk^{p6},aub^{QC42}	40	59	1
$ligIV^{5}$/ $ligIV^{5}$;aub^{HN2}/aub^{QC42}	73	11	16
$armi^{1}$/$armi^{72.1}$	88	10	2
mnk^{p6}/mnk^{p6};$armi^{1}$/$armi^{72.1}$	77	13	11
$ligIV^{5}$/$ligIV^{5}$;$armi^{1}$/$armi^{72.1}$	92	2	7

The remaining embryos appear to be progressing through the cleavage divisions, and some cellularization and gastrulation stage embryos are observed. However, chromosome bridges/lagging chromosomes were present in 50% to 70% of the cleavage stage anaphase and early telophase figures (Figure 2.3B and Figure 2.4C).

Chromatin fragmentation could result from replication of broken chromosomes inherited from the female, or from post-fertilization fragmentation of the zygotic genome. To directly assay zygotic genome integrity, mutant females were mated to wild type males and dual-label FISH was used to monitor physically separate regions of the Y chromosome. In male embryos derived from wild type females, the two Y chromosome probes always co-segregated through anaphase and telophase (Figure 2.3C, D). Mutant embryos showing chromatin fragmentation, by contrast, contained chromatin clusters that did not label for either Y chromosome probe, or that labeled for only one of the two probes (Figure 2.3C). In mutant embryos that proceeded through cleavage stage mitotic cycles, the majority of segregating chromatids retained both Y chromosome markers, indicating that chromosome continuity had been maintained. Chromatids with only one of two markers were observed, however, indicating that breaks had separated regions on a Y chromosome arm from the centromere (Figure 2.3D). The axial patterning defects associated with piRNA mutations are suppressed by mutations in *mnk* (Chen et al., 2007; Klattenhoff et al., 2007), but *mnk* did not suppress either the chromatin fragmentation or segregation defects linked to *aub* and *armi* (Table 2.2, Figure 2.5). Mutations in *aub* and *armi* thus destabilize the genome of the zygote and disrupt chromosome resolution during the cleavage divisions through processes that are independent of DNA damage signaling.

Figure 2.4: Chromatin bridges in piRNA mutants are *ligIV* – dependent telomere fusions.

A. Two-color FISH for a pair of daughter nuclei in anaphase, labeled for centromeric *dodeca* satellite (green) and telomeric transposon, *HeT-A* (red) with DNA (blue) showing telomeres are fused in piRNA mutants.

B. Immunostaining for microtubules (green) and DNA (blue) in 0-3 hr-old embryos showing suppression of chromatin bridge formation in *ligIV;aub* embryos. Scale bar is 10μM.

C. Ratio of anaphase/telophase bridges to total anaphase/telophase figures in different genotypes. The data for multiple samples were compared using Anova test, and sample mean was plotted with standard error of mean (SEM) as error bars. A two-tailed t-test was performed for certain pairs and p-values are noted on the graph.

Figure 2.4

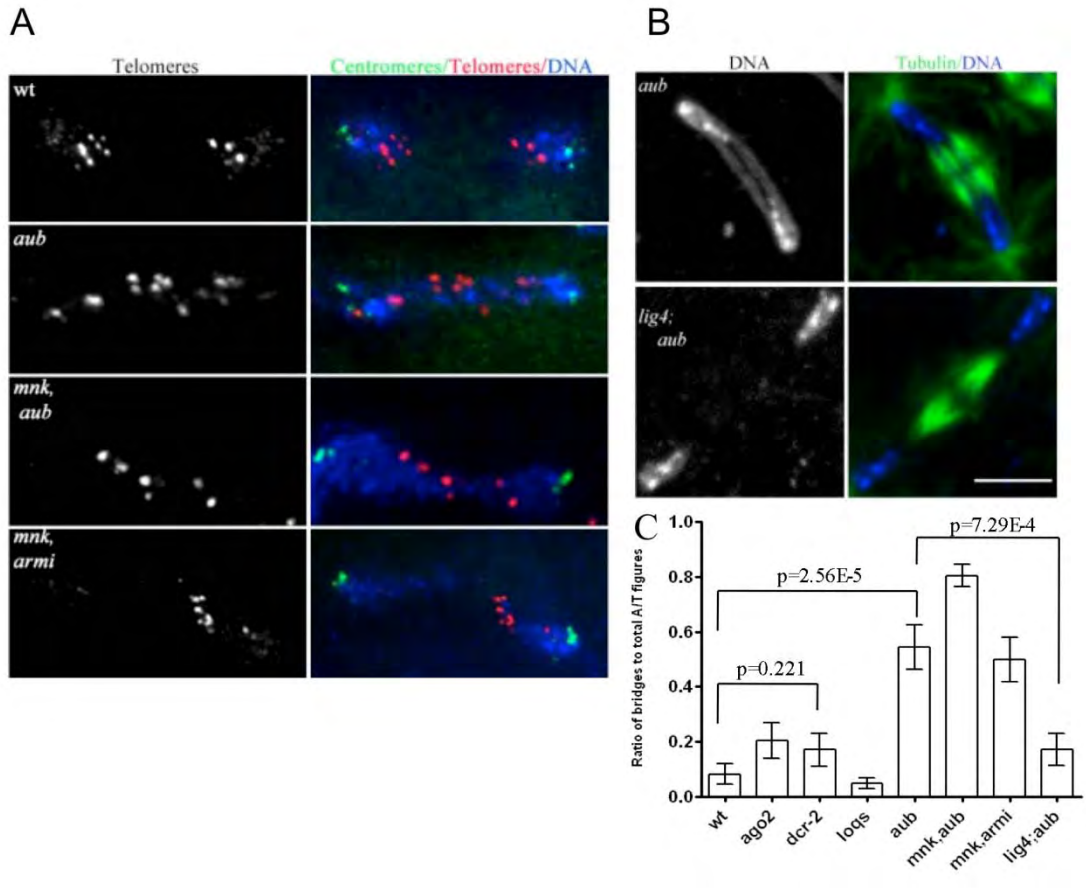
A
Telomeres
Centromeres/Telomeres/DNA
wt
aub
mnk,
aub
mnk,
armi
B
DNA
Tubulin/DNA
aub
lig4;
aub
C
Ratio of bridges to total A/T figures
1.0
0.8
0.6
0.4
0.2
0.0
p=2.56E-5
p=7.29E-4
p=0.221
wt
ago2
dcr-2
loqs
aub
mnk,aub
mnk,armi
lig4;aub

Figure 2.5: DNA bridges in piRNA mutants are independent of Chk2 activation

Immunostaining of DNA (blue) and microtubules (green) in embryos from *mnk*, *mnk armi* and *mnk aub* showing chromatin bridges and chromatin fragmentation during syncytial mitotic divisions.

Figure 2.5

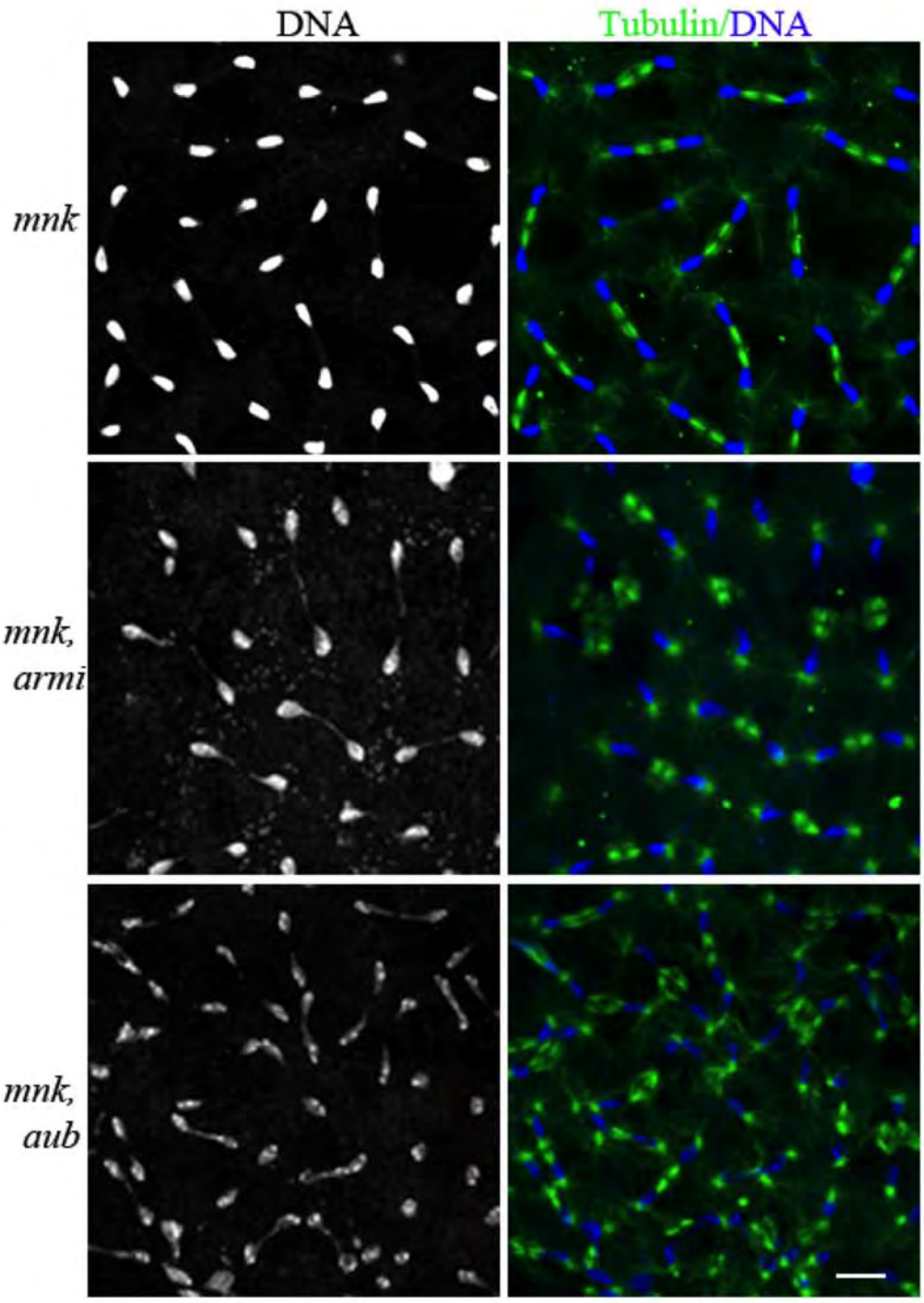

Mutations in the *armi* and *aub* genes disrupt piRNA production and transposon silencing, but have also been reported to inhibit homology dependent target cleavage by siRNAs (Kennerdell et al., 2002; Tomari et al., 2004). In addition, null mutations in *argonaute2 (ago2),* which block siRNA based silencing, have been reported to disrupt mitosis during the syncytial blastoderm stage (Deshpande et al., 2005). These observations raise the possibility that chromatin fragmentation and fusion in *aub* and *armi* mutants result from defects in the siRNA pathway. We therefore analyzed cleavage in embryos from females homozygous for null mutations in *ago2* and *dcr2,* which block siRNA production and silencing (Lee et al., 2004). Consistent with previous studies, we find that embryos from *ago2* and *dcr2* mutant females are viable (Deshpande et al., 2005; Lee et al., 2004). In addition, we did not observe chromosome fragmentation or a statistically significant increase in anaphase bridge formation relative to wild type controls (Figure 2.4C, Figure 2.6). The *loquacious* (*loqs)* gene encodes a Dicer-1 binding protein required for miRNA production (Park et al., 2007), and we find that embryos from *loqs* mutant females also proceed through normal cleavage stage divisions (Figure 2.4C, Figure 2.6). Chromosome segregation and maintenance of zygotic genome integrity during early embryogenesis are therefore independent of siRNAs and miRNAs, but require at least two components of the piRNA pathway.

Telomere fusions in *aub* and *armi* embryos

In *S. pombe*, mutations in *ago1*, *dcr1* and *rdp1* disrupt kinetochore assembly and thus lead to lagging mitotic chromosomes due to defects in centromere movement to the spindle poles (Hall et al., 2003). To determine if *Drosophila* piRNA mutations disrupt kinetochore assembly,

we performed dual label FISH for centromeric dodeca-satellite sequences (Abad et al., 1992) and the telomere-specific transposon *HeT-A*. In *aub* and *armi* mutants, centromeric sequences segregated to the spindle poles in essentially every anaphase figure, but telomere specific sequences were consistently present at the chromatin bridges (Figure 2.4A). These observations indicate that *armi* and *aub* are not required for kinetochore assembly, but are needed for telomere resolution.

Figure 2.6: Chromosome segregation in RNAi and miRNA mutants. Immunostaining of DNA (blue) and microtubules (green) in embryos from *ago2*, *dcr2* and *loquacious* (*loqs*) showing normal chromosome segregation during syncytial mitotic divisions.

Figure 2.6

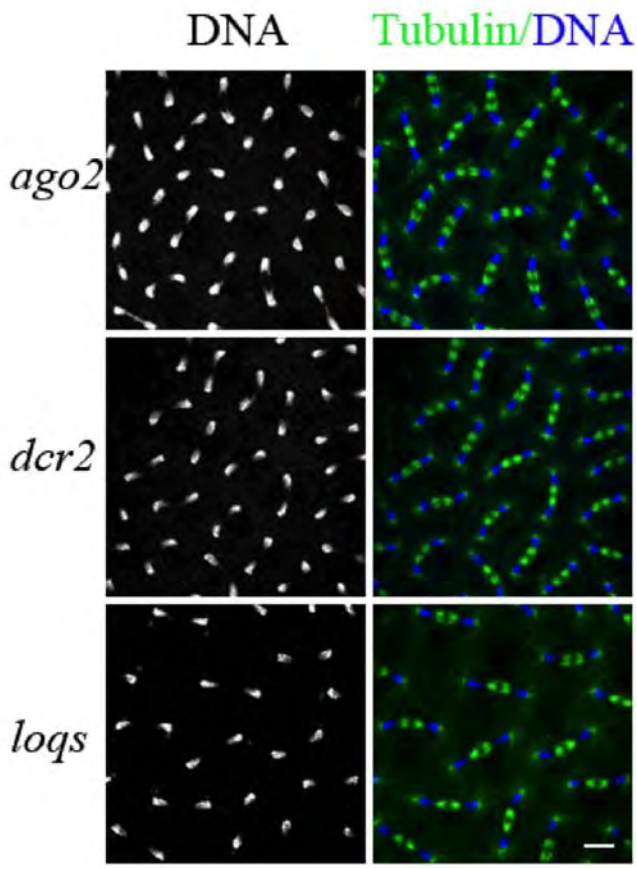

Telomeres are protected from recognition as DNA double strand breaks by the telomere-protection complex (TPC) and defects in telomere protection thus lead to covalent ligation of chromosome ends by the non-homologous end-joining (NHEJ) pathway (Bi et al., 2005; Smogorzewska et al., 2002). DNA Ligase IV is required for NHEJ, and *ligase IV* mutations suppress fusions that result from covalent joining of unprotected chromosome ends (Bi et al., 2005; Smogorzewska et al., 2002). To determine if chromosome fusions in *aub* and *armi* are due to NHEJ, we generated *ligIV;aub* and *ligIV;armi* double mutant females and analyzed chromosome segregation in the resulting embryos. In *aub* single mutant embryos, 50% of anaphase figures show bridges, but anaphase bridges are present in only 15% of *ligIV;aub* double mutants (Figure 2.4B and C). By contrast, the fraction of embryos showing chromosome fragmentation increases in *ligIV;aub* double mutants (Table 2.2). Chromosome fragmentation also increased in *ligIV;armi* mutant embryos, and as a result morphologically normal anaphase figures could not be observed (Table 2.2). These findings strongly suggest that lagging chromosomes are the result of aberrant covalent ligation of chromosome ends by the NHEJ pathway, while chromatin fragmentation results from DNA breaks that are repaired by NHEJ pathway. Mutations in *armi* and *aub* lead to significant over-expression of transposable elements (Klattenhoff et al., 2009b; Li et al., 2009; Vagin et al., 2006), including DNA elements that are mobilized by a "cut and paste" mechanism that directly produces double strand breaks (Wicker et al., 2007). In addition, NHEJ pathway has been implicated in repair of gapped retroviral integration intermediates (Li et al., 2001). Chromosome fragmentation may therefore result from transposon over-expression and mobilization, which induces breaks that overwhelm the NHEJ pathway. Telomere fusions, by contrast, appear to result from defects in telomere protection, which prevent chromosome end recognition by the NHEJ pathway.

Assembly of the telomere protection complex

The *Drosophila* TPC includes HOAP and Modigliani (Moi), which may function only at chromosome ends, and HP1a and the MRN complex, which have additional roles in heterochromatic silencing and DNA repair (Bi et al., 2004; Cenci et al., 2003; Perrini et al., 2004; Raffa et al., 2009). To directly assay for TPC recruitment, we used chromatin immunoprecipitation (ChIP) to measure HP1a and HOAP binding to the telomere specific transposon *HeT-A* (Figure 2.7B, C). In wild type ovaries, HOAP and HP1a bind to multiple regions of *HeT*-A (Figure 2.7B and C). In *armi* and *aub* mutants, by contrast, HOAP and HP1a binding to the *Het-A* 5'-UTR and ORF are significantly reduced (Figure 2.7B and C). The 5'end of *Het-A* is oriented toward the chromosome end, and is therefore likely to lie at the telomere. Ovarian tissue consists of germ cells with a surrounding layer of somatic cells which complicate interpretation of these biochemical studies. We therefore performed ChIP on 0-3 hour old embryos from *aub* and *mnk,aub* mutant females, which showed significant reduction in HOAP binding at the *HeT-A* 5'-UTR (Figure 2.8). These findings indicate that *aub* and *armi* are required for TPC recruitment, supporting the hypothesis that these mutations lead to covalent ligation of chromosome ends.

To determine if other piRNA pathway mutations disrupt telomere protection, we analyzed the cleavage stage embryonic divisions in *ago3* and *rhi* mutants. The *ago3* locus encodes a PIWI clade protein that primarily binds sense strand piRNAs, and *rhi* encodes a rapidly evolving HP1 homologue required for production of precursor RNAs from a subset of piRNA clusters (Klattenhoff et al., 2009b; Li et al., 2009). Essentially all of the *rhi* and *ago3* mutant embryos showed chromatin fragmentation, as observed in the majority of *aub* and *armi* mutants (Figure 2.9).

Figure 2.7: Mutations in *aub* and *armi* disrupt assembly of the telomere protection complex.

A. Schematic showing transposon arrays at *Drosophila* telomeres. The *HeT-A* transposon 3' and 5'-UTRs are in red and yellow respectively, and the ORF is in blue.

B and C. Binding of the telomere protection complex proteins HOAP and HP1 to *HeT-A.* Chromatin Immunoprecipitation (ChIP) was used to recover bound DNA, and the percent of input chromatin precipitated was determined by qPCR. Fold change in binding relative to wild type is shown, and was calculated by dividing mutant by wild type (wt) values.

D. Genomic copy number for *HeT-A* and *TART*. Copy number was determined by qPCR, using the single copy Rp49 gene as an internal standard. *Gaiano* is a wild-type stock previously shown to carry additional telomeric transposon repeats.

Figure 2.7

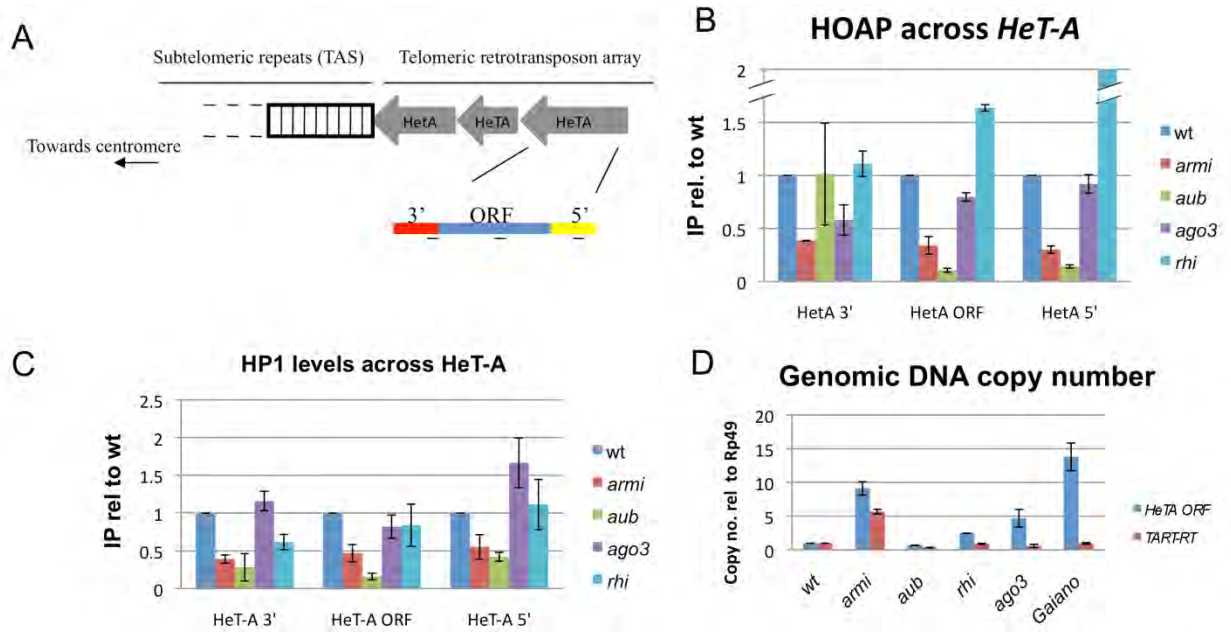
A
Subtelomeric repeats (TAS)
Telomeric retrotransposon array
Towards centromere
HetA
HeTA
HeTA
3'
ORF
5'
B
HOAP across HeT-A
IP rel. to wt
2
1.5
1
0.5
0
HetA 3'
HetA ORF
HetA 5'
wt
armi
aub
ago3
rhi
C
HP1 levels across HeT-A
IP rel to wt
2.5
2
1.5
1
0.5
0
HeT-A 3'
HeT-A ORF
HeT-A 5'
wt
armi
aub
ago3
rhi
D
Genomic DNA copy number
Copy no. rel to Rp49
20
15
10
5
0
wt
armi
aub
rhi
ago3
Gaiano
HeTA ORF
TART-RT

Figure 2.8: HOAP recruitment defect in early embryos

ChIP-qPCR analysis of HOAP antibody from 0-3-hr old embryos in *wt*, *aub* and *mnk aub*across telomeric regions.

Figure 2.8

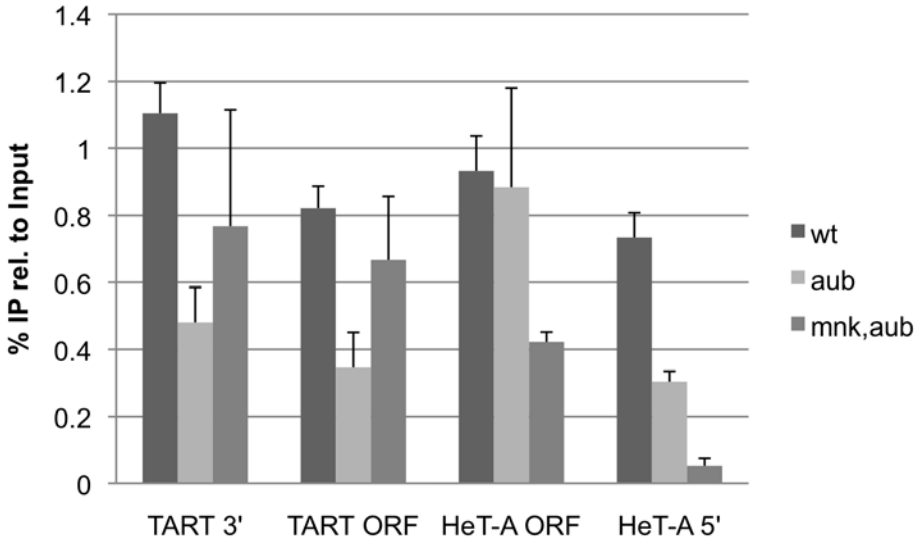
1.4
1.2
1
0.8
0.6
0.4
0.2
0
% IP rel. to Input
TART 3'
TART ORF
HeT-A ORF
HeT-A 5'
wt
aub
mnk,aub

Figure 2.9: Chromatin defects in piRNA mutants are independent of telomeric length. Immunostaining for microtubules (green) and DNA (blue) in 0-3 hr old embryos from *rhi*, *ago3* and *Gaiano*. All these samples show longer *HeT-A* arrays, however, *Gaiano* stocks show no signs of chromatin defects.

Figure 2.9

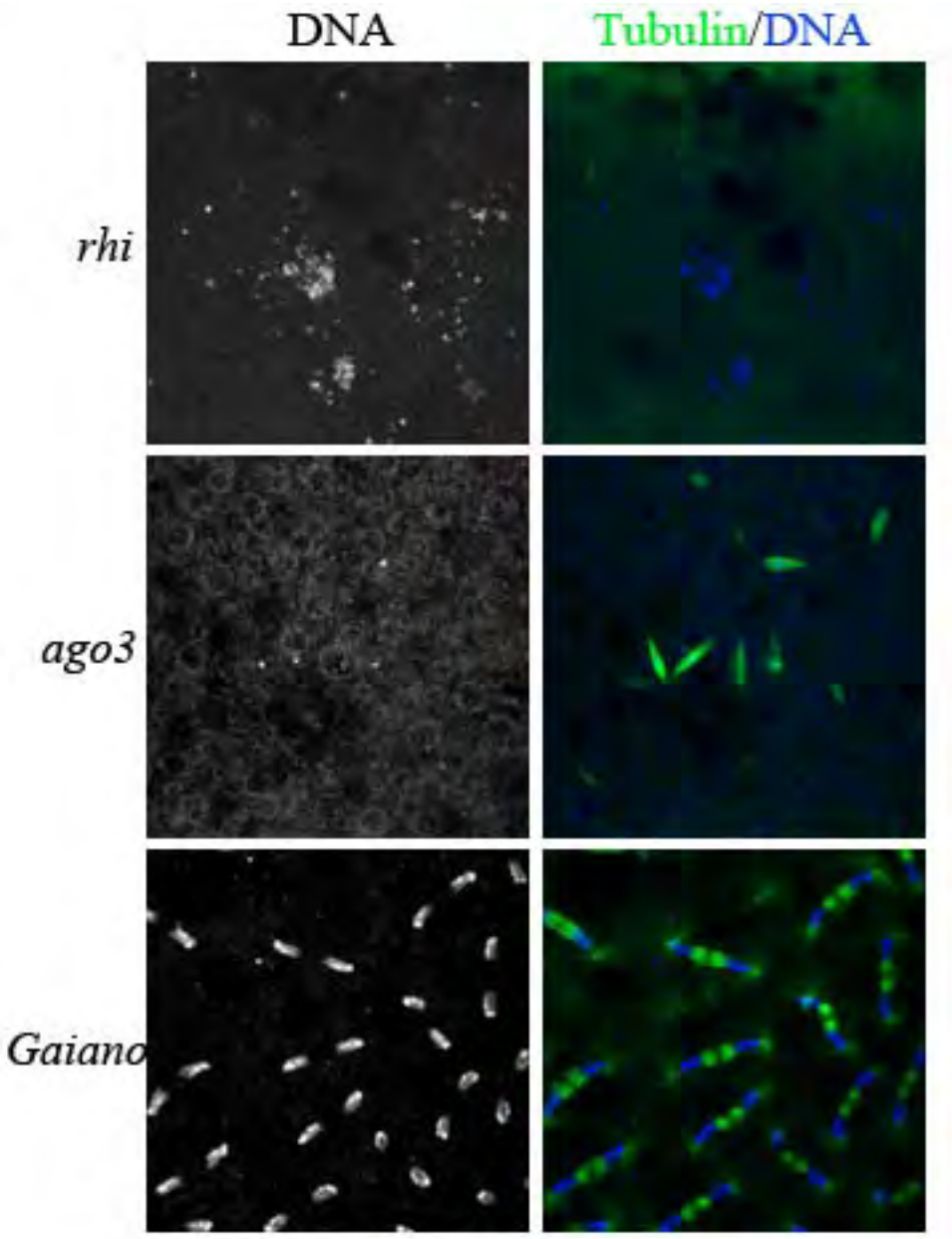

We therefore biochemically assayed for telomere protection complex assembly in ovarian chromatin using ChIP for HOAP and HP1a. Surprisingly, neither *ago3* nor *rhi* mutations disrupt HOAP or HP1a binding to *Het-A* (Figure 2.7B and C). Since the *ago3* mutations assayed appear to be null, the absence of TPC assembly defects are not due to residual protein function. The *rhi* mutations are strong hypomorphs, but show greater than wild type levels of HOAP binding to *Het-A.* By contrast, these alleles reduce total piRNA production by 10 fold (Klattenhoff et al., 2009b). It is therefore unlikely that *rhi* functions in telomere protection. Instead, these findings suggest that *aub* and *armi* have a function in telomere protection that is not shared with *ago3* or *rhi*.

In *Drosophila*, chromosome breaks can be converted to stable telomeres (Biessmann et al., 1990), called terminal deletions, which accumulate additional copies of the telomeric elements *HeT-A* and *TART*. When terminal deletions are passaged in animals heterozygous for *aub* or the piRNA pathway gene *spnE,* the number of terminal *TART* repeats increase (Savitsky et al., 2006). Therefore, the defects in TPC assembly in *aub* and *armi* could be secondary to increased *HeT-A* and *TART* copy number, which could titrate telomere binding proteins. We therefore assayed telomeric transposon copy number in *aub* and *armi* mutants, which show defects in TPC assembly, and in *rhi* and *ago3* mutants, which do not. We also assayed telomeric transposon copy number and mitotic chromosome segregation in a wild-type variant, *Gaiano*, that has been reported to carry additional *HeT-A* repeats (Siriaco et al., 2002). Consistent with previous reports, we find that *Gaiano* has 10 to 15 fold more *HeT-A* copies than *OregonR* controls (Figure 2.7 D). Despite the increase in telomere length, this stock is viable and fertile, and we did not observe telomere fusions or lagging chromosomes during the cleavage stage embryonic divisions (Figure 2.9). In addition, we found that *aub* mutants that show defects in

TPC assembly do not accumulate additional copies of *HeT-A* or *TART*, while *rhi* and *ago3* mutants that are wild type for TPC binding show an increase in telomere-specific transposon copy number (Figure 2.7 D). Assembly of the TPC is therefore independent of telomere specific transposon copy number (Figure 2.9).

Aub and Armi are required for production of a subpopulation of 19-22 nt piRNAs

piRNAs are proposed to guide PIWI clade proteins to targets through sequence specific interactions. Our observations thus raised the possibility that *armi* and *aub* promote production of piRNAs that direct assembly of the telomere protection complex. All four mutations analyzed here reduce total piRNA production (Klattenhoff et al., 2009b; Li et al., 2009; Malone et al., 2009). We therefore focused on small RNA species derived from a fourth chromosome cluster, defined by a high density of uniquely mapping piRNAs, containing multiple repeats of the telomeric transposons (Brennecke et al., 2007). Bioinformatic analysis indicates that 70-80% of telomere specific piRNAs match this cluster (Figure 2.10, Table 3). Figure 2.10 shows length histograms for small RNAs mapping to this cluster from wt, *rhi, ago3, aub* and *armi* mutant ovaries. Data are normalized to sequencing depth, and small RNAs mapping to the plus genomic strand are represented in blue and RNAs mapping to the minus strand are in red. Significantly, *aub* and *armi* mutations lead to a preferential loss of shorter piRNAs mapping to the minus genomic strand (Figure 2.10B and C). Loss of these shorter RNAs highlights the peak at 21 nt, which is retained in all of the mutants and likely represent endogenous siRNAs (Figure 2.10A, black arrow). The telomeric elements (*HeT-A* and *TART*) are almost exclusively on the minus genomic strand in this cluster, and the RNAs that are lost in *aub* and *armi* thus correspond to the sense strand of the target elements. Ovaries mutant for *ago3* and *rhi*, by contrast, retain these shorter sense strand RNAs.

Figure 2.10: piRNAs linked to a 4th chromosome cluster containing telomeric transposon fragments.

A. Length histograms showing plus genomic strand (blue) and minus genomic strand (red) mapping piRNAs in wt, *armi*, *aub*, *rhi* and *ago3* mutants. The datasets are taken from published work by Klattenhoff et.al 2009, Li et.al, 2009 and Malone et.al, 2009. The relative abundance is normalized to sequencing depth and is plotted on the y-axis. Note that sense strand of the transposon fragments in this cluster are on the minus genomic strand, and that the scales differ. Preferential loss of shorter piRNAs from *aub* and *armi* leads to a prominent endo-siRNA peak at 21 nt (marked by a black arrow).

B. Abundance of longer (23-29 nt) plus strand (blue) and minus strand (red) piRNAs in the indicated mutants relative to their respective wild-type controls. All four mutations reduce plus strand piRNAs, which are anti-sense to the telomeric transposons.

C. 19-22 nt genomic plus and minus strand piRNAs in the indicated mutants. All four mutations reduce plus strand RNAs. However, minus strand species are retained at near wild type levels in both *rhi* and *ago3* mutants. For panels B and C, bars show normalized reads in mutants divided by normalized reads in wild-type controls.

Figure 2.10

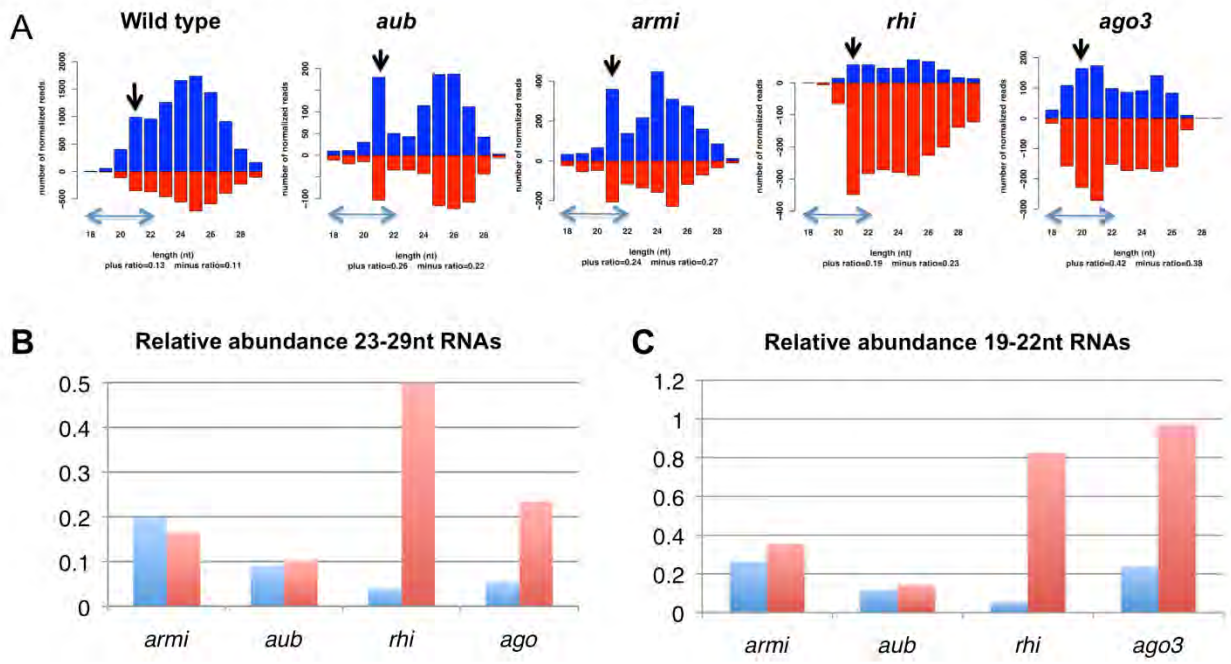
A
Wild type
aub
armi
rhi
ago3
number of normalized reads
length (nt)
plus ratio=0.13 minus ratio=0.11
plus ratio=0.26 minus ratio=0.22
plus ratio=0.24 minus ratio=0.27
plus ratio=0.19 minus ratio=0.23
plus ratio=0.42 minus ratio=0.38
B
Relative abundance 23-29nt RNAs
0.5
0.4
0.3
0.2
0.1
0
armi
aub
rhi
ago
C
Relative abundance 19-22nt RNAs
1.2
1
0.8
0.6
0.4
0.2
0
armi
aub
rhi
ago3

Table 2.3: Contribution of 4th chromosome telomeric cluster to piRNAs against telomeric transposons

Telomeric element	piRNAs unique to chr. 4 telomeric cluster	piRNAs unique to other chromosomes	Total piRNAs shared	Fraction coming from chr. 4
HeT A	2907	3108	9172	0.79
TART-A	2355	3274	6506	0.73
TAHRE	1631	3167	6507	0.71

We quantified the relative abundance of typical 23-29nt long piRNAs and the shorter 19-22nt species, excluding the 21nt endo-siRNA peak. All four mutations significantly reduce 23 to 29 nt piRNAs, although *rhi* mutants retain approximately 50% of wild type minus strand species. Loss of these piRNAs is consistent with over-expression of transposons matching this cluster (Figure 2.11). By contrast, the shorter minus strand RNAs are reduced by 3 to 10 fold in *armi* and *aub*, but remain at 80% to 95% of wild type levels in *ago3* and *rhi* (Figure 2.10B and C). In addition, short piRNA species from the telomeric cluster co-immunoprecipitate with Piwi protein (Li et al., 2009; Malone et al., 2009), which localizes to the nucleus and is the likely effector of chromatin functions for the piRNA pathway (Figure 2.12). In addition, binding of this subpopulation of piRNAs by Piwi is retained in *ago3* mutants, which assemble the TPC, but significantly reduced in *armi* mutants, which block assembly of the TPC (Figure 2.12).

Taken together, these observations indicate that the piRNA pathway has two genetically distinct functions during oogenesis and early embryogenesis. The pathway prevents DNA damage during oogenesis and maintains the integrity of the zygotic genome during the embryonic cleavage divisions, which likely reflects the established role for piRNAs in transposon silencing (Klattenhoff et al., 2007; Klattenhoff et al., 2009b; Li et al., 2009; Vagin et al., 2006). This function requires *aub*, *armi*, *rhi* and *ago3*, which are also required for wild type piRNA production. In addition, our studies reveal a novel function for the piRNA genes *aub* and *armi* in telomere protection and production of a novel class of short RNAs that bind to Piwi. Intriguingly, germline clones of *piwi* null alleles do not significantly disrupt oogenesis, but lead to maternal effect embryonic lethality and severe chromosome segregation defects during the cleavage divisions (Cox et al., 2000). We therefore speculate that *aub* and *armi* are required for production of a subset of piRNAs that bind to Piwi and direct assembly of the TPC.

Figure 2.11: Transcript expression levels of telomeric transposons.

Genome browser view showing the 4th chromosome telomeric piRNA cluster, with the expression levels of telomeric transposons in piRNA mutants. Note the variability of fold expression change in these mutants irrespective of their effects on telomeric protection.

Figure 2.11

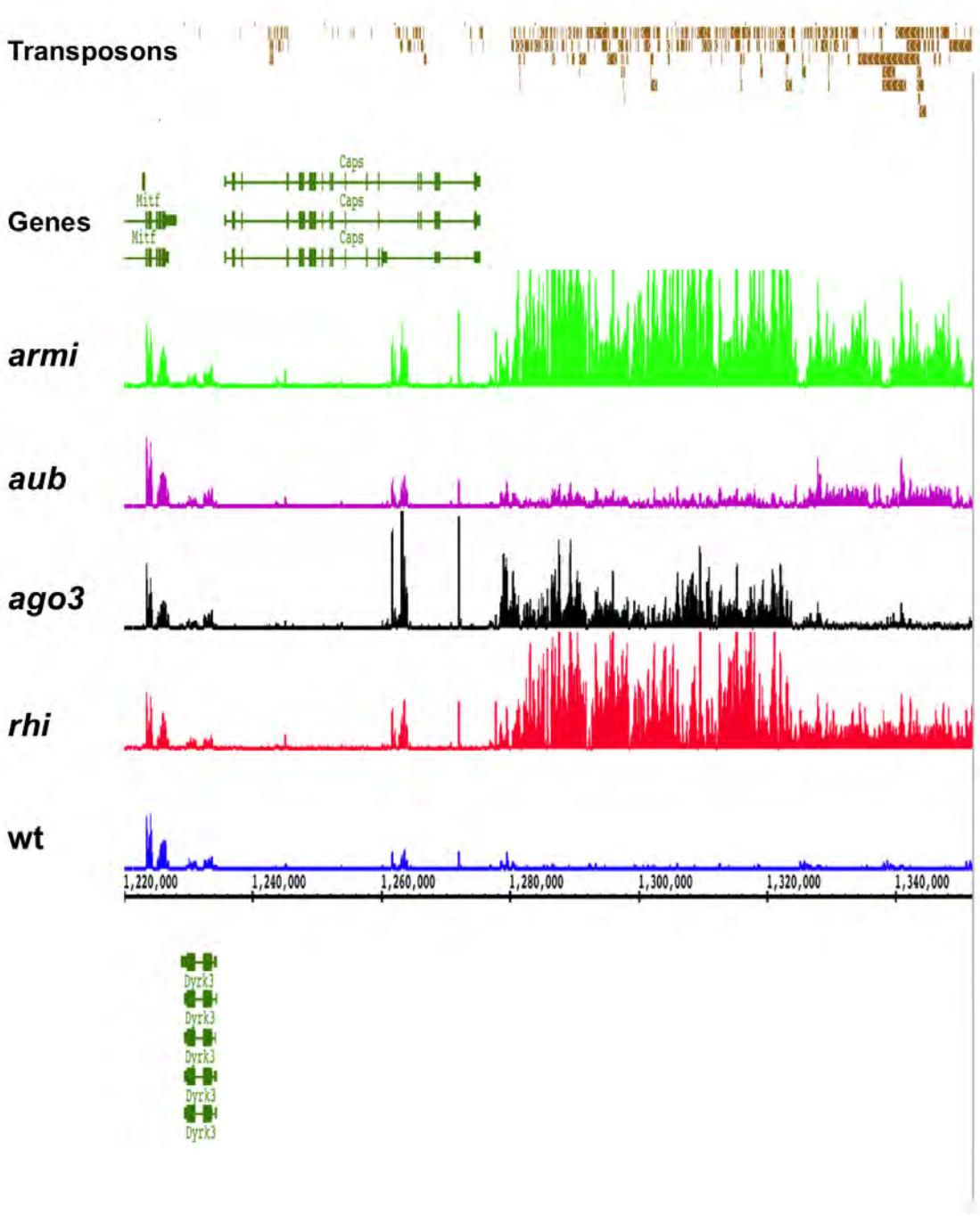
Transposons
Genes
Mitf
Mitf
Caps
Caps
Caps
armi
aub
ago3
rhi
wt
1,220,000
1,240,000
1,260,000
1,280,000
1,300,000
1,320,000
1,340,000
Dyrk3
Dyrk3
Dyrk3
Dyrk3
Dyrk3

Figure 2.12: Analysis of Piwi-small RNA IP datasets in *ago3* and *armi* mutants.

(A) shows the small RNA length distribution on X-axis and Piwi-bound piRNAs on Y-axis in wt, *armi* and *ago3* with piRNAs from genomic plus strand in blue and piRNAs from genomic minus strand in red. (B) shows the abundance of piRNAs mapping to the 4^{th} chromosome telomeric cluster. The height of the spikes denotes the number of piRNA sequence reads coming from that region. There is a preferential retention of Piwi-bound minus strand piRNAs in *ago3* versus *armi*.

Figure 2.12

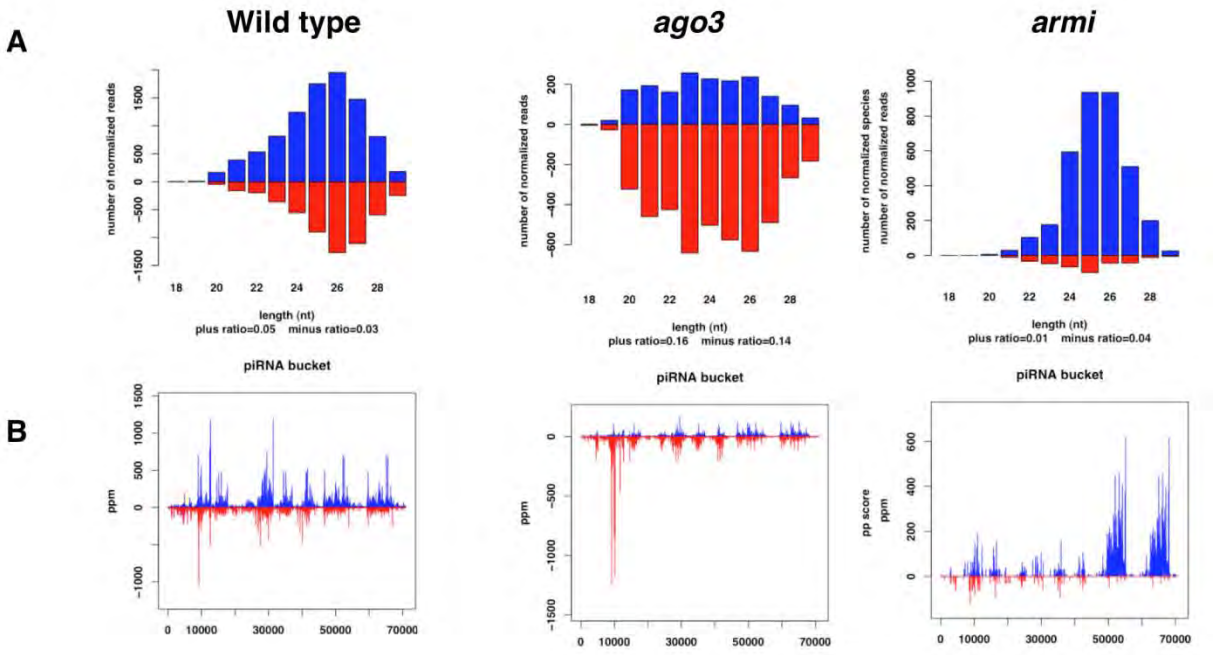
A
Wild type
ago3
armi
number of normalized reads
number of normalized species
length (nt)
plus ratio=0.05 minus ratio=0.03
plus ratio=0.16 minus ratio=0.14
plus ratio=0.01 minus ratio=0.04
B
piRNA bucket
ppm
pp score

Model for telomere protection

The mutations in *aub* and *armi* affect telomere resolution during chromosome segregation, while *rhi* and *ago3* maintain proper telomere protection complex. To confirm whether recruitment of telomere protection complex involves Aub and Armi-dependent piRNAs, we probed the relative abundance of small RNAs mapping to the major telomeric piRNA cluster on the 4th chromosome using published small RNA datasets. While all the aforementioned mutants reduce 23-29 nt small RNAs from this cluster to varying degrees, *rhi* and *ago3* maintain a population of sense-strand 19-22 nt small RNAs. Thus, there is a correlation between loss of these 19-22 Piwi-bound small RNAs and loss of telomere protection. A number of observations suggest that Piwi is also involved in telomere protection. Piwi depletion from the germline results in mitotic defects in early embryos (Cox et al., 2000). In addition, Piwi binds HP1, a component of telomere protection complex, in somatic cells and whole ovarian extracts (Brower-Toland et al., 2007b and Appendix I, this thesis). Since, these Piwi-bound telomeric small RNAs are drastically reduced in *armi*, and largely unaffected in *ago3* mutants, I propose that Piwi functions in concert with Aub and Armi in recruiting the telomere protection complex. Thus, in this model, Aub and Piwi are involved in production of telomeric 19-22 small RNAs. *armi* might directly affect Piwi activity or nuclear entry, as has been shown in ovarian somatic cells (Saito et al., 2010). Inside the nucleus, Piwi-piRNA complexes recruit HP1 which further recruits HOAP at the telomeric ends. Thus, the cycle collapses in *aub* and *armi* mutants, compromising telomere protection.

Figure 2.13: Model for telomere protection

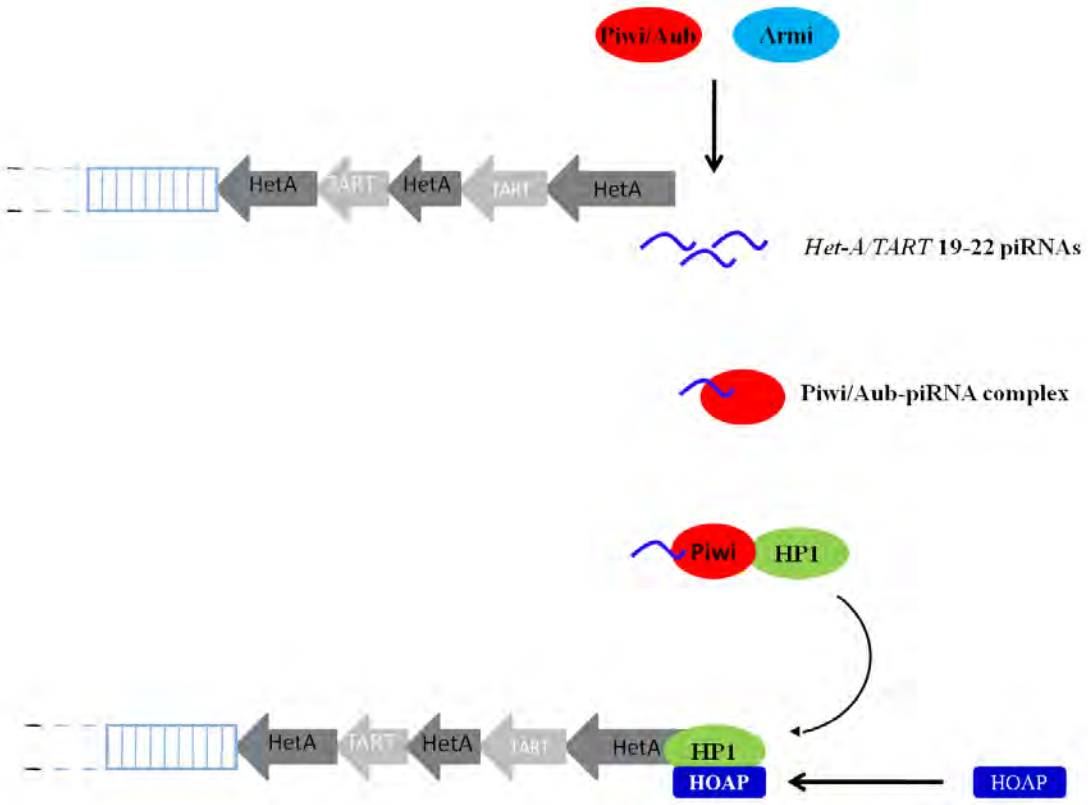

Materials and Methods

Fly stocks

Flies were reared at 25ºC on standard corn meal medium. *OregonR* and *w1118* were used as controls. Stocks carrying the following alleles were obtained from the Bloomington Stock Center: $ago2^{51B}$, $ago2^{Df}$, aub^{HN2}, aub^{QC42}, $dcr2^{L811fsX}$, mnk^{P6}, $ligIV^{5}$, rhi^{02086} and $rhi^{KG00910}$. $ago2^{51B}$ is an imprecise P-element induced deletion of the first two exons of *ago2* locus. aub^{HN2} and $aub^{QC42}$are both EMS-induced point mutations (Harris and Macdonald, 2001; Schupbach and Wieschaus, 1991). $dcr2^{L811fsX}$ is an EMS-induced loss-of-function allele described in (Lee et al., 2004). rhi^{02086} and $rhi^{KG00910}$ are both P-element insertion alleles, which act as strong hypomorphs (Volpe et al., 2001). Both $armi^{1}$and $armi^{72.1}$alleles are strong hypomorphic alleles which produce *armi* transcript at low levels(Cook et al., 2004). mnk^{P6},aub^{HN2} and mnk^{P6},aub^{QC42} (Klattenhoff et al., 2007) recombinants were generated using standard genetic procedures. The $loqs^{f00791}$ and $loqs^{KO}$ alleles were from Bloomington and Dennis McKearin(Park et al., 2007), respectively. Stocks carrying $ago3^{4931}$and $ago3^{3658}$, which are loss-of-function alleles with premature stop codons(Li et al., 2009), were obtained from the Zamore lab (University of Massachusetts Medical School).

Immunostaining and Fluorescence in situ Hybridization

0-30-min-old or 0-3-hr-old embryos were fixed in methanol and immunostained for α-tubulin (Dm1α, Sigma Chemical Co., 1:300) and 0.2μM TOTO-3 (Molecular Probes) using standard procedures (Theurkauf, 1994). For staining of egg chambers, the ovaries were dissected in Robb's medium and fixed in 4% formaldehyde as described (Klattenhoff et al., 2007). γ-H2Av antibody was generously provided by Kim McKim (Rutgers) and was used at 1:500 dilution. The dodeca-satellite probe for the fluorescent in situ hybridization was made by 3' end labeling

using terminal deoxynucleotidyl transferase (Roche), followed by direct fluorophore conjugation using ARES DNA labeling kit as described by the manufacturer (Molecular Probes). The dodeca satellite sequence from the pBK6E218 plasmid was amplified using T3 and T7 primers(Abad et al., 1992). The telomeric probe was made by indirect substitution of DIG-dUTP using the PCR DIG probe synthesis kit (Roche). The sequence was amplified from genomic DNA using the following primers- telF- 5'-GACAATGCACGACAGAGGAA-3' and telR- 5'-GTCTTTTTGGGTTTGCGGTA-3'. The Y-chromosome satellites (AATAC)n and (AATAAAC)n were purchased as oligos with direct conjugation of FAM and Cy-3 fluorophores at the 3'end (IDT). Hybridization was performed as described previously (Blumenstiel et al., 2008). Fluorescently labeled samples were imaged using a Leica TCS-SP inverted scanning confocal microscope or a Nikon TE-2000E2 inverted microscope and captured using Metamorph software (Universal Imaging). All images were processed using Image J (Rasband, W.S., ImageJ, U.S. National Institutes of Health, Bethesda, Maryland, USA, http://rsb.info.nih.gov/ij/, 1997-2006) and Adobe Photoshop.

Chromatin bridges quantification

To quantify chromatin bridges, the ratio of anaphase/telophase (A/T) bridges to total A/T figures was calculated for 10 to 30 embryos. The mean bridge frequency was determined by designating each embryo as an independent experiment, and the standard error was determined using an Anova test. Two-tailed t-tests were also used to compare specific data sets, using α=0.05. P-values are noted on the graphs.

Chromatin Immunoprecipitation and quantitative PCR (qPCR)

Whole ovaries were dissected from 2-5-day old flies and fixed using 1.8% formaldehyde for 10 minutes at room temperature. For ChIP using embryos, 0-3hr old embryos were collected and fixed using 1.8% formaldehyde for 20 minutes at room temperature. The ChIP assay was performed as per manufacturer's instructions (Invitrogen) and as previously described with some modifications (Klattenhoff et al., 2009b). Immunoprecipitation was done using HOAP polyclonal serum previously described (Klattenhoff et al., 2009b) or the monoclonal HP1 antibody (Developmental Studies Hybridoma Bank, IA). The purified DNA was subjected to qPCR using Applied Biosystems 7500 system, and data was analyzed by calculating the % of immunoprecipitated DNA compared to the input DNA sample. All ChIPs were performed at least twice and the data presented is an average of two different biological replicates with technical triplicates for each of them. The data was plotted with error bars representing standard deviations for individual samples. The difference between primer efficiencies was calculated by preparing standard curves and was taken into consideration while calculating % IP values. The primer sequences are available upon request.

Sequence extraction and annotation

For each sequence read, the first occurrence of the 6-mer perfectly matching the 5′-end of the 3′-linker was identified. Sequences without a match were discarded. The extracted inserts for sequences that contained the 3′-linker were then mapped to the female *Drosophila melanogaster* genome (Release R5.5, excluding chromosome YHet). Inserts that matched fully to a genomic sequence were collected using Bowtie (Langmead et al., 2009) and the corresponding genomic coordinates were determined for downstream functional analysis. Sequences corresponding to pre-miRNAs or non-coding RNAs (ncRNAs) were identified and removed. For analysis of the

telomeric cluster, small RNA length distributions were determined for reads that mapping to chr4:1280000-1350999, normalizing for sequencing depth (genome mapping reads excluding ncRNAs).

CHAPTER 3

piRNA-mediated adaptation to a new transposon infection in *Drosophila* within a single generation

Summary

Transposons are prominent features of all eukaryotic genomes, and mobilization of these elements triggers genetic instability, generates disease associated mutations, and drives genome evolution. Maternally deposited PIWI-interacting RNAs (piRNAs), derived from heterochromatic clusters, mediate sequence-specific transposon silencing during *Drosophila* germline development and embryogenesis. New mobile elements, introduced into the zygote through males, thus escape silencing and trigger hybrid dysgenesis, a syndrome characterized by genome instability and reduced hybrid fertility. We show that *P-element* transposon induced hybrid dysgenesis leads to over-expression and mobilization of P-elements, but also triggers mobilization of over 98% of resident transposon families. However, hybrid fertility progressively increases with age, as P-elements and resident transposons are silenced. Restoration of fertility is associated with transposition of resident elements into piRNA clusters, and these new insertions are inherited with high fidelity by the fertile offspring of dysgenic females. By contrast, new *P-element* insertions are not biased toward clusters or inherited. Instead, *P-element* silencing is associated with *de novo* production of piRNAs derived from a paternally inherited cluster. *P-element* transposon invasion thus triggers genome-wide transposon mobilization, and restoration of transposon silencing and genome stability is linked to *de novo* piRNA processing and genetic modification of the germline.

Results and Discussion

Developmental defects in inter-strain hybrids

Transposons are genetic parasites and natural residents of all characterized eukaryotic genomes. Their mobilization has been linked to many disease causing mutations (Chen et al., 2005; Deininger and Batzer, 1999; Iskow et al., 2010; Vidal et al., 2002). Exploring the transposon landscape of human genome reveals that most (99.95%) of the transposons are inactive and thus have been tamed by the host (Mills et al., 2007). Small non-coding RNAs bound to PIWI-clade of Argonaute proteins appear to play an evolutionarily conserved role in transposon silencing (reviewed in (Ghildiyal and Zamore, 2009; Klattenhoff and Theurkauf, 2007)). In *Drosophila*, maternally supplied PIWI-interacting RNAs (piRNAs) provide immunity against transposons during embryogenesis (Blumenstiel and Hartl, 2005; Brennecke et al., 2008). New transposons, introduced into the zygote through the male, thus escape piRNA-based silencing and are mobilized (Bucheton et al., 1976; Kidwell et al., 1977). Inter-strain crosses in *D.melanogaster* can thus lead to a syndrome termed hybrid dysgenesis that includes increased mutability, sterility, chromosome rearrangements and male recombination (Bucheton, 1973; Hiraizumi, 1971; Kidwell et al., 1977; Picard et al., 1972). P and M strains of *D.melanogaster* are defined by the presence or absence of *P-element* transposon in their genome, respectively (Kidwell et al., 1977; Rubin et al., 1982). Crosses between P strain males and M strain females lead to non-reciprocal sterility in the progeny, which is linked to an absence of maternally deposited piRNAs against the *P-element*(Brennecke et al., 2008).

In order to monitor the host responses following a transposon-mediated genetic stress, I crossed w^1 females (a reference M strain) and Harwich males (a reference P strain) to induce *P-element* transposition and studied oogenesis in the hybrid progeny (Figure 3.1A).

Figure 3.1: Developmental defects in inter-strain hybrids.

A. Schematic of the cross between Harwich (Har) and w^1 flies. Cross between w^1 females and Harwich males (bottom panel) produces sterile, dysgenic F1 progeny (*w* x Har). The F1 progeny (Har x *w*) from the reciprocal cross (top panel) are fertile.

B. Confocal micrograph showing the projection of stacks of images collected from ovaries stained for H2Av-p (green) and DNA (blue). The oocyte is highlighted by the dotted line. Magnified view of the karyosome is shown in the inset at the top left corner with the arrowhead pointing to the aberrant karyosome morphology and positive signal for H2Av-p in *w* x Har 2-4 samples, which are repaired in the *w* x Har 21 day old flies similar to the Har x *w* reciprocal control.

C. Confocal micrograph of stage 4 egg chambers showing ovaries stained for Vasa (red) and DNA (blue). The Vasa is localized to the perinuclear 'nuage' in the nurse cell nuclei of Har x *w* reciprocal control flies. It is dispersed in the cytoplasm in *w* x Har 2-4 day old progeny, but becomes perinuclear in *w* x Har 21 day old flies.

Figure 3.1

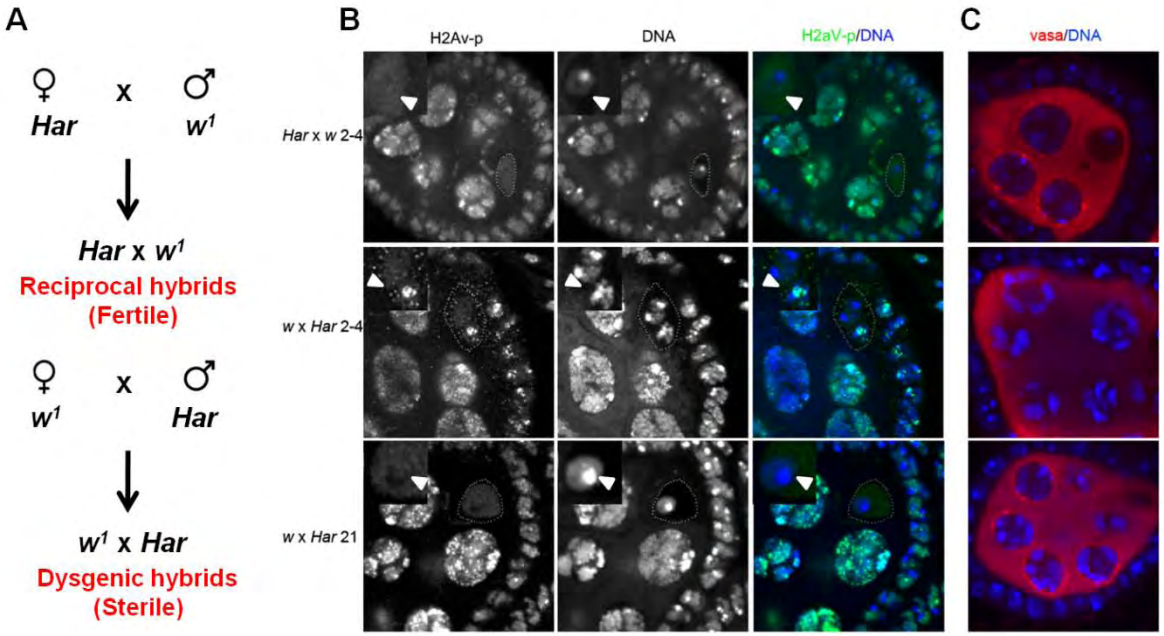
A
♀ x ♂
Har w1
Har x w1
Reciprocal hybrids
(Fertile)
♀ x ♂
w1 Har
w1 x Har
Dysgenic hybrids
(Sterile)
B
H2Av-p
DNA
H2aV-p/DNA
Har x w 2-4
w x Har 2-4
w x Har 21
C
vasa/DNA

Wild-type ovaries consist of multiple strings of progressively developing cysts called ovarioles. At the tip of each ovariole lies a pair of germline stem cells which differentiate to produce cysts (Spradling et al., 1997). The ovaries from young dysgenic hybrids (*w* x Har) show severely compromised oogenesis progression as compared to the reciprocal control hybrids (Har x *w*). Most of the ovaries were rudimentary, with few or no vitellogenic stages, implying an arrest in oogenesis. The few embryos produced by the *w* x Har females arrested in development and manifested changes in egg shell morphology characteristic of axial patterning defects during oogenesis (Figure 3.2B and C). Axis specification in *Drosophila* involves polarized localization of RNA and protein morphogens in the oocyte, and this process is disrupted when the ATR/Chk2 dependent DNA damage checkpoint is activated, which has been observed in both DNA repair and piRNA pathway mutations (Abdu et al., 2002; Chen et al., 2007; Ghabrial and Schupbach, 1999; Klattenhoff et al., 2007; Pane et al., 2007). To cytologically assay for DNA damage, I labeled ovaries from *w* x Har and Har x *w* for γ-H2Av, a marker for DNA double-strand breaks (Madigan et al., 2002). Meiotic DNA breaks form while germline cysts are in the germarium and are repaired by stage 2 of oogenesis, when the oocyte nucleus has formed a compact structure called the karyosome (McKim et al., 2002). Karyosome structure is impaired in *w* x Har ovaries (Figure 3.1B inset) and the oocyte nucleus stained positive for γ-H2Av throughout oogenesis, presumably due to the presence of breaks caused by *P-element* transposon mobilization (Figure 3.1B).

Most of the piRNA pathway mutations that lead to germline DNA damage also disrupt assembly of nuage, a perinuclear structure implicated in piRNA function and transposon silencing (Chen et al., 2007; Klattenhoff et al., 2007; Klattenhoff et al., 2009b; Li et al., 2009; Lim and Kai, 2007). I labeled the ovaries from hybrid progeny for Vasa, an evolutionarily

conserved RNA helicase involved in piRNA biogenesis which localizes at nuage (Liang et al., 1994; Malone et al., 2009). Vasa was dispersed in the cytoplasm in dysgenic hybrids, but formed normal perinuclear foci in control hybrids (Figure 3.1C). P-M dysgenesis thus triggers germline DNA damage and nuage defects characteristic of piRNA pathway mutations.

Figure 3.2: Restoration of *P-element* induced phenotypic effects.

Fertility for the *w* x Har F1 females was scored by plotting the average number of eggs per female per day (A) and the percentage of embryos which hatch into larvae (hatch rates) (B) as a function of age (in days). The axial patterning of the embryos laid down by the F1 females is represented by the % of embryos with wild-type appendages (two) as a function of age (C). The abundance of the 19-27 nt small RNAs mapping to the sense (blue) or the antisense (red) strand of the *P-element* sequence (D). The *P-element* nucleotide positions are plotted on the x-axis. There is a dramatic induction of *P-element* piRNAs in the *w* x Har 21 day old flies (bottom right) as compared to the *w* x Har 2-4 day old flies (top right). Their reciprocal controls (Har x *w)* at 2-4 days and 21 days are presented on the left. This piRNA production at 21 days is linked to the *P-element* transcript silencing (F). (F) shows the results from a Reverse-Transcriptase-quantitative PCR (qRT-PCR) from RNA collected from whole ovaries and analyzed for *P-element* transposase sequence, using *vasa* as the internal control. (G) Strand-specific qRT-PCR analysis for longer transcripts derived specifically from the P-element containing piRNA cluster at chromosome 4^{th} (4-P) in RNA derived from the F1 dysgenic hybrids or control hybrids at 2-4 days or 21 days. (+) or (-) refer to the plus or minus strands analyzed. The cl. 5 refers to an independent major piRNA cluster at chr 2L, which shows no significant change between the samples and acts as a control. The transcript levels were normalized against piRNA precursors from 42AB cluster. Error bars represent the standard deviation from three independent biological replicates.

Figure 3.2

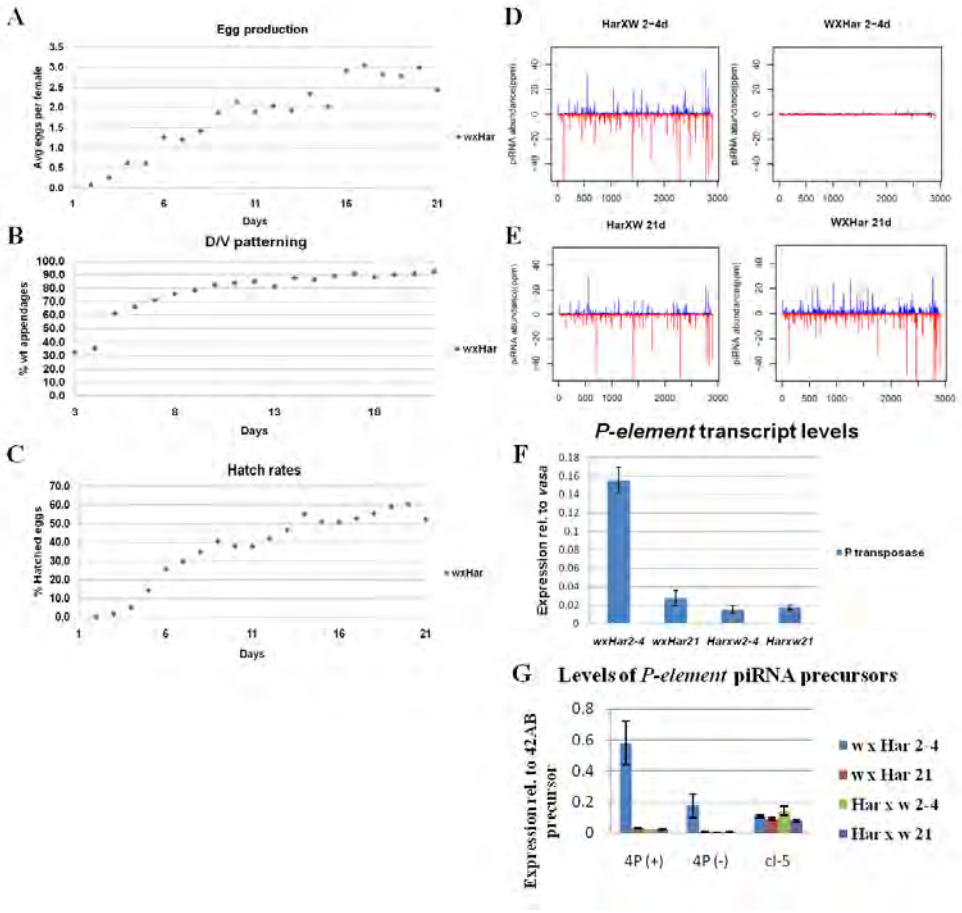
A
Egg production
Avg eggs per female
Days
wxHar
B
D/V patterning
% wt appendages
Days
wxHar
C
Hatch rates
% Hatched eggs
Days
wxHar
D
HarXW 2-4d
WXHar 2-4d
E
HarXW 21d
WXHar 21d
P-element transcript levels
F
Expression rel. to vasa
P transposase
wxHar2-4 wxHar21 Harxw2-4 Harxw21
G
Levels of P-element piRNA precursors
Expression rel. to 42AB precursor
w x Har 2-4
w x Har 21
Har x w 2-4
Har x w 21
4P (+)
4P (-)
cl-5

Restoration of *P-element* induced phenotypes

Despite the dramatic developmental defects in *w* x *Har* progeny, there was a partial restoration in fertility of F1 females with age. I found a gradual and progressive improvement in the fecundity of the *w* x *Har* females as witnessed by an increase in egg production from approximately 0.5 eggs per female per day at 2-4 days to 2.5 eggs per female per day at 21 days (Figure 3.2A). The egg hatch rates, reflecting the percentage of embryos developing into larvae, increased from 3% to 52% over the same 3 week period (Figure 3.2B). Similarly, the fraction of eggs with normal dorsal patterning increased from 32% to 92% (Figure 3.2C). In addition, I observed a dramatic reduction in γ-H2Av foci in oocyte nuclei as the F1 hybrids aged (Figure 3.1B). In addition, nuage showed essentially wild type morphology in 21-day old dysgenic females (Figure 3.1C). The fertility restoration at 21 days is linked to an improvement in oogenesis progression. Many ovarioles are populated with vitellogenic stages and mature eggs in 21 day old dysgenic ovaries. However, a continuum of phenotypes was still visible. Figure 3.3 summarizes the percentage of flies showing variable ovarian morphology at both ages in *w* x Har flies. The results from a χ^2 test suggest that the temporal re-population of ovarioles is a co-operative event (Figure 3.3). The overt phenotypic effects of hybrid dysgenesis are therefore reversed as the *w* x Har age, suggesting that transposon silencing is established within a single generation.

Figure 3.3 Summary of ovarian phenotypes in dysgenic hybrids

This figure summarizes the data for various ovarian phenotypes observed in w x Har 2-4 or 21 day old F1 progeny. The dissected ovaries were categorized into 'both rudimentary' when both the ovaries were rudimentary, 'only 1 ovariole' when only one ovarioles showed any mature vitellogenic stages, '3-5 ovarioles' or multiple when the ovaries showed 3-5 or multiple ovarioles with mature stages. The observed and expected frequency for all the phenotypes is presented. χ^2 test values suggest that the occurrence of observed phenotypes is independent of each other.

Figure 3.3

Observed

	Both rudimentary	Only 1 ovariole	3-5 ovarioles	Multiple
w x Har 2-4	91	19	8	1
w x Har 21	54	3	11	21
Total	145	22	19	22

Expected

w x Har 2-4	82.957	12.587	10.870	12.587
w x Har 21	62.043	9.413	8.130	9.413

Chi- square test value

6.93223E-08

de novo P-element piRNA biogenesis in adult females

piRNAs in *Drosophila* are maternally deposited and an absence of specific maternally deposited piRNAs is linked to hybrid dysgenesis (Aravin et al., 2003; Blumenstiel and Hartl, 2005; Brennecke et al., 2008; Malone et al., 2009). However, we observe that the *w* x *Har* dysgenic hybrids show signs of improved fertility in absence of maternally deposited *P-element* piRNAs. To determine if the age dependent improvement in F1 hybrid fertility is associated with changes in piRNA production, we isolated and deep sequenced small RNAs from *w* x Har 2-4 day old and 21-day female ovaries, with their respective reciprocal controls. We obtained roughly 3.8 to 6.8 million small RNA genome-mapping reads from all our samples. A detailed analysis of small RNAs matching major transposon families in all four samples is presented in Supplementary Figure 3.1. 19-27 nt small RNAs uniquely mapping to the *P-element* sequence were plotted for all four samples (Figure 3.2D). Very few *P-element* reads were detected in 2-4 day old dysgenic ovaries, but the abundance of these RNAs increased to control levels by 21 days. Since these females are derived from embryos that lacked maternally deposited *P-element* piRNAs, this increase represents *de novo* production in the adult germline. In addition, qPCR showed that *de novo* piRNA production is linked to a 6-fold drop in *P-element* transcripts, bringing them to levels comparable to reciprocal hybrid controls (Figure 3.2F).

Transposon silencing in older dysgenic hybrids

Our deep sequencing studies revealed a reduction for piRNAs against a number of transposons in 2-4 day old dysgenic ovaries, which also show defects in nuage organization (Figure3.4B). These findings suggested that P-M hybrid dysgenesis may trigger defects in silencing other transposon families.

Figure 3.4: Transposon silencing is linked to increased piRNA abundance in older hybrids.

A) Tiling array analysis of transposon transcript expression levels in ovaries from w^1 versus Harwich, *w* x Har 2-4 or 21 day old flies in log2 scale. Each hollow circle represents a single transposon family. The circles in blue represent samples with no significant change (FDR>0.5). The pink circles show samples with FDR<0.15. The red circles show significant change between the samples with more than 99% certainty (FDR<0.01).

B) Comparison for piRNA abundance in *w* x Har versus Har x *w* 2-4 days (left, correlation coefficient = 0.84) or 21-day old (right, correlation coefficient = 0.98) samples for all the annotated transposon families in the *D.melanogaster* genome and the *P-element*, with each hollow blue circle representing a single transposon and the *P-element* depicted with the red circle.

Figure 3.4

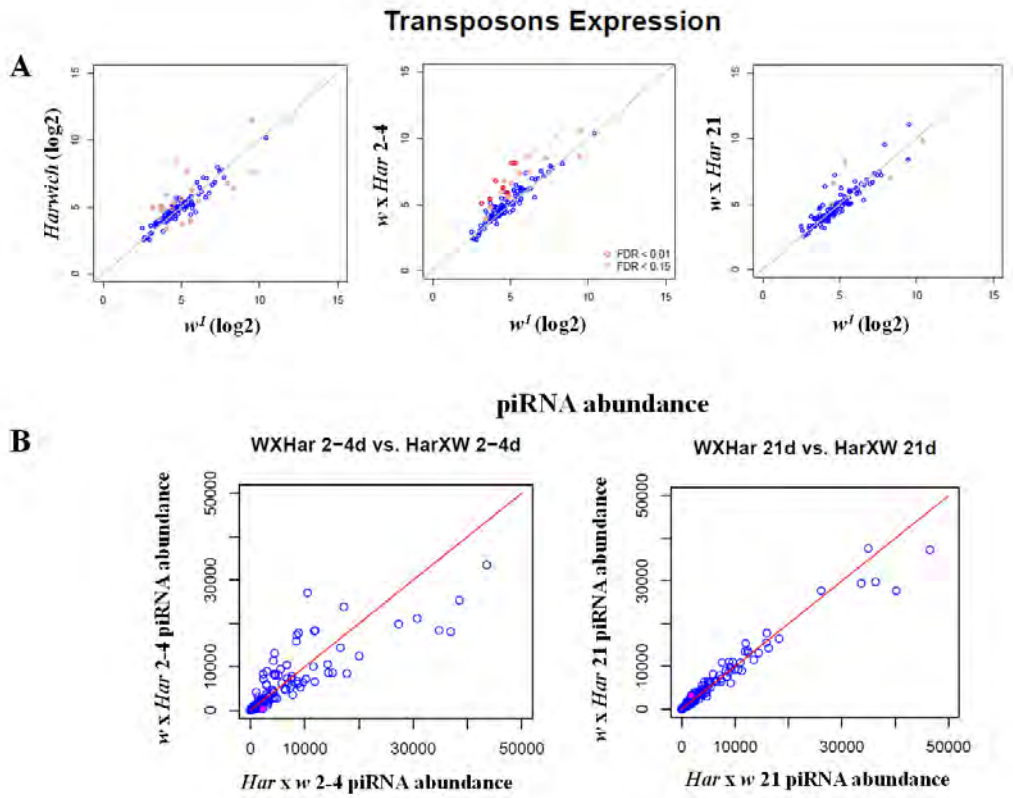
Transposons Expression
A
Harwich (log2)
w1 (log2)
w x Har 2-4
FDR < 0.01
FDR < 0.15
w x Har 21
piRNA abundance
B
WXHar 2-4d vs. HarXW 2-4d
w x Har 2-4 piRNA abundance
Har x w 2-4 piRNA abundance
WXHar 21d vs. HarXW 21d
w x Har 21 piRNA abundance
Har x w 21 piRNA abundance

I therefore used whole-genome tiling arrays to assay expression of protein coding genes and transposons in controls and dysgenic ovaries. *w* x *Har* F1 ovaries at both 2-4 and 21days showed gene expression profiles that were essentially identical to parental w^1 and Harwich strains (Figure 3.6). However, 7 transposon classes show 2-fold or greater increase in expression in 2-4 day old dysgenic ovaries (FDR< 0.01) (Figure 3.4A). Strikingly, none of these transposon families show a statistically significant increase in expression in 21-day old sample (Figure 3.4B). P-M dysgenesis thus disrupts silencing of other transposon families, but silencing of these resident elements is re-established, and silencing of *P-element* transposons is imposed, as hybrid females age (Figure 3.1F and 3.4A). It is possible that the genetic stress caused by *P-element* mobilization triggers a transient collapse of the host transposon silencing system, without any detrimental effects on single-copy gene expression.

Transposon mobilization during P-M dysgenesis

Primary piRNAs produced from heterochromatic clusters appear to trans-silence target transposons elsewhere in the genome (Brennecke et al., 2007; Gunawardane et al., 2007; Mével-Ninio et al., 2007; Sarot et al., 2004). Silencing of P-elements and activated resident elements as *w* x Har females age could therefore be a result, in part, from transposition into functional piRNA clusters. To explore this possibility, we used paired end genomic DNA deep sequencing to directly assay transposon mobilization in w^1 and Harwich parental stains, F1 progeny at 2-4, 12 and 21 days, and the offspring of 12 and 21 day old F1 dysgenic hybrids that had been back crossed to w^1 males. The schematic of the cross is presented in Figure 3.5.

Figure 3.5 Schematic of the dysgenic cross.

Females from w1 strain were mated to Harwich males. The F1 progeny were aged for different times- 2-4, 12-14, 21-23 days (named F1-2-4, F1-12, F1-21, hereafter), and then back-crossed to w1 males. The resulting progeny were named F2-12 and F2-21. No viable adults were obtained from F1-2-4. Genomic DNA from the genotypes circled in red was then sequenced with the Illumina paired-end sequencing.

Figure 3.5

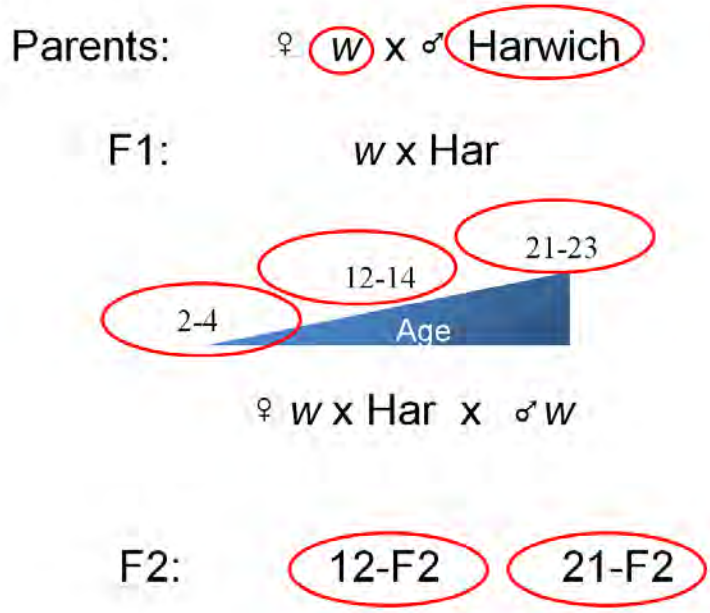
Parents:
♀ w x ♂ Harwich
F1:
w x Har
21-23
12-14
2-4
Age
♀ w x Har x ♂ w
F2:
12-F2
21-F2

Figure 3.6: Gene expression profiles for the dysgenic hybrids.

Tiling array gene expression analysis from total Poly(A)+ RNA from w^1, *Har*, *w* x *Har* 2-4 and 21 days. The results are plotted on a log2 scale. Each blue dot represents a single gene represented on the Affymetrix Tiling Array 2.0. No significant change between gene expression profiles (FDR>0.5) between the parents and the progeny.

Figure 3.6

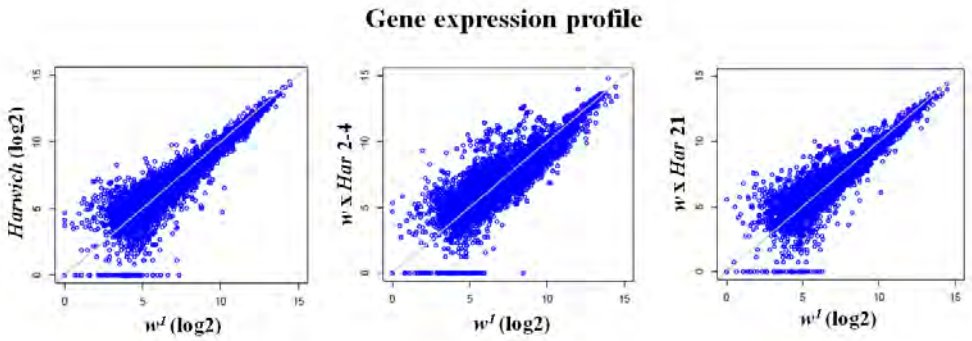
Gene expression profile
Harwich (log2)
w1 (log2)
w1 X Har 2-4
w1 (log2)
w1 X Har 21
w1 (log2)

To map TE insertions, we scored paired-end reads with one end uniquely mapping to the annotated genome and other end mapping to a canonical transposon family. These studies revealed 288 *P-element* insertions in the parental Harwich genome, but only 2 of these insertions were in known piRNA clusters, of which one (chrX:21,815,719-21,816,219) was defined by a single paired end read in a region with approximately 16 fold genome coverage, indicating that it is a rare polymorphism. The second cluster insertion (chr4:1,272,392-1,272,191) (hereby named 4-P) is defined by 20 reads in a region with 23-fold coverage, indicating that most Harwich individuals are homozygous for this allele, and suggesting that it is the source of primary *P-element* piRNAs in Harwich (Figure 3.7). We detected 359 new *P-element* insertions in F1 dysgenic progeny, but only one of these insertions, defined by a single paired end read, mapped to a piRNA cluster. Furthermore, this insertion was not transmitted to fertile F2 progeny of dysgenic females, indicating that it is not linked to *P-element* silencing (single gray line, Figure 3.8B). So, we reasoned that the active piRNA production from paternal 4-P insertion might be linked to the P-element silencing at 21 days. Strand-specific RT-PCR for transcripts specifically coming from the *P-element* at 4-P revealed that there is an 18-19-fold excess of longer transcripts from both strands at 2-4 days in *w* x Har progeny in comparison to the *w* x Har 21 day old progeny or their respective reciprocal controls (Figure 3.2G). These longer transcripts likely represent the precursor RNAs which eventually get processed into mature piRNAs by the PIWI-mediated cleavage. Thus, the primary source of paternal *P-element* piRNAs is actively producing potential *P-element* piRNA precursors and thus adaptation to the *P-element* is linked to the processing of these transcripts into effector piRNAs at 21 days.

Figure 3.7 Primary source of *P-element* piRNAs stably inherited in all samples

Screenshot from the genome browser showing the sole *P-element* containing piRNA cluster (4-P) on the 4th chromosome in parental strain, Harwich, F1 progeny at 2-4, 12 and 21 days and resulting F2 progeny at 12 and 21 days. The blue and red bars with arrows show confirming sequence reads from both the strands, one matching the annotated genome and the other mapping in the P-element sequence.

Figure 3.7

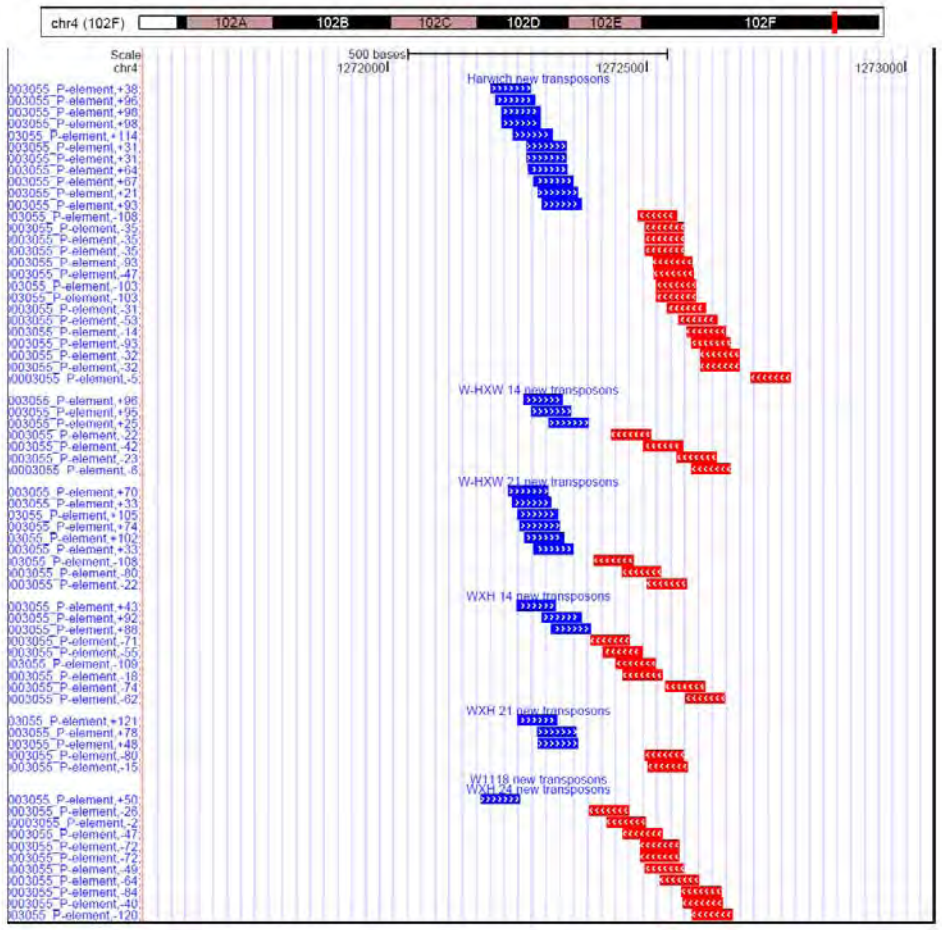
chr4 (102F)
102A
102B
102C
102D
102E
102F
Scale
chr4
500 bases
1272000
1272500
1273000
Harwich new transposons
W-HXW 14 new transposons
W-HXW 21 new transposons
WXH 14 new transposons
WXH 21 new transposons
W1118 new transposons
WXH 24 new transposons

Figure 3.8: *P-element* insertions are not stably inherited in the hybrid progeny

A) The number of TE insertions shared in parents (blue) which are transmitted to the next generation. The new insertions in F1 and F2 are labeled in green and orange respectively. Only half of the insertions in *Harwich* are inherited to the F1, and very few from F1 to F2 progeny. The *P-element* inheritance shows the opposite trend from other transposons. *roo* transposon is shown as a representative example.

B) A circos plot showing the number of new insertions shared between the progeny. The colored blocks around the circle represent the different progeny, red-F1-2-4, blue-F1-14, orange-F1-21, green-F2-14 and yellow-F2-21. The chromosomes are given in the order-chr2L, 2LHet, 2R, 2RHet, 3L, 3LHet, 3R, 3RHet, 4, X, XHet and chrU. The links between different progeny in the middle of the circle show the inheritance of insertions for the *P-element* (left) and *roo* (right), and the thickness of the lines represents the number of supported reads. Grey lines are shared between all progeny, red lines are insertions shared between all F1, blue lines that are inherited from F1-14 to F1-14 and green lines are insertions inherited from F1-21 to F2-21. Note that few *P-element* insertions are inherited by the progeny, as compared to the *roo* insertions (grey links).

Figure 3.8

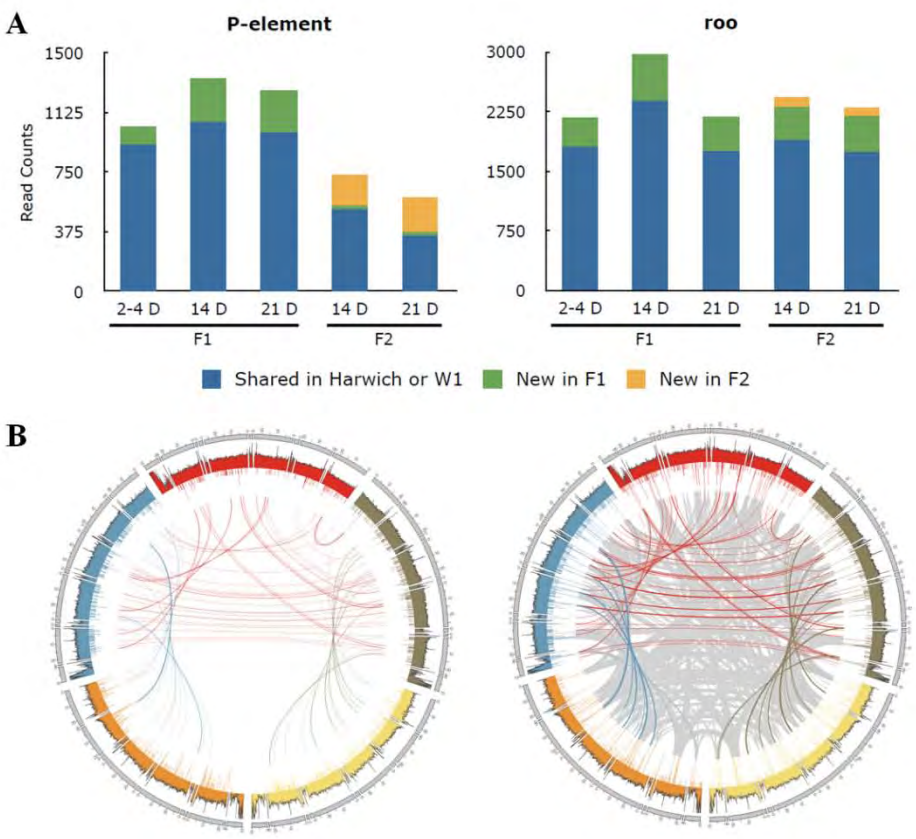
A
P-element
roo
Read Counts
1500
1125
750
375
0
3000
2250
1500
750
0
2-4 D
14 D
21 D
14 D
21 D
F1
F2
Shared in Harwich or W1
New in F1
New in F2
B

Surprisingly, these studies also revealed new insertions of almost every resident transposon family in the dysgenic hybrids, and some resident elements showed higher activity than the P-elements that triggered dysgenesis. For example, we detected 656 new *P-element* insertions in F1 dysgenic ovaries, and 1274 new *roo* insertions in the same samples (Figure 3.8A). While most new insertions were defined by single paired end reads, for a subset of genomic sites we observed a steady increase in transposon occupancy, indicated by the ratio of total TE insertion reads divided by the sum of TE insertion mapping reads and insertion reads spanning the junction in the genomic DNA. Strikingly, this class of insertion was inherited with very high fidelity by F2 progeny, demonstrating that the insertions are in germline DNA. Since F1 progeny were back-crossed to w^1, one-quarter of the F2 progeny should inherit new TE insertions that are heterozygous in the F1 germline. We identified 50 cases of new TE insertions with transposon occupancy greater than 0.25%, and 6 of these insertions (~12% of total) were in known piRNA clusters, which represent only 1% of the genome. These 6 TEs are summarized in Table 3.1. The bias toward cluster transposition among heritable TE insertions is consistent with a function linked to transposon silencing and restoration of fertility (Table 3.1). Significantly, this bias does not appear to reflect simple site preferences, since insertions into these sites are not observed in piRNA mutants that lead to a general increase in transposon activity (Nowosielska, A and Theurkauf, W, unpublished observation).

Table 3.1: Summary of stably inherited TEs in piRNA clusters

Chromosome	**Genome coordinates**	**Transposon insertion**	**Relative effect in F1-21**
2R	731002-731326	*Transpac*	Ping-pong improves
2R	2213117-2213729	*Ivk*	Increase in piRNA abundance ping-pong improves
2R	2352978-2353716	*Bari1*	Ping-pong improves
2R	2379297-2380125	*Copia*	No change
2RHet	2270957-2271263	*Mdg3*	No change
3LHet	2007277-2007950	*Roo*	Slight increase

An *Ivk* insertion into the major 42AB cluster falls into this class of heritable genetic modifications (Figure 3.9). Interestingly, this is the only *Ivk* insertion passed on to the F2 generation, and *Ivk* piRNAs increase in abundance as the F1 hybrids age (Figure 3.9). Furthermore, we detect piRNA mapping to the junction of this insertion and the 42AB cluster in F1 datasets, indicating that the inserted element is incorporated into piRNA precursors (Figure 3.9).

Figure 3.9: piRNA production from stably inherited *Ivk* TE insertion in 42AB piRNA cluster

Genome browser view of the 42AB piRNA cluster on chromosome 2R between 2213100-2213700, highlighting the insertion site for *Ivk* transposon (in brown). Blue and red bars represent the sequence reads confirming the *Ivk* insertion at this site in the hybrid progeny. Note the absence of these reads in either parent. This insertion leads to production of new unique mapping piRNAs matching the junction between *Ivk* and the 42AB cluster.

Figure 3.9

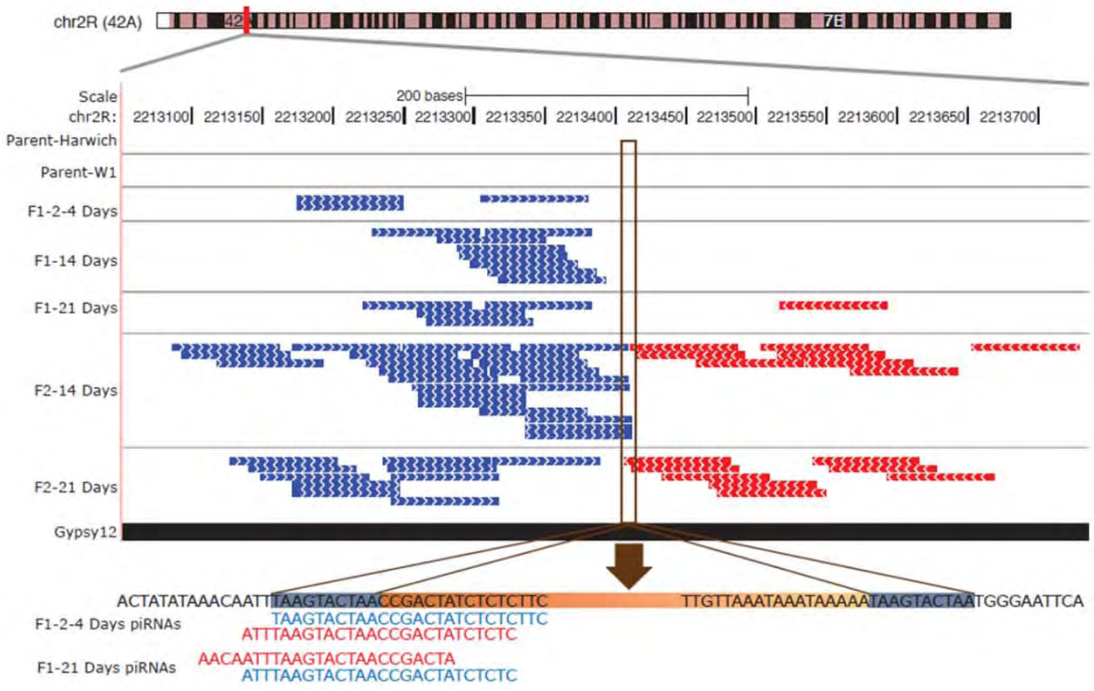
chr2R (42A)
42
7B
Scale
200 bases
chr2R:
2213100
2213150
2213200
2213250
2213300
2213350
2213400
2213450
2213500
2213550
2213600
2213650
2213700
Parent-Harwich
Parent-W1
F1-2-4 Days
F1-14 Days
F1-21 Days
F2-14 Days
F2-21 Days
Gypsy12
ACTATATAAACAATTTAAGTACTAACCGACTATCTCTCTTC
TTGTTAAATAAATAAAAATAAGTACTAATGGGAATTCA
F1-2-4 Days piRNAs
TAAGTACTAACCGACTATCTCTCTTC
ATTTAAGTACTAACCGACTATCTCTC
F1-21 Days piRNAs
AACAATTTAAGTACTAACCGACTA
ATTTAAGTACTAACCGACTATCTCTC

Thus, adaptation to *P-element* infection is linked to both *de novo* processing of piRNAs from existing paternal clusters and biased insertion of resident TEs into piRNA clusters, which leads to piRNA production from the resulting modified RNAs.

Active transposons pose a major threat to the host genome. Using an inducible transposon mobilization system, we show that activation of a single transposon can disrupt silencing of other resident transposons, which is linked to severely reduced fertility. This is accompanied by mobilization of P-elements and almost all other transposon families in the genome. With age, however, transposon silencing is restored and the TE-induced DNA damage is repaired. Our observations suggest that two distinct processes drive this adaptation process. For the newly introduced *P-element, de novo* processing of paternal transcripts appears to generate piRNAs that silence expression. On the other hand, piRNA production and resident transposon silencing are associated with new insertions into piRNA clusters. These genetic modifications are inherited by the next generation, demonstrating that they are carried in the germline and consistent with the hypothesis that they provide a selective advantage. This could reflect incorporation of the inserted sequences into primary piRNA precursors, which would presumably increase silencing. However, this is difficult to prove and other explanations are possible. In summary, we show that genomic stress posed by a single transposon infection can destabilize the host genome, and present evidence that genetic and epigenetic processes may contribute to piRNA pathway mediated adaptation to this challenge.

Supplementary Figure 3a

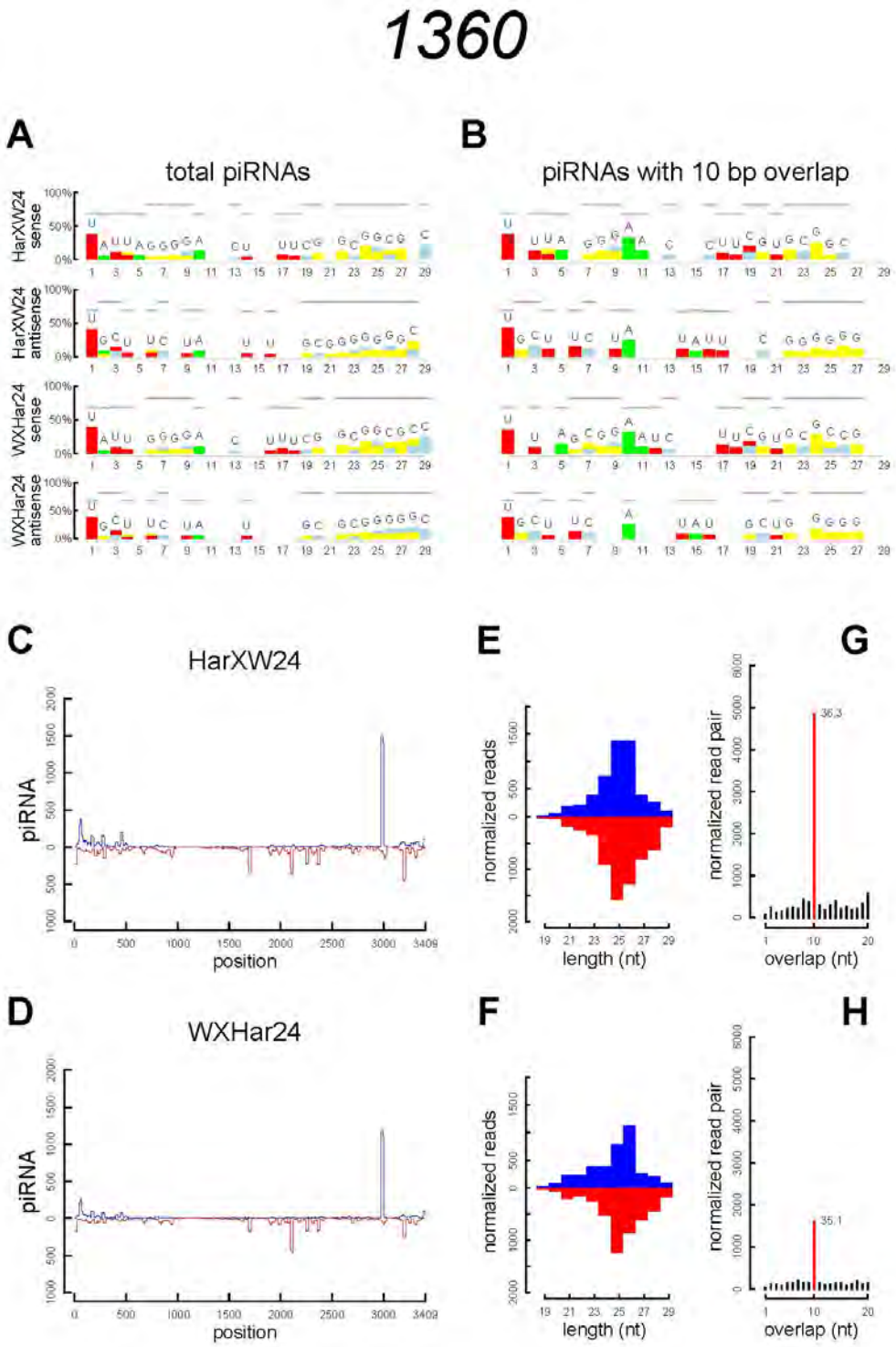

1731

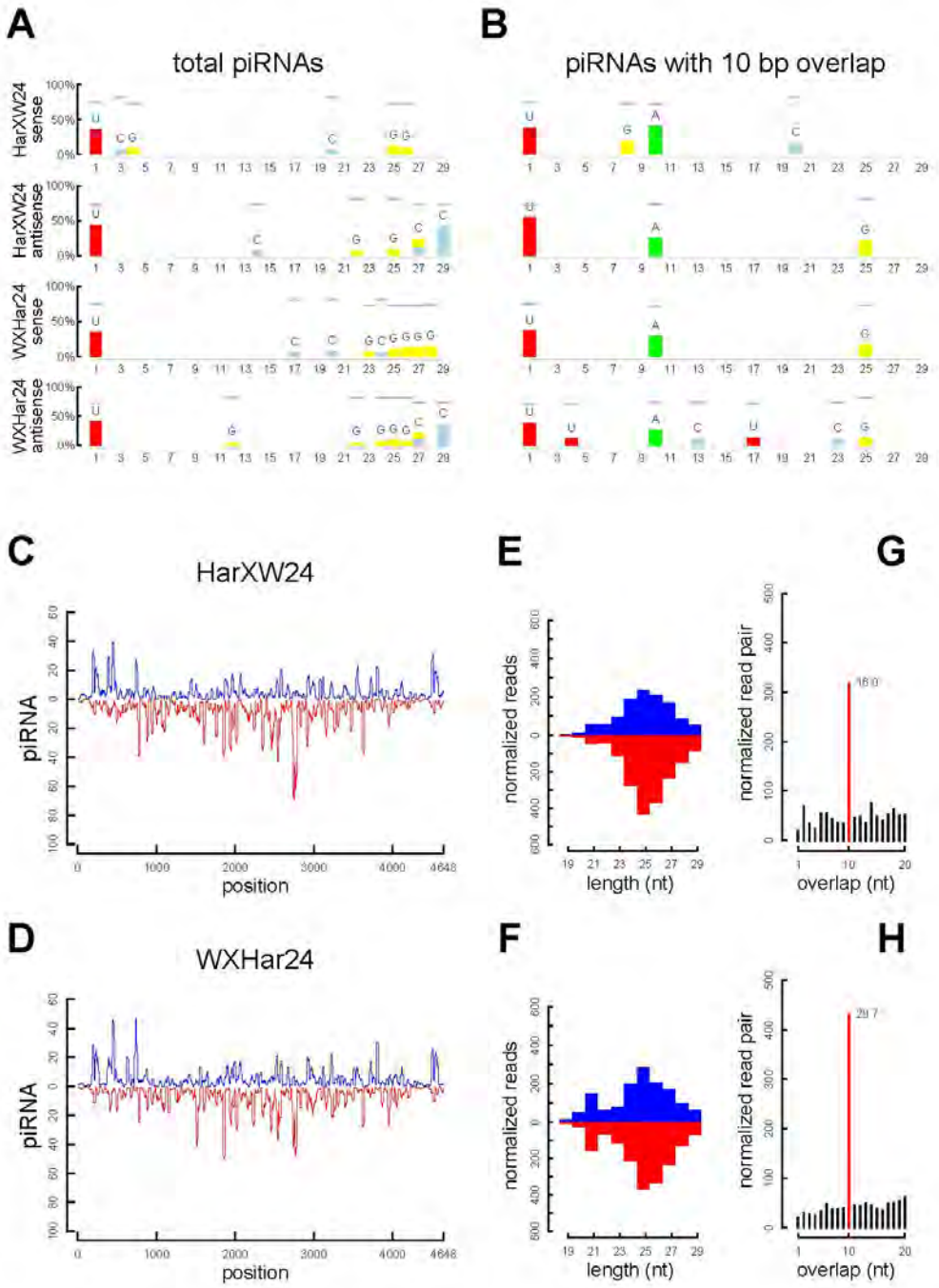
A
total piRNAs
B
piRNAs with 10 bp overlap
HarXW24 sense
HarXW24 antisense
WXHar24 sense
WXHar24 antisense
C
HarXW24
piRNA
position
D
WXHar24
piRNA
position
E
normalized reads
length (nt)
F
normalized reads
length (nt)
G
normalized read pair
overlap (nt)
H
normalized read pair
overlap (nt)

17.6

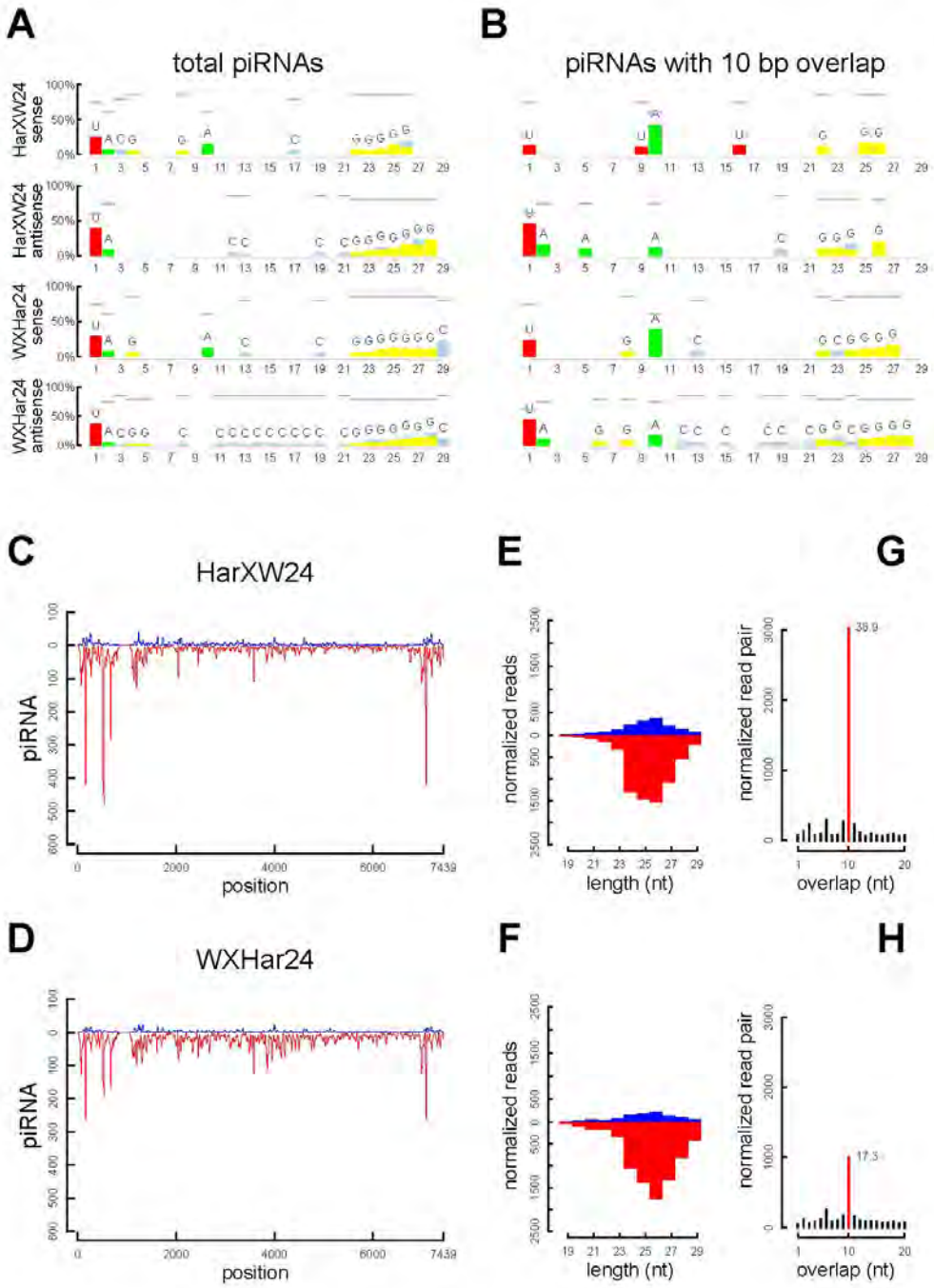
A
total piRNAs
B
piRNAs with 10 bp overlap
HarXW24 sense
HarXW24 antisense
WXHar24 sense
WXHar24 antisense
C
HarXW24
D
WXHar24
piRNA
position
E
F
normalized reads
length (nt)
G
H
normalized read pair
overlap (nt)
36.9
17.3

297

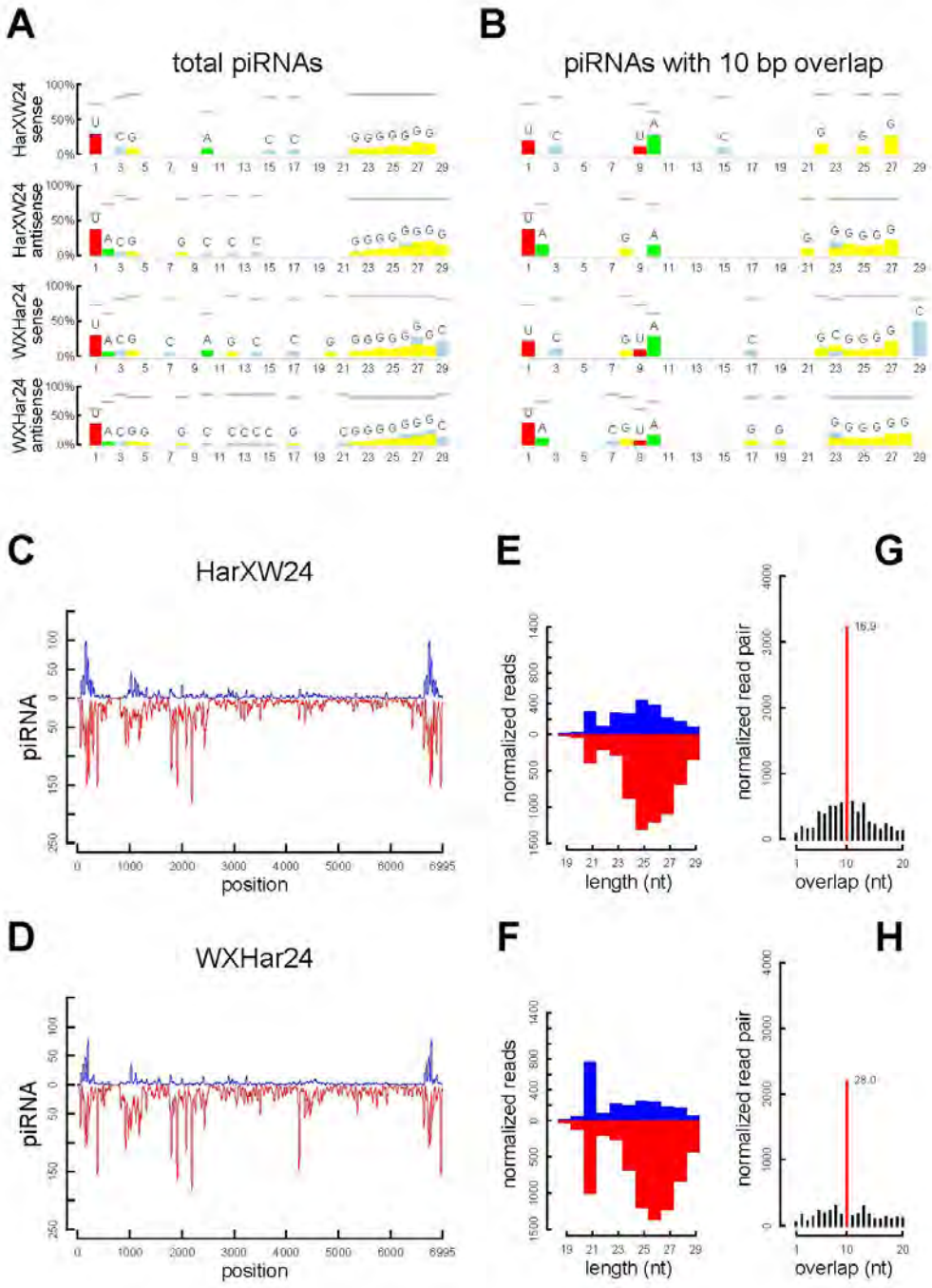
A
total piRNAs
B
piRNAs with 10 bp overlap
HarXW24 sense
HarXW24 antisense
WXHar24 sense
WXHar24 antisense
C
HarXW24
D
WXHar24
piRNA
position
E
F
normalized reads
length (nt)
G
H
normalized read pair
overlap (nt)
16.0
28.0

3S18

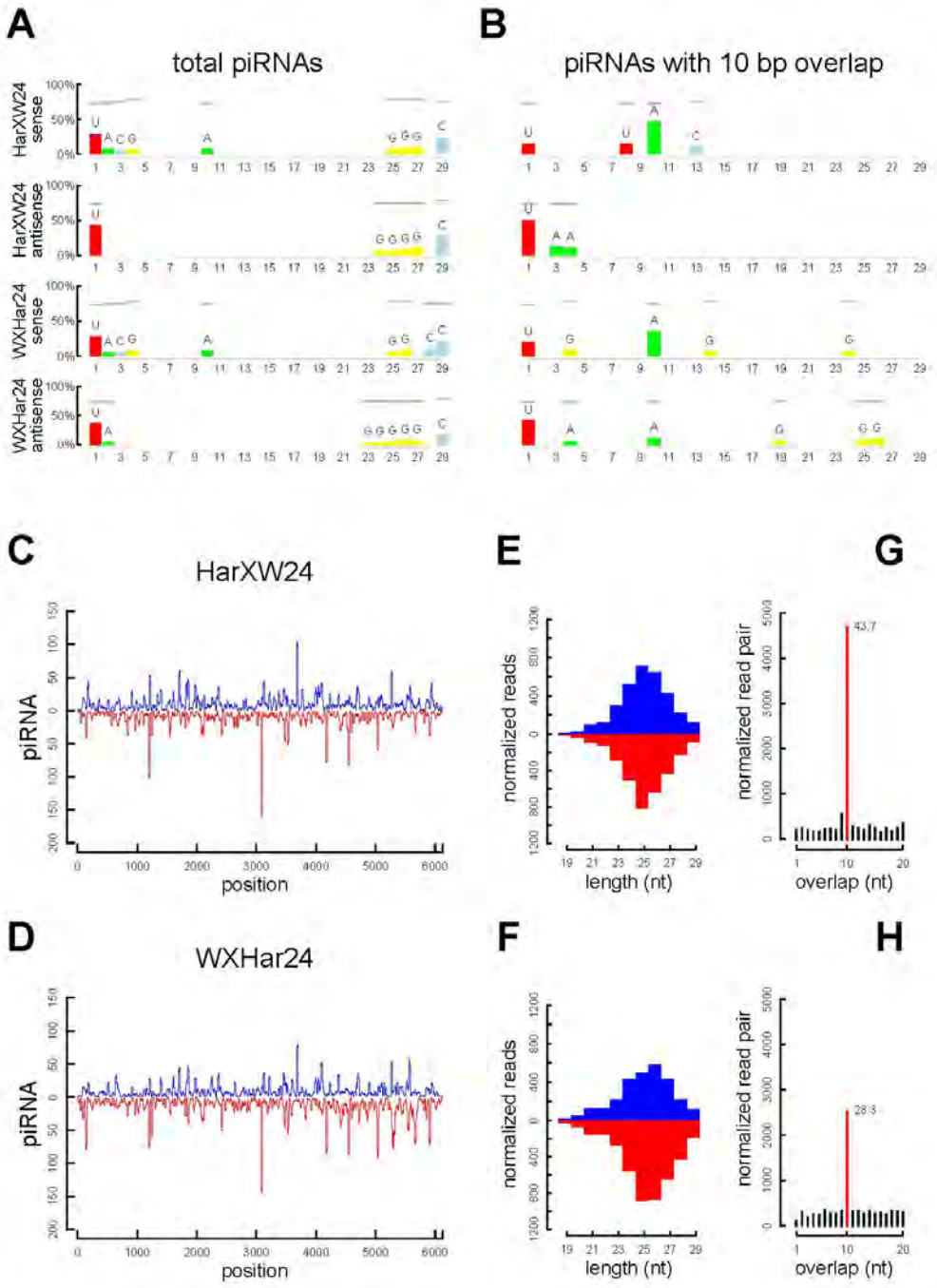
A
total piRNAs
B
piRNAs with 10 bp overlap
HarXW24 sense
HarXW24 antisense
WXHar24 sense
WXHar24 antisense
C
HarXW24
piRNA
position
D
WXHar24
piRNA
position
E
normalized reads
length (nt)
F
normalized reads
length (nt)
G
normalized read pair
43.7
overlap (nt)
H
normalized read pair
28.3
overlap (nt)

412

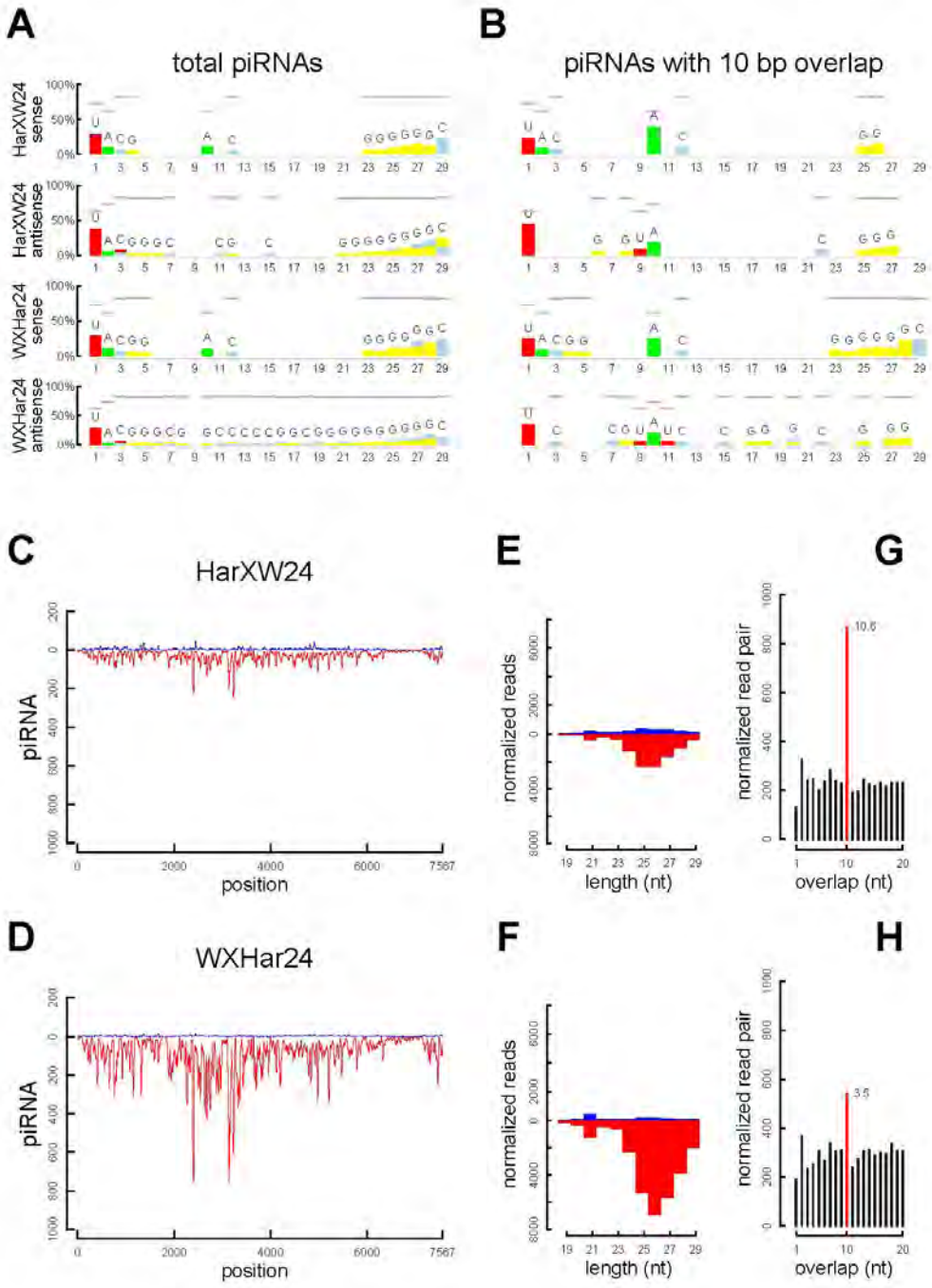
A
total piRNAs
B
piRNAs with 10 bp overlap
HarXW24 sense
HarXW24 antisense
WXHar24 sense
WXHar24 antisense
C
HarXW24
D
WXHar24
piRNA
position
E
F
normalized reads
length (nt)
G
H
normalized read pair
overlap (nt)
10.6
3.5

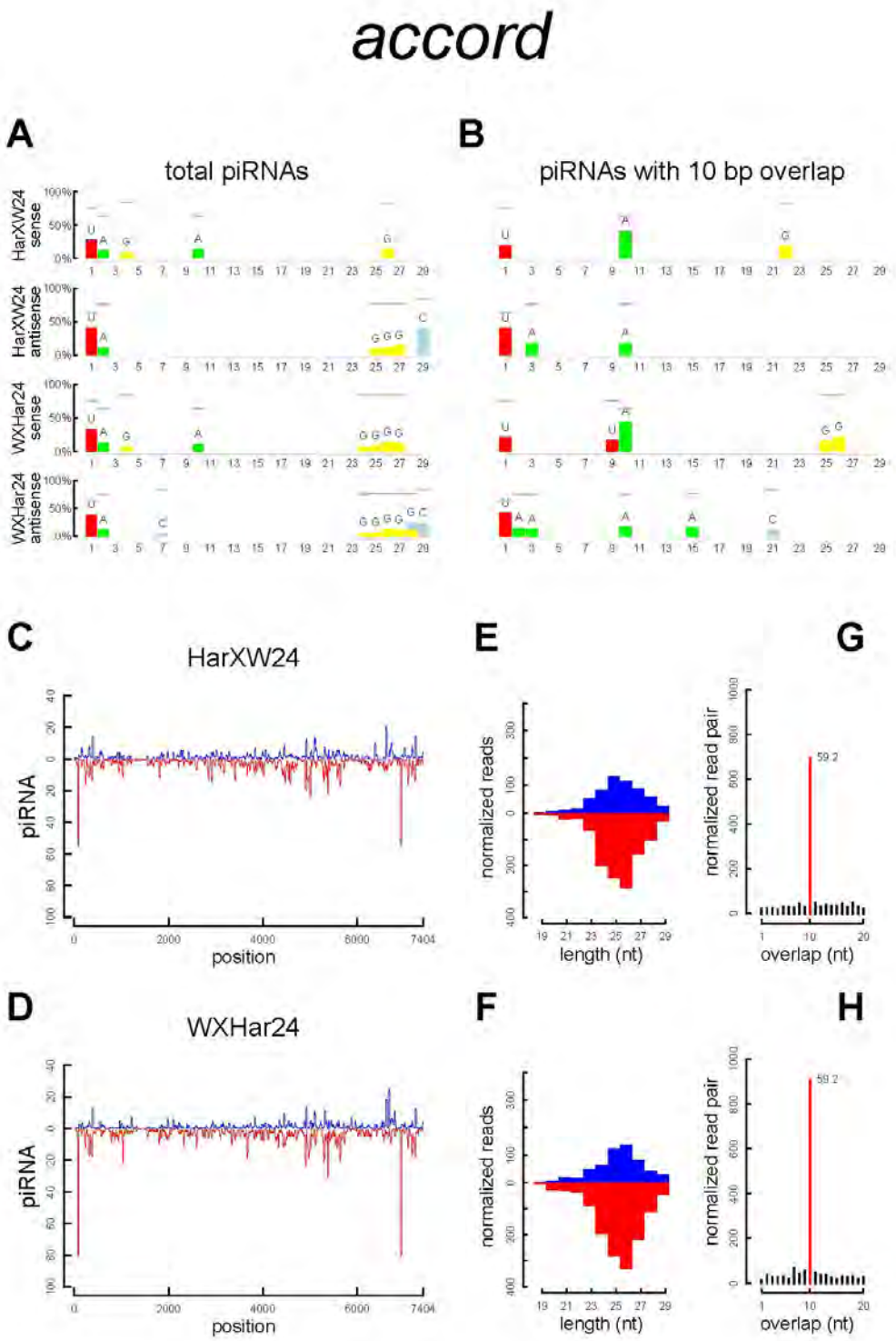
accord
A
total piRNAs
B
piRNAs with 10 bp overlap
HarXW24 sense
HarXW24 antisense
WXHar24 sense
WXHar24 antisense
C
HarXW24
D
WXHar24
piRNA
position
E
F
normalized reads
length (nt)
G
H
normalized read pair
overlap (nt)
59.2

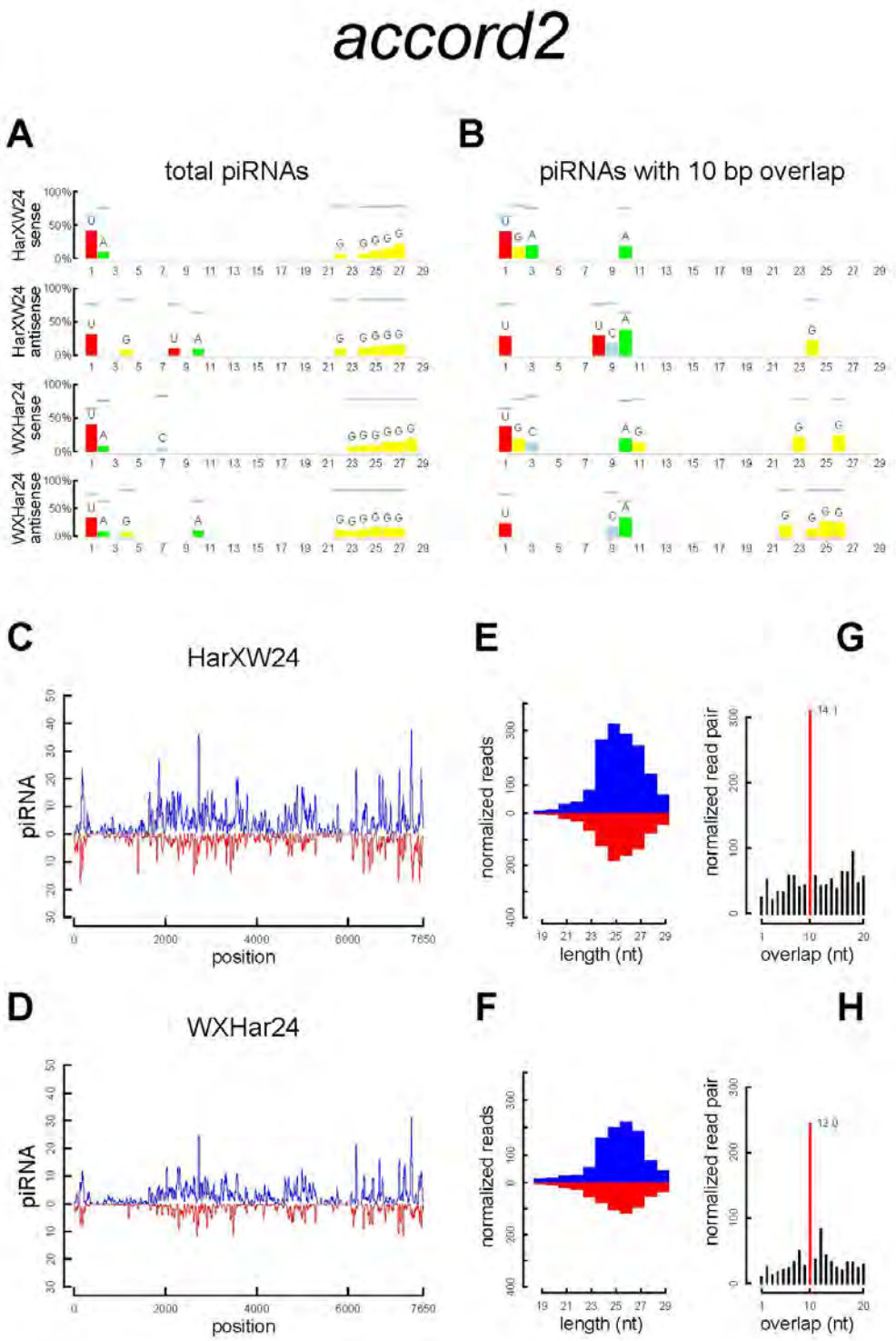
accord2
A
total piRNAs
B
piRNAs with 10 bp overlap
HarXW24 sense
HarXW24 antisense
WXHar24 sense
WXHar24 antisense
C
HarXW24
D
WXHar24
piRNA
position
E
F
normalized reads
length (nt)
G
H
normalized read pair
overlap (nt)

aurora element

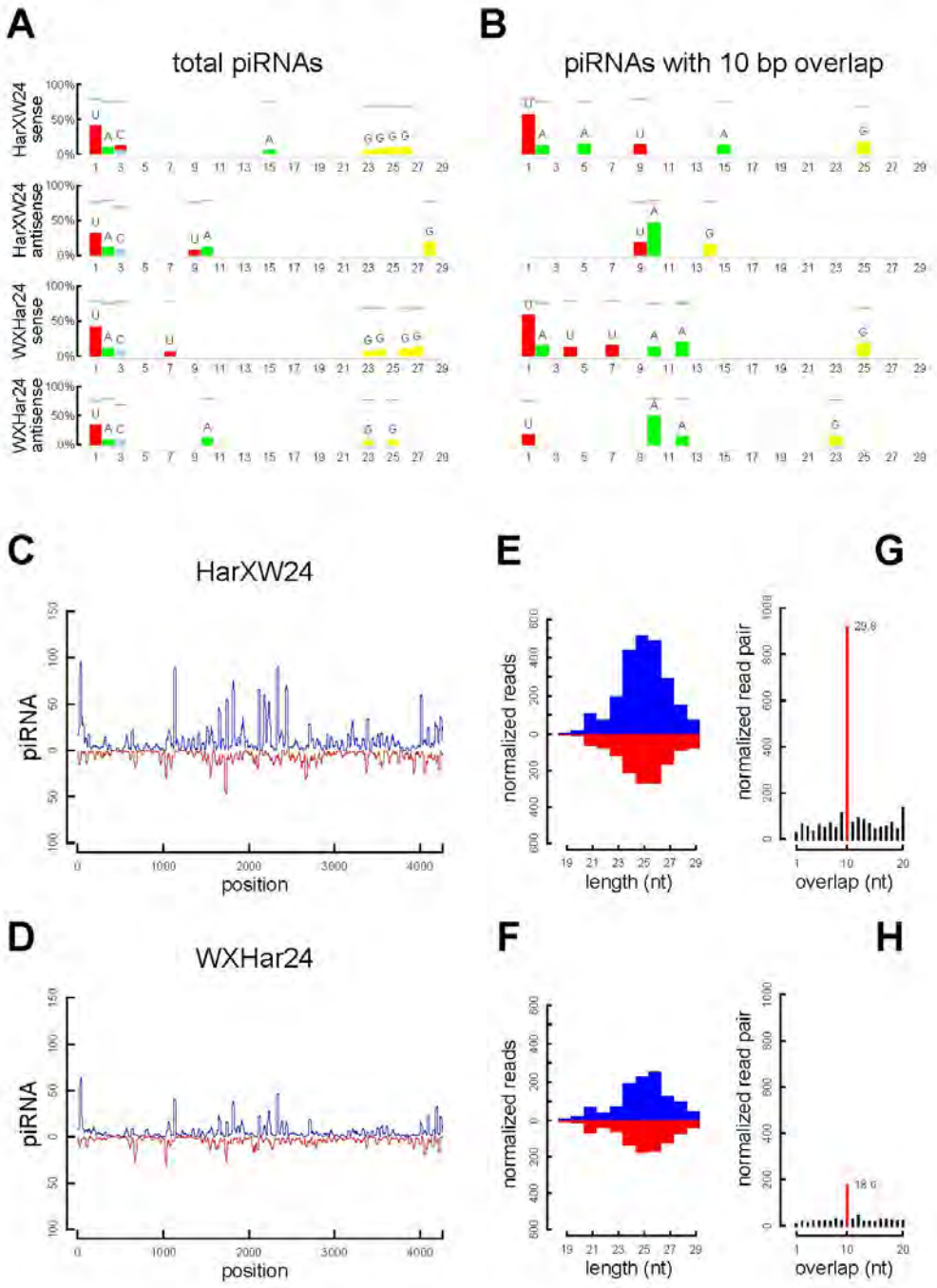

baggins

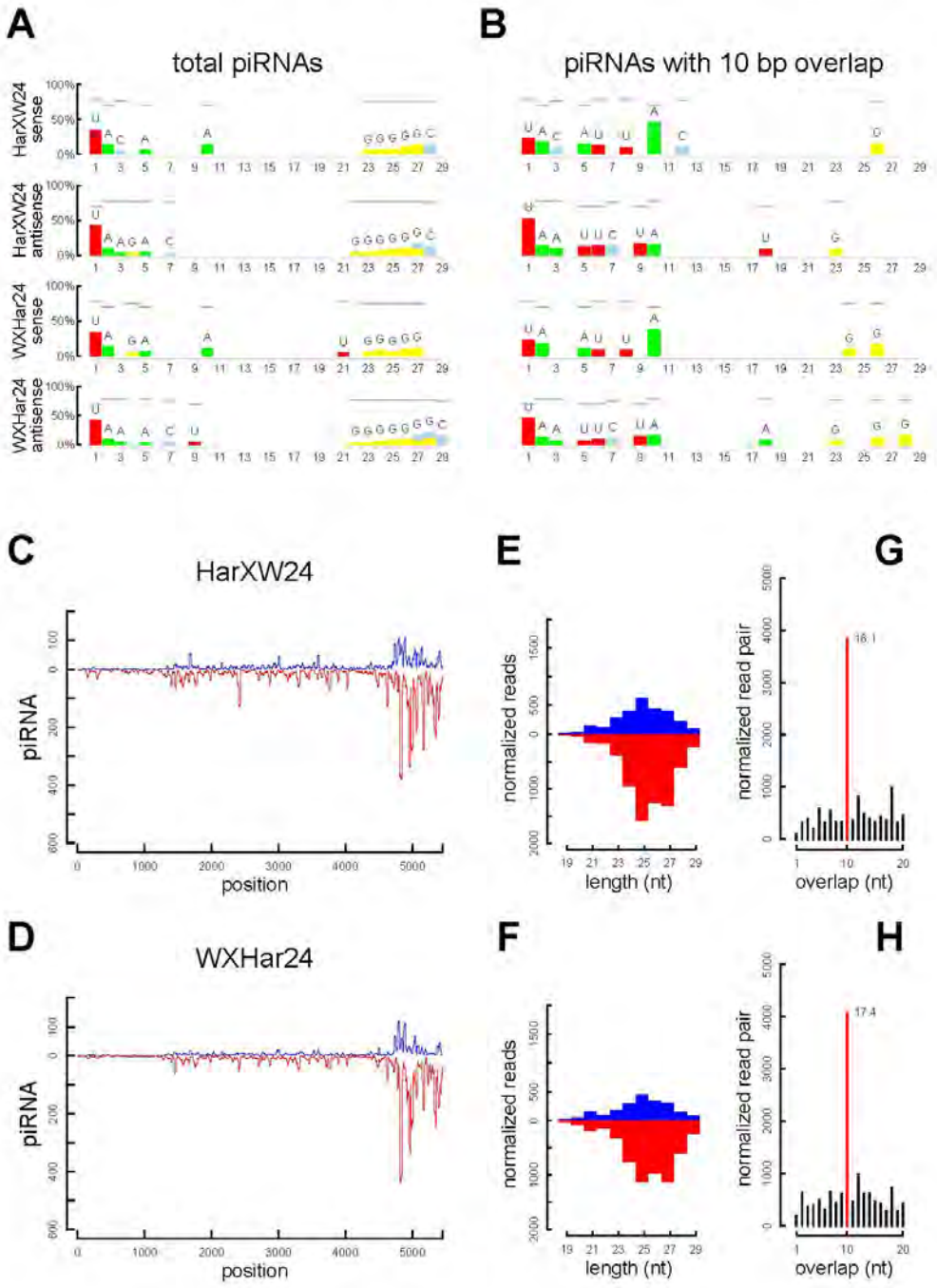
A
total piRNAs
B
piRNAs with 10 bp overlap
HarXW24 sense
HarXW24 antisense
WXHar24 sense
WXHar24 antisense
C
HarXW24
D
WXHar24
piRNA
position
E
F
normalized reads
length (nt)
G
H
normalized read pair
overlap (nt)

Bari1

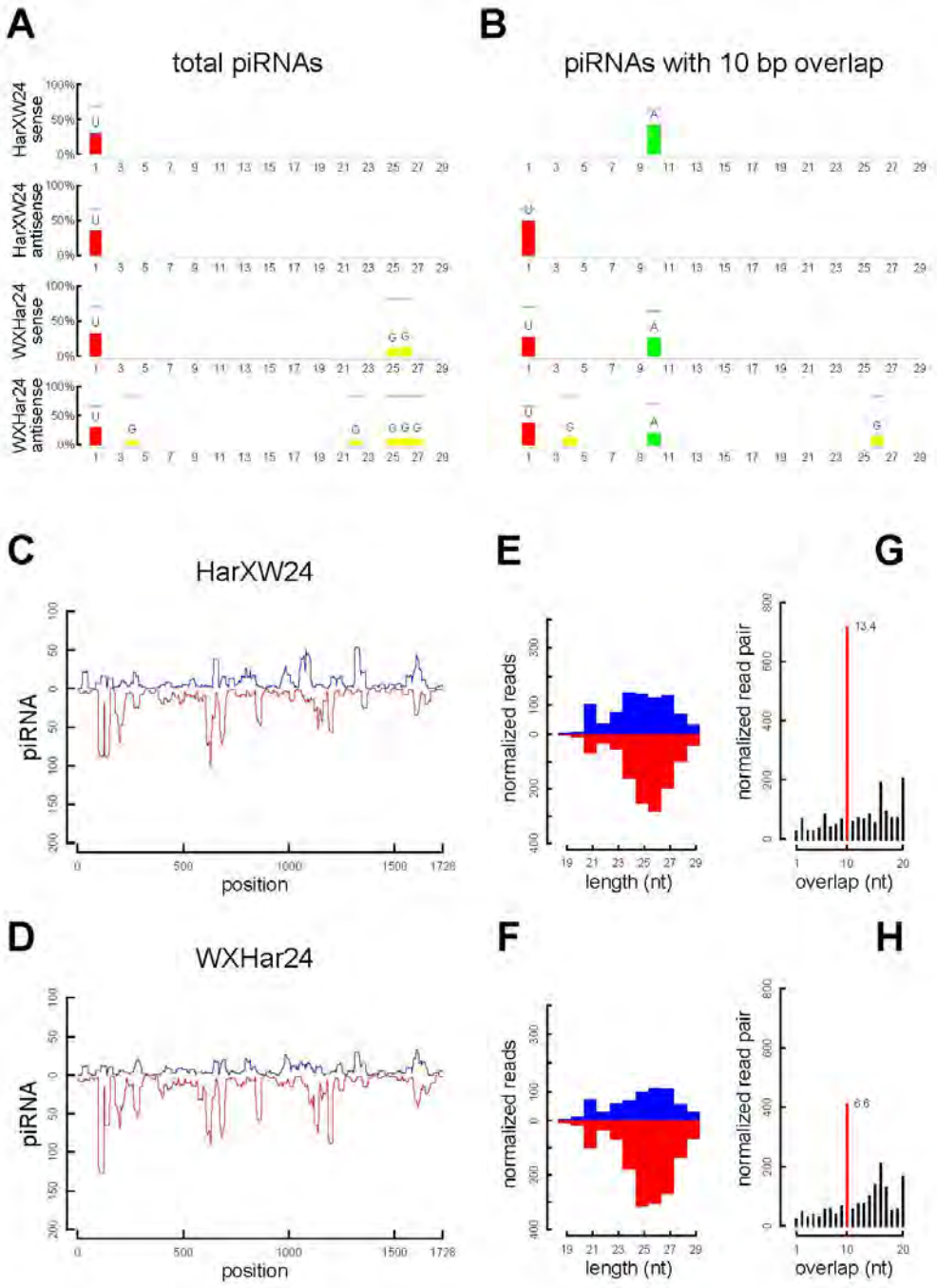
A
total piRNAs
B
piRNAs with 10 bp overlap
HarXW24 sense
HarXW24 antisense
WXHar24 sense
WXHar24 antisense
C
HarXW24
D
WXHar24
piRNA
position
E
F
normalized reads
length (nt)
G
H
normalized read pair
overlap (nt)
13.4
6.6

Bari2

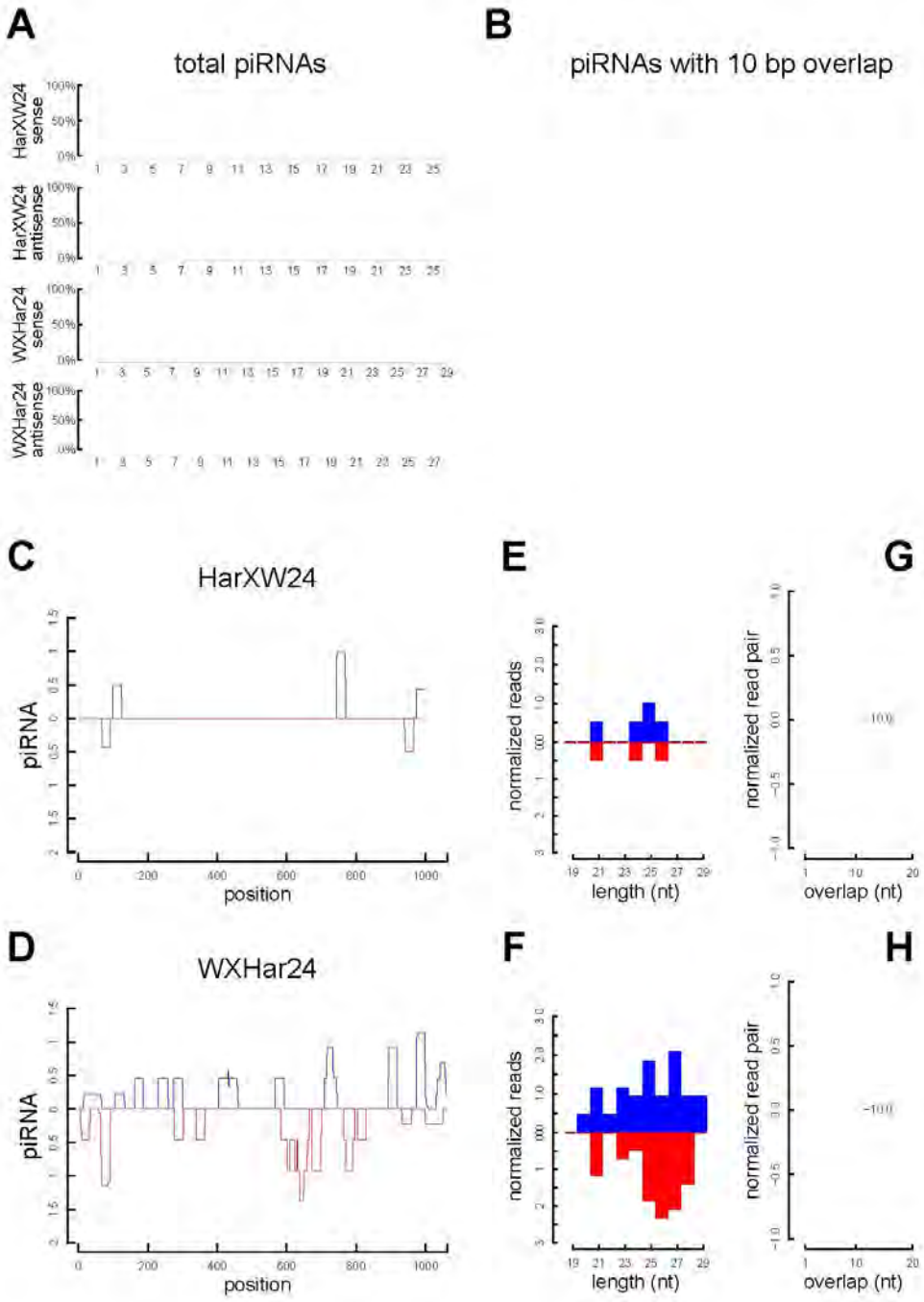
A
total piRNAs
B
piRNAs with 10 bp overlap
HarXW24 sense
HarXW24 antisense
WXHar24 sense
WXHar24 antisense
C
HarXW24
D
WXHar24
piRNA
position
E
F
normalized reads
length (nt)
G
H
normalized read pair
overlap (nt)

blood

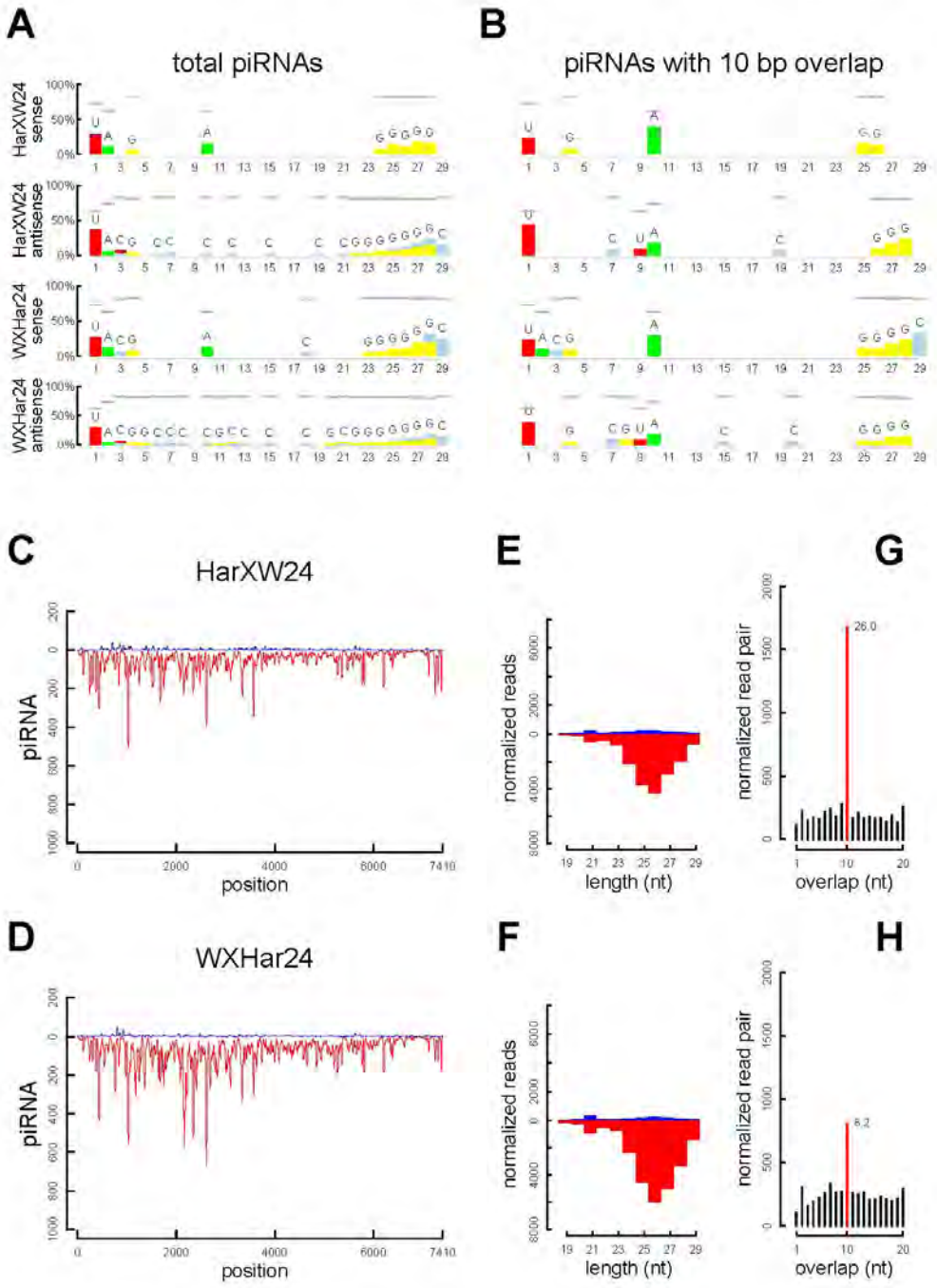
A
total piRNAs
B
piRNAs with 10 bp overlap
HarXW24 sense
HarXW24 antisense
WXHar24 sense
WXHar24 antisense
C
HarXW24
D
WXHar24
piRNA
position
E
F
normalized reads
length (nt)
G
H
normalized read pair
overlap (nt)
26.0
8.2

BS

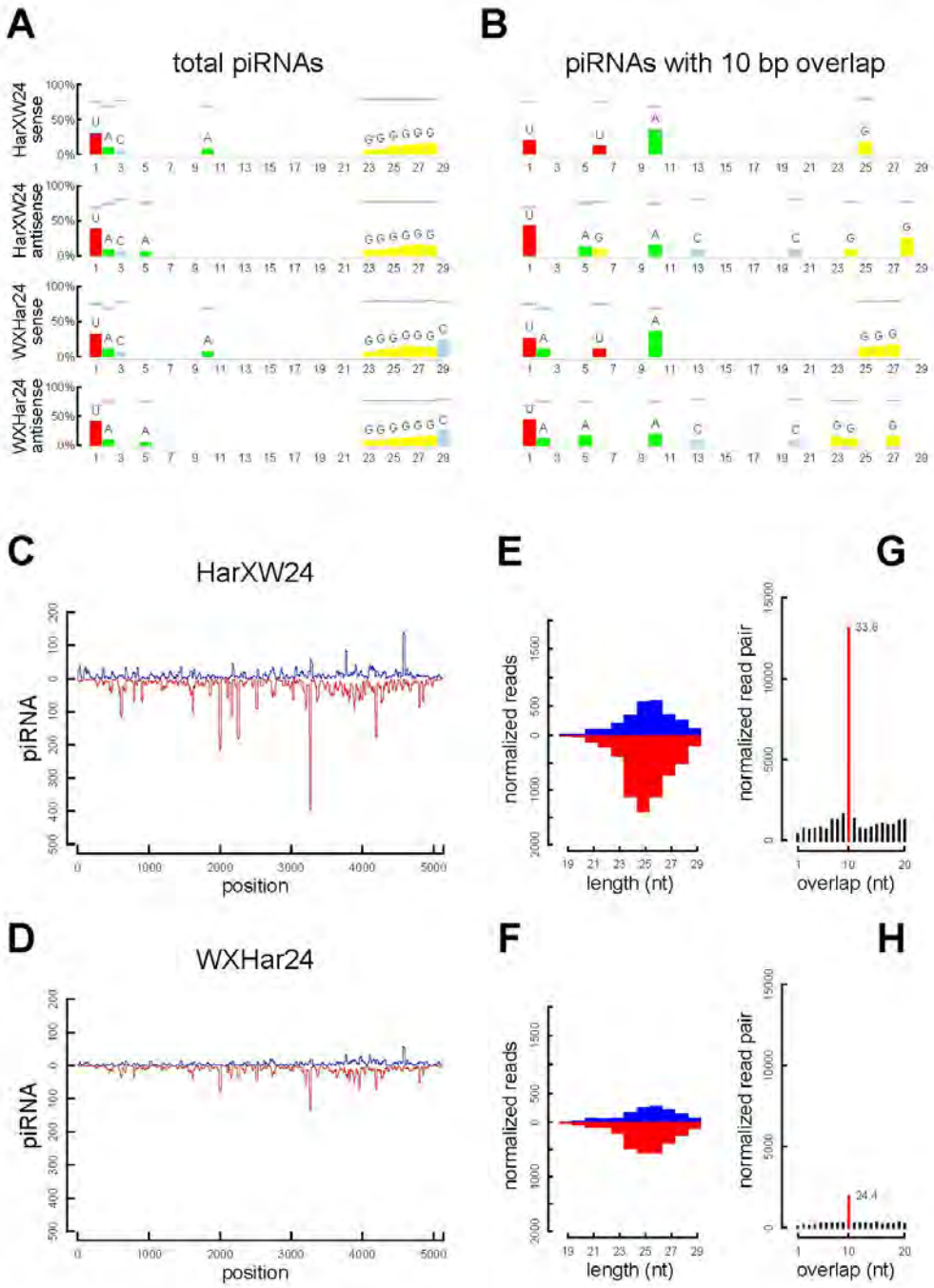
A
total piRNAs
B
piRNAs with 10 bp overlap
HarXW24 sense
HarXW24 antisense
WXHar24 sense
WXHar24 antisense
C
HarXW24
piRNA
position
D
WXHar24
piRNA
position
E
normalized reads
length (nt)
F
normalized reads
length (nt)
G
normalized read pair
33.8
overlap (nt)
H
normalized read pair
24.4
overlap (nt)

BS3

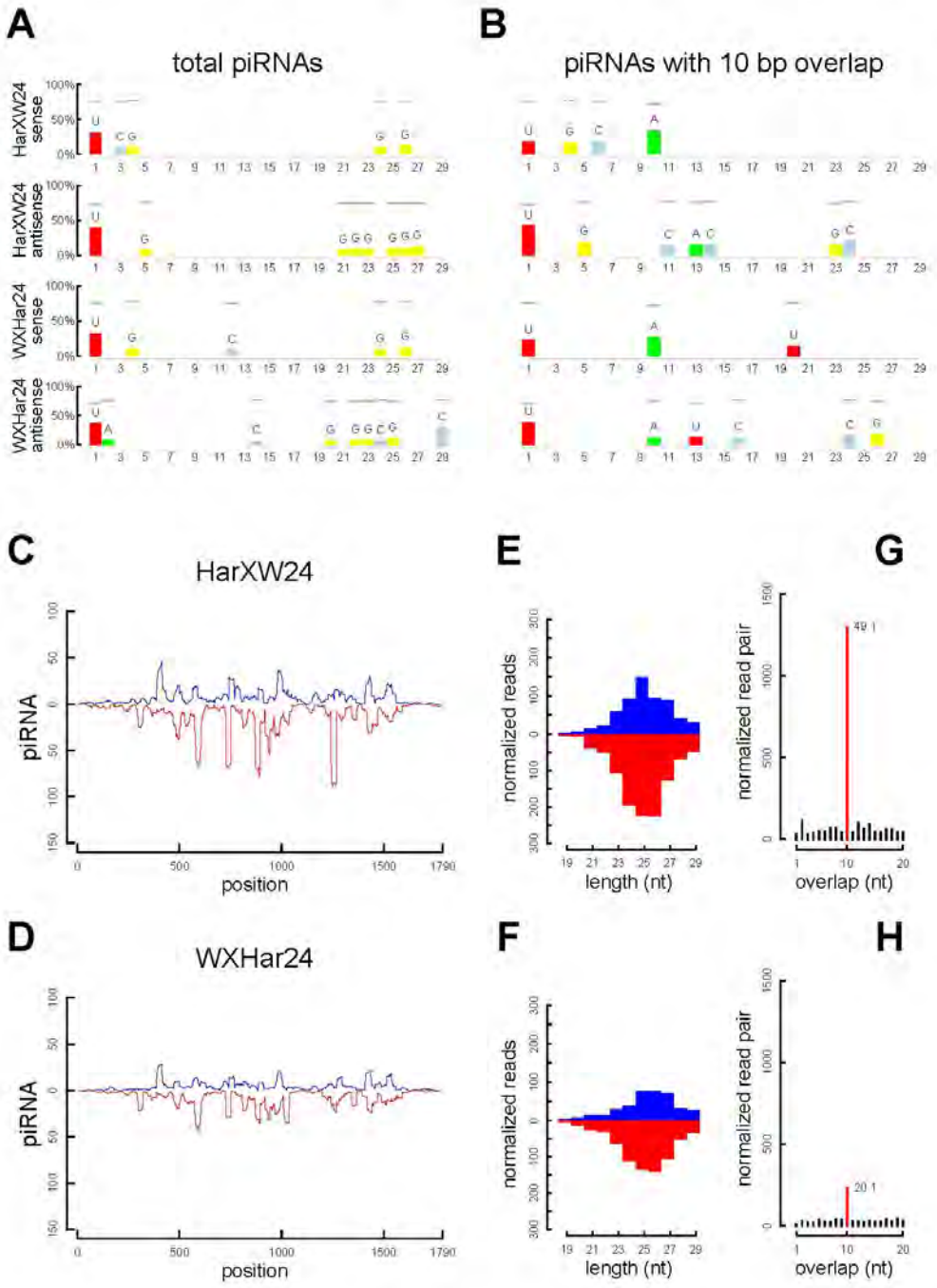
A
total piRNAs
B
piRNAs with 10 bp overlap
HarXW24 sense
HarXW24 antisense
WXHar24 sense
WXHar24 antisense
C
HarXW24
D
WXHar24
piRNA
position
E
F
normalized reads
length (nt)
G
H
normalized read pair
overlap (nt)

BS3#2

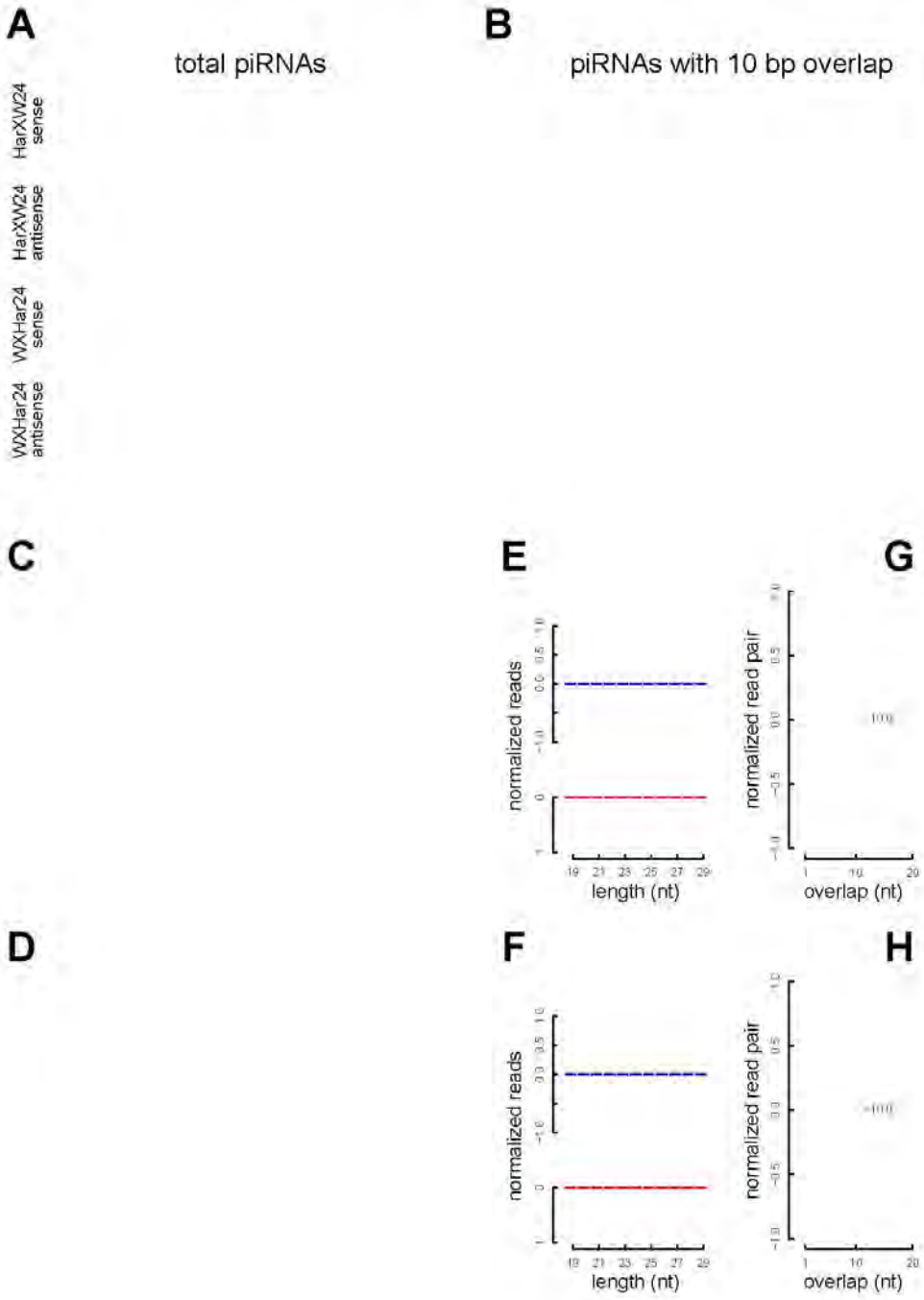
A
total piRNAs
HarXW24 sense
HarXW24 antisense
WXHar24 sense
WXHar24 antisense
B
piRNAs with 10 bp overlap
C
D
E
normalized reads
length (nt)
F
normalized reads
length (nt)
G
normalized read pair
overlap (nt)
H
normalized read pair
overlap (nt)

Burdock

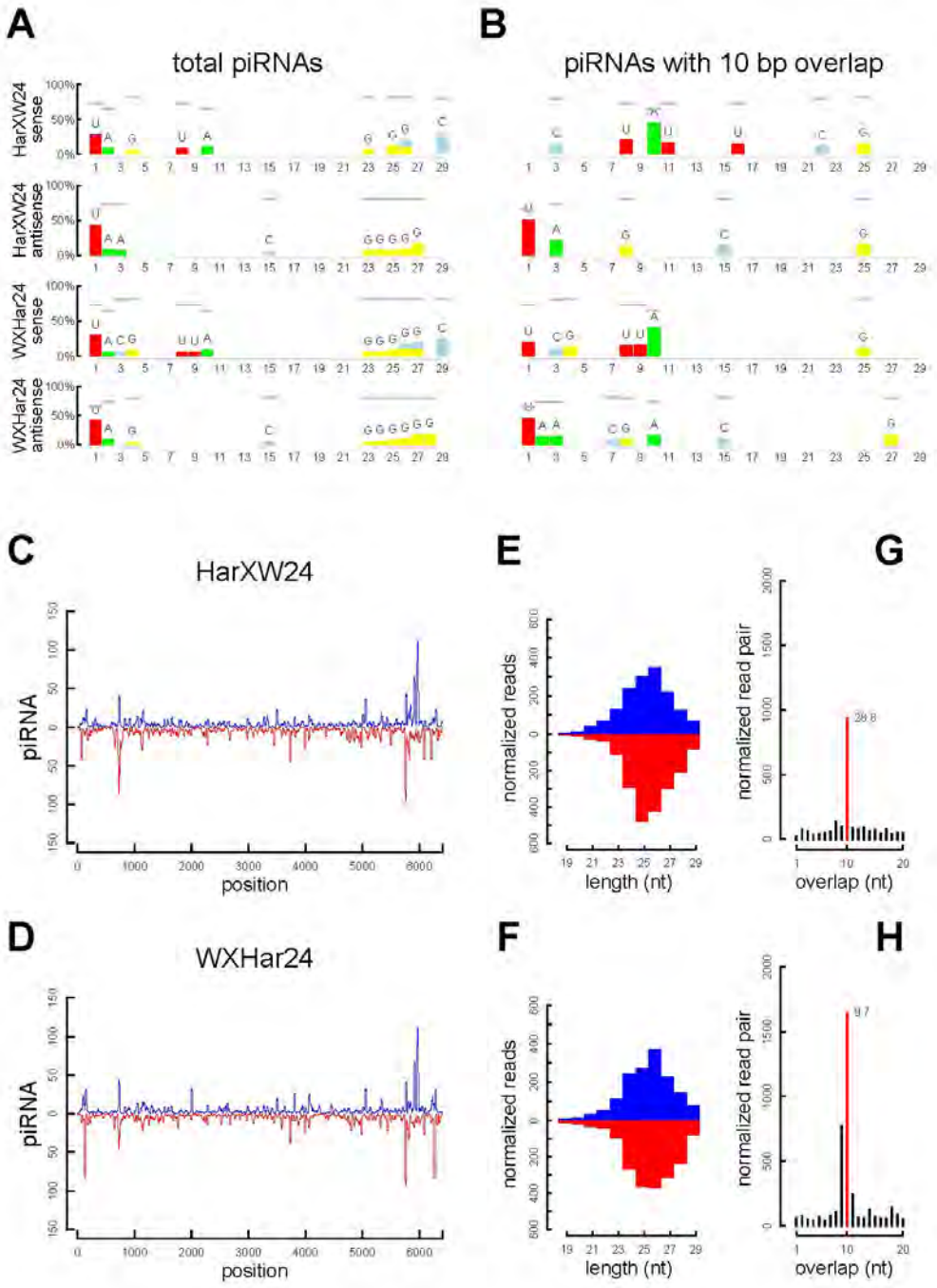
A
total piRNAs
B
piRNAs with 10 bp overlap
HarXW24 sense
HarXW24 antisense
WXHar24 sense
WXHar24 antisense
C
HarXW24
D
WXHar24
piRNA
position
E
F
normalized reads
length (nt)
G
H
normalized read pair
overlap (nt)

Circe

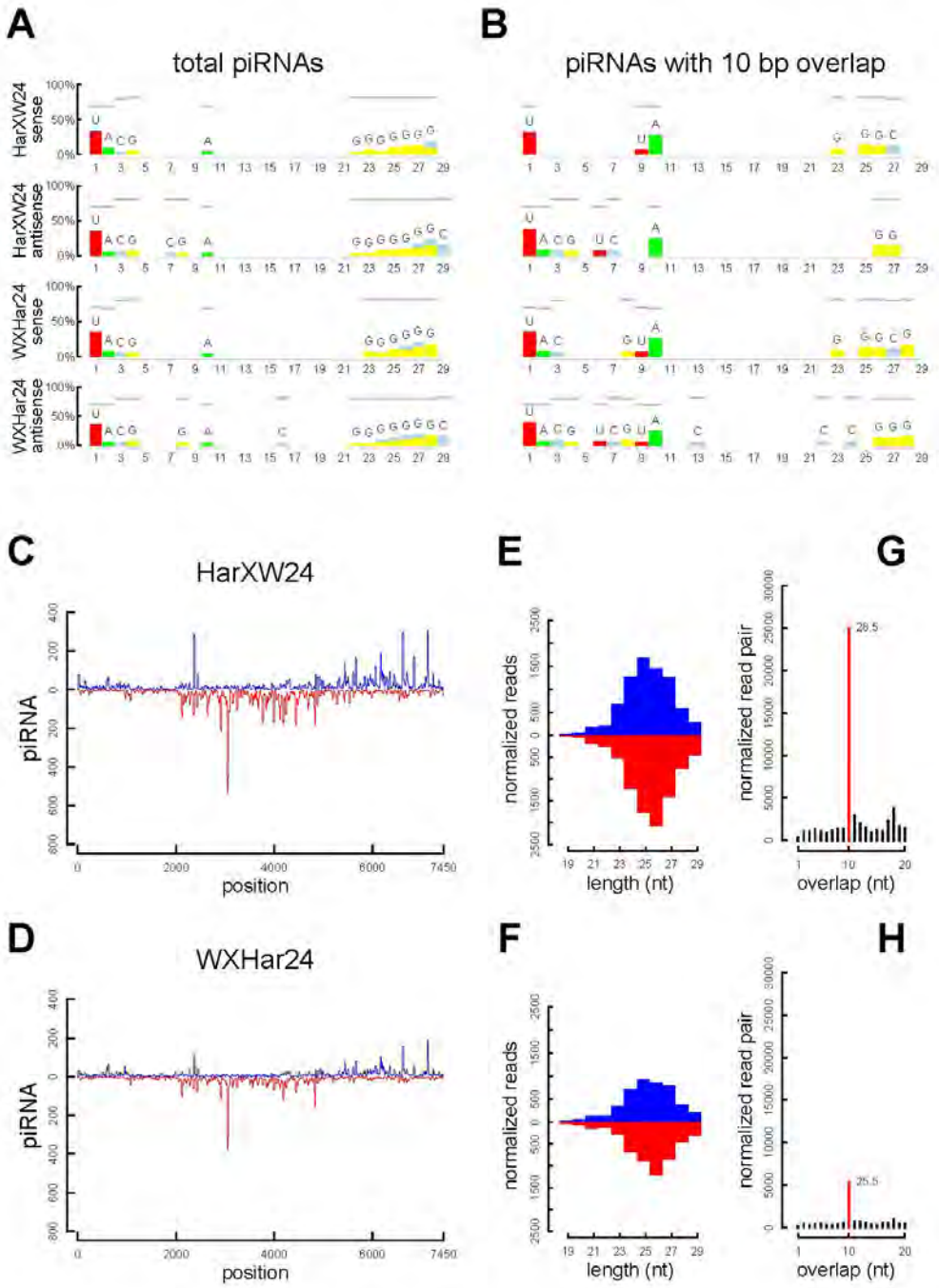
A
total piRNAs
B
piRNAs with 10 bp overlap
HarXW24 sense
HarXW24 antisense
WXHar24 sense
WXHar24 antisense
C
HarXW24
piRNA
position
D
WXHar24
piRNA
position
E
normalized reads
length (nt)
F
normalized reads
length (nt)
G
normalized read pair
overlap (nt)
26.5
H
normalized read pair
overlap (nt)
25.5

copia

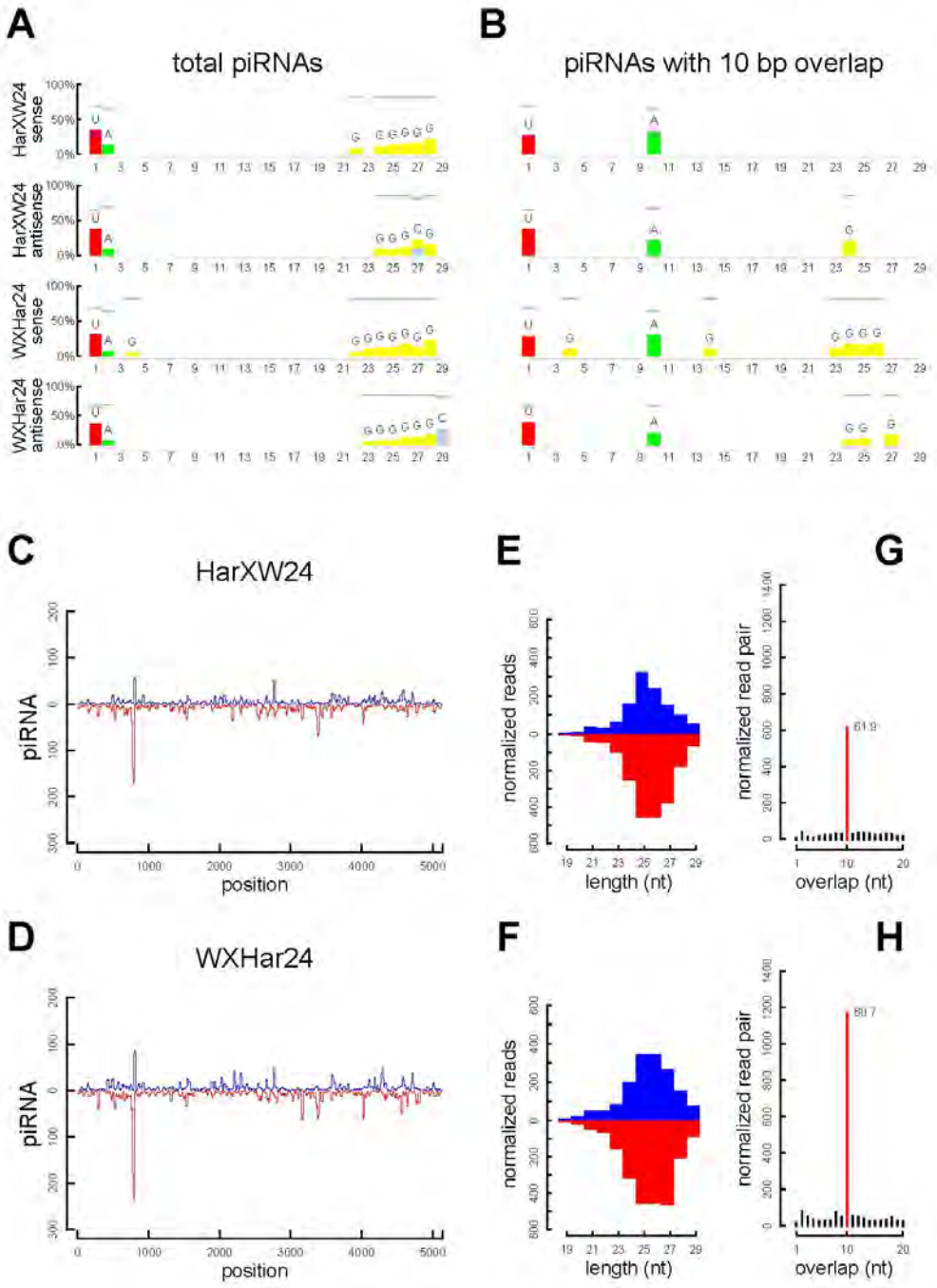
A
total piRNAs
B
piRNAs with 10 bp overlap
HarXW24 sense
HarXW24 antisense
WXHar24 sense
WXHar24 antisense
C
HarXW24
D
WXHar24
piRNA
position
E
F
normalized reads
length (nt)
G
H
normalized read pair
overlap (nt)
61.9
80.7

Cr1a

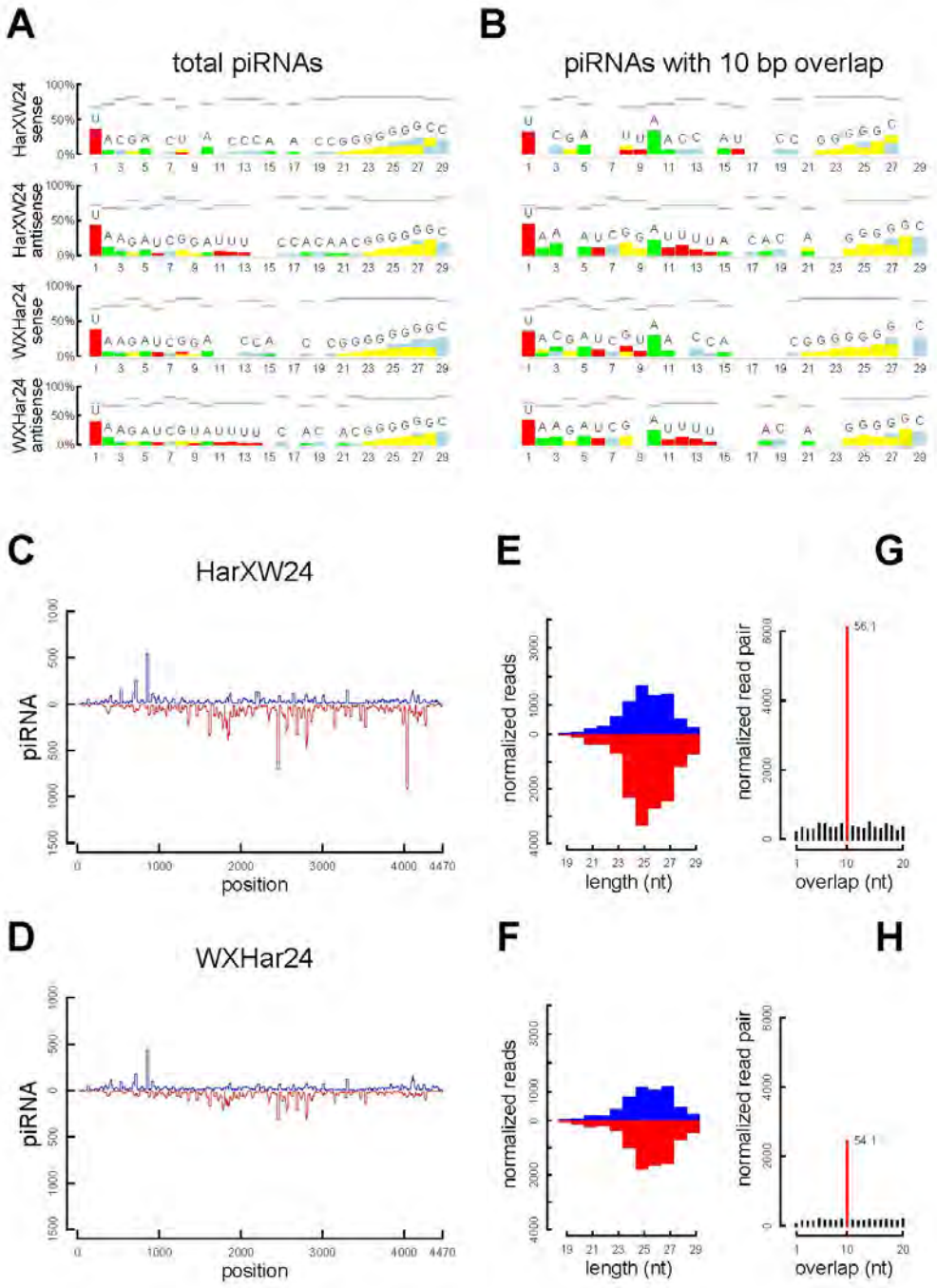
A
total piRNAs
B
piRNAs with 10 bp overlap
HarXW24 sense
HarXW24 antisense
WXHar24 sense
WXHar24 antisense
C
HarXW24
piRNA
position
D
WXHar24
piRNA
position
E
normalized reads
length (nt)
F
normalized reads
length (nt)
G
normalized read pair
overlap (nt)
56.1
H
normalized read pair
overlap (nt)
54.1

diver

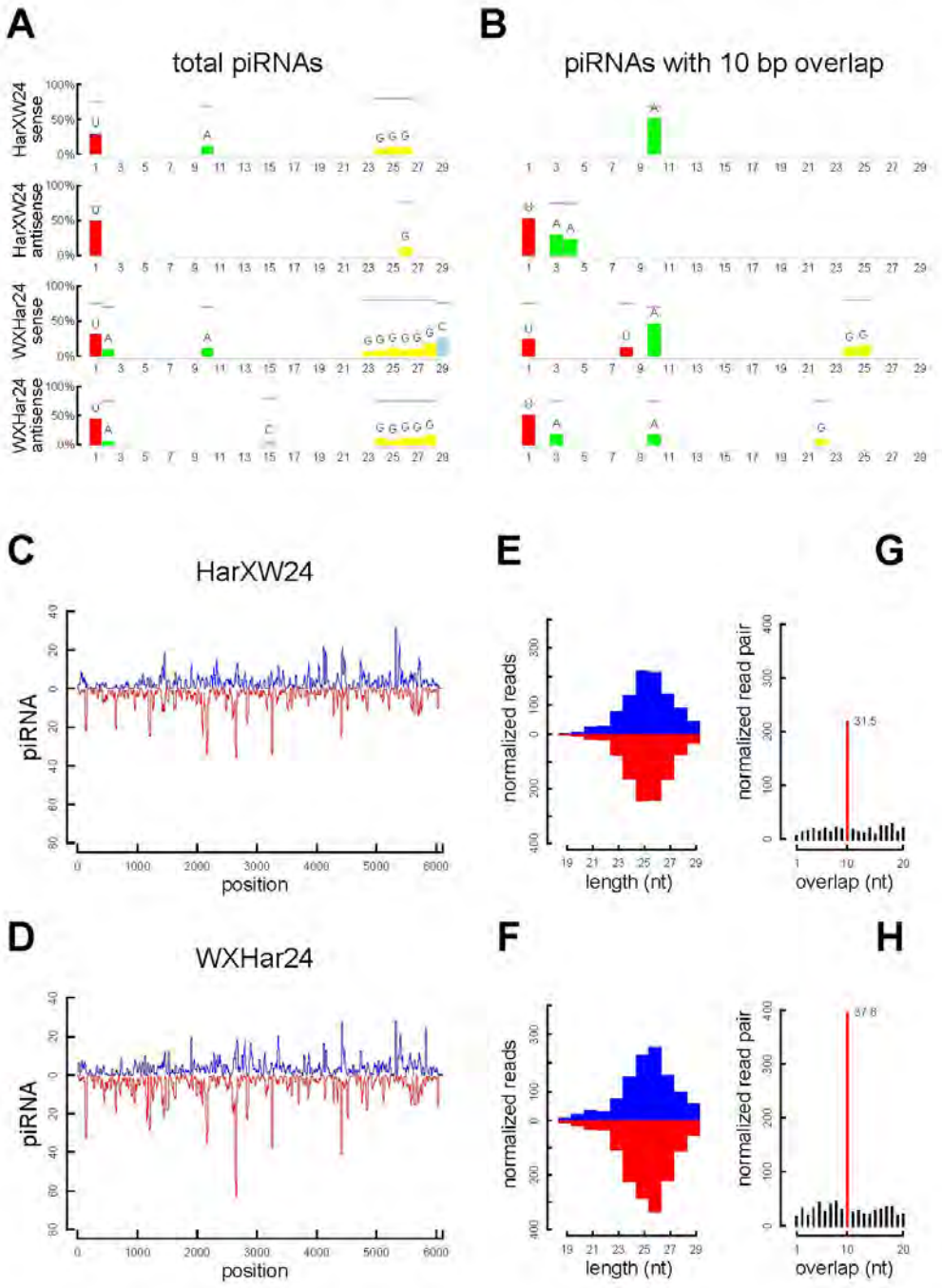
A
total piRNAs
B
piRNAs with 10 bp overlap
HarXW24 sense
HarXW24 antisense
WXHar24 sense
WXHar24 antisense
C
HarXW24
D
WXHar24
piRNA
position
E
F
normalized reads
length (nt)
G
H
normalized read pair
overlap (nt)
31.5
57.8

diver2

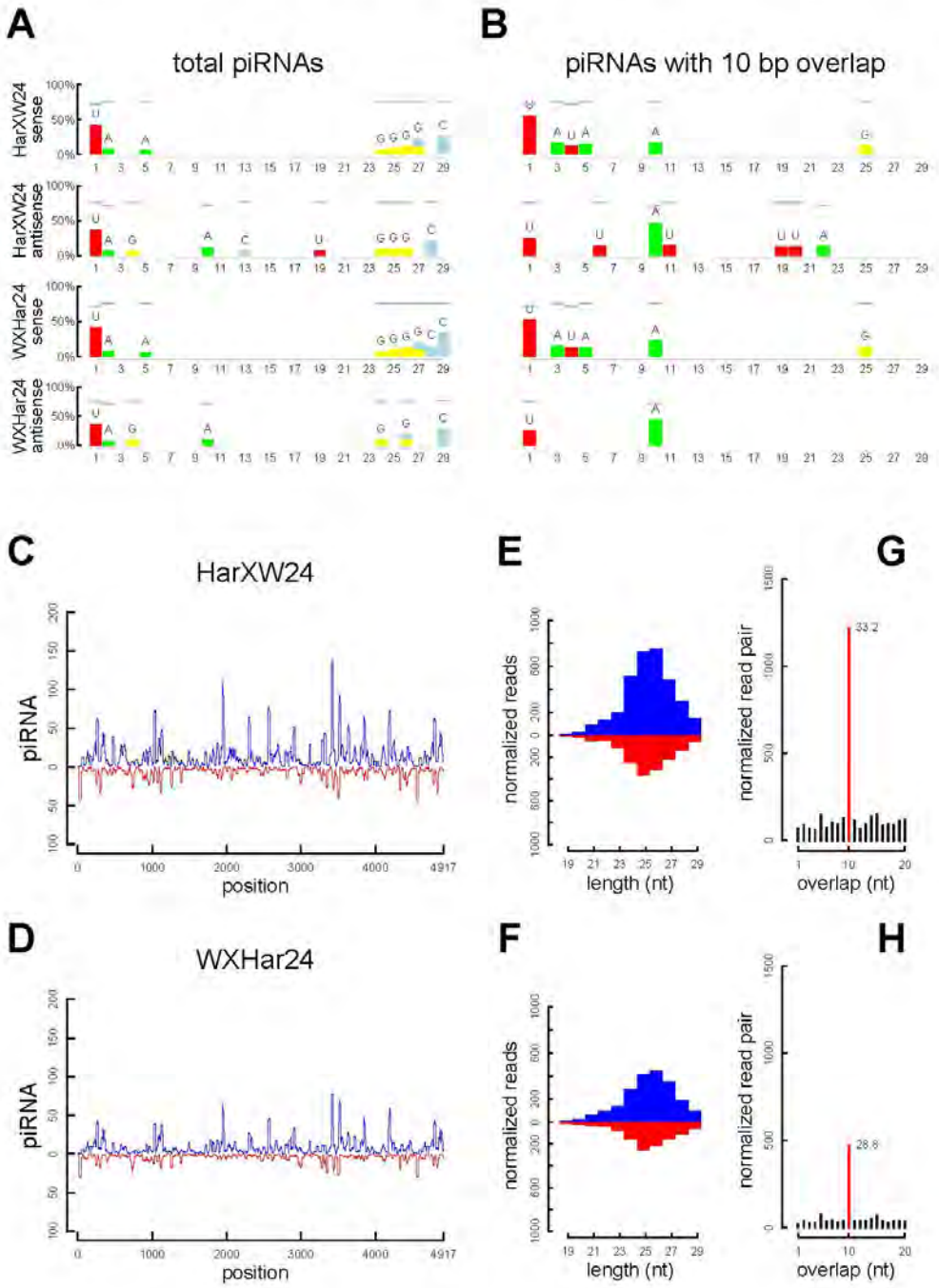
A
total piRNAs
B
piRNAs with 10 bp overlap
HarXW24 sense
HarXW24 antisense
WXHar24 sense
WXHar24 antisense
C
HarXW24
piRNA
position
D
WXHar24
piRNA
position
E
normalized reads
length (nt)
F
normalized reads
length (nt)
G
normalized read pair
overlap (nt)
33.2
H
normalized read pair
overlap (nt)
28.8

Dm88

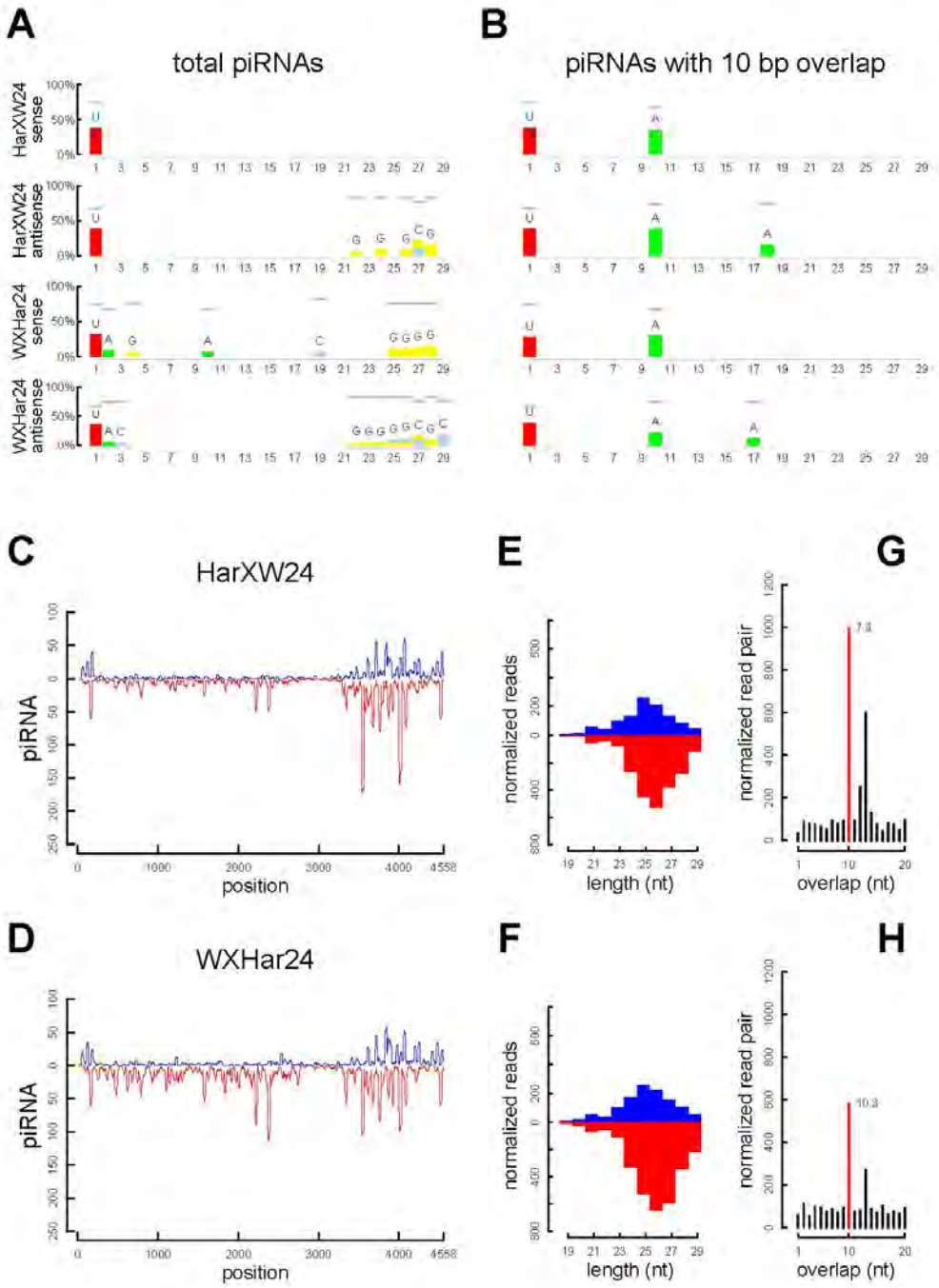
A
total piRNAs
B
piRNAs with 10 bp overlap
HarXW24 sense
HarXW24 antisense
WXHar24 sense
WXHar24 antisense
C
HarXW24
piRNA
position
D
WXHar24
piRNA
position
E
normalized reads
length (nt)
F
normalized reads
length (nt)
G
normalized read pair
overlap (nt)
H
normalized read pair
overlap (nt)

Doc

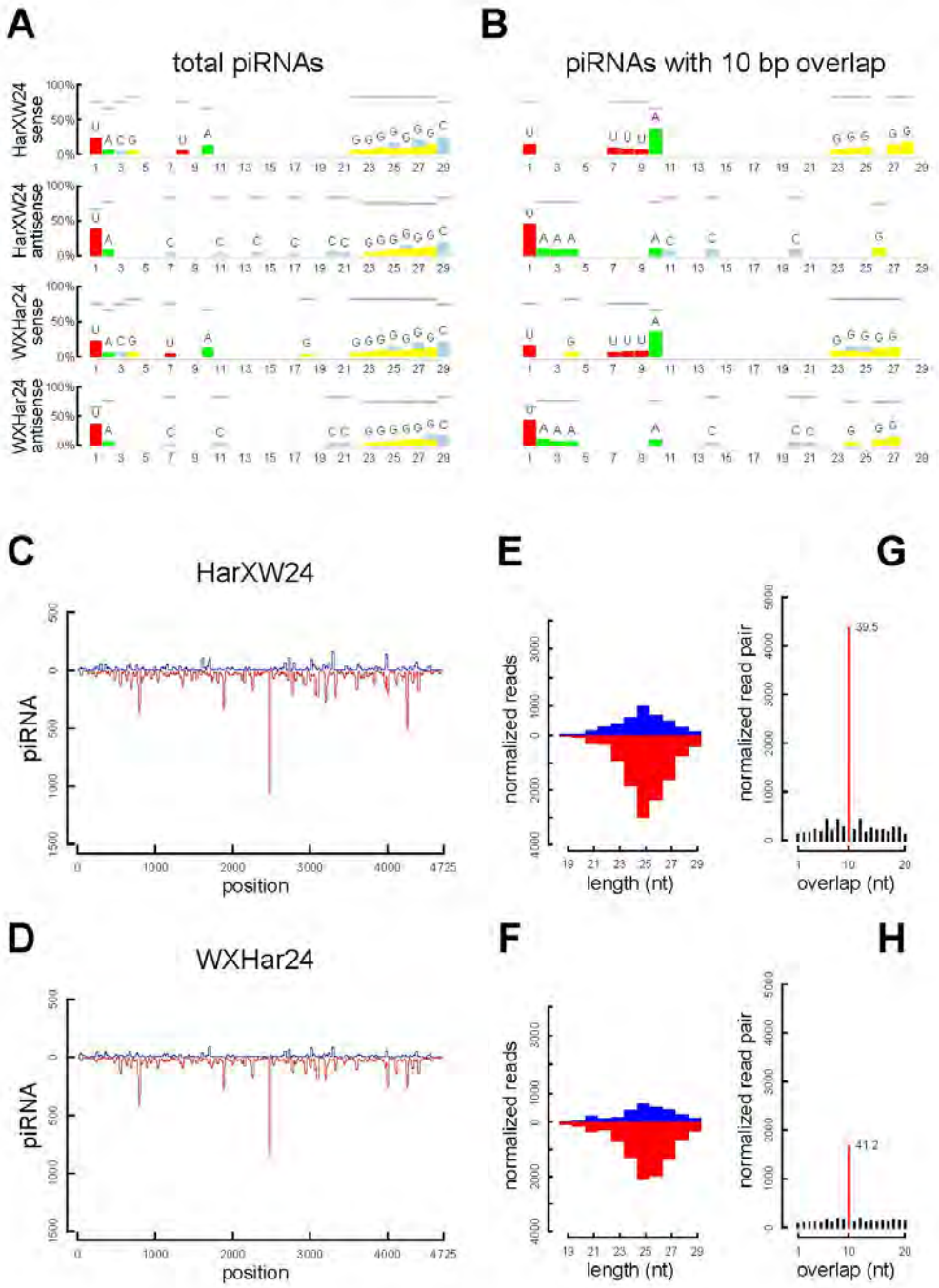
A
total piRNAs
B
piRNAs with 10 bp overlap
HarXW24 sense
HarXW24 antisense
WXHar24 sense
WXHar24 antisense
C
HarXW24
piRNA
position
D
WXHar24
E
F
normalized reads
length (nt)
G
H
normalized read pair
overlap (nt)
39.5
41.2

Doc2 element

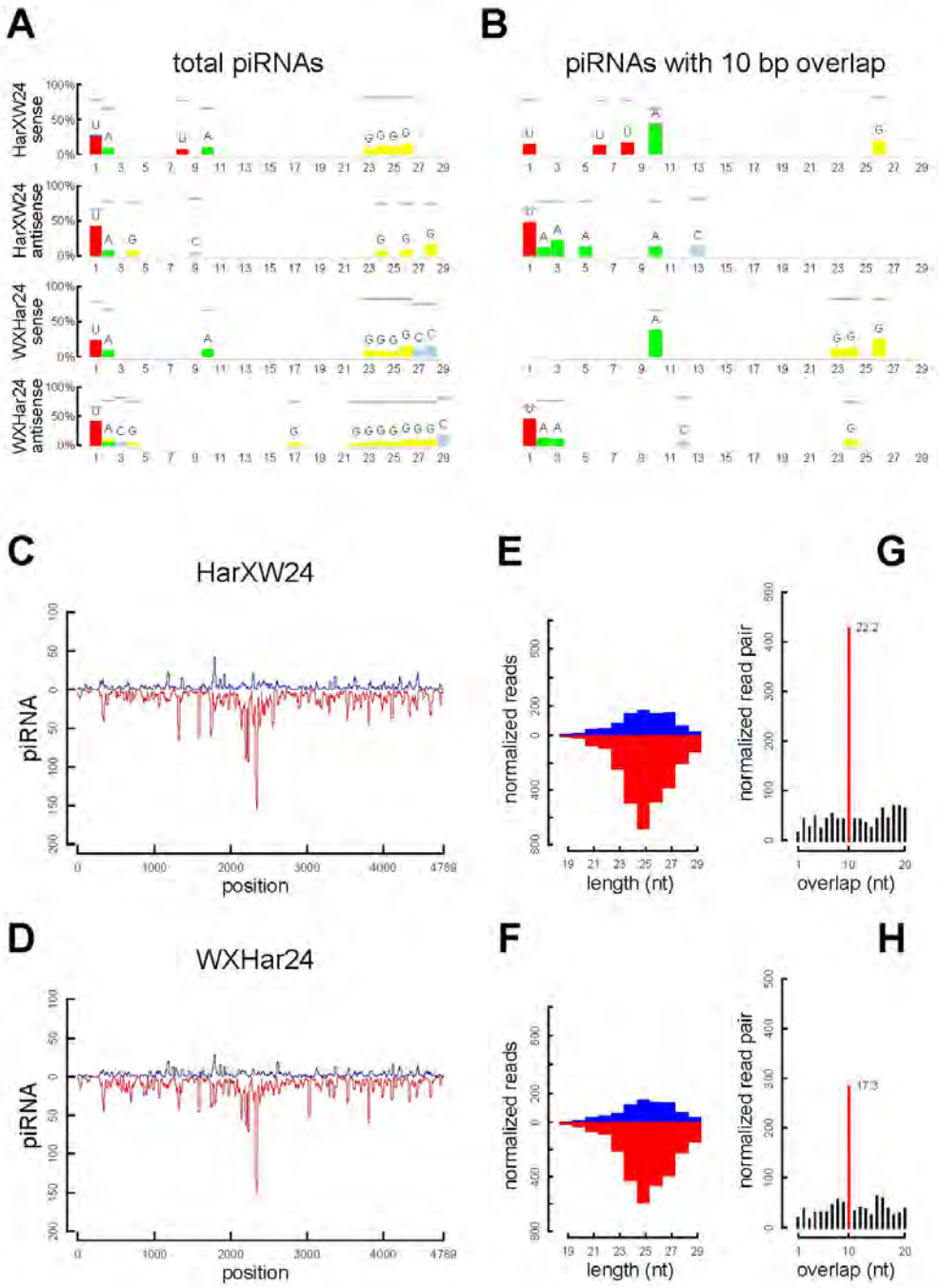

Doc3 element

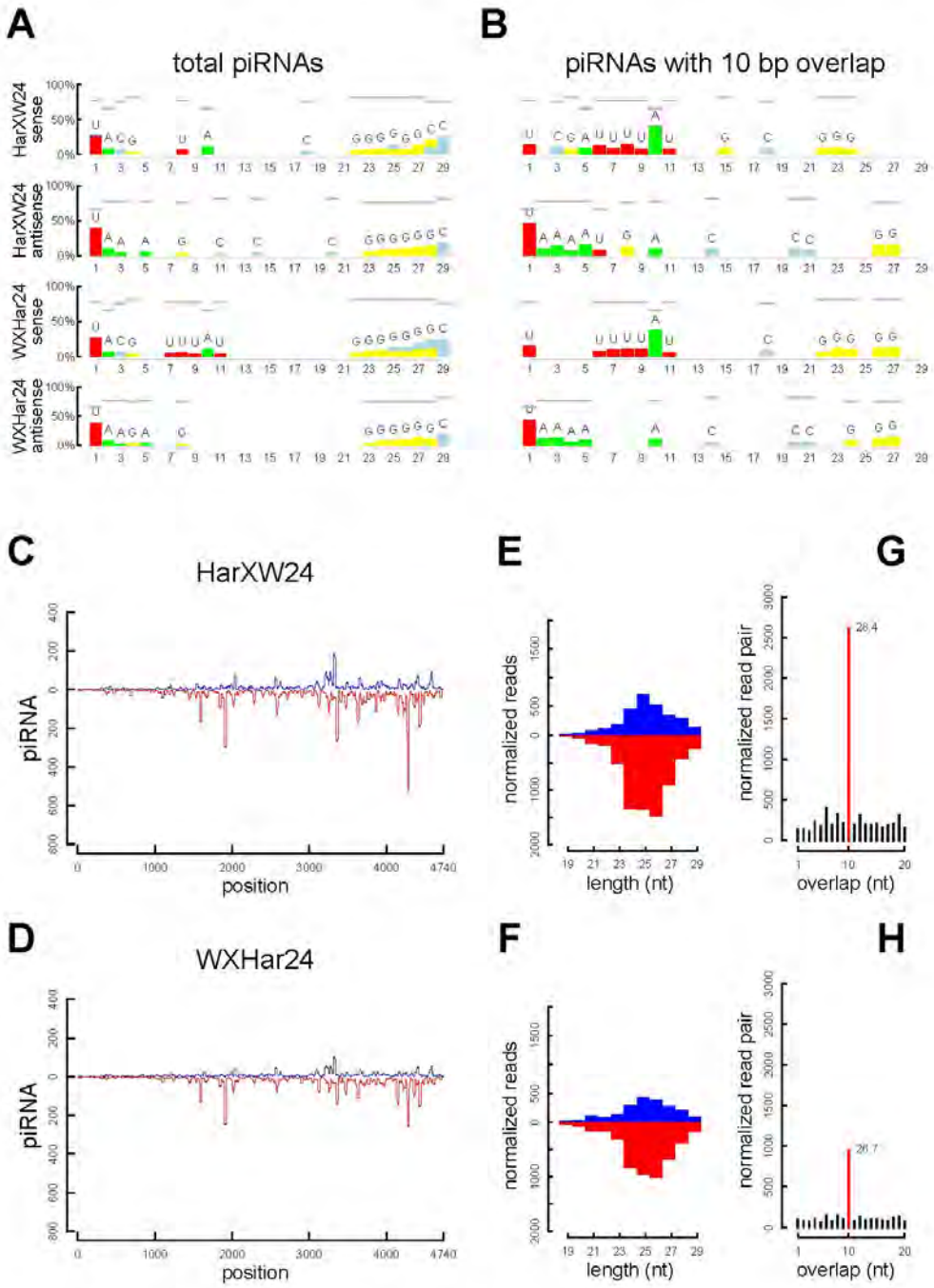

Doc4 element

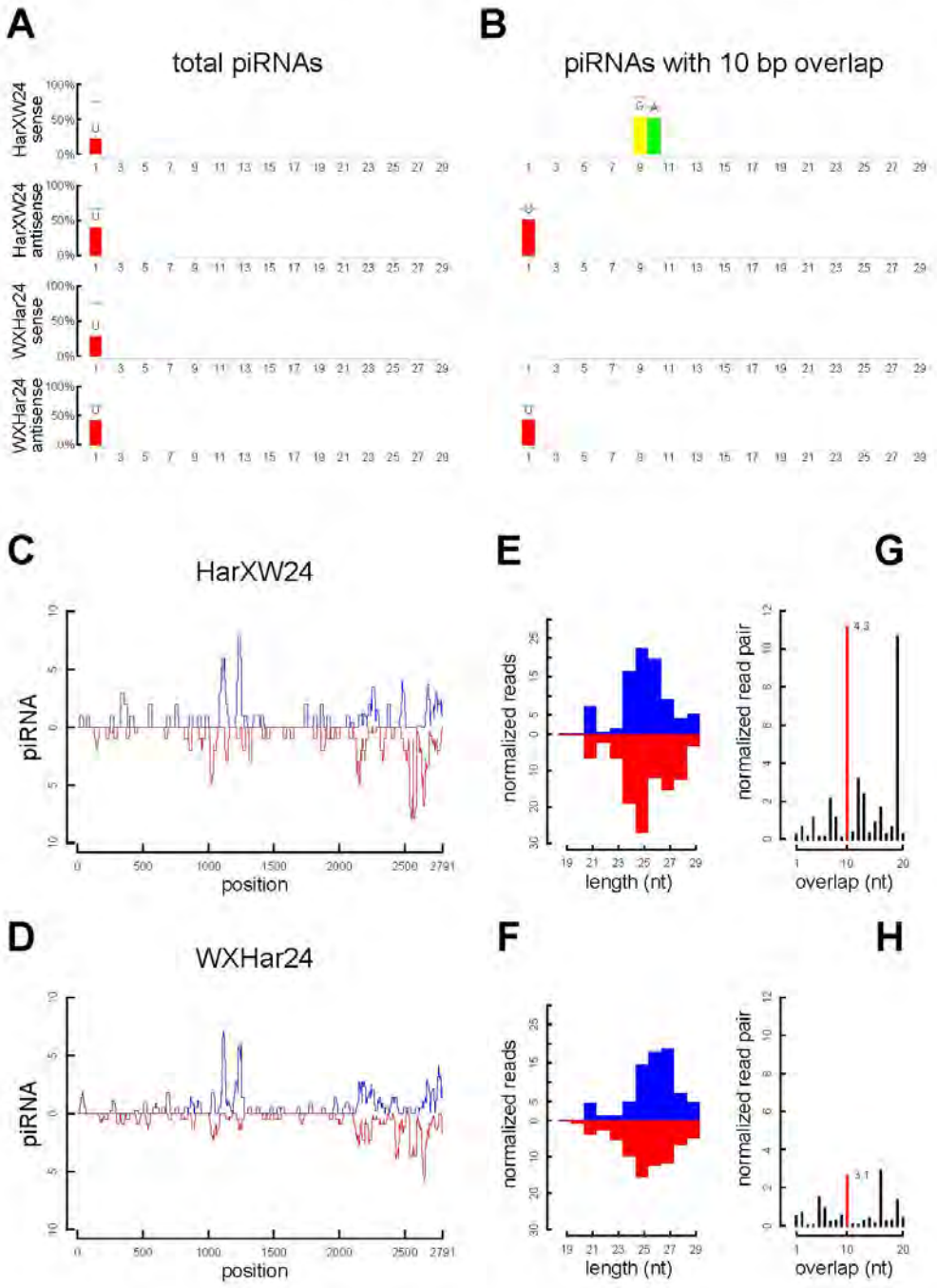

FB

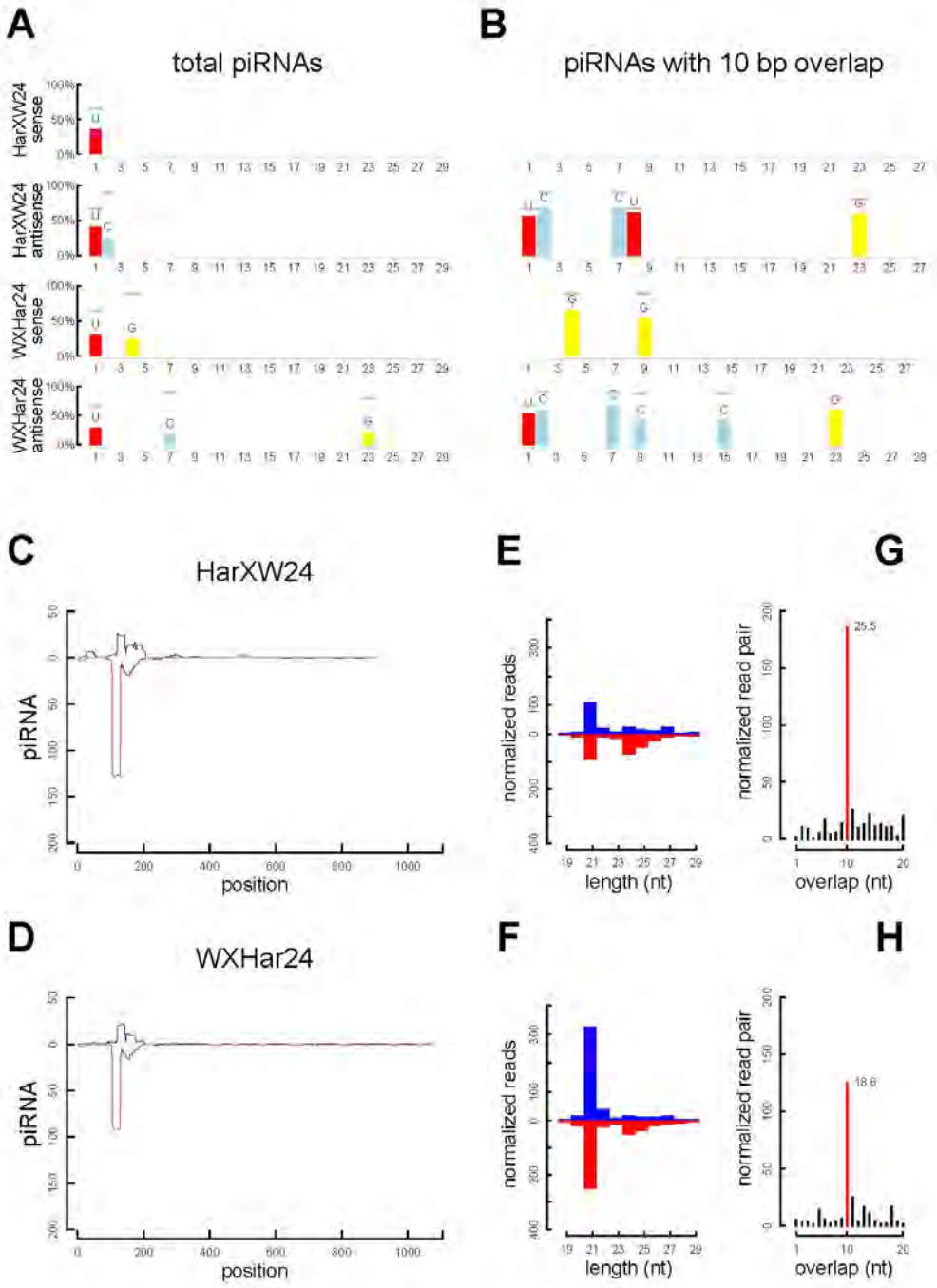
A
total piRNAs
B
piRNAs with 10 bp overlap
HarXW24 sense
HarXW24 antisense
WXHar24 sense
WXHar24 antisense
C
HarXW24
piRNA
position
D
WXHar24
piRNA
position
E
normalized reads
length (nt)
F
normalized reads
length (nt)
G
normalized read pair
25.5
overlap (nt)
H
normalized read pair
18.6
overlap (nt)

FBgn0063571

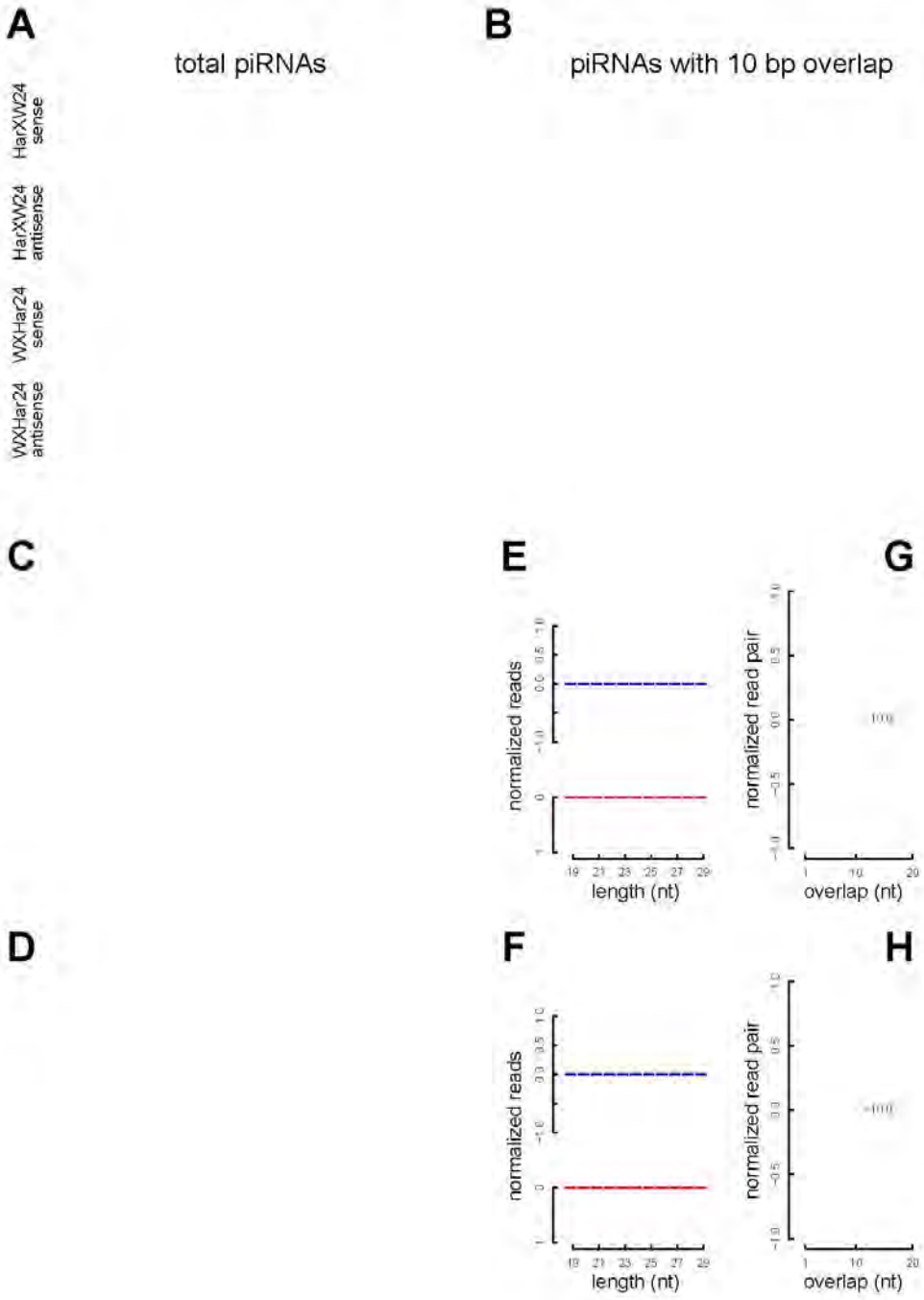

F element

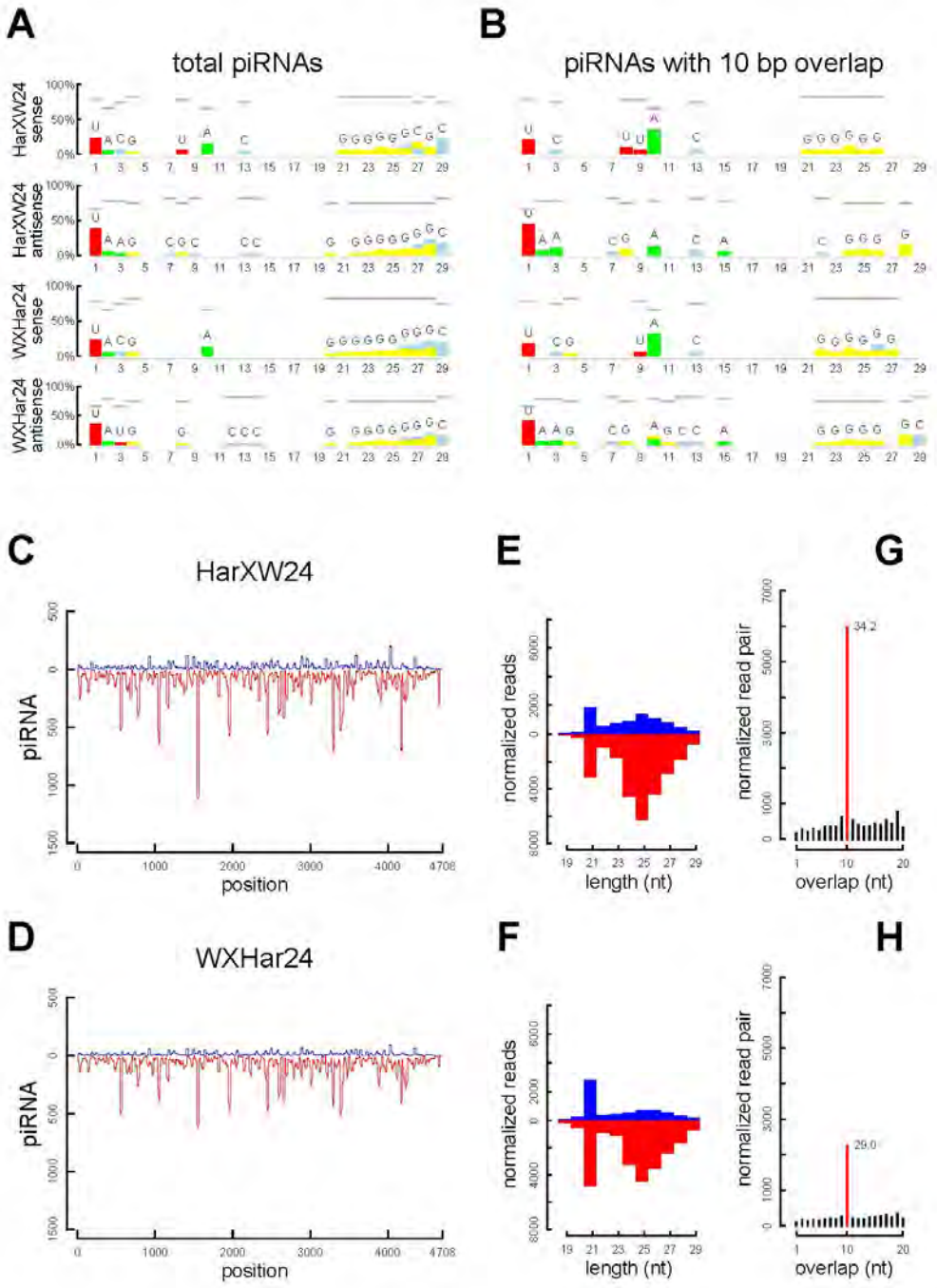
A
total piRNAs
B
piRNAs with 10 bp overlap
HarXW24 sense
HarXW24 antisense
WXHar24 sense
WXHar24 antisense
C
HarXW24
piRNA
position
D
WXHar24
piRNA
position
E
normalized reads
length (nt)
F
normalized reads
length (nt)
G
normalized read pair
34.2
overlap (nt)
H
normalized read pair
29.0
overlap (nt)

flea

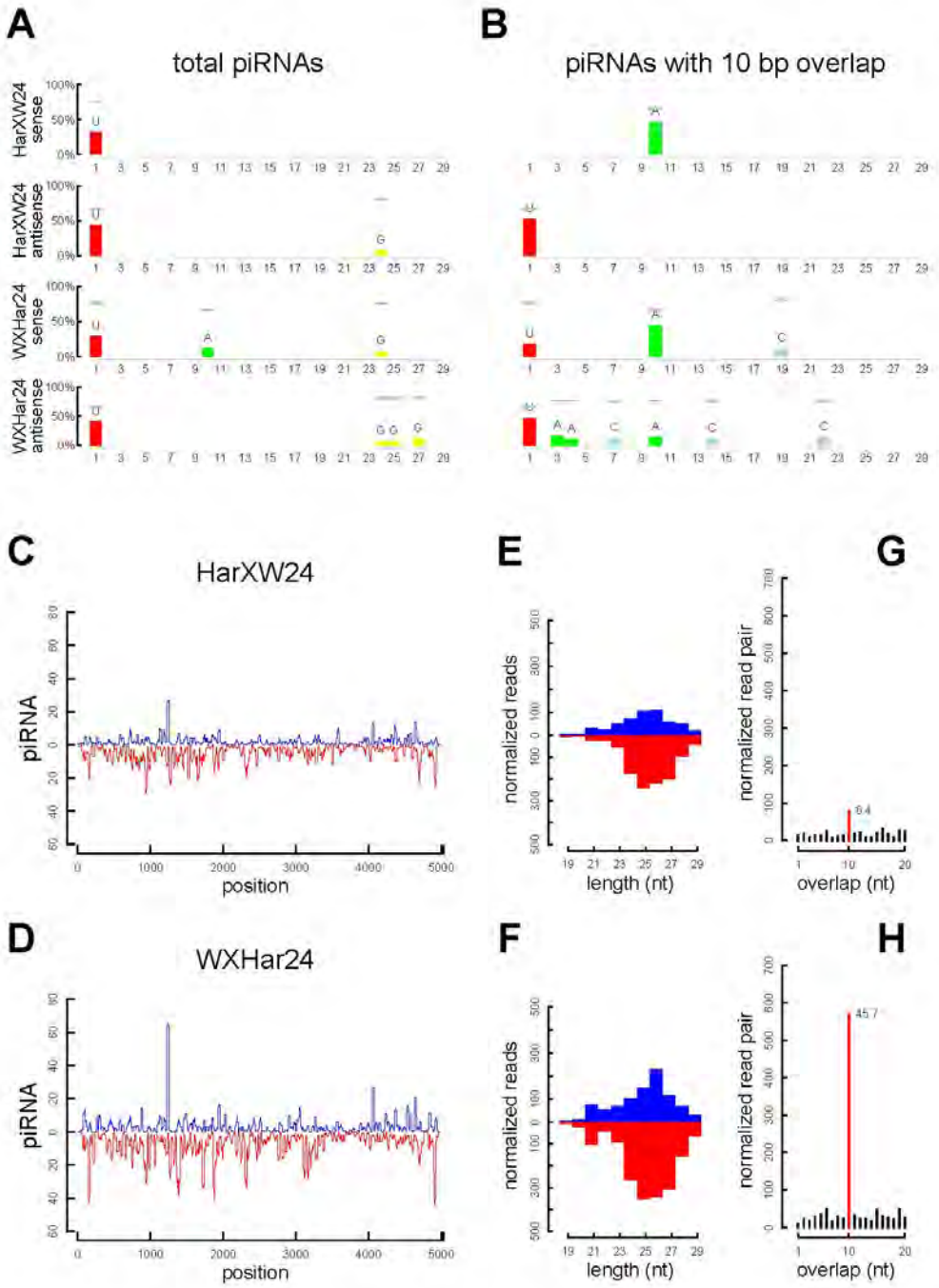
A
total piRNAs
HarXW24 sense
HarXW24 antisense
WXHar24 sense
WXHar24 antisense
B
piRNAs with 10 bp overlap
C
HarXW24
piRNA
position
D
WXHar24
piRNA
position
E
normalized reads
length (nt)
F
normalized reads
length (nt)
G
normalized read pair
6.4
overlap (nt)
H
normalized read pair
45.7
overlap (nt)

frogger

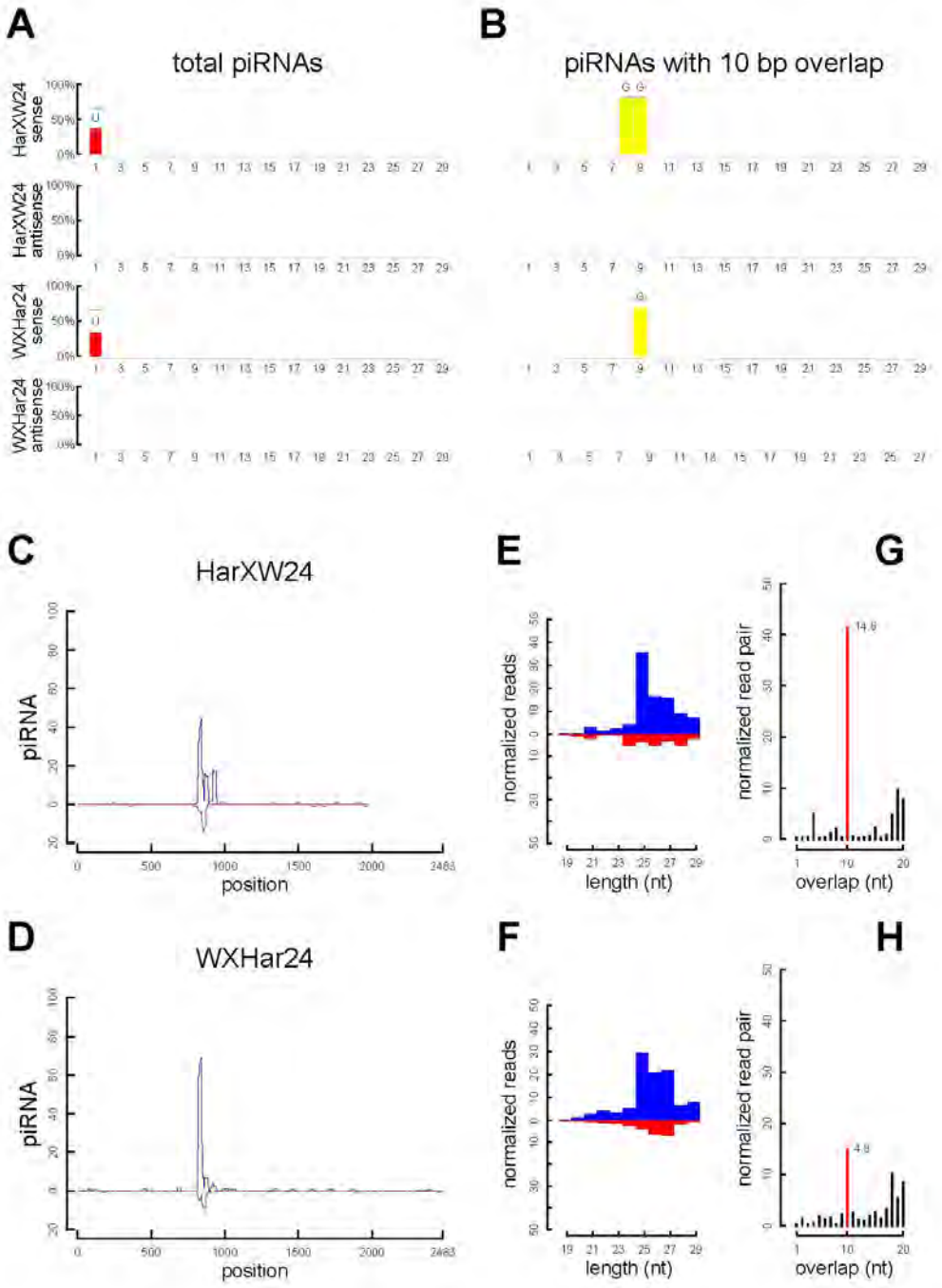
A
total piRNAs
B
piRNAs with 10 bp overlap
HarXW24 sense
HarXW24 antisense
WXHar24 sense
WXHar24 antisense
C
HarXW24
D
WXHar24
piRNA
position
E
F
normalized reads
length (nt)
G
H
normalized read pair
overlap (nt)

Fw2

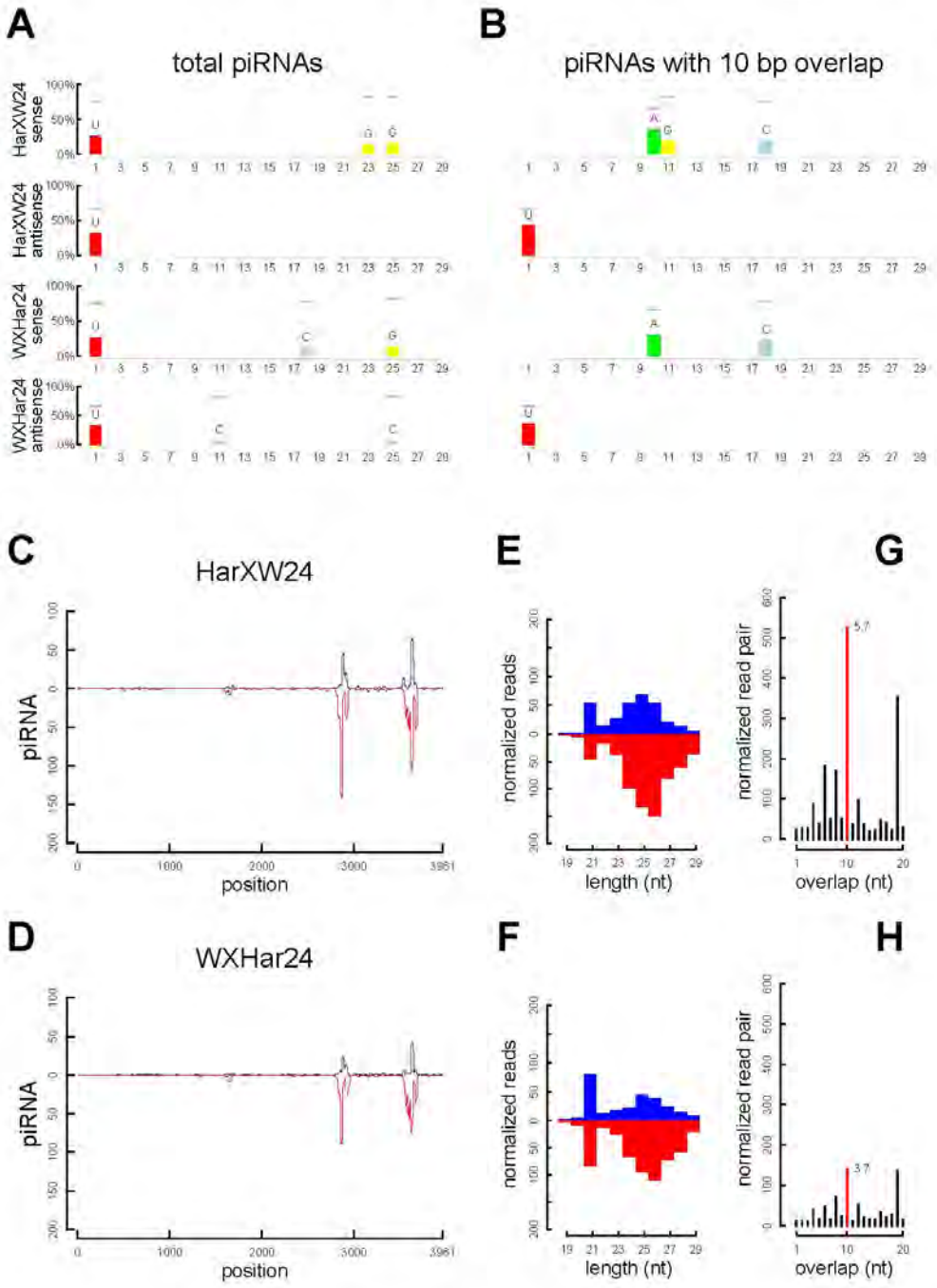
A
total piRNAs
B
piRNAs with 10 bp overlap
HarXW24 sense
HarXW24 antisense
WXHar24 sense
WXHar24 antisense
C
HarXW24
D
WXHar24
piRNA
position
E
F
normalized reads
length (nt)
G
H
normalized read pair
overlap (nt)
5.7
3.7

Fw3

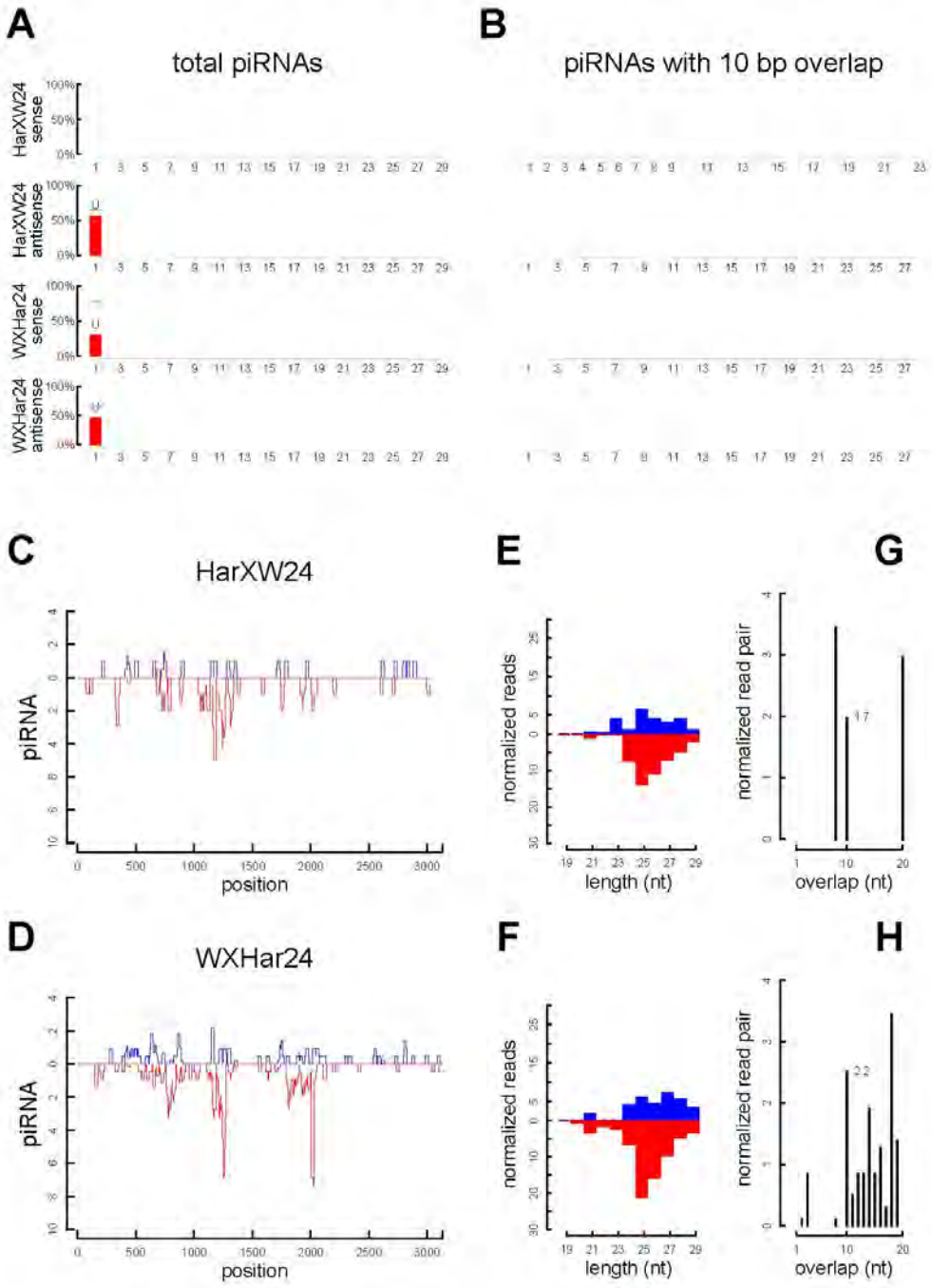
A
total piRNAs
B
piRNAs with 10 bp overlap
HarXW24 sense
HarXW24 antisense
WXHar24 sense
WXHar24 antisense
C
HarXW24
D
WXHar24
piRNA
position
E
F
normalized reads
length (nt)
G
H
normalized read pair
overlap (nt)

G2

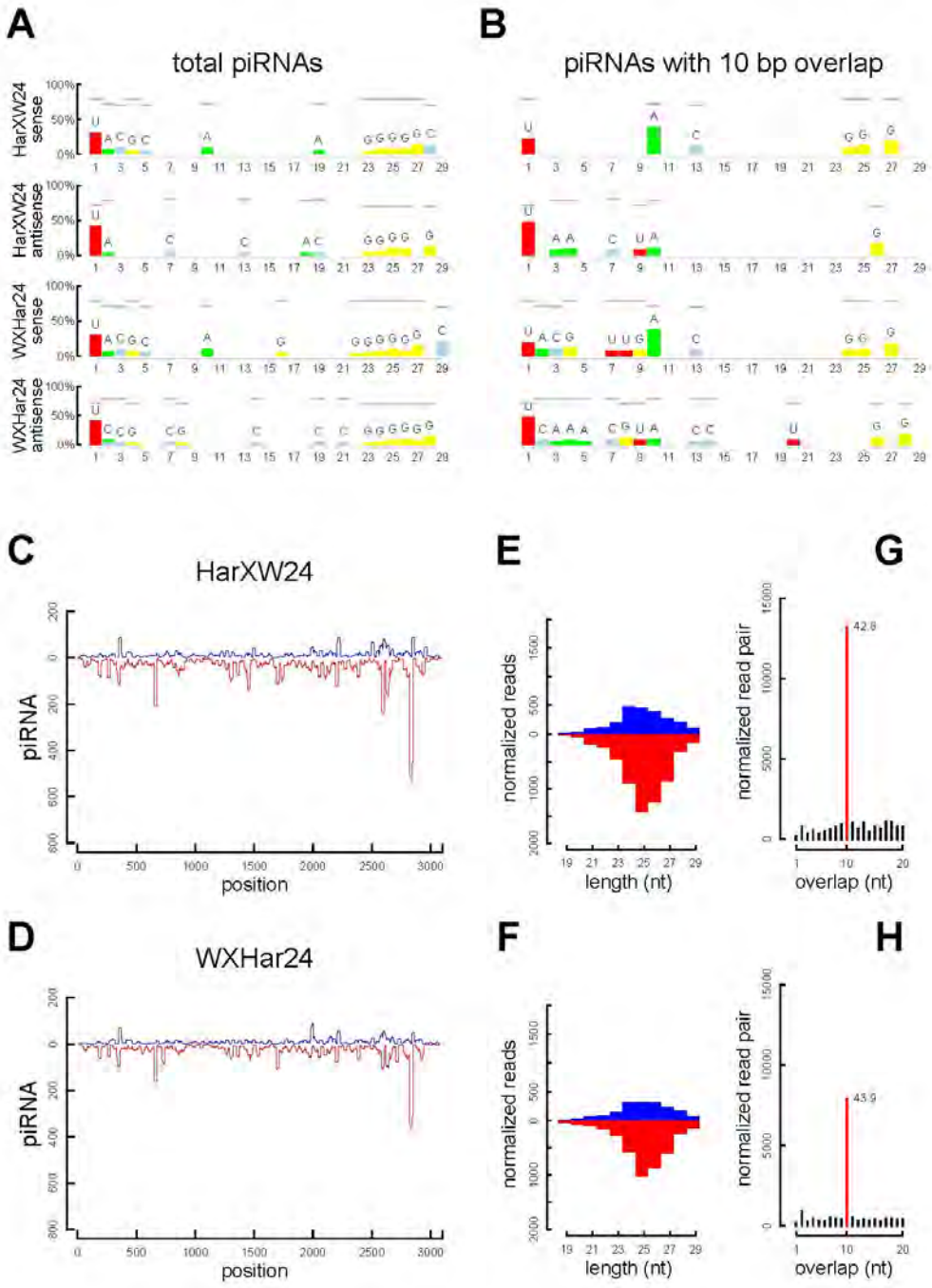
A
total piRNAs
B
piRNAs with 10 bp overlap
HarXW24 sense
HarXW24 antisense
WXHar24 sense
WXHar24 antisense
C
HarXW24
piRNA
position
D
WXHar24
piRNA
position
E
normalized reads
length (nt)
F
normalized reads
length (nt)
G
normalized read pair
42.8
overlap (nt)
H
normalized read pair
43.9
overlap (nt)

G3

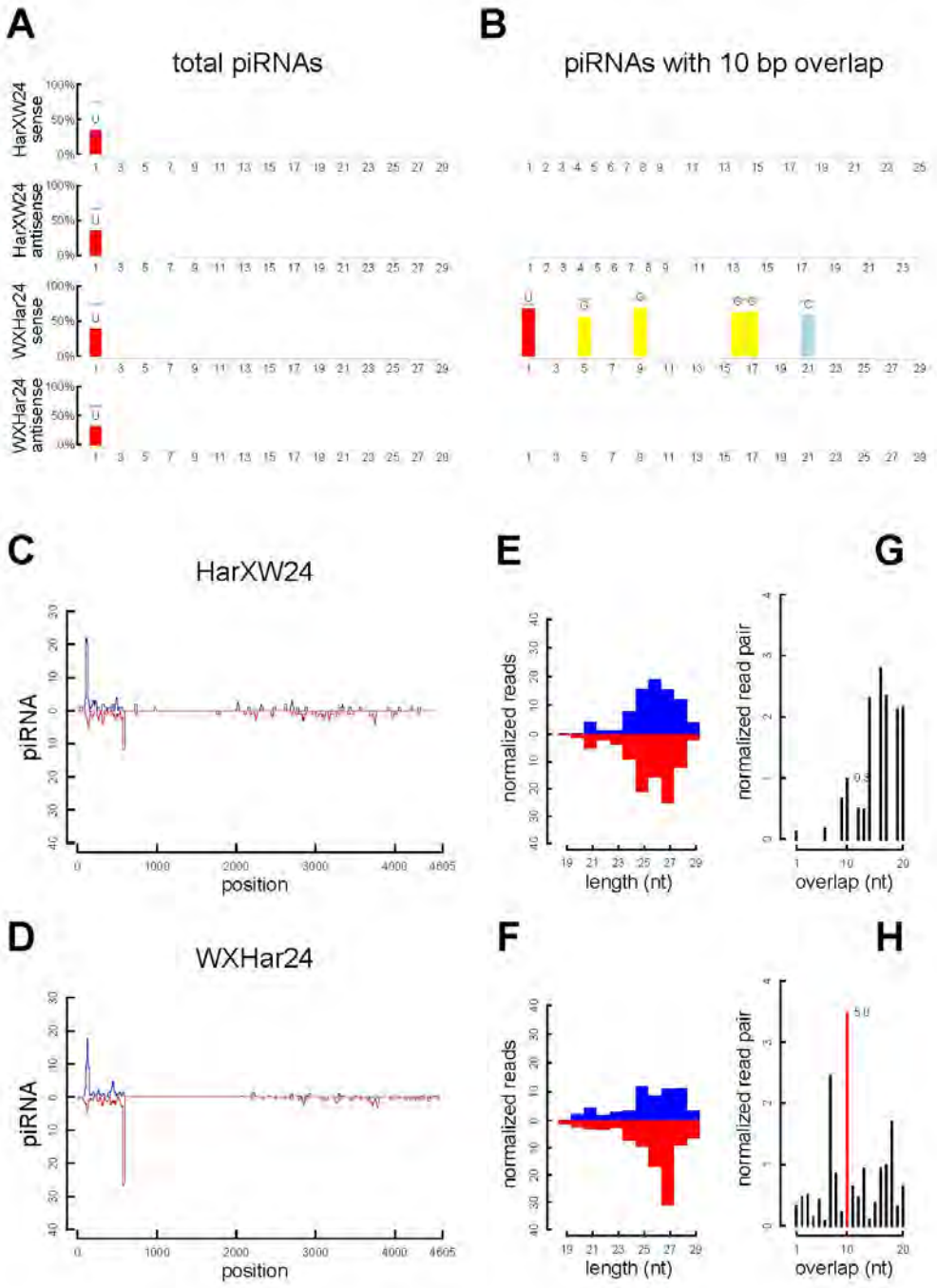
A
total piRNAs
B
piRNAs with 10 bp overlap
HarXW24 sense
HarXW24 antisense
WXHar24 sense
WXHar24 antisense
C
HarXW24
D
WXHar24
piRNA
position
E
F
normalized reads
length (nt)
G
H
normalized read pair
overlap (nt)

G4

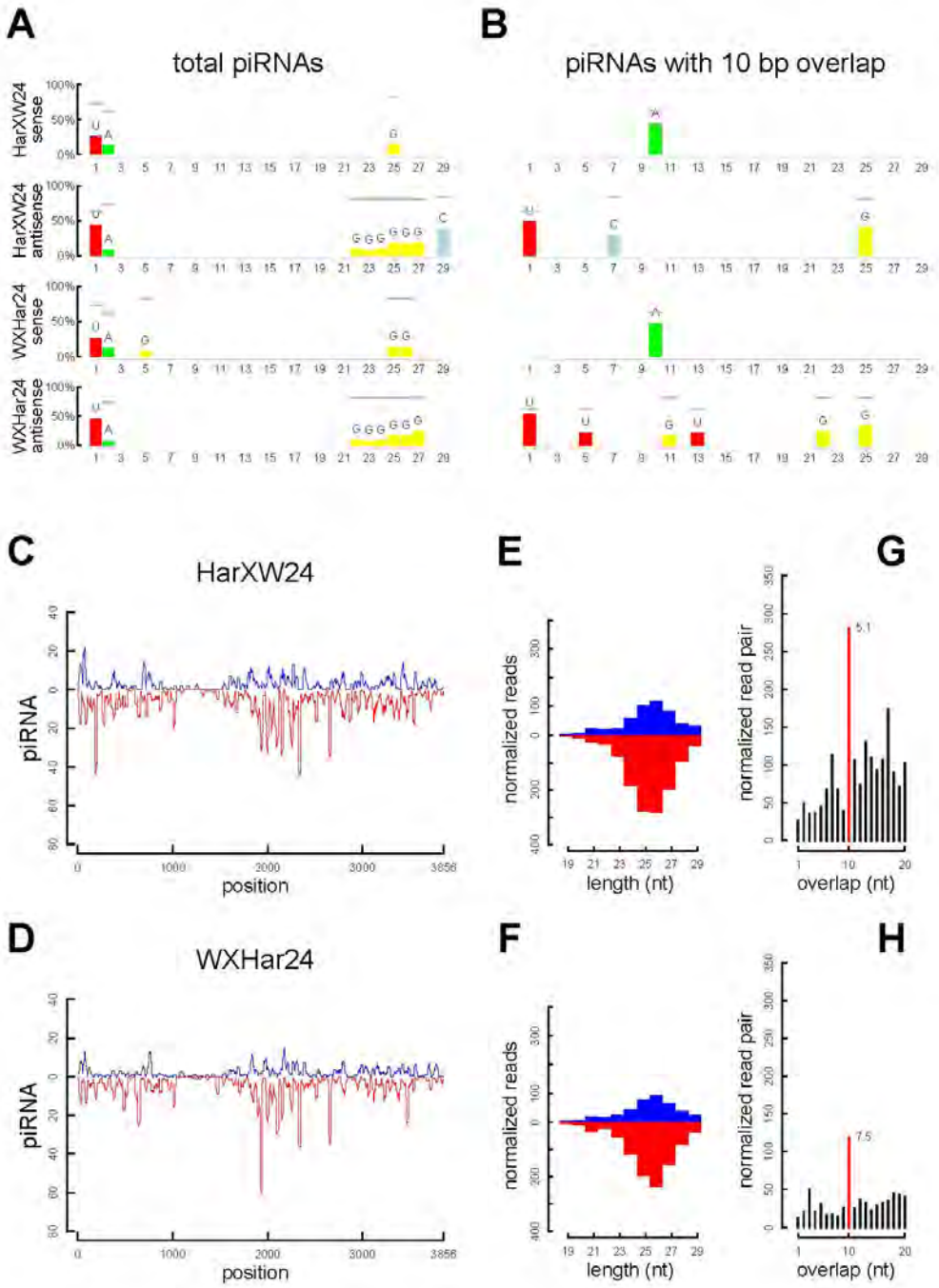
A
total piRNAs
B
piRNAs with 10 bp overlap
HarXW24 sense
HarXW24 antisense
WXHar24 sense
WXHar24 antisense
C
HarXW24
D
WXHar24
piRNA
position
E
F
normalized reads
length (nt)
G
H
normalized read pair
overlap (nt)
5.1
7.5

G5

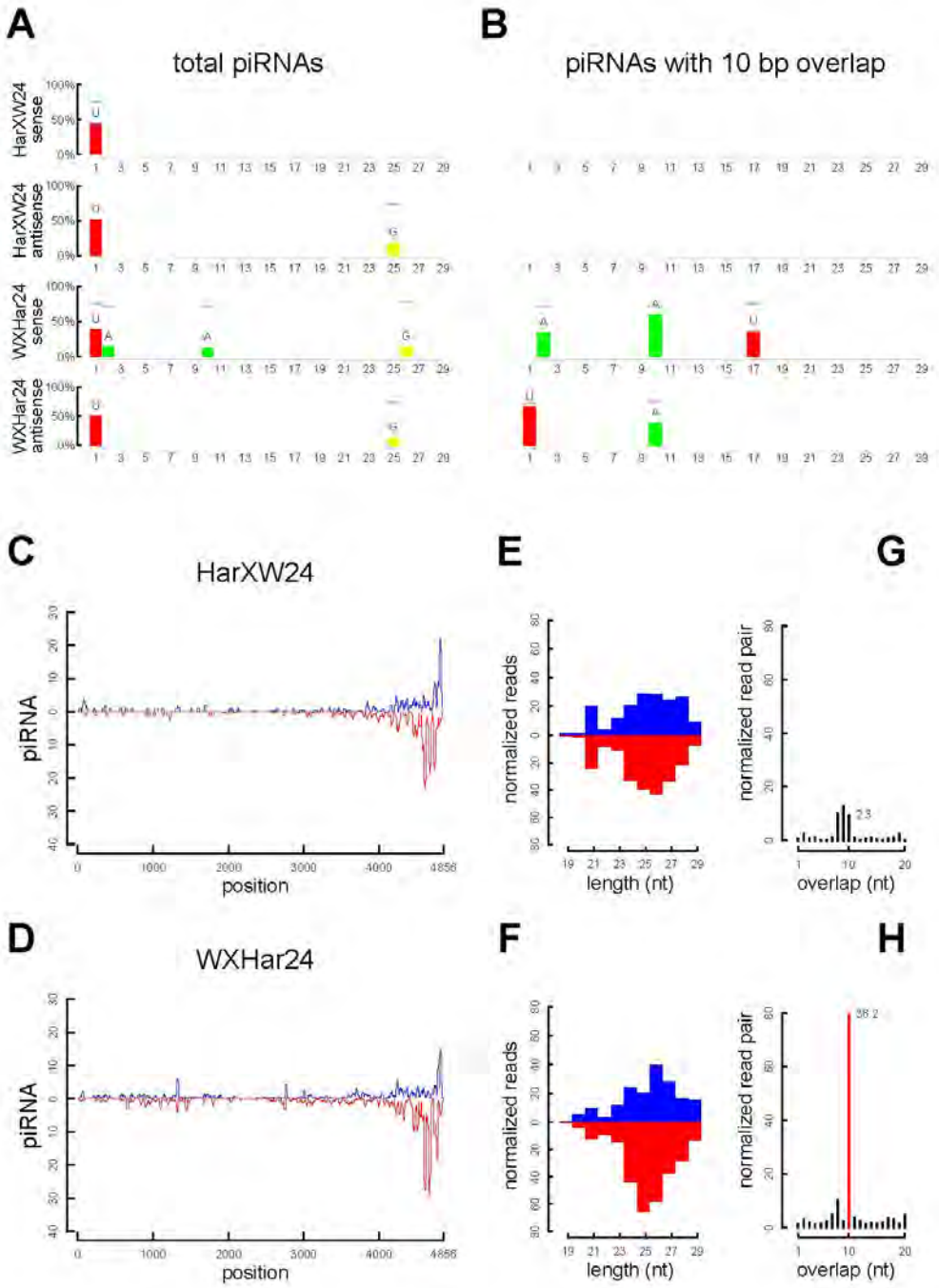
A
total piRNAs
B
piRNAs with 10 bp overlap
HarXW24 sense
HarXW24 antisense
WXHar24 sense
WXHar24 antisense
C
HarXW24
D
WXHar24
piRNA
position
E
F
normalized reads
length (nt)
G
H
normalized read pair
overlap (nt)

G5A

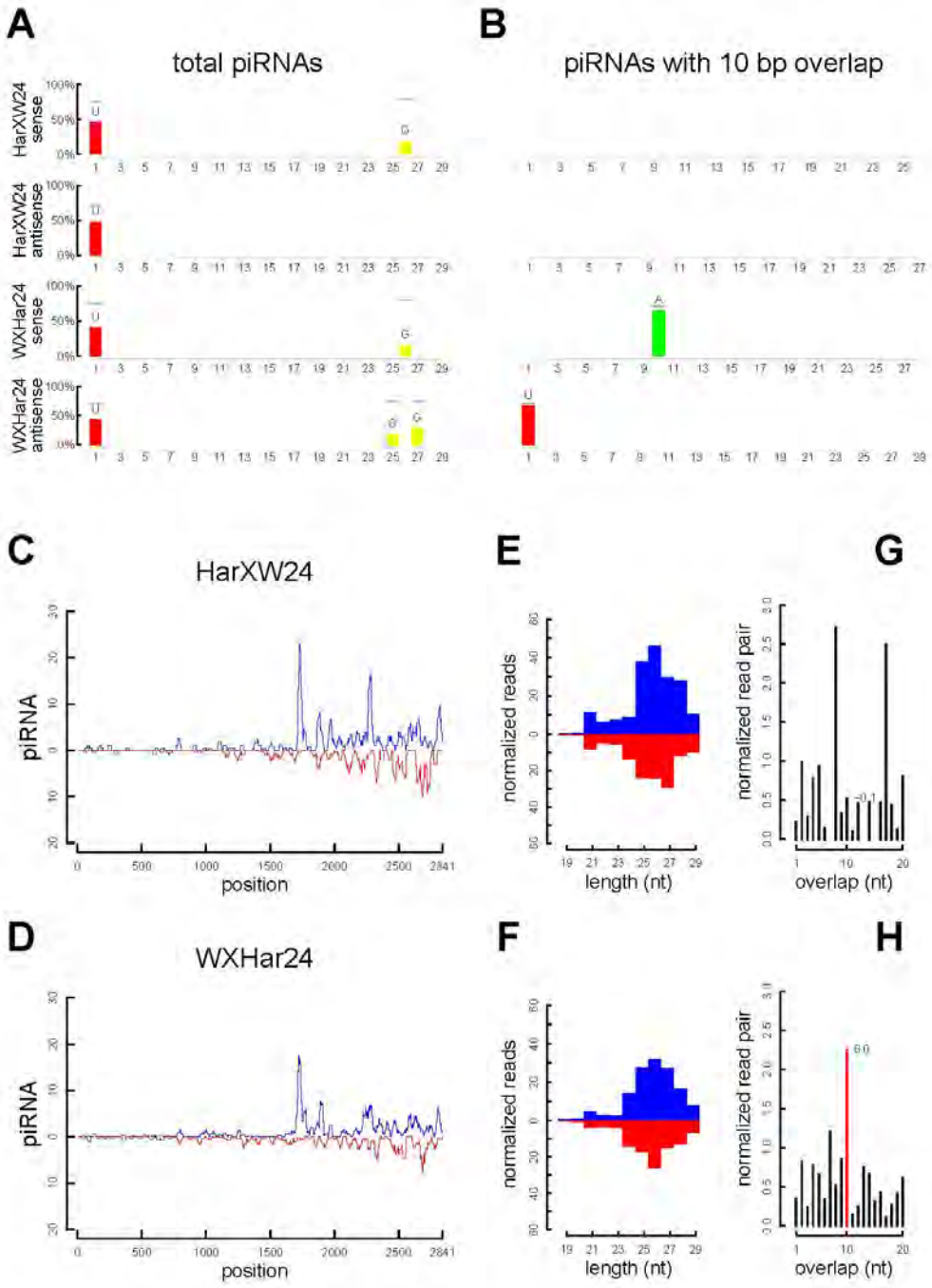
A
total piRNAs
HarXW24 sense
HarXW24 antisense
WXHar24 sense
WXHar24 antisense
B
piRNAs with 10 bp overlap
C
HarXW24
piRNA
position
D
WXHar24
piRNA
position
E
normalized reads
length (nt)
F
normalized reads
length (nt)
G
normalized read pair
overlap (nt)
H
normalized read pair
overlap (nt)

G6

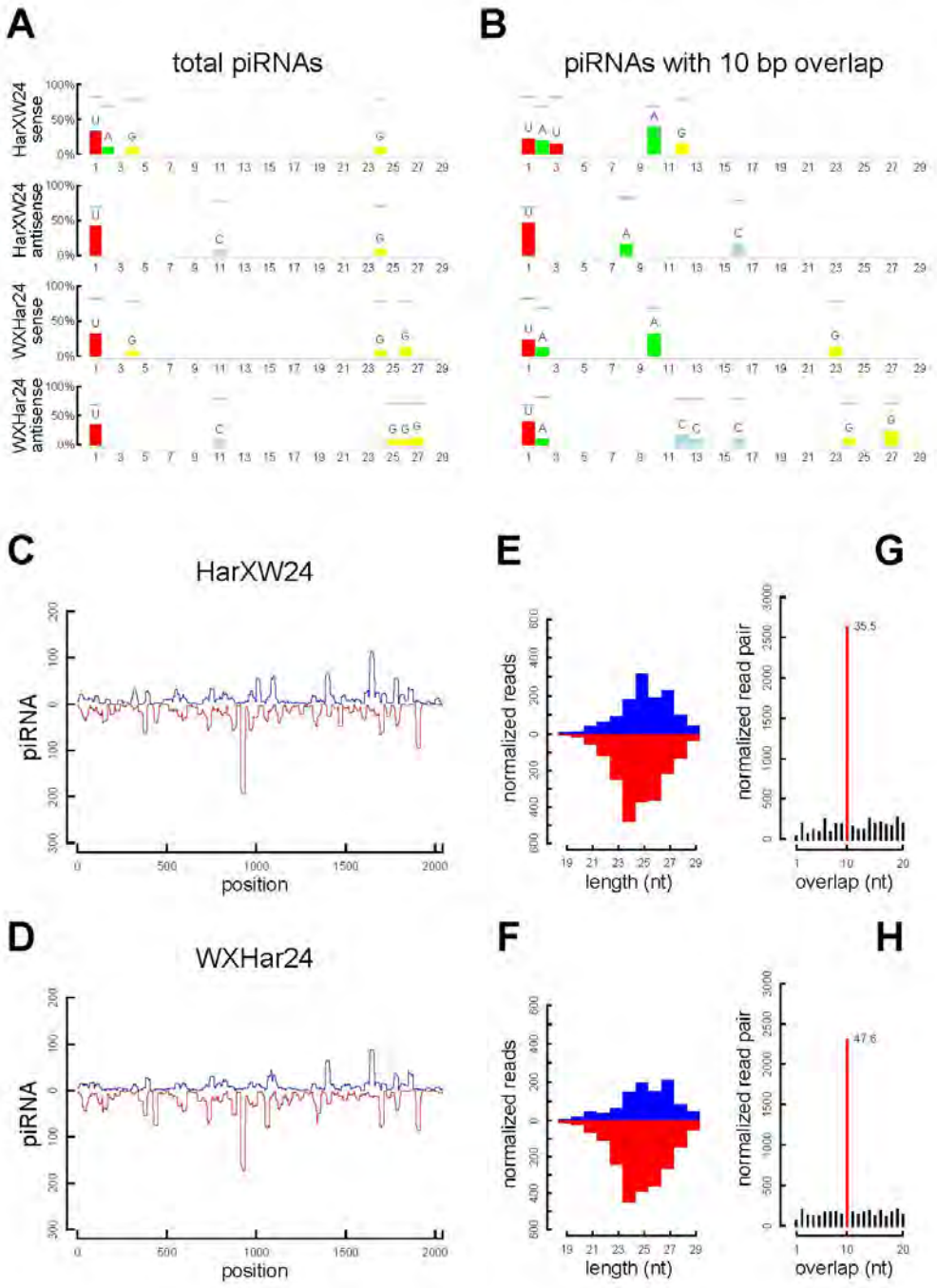
A
total piRNAs
B
piRNAs with 10 bp overlap
HarXW24 sense
HarXW24 antisense
WXHar24 sense
WXHar24 antisense
C
HarXW24
D
WXHar24
piRNA
position
E
F
normalized reads
length (nt)
G
H
normalized read pair
overlap (nt)
35.5
47.6

G7

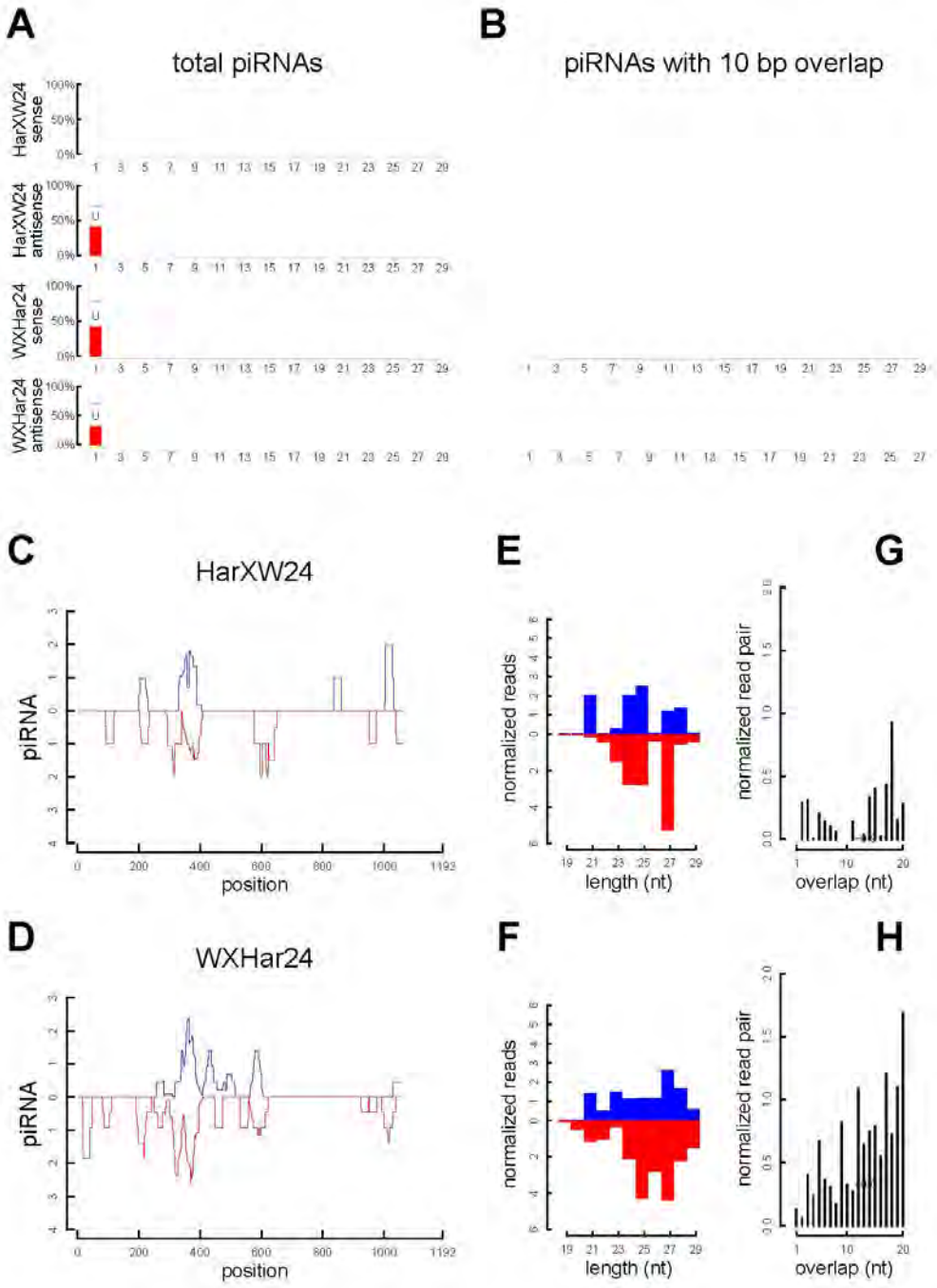
A
total piRNAs
B
piRNAs with 10 bp overlap
HarXW24 sense
HarXW24 antisense
WXHar24 sense
WXHar24 antisense
C
HarXW24
D
WXHar24
piRNA
position
E
F
normalized reads
length (nt)
G
H
normalized read pair
overlap (nt)

GATE

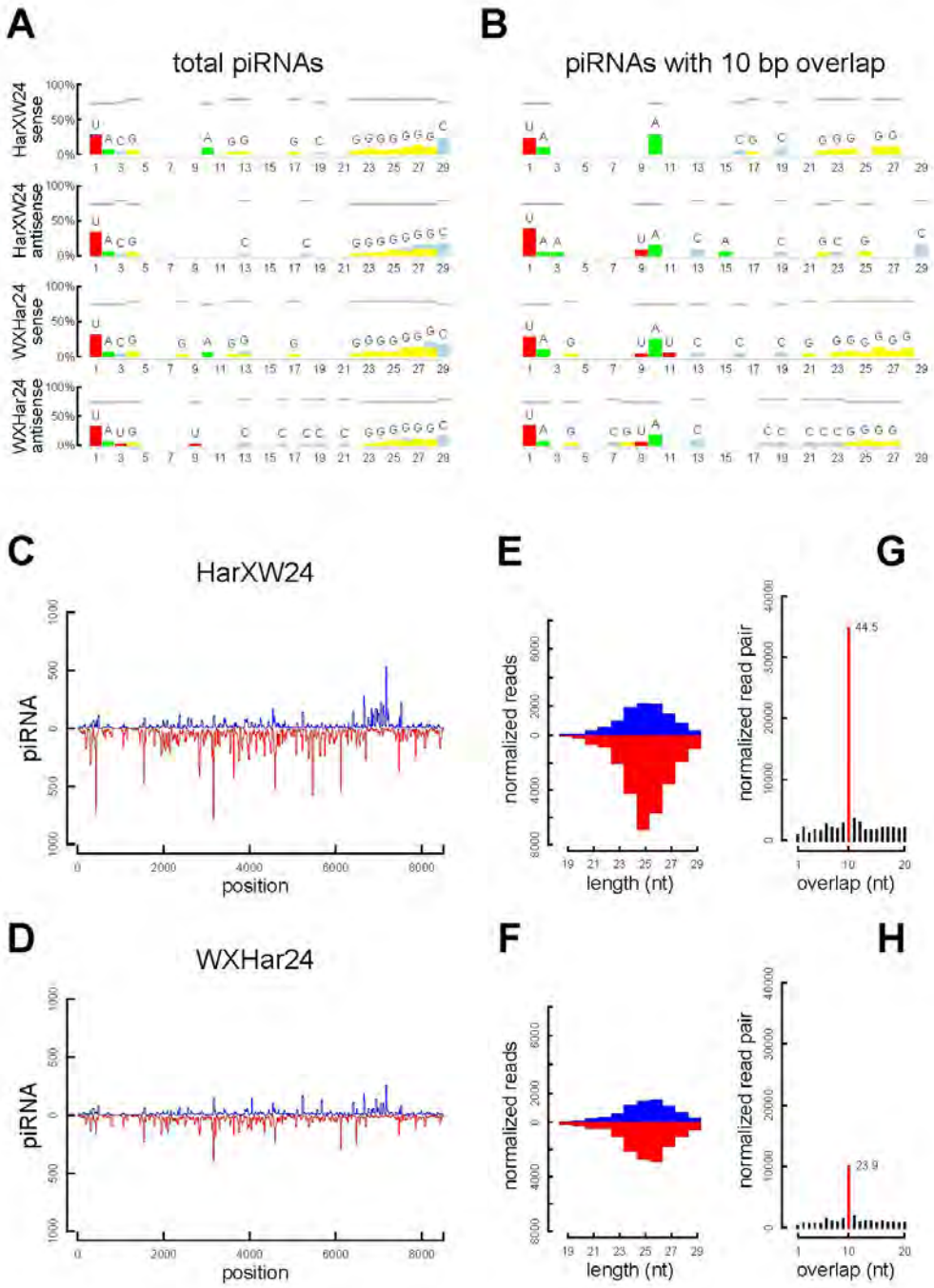
A
total piRNAs
HarXW24 sense
HarXW24 antisense
WXHar24 sense
WXHar24 antisense
B
piRNAs with 10 bp overlap
C
HarXW24
piRNA
position
D
WXHar24
piRNA
position
E
normalized reads
length (nt)
F
normalized reads
length (nt)
G
normalized read pair
44.5
overlap (nt)
H
normalized read pair
23.9
overlap (nt)

G element

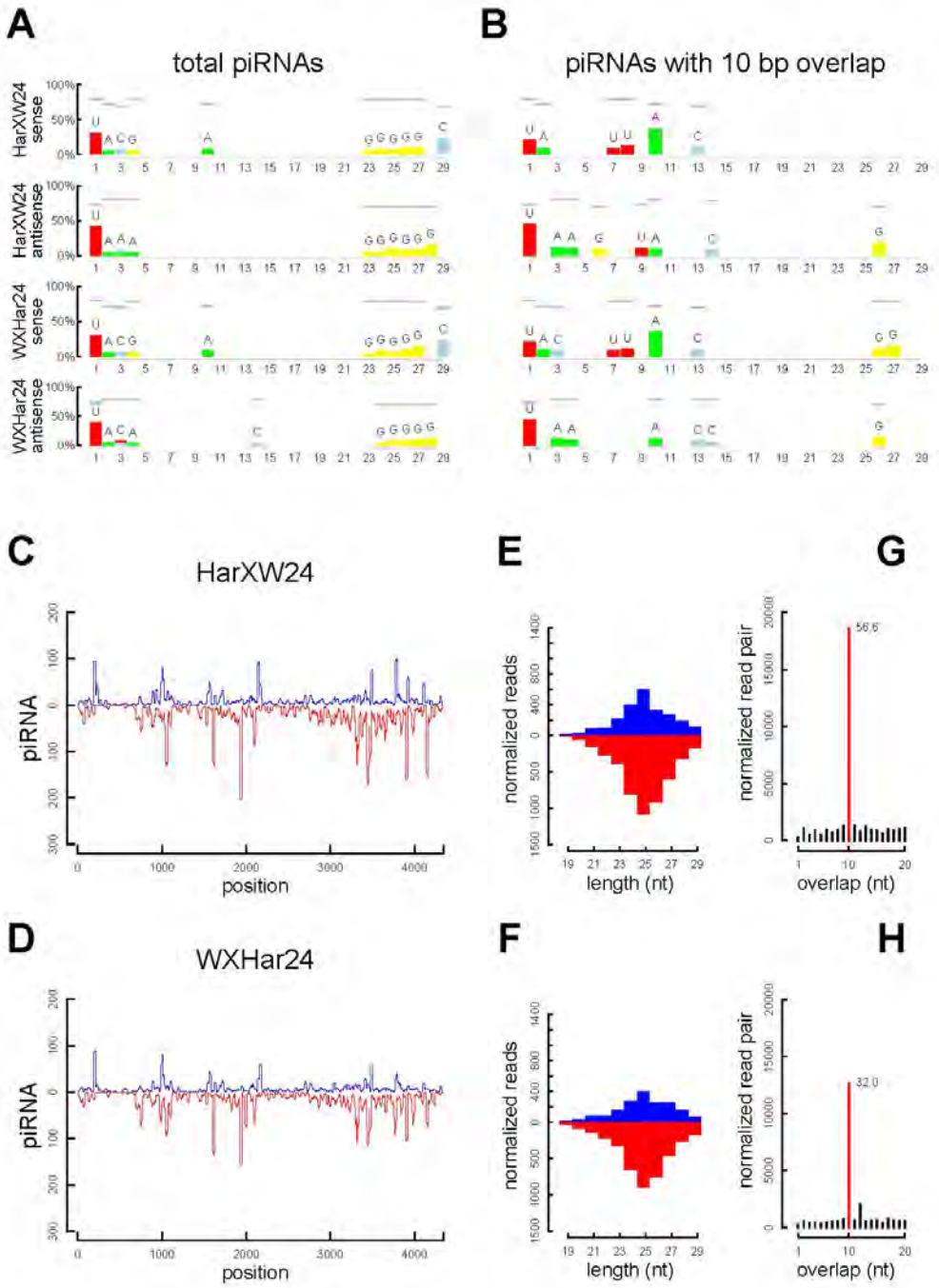
A
total piRNAs
B
piRNAs with 10 bp overlap
HarXW24 sense
HarXW24 antisense
WXHar24 sense
WXHar24 antisense
C
HarXW24
D
WXHar24
piRNA
position
E
F
normalized reads
length (nt)
G
H
normalized read pair
overlap (nt)
56.6
32.0

gtwin

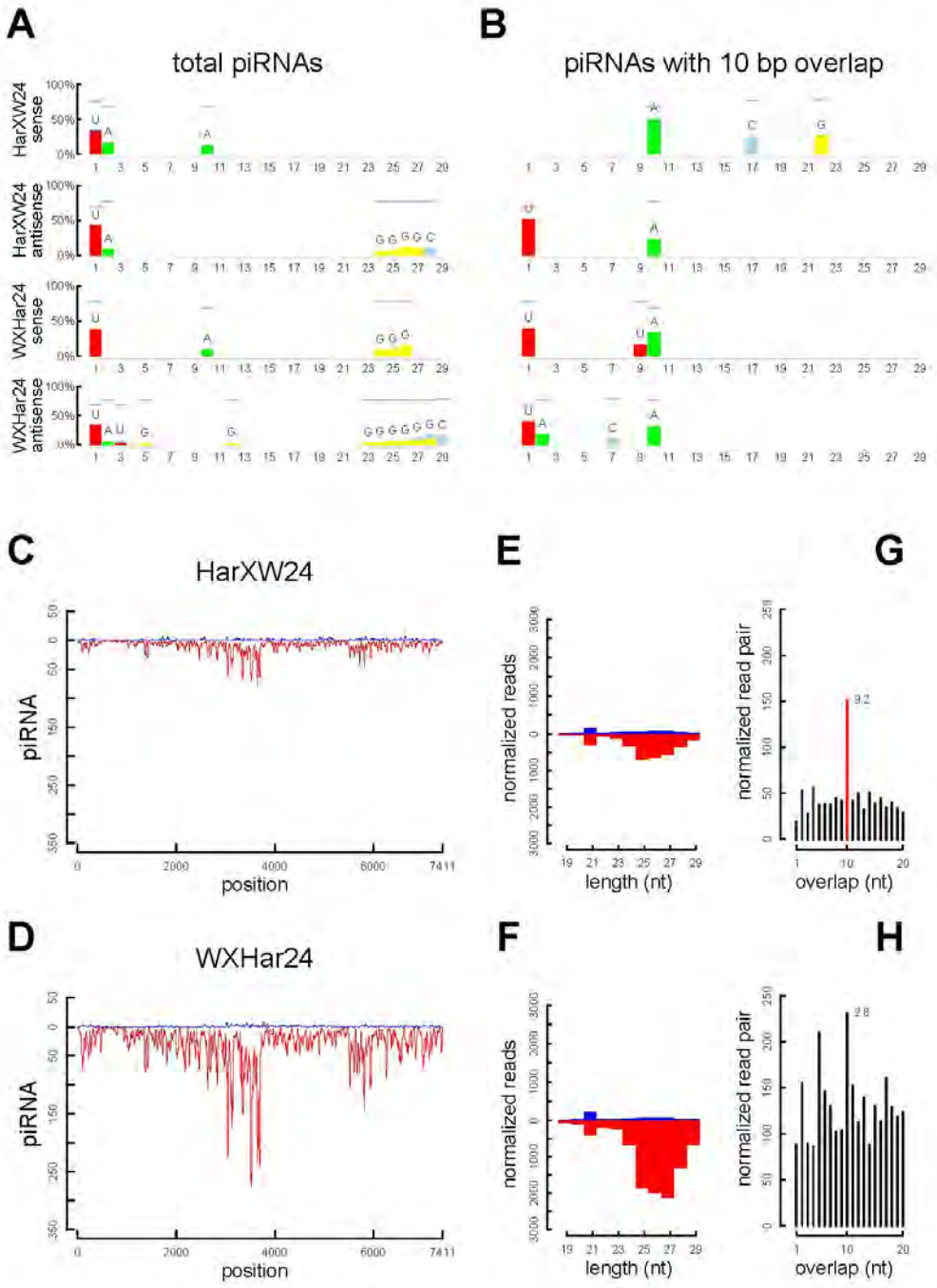
A
total piRNAs
B
piRNAs with 10 bp overlap
HarXW24 sense
HarXW24 antisense
WXHar24 sense
WXHar24 antisense
C
HarXW24
D
WXHar24
piRNA
position
E
F
normalized reads
length (nt)
G
H
normalized read pair
overlap (nt)

gypsy

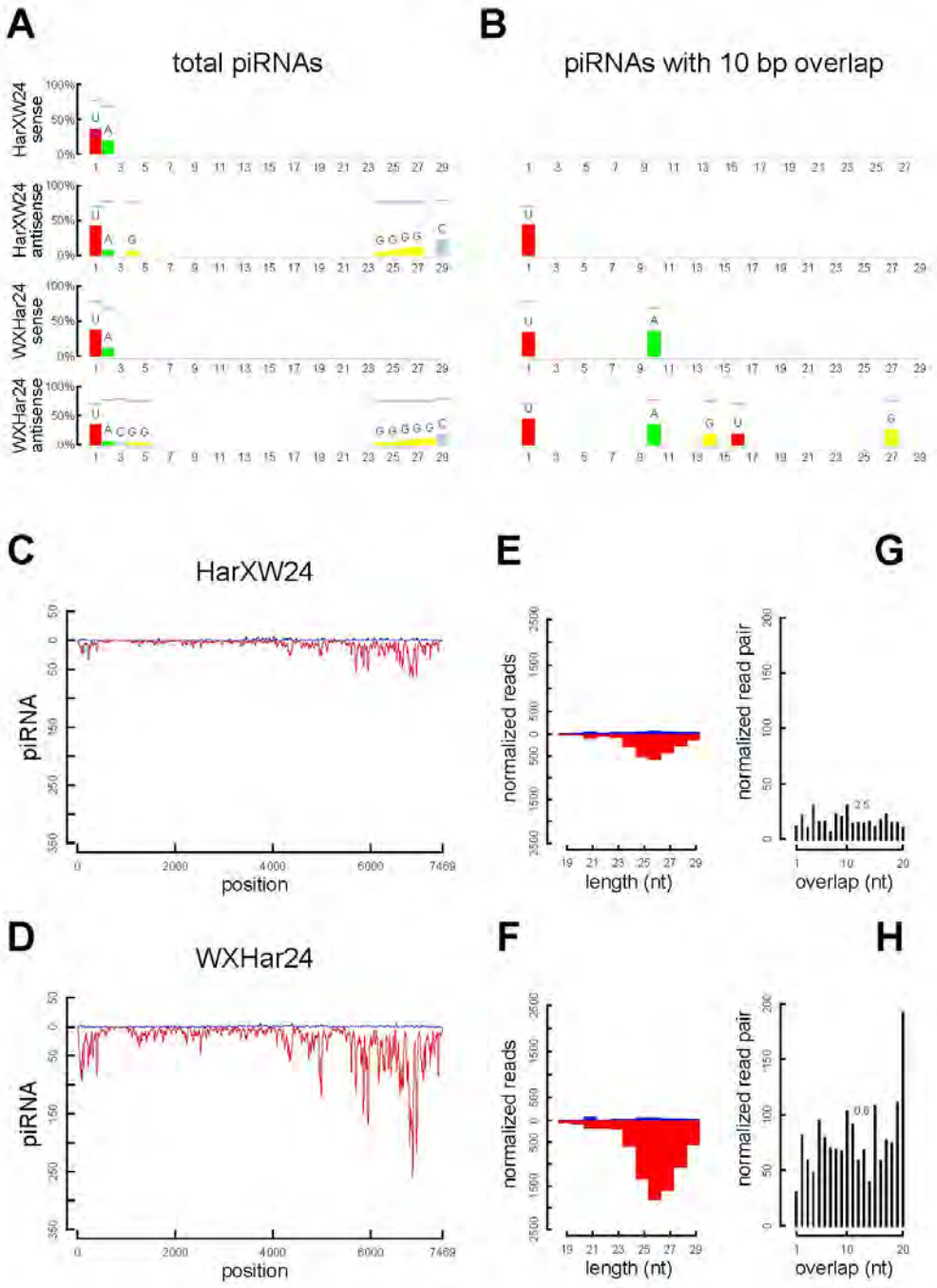
A
total piRNAs
B
piRNAs with 10 bp overlap
HarXW24 sense
HarXW24 antisense
WXHar24 sense
WXHar24 antisense
C
HarXW24
D
WXHar24
piRNA
position
E
F
normalized reads
length (nt)
G
H
normalized read pair
overlap (nt)

gypsy10

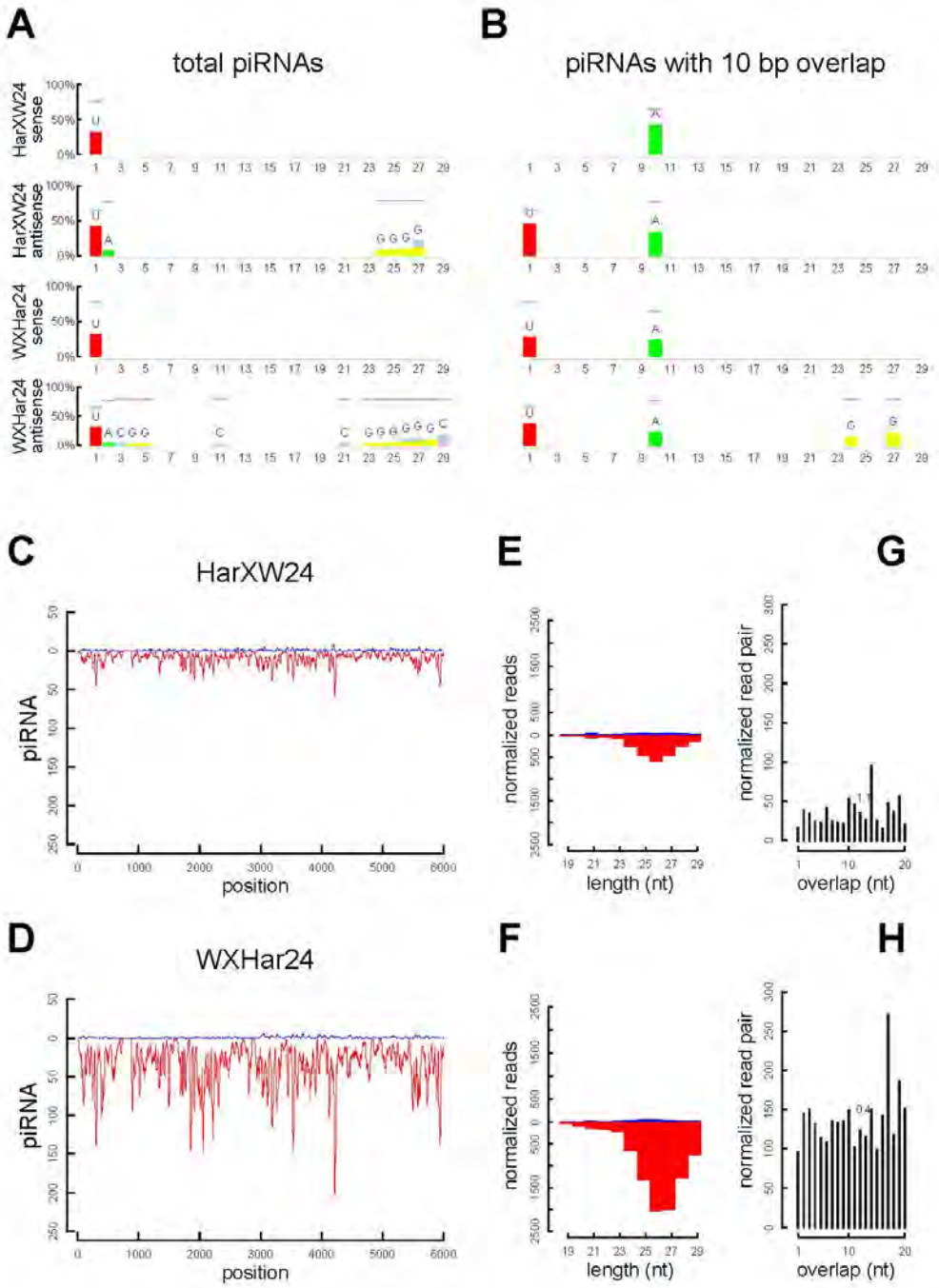
A
total piRNAs
B
piRNAs with 10 bp overlap
HarXW24 sense
HarXW24 antisense
WXHar24 sense
WXHar24 antisense
C
HarXW24
D
WXHar24
piRNA
position
E
F
normalized reads
length (nt)
G
H
normalized read pair
overlap (nt)

gypsy11

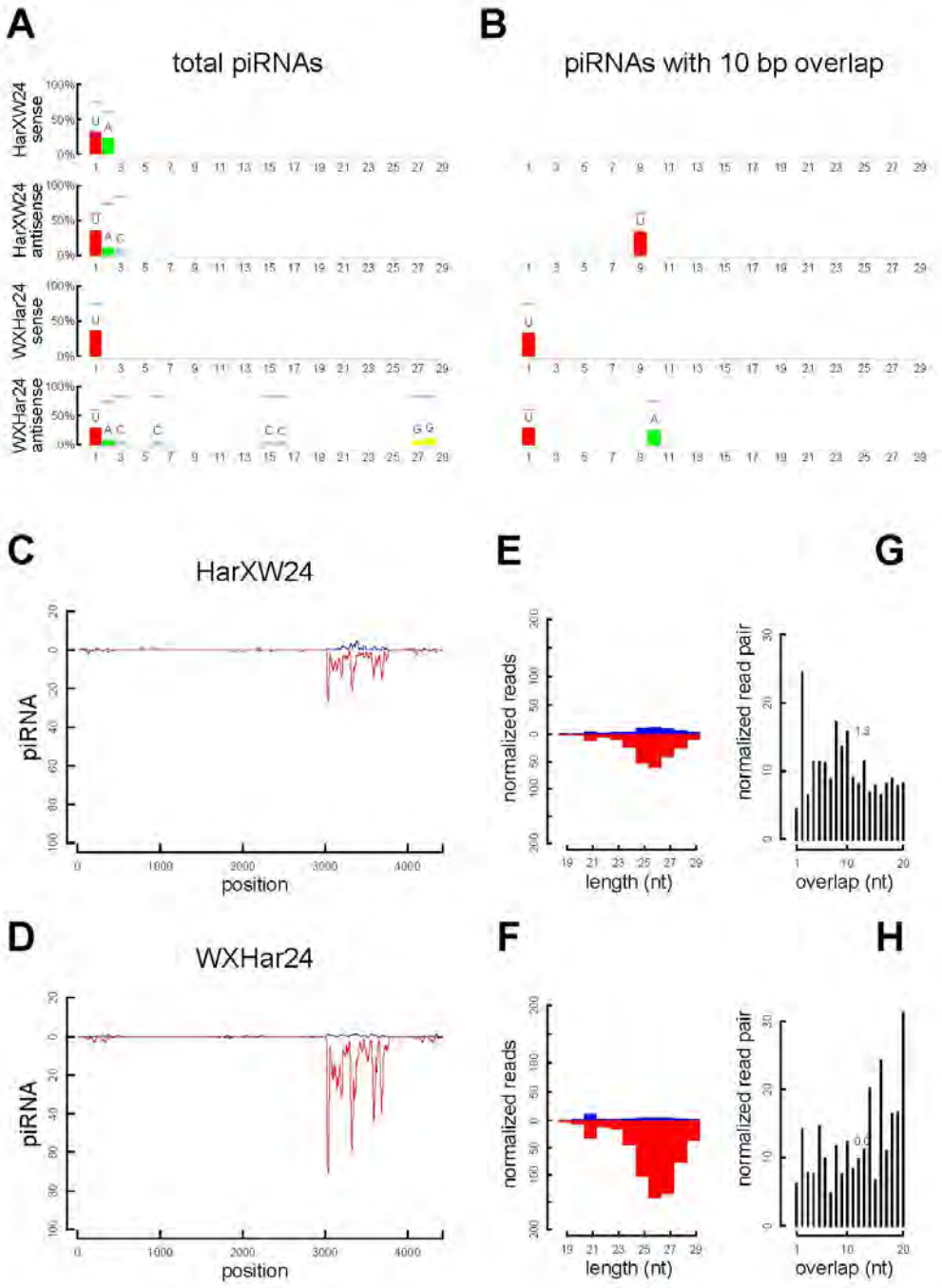
A
total piRNAs
B
piRNAs with 10 bp overlap
HarXW24 sense
HarXW24 antisense
WXHar24 sense
WXHar24 antisense
C
HarXW24
D
WXHar24
piRNA
position
E
F
normalized reads
length (nt)
G
H
normalized read pair
overlap (nt)

gypsy12

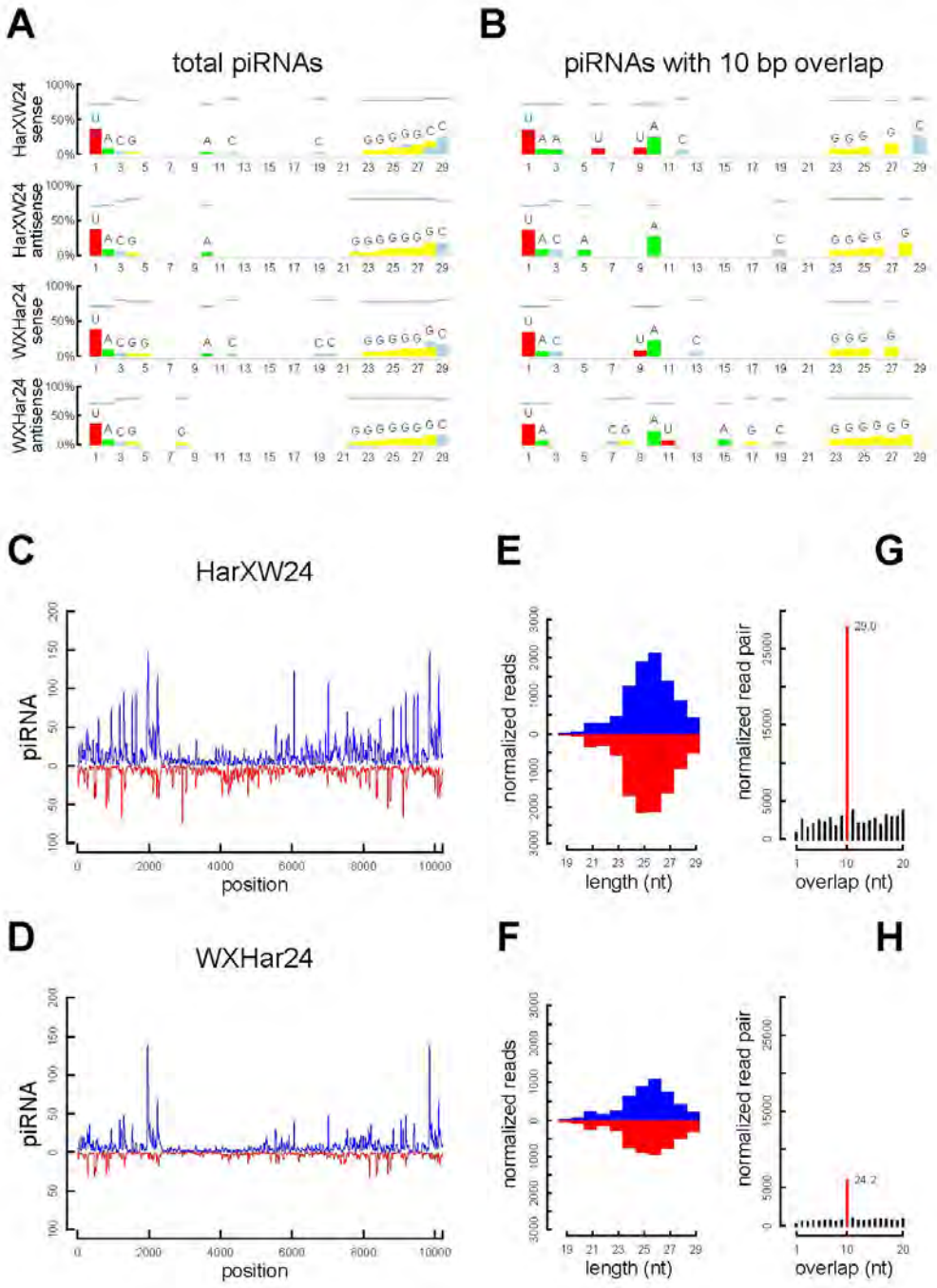
A
total piRNAs
B
piRNAs with 10 bp overlap
HarXW24 sense
HarXW24 antisense
WXHar24 sense
WXHar24 antisense
C
HarXW24
D
WXHar24
piRNA
position
E
F
normalized reads
length (nt)
G
H
normalized read pair
overlap (nt)
29.0
24.2

gypsy12#2

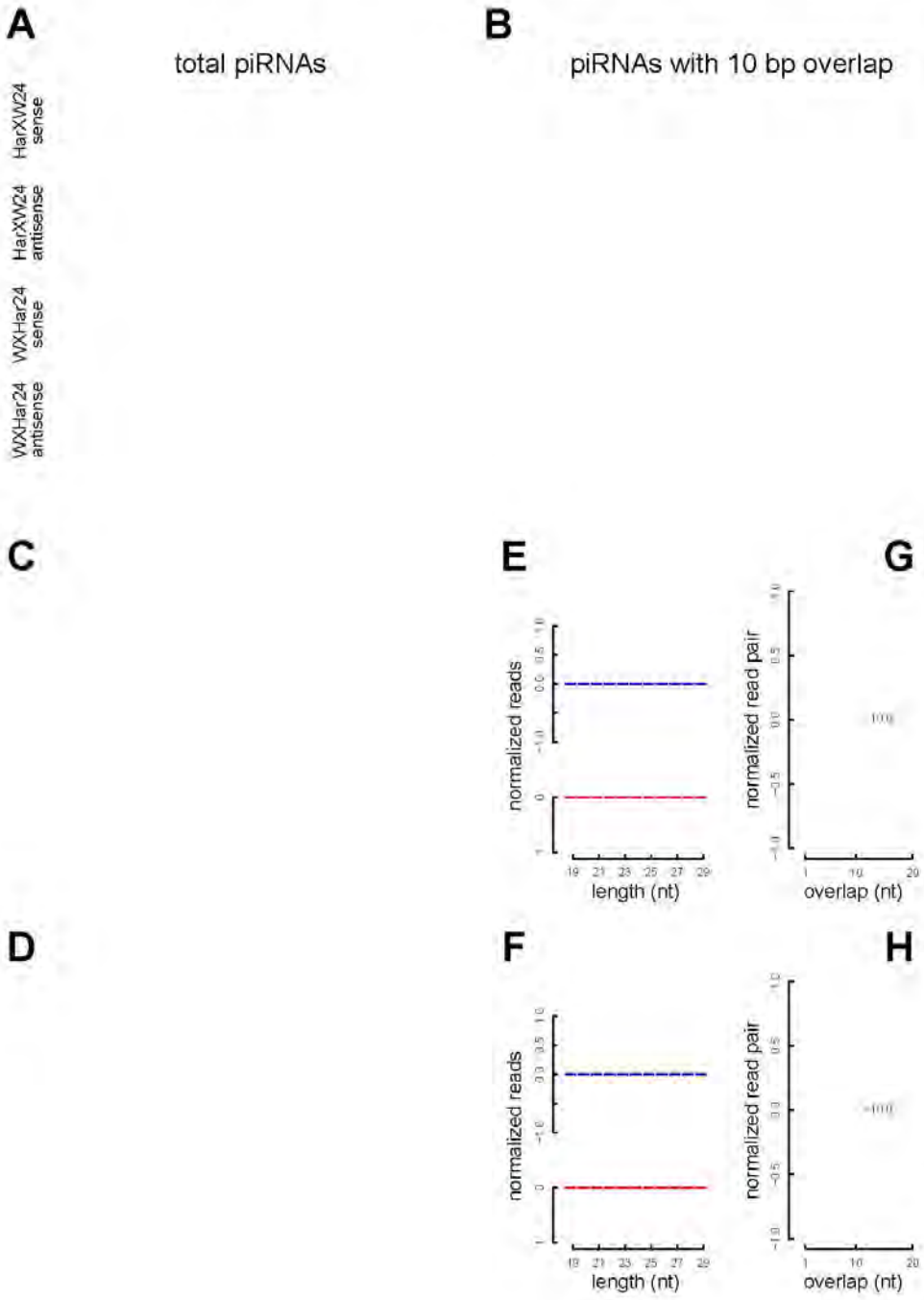
A
total piRNAs
B
piRNAs with 10 bp overlap
HarXW24 sense
HarXW24 antisense
WXHar24 sense
WXHar24 antisense
C
D
E
F
G
H
normalized reads
length (nt)
normalized read pair
overlap (nt)

gypsy2

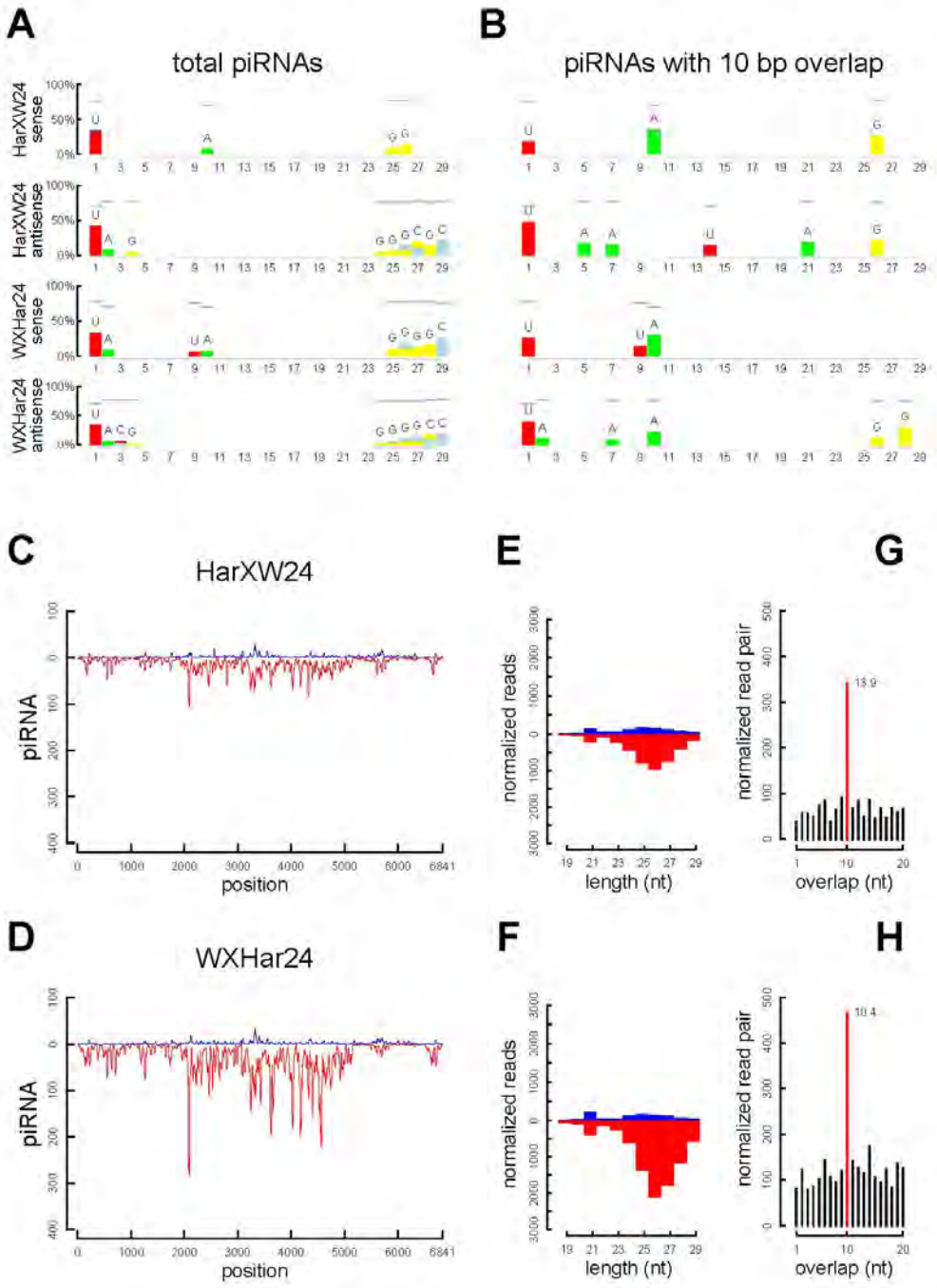
A
total piRNAs
B
piRNAs with 10 bp overlap
HarXW24 sense
HarXW24 antisense
WXHar24 sense
WXHar24 antisense
C
HarXW24
D
WXHar24
piRNA
position
E
F
normalized reads
length (nt)
G
H
normalized read pair
overlap (nt)
13.9
10.4

gypsy3

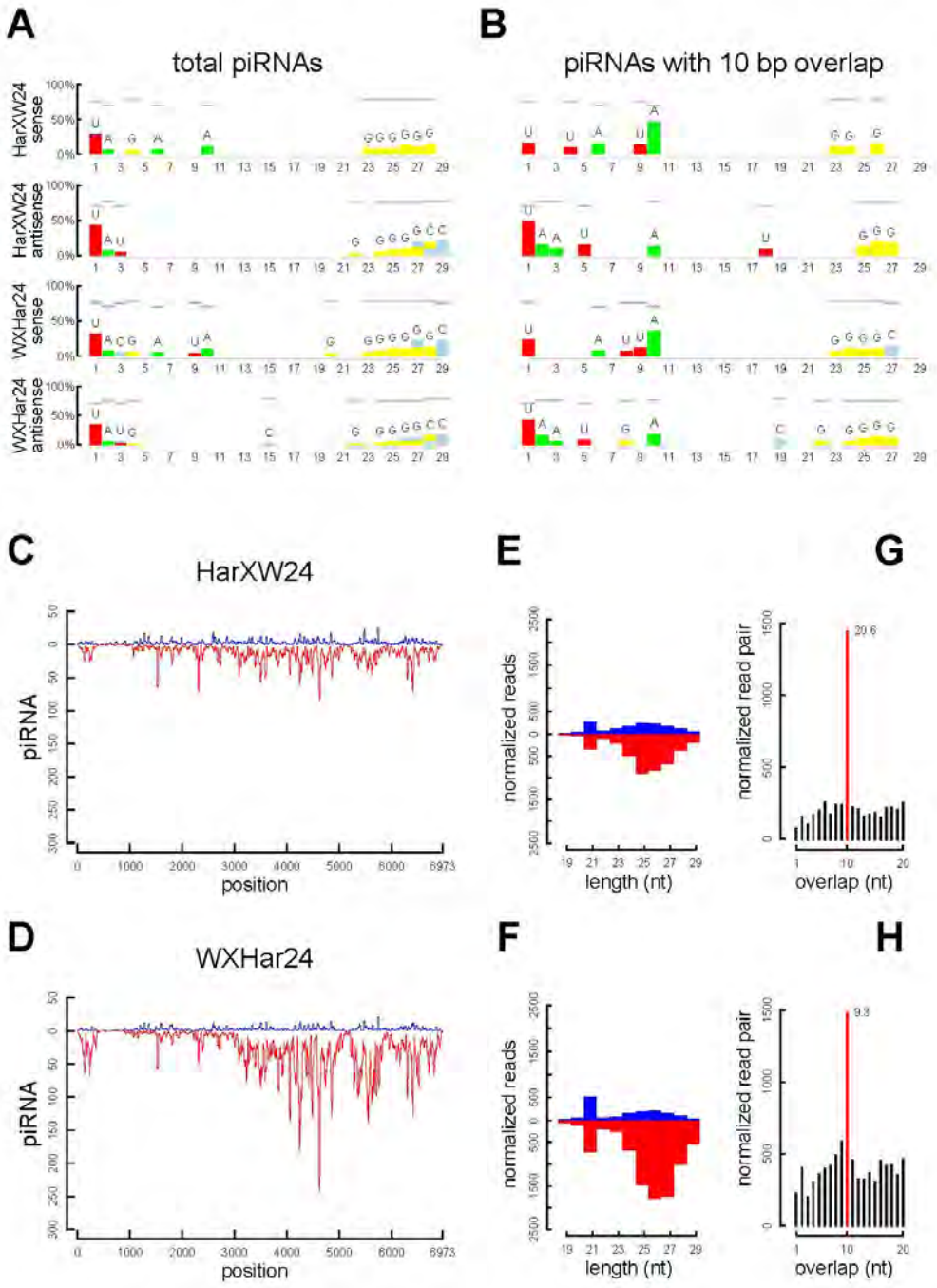
A
total piRNAs
B
piRNAs with 10 bp overlap
HarXW24 sense
HarXW24 antisense
WXHar24 sense
WXHar24 antisense
C
HarXW24
D
WXHar24
piRNA
position
E
F
normalized reads
length (nt)
G
H
normalized read pair
overlap (nt)
20.6
9.3

gypsy4

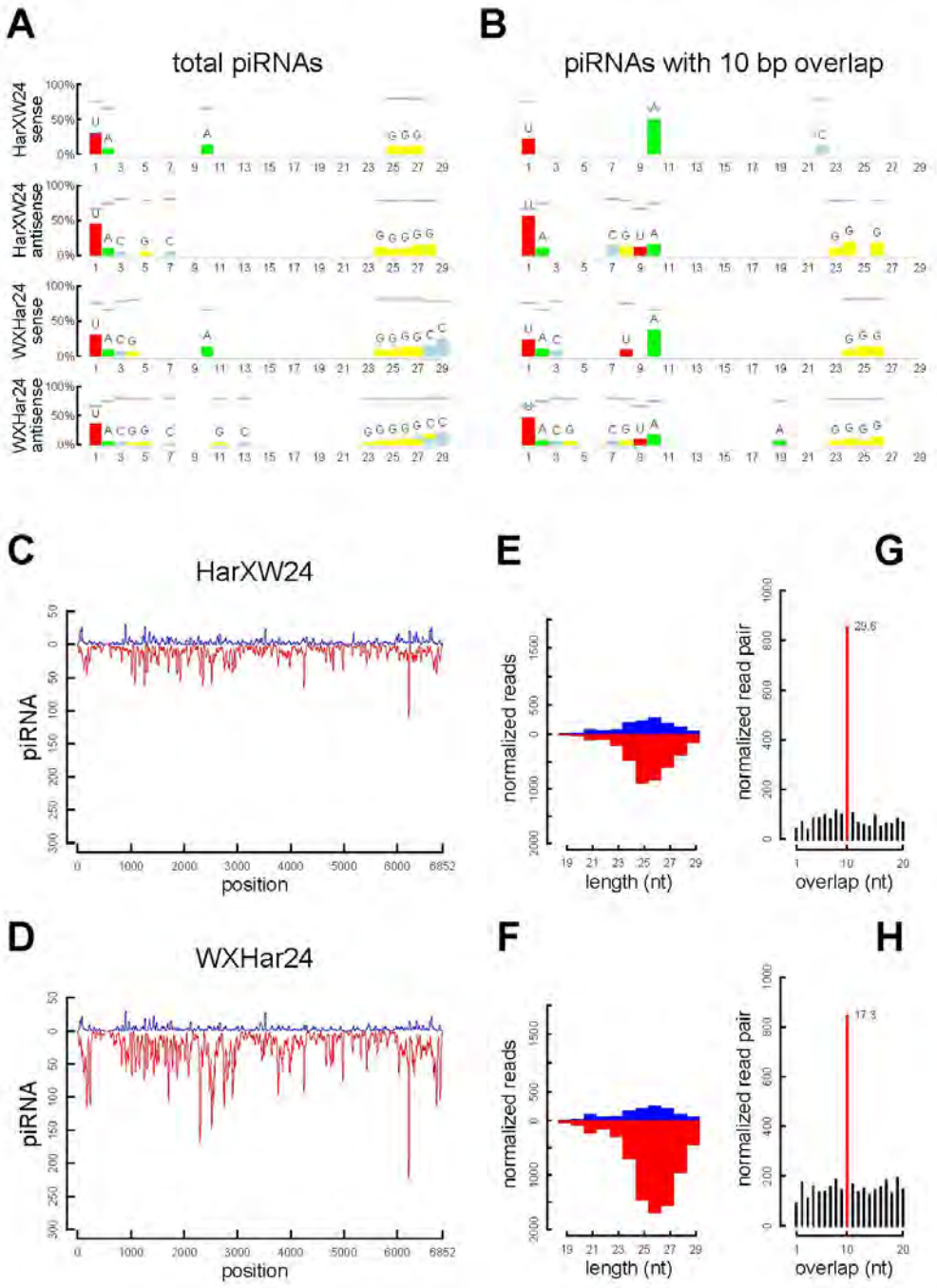
A
total piRNAs
B
piRNAs with 10 bp overlap
HarXW24 sense
HarXW24 antisense
WXHar24 sense
WXHar24 antisense
C
HarXW24
D
WXHar24
piRNA
position
E
F
normalized reads
length (nt)
G
H
normalized read pair
overlap (nt)
29.6
17.3

gypsy5

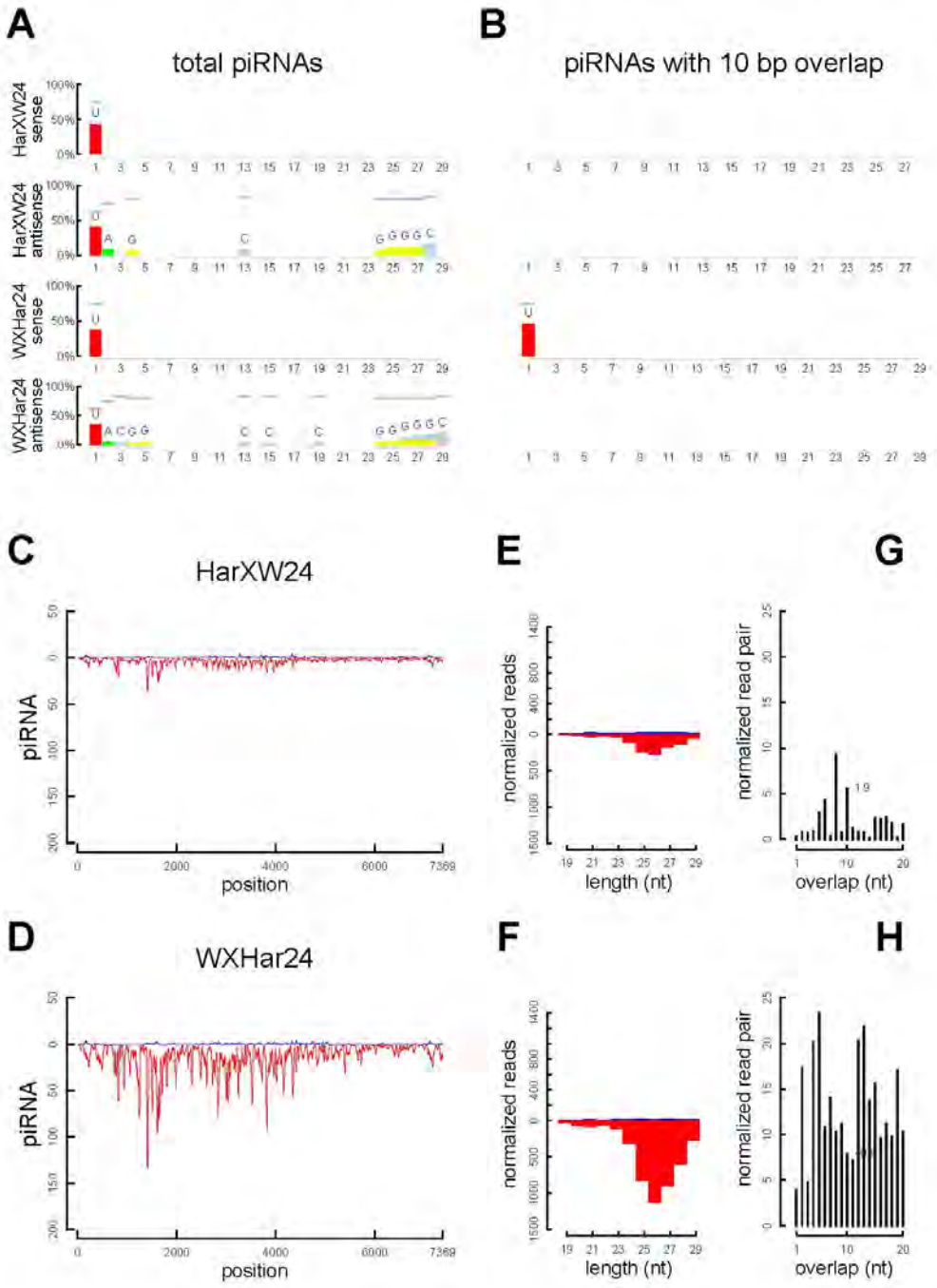
A
total piRNAs
B
piRNAs with 10 bp overlap
HarXW24 sense
HarXW24 antisense
WXHar24 sense
WXHar24 antisense
C
HarXW24
D
WXHar24
piRNA
position
E
F
normalized reads
length (nt)
G
H
normalized read pair
overlap (nt)

gypsy6

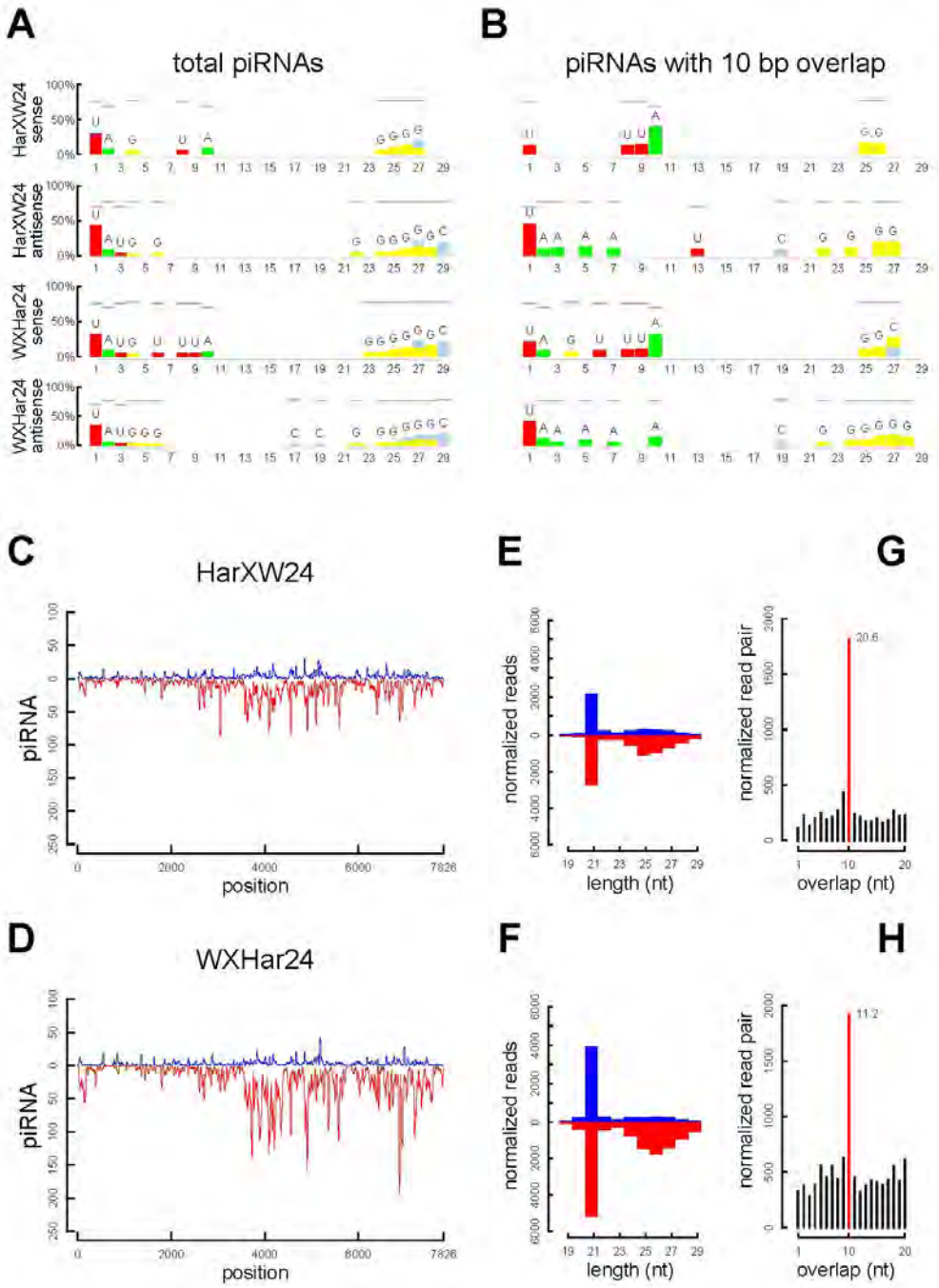
A
total piRNAs
B
piRNAs with 10 bp overlap
HarXW24 sense
HarXW24 antisense
WXHar24 sense
WXHar24 antisense
C
HarXW24
D
WXHar24
piRNA
position
E
F
normalized reads
length (nt)
G
H
normalized read pair
overlap (nt)
20.6
11.2

gypsy7

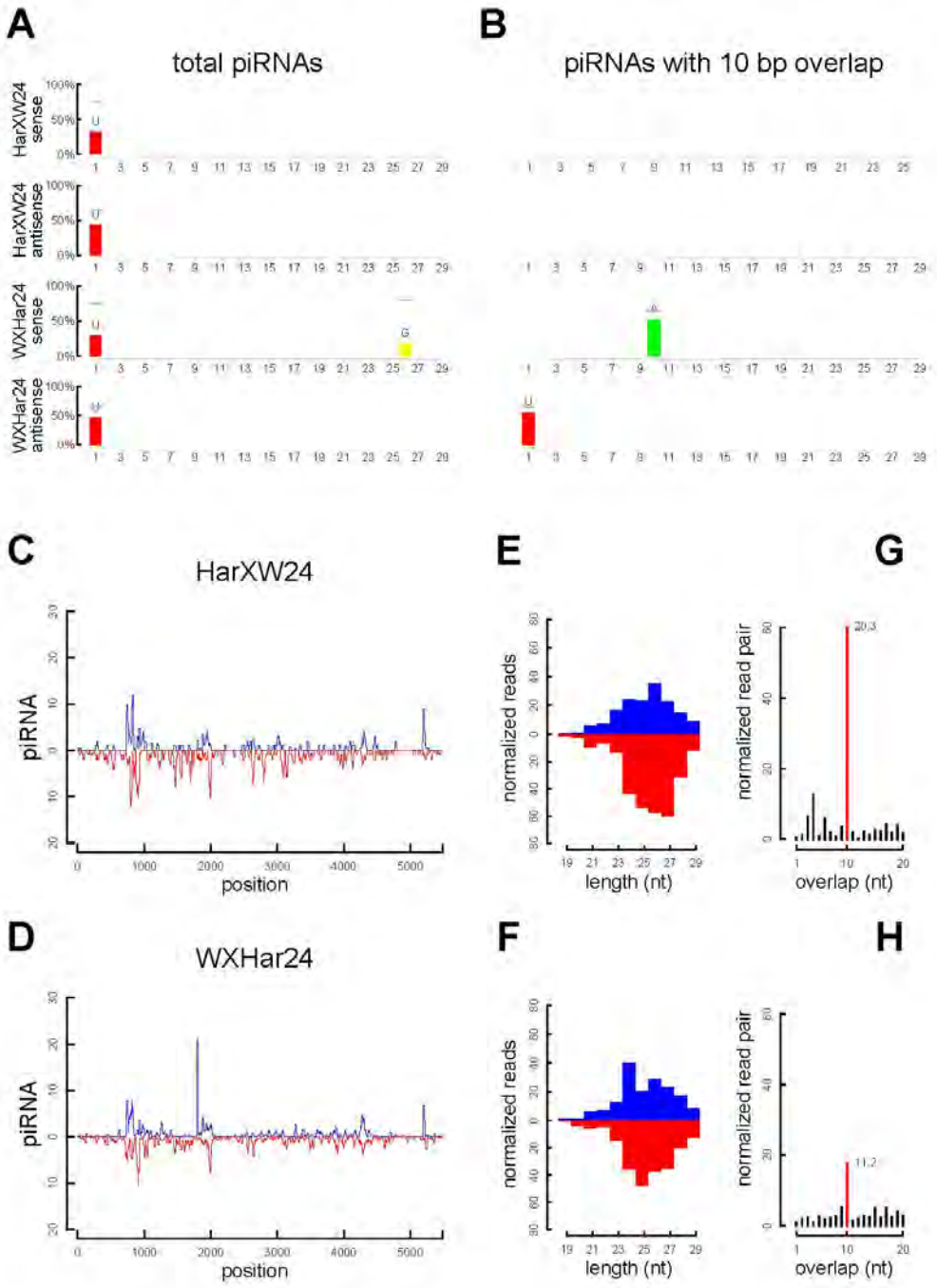
A
total piRNAs
HarXW24 sense
HarXW24 antisense
WXHar24 sense
WXHar24 antisense
B
piRNAs with 10 bp overlap
C
HarXW24
piRNA
position
D
WXHar24
piRNA
position
E
normalized reads
length (nt)
F
normalized reads
length (nt)
G
normalized read pair
overlap (nt)
20.3
H
normalized read pair
overlap (nt)
11.2

gypsy8

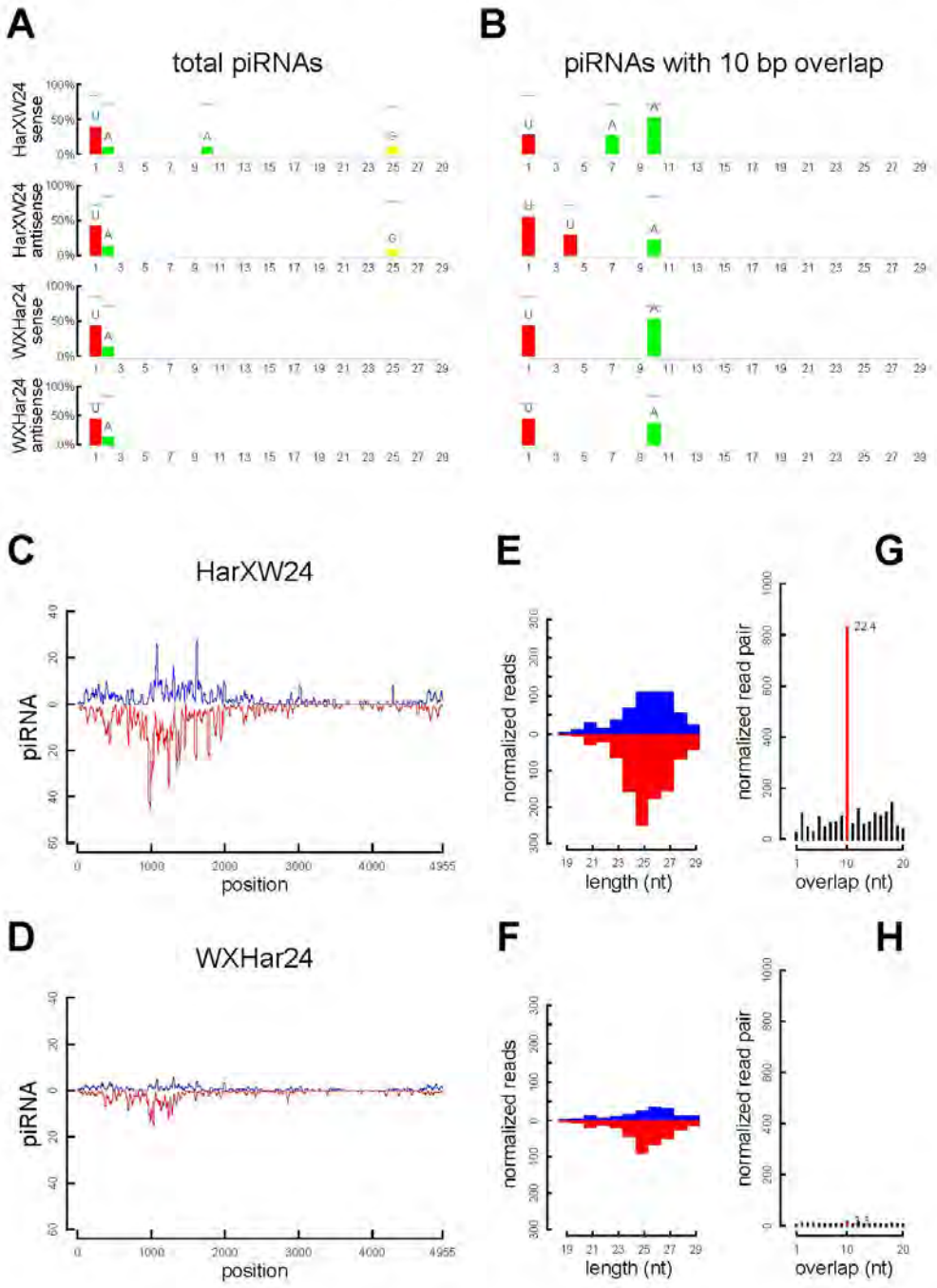
A
total piRNAs
B
piRNAs with 10 bp overlap
HarXW24 sense
HarXW24 antisense
WXHar24 sense
WXHar24 antisense
C
HarXW24
D
WXHar24
piRNA
position
E
F
normalized reads
length (nt)
G
H
normalized read pair
overlap (nt)
224

gypsy9

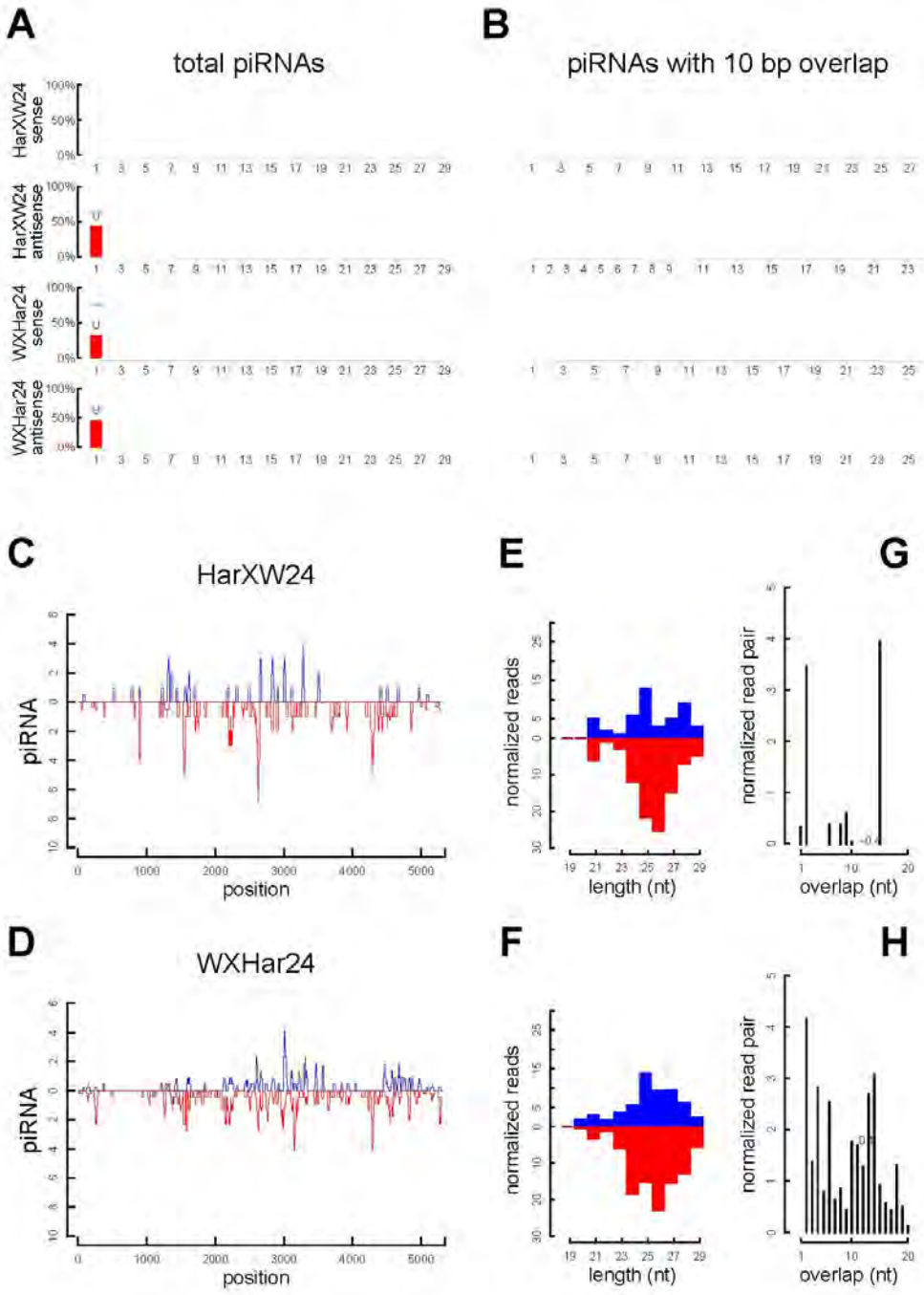
A
total piRNAs
B
piRNAs with 10 bp overlap
HarXW24 sense
HarXW24 antisense
WXHar24 sense
WXHar24 antisense
C
HarXW24
piRNA
position
D
WXHar24
E
normalized reads
length (nt)
F
G
normalized read pair
overlap (nt)
H

HB

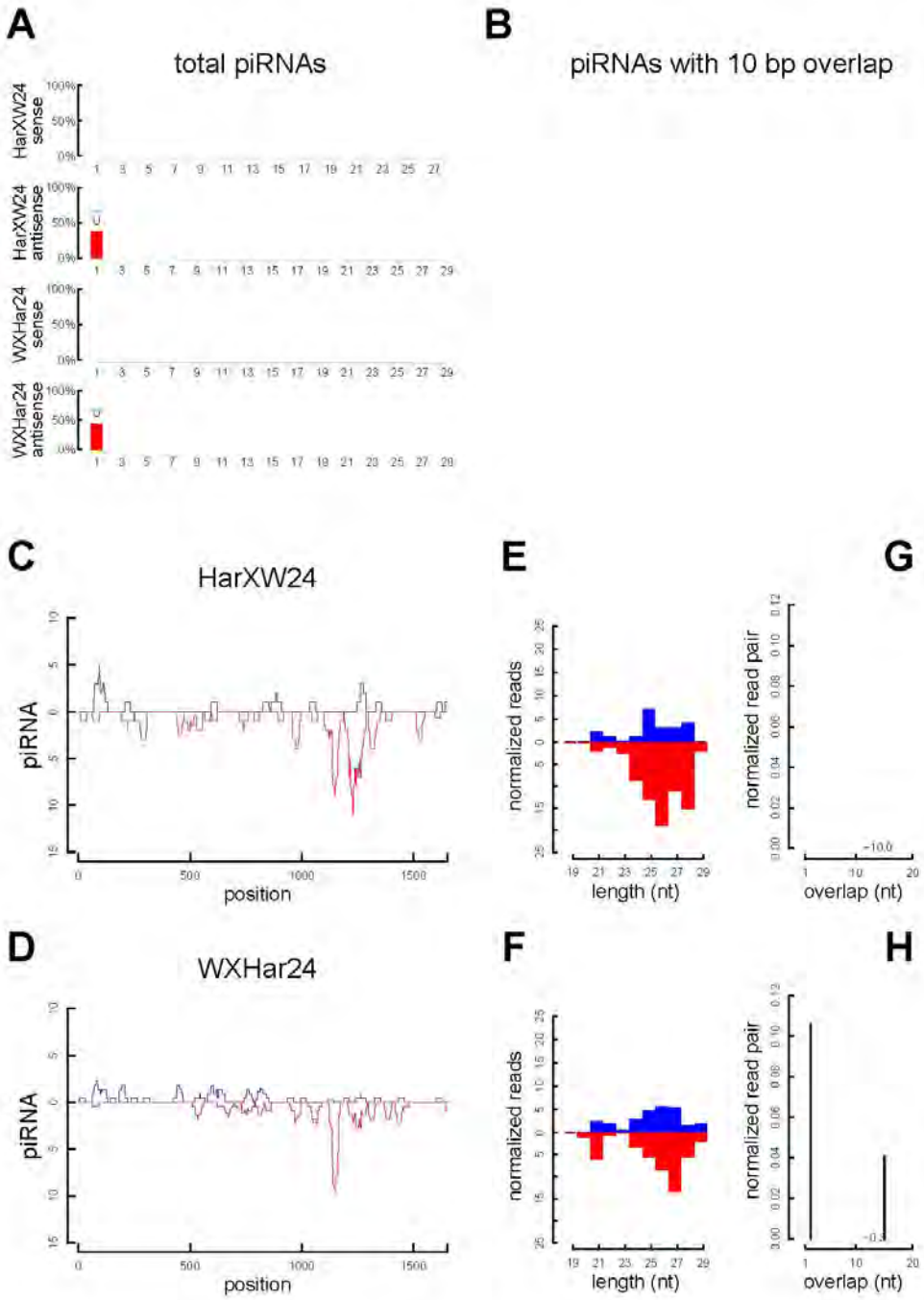
A
total piRNAs
B
piRNAs with 10 bp overlap
HarXW24 sense
HarXW24 antisense
WXHar24 sense
WXHar24 antisense
C
HarXW24
piRNA
position
D
WXHar24
piRNA
position
E
normalized reads
length (nt)
F
normalized reads
length (nt)
G
normalized read pair
overlap (nt)
H
normalized read pair
overlap (nt)

Helena

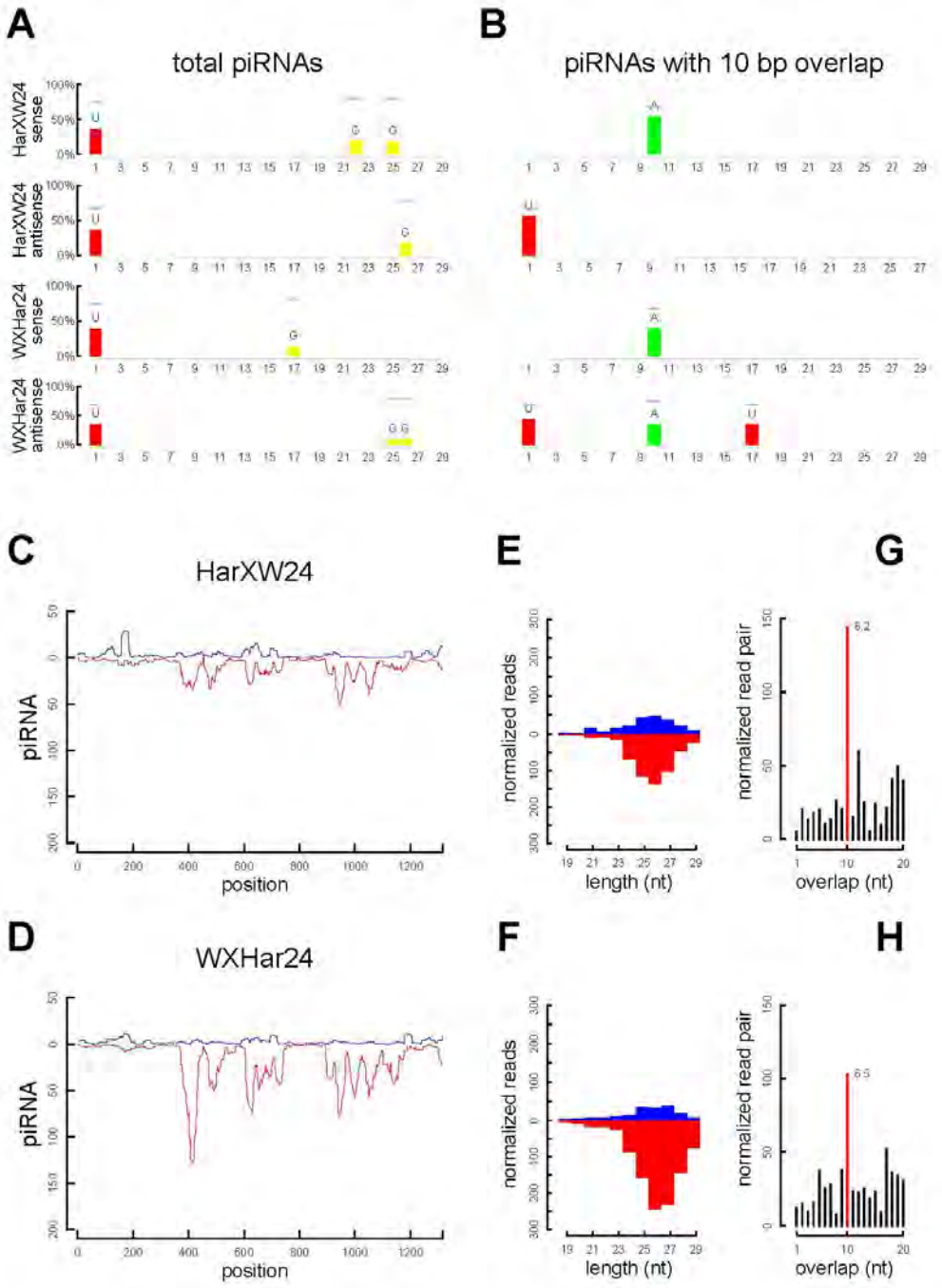
A
total piRNAs
B
piRNAs with 10 bp overlap
HarXW24 sense
HarXW24 antisense
WXHar24 sense
WXHar24 antisense
C
HarXW24
D
WXHar24
piRNA
position
E
F
normalized reads
length (nt)
G
H
normalized read pair
overlap (nt)

Helitron

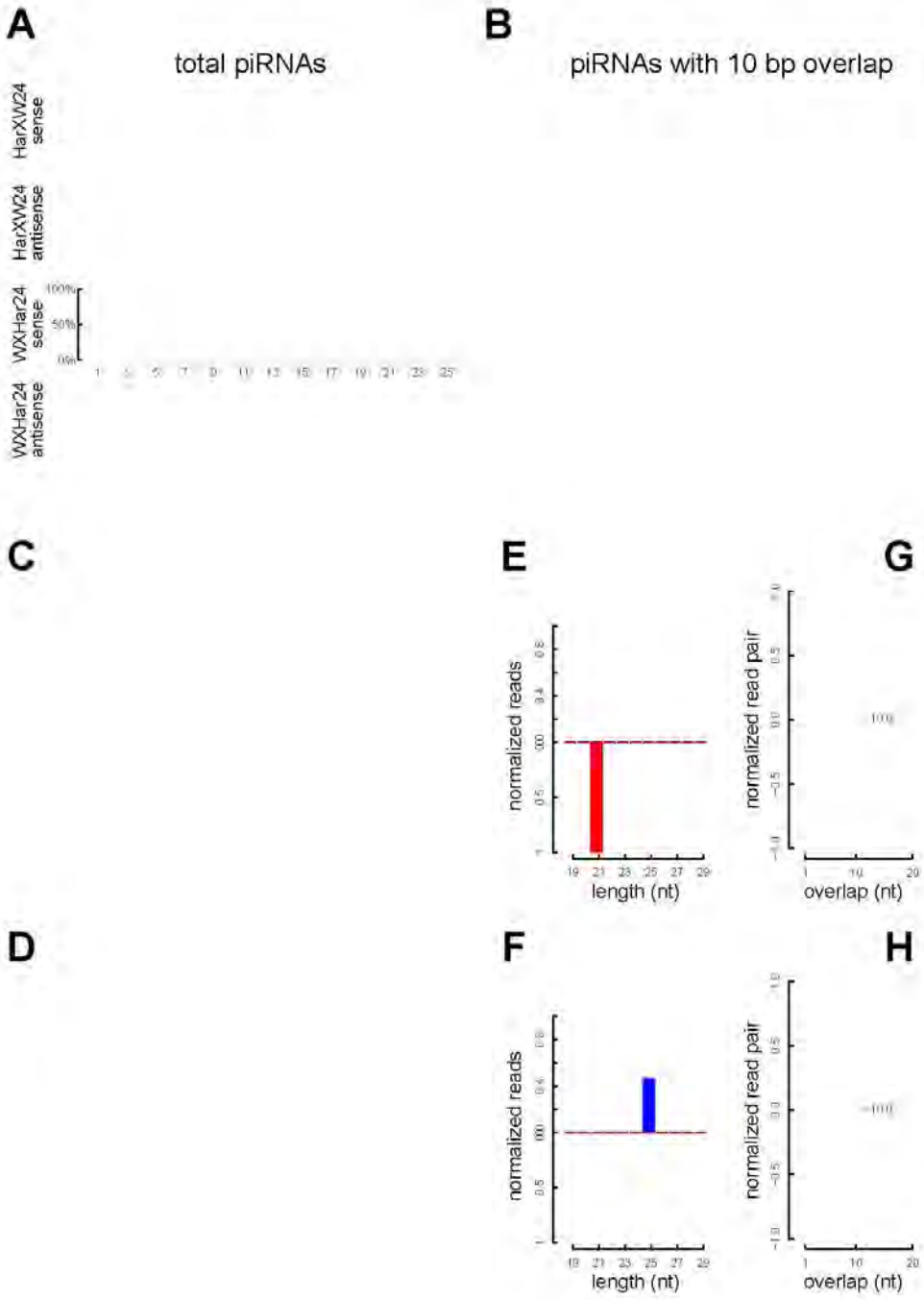
A
total piRNAs
B
piRNAs with 10 bp overlap
HarXW24 sense
HarXW24 antisense
WXHar24 sense
WXHar24 antisense
100%
50%
0%
C
D
E
F
G
H
normalized reads
length (nt)
normalized read pair
overlap (nt)

HeT A

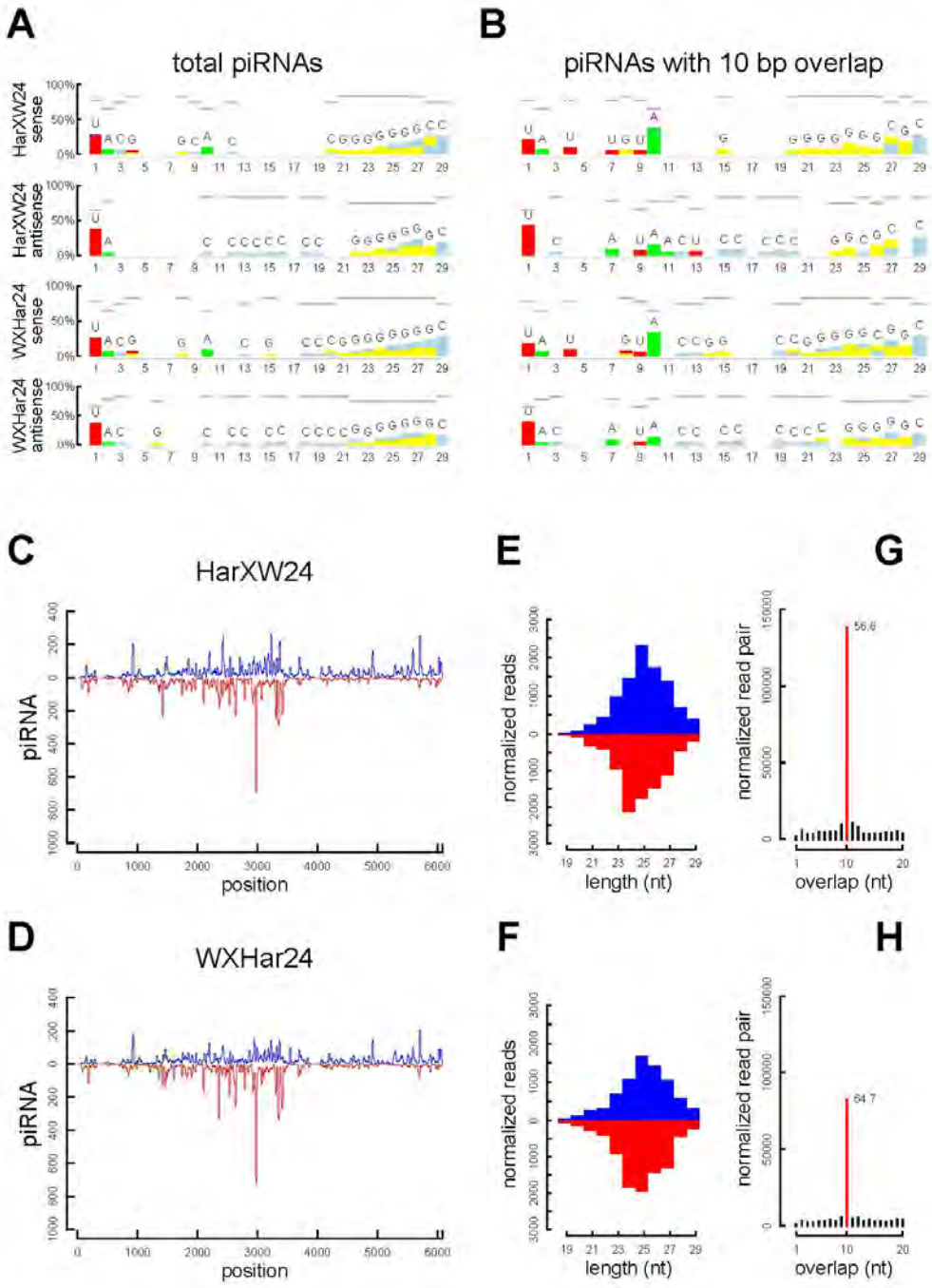
A
total piRNAs
B
piRNAs with 10 bp overlap
HarXW24 sense
HarXW24 antisense
WXHar24 sense
WXHar24 antisense
C
HarXW24
D
WXHar24
piRNA
position
E
F
normalized reads
length (nt)
G
H
normalized read pair
overlap (nt)
56.6
64.7

HMS Beagle

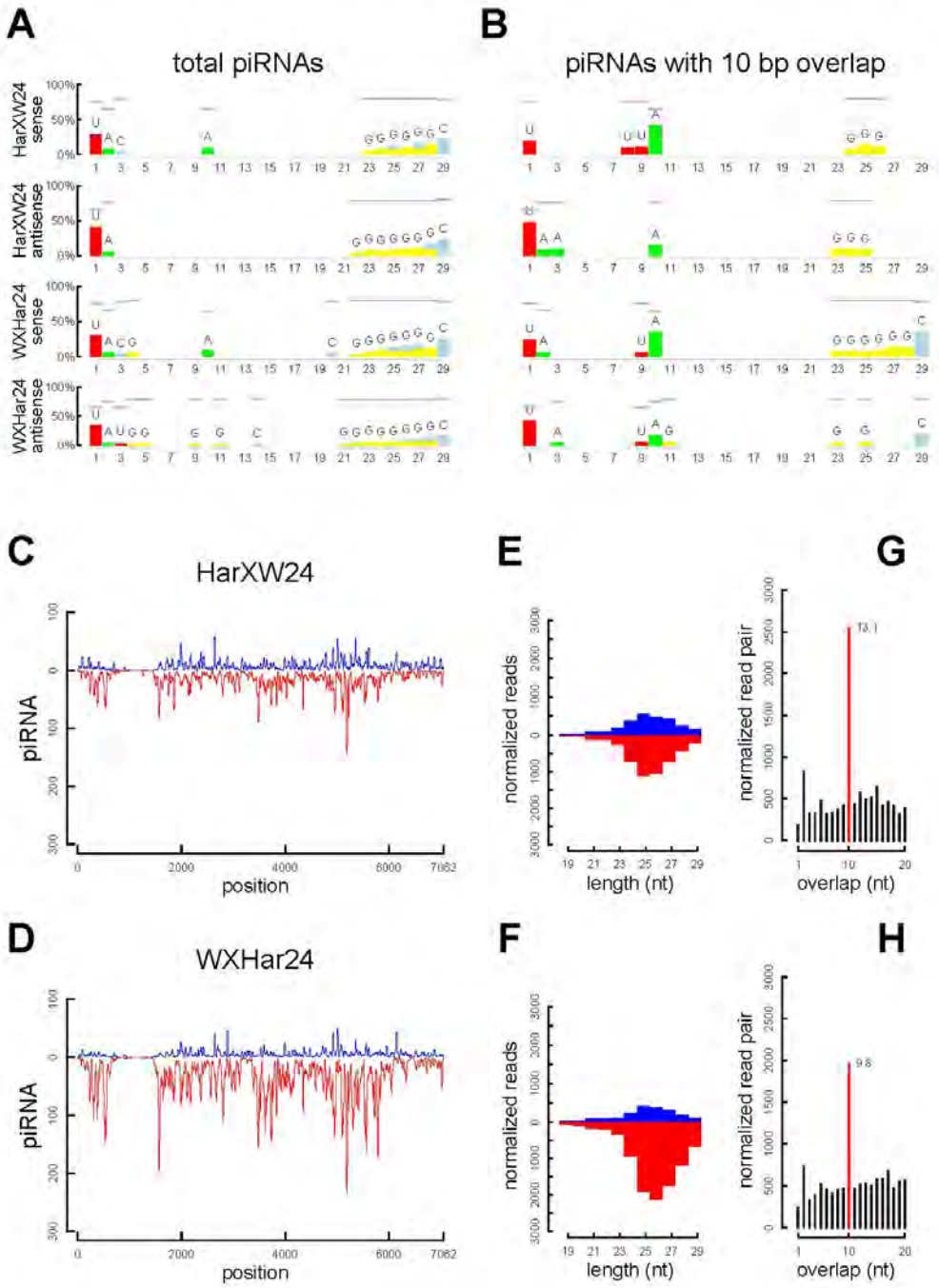
A
total piRNAs
B
piRNAs with 10 bp overlap
HarXW24 sense
HarXW24 antisense
WXHar24 sense
WXHar24 antisense
C
HarXW24
piRNA
position
D
WXHar24
piRNA
position
E
normalized reads
length (nt)
F
normalized reads
length (nt)
G
normalized read pair
overlap (nt)
H
normalized read pair
overlap (nt)

HMS Beagle2

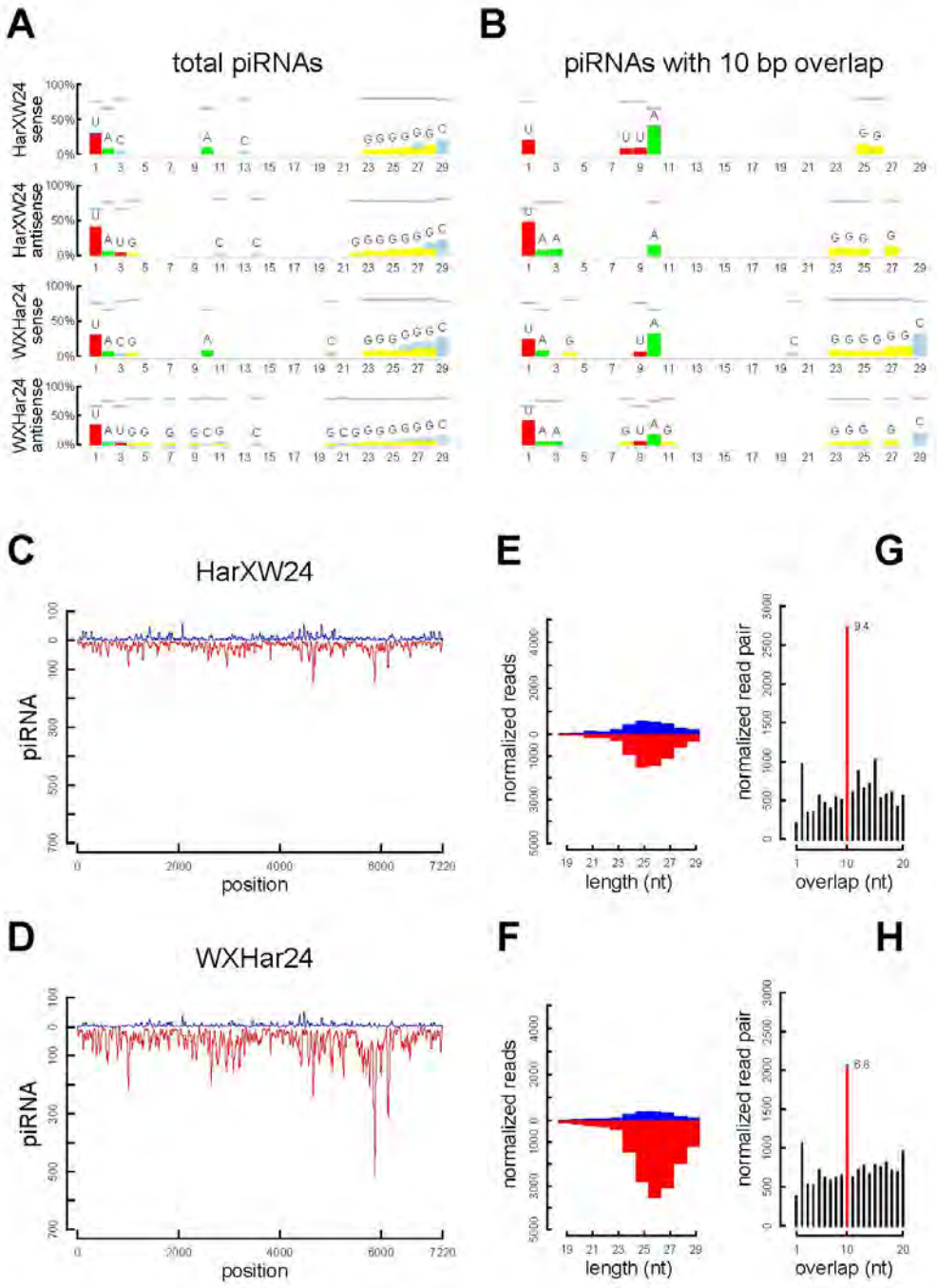
A
total piRNAs
B
piRNAs with 10 bp overlap
HarXW24 sense
HarXW24 antisense
WXHar24 sense
WXHar24 antisense
C
HarXW24
D
WXHar24
piRNA
position
E
F
normalized reads
length (nt)
G
H
normalized read pair
overlap (nt)
9.4
6.6

hobo

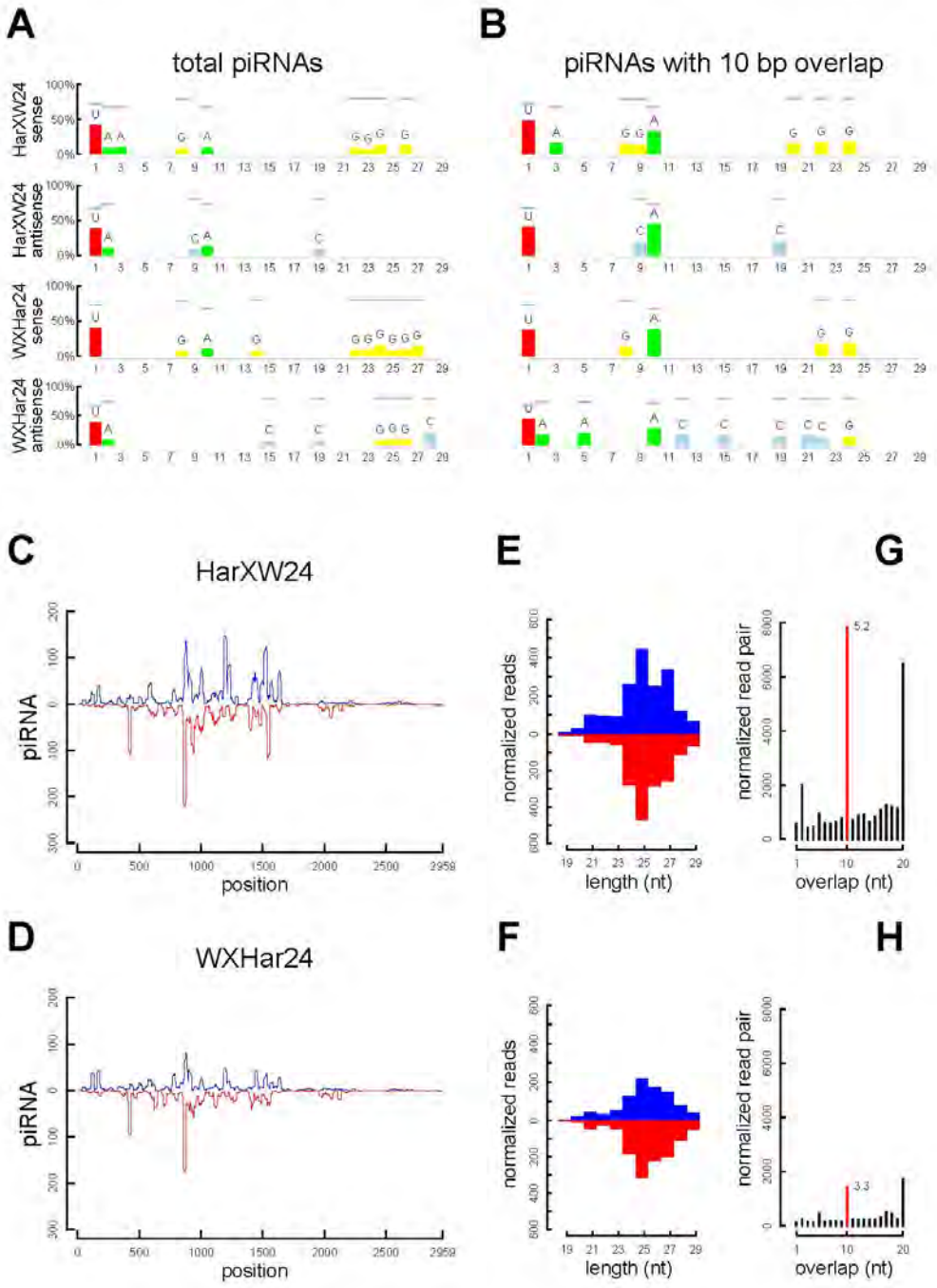
A
total piRNAs
B
piRNAs with 10 bp overlap
HarXW24 sense
HarXW24 antisense
WXHar24 sense
WXHar24 antisense
C
HarXW24
D
WXHar24
piRNA
position
E
F
normalized reads
length (nt)
G
H
normalized read pair
overlap (nt)
5.2
3.3

hopper

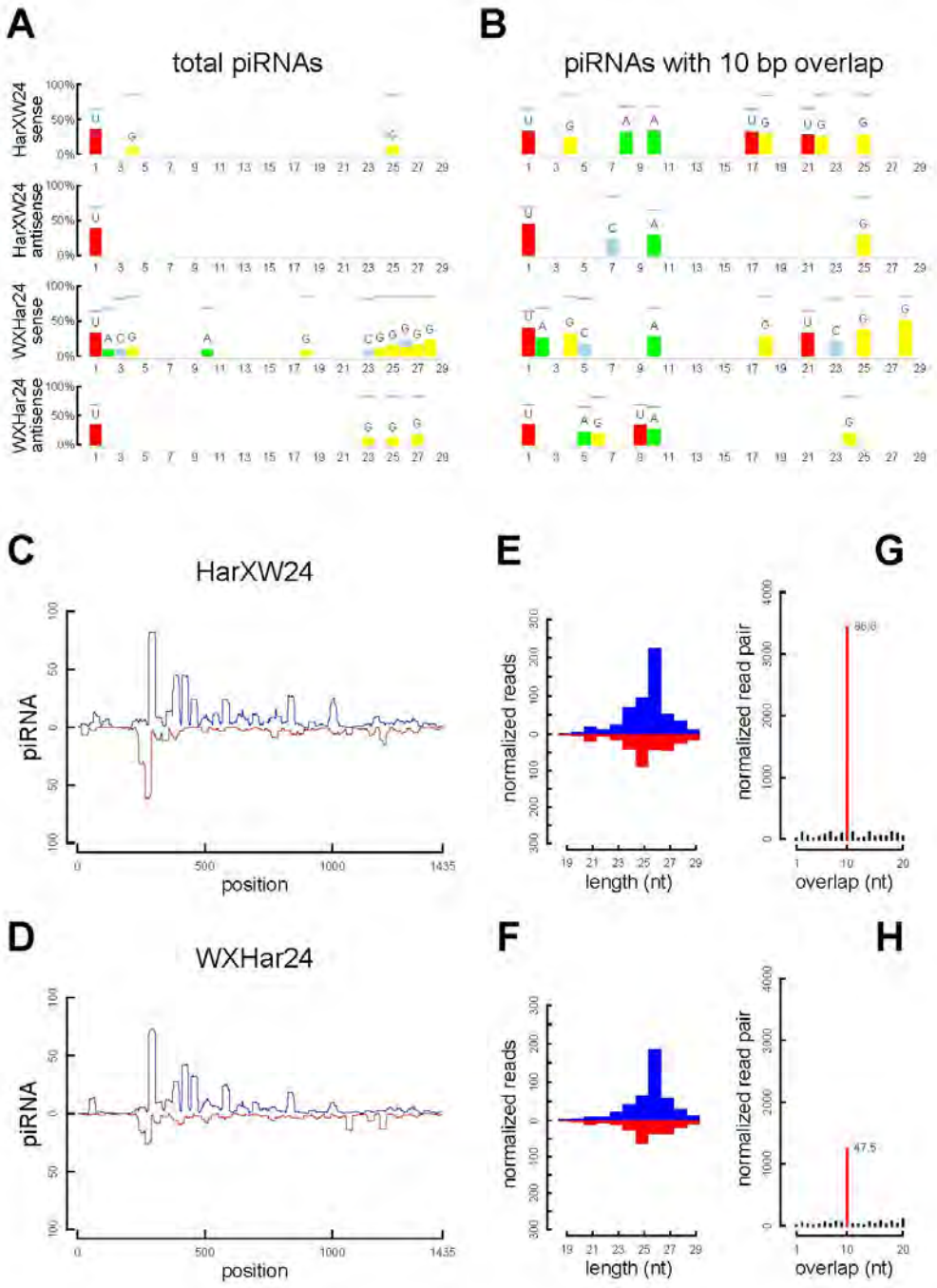
A
total piRNAs
B
piRNAs with 10 bp overlap
HarXW24 sense
HarXW24 antisense
WXHar24 sense
WXHar24 antisense
C
HarXW24
piRNA
position
D
WXHar24
E
F
normalized reads
length (nt)
G
H
normalized read pair
overlap (nt)
86.6
47.5

hopper2

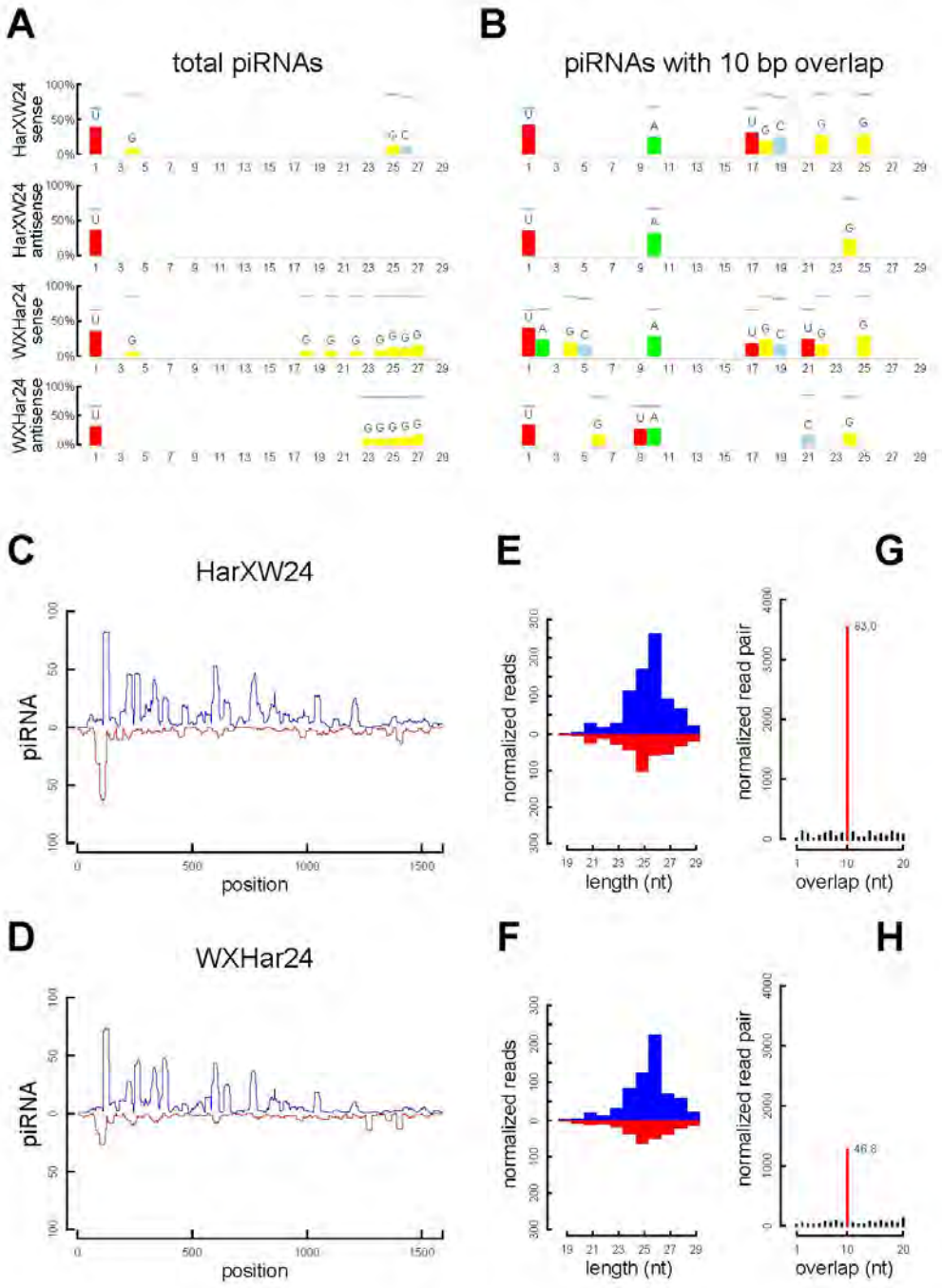
A
total piRNAs
B
piRNAs with 10 bp overlap
HarXW24 sense
HarXW24 antisense
WXHar24 sense
WXHar24 antisense
C
HarXW24
piRNA
position
D
WXHar24
piRNA
position
E
normalized reads
length (nt)
F
normalized reads
length (nt)
G
normalized read pair
overlap (nt)
63.0
H
normalized read pair
overlap (nt)
46.8

Idefix

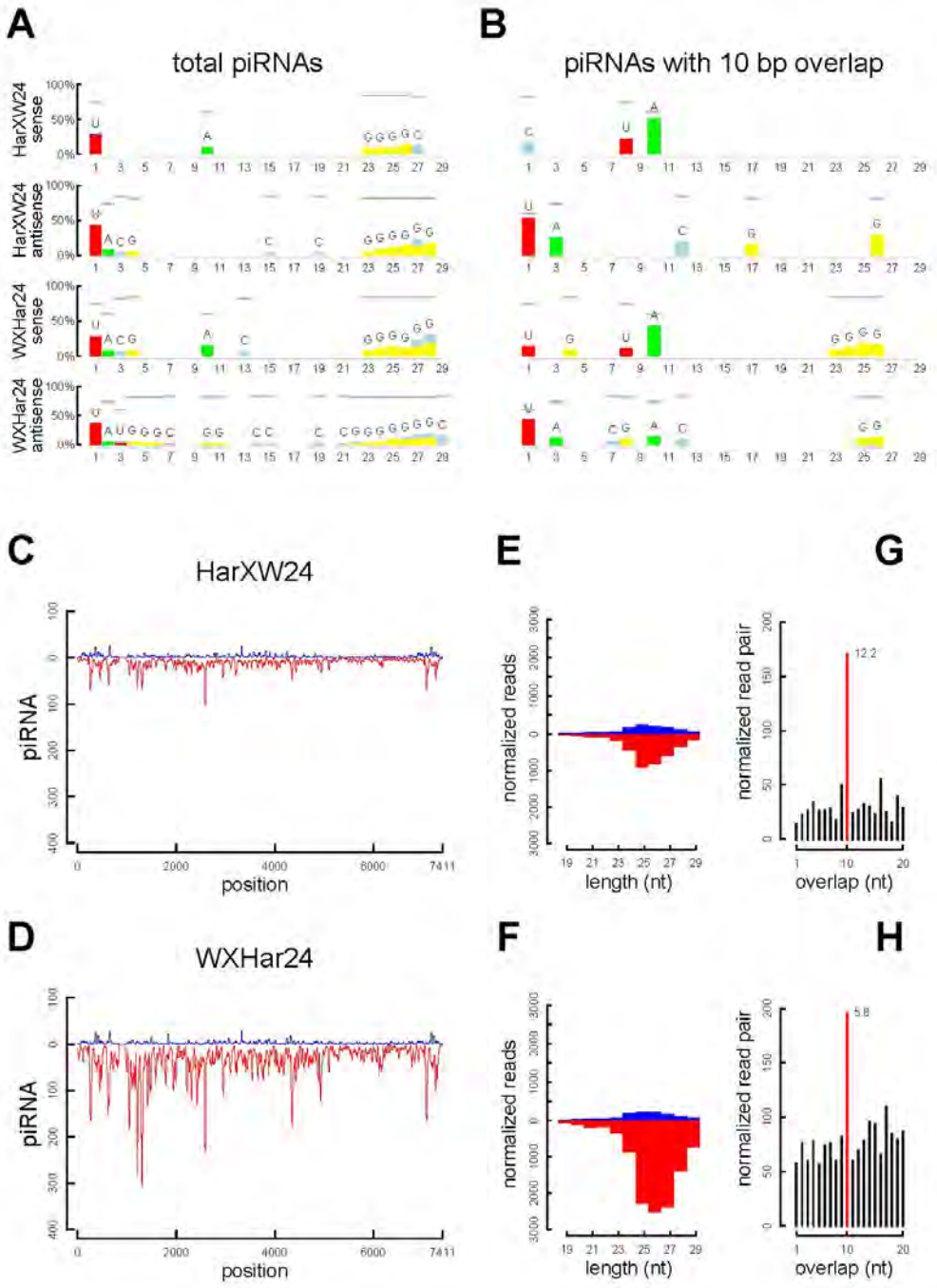
A
total piRNAs
B
piRNAs with 10 bp overlap
HarXW24 sense
HarXW24 antisense
WXHar24 sense
WXHar24 antisense
C
HarXW24
D
WXHar24
piRNA
position
E
F
normalized reads
length (nt)
G
H
normalized read pair
overlap (nt)
12.2
5.8

I element

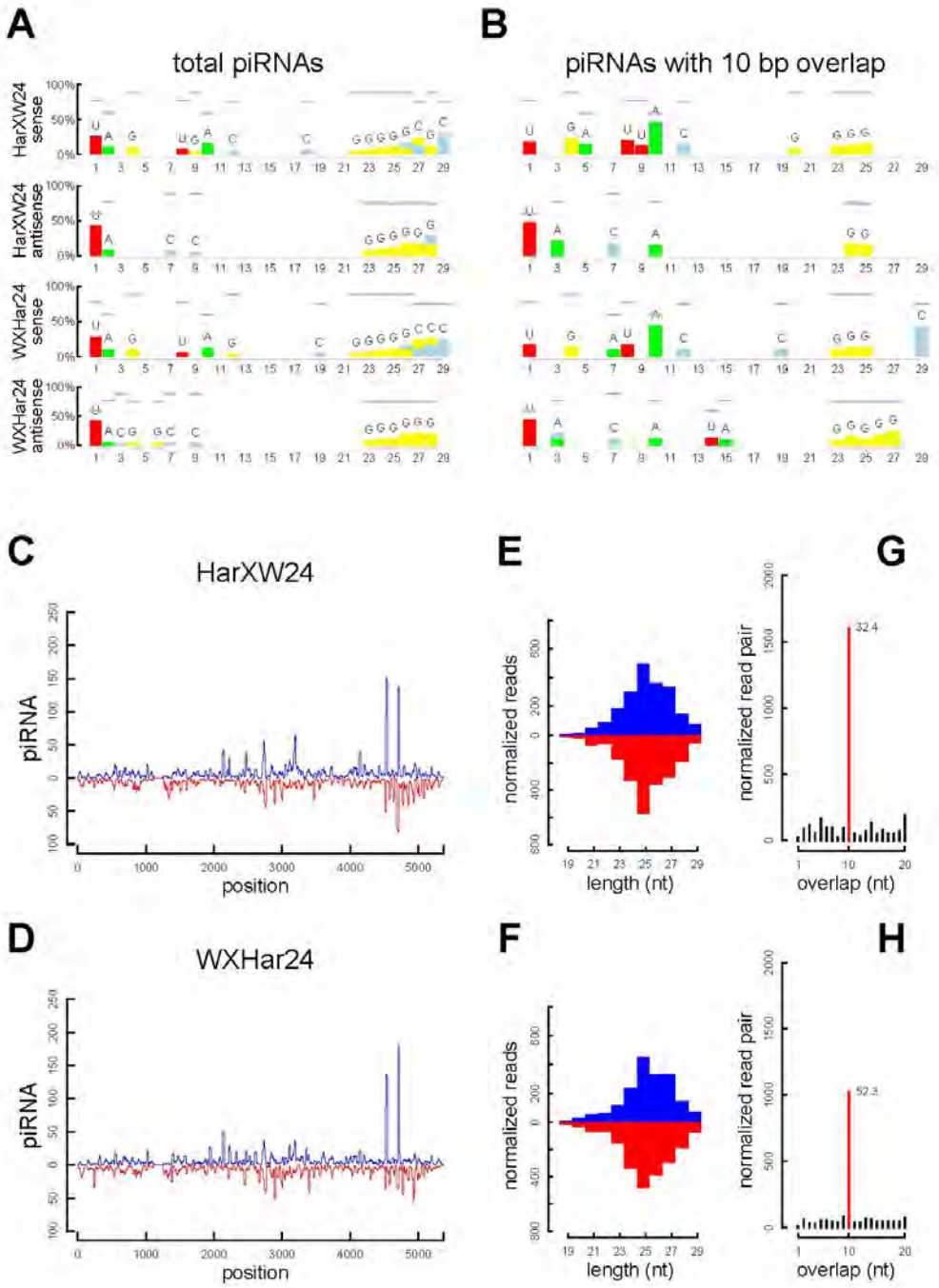
A
total piRNAs
B
piRNAs with 10 bp overlap
HarXW24 sense
HarXW24 antisense
WXHar24 sense
WXHar24 antisense
C
HarXW24
piRNA
position
D
WXHar24
piRNA
position
E
normalized reads
length (nt)
F
normalized reads
length (nt)
G
normalized read pair
32.4
overlap (nt)
H
normalized read pair
52.3
overlap (nt)

INE 1

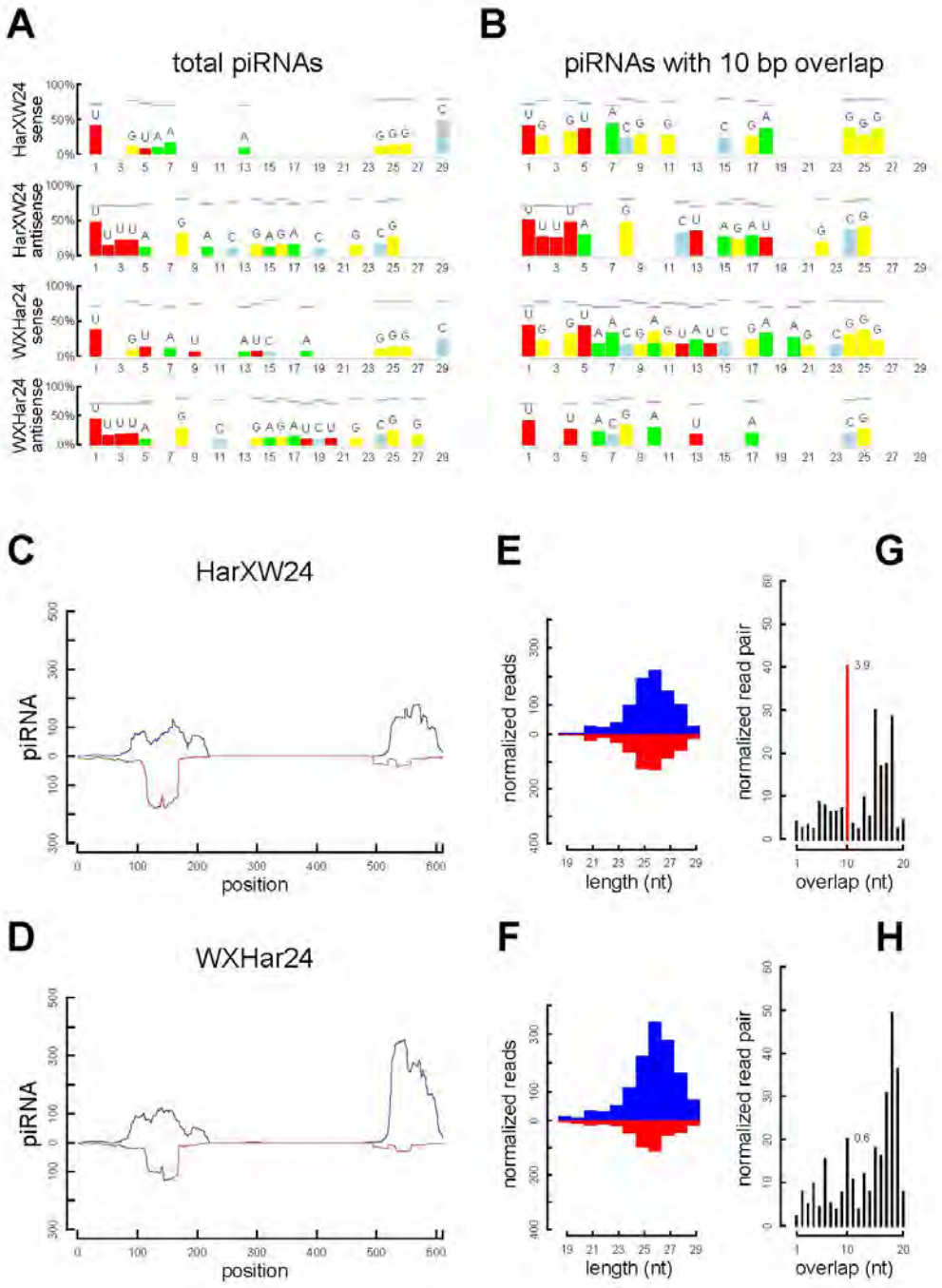
A
total piRNAs
B
piRNAs with 10 bp overlap
HarXW24 sense
HarXW24 antisense
WXHar24 sense
WXHar24 antisense
C
HarXW24
D
WXHar24
piRNA
position
E
F
normalized reads
length (nt)
G
H
normalized read pair
overlap (nt)
3.9
0.6

invader1

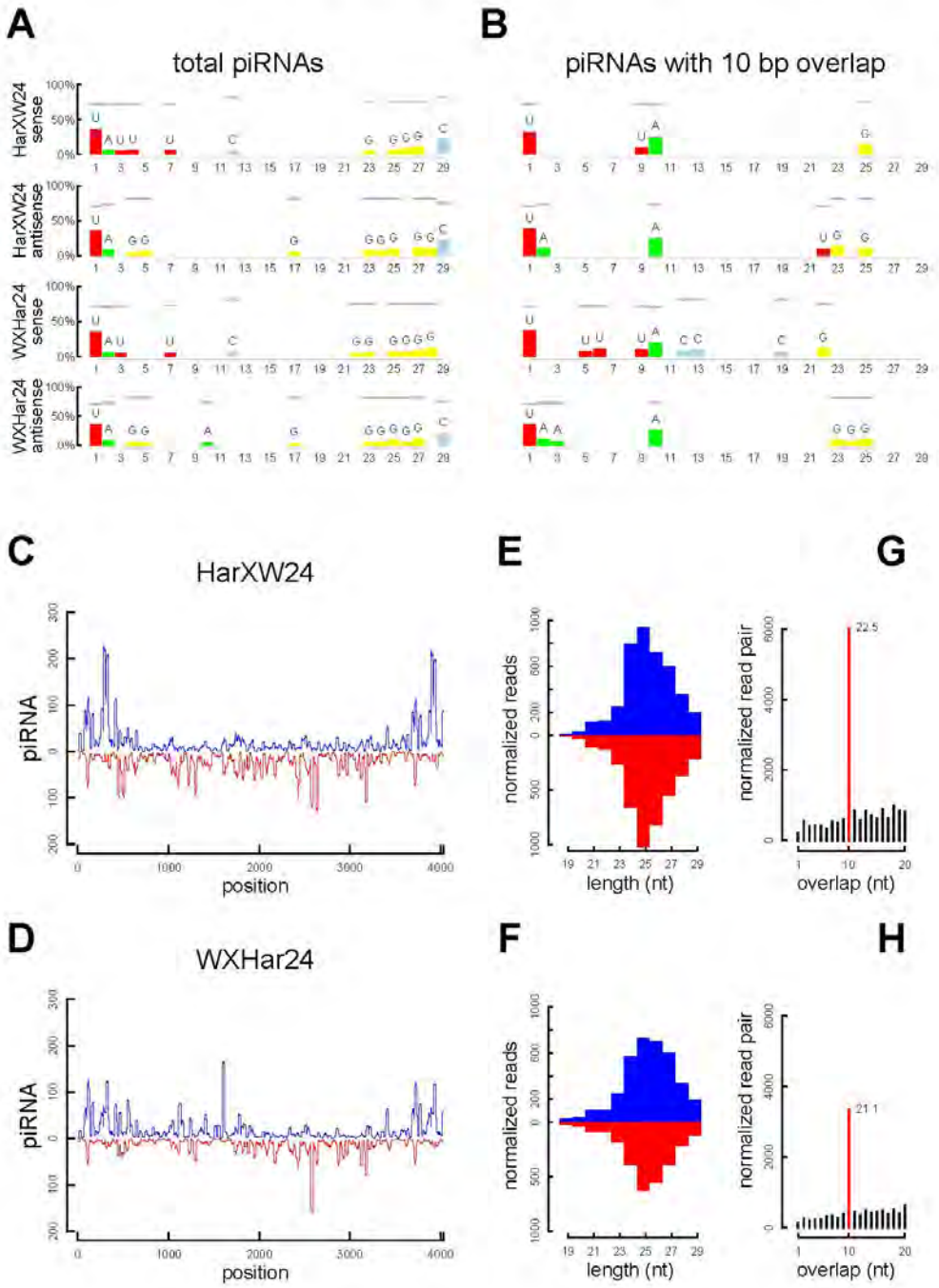
A
total piRNAs
B
piRNAs with 10 bp overlap
HarXW24 sense
HarXW24 antisense
WXHar24 sense
WXHar24 antisense
C
HarXW24
D
WXHar24
piRNA
position
E
F
normalized reads
length (nt)
G
H
normalized read pair
overlap (nt)
22.5
21.1

invader2

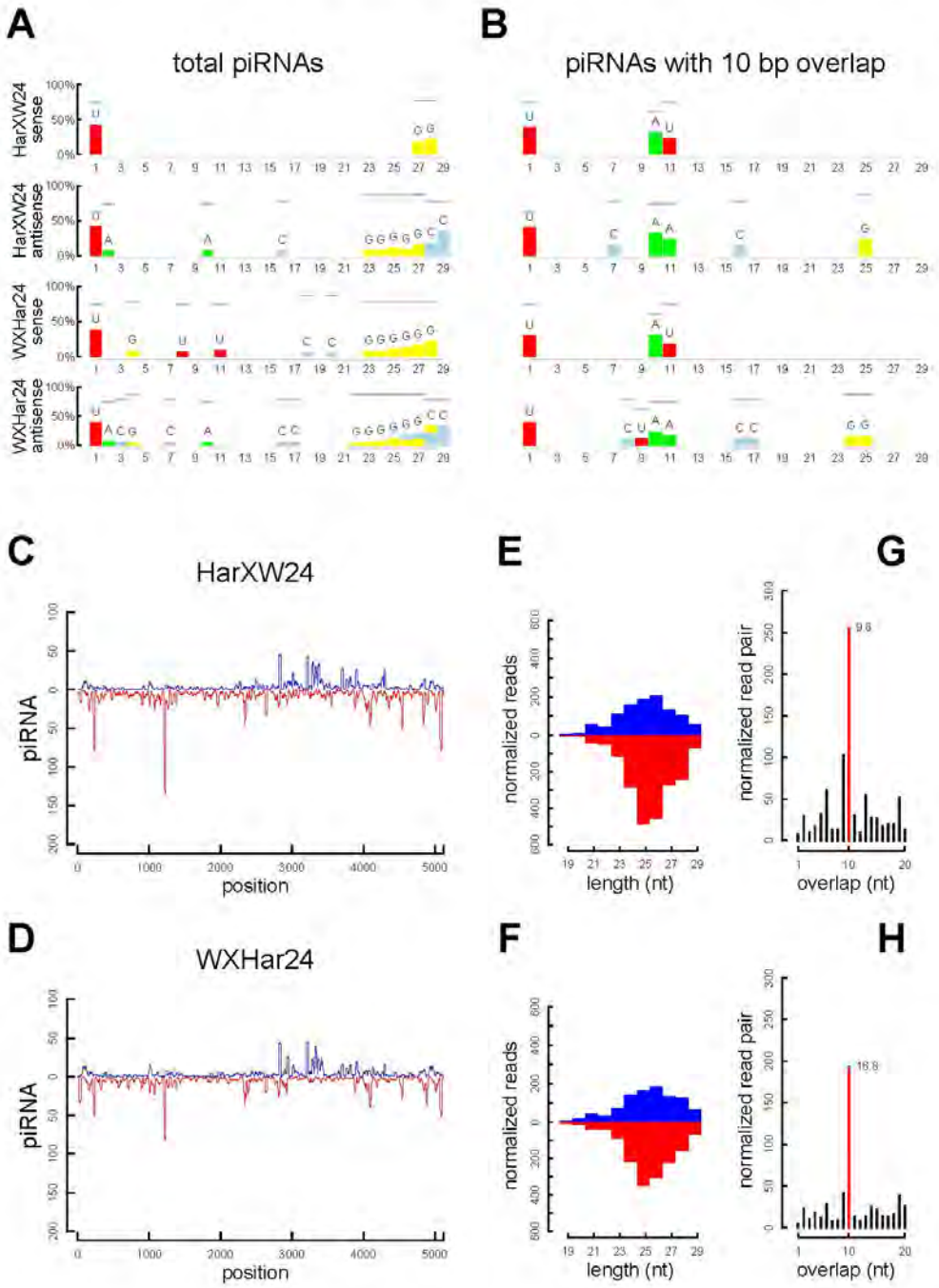
A
total piRNAs
B
piRNAs with 10 bp overlap
HarXW24 sense
HarXW24 antisense
WXHar24 sense
WXHar24 antisense
C
HarXW24
D
WXHar24
piRNA
position
E
F
normalized reads
length (nt)
G
H
normalized read pair
overlap (nt)
9.6
16.8

invader3

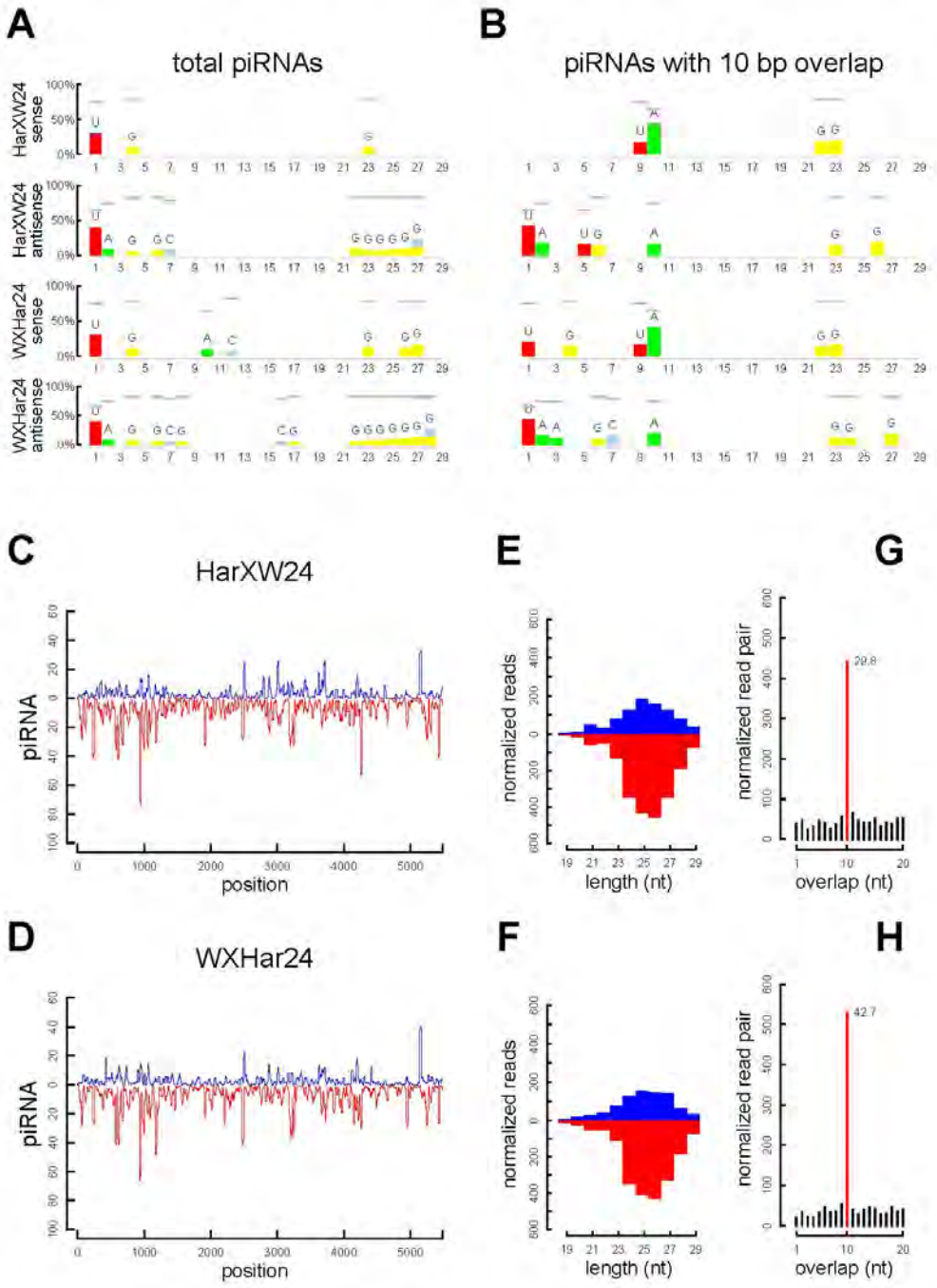
A
total piRNAs
B
piRNAs with 10 bp overlap
HarXW24 sense
HarXW24 antisense
WXHar24 sense
WXHar24 antisense
C
HarXW24
D
WXHar24
piRNA
position
E
F
normalized reads
length (nt)
G
H
normalized read pair
overlap (nt)
29.8
42.7

invader4

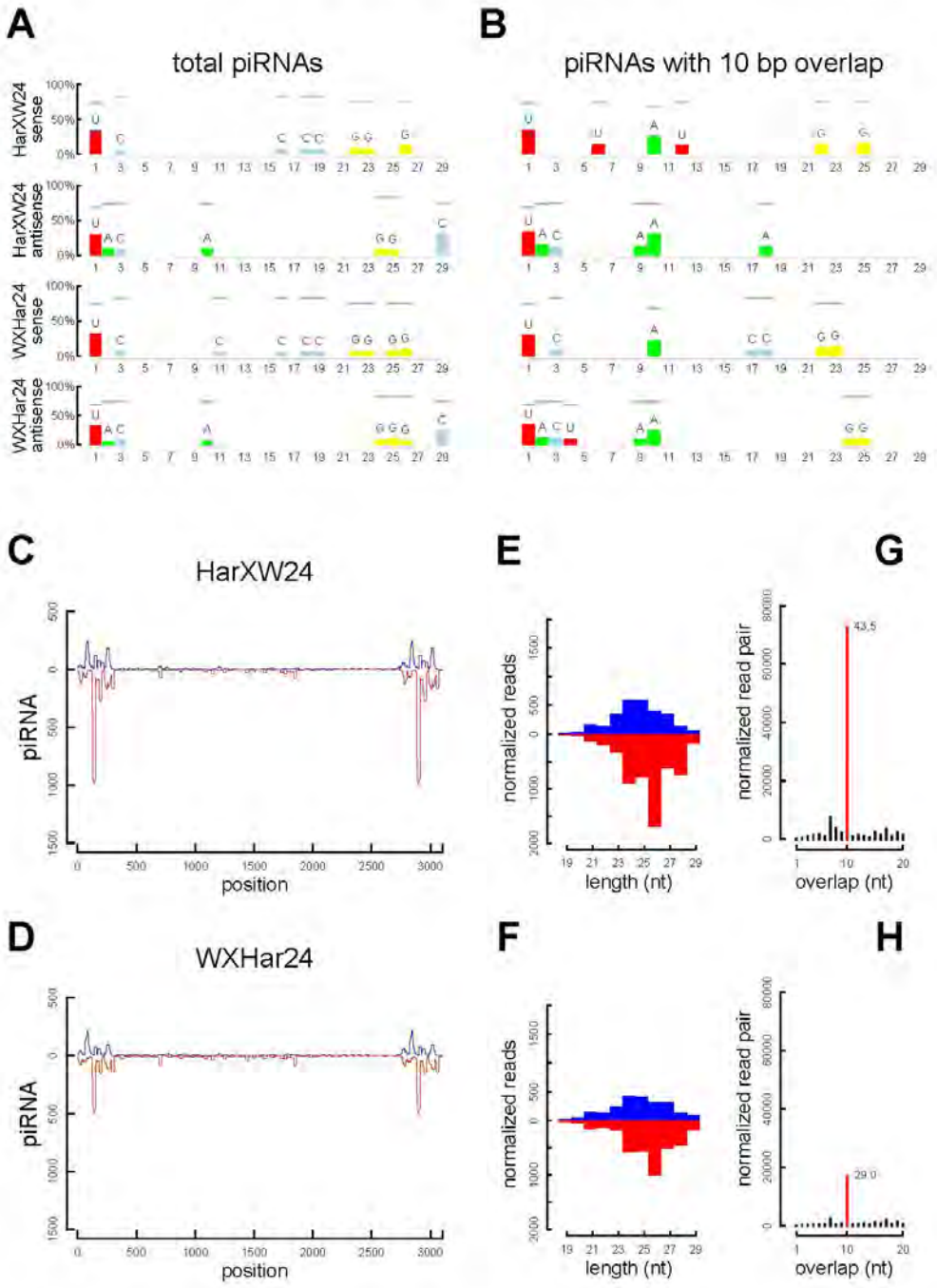
A
total piRNAs
B
piRNAs with 10 bp overlap
HarXW24 sense
HarXW24 antisense
WXHar24 sense
WXHar24 antisense
C
HarXW24
piRNA
position
D
WXHar24
E
F
normalized reads
length (nt)
G
H
normalized read pair
overlap (nt)
43.5
29.0

invader5

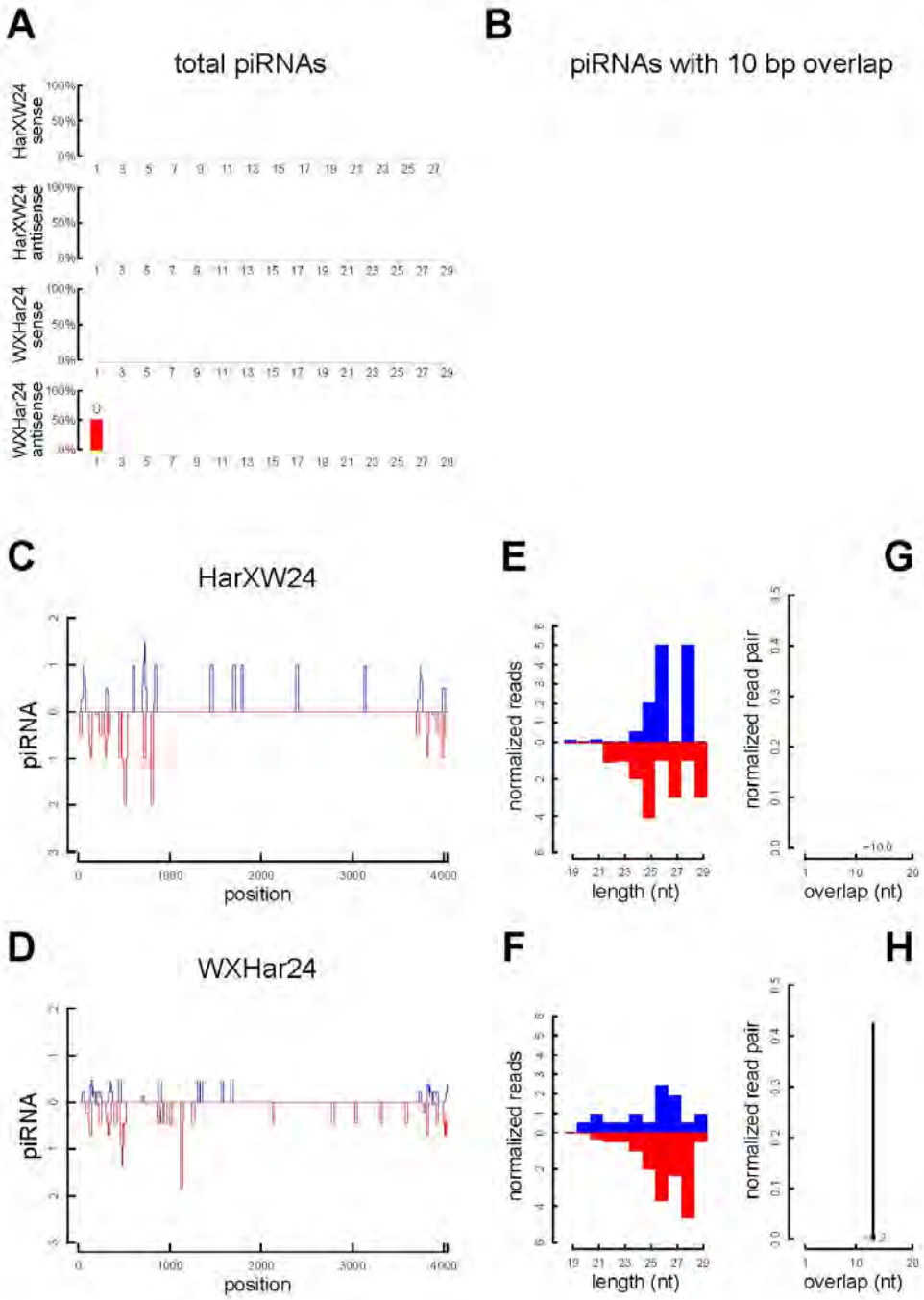
A
total piRNAs
HarXW24 sense
HarXW24 antisense
WXHar24 sense
WXHar24 antisense
B
piRNAs with 10 bp overlap
C
HarXW24
piRNA
position
D
WXHar24
piRNA
position
E
normalized reads
length (nt)
F
normalized reads
length (nt)
G
normalized read pair
overlap (nt)
H
normalized read pair
overlap (nt)

lvk

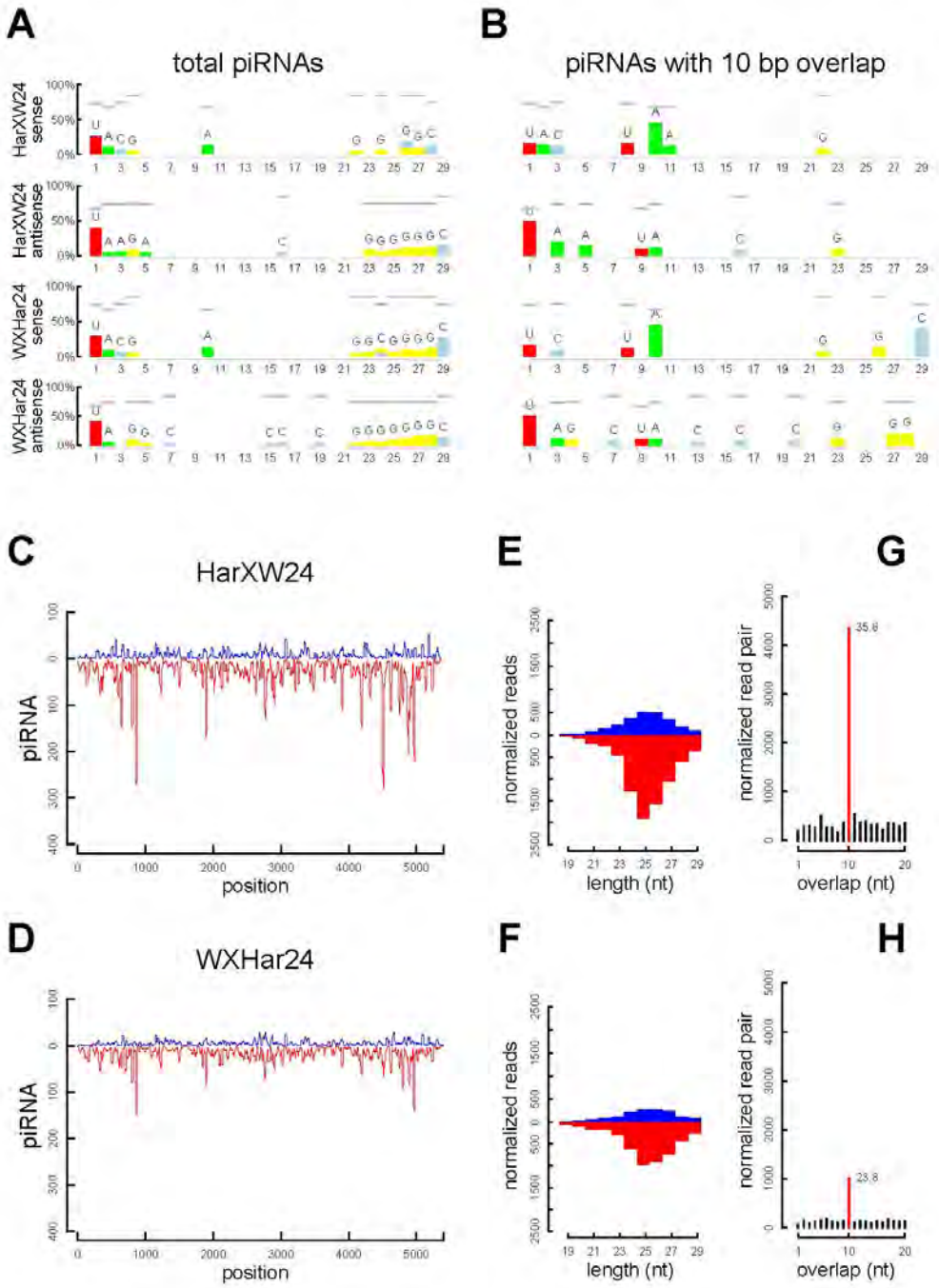
A
total piRNAs
B
piRNAs with 10 bp overlap
HarXW24 sense
HarXW24 antisense
WXHar24 sense
WXHar24 antisense
C
HarXW24
piRNA
position
D
WXHar24
E
normalized reads
length (nt)
F
G
normalized read pair
overlap (nt)
35.8
H
23.8

jockey

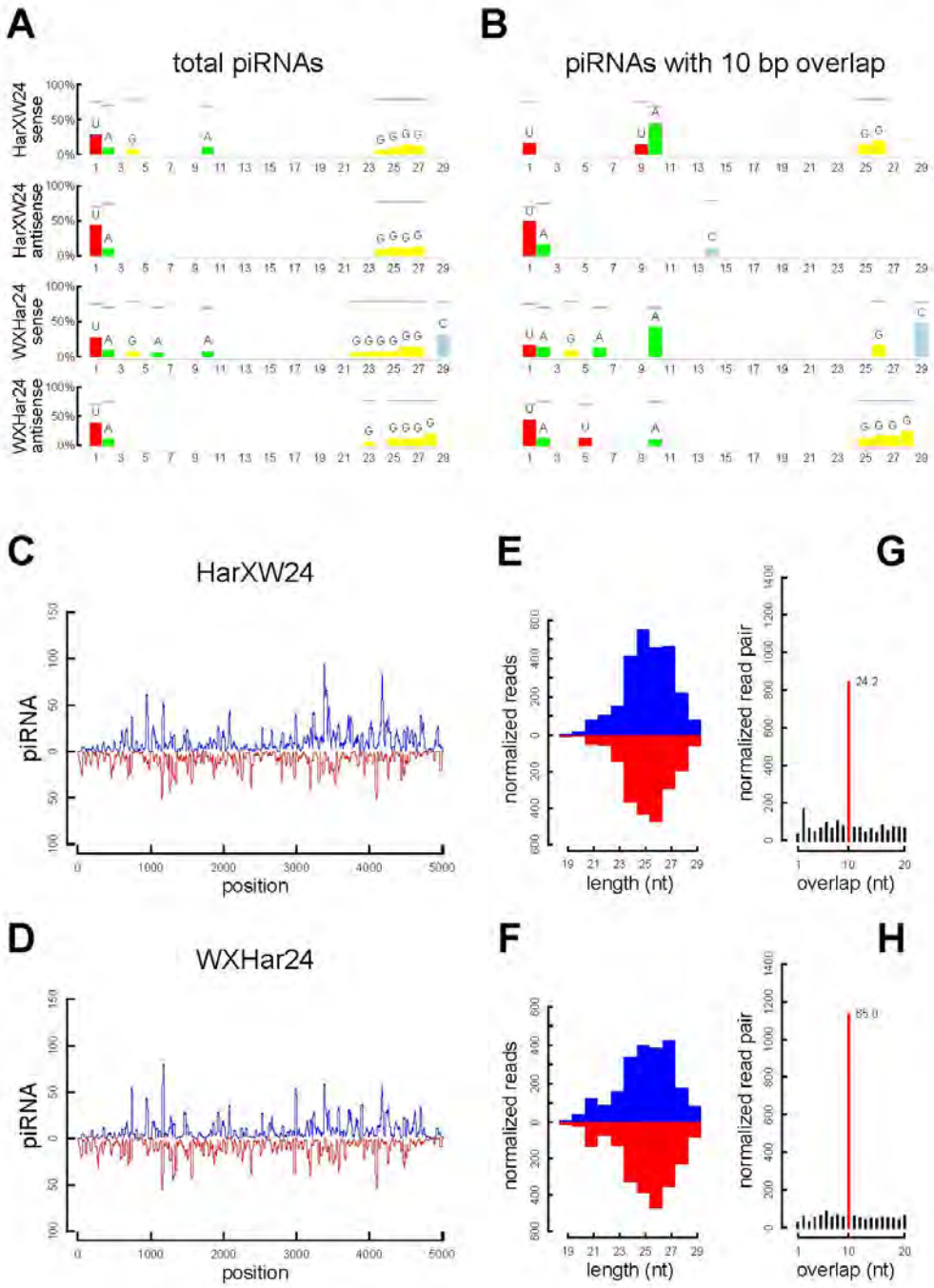
A
total piRNAs
B
piRNAs with 10 bp overlap
HarXW24 sense
HarXW24 antisense
WXHar24 sense
WXHar24 antisense
C
HarXW24
piRNA
position
D
WXHar24
E
F
normalized reads
length (nt)
G
H
normalized read pair
overlap (nt)
24.2
85.0

jockey2

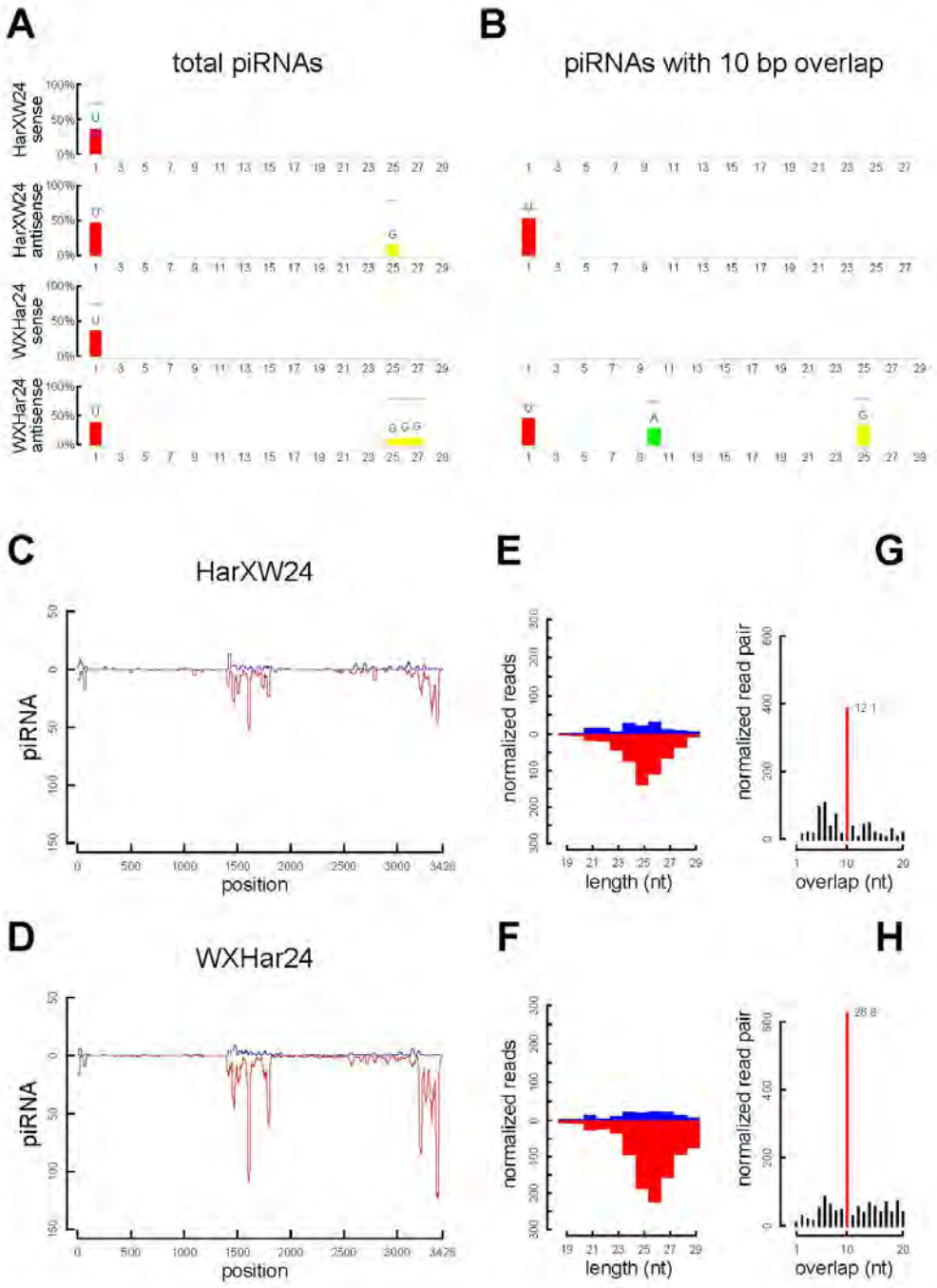
A
total piRNAs
B
piRNAs with 10 bp overlap
HarXW24 sense
HarXW24 antisense
WXHar24 sense
WXHar24 antisense
C
HarXW24
D
WXHar24
piRNA
position
E
F
normalized reads
length (nt)
G
H
normalized read pair
overlap (nt)

Juan

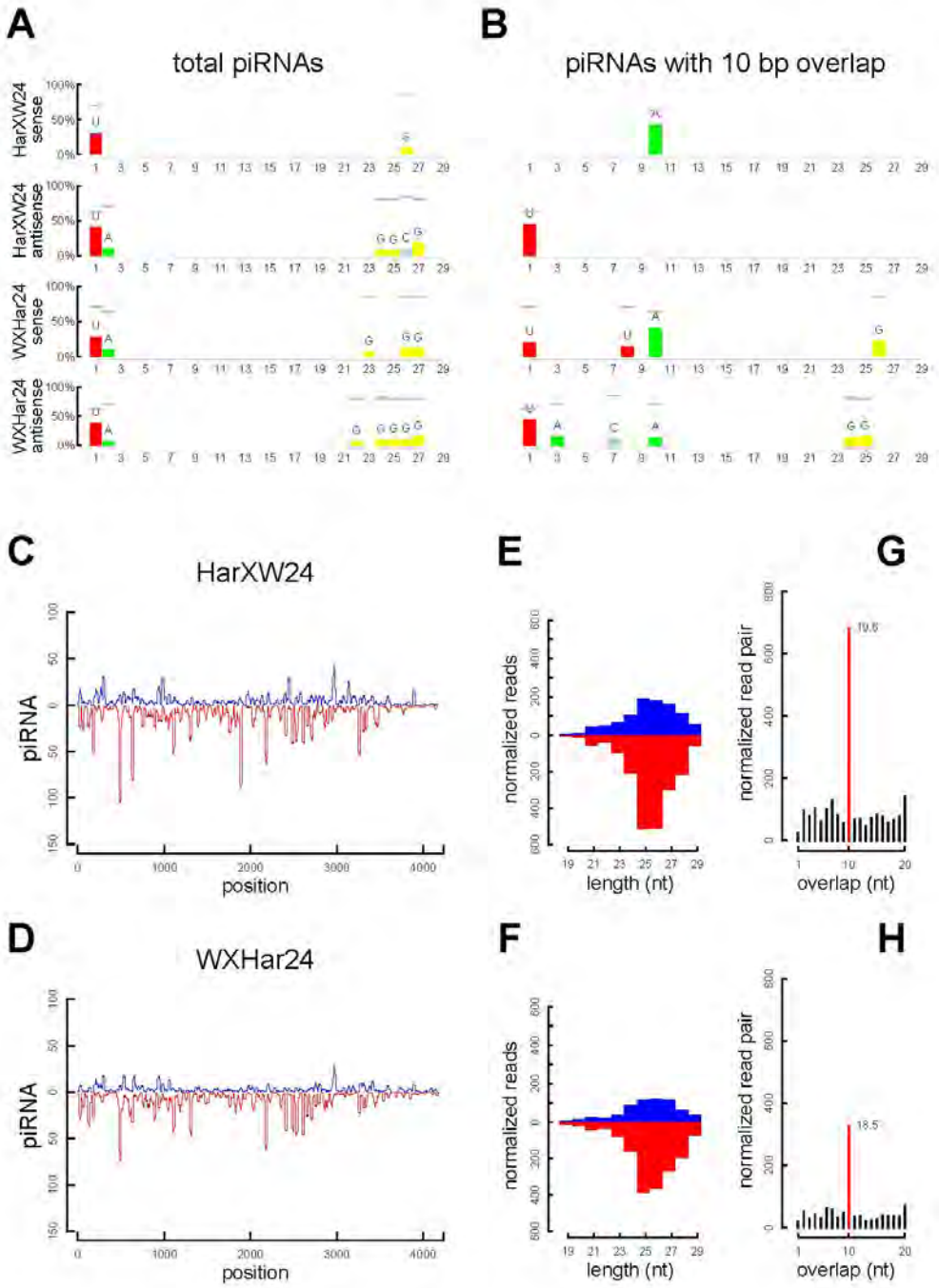
A
total piRNAs
B
piRNAs with 10 bp overlap
HarXW24 sense
HarXW24 antisense
WXHar24 sense
WXHar24 antisense
C
HarXW24
piRNA
position
D
WXHar24
piRNA
position
E
normalized reads
length (nt)
F
normalized reads
length (nt)
G
normalized read pair
overlap (nt)
19.6
H
normalized read pair
overlap (nt)
18.5

looper1

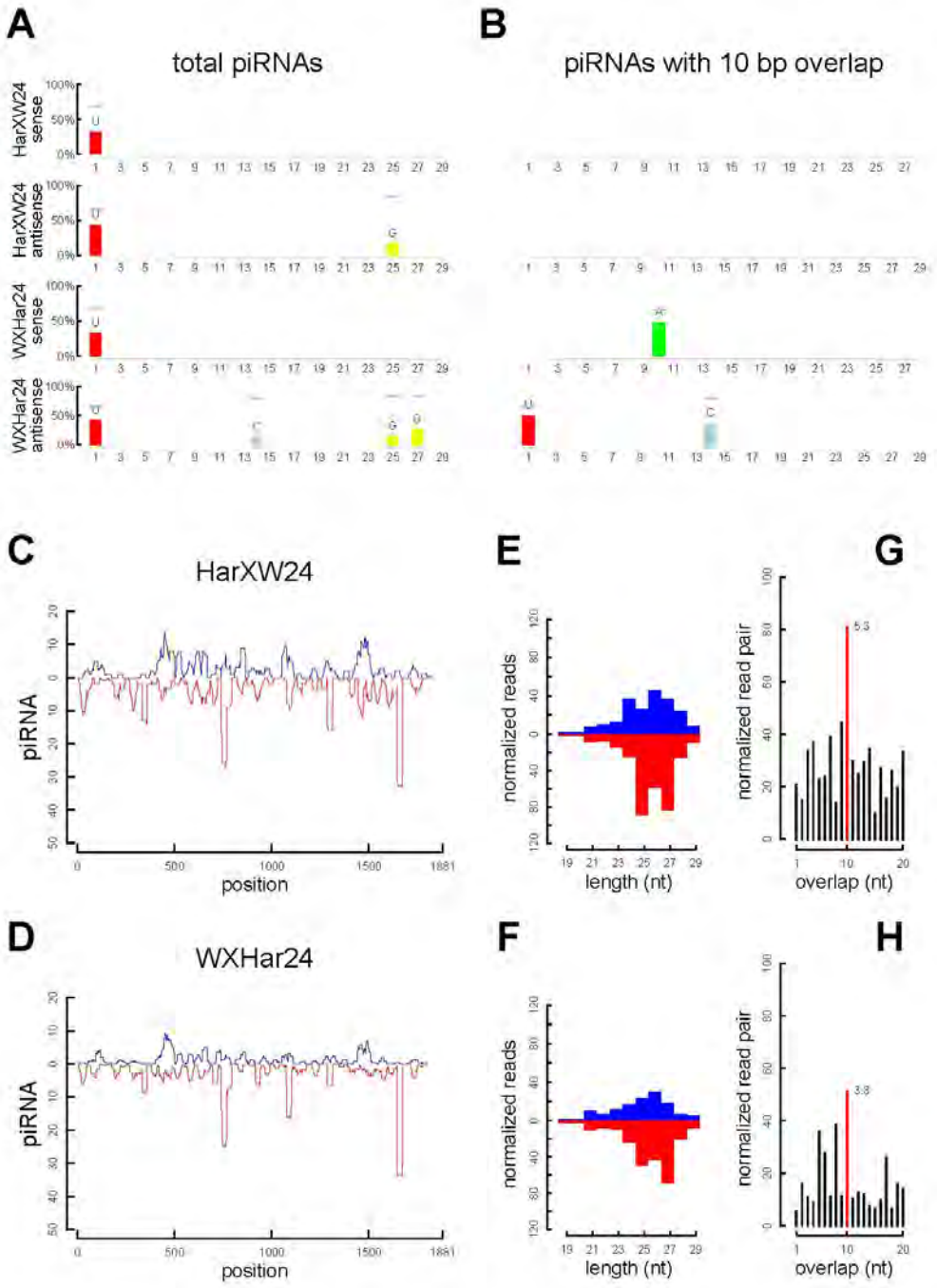
A
total piRNAs
B
piRNAs with 10 bp overlap
HarXW24 sense
HarXW24 antisense
WXHar24 sense
WXHar24 antisense
C
HarXW24
piRNA
position
D
WXHar24
piRNA
position
E
normalized reads
length (nt)
F
normalized reads
length (nt)
G
normalized read pair
overlap (nt)
5.3
H
normalized read pair
overlap (nt)
3.8

mariner2

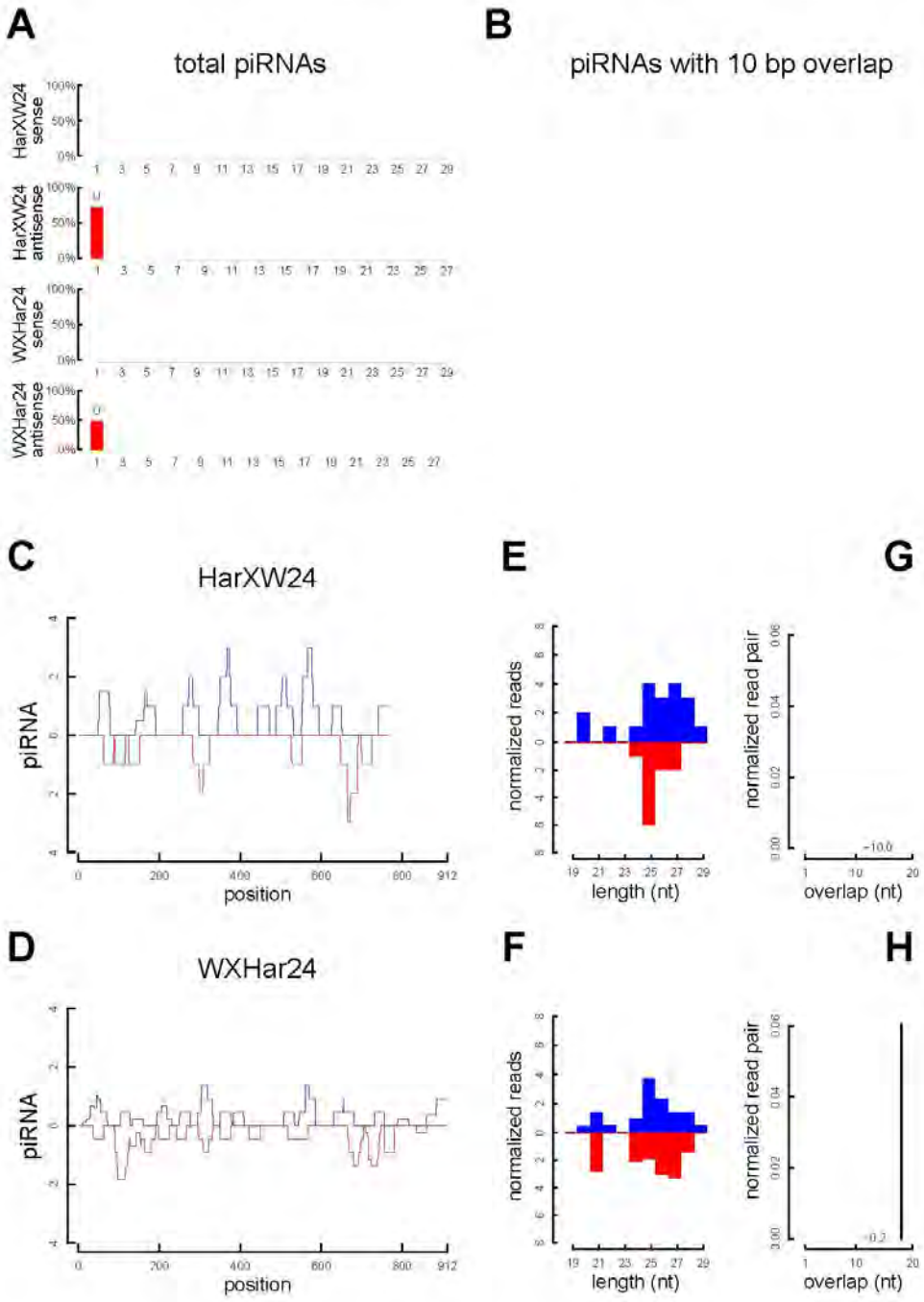
A
total piRNAs
B
piRNAs with 10 bp overlap
HarXW24 sense
HarXW24 antisense
WXHar24 sense
WXHar24 antisense
C
HarXW24
D
WXHar24
piRNA
position
E
F
normalized reads
length (nt)
G
H
normalized read pair
overlap (nt)

Max element

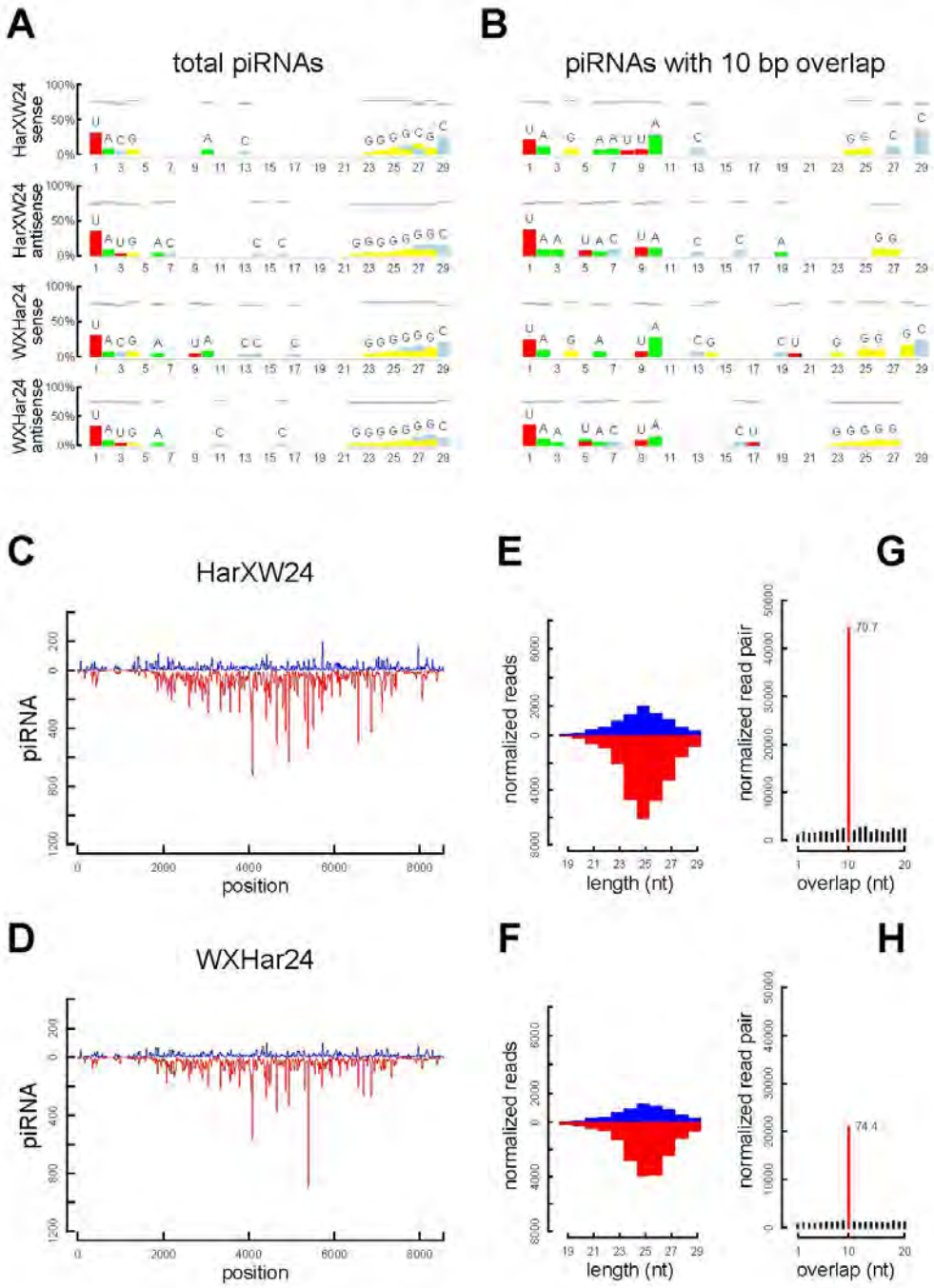
A
total piRNAs
B
piRNAs with 10 bp overlap
HarXW24 sense
HarXW24 antisense
WXHar24 sense
WXHar24 antisense
C
HarXW24
D
WXHar24
piRNA
position
E
F
normalized reads
length (nt)
G
H
normalized read pair
overlap (nt)
70.7
74.4

McClintock

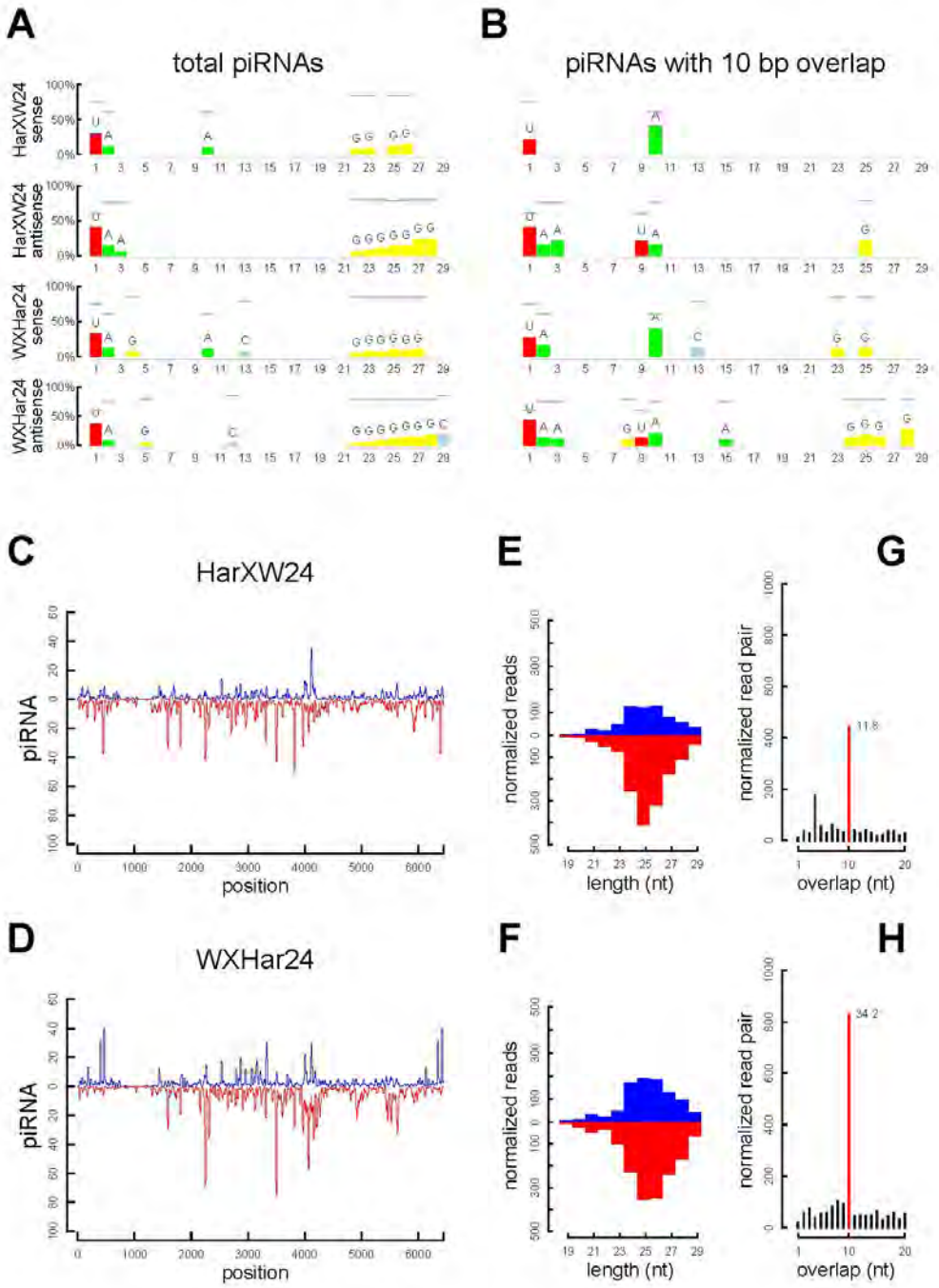
A
total piRNAs
B
piRNAs with 10 bp overlap
HarXW24 sense
HarXW24 antisense
WXHar24 sense
WXHar24 antisense
C
HarXW24
D
WXHar24
piRNA
position
E
F
normalized reads
length (nt)
G
H
normalized read pair
overlap (nt)
11.8
34.2

mdg1

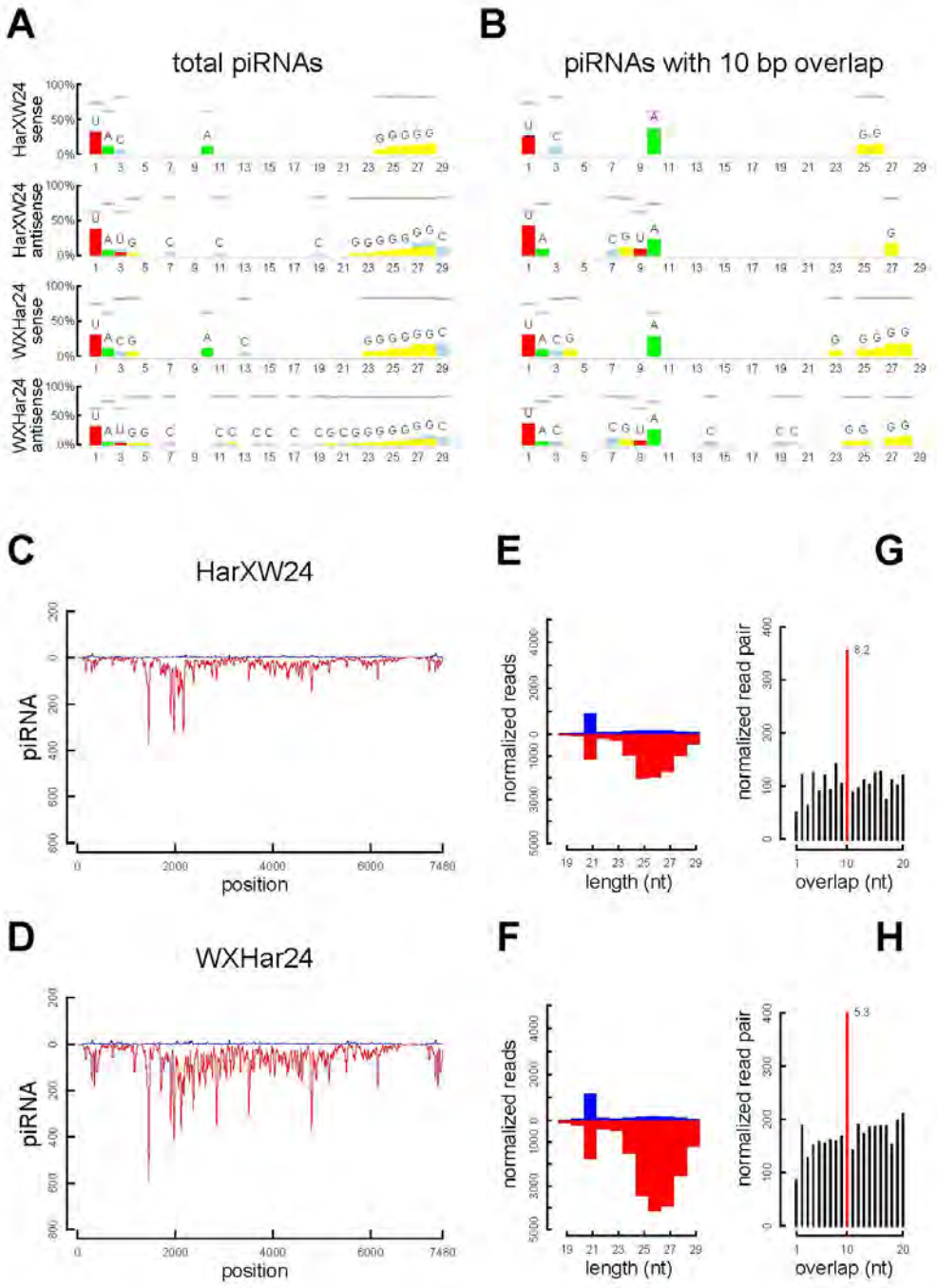
A
total piRNAs
B
piRNAs with 10 bp overlap
HarXW24 sense
HarXW24 antisense
WXHar24 sense
WXHar24 antisense
C
HarXW24
D
WXHar24
piRNA
position
E
F
normalized reads
length (nt)
G
H
normalized read pair
overlap (nt)
8.2
5.3

mdg3

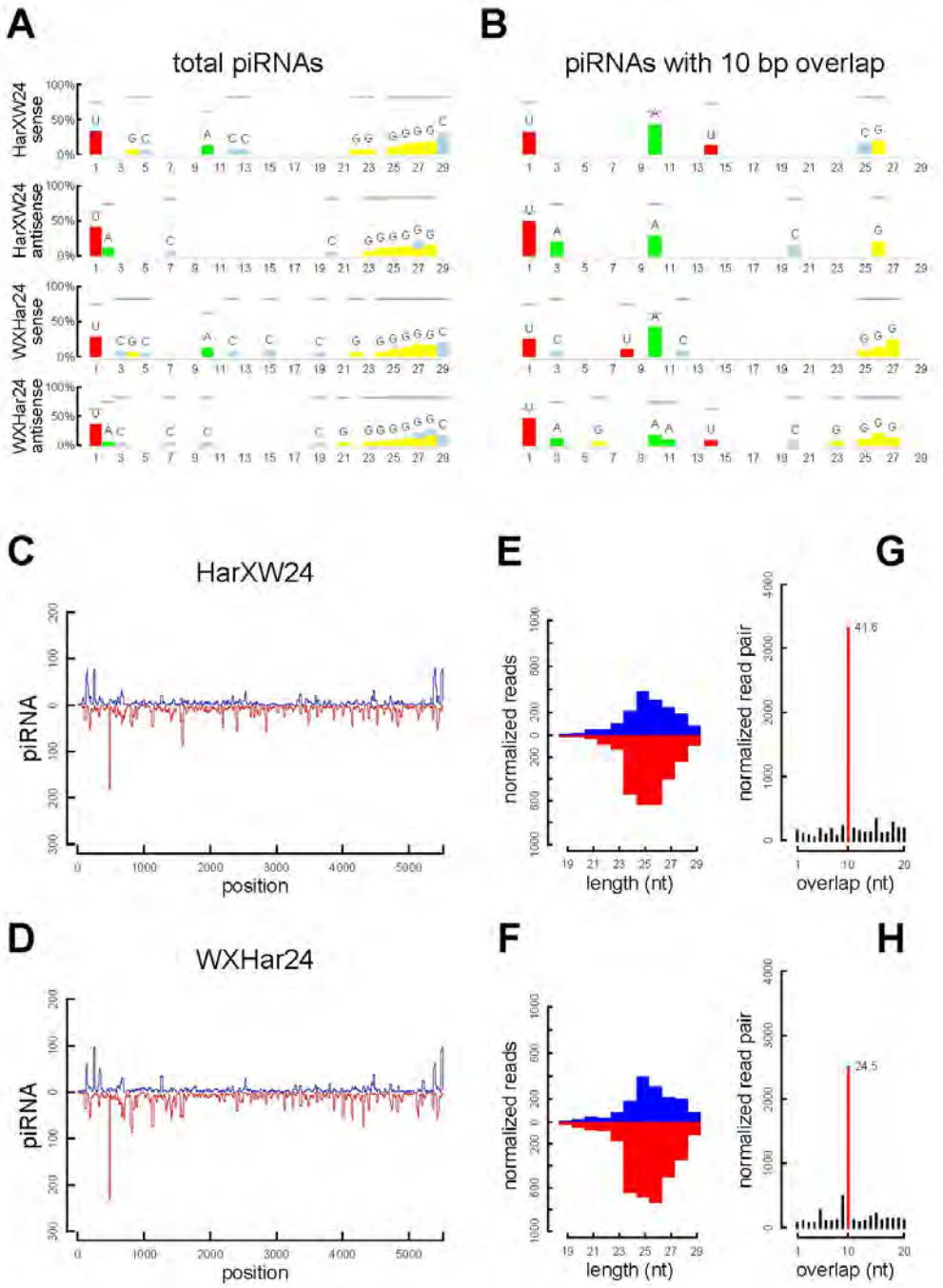
A
total piRNAs
B
piRNAs with 10 bp overlap
HarXW24 sense
HarXW24 antisense
WXHar24 sense
WXHar24 antisense
C
HarXW24
D
WXHar24
piRNA
position
E
F
normalized reads
length (nt)
G
H
normalized read pair
overlap (nt)
41.6
24.5

micropia

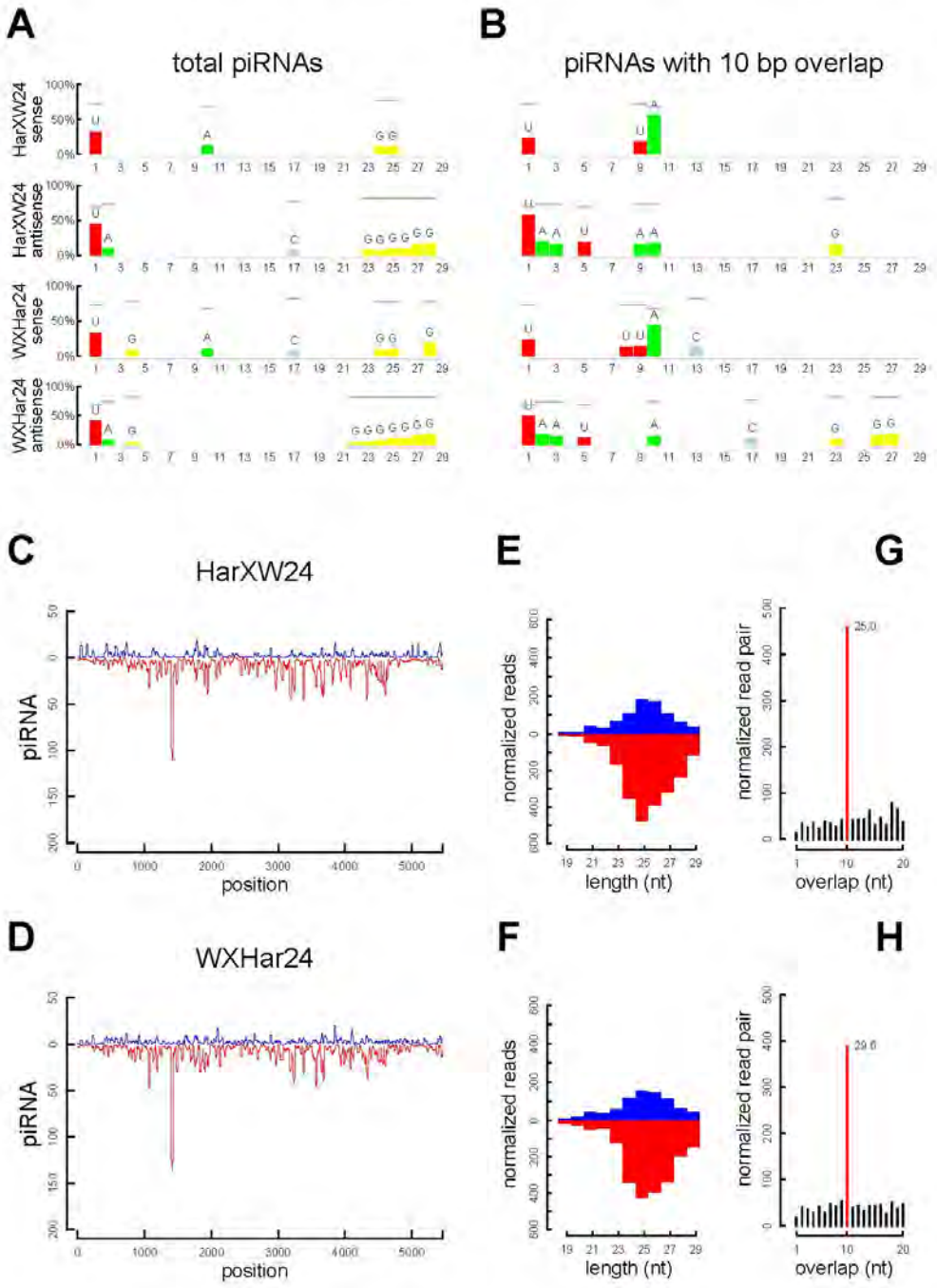
A
total piRNAs
B
piRNAs with 10 bp overlap
HarXW24 sense
HarXW24 antisense
WXHar24 sense
WXHar24 antisense
C
HarXW24
D
WXHar24
piRNA
position
E
F
normalized reads
length (nt)
G
H
normalized read pair
overlap (nt)

NOF

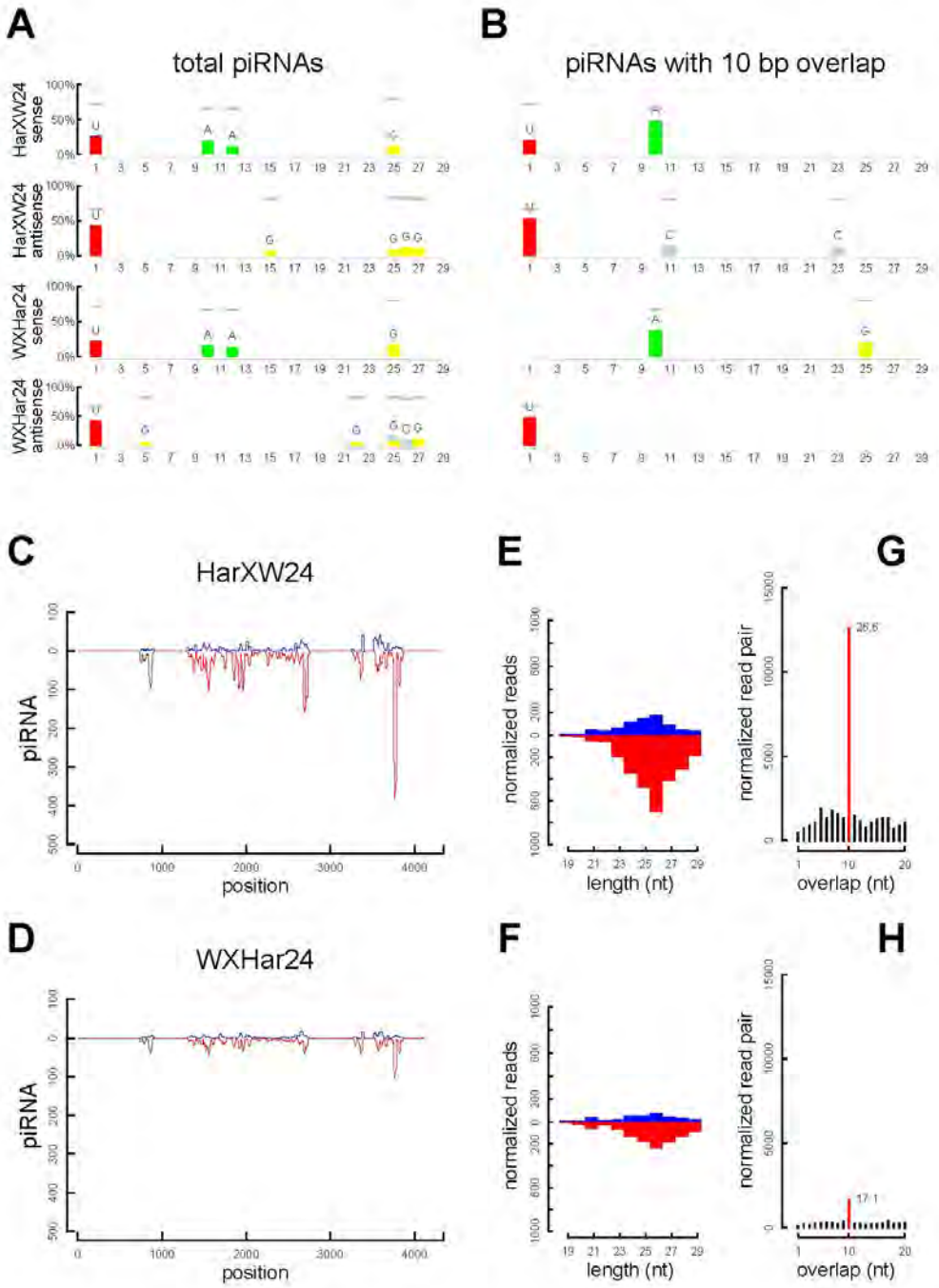
A
total piRNAs
B
piRNAs with 10 bp overlap
HarXW24 sense
HarXW24 antisense
WXHar24 sense
WXHar24 antisense
C
HarXW24
D
WXHar24
piRNA
position
E
F
normalized reads
length (nt)
G
H
normalized read pair
overlap (nt)

opus

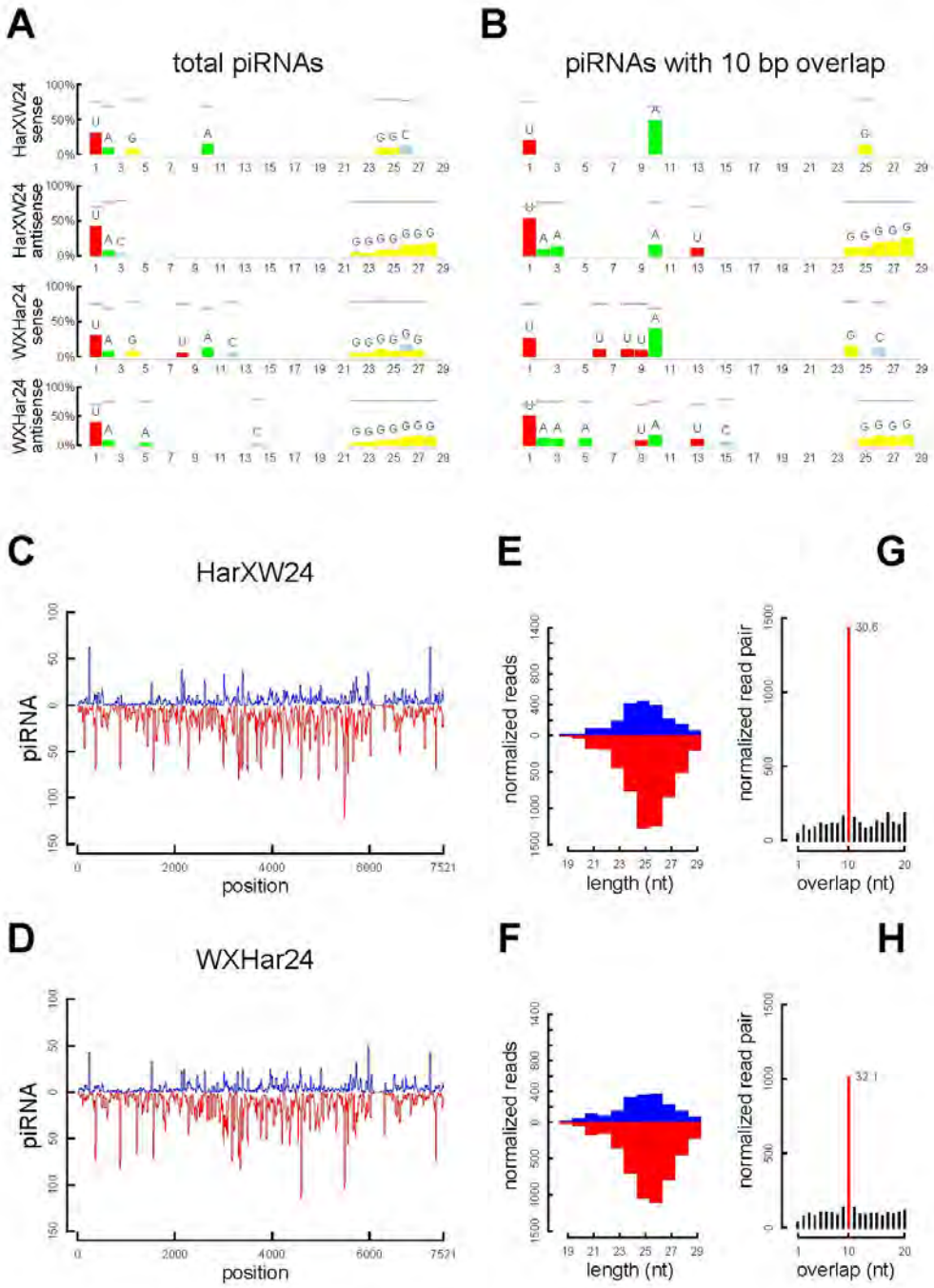
A
total piRNAs
B
piRNAs with 10 bp overlap
HarXW24 sense
HarXW24 antisense
WXHar24 sense
WXHar24 antisense
C
HarXW24
piRNA
position
D
WXHar24
E
normalized reads
length (nt)
F
G
normalized read pair
overlap (nt)
30.6
H
32.1

Osvaldo

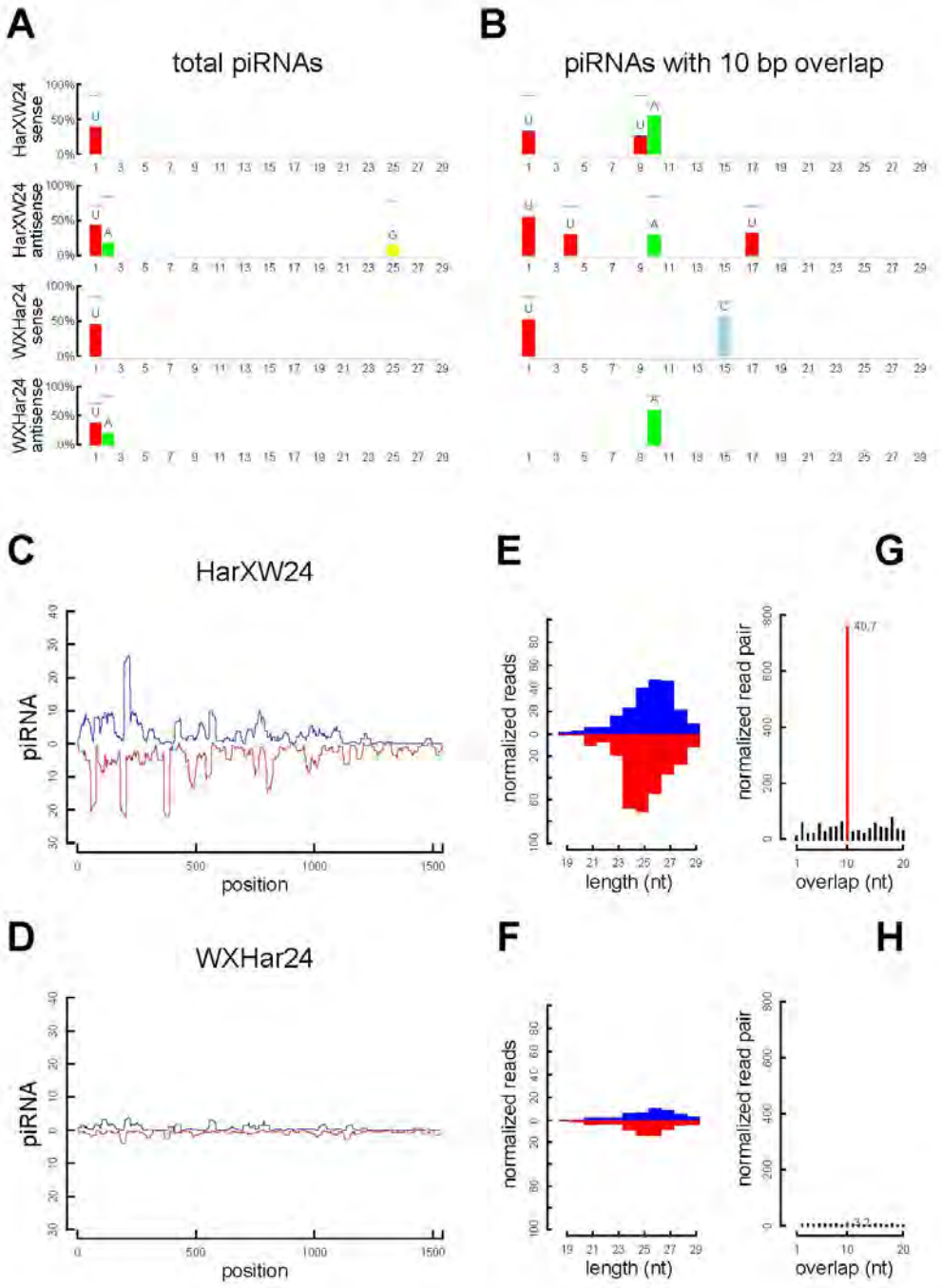
A
total piRNAs
HarXW24 sense
HarXW24 antisense
WXHar24 sense
WXHar24 antisense
B
piRNAs with 10 bp overlap
C
HarXW24
piRNA
position
D
WXHar24
piRNA
position
E
normalized reads
length (nt)
F
normalized reads
length (nt)
G
normalized read pair
overlap (nt)
40.7
H
normalized read pair
overlap (nt)

P element

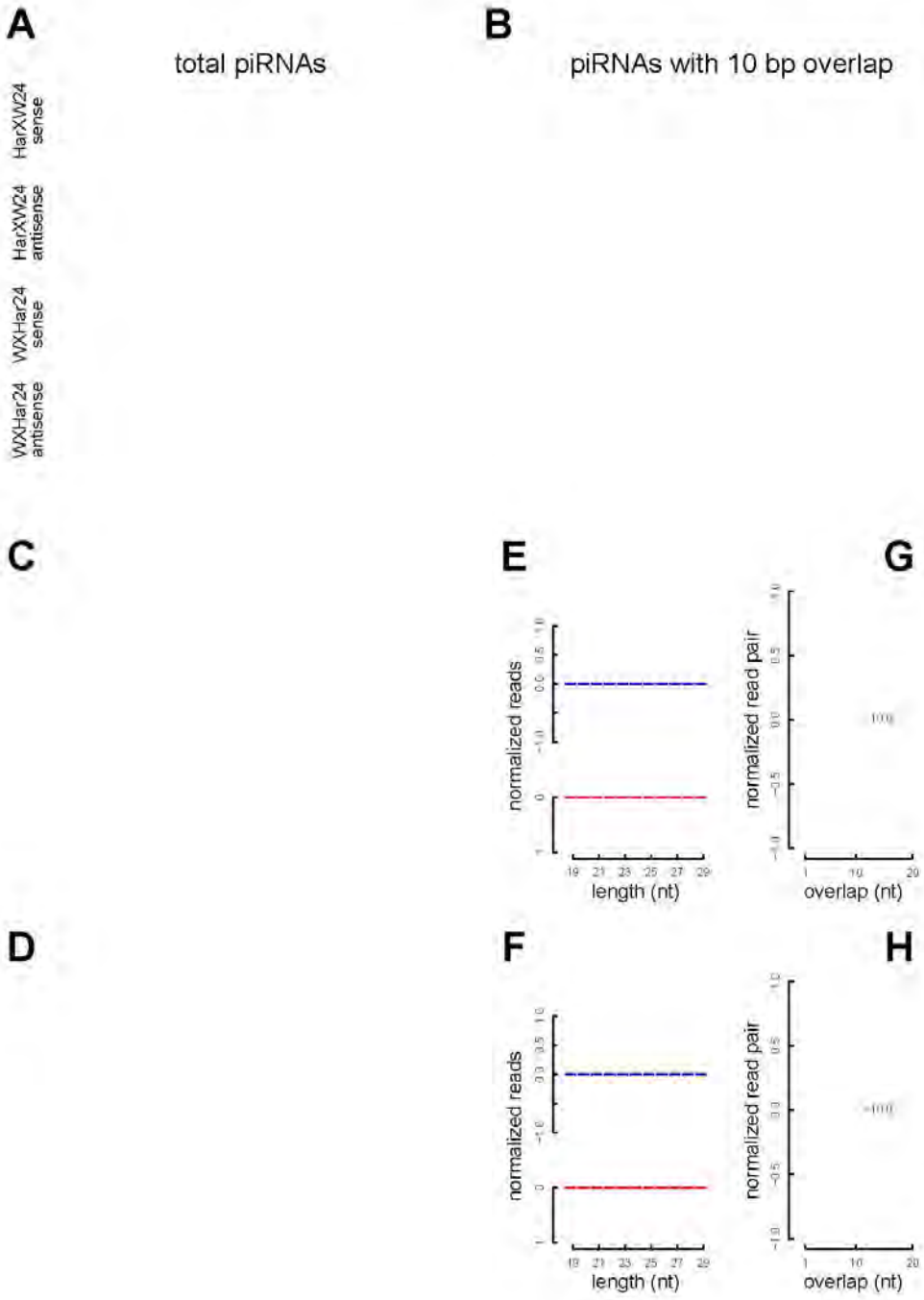
A
total piRNAs
B
piRNAs with 10 bp overlap
HarXW24 sense
HarXW24 antisense
WXHar24 sense
WXHar24 antisense
C
D
E
F
G
H
normalized reads
length (nt)
normalized read pair
overlap (nt)

Penelope

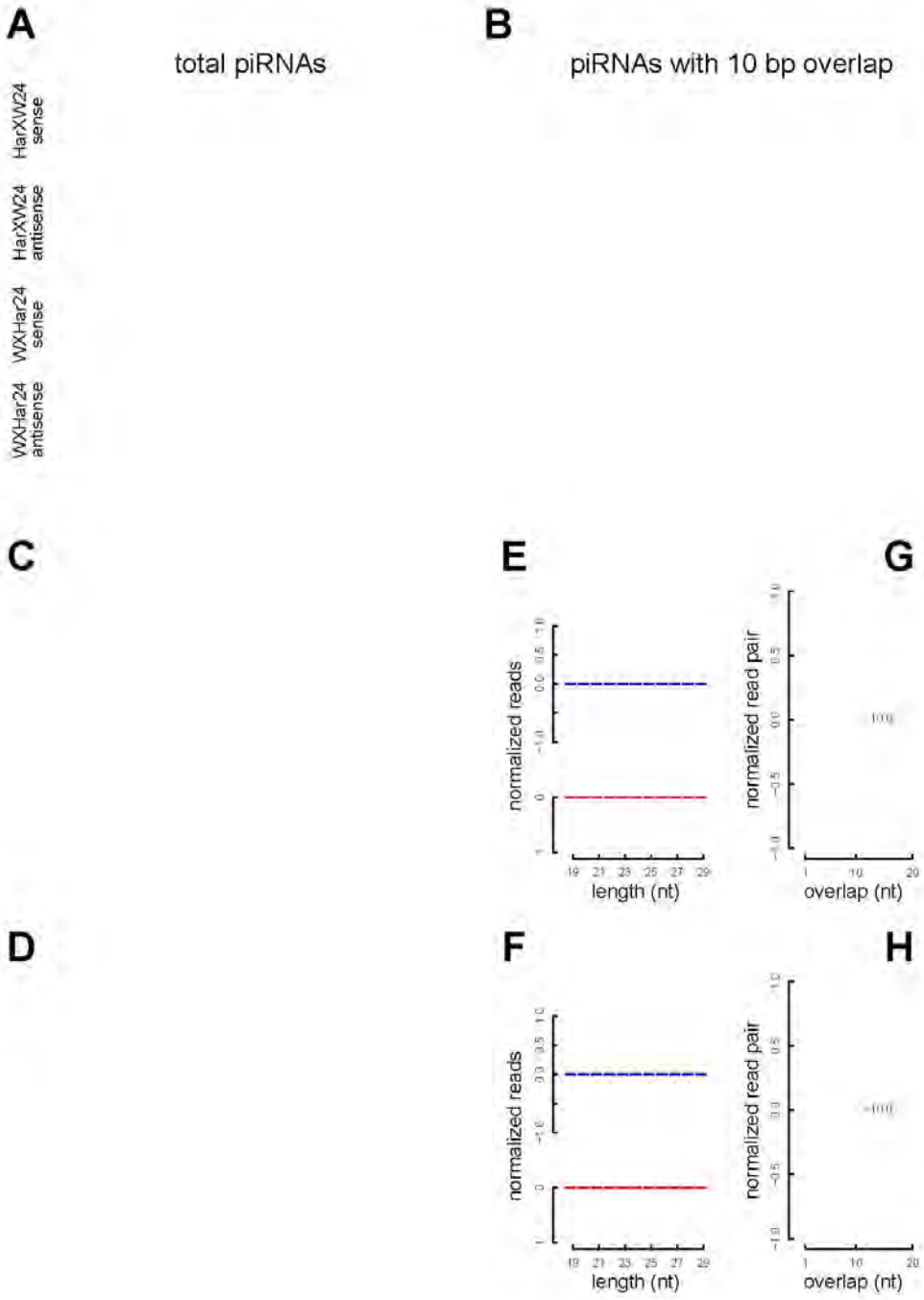
A
total piRNAs
HarXW24 sense
HarXW24 antisense
WXHar24 sense
WXHar24 antisense
B
piRNAs with 10 bp overlap
C
D
E
normalized reads
length (nt)
F
normalized reads
length (nt)
G
normalized read pair
overlap (nt)
H
normalized read pair
overlap (nt)

pogo

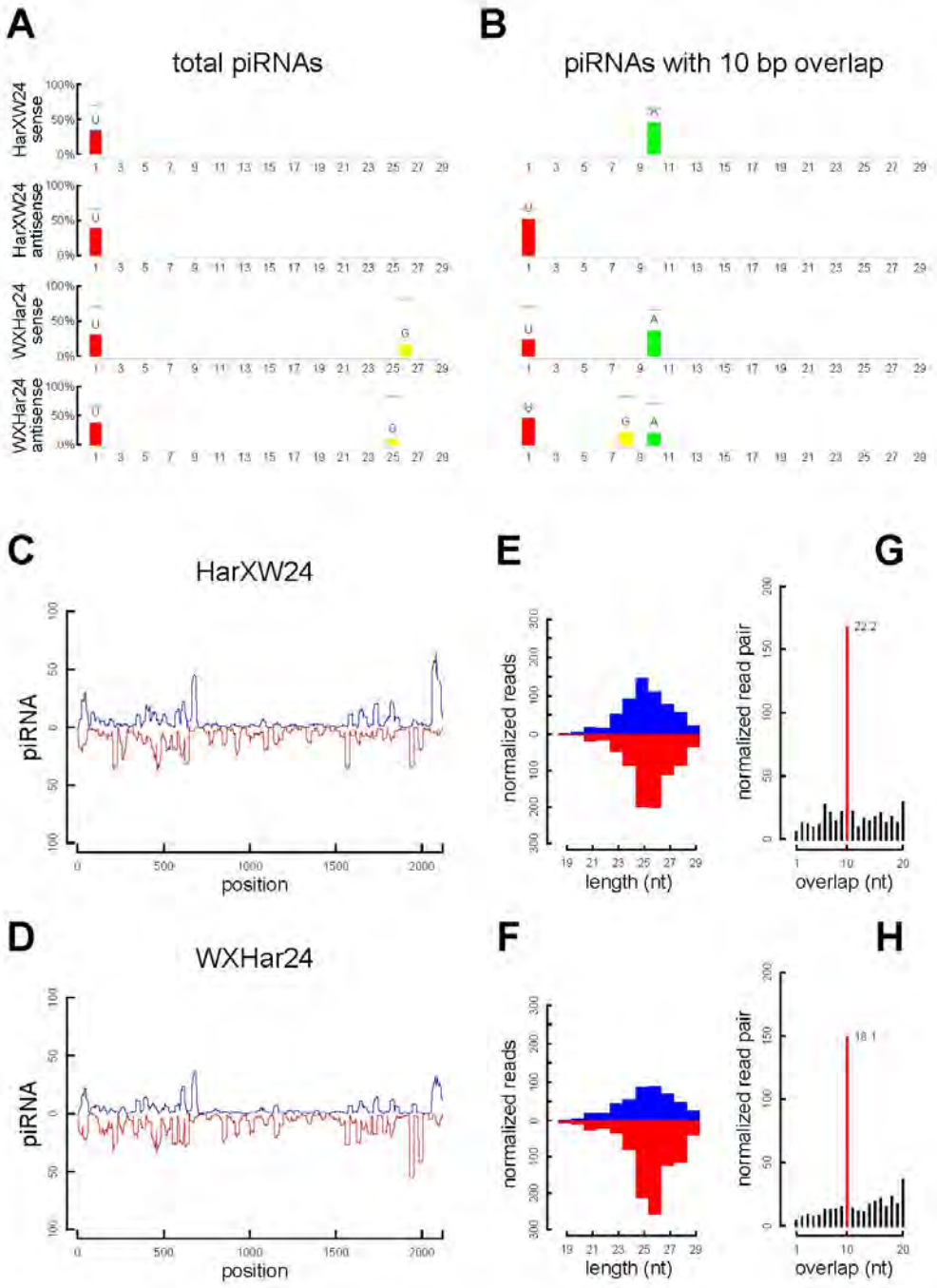
A
total piRNAs
B
piRNAs with 10 bp overlap
HarXW24 sense
HarXW24 antisense
WXHar24 sense
WXHar24 antisense
C
HarXW24
D
WXHar24
piRNA
position
E
F
normalized reads
length (nt)
G
H
normalized read pair
overlap (nt)
22.2
18.1

Porto1

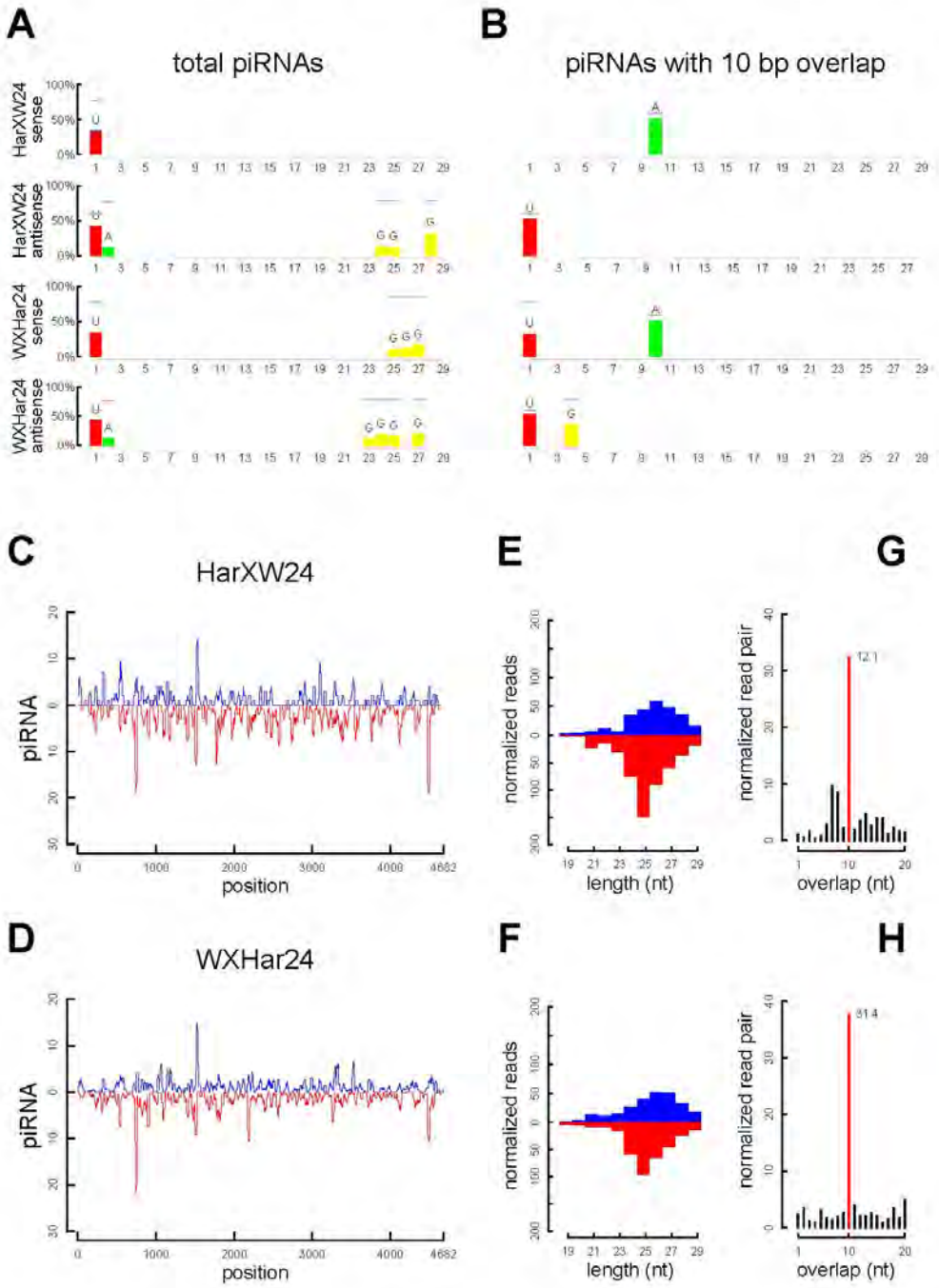
A
total piRNAs
B
piRNAs with 10 bp overlap
HarXW24 sense
HarXW24 antisense
WXHar24 sense
WXHar24 antisense
C
HarXW24
D
WXHar24
piRNA
position
E
F
normalized reads
length (nt)
G
H
normalized read pair
overlap (nt)

Q element

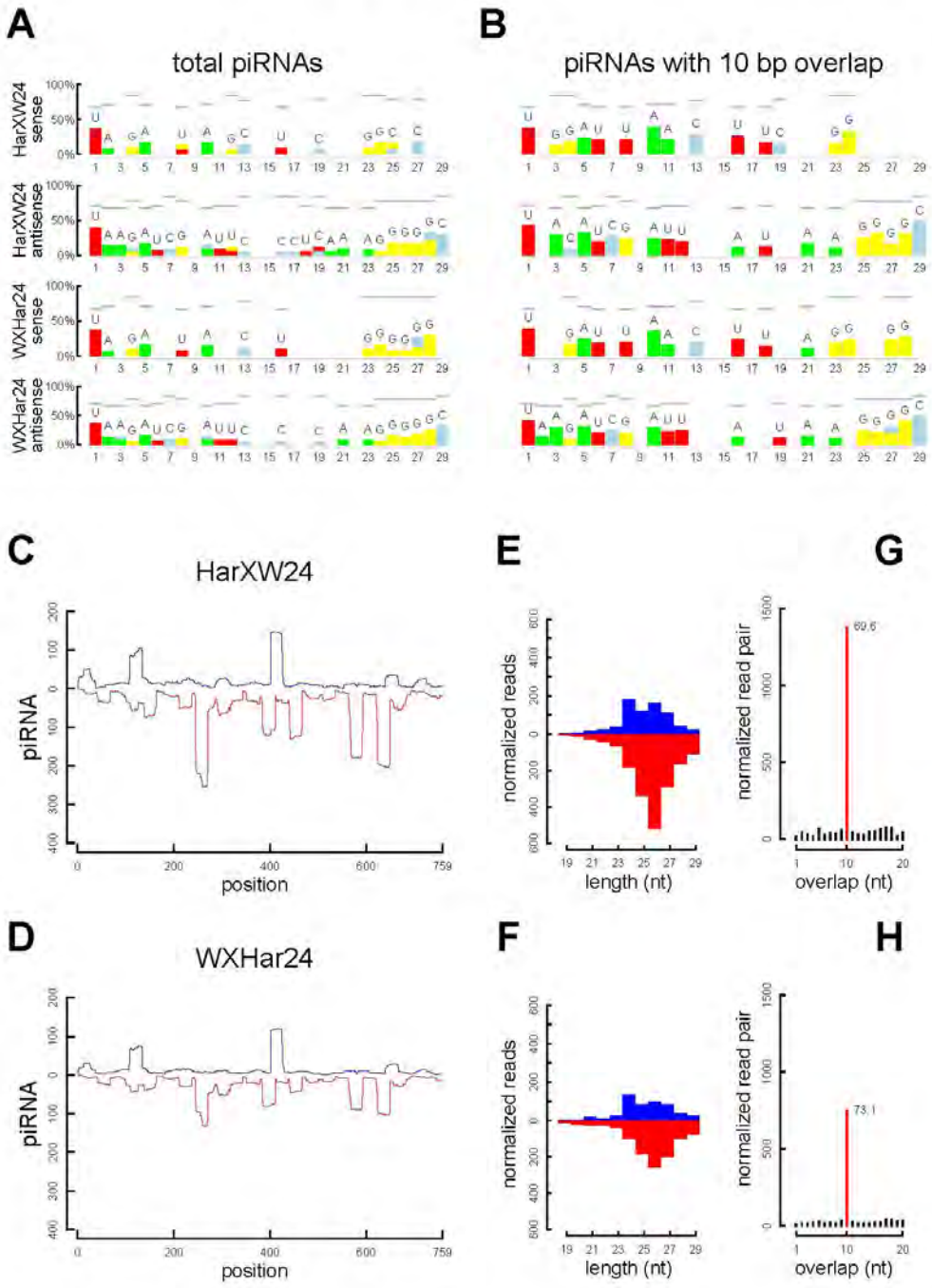
A
total piRNAs
B
piRNAs with 10 bp overlap
HarXW24 sense
HarXW24 antisense
WXHar24 sense
WXHar24 antisense
C
HarXW24
piRNA
position
D
WXHar24
E
F
normalized reads
length (nt)
G
H
normalized read pair
overlap (nt)
69.6
73.1

Quasimodo

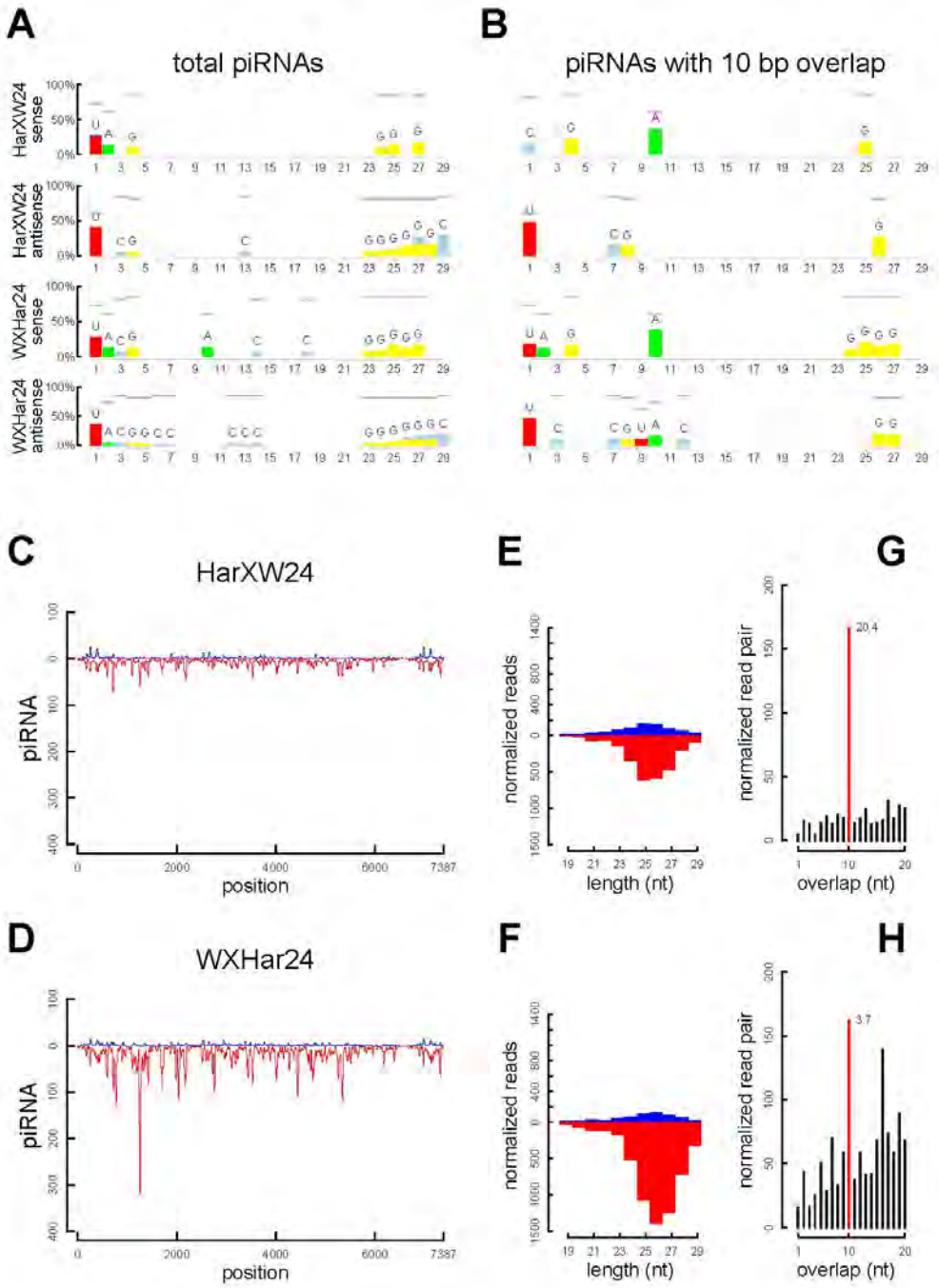
A
total piRNAs
B
piRNAs with 10 bp overlap
HarXW24 sense
HarXW24 antisense
WXHar24 sense
WXHar24 antisense
C
HarXW24
D
WXHar24
piRNA
position
E
F
normalized reads
length (nt)
G
H
normalized read pair
overlap (nt)
20.4
3.7

R1 2

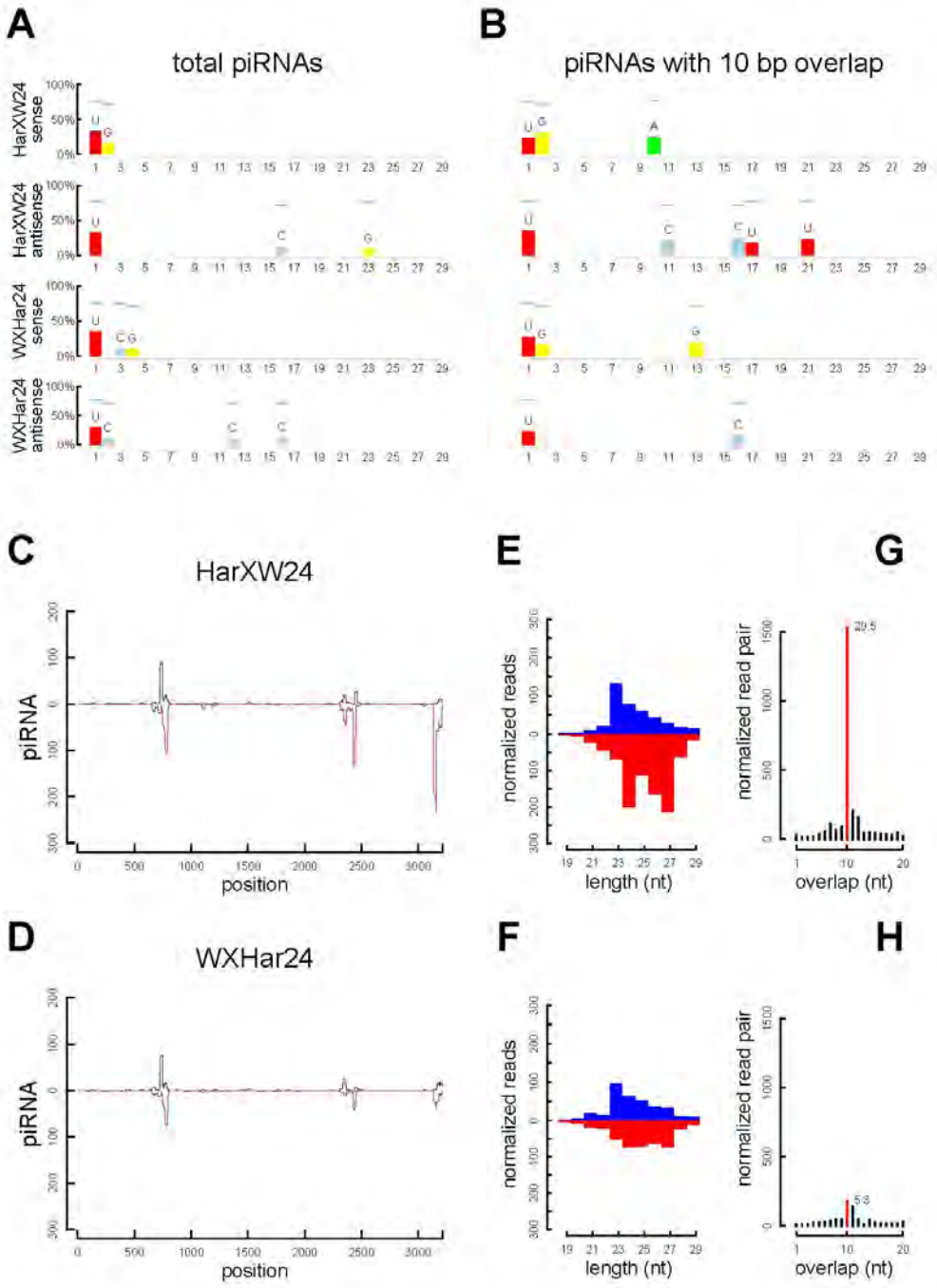
A
total piRNAs
B
piRNAs with 10 bp overlap
HarXW24 sense
HarXW24 antisense
WXHar24 sense
WXHar24 antisense
C
HarXW24
D
WXHar24
piRNA
position
E
F
normalized reads
length (nt)
G
H
normalized read pair
overlap (nt)
29.5
5.8

R1A1 element

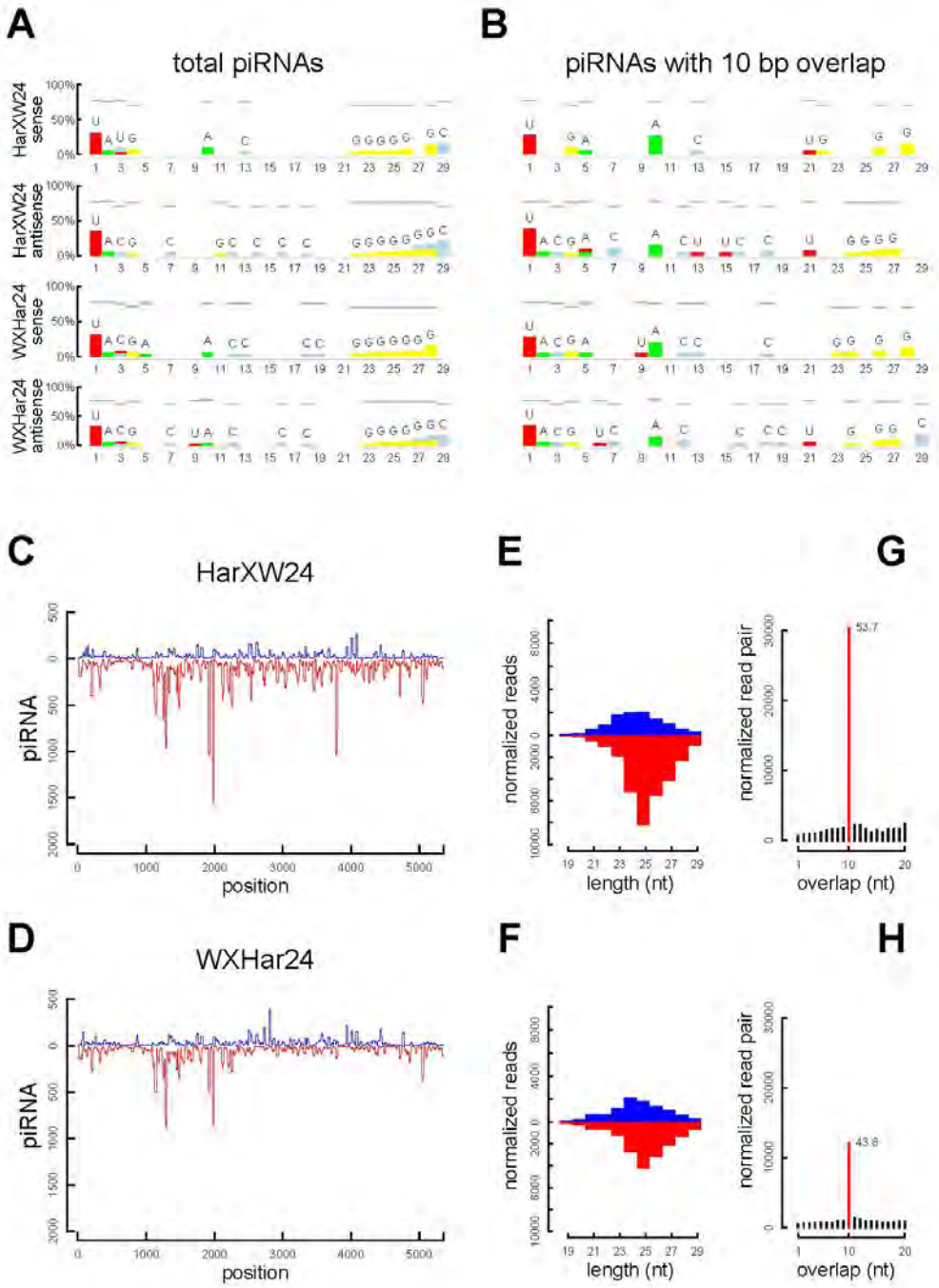

R2 element

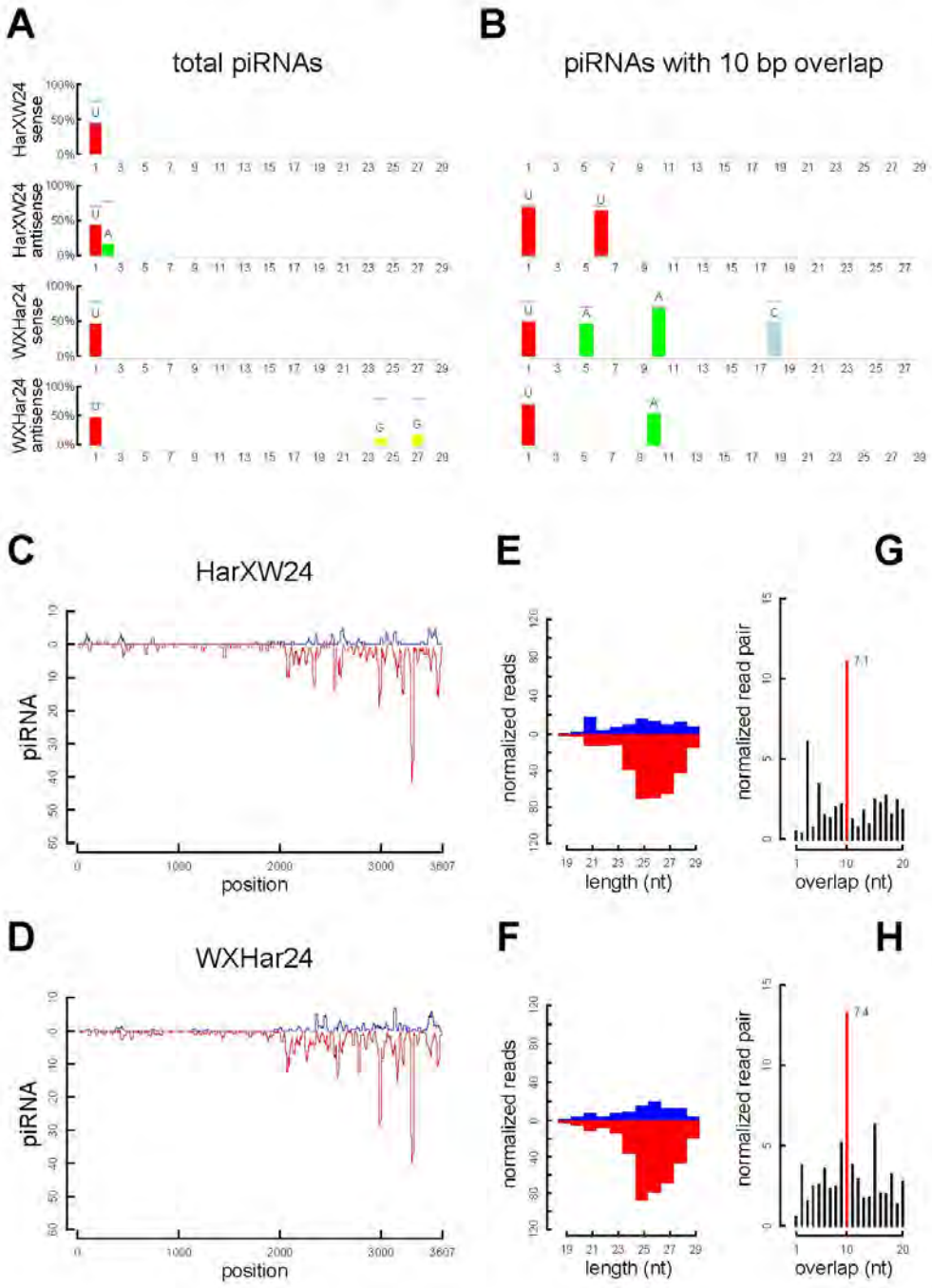
A
total piRNAs
B
piRNAs with 10 bp overlap
HarXW24 sense
HarXW24 antisense
WXHar24 sense
WXHar24 antisense
C
HarXW24
D
WXHar24
piRNA
position
E
F
normalized reads
length (nt)
G
H
normalized read pair
overlap (nt)

roo

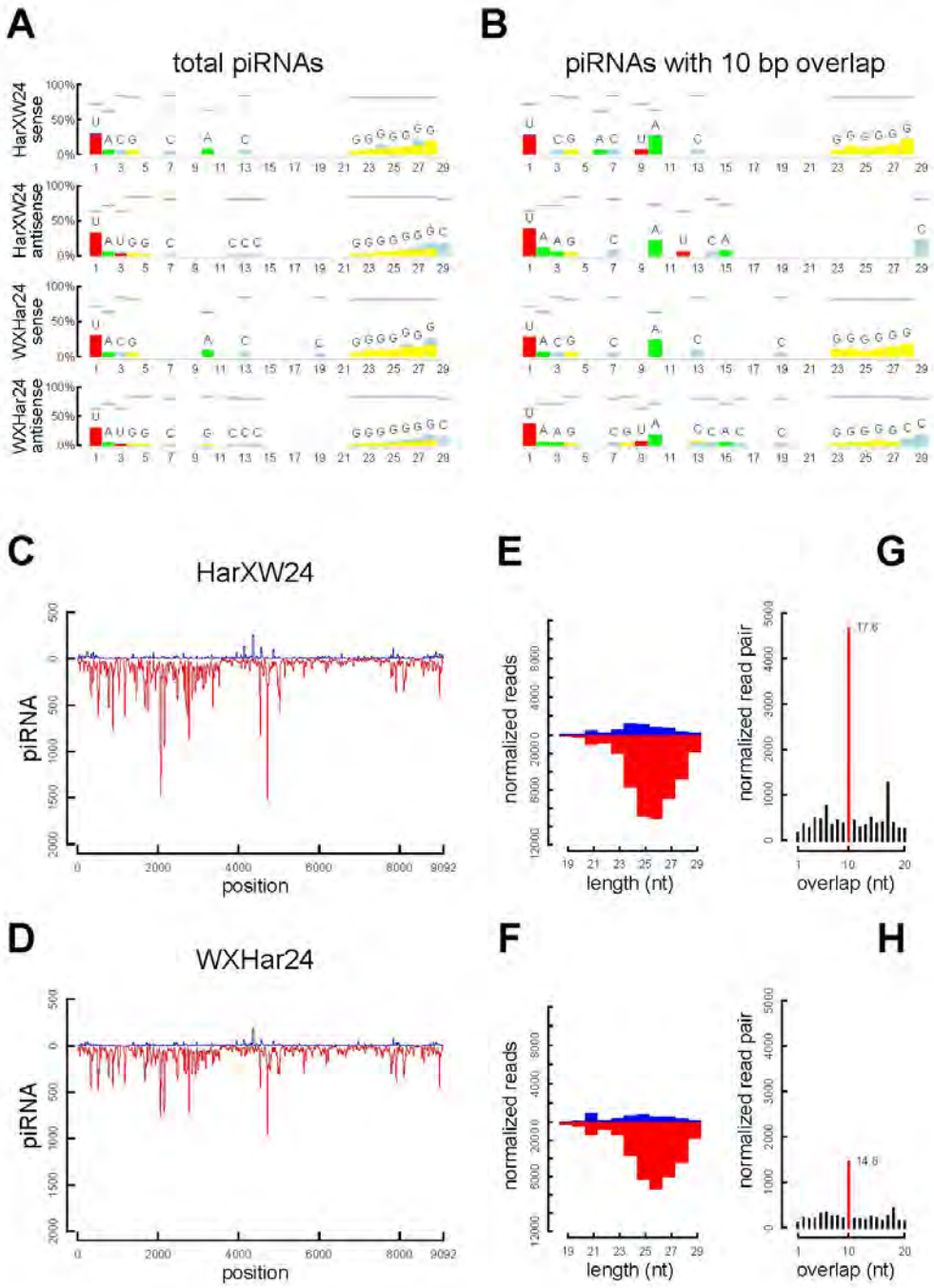
A
total piRNAs
B
piRNAs with 10 bp overlap
HarXW24 sense
HarXW24 antisense
WXHar24 sense
WXHar24 antisense
C
HarXW24
D
WXHar24
piRNA
position
E
F
normalized reads
length (nt)
G
H
normalized read pair
overlap (nt)
17.6
14.8

rooA

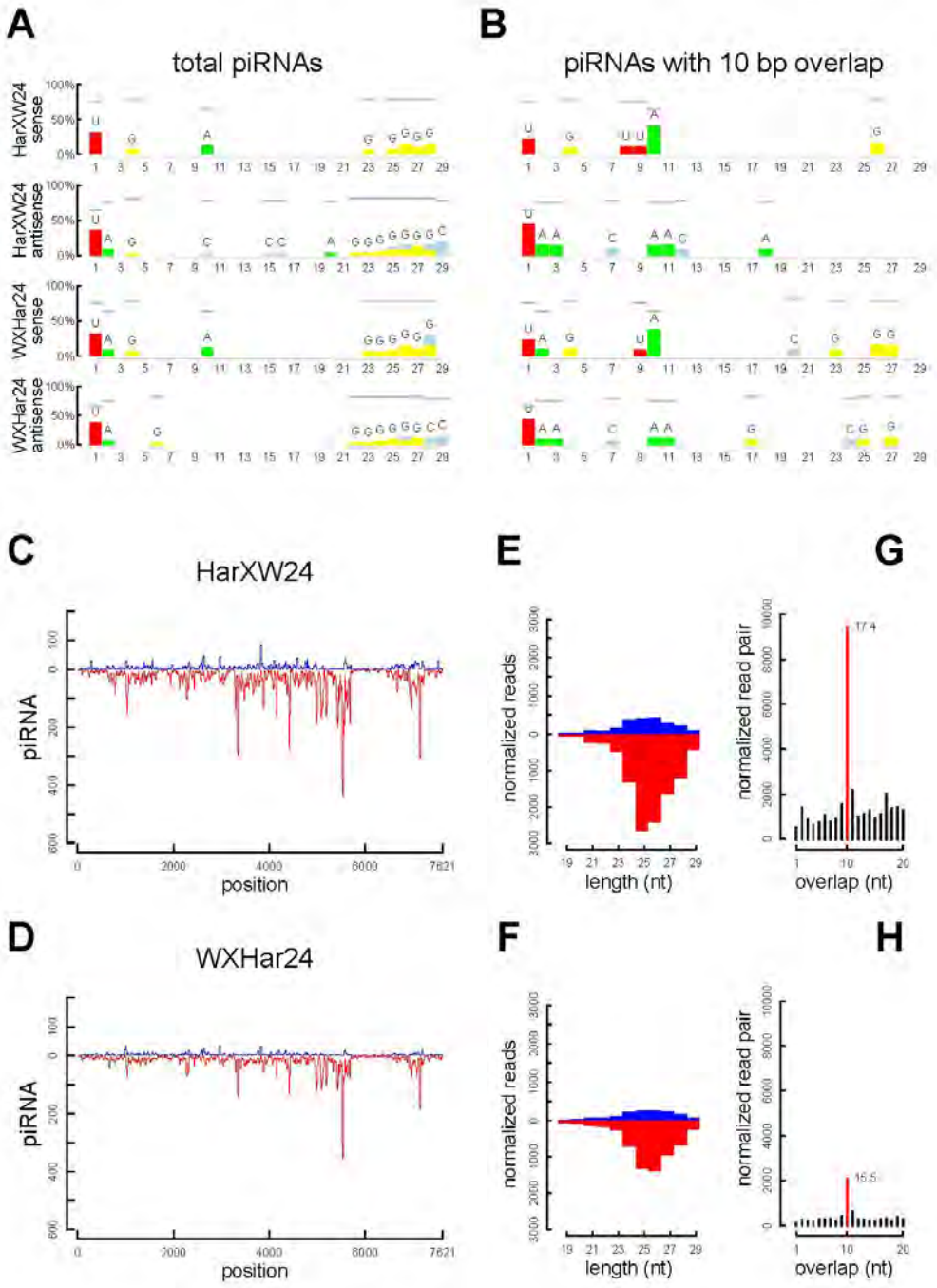
A
total piRNAs
B
piRNAs with 10 bp overlap
HarXW24 sense
HarXW24 antisense
WXHar24 sense
WXHar24 antisense
C
HarXW24
D
WXHar24
piRNA
position
E
F
normalized reads
length (nt)
G
H
normalized read pair
overlap (nt)
17.4
16.5

rover

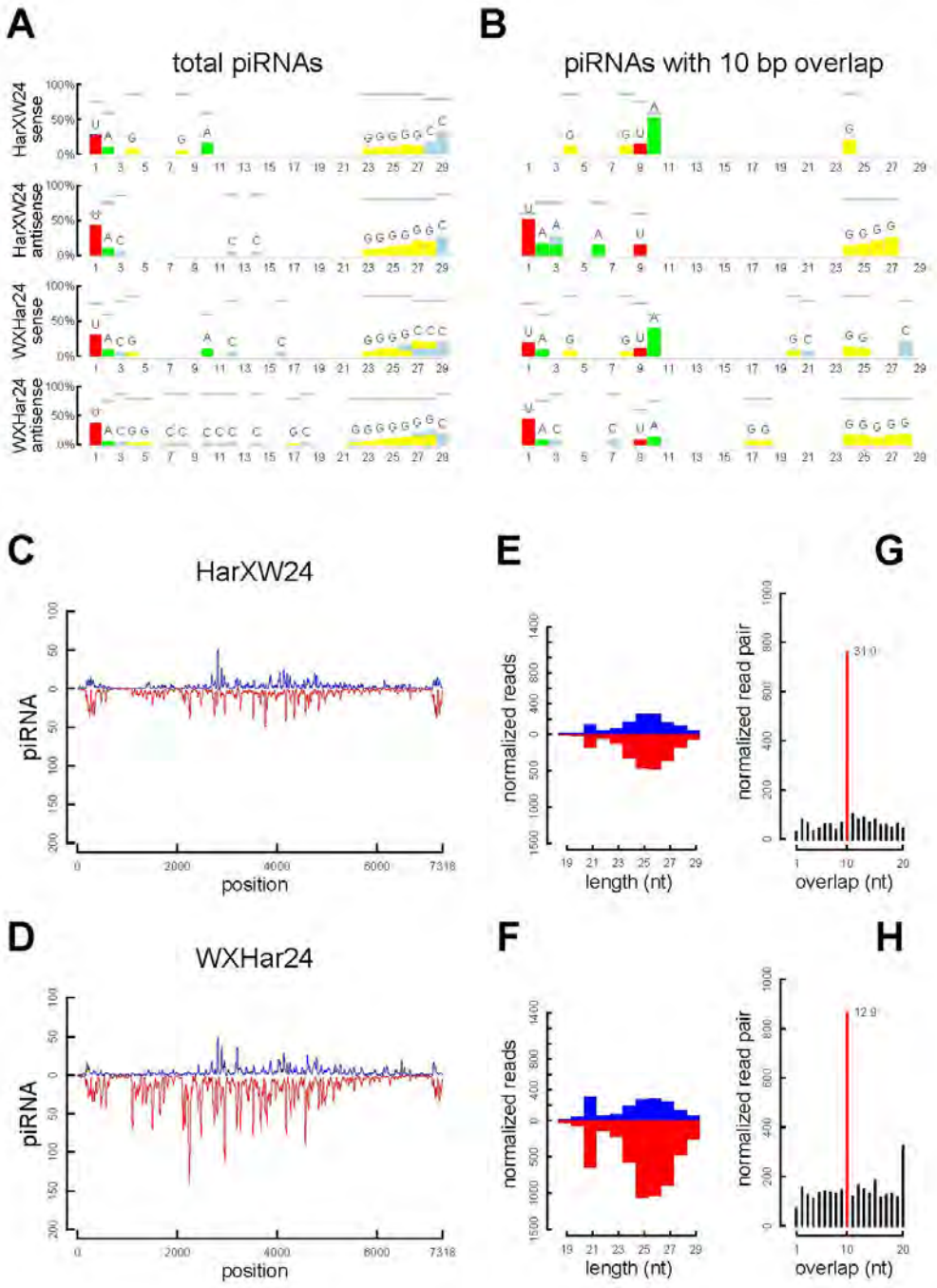
A
total piRNAs
B
piRNAs with 10 bp overlap
HarXW24 sense
HarXW24 antisense
WXHar24 sense
WXHar24 antisense
C
HarXW24
piRNA
position
D
WXHar24
piRNA
position
E
normalized reads
length (nt)
F
normalized reads
length (nt)
G
normalized read pair
overlap (nt)
H
normalized read pair
overlap (nt)

Rt1a

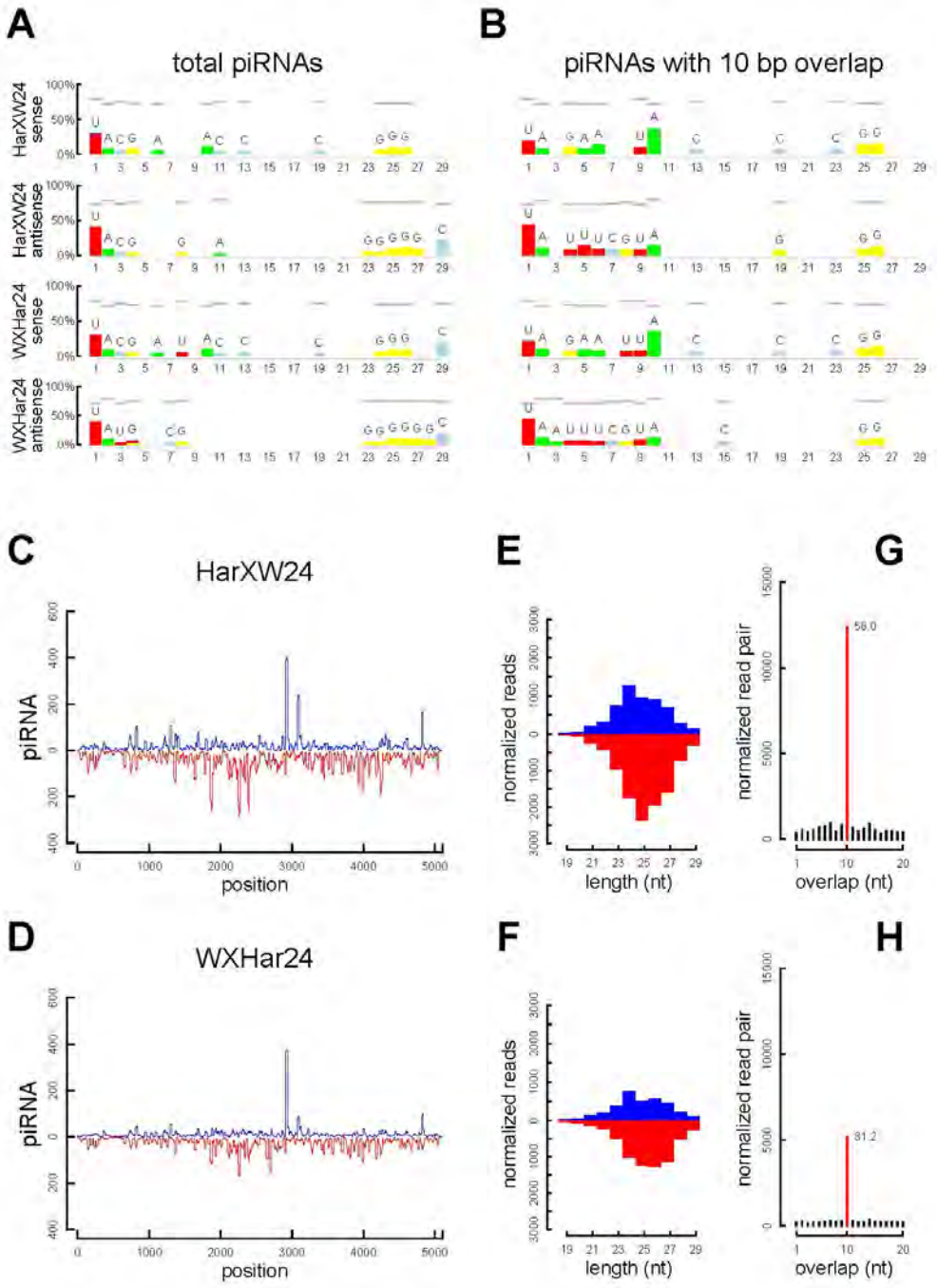
A
total piRNAs
B
piRNAs with 10 bp overlap
HarXW24 sense
HarXW24 antisense
WXHar24 sense
WXHar24 antisense
C
HarXW24
piRNA
position
D
WXHar24
E
F
normalized reads
length (nt)
G
H
normalized read pair
overlap (nt)
56.0
81.2

Rt1b

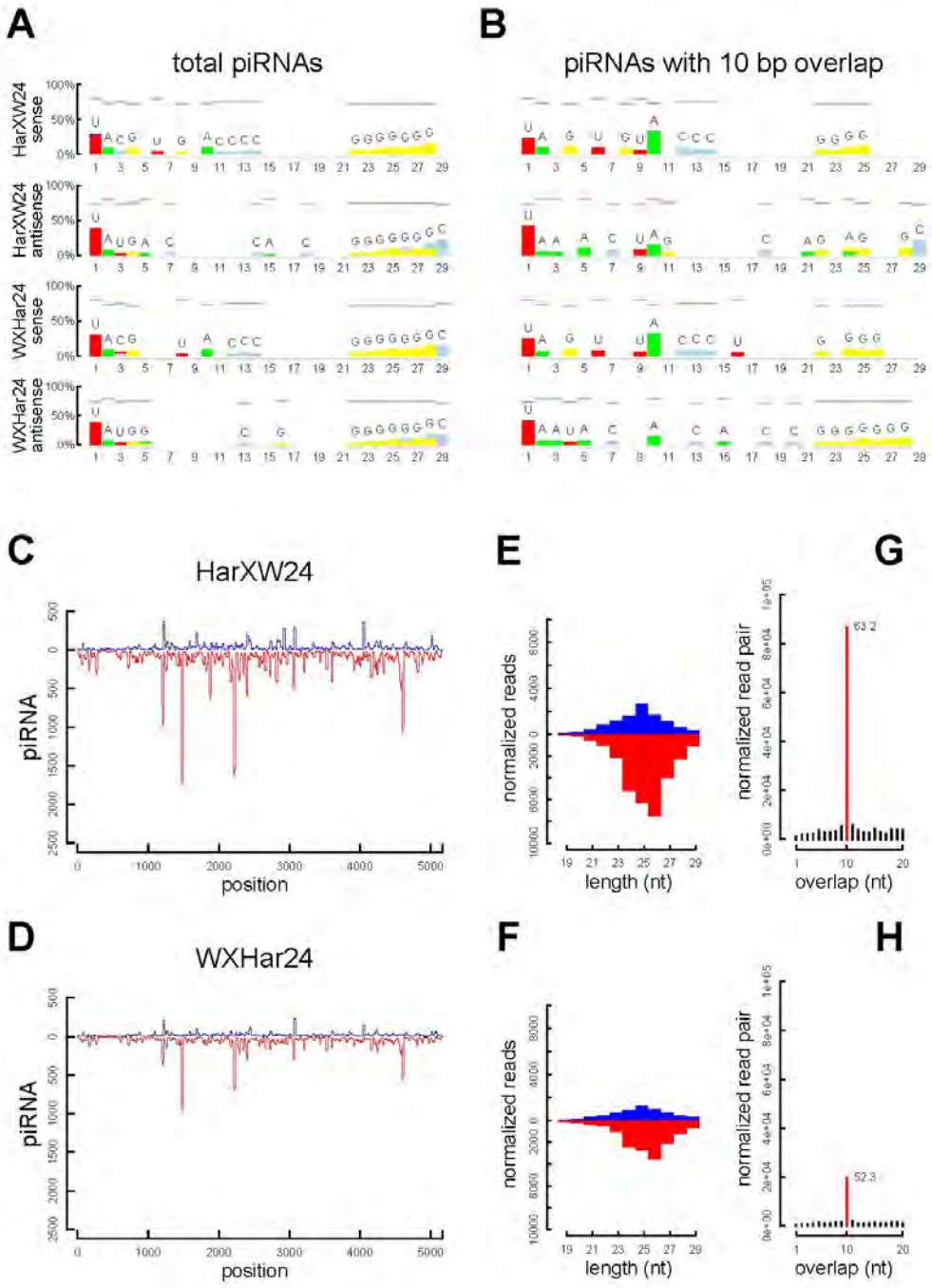
A
total piRNAs
B
piRNAs with 10 bp overlap
HarXW24 sense
HarXW24 antisense
WXHar24 sense
WXHar24 antisense
C
HarXW24
piRNA
position
D
WXHar24
E
normalized reads
length (nt)
F
G
normalized read pair
overlap (nt)
63.2
H
52.3

Rt1c

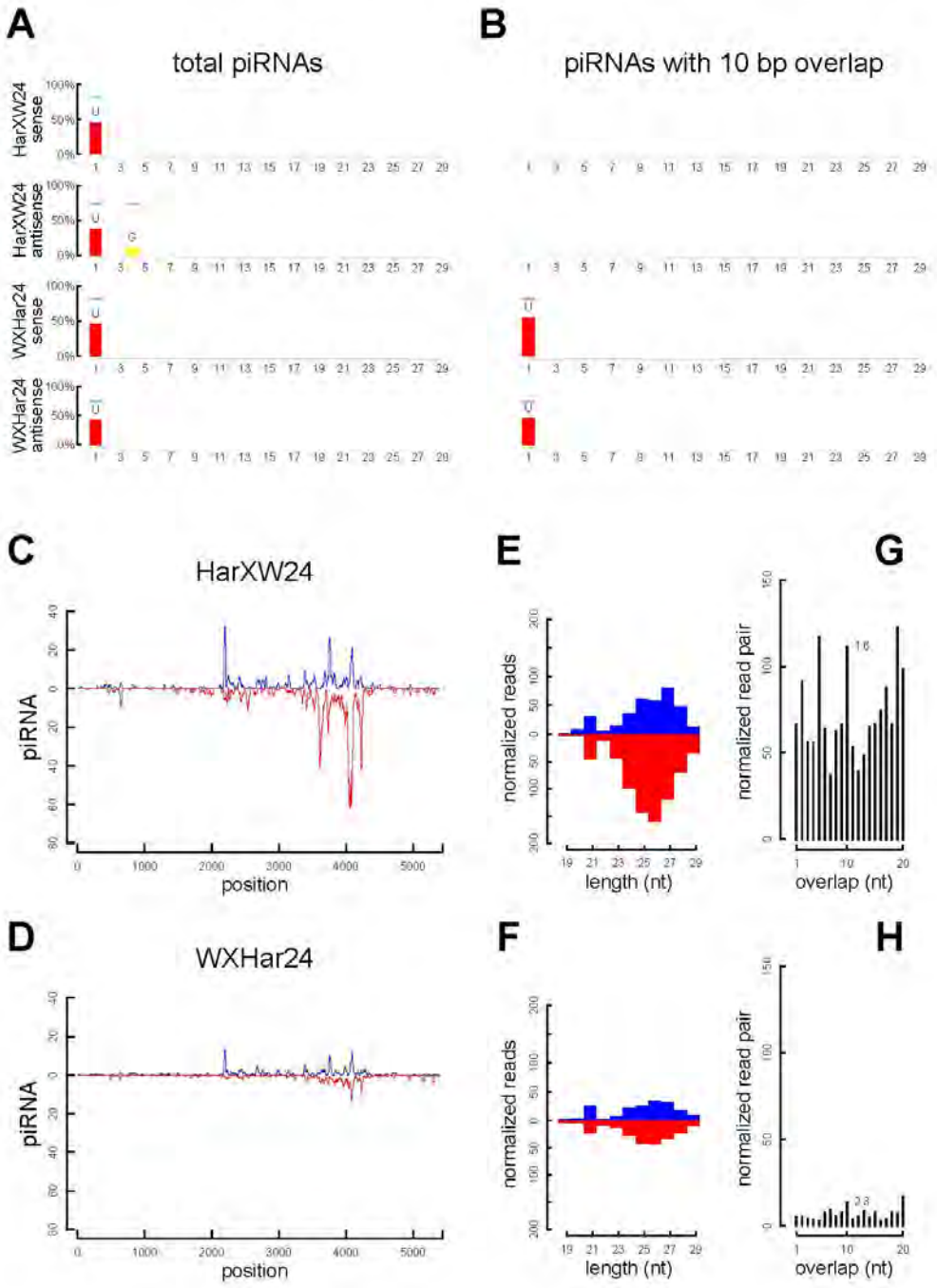
A
total piRNAs
B
piRNAs with 10 bp overlap
HarXW24 sense
HarXW24 antisense
WXHar24 sense
WXHar24 antisense
C
HarXW24
D
WXHar24
piRNA
position
E
F
normalized reads
length (nt)
G
H
normalized read pair
overlap (nt)

S2

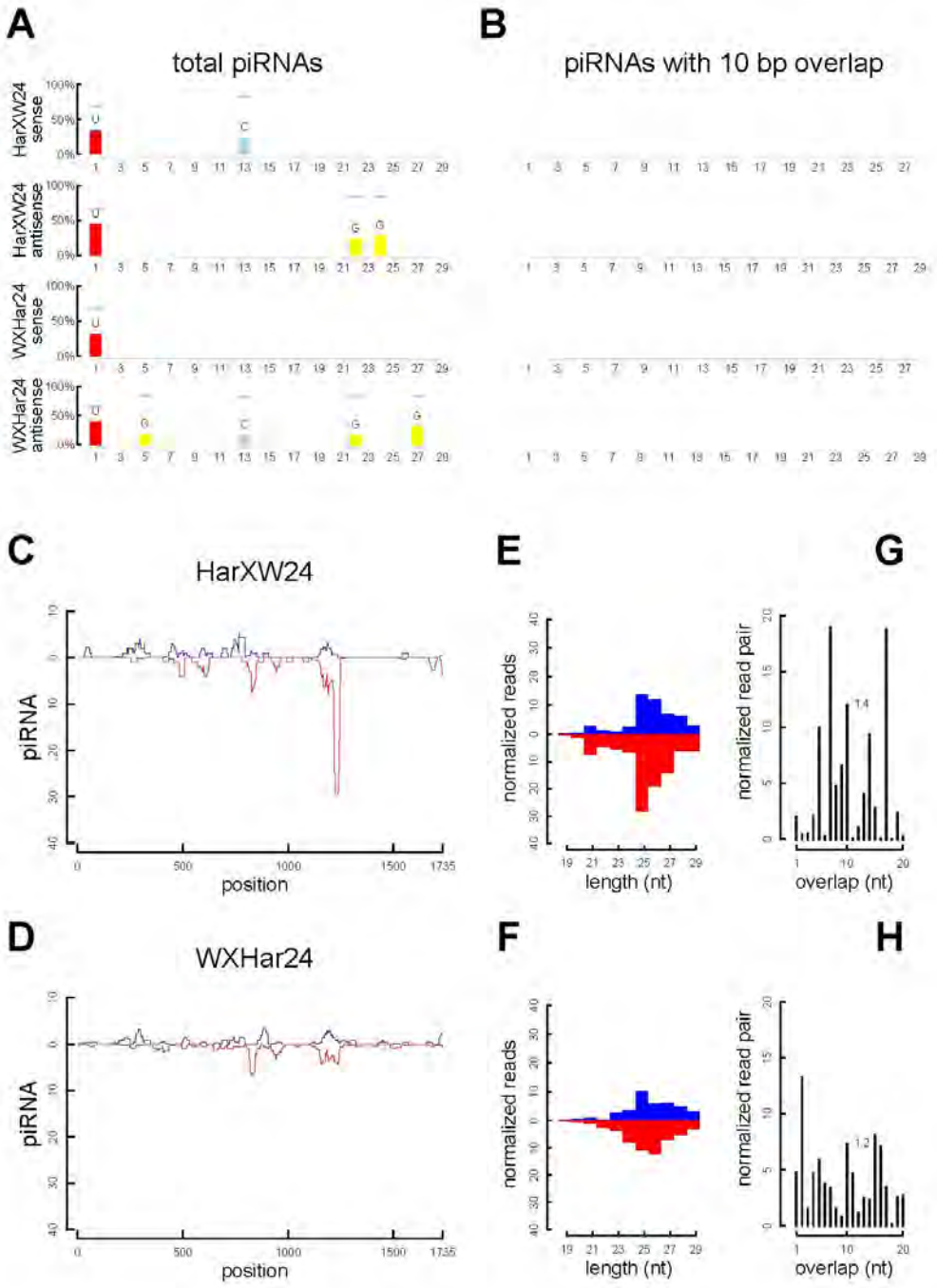
A
total piRNAs
B
piRNAs with 10 bp overlap
HarXW24 sense
HarXW24 antisense
WXHar24 sense
WXHar24 antisense
C
HarXW24
D
WXHar24
piRNA
position
E
F
normalized reads
length (nt)
G
H
normalized read pair
overlap (nt)

S element

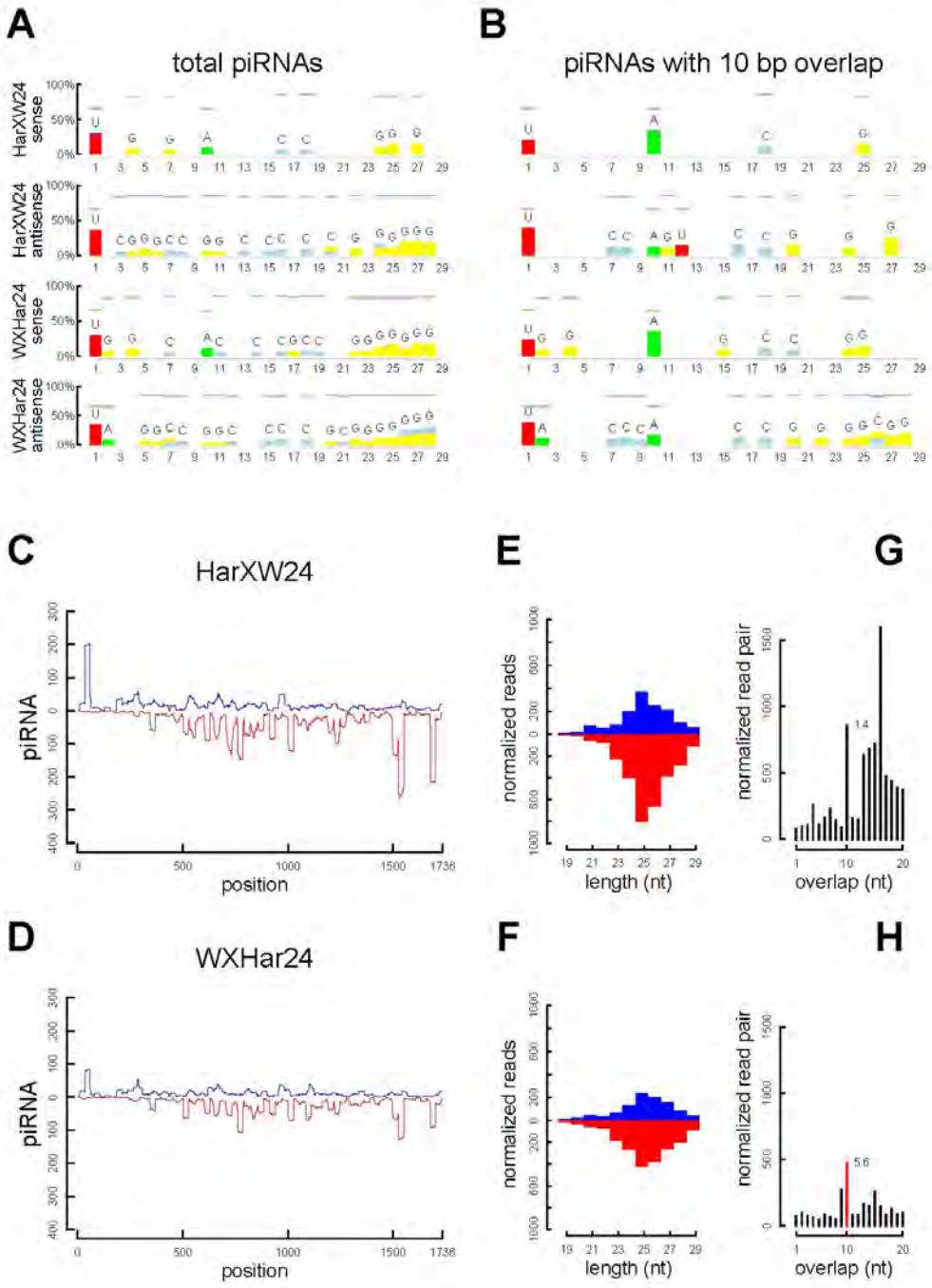
A
total piRNAs
B
piRNAs with 10 bp overlap
HarXW24 sense
HarXW24 antisense
WXHar24 sense
WXHar24 antisense
C
HarXW24
piRNA
position
D
WXHar24
piRNA
position
E
normalized reads
length (nt)
F
normalized reads
length (nt)
G
normalized read pair
overlap (nt)
1.4
H
normalized read pair
overlap (nt)
5.6

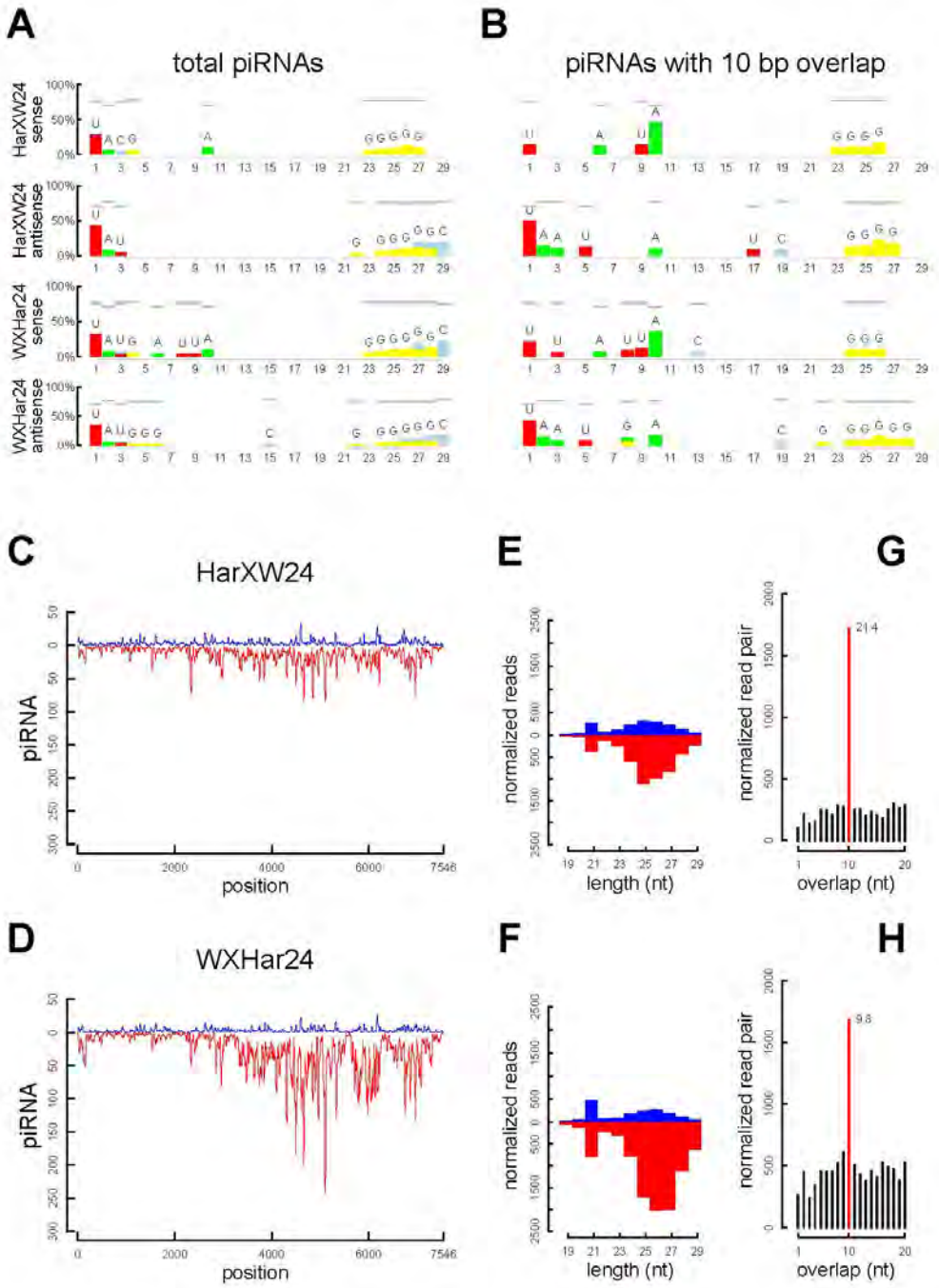
A
total piRNAs
B
piRNAs with 10 bp overlap
HarXW24 sense
HarXW24 antisense
WXHar24 sense
WXHar24 antisense
C
HarXW24
piRNA
position
D
WXHar24
piRNA
position
E
normalized reads
length (nt)
F
normalized reads
length (nt)
G
normalized read pair
overlap (nt)
214
H
normalized read pair
overlap (nt)
9.8

Stalker

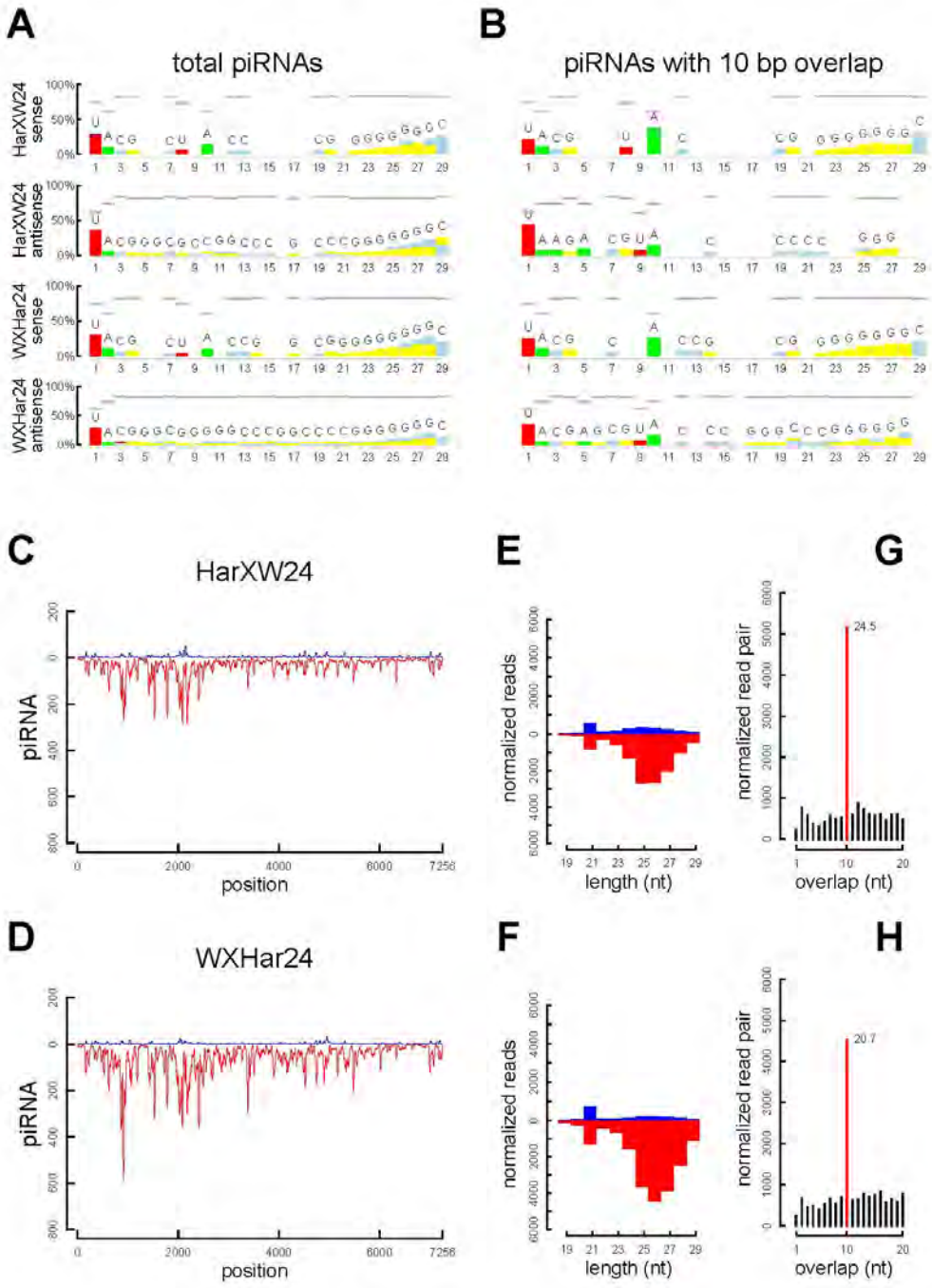
A
total piRNAs
B
piRNAs with 10 bp overlap
HarXW24 sense
HarXW24 antisense
WXHar24 sense
WXHar24 antisense
C
HarXW24
piRNA
position
D
WXHar24
piRNA
position
E
normalized reads
length (nt)
F
normalized reads
length (nt)
G
normalized read pair
24.5
overlap (nt)
H
normalized read pair
20.7
overlap (nt)

Stalker2

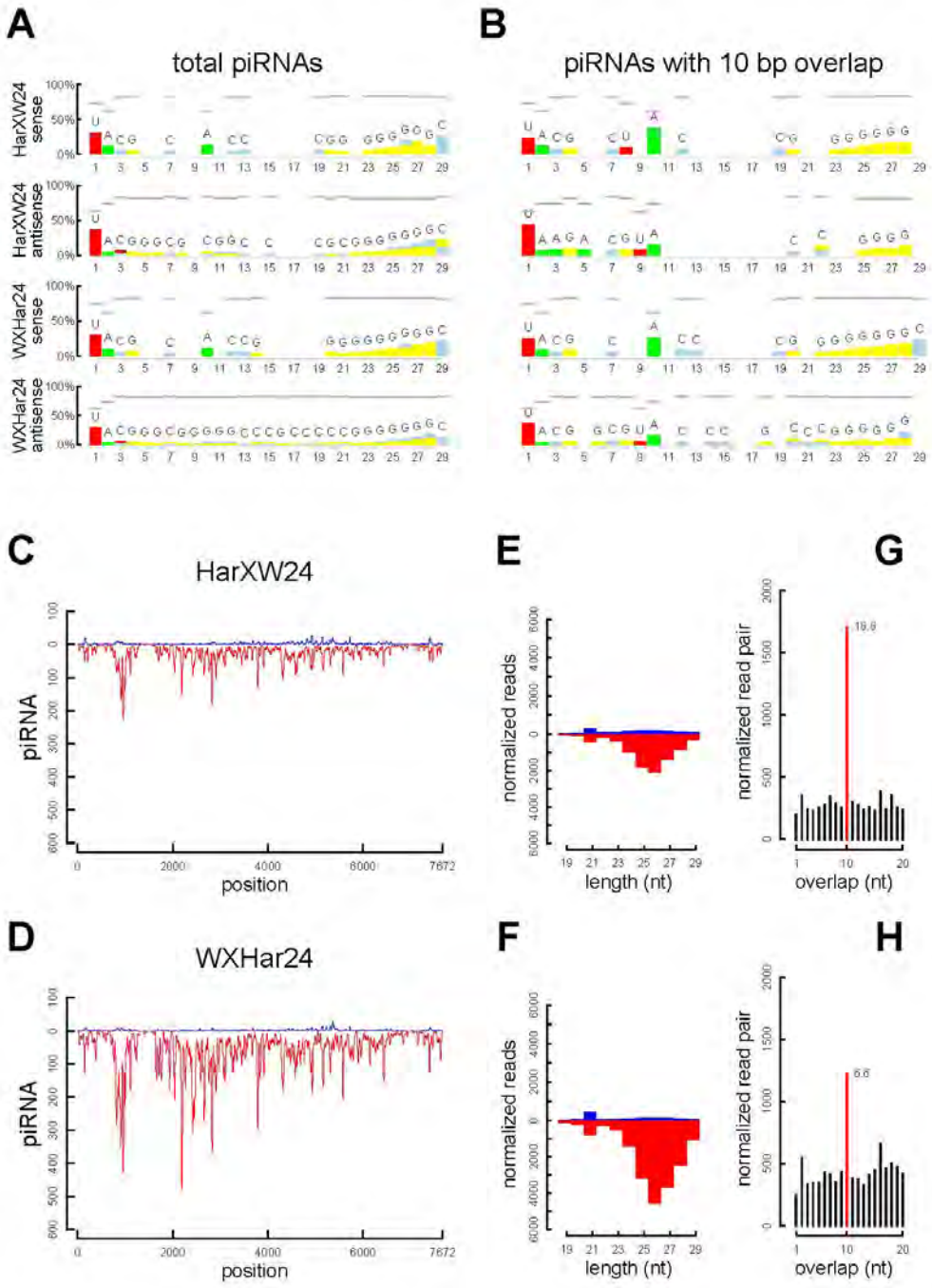
A
total piRNAs
B
piRNAs with 10 bp overlap
HarXW24 sense
HarXW24 antisense
WXHar24 sense
WXHar24 antisense
C
HarXW24
D
WXHar24
piRNA
position
E
F
normalized reads
length (nt)
G
H
normalized read pair
overlap (nt)
19.8
6.6

Stalker3

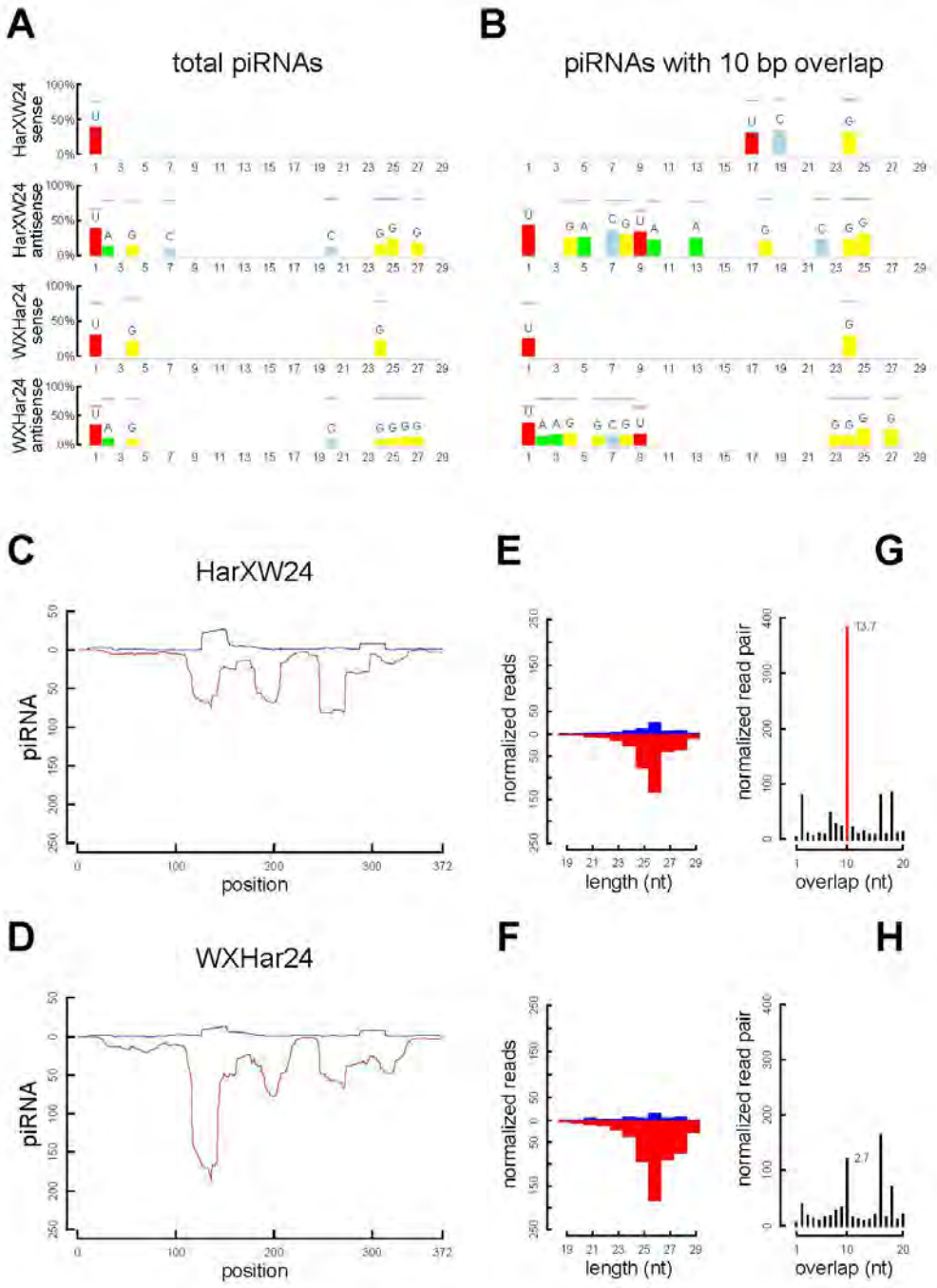
A
total piRNAs
B
piRNAs with 10 bp overlap
HarXW24 sense
HarXW24 antisense
WXHar24 sense
WXHar24 antisense
C
HarXW24
piRNA
position
D
WXHar24
piRNA
position
E
normalized reads
length (nt)
F
normalized reads
length (nt)
G
normalized read pair
overlap (nt)
13.7
H
normalized read pair
overlap (nt)
2.7

Stalker4

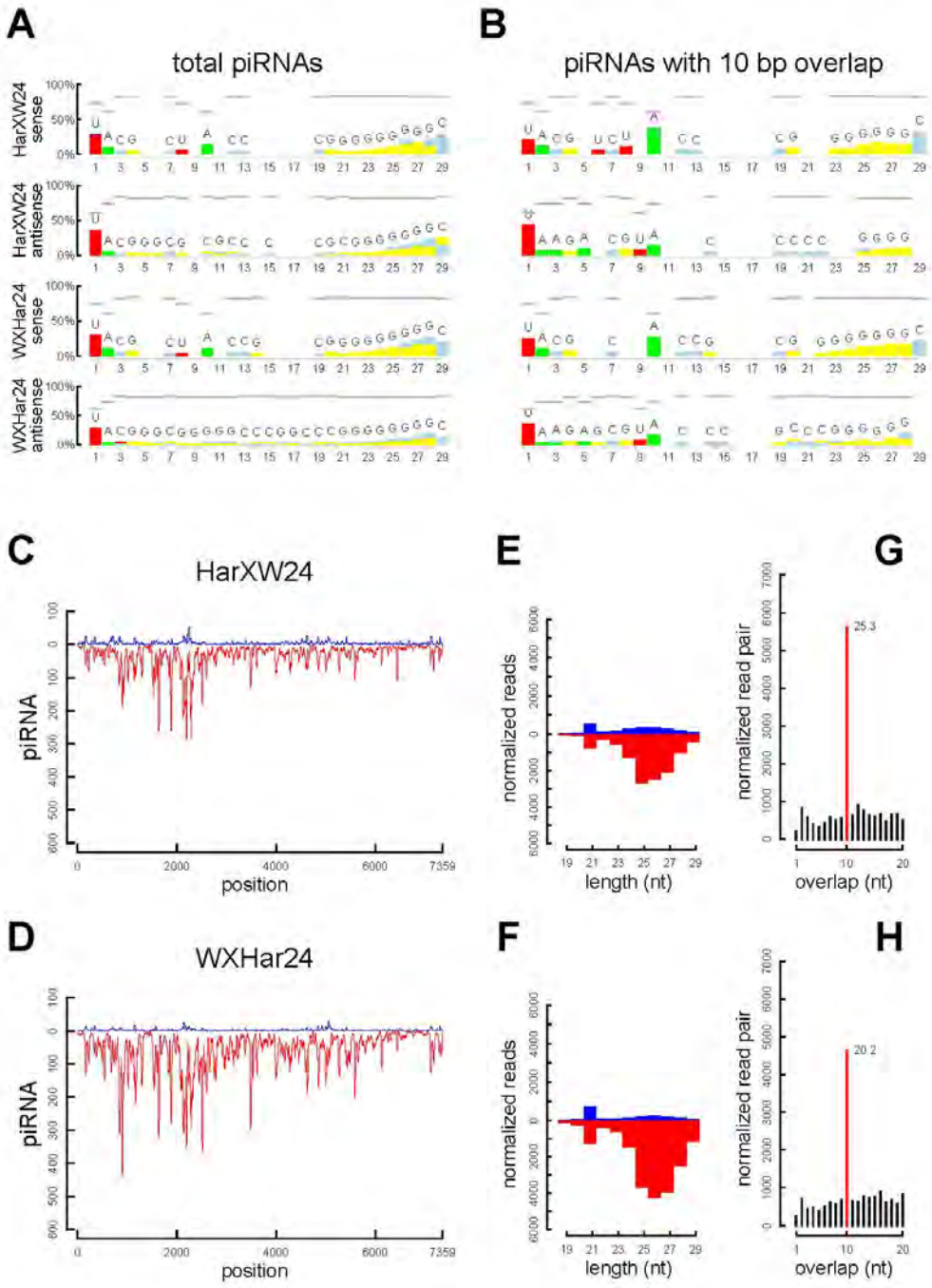
A
total piRNAs
B
piRNAs with 10 bp overlap
HarXW24 sense
HarXW24 antisense
WXHar24 sense
WXHar24 antisense
C
HarXW24
D
WXHar24
piRNA
position
E
F
normalized reads
length (nt)
G
H
normalized read pair
overlap (nt)
25.3
20.2

Tabor

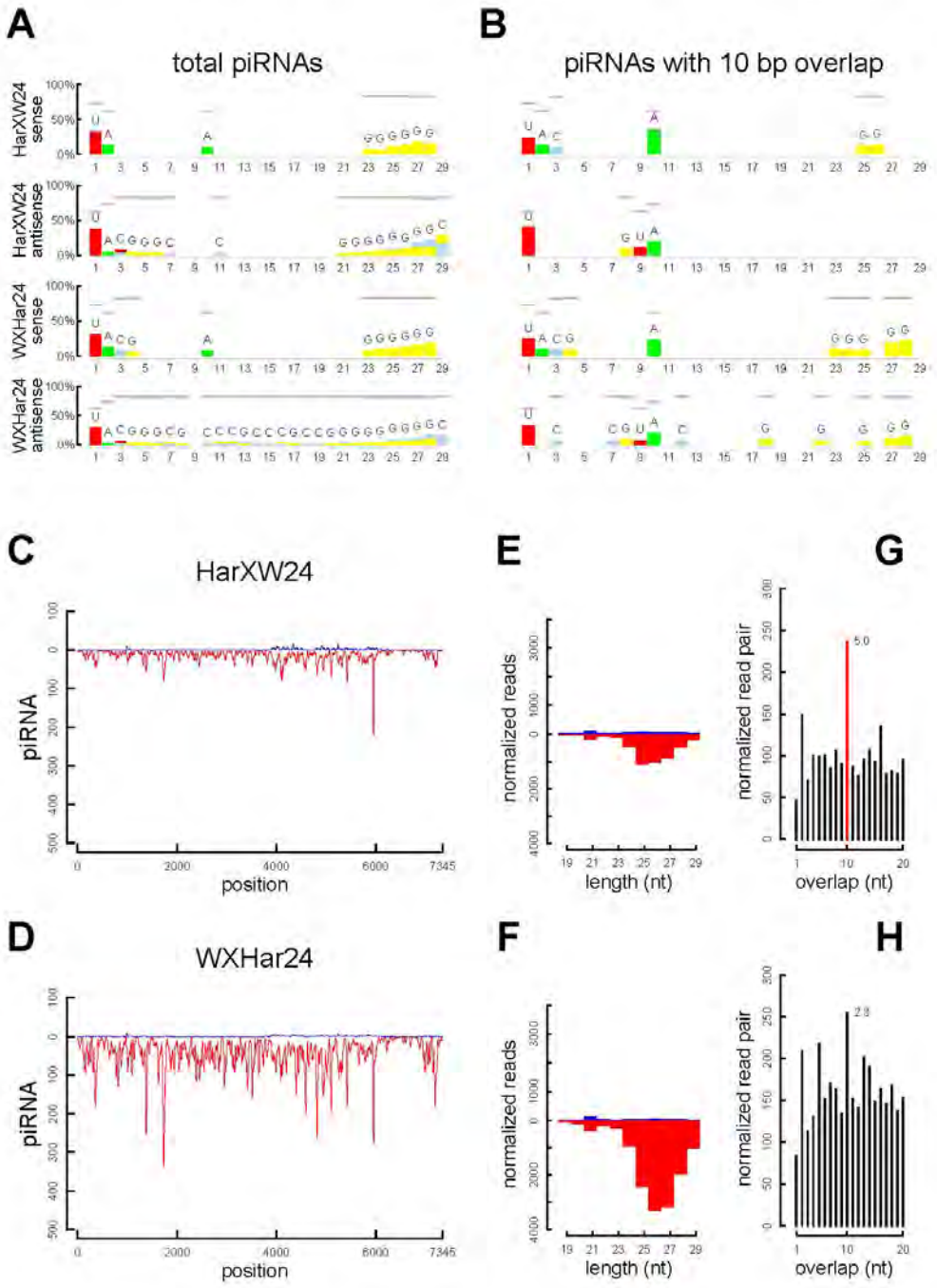
A
total piRNAs
B
piRNAs with 10 bp overlap
HarXW24 sense
HarXW24 antisense
WXHar24 sense
WXHar24 antisense
C
HarXW24
piRNA
position
D
WXHar24
piRNA
position
E
normalized reads
length (nt)
F
normalized reads
length (nt)
G
normalized read pair
overlap (nt)
5.0
H
normalized read pair
overlap (nt)
2.8

TAHRE

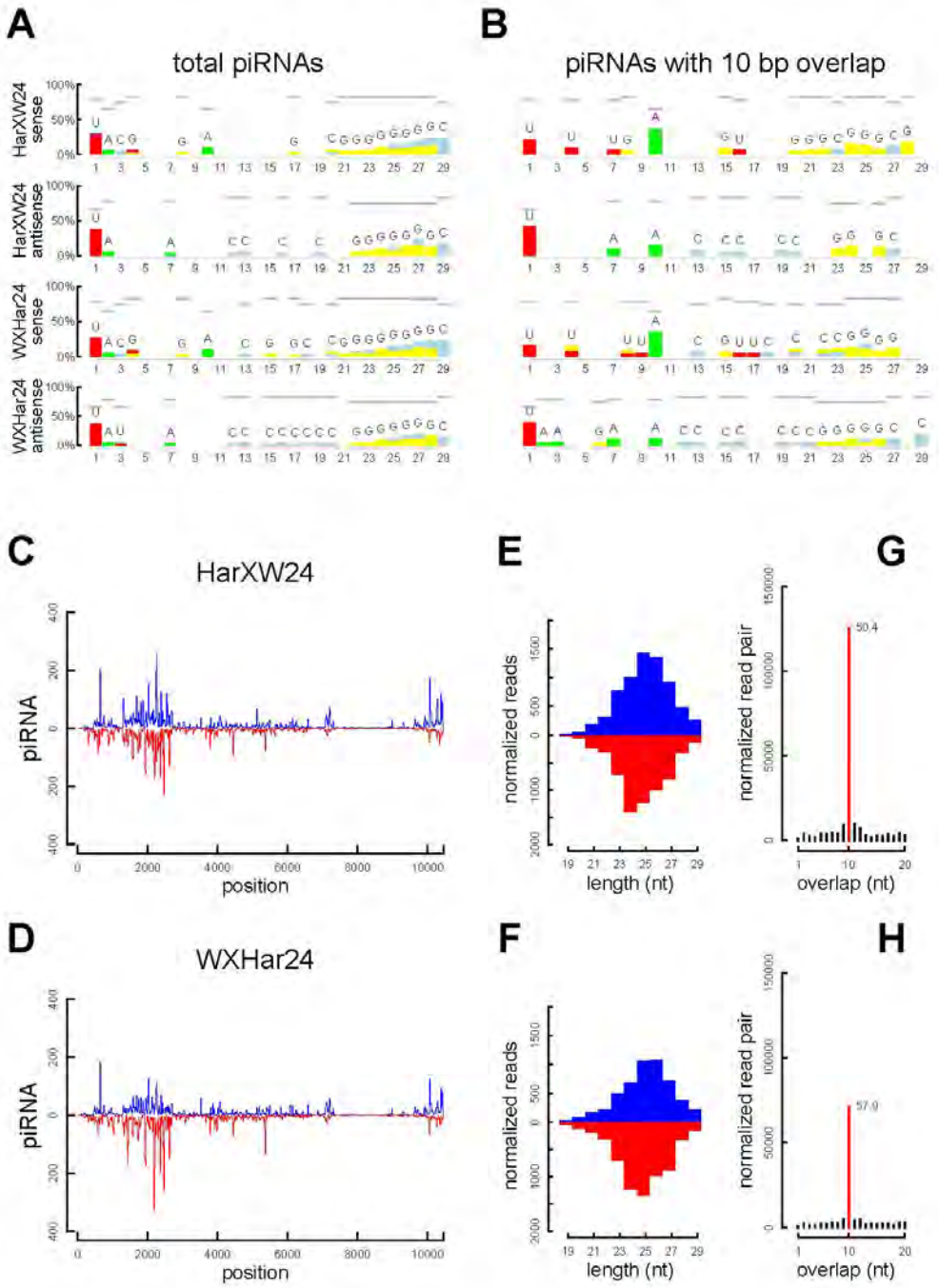
A
total piRNAs
B
piRNAs with 10 bp overlap
HarXW24 sense
HarXW24 antisense
WXHar24 sense
WXHar24 antisense
C
HarXW24
piRNA
position
D
WXHar24
piRNA
position
E
normalized reads
length (nt)
F
normalized reads
length (nt)
G
normalized read pair
overlap (nt)
50.4
H
normalized read pair
overlap (nt)
57.9

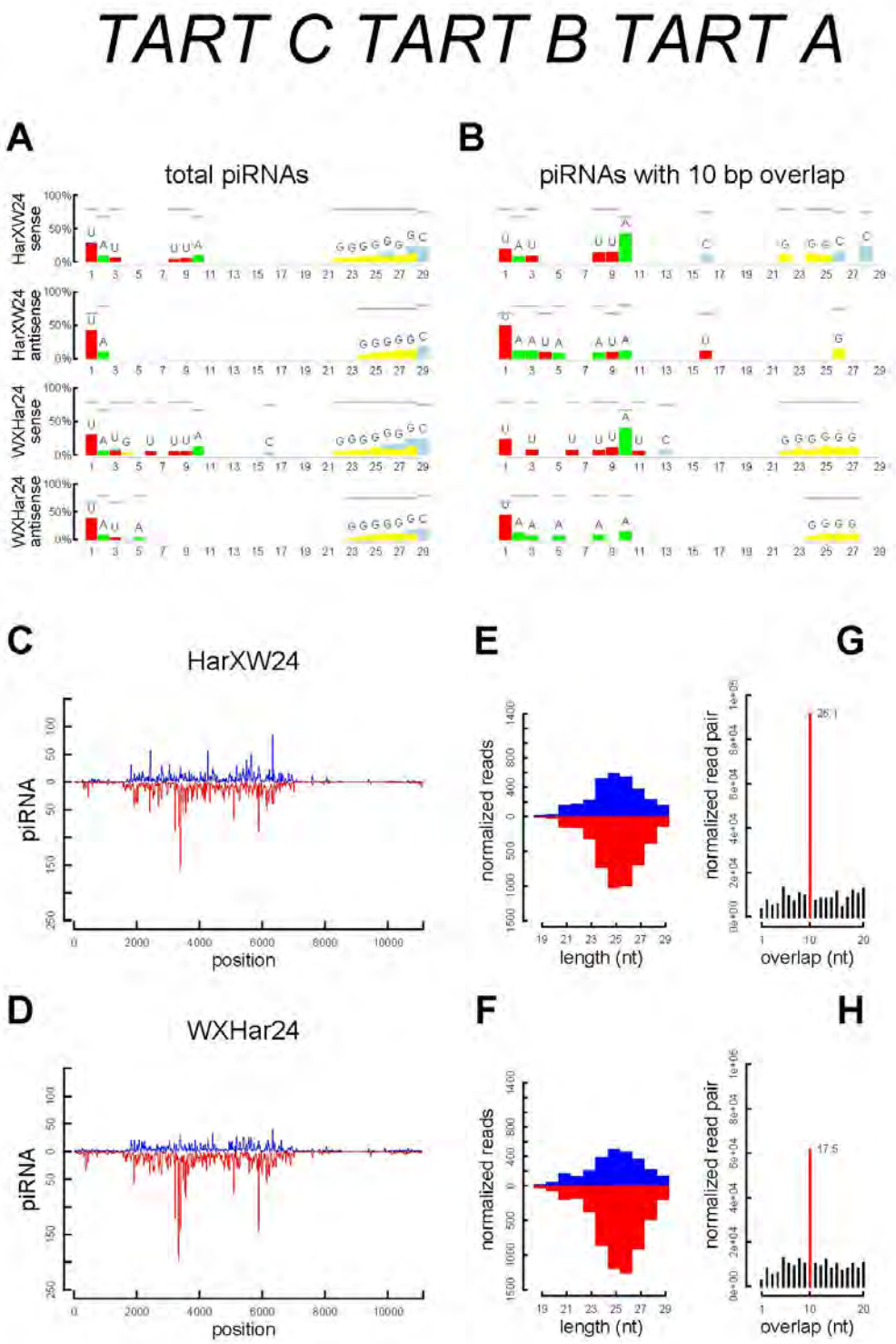
TART C TART B TART A
A
total piRNAs
B
piRNAs with 10 bp overlap
HarXW24 sense
HarXW24 antisense
WXHar24 sense
WXHar24 antisense
C
HarXW24
piRNA
position
D
WXHar24
E
normalized reads
length (nt)
F
G
normalized read pair
overlap (nt)
26.1
H
17.5

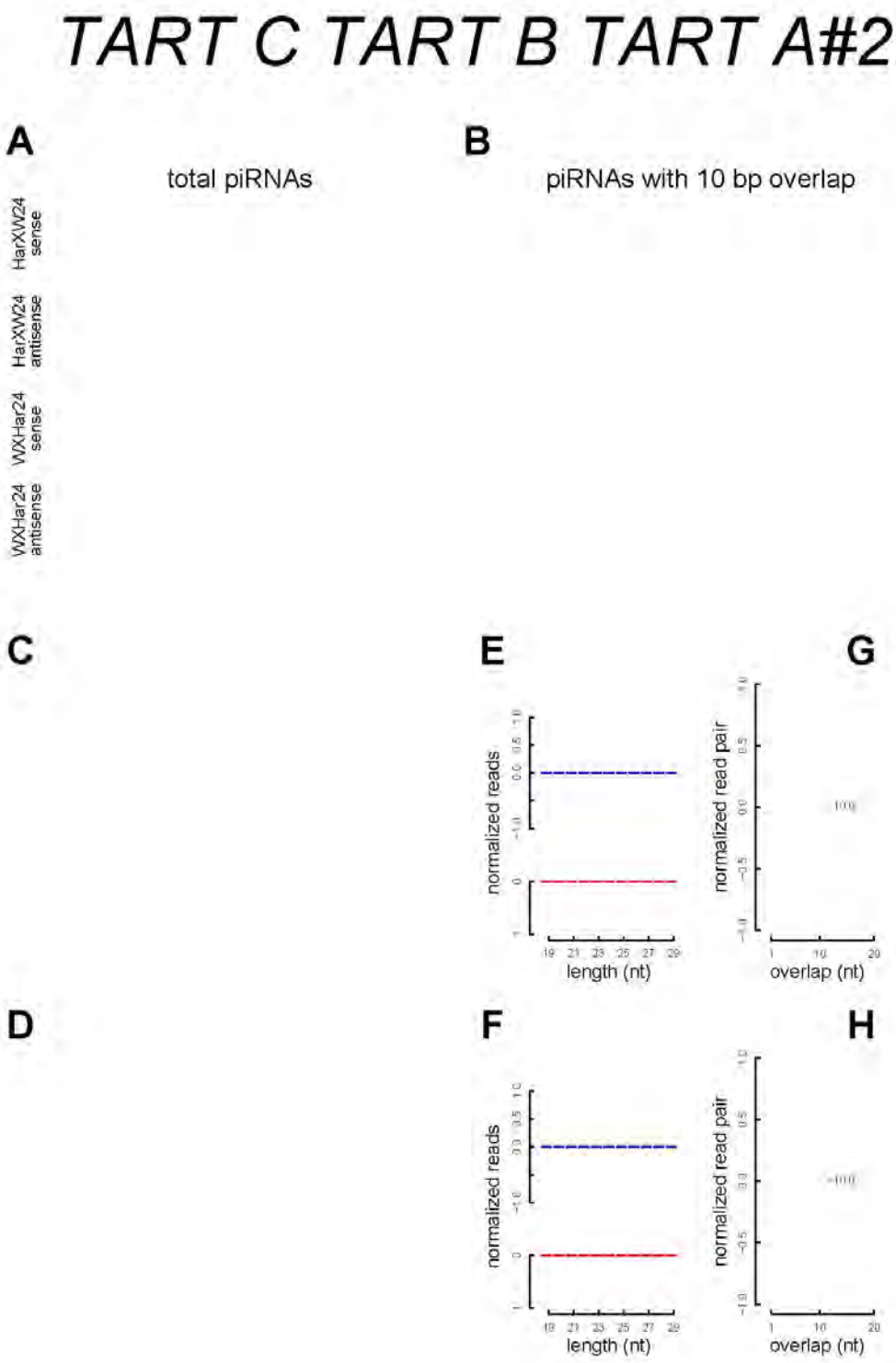
TART C TART B TART A#2
A
total piRNAs
B
piRNAs with 10 bp overlap
HarXW24 sense
HarXW24 antisense
WXHar24 sense
WXHar24 antisense
C
D
E
F
G
H
normalized reads
length (nt)
normalized read pair
overlap (nt)

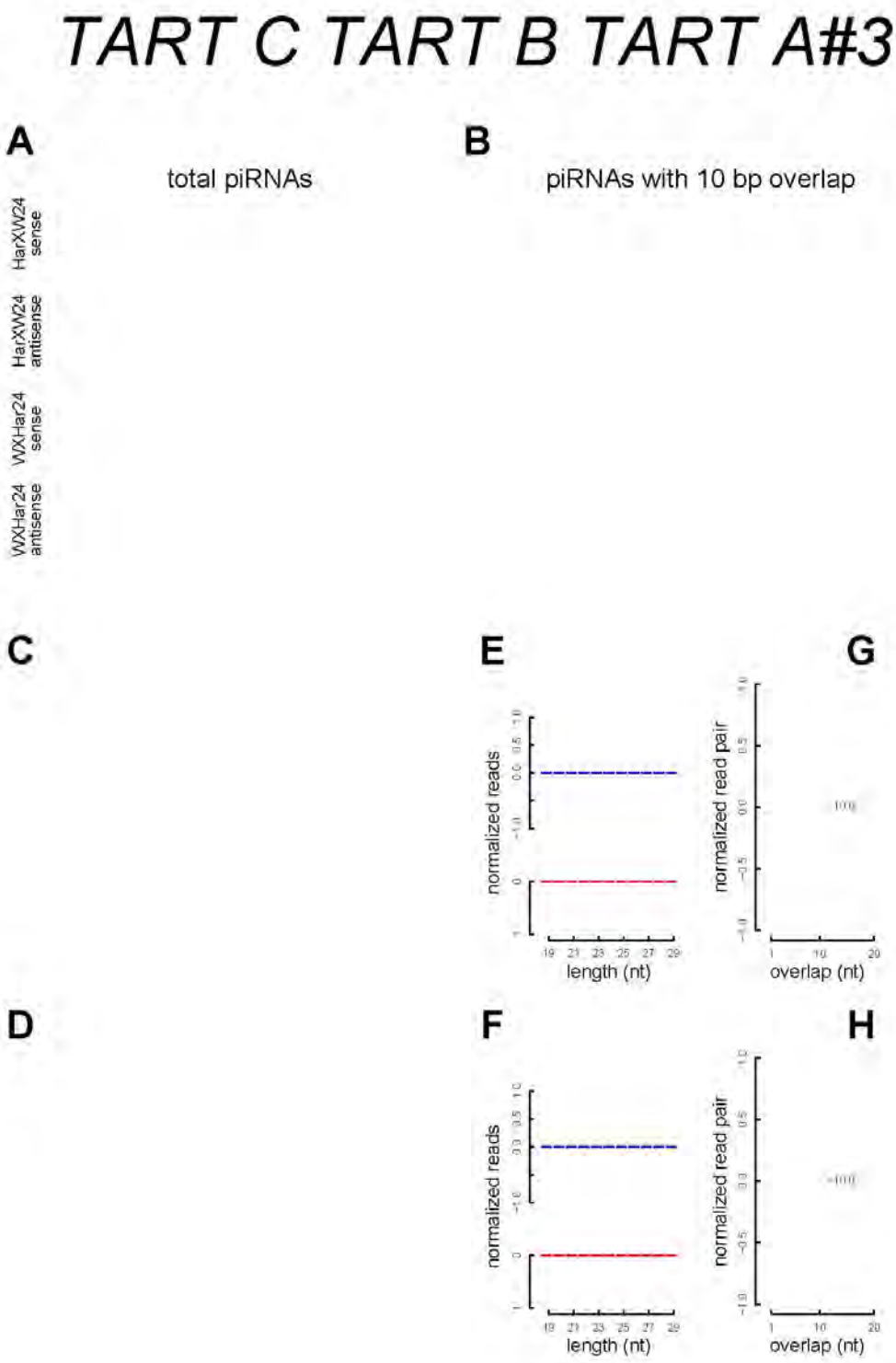
TART C TART B TART A#3
A
total piRNAs
B
piRNAs with 10 bp overlap
HarXW24 sense
HarXW24 antisense
WXHar24 sense
WXHar24 antisense
C
D
E
G
F
H
normalized reads
normalized read pair
length (nt)
overlap (nt)

Tc1

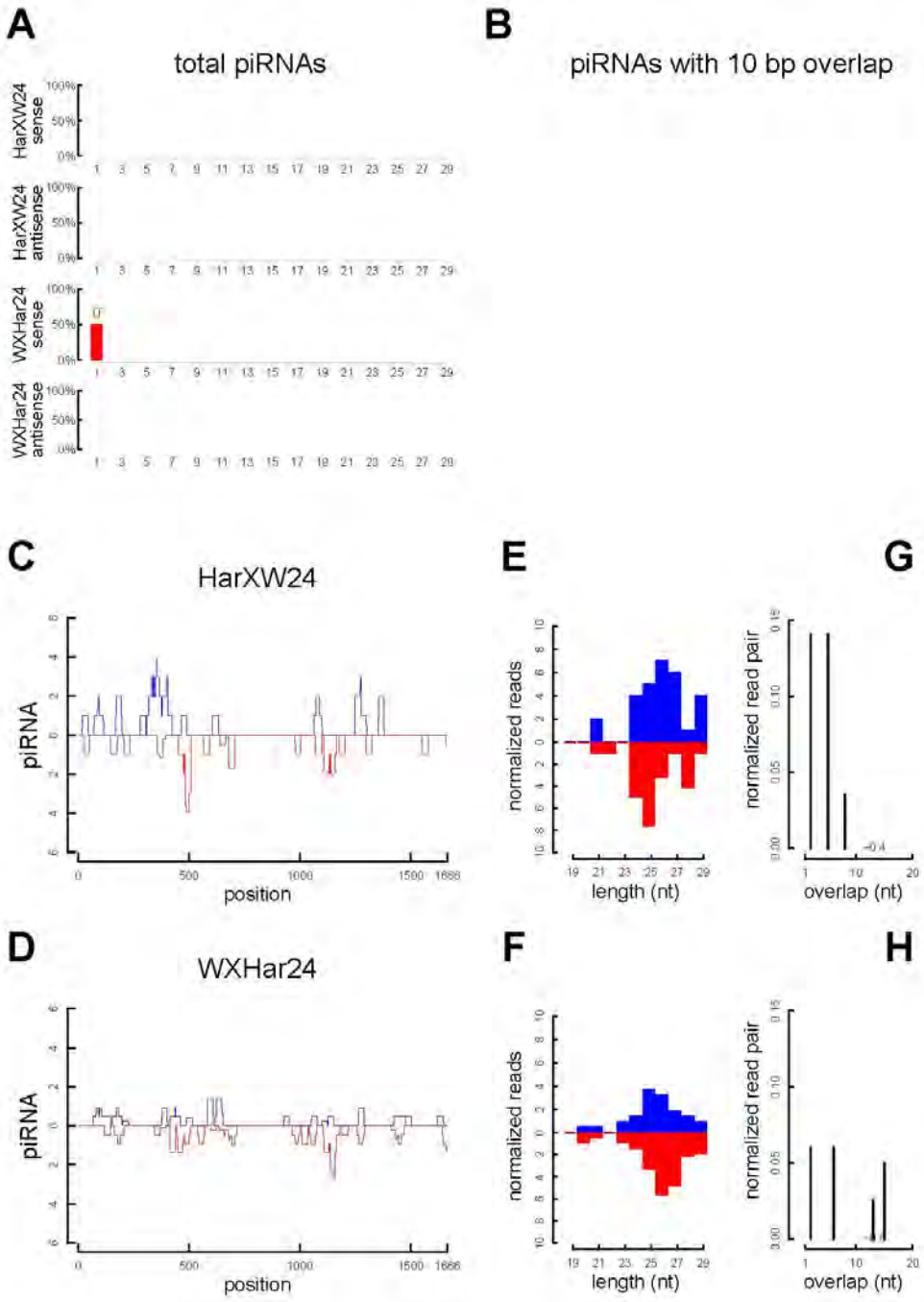
A
total piRNAs
B
piRNAs with 10 bp overlap
HarXW24 sense
HarXW24 antisense
WXHar24 sense
WXHar24 antisense
C
HarXW24
D
WXHar24
piRNA
position
E
F
normalized reads
length (nt)
G
H
normalized read pair
overlap (nt)

Tc1 2

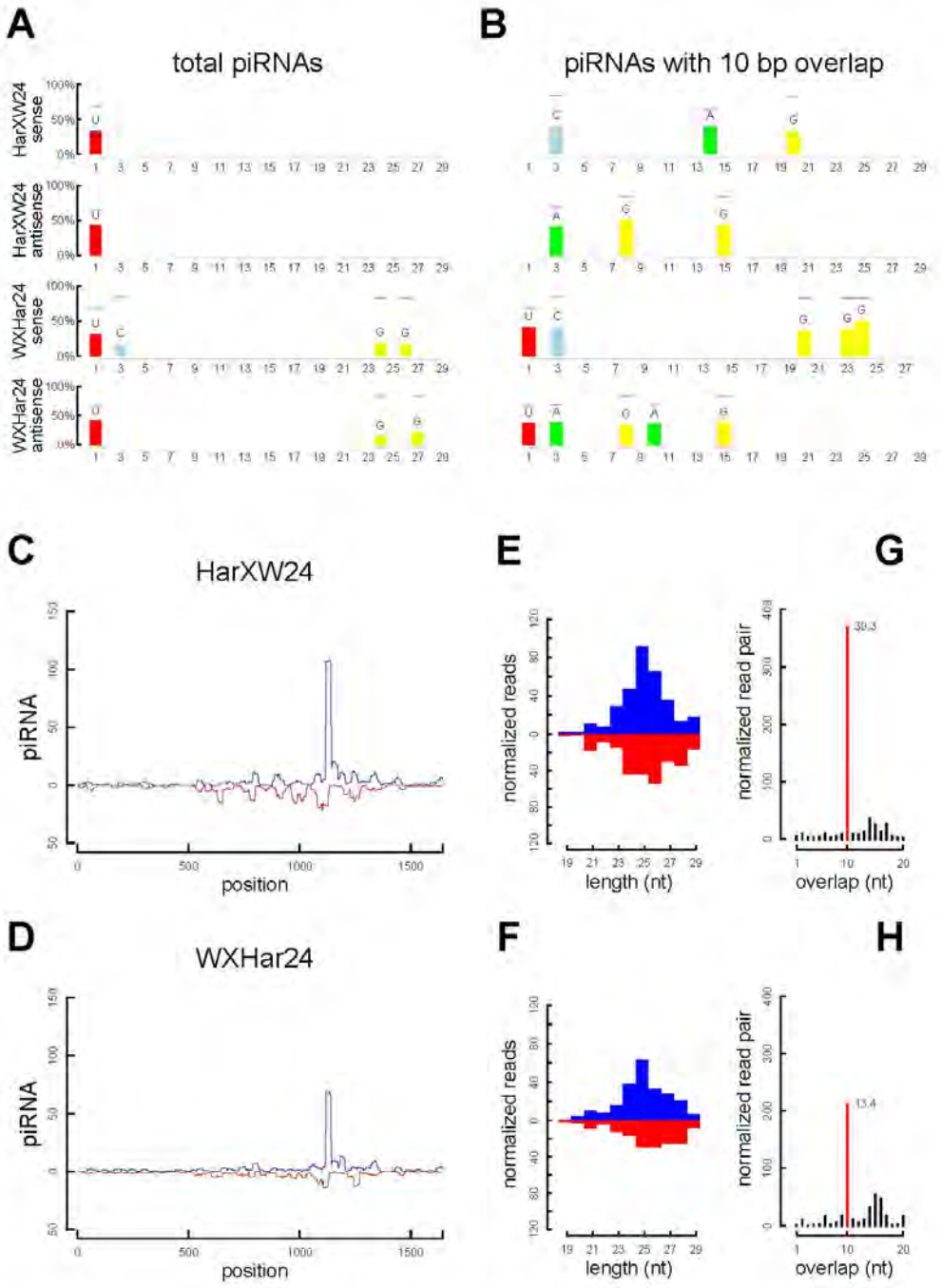
A
total piRNAs
B
piRNAs with 10 bp overlap
HarXW24 sense
HarXW24 antisense
WXHar24 sense
WXHar24 antisense
C
HarXW24
D
WXHar24
piRNA
position
E
F
normalized reads
length (nt)
G
H
normalized read pair
overlap (nt)
39.3
13.4

Tc3

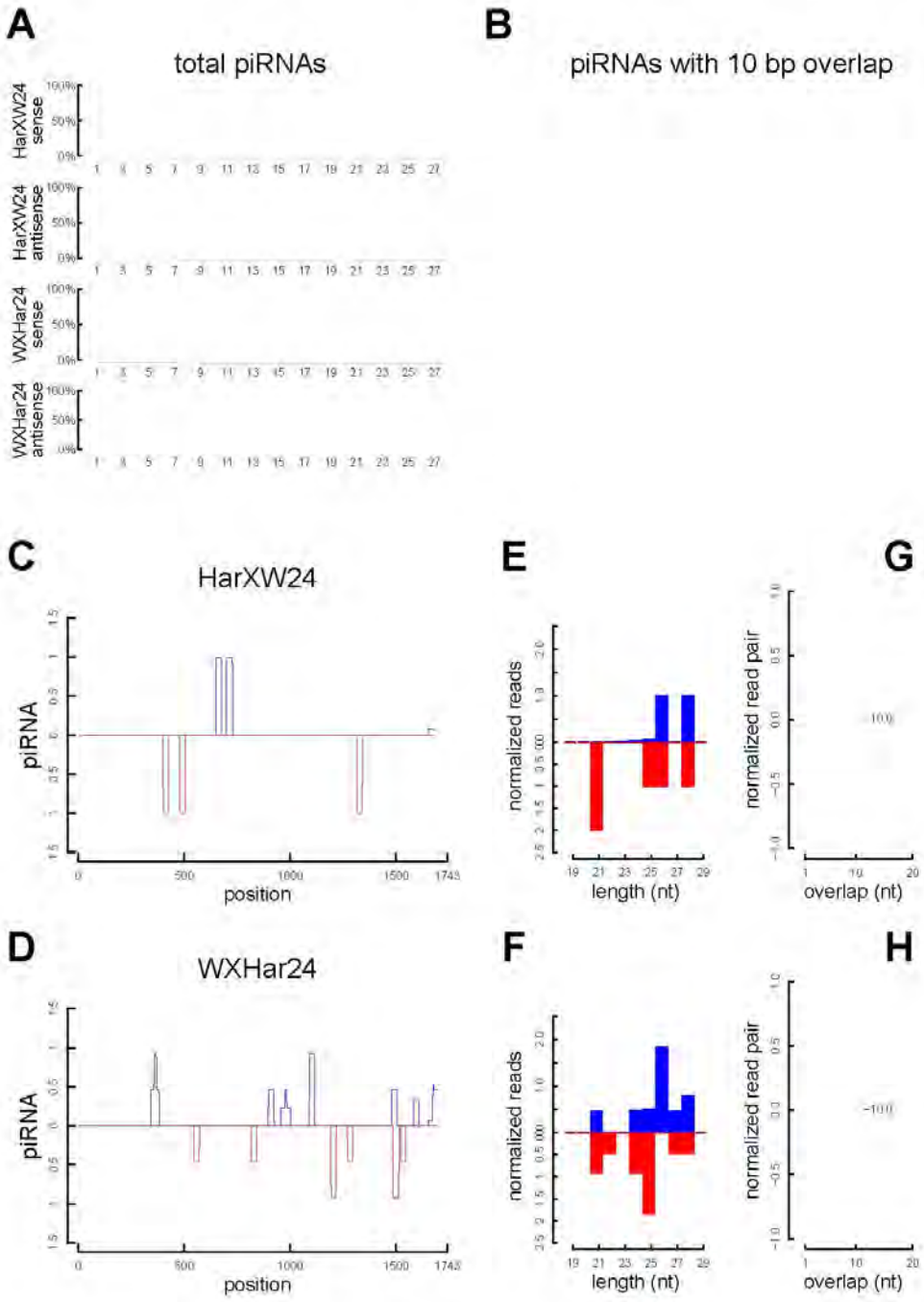
A
total piRNAs
B
piRNAs with 10 bp overlap
HarXW24 sense
HarXW24 antisense
WXHar24 sense
WXHar24 antisense
C
HarXW24
D
WXHar24
piRNA
position
E
F
normalized reads
length (nt)
G
H
normalized read pair
overlap (nt)

Tirant

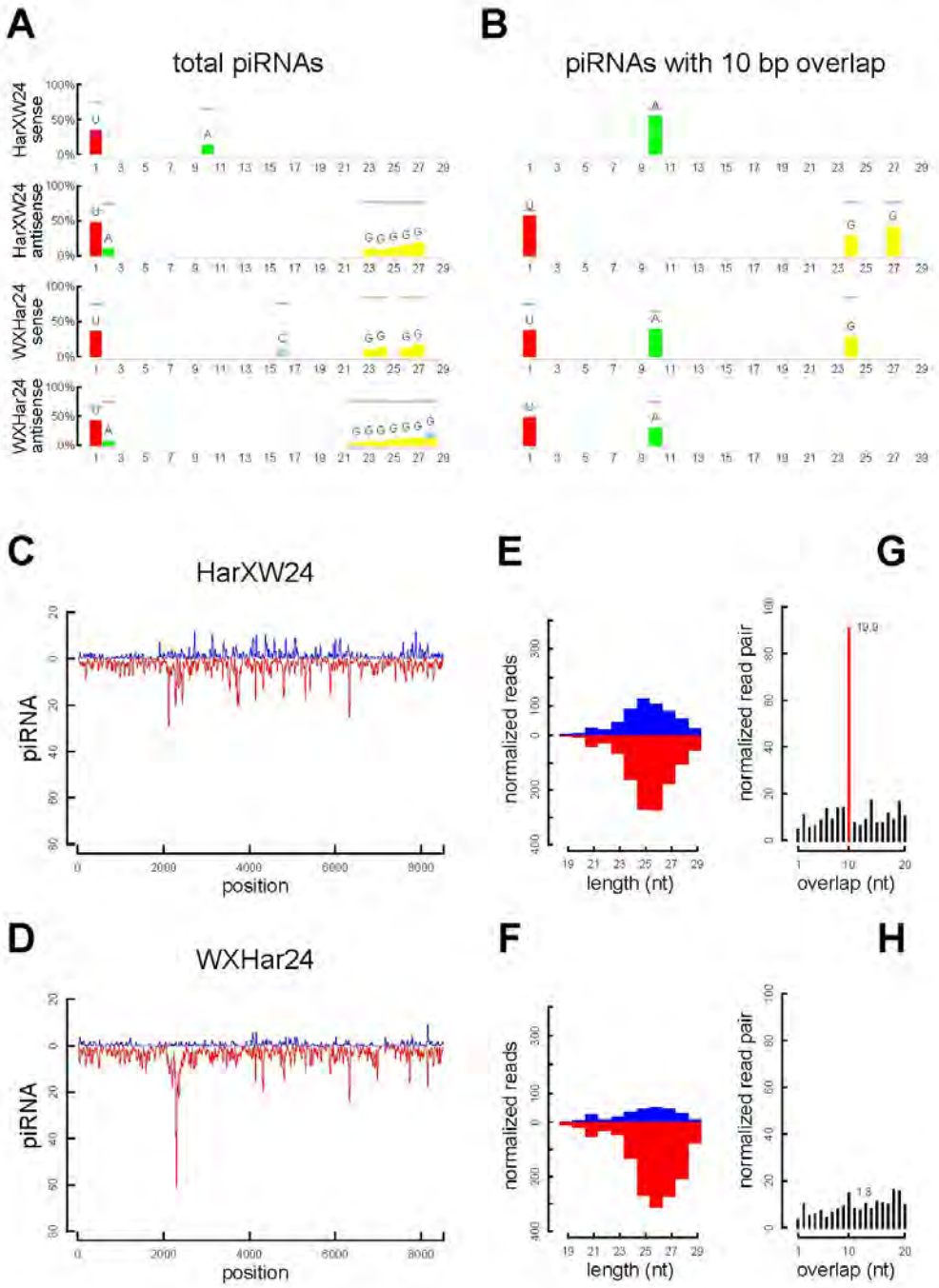
A
total piRNAs
B
piRNAs with 10 bp overlap
HarXW24 sense
HarXW24 antisense
WXHar24 sense
WXHar24 antisense
C
HarXW24
D
WXHar24
piRNA
position
E
F
normalized reads
length (nt)
G
H
normalized read pair
overlap (nt)

Tom1

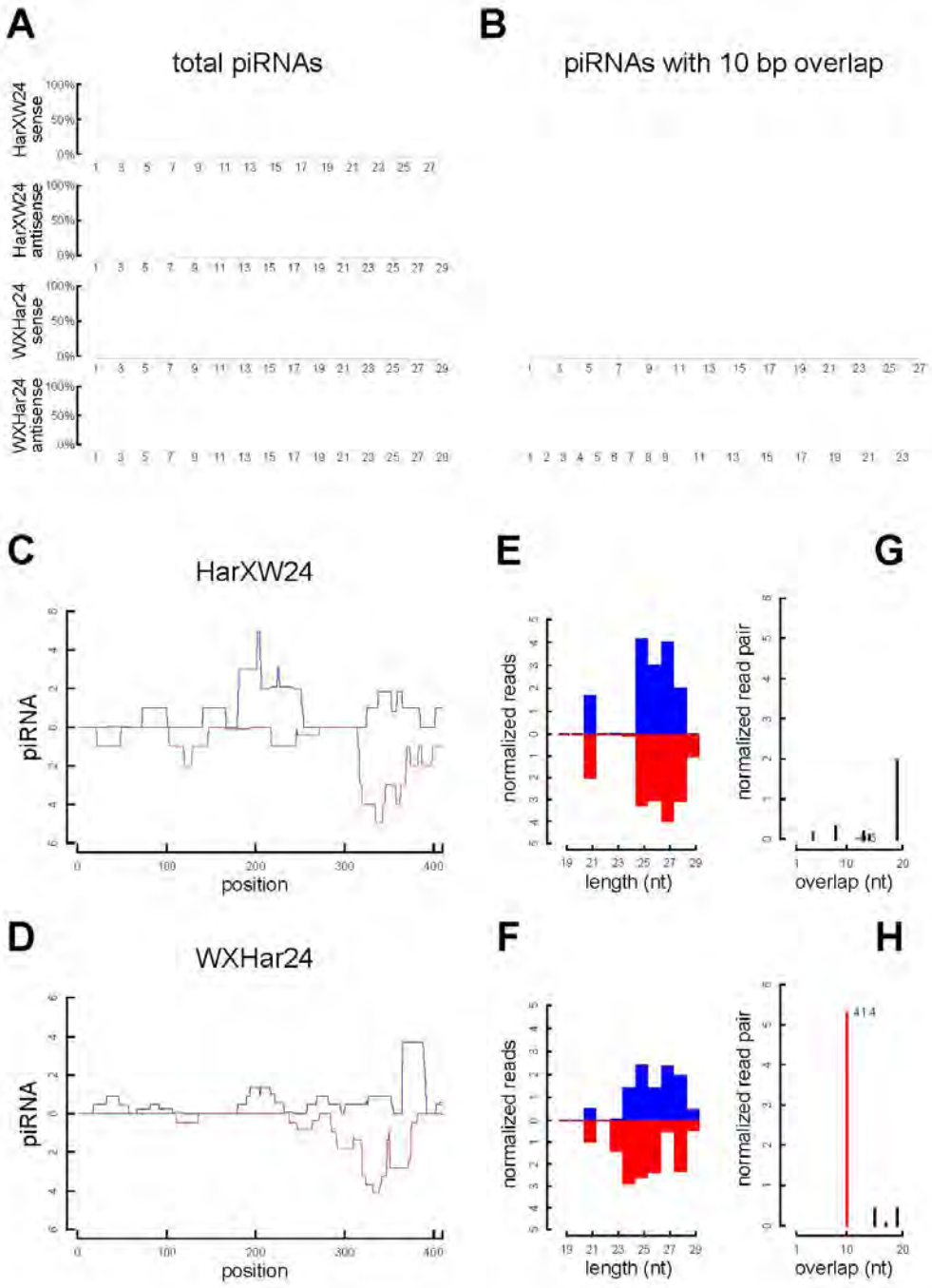
A
total piRNAs
HarXW24 sense
HarXW24 antisense
WXHar24 sense
WXHar24 antisense
B
piRNAs with 10 bp overlap
C
HarXW24
piRNA
position
D
WXHar24
piRNA
position
E
normalized reads
length (nt)
F
normalized reads
length (nt)
G
normalized read pair
overlap (nt)
H
normalized read pair
overlap (nt)
414

transib1

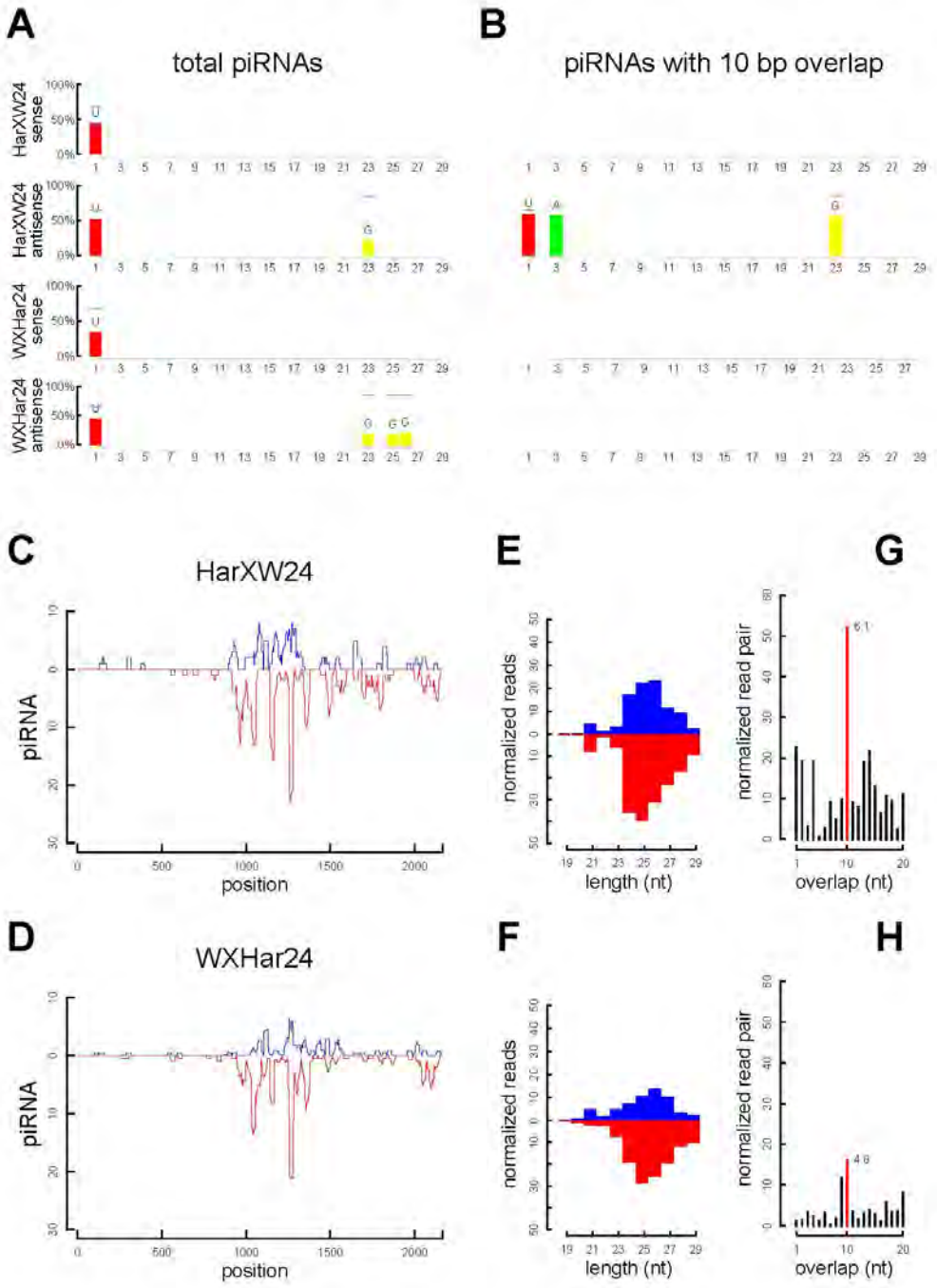
A
total piRNAs
B
piRNAs with 10 bp overlap
HarXW24 sense
HarXW24 antisense
WXHar24 sense
WXHar24 antisense
C
HarXW24
piRNA
position
D
WXHar24
piRNA
position
E
normalized reads
length (nt)
F
normalized reads
length (nt)
G
normalized read pair
overlap (nt)
H
normalized read pair
overlap (nt)

transib2

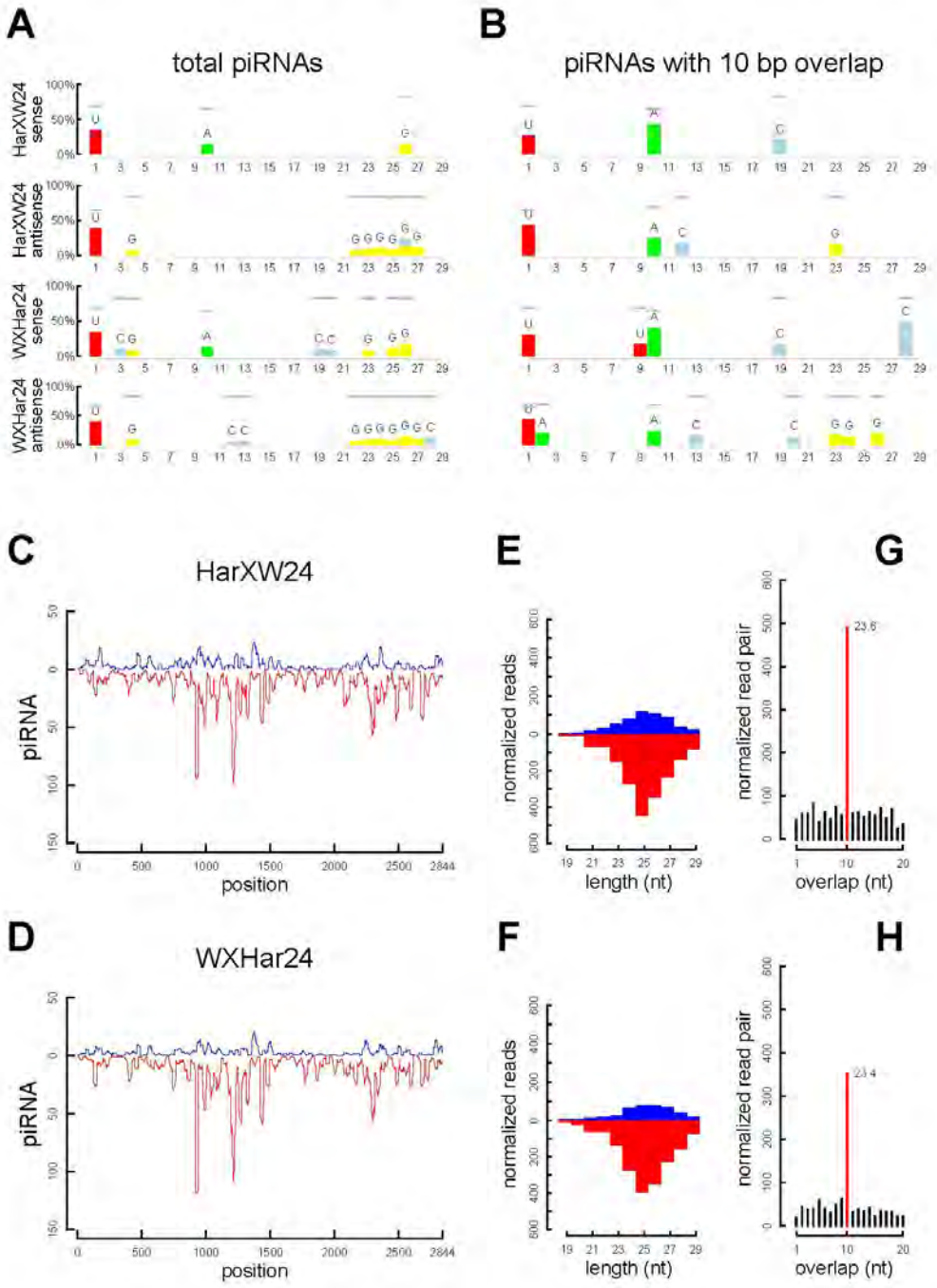
A
total piRNAs
B
piRNAs with 10 bp overlap
HarXW24 sense
HarXW24 antisense
WXHar24 sense
WXHar24 antisense
C
HarXW24
piRNA
position
D
WXHar24
piRNA
position
E
normalized reads
length (nt)
F
normalized reads
length (nt)
G
normalized read pair
23.6
overlap (nt)
H
normalized read pair
23.4
overlap (nt)

transib3

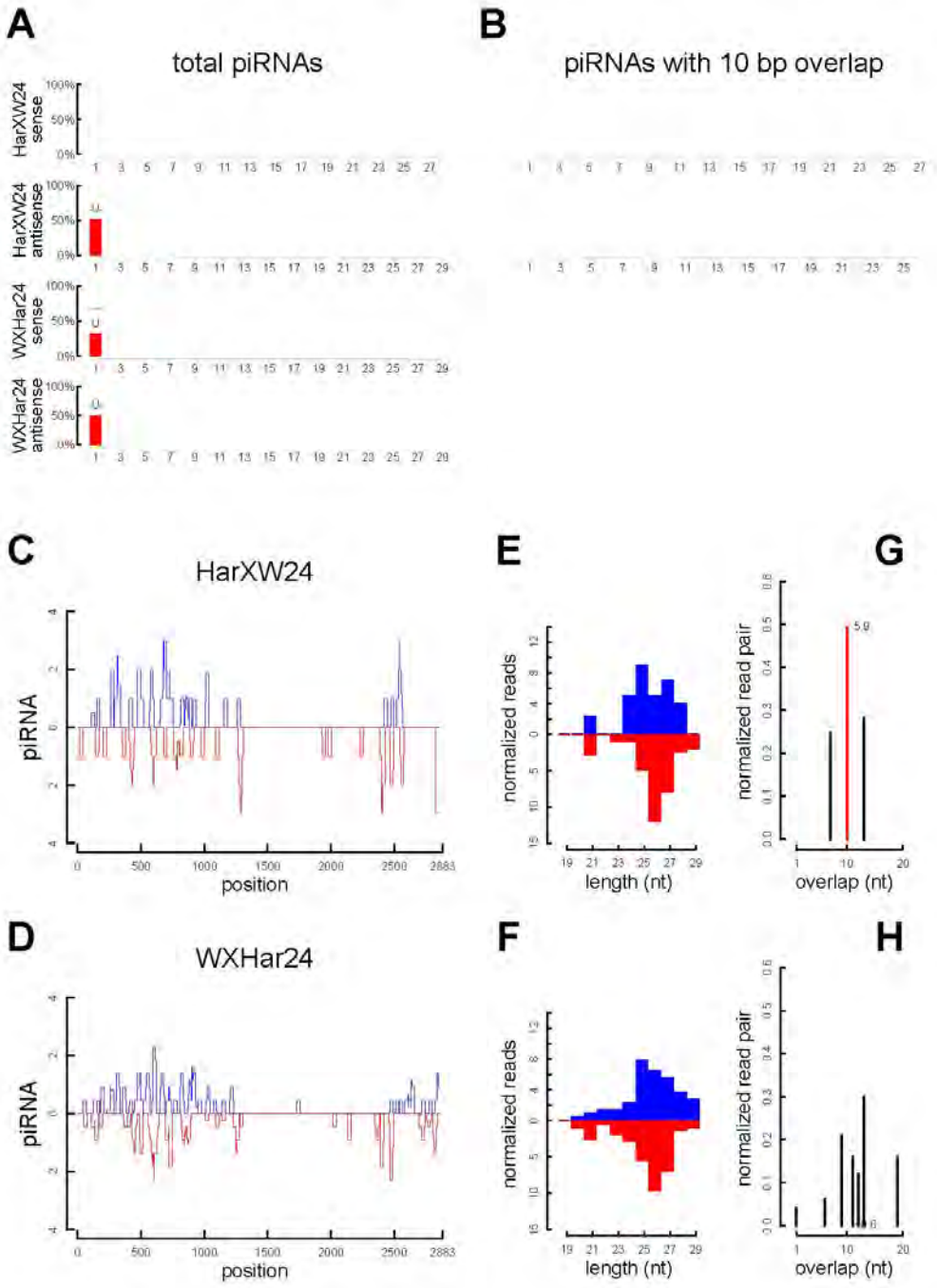
A
total piRNAs
B
piRNAs with 10 bp overlap
HarXW24 sense
HarXW24 antisense
WXHar24 sense
WXHar24 antisense
C
HarXW24
D
WXHar24
piRNA
position
E
F
normalized reads
length (nt)
G
H
normalized read pair
overlap (nt)

transib4

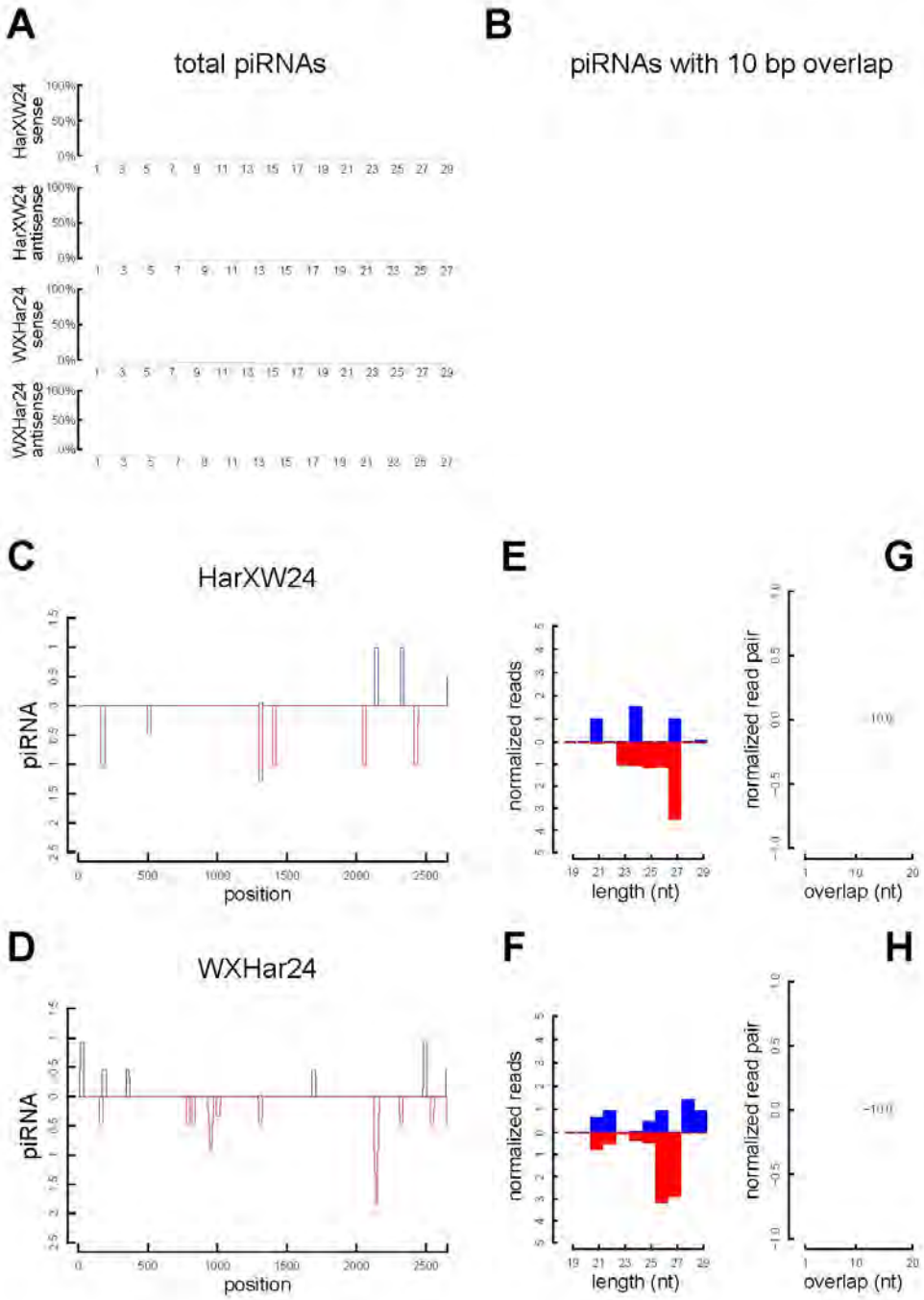
A
total piRNAs
HarXW24 sense
HarXW24 antisense
WXHar24 sense
WXHar24 antisense
B
piRNAs with 10 bp overlap
C
HarXW24
piRNA
position
D
WXHar24
piRNA
position
E
normalized reads
length (nt)
F
normalized reads
length (nt)
G
normalized read pair
overlap (nt)
H
normalized read pair
overlap (nt)

Transpac

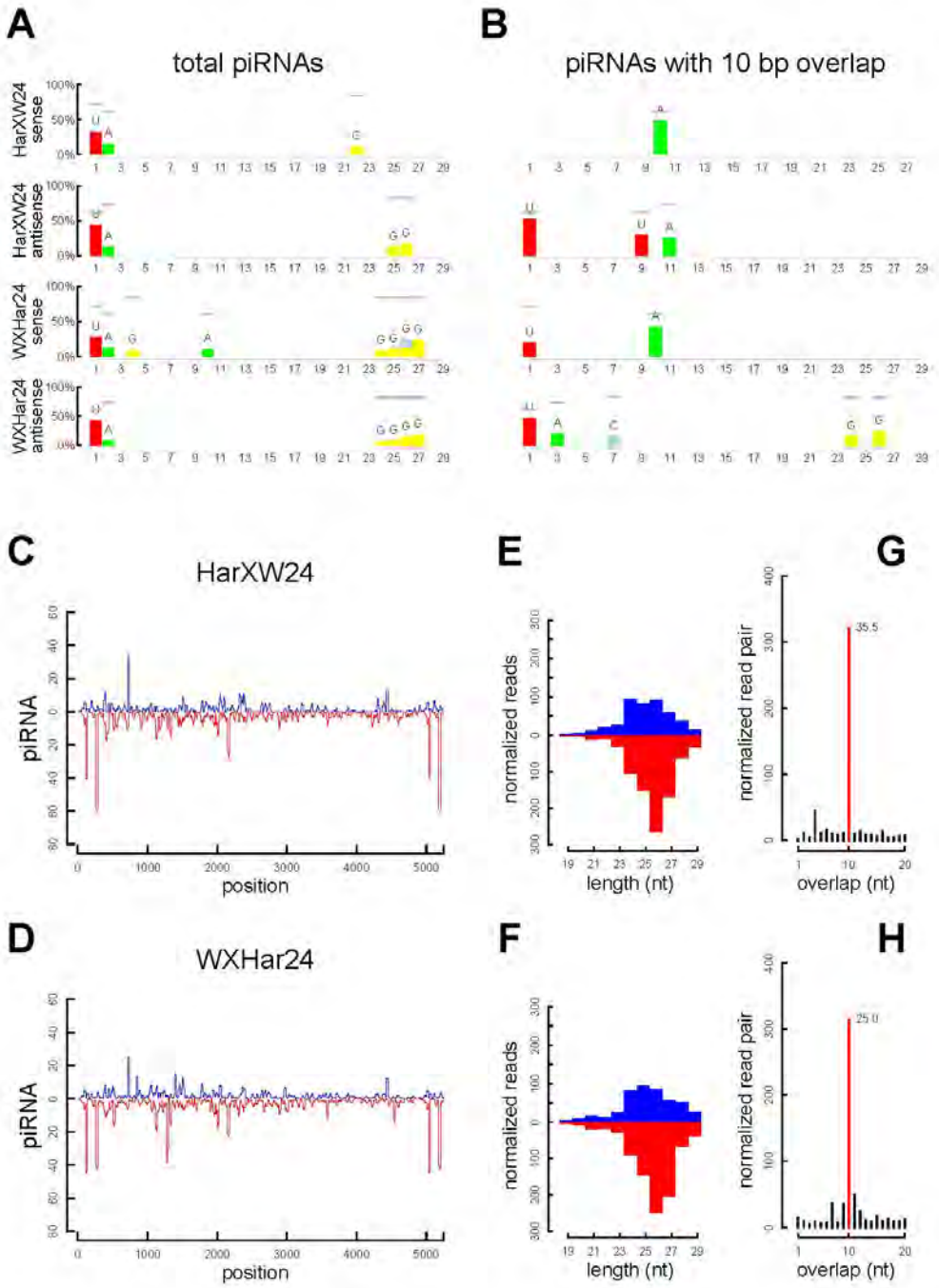
A
total piRNAs
B
piRNAs with 10 bp overlap
HarXW24 sense
HarXW24 antisense
WXHar24 sense
WXHar24 antisense
C
HarXW24
piRNA
position
D
WXHar24
piRNA
position
E
normalized reads
length (nt)
F
normalized reads
length (nt)
G
normalized read pair
35.5
overlap (nt)
H
normalized read pair
25.0
overlap (nt)

X element

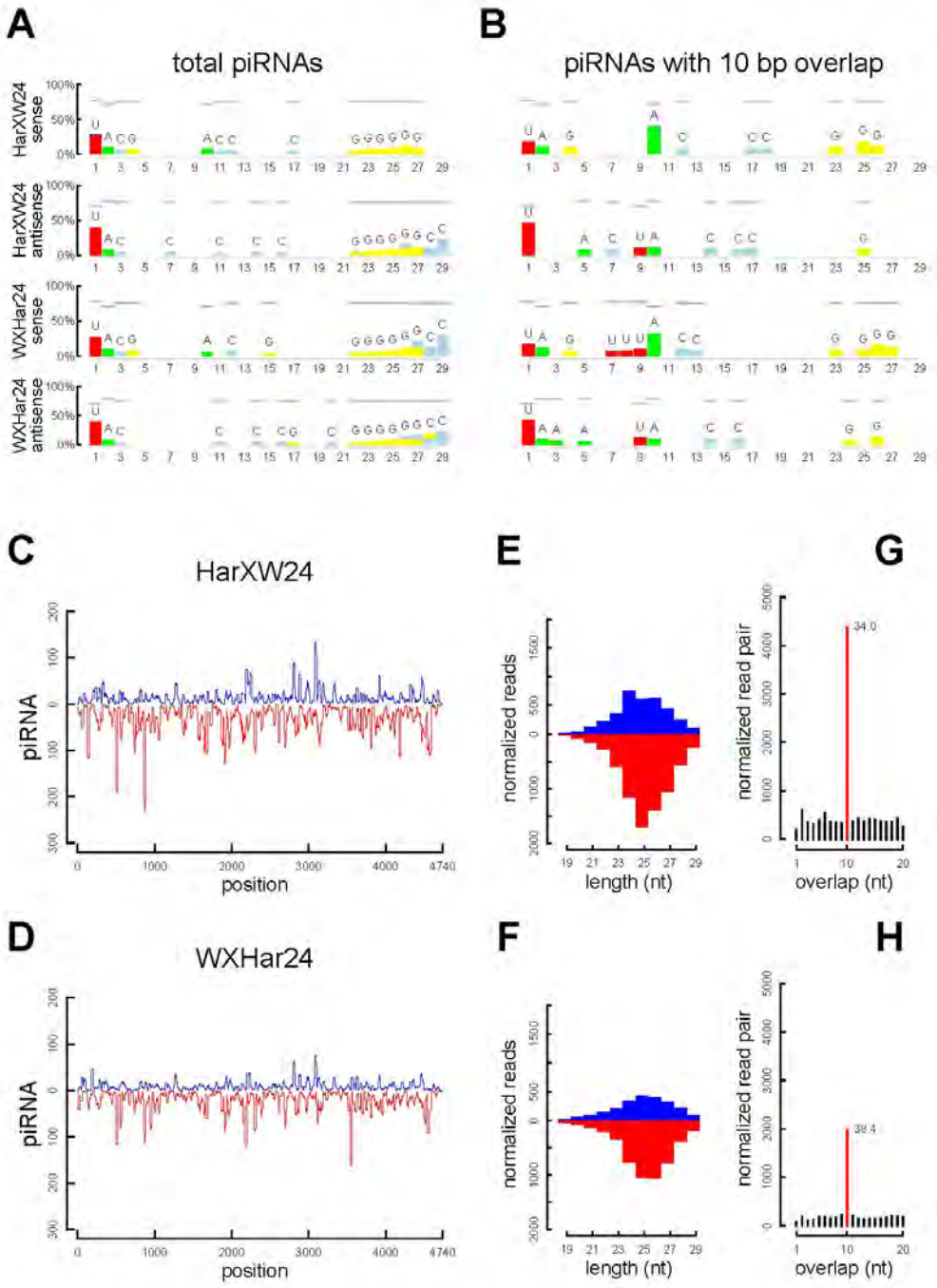
A
total piRNAs
B
piRNAs with 10 bp overlap
HarXW24 sense
HarXW24 antisense
WXHar24 sense
WXHar24 antisense
C
HarXW24
piRNA
position
D
WXHar24
piRNA
position
E
normalized reads
length (nt)
F
normalized reads
length (nt)
G
normalized read pair
34.0
overlap (nt)
H
normalized read pair
39.4
overlap (nt)

ZAM

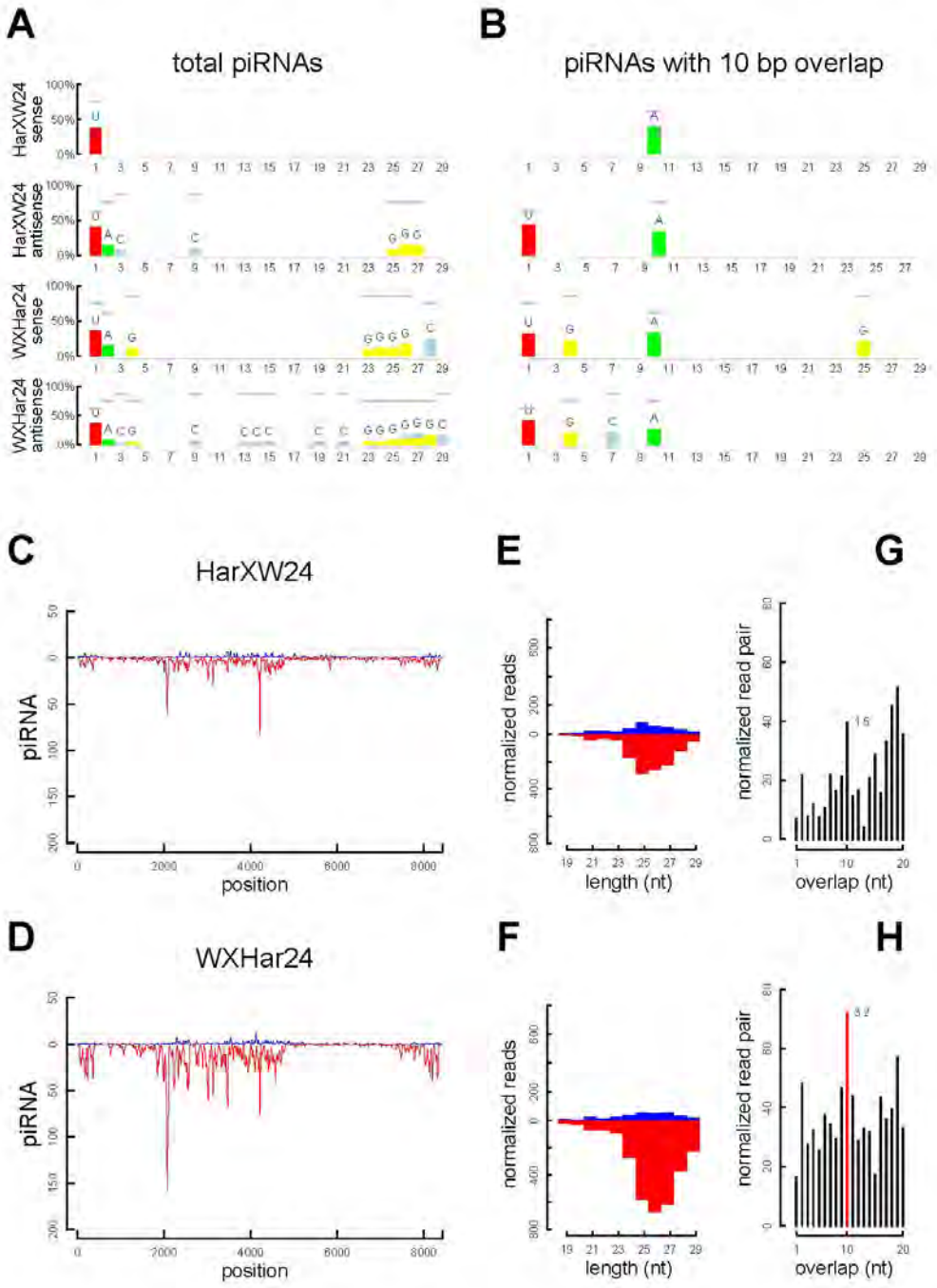
A
total piRNAs
B
piRNAs with 10 bp overlap
HarXW24 sense
HarXW24 antisense
WXHar24 sense
WXHar24 antisense
C
HarXW24
D
WXHar24
piRNA
position
E
F
normalized reads
length (nt)
G
H
normalized read pair
overlap (nt)

mst40

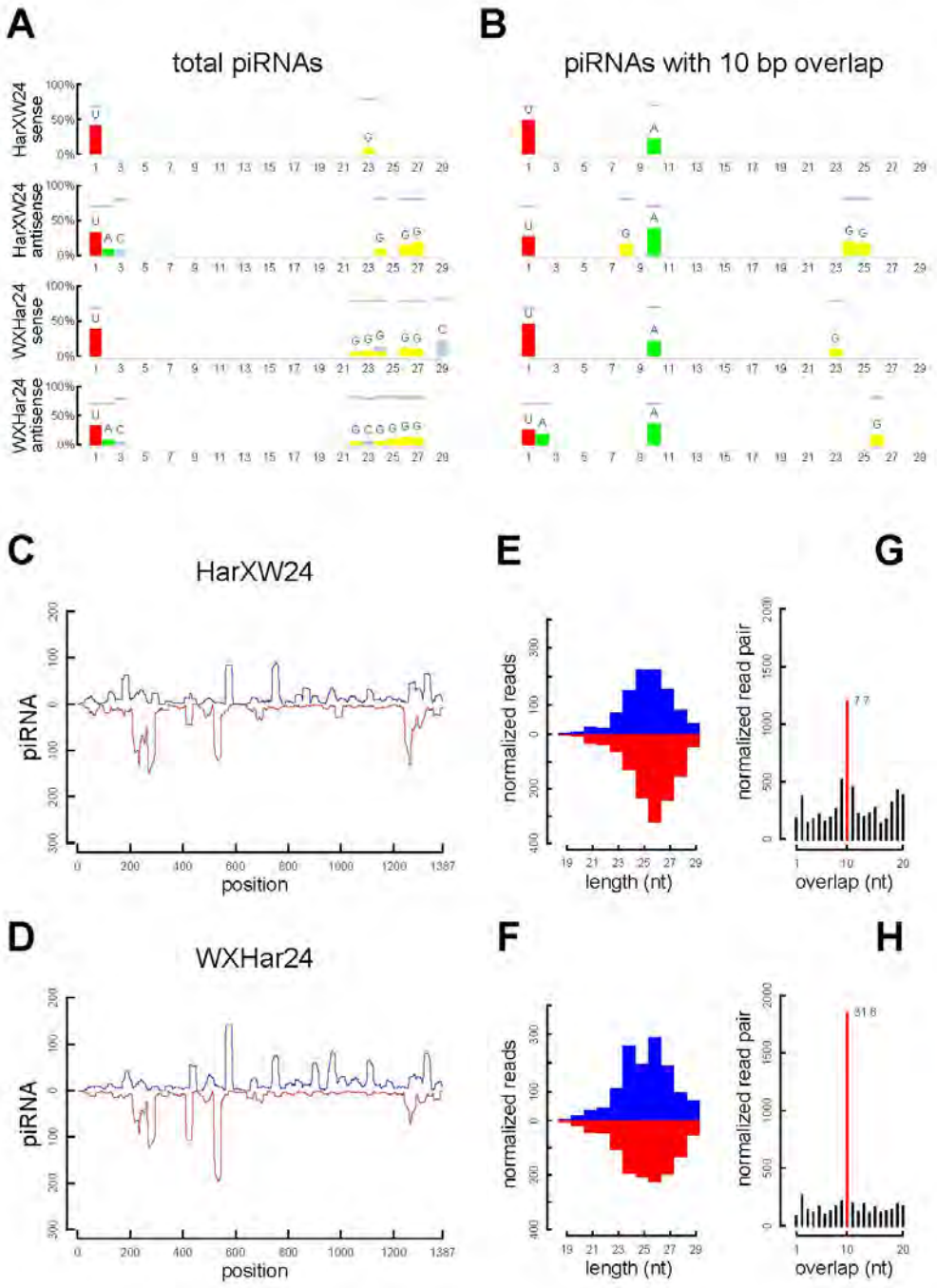
A
total piRNAs
B
piRNAs with 10 bp overlap
HarXW24 sense
HarXW24 antisense
WXHar24 sense
WXHar24 antisense
C
HarXW24
D
WXHar24
piRNA
position
E
F
normalized reads
length (nt)
G
H
normalized read pair
overlap (nt)

suffix

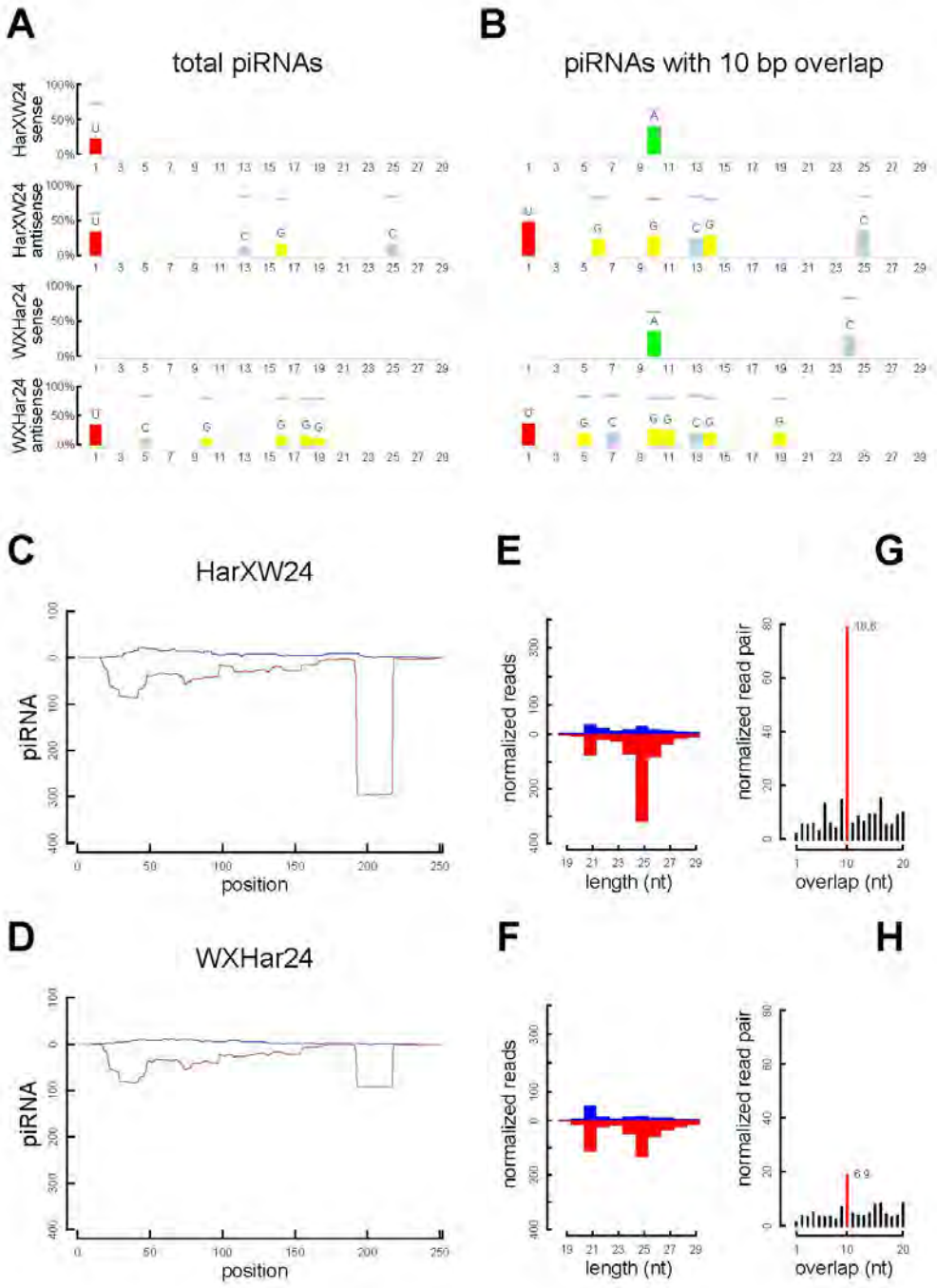
A
total piRNAs
B
piRNAs with 10 bp overlap
HarXW24 sense
HarXW24 antisense
WXHar24 sense
WXHar24 antisense
C
HarXW24
D
WXHar24
piRNA
position
E
F
normalized reads
length (nt)
G
H
normalized read pair
overlap (nt)
10.6
6.9

satellite

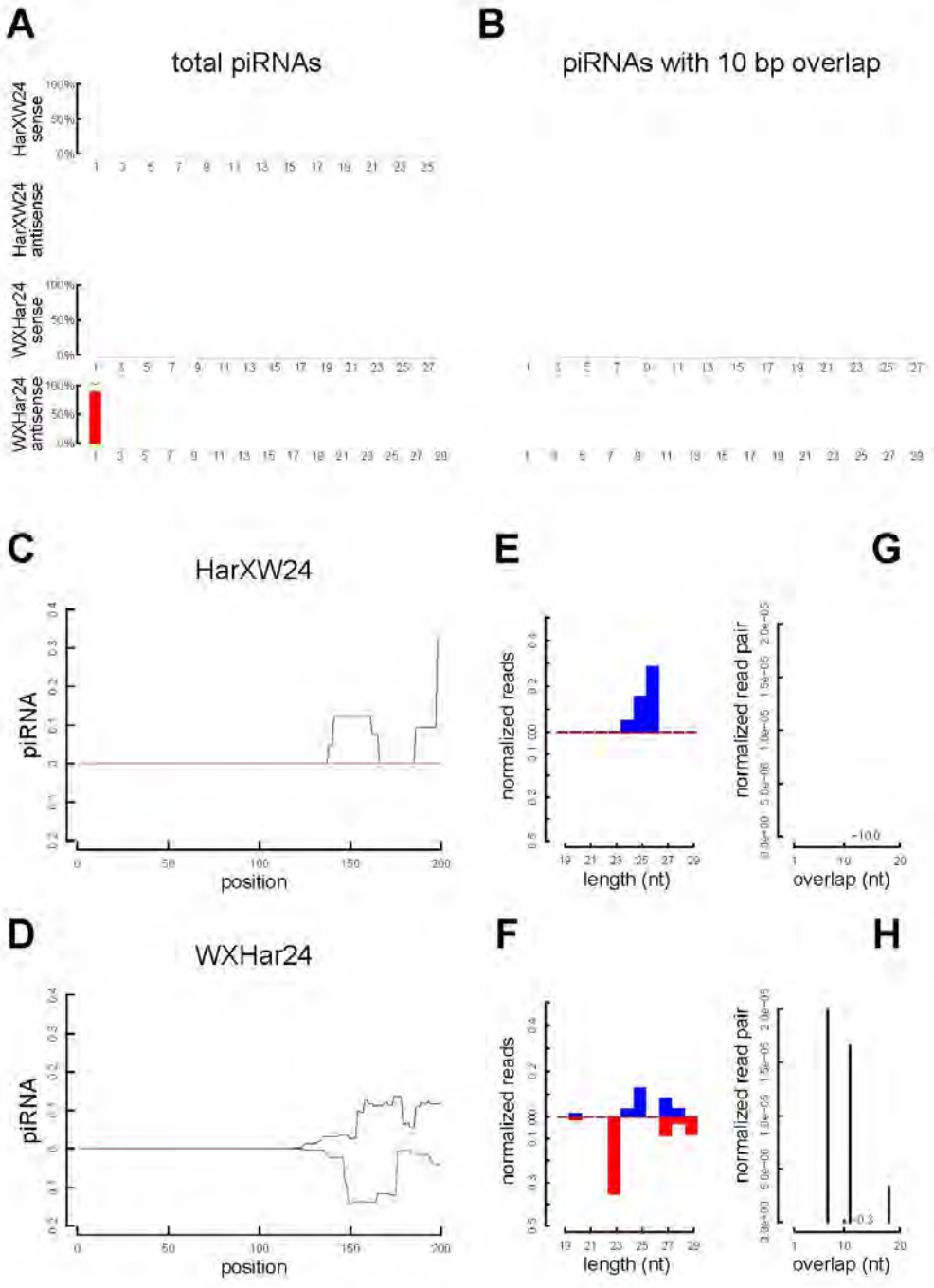
A
total piRNAs
B
piRNAs with 10 bp overlap
HarXW24 sense
HarXW24 antisense
WXHar24 sense
WXHar24 antisense
C
HarXW24
D
WXHar24
piRNA
position
E
F
normalized reads
length (nt)
G
H
normalized read pair
overlap (nt)

stellate

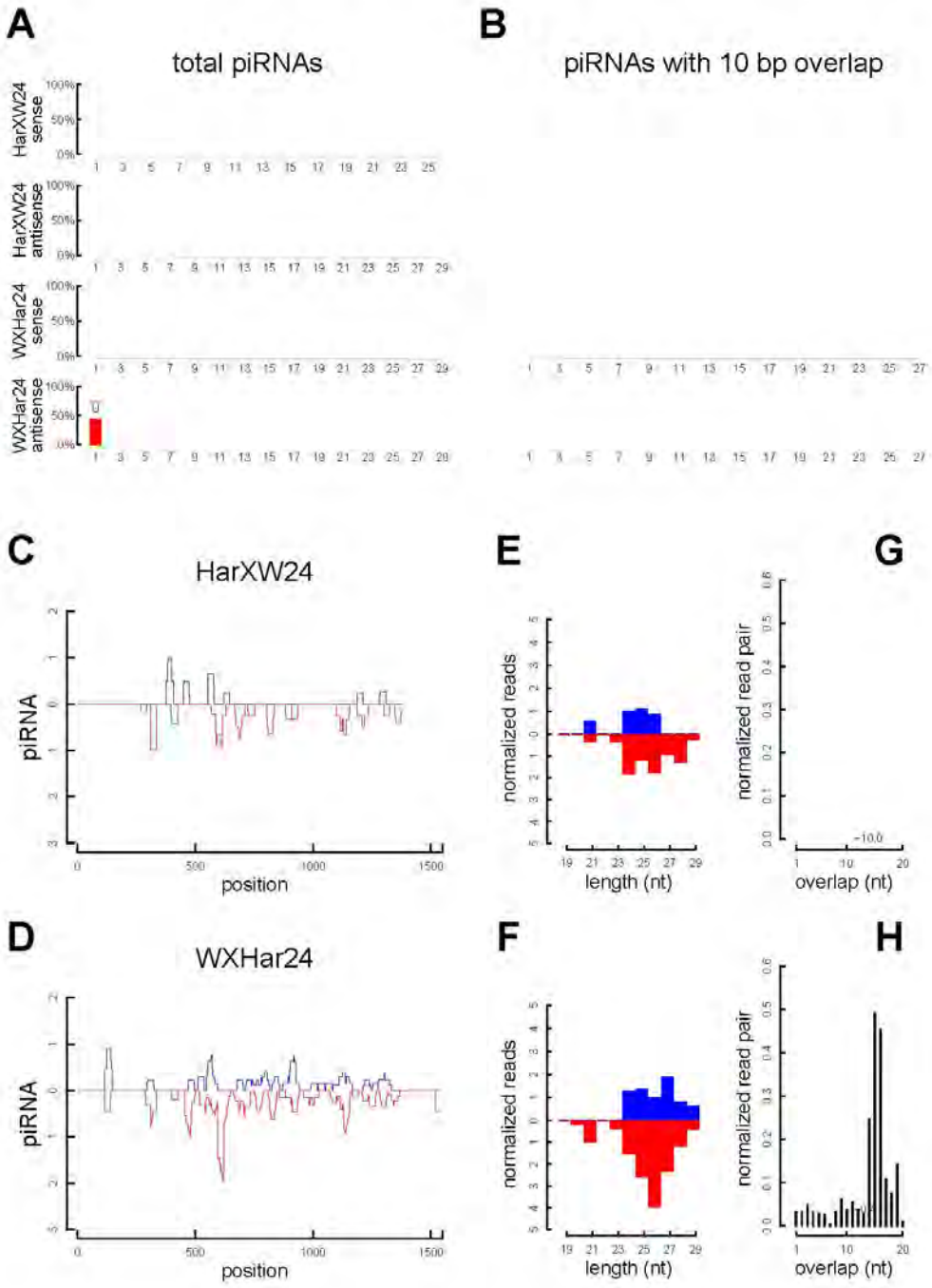
A
total piRNAs
HarXW24 sense
HarXW24 antisense
WXHar24 sense
WXHar24 antisense
B
piRNAs with 10 bp overlap
C
HarXW24
piRNA
position
D
WXHar24
piRNA
position
E
normalized reads
length (nt)
F
normalized reads
length (nt)
G
normalized read pair
overlap (nt)
H
normalized read pair
overlap (nt)

stellateHet

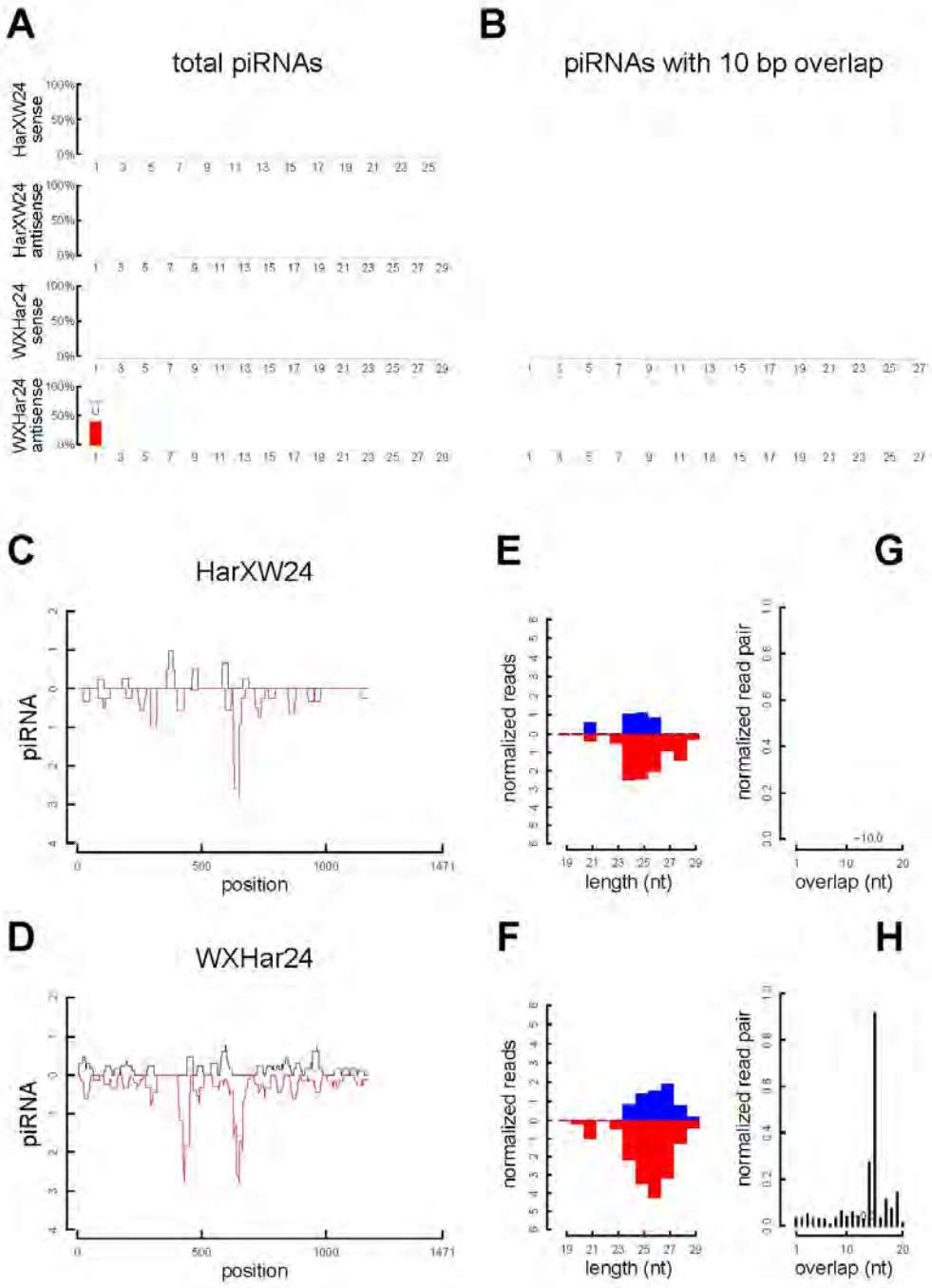

suste

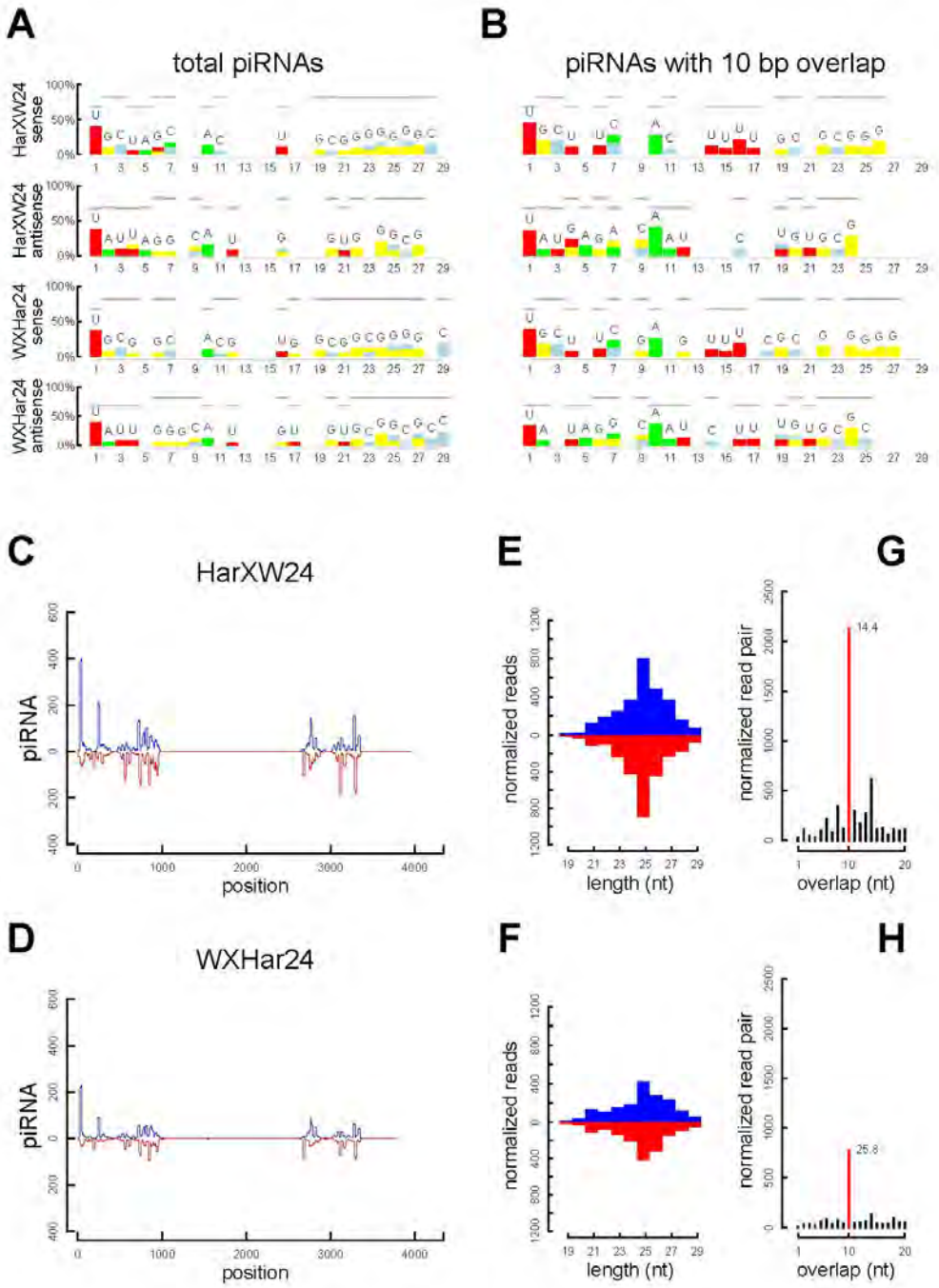
A
total piRNAs
HarXW24 sense
HarXW24 antisense
WXHar24 sense
WXHar24 antisense
B
piRNAs with 10 bp overlap
C
HarXW24
piRNA
position
D
WXHar24
piRNA
position
E
normalized reads
length (nt)
F
normalized reads
length (nt)
G
normalized read pair
14.4
overlap (nt)
H
normalized read pair
25.8
overlap (nt)

TARTA

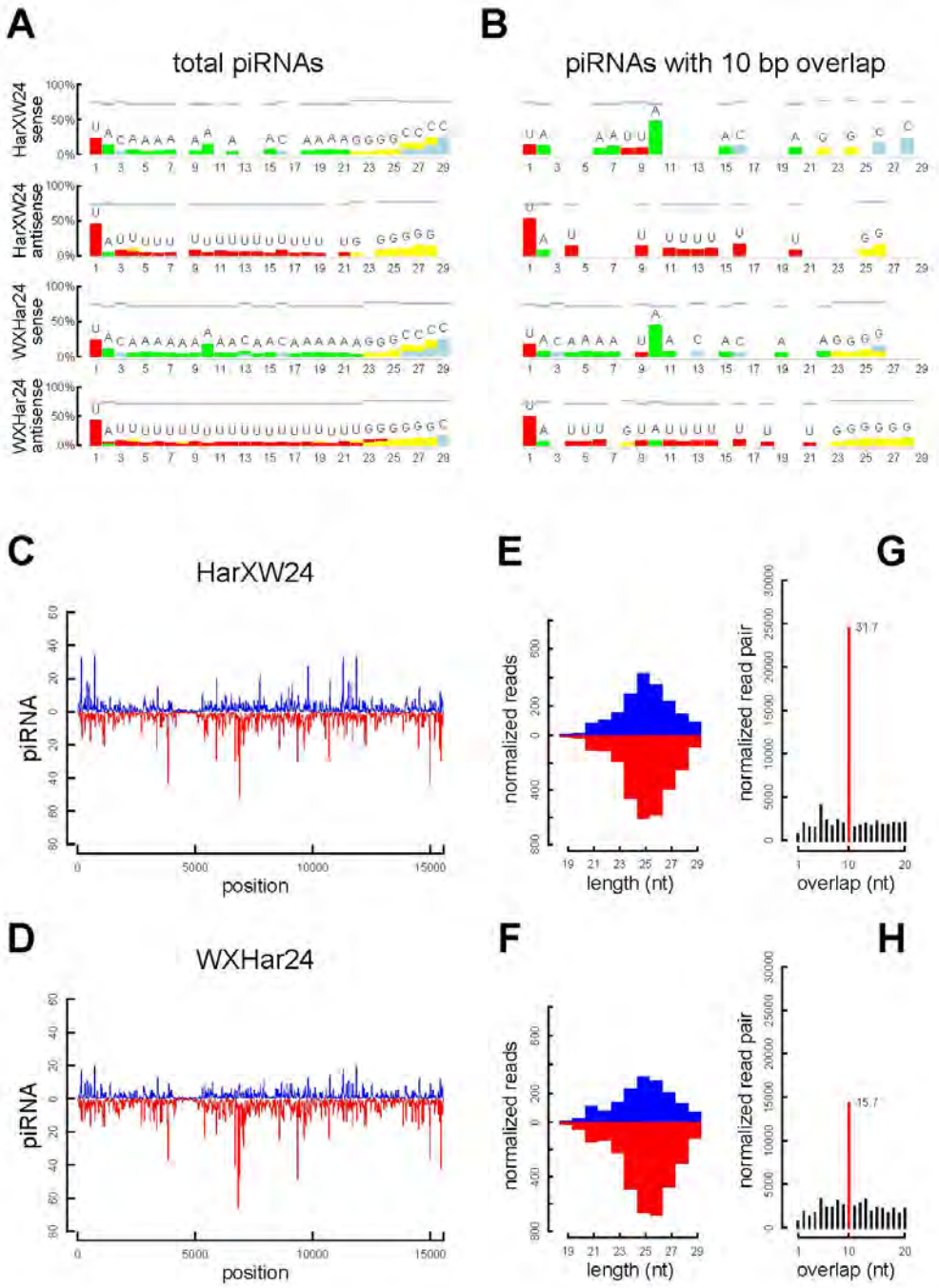
A
total piRNAs
B
piRNAs with 10 bp overlap
HarXW24 sense
HarXW24 antisense
WXHar24 sense
WXHar24 antisense
C
HarXW24
D
WXHar24
piRNA
position
E
F
normalized reads
length (nt)
G
H
normalized read pair
overlap (nt)
31.7
15.7

P-element

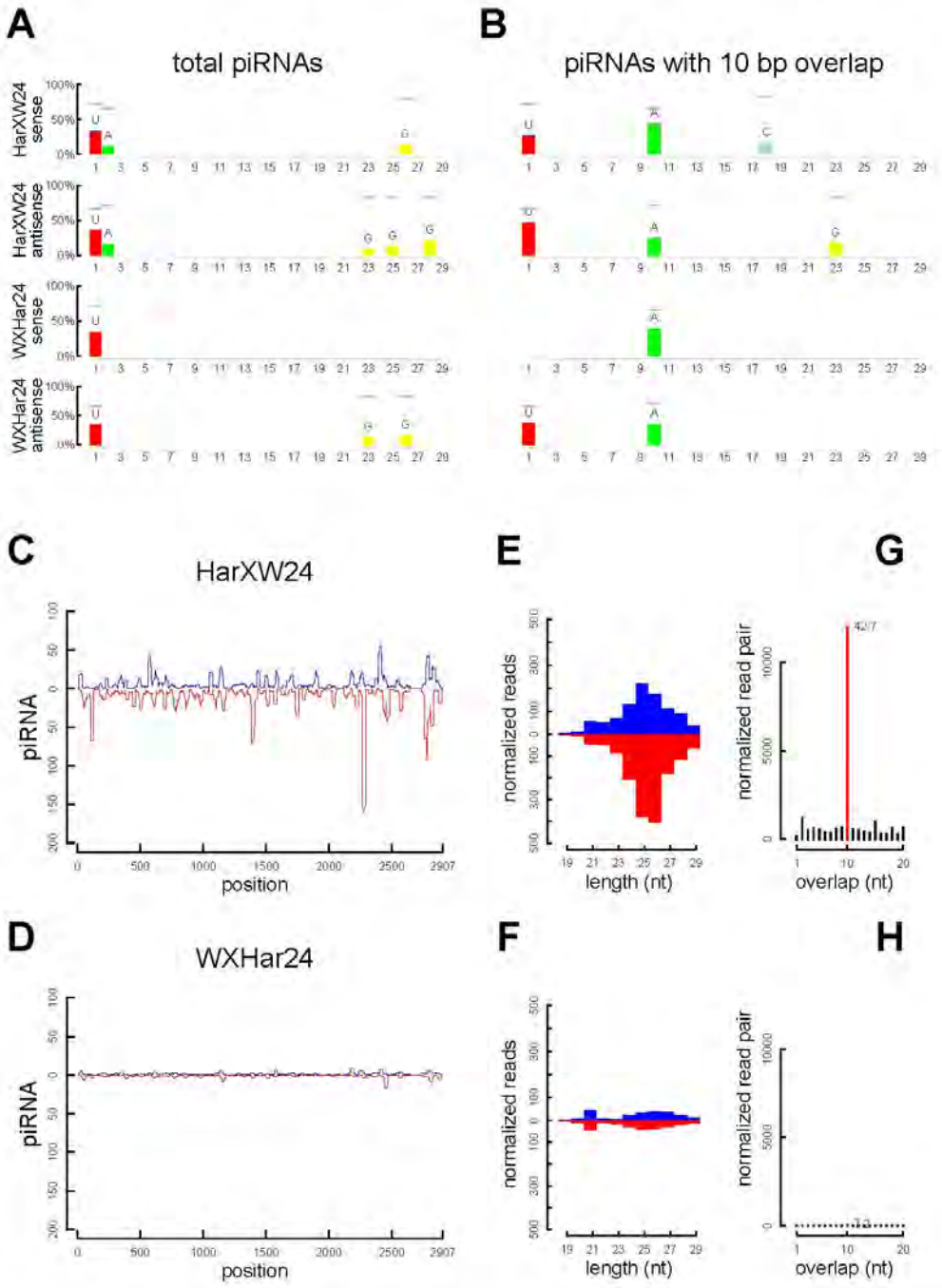
A
total piRNAs
B
piRNAs with 10 bp overlap
HarXW24 sense
HarXW24 antisense
WXHar24 sense
WXHar24 antisense
C
HarXW24
D
WXHar24
piRNA
position
E
F
normalized reads
length (nt)
G
H
normalized read pair
overlap (nt)

Supplementary Figure 3b

1360

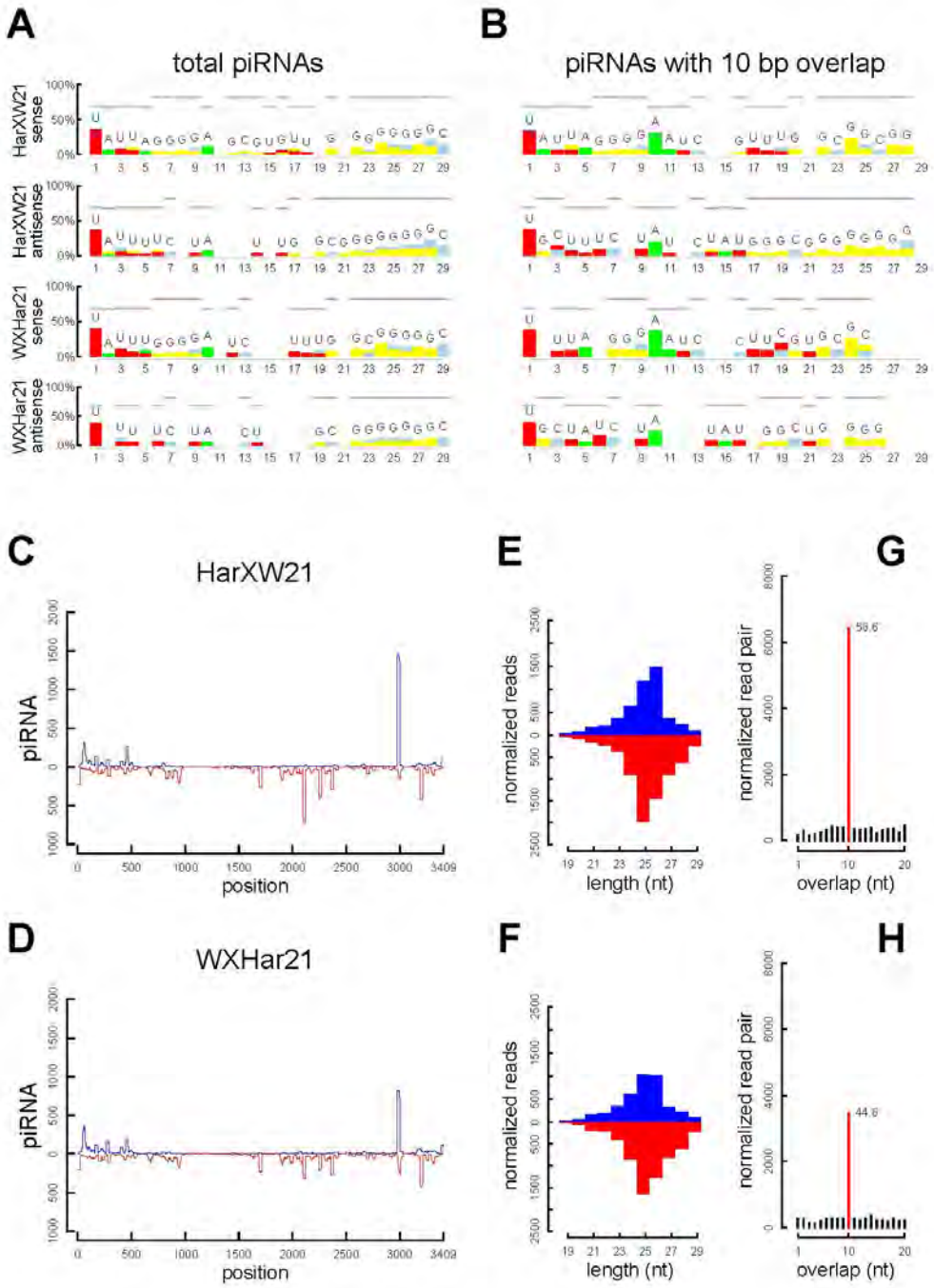
A
total piRNAs
B
piRNAs with 10 bp overlap
HarXW21 sense
HarXW21 antisense
WXHar21 sense
WXHar21 antisense
C
HarXW21
piRNA
position
D
WXHar21
piRNA
position
E
normalized reads
length (nt)
F
normalized reads
length (nt)
G
normalized read pair
overlap (nt)
56.6
H
normalized read pair
overlap (nt)
44.8

1731

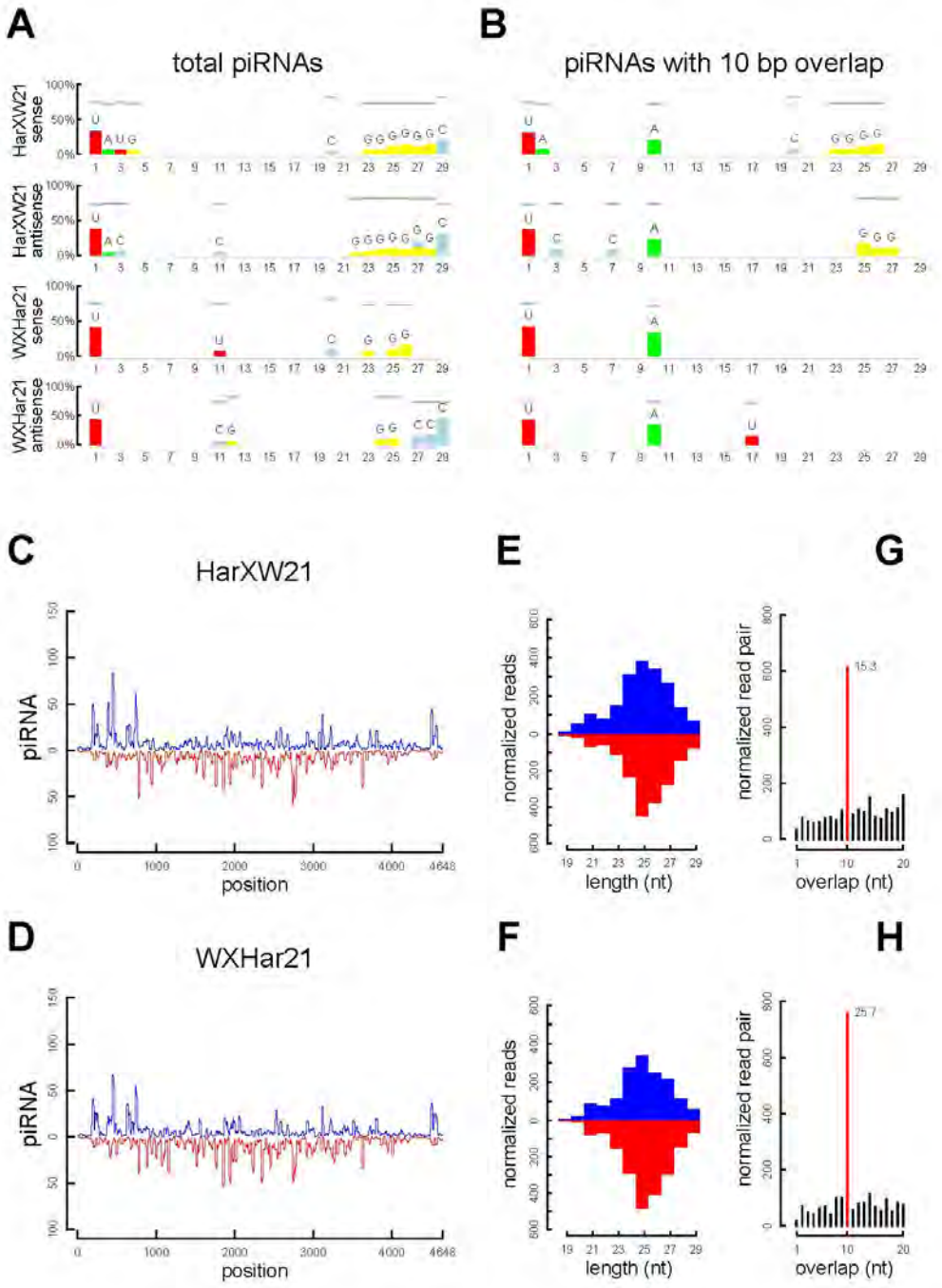
A
total piRNAs
B
piRNAs with 10 bp overlap
HarXW21 sense
HarXW21 antisense
WXHar21 sense
WXHar21 antisense
C
HarXW21
D
WXHar21
piRNA
position
E
F
normalized reads
length (nt)
G
H
normalized read pair
overlap (nt)
15.3
25.7

17.6

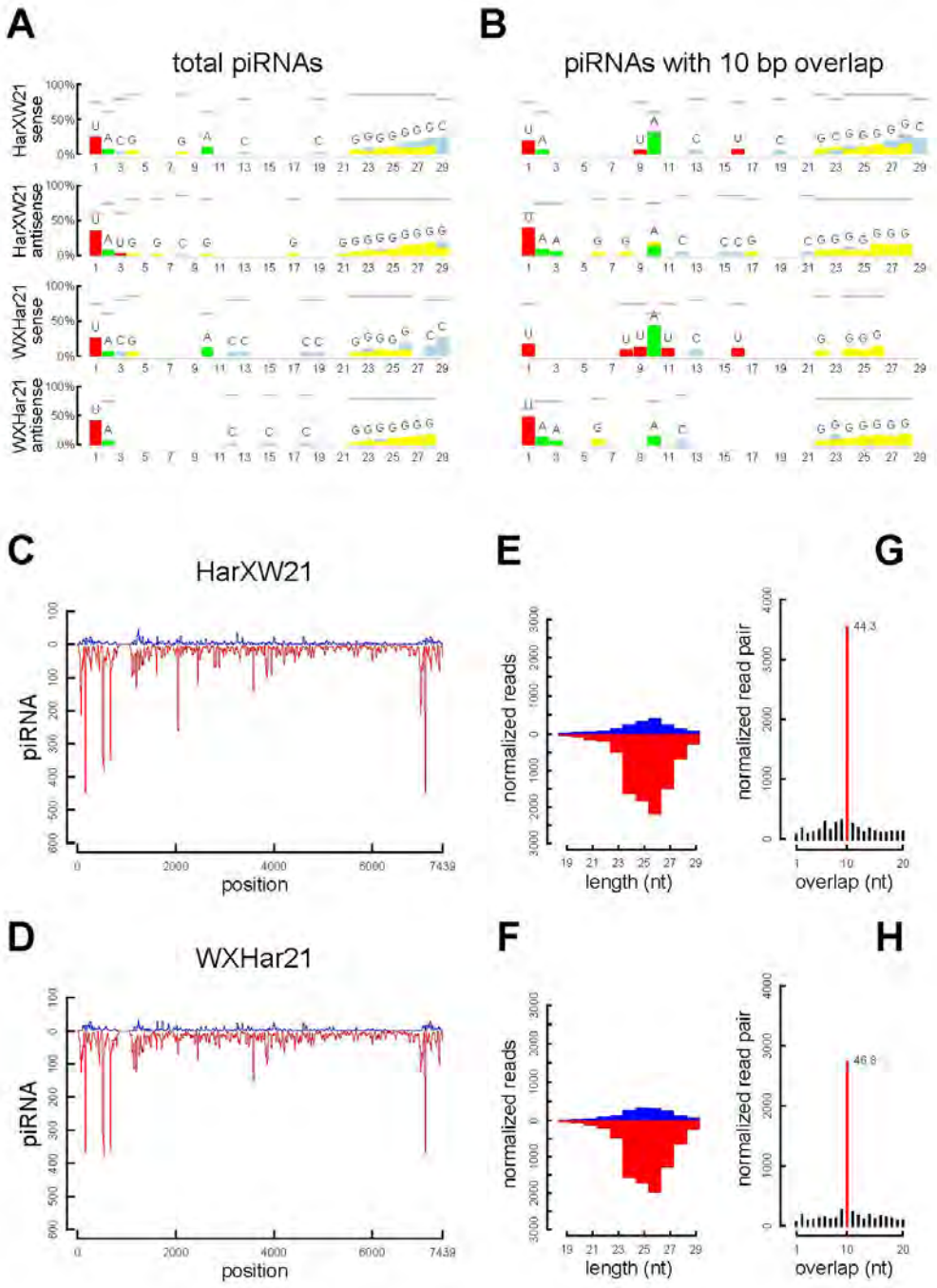
A
total piRNAs
B
piRNAs with 10 bp overlap
HarXW21 sense
HarXW21 antisense
WXHar21 sense
WXHar21 antisense
C
HarXW21
piRNA
position
D
WXHar21
piRNA
position
E
normalized reads
length (nt)
F
normalized reads
length (nt)
G
normalized read pair
44.3
overlap (nt)
H
normalized read pair
46.8
overlap (nt)

297

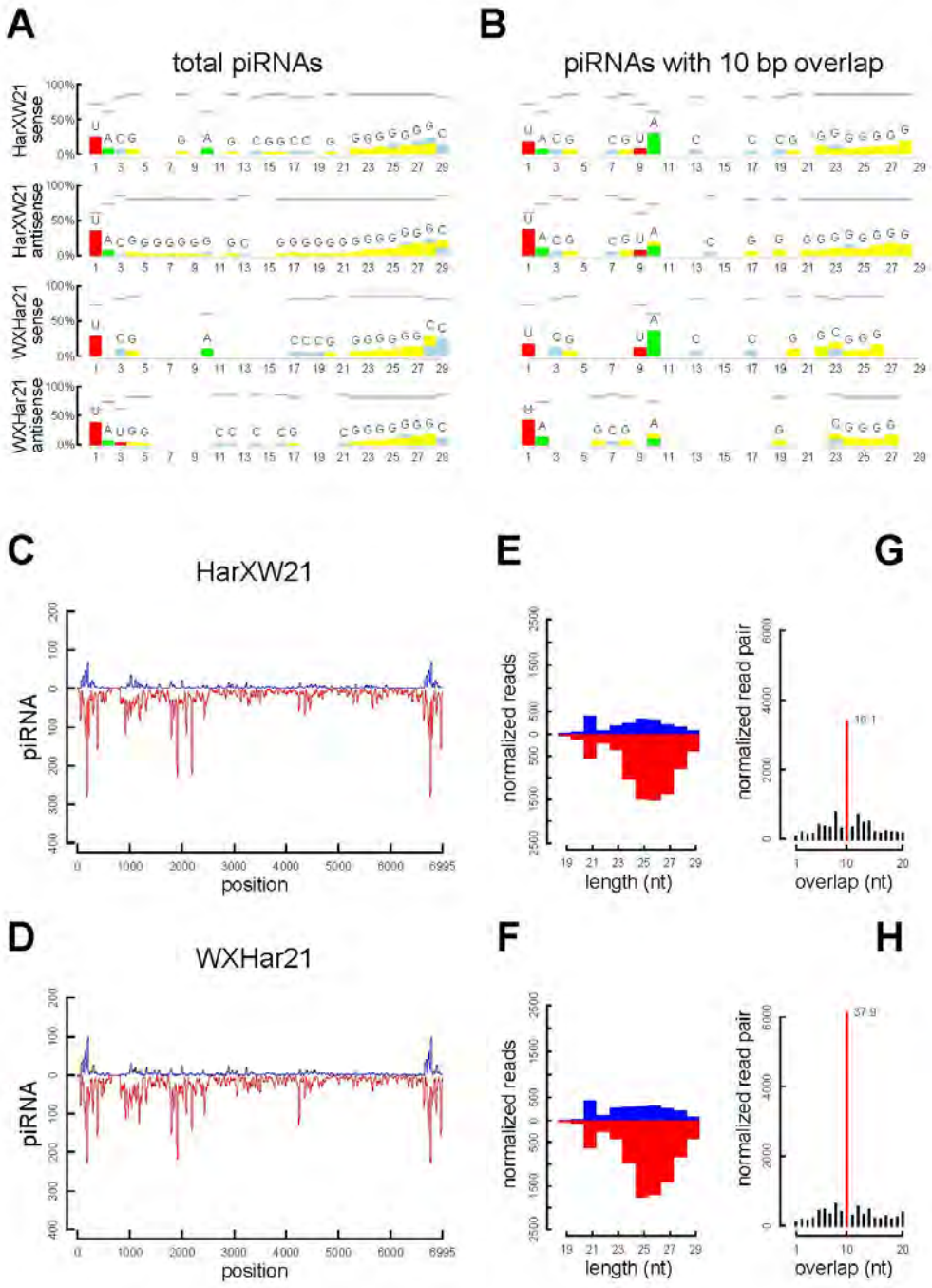
A
total piRNAs
B
piRNAs with 10 bp overlap
HarXW21 sense
HarXW21 antisense
WXHar21 sense
WXHar21 antisense
C
HarXW21
D
WXHar21
piRNA
position
E
F
normalized reads
length (nt)
G
H
normalized read pair
overlap (nt)
10.1
37.9

3S18

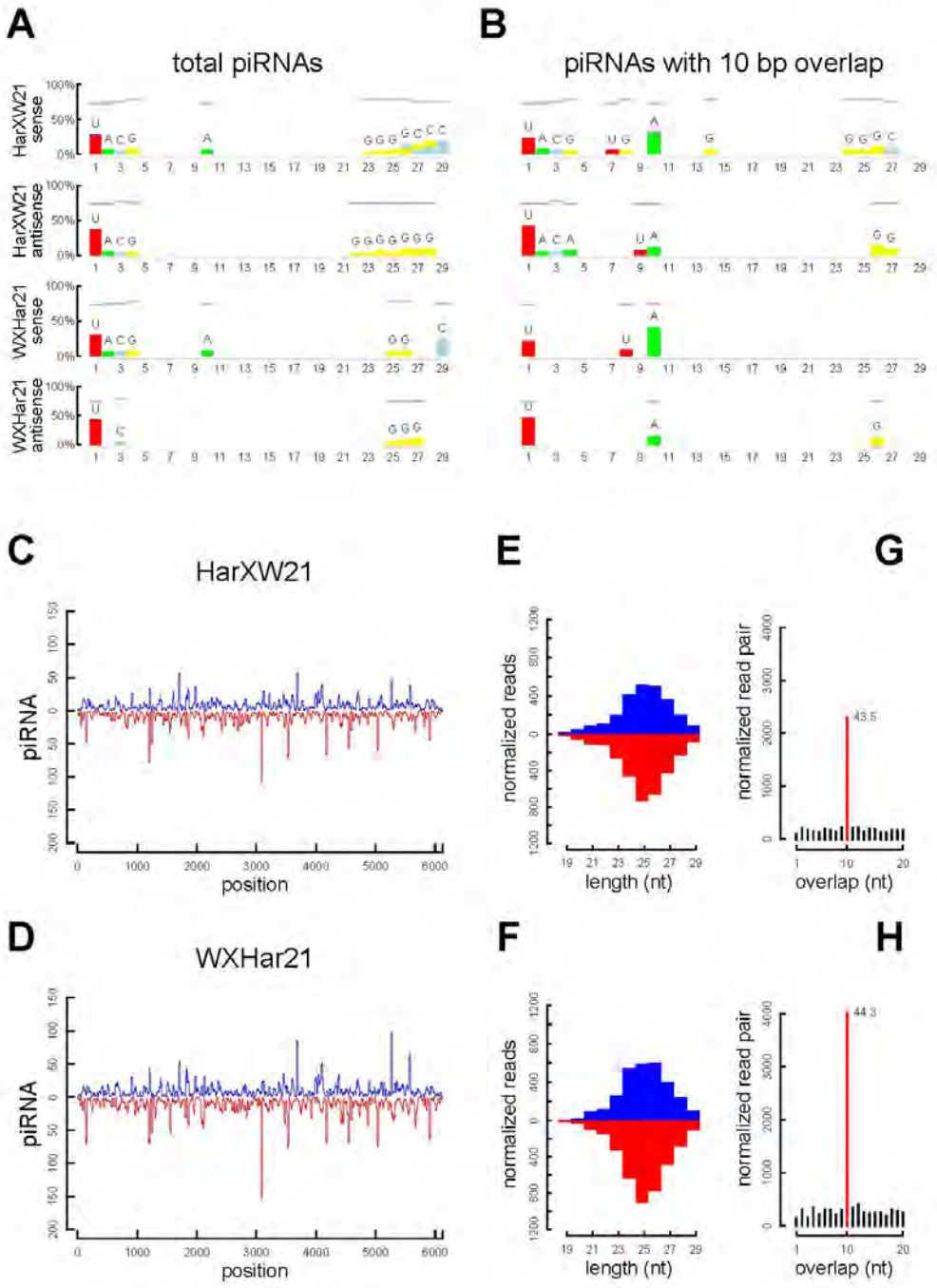
A
total piRNAs
B
piRNAs with 10 bp overlap
HarXW21 sense
HarXW21 antisense
WXHar21 sense
WXHar21 antisense
C
HarXW21
D
WXHar21
piRNA
position
E
F
normalized reads
length (nt)
G
H
normalized read pair
overlap (nt)
43.5
44.3

412

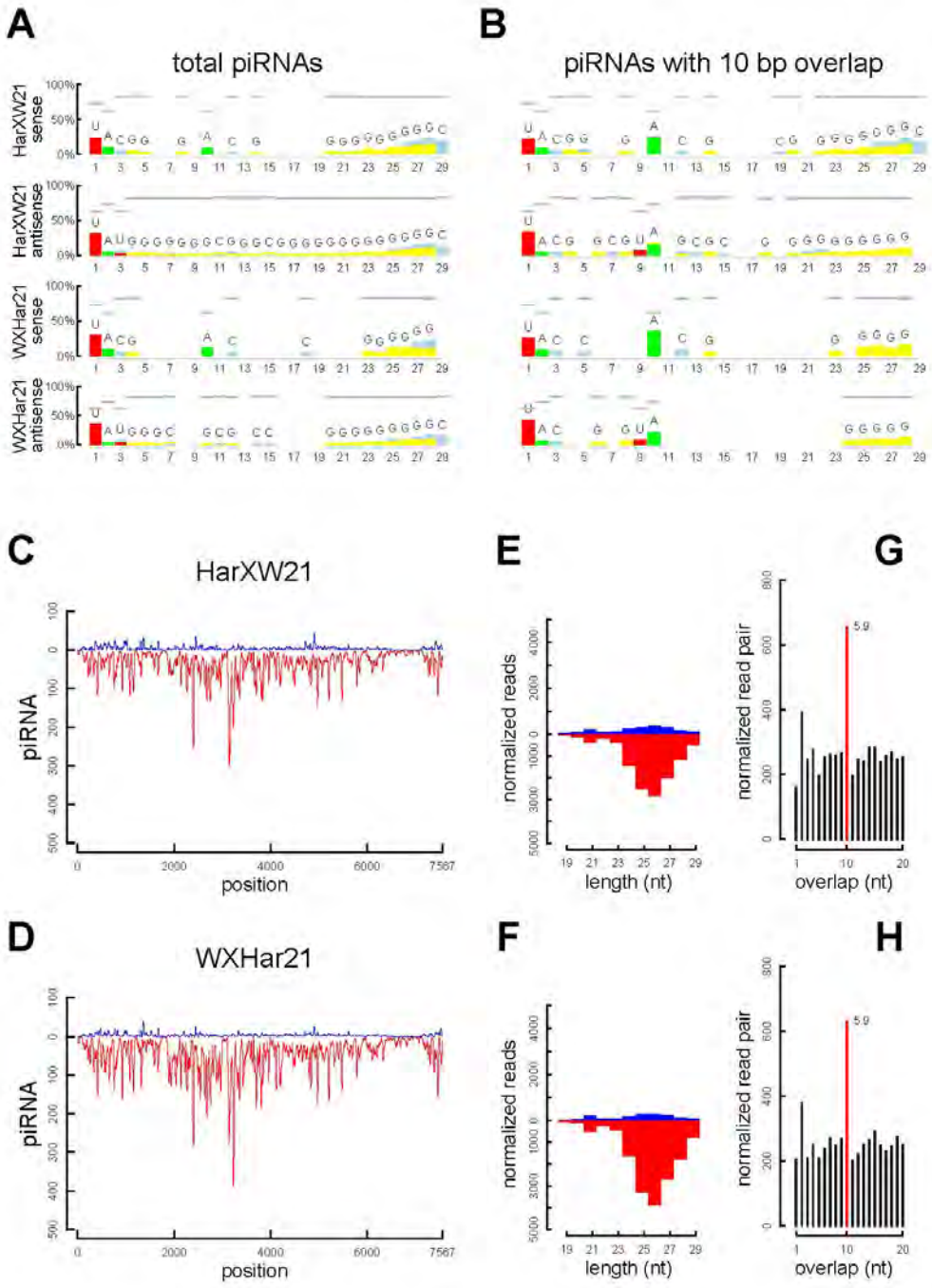
A
total piRNAs
B
piRNAs with 10 bp overlap
HarXW21 sense
HarXW21 antisense
WXHar21 sense
WXHar21 antisense
C
HarXW21
piRNA
position
D
WXHar21
piRNA
position
E
normalized reads
length (nt)
F
normalized reads
length (nt)
G
normalized read pair
overlap (nt)
5.9
H
normalized read pair
overlap (nt)
5.9

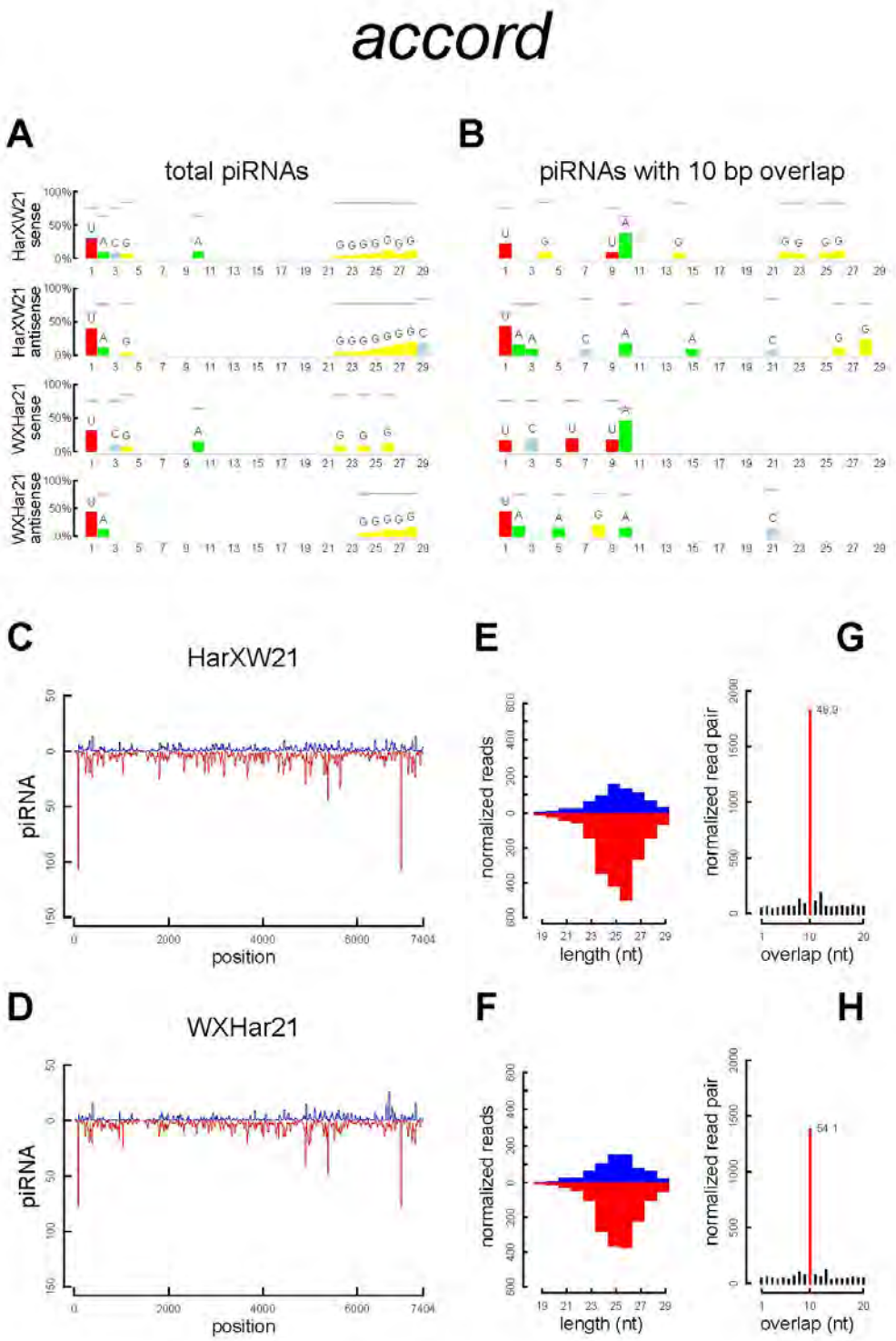
accord
A
total piRNAs
B
piRNAs with 10 bp overlap
HarXW21 sense
HarXW21 antisense
WXHar21 sense
WXHar21 antisense
C
HarXW21
D
WXHar21
piRNA
position
E
F
normalized reads
length (nt)
G
H
normalized read pair
overlap (nt)

accord2

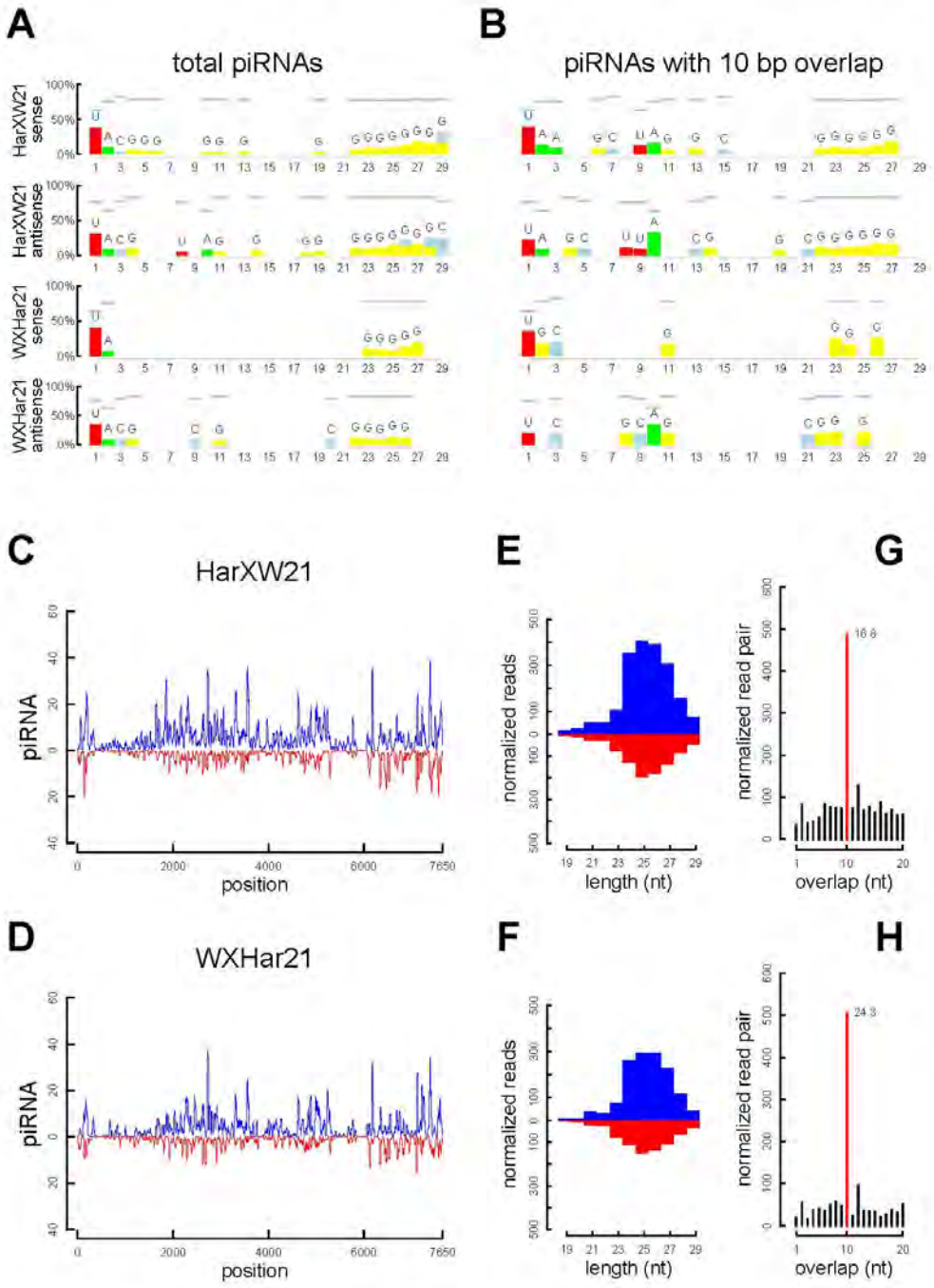
A
total piRNAs
B
piRNAs with 10 bp overlap
HarXW21 sense
HarXW21 antisense
WXHar21 sense
WXHar21 antisense
C
HarXW21
D
WXHar21
piRNA
position
E
F
normalized reads
length (nt)
G
H
normalized read pair
overlap (nt)
16.6
24.3

aurora element

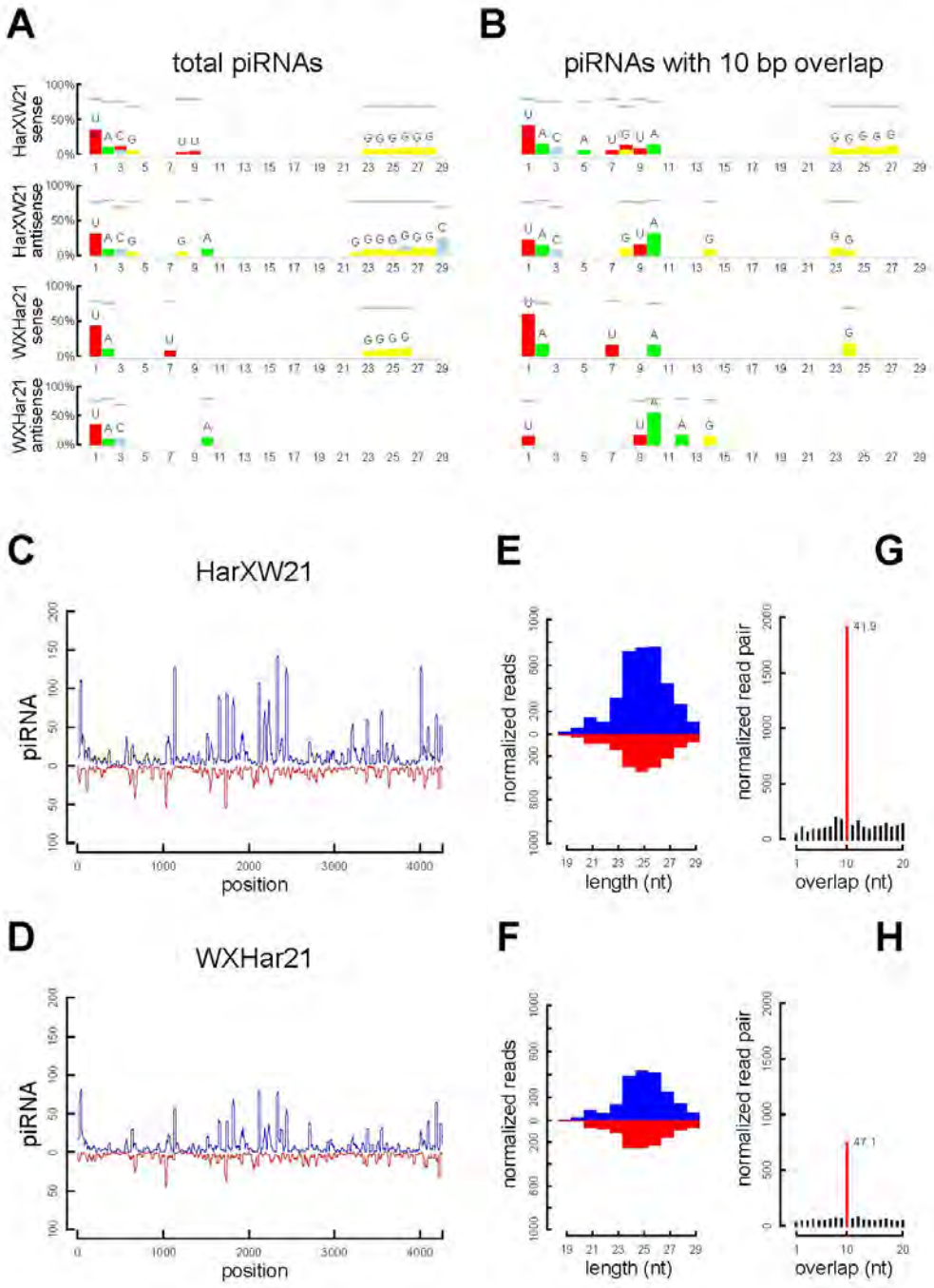

baggins

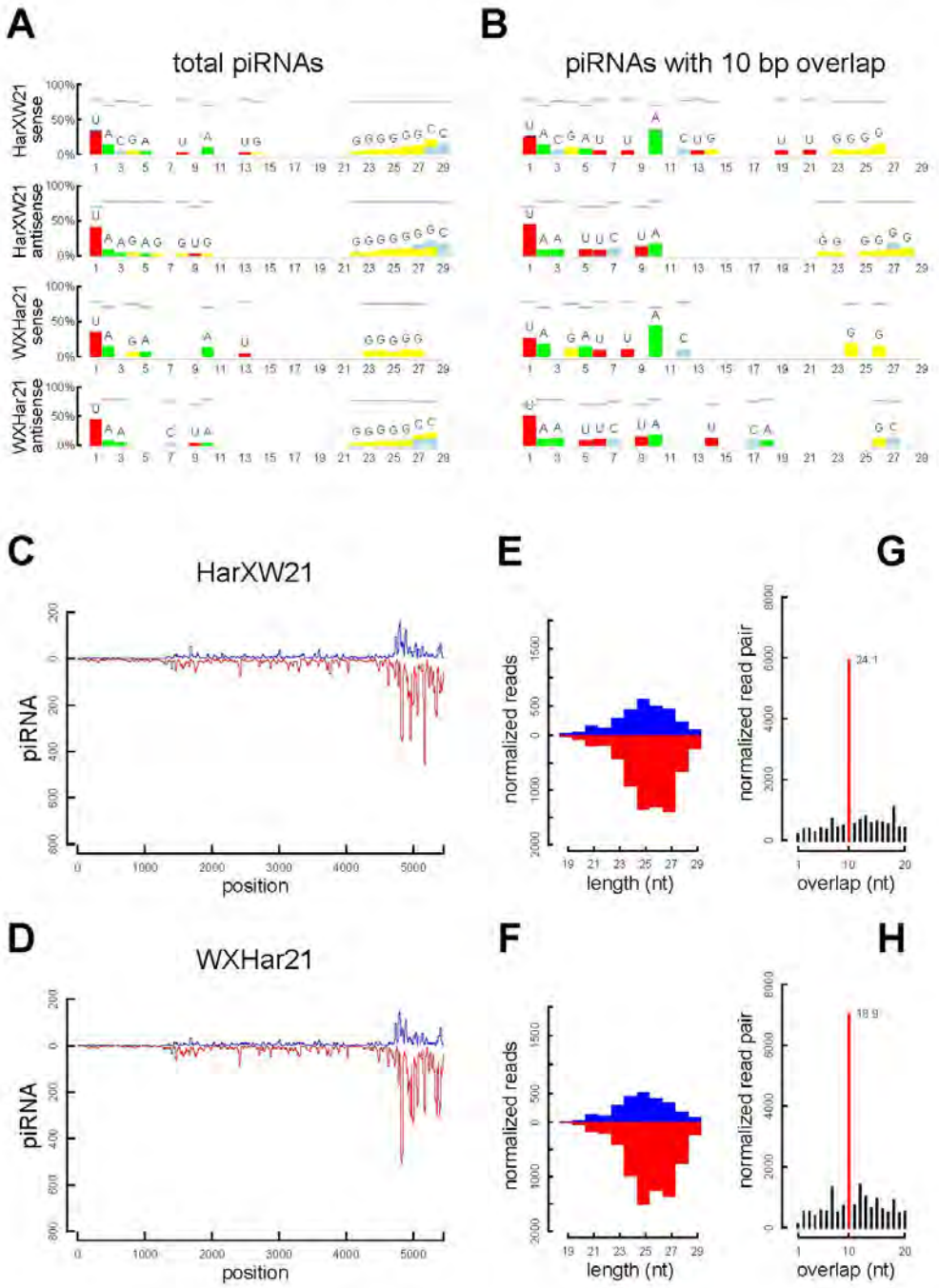
A
total piRNAs
B
piRNAs with 10 bp overlap
HarXW21 sense
HarXW21 antisense
WXHar21 sense
WXHar21 antisense
C
HarXW21
D
WXHar21
piRNA
position
E
F
normalized reads
length (nt)
G
H
normalized read pair
overlap (nt)
24.1
18.9

Bari1

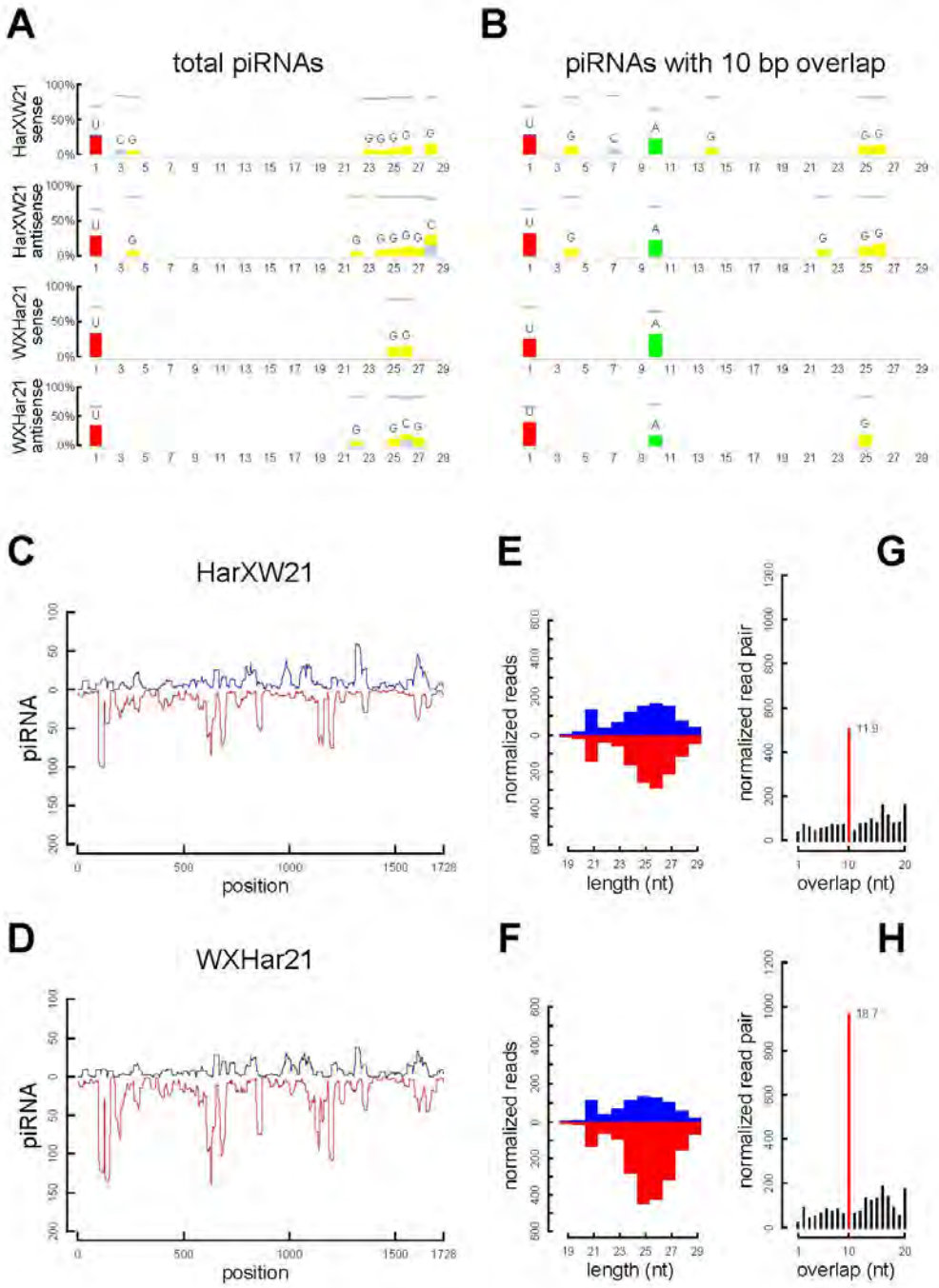
A
total piRNAs
B
piRNAs with 10 bp overlap
HarXW21 sense
HarXW21 antisense
WXHar21 sense
WXHar21 antisense
C
HarXW21
piRNA
position
D
WXHar21
piRNA
position
E
normalized reads
length (nt)
F
normalized reads
length (nt)
G
normalized read pair
overlap (nt)
11.9
H
normalized read pair
overlap (nt)
18.7

Bari2

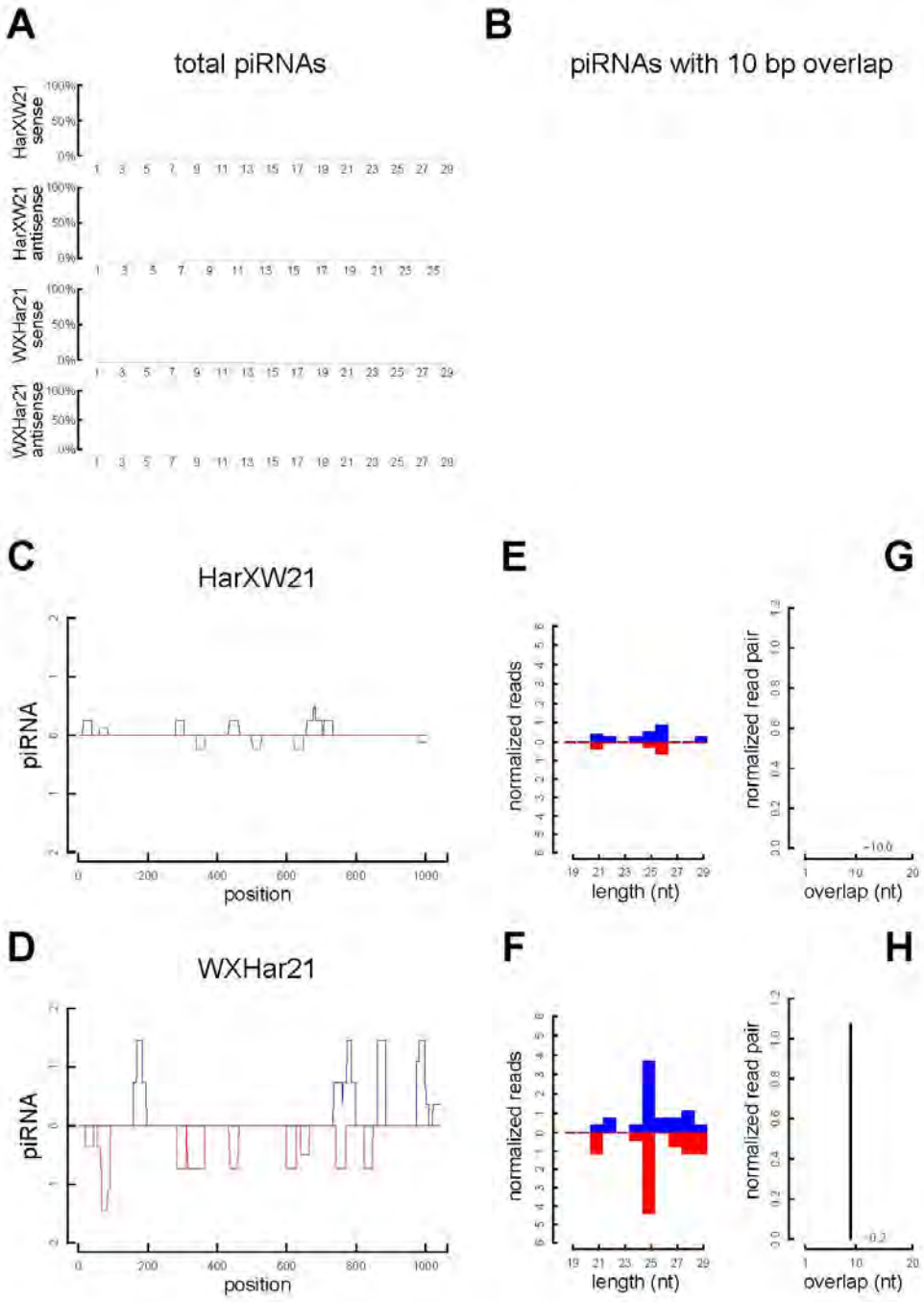
A
total piRNAs
B
piRNAs with 10 bp overlap
HarXW21 sense
HarXW21 antisense
WXHar21 sense
WXHar21 antisense
C
HarXW21
D
WXHar21
piRNA
position
E
F
normalized reads
length (nt)
G
H
normalized read pair
overlap (nt)

blood

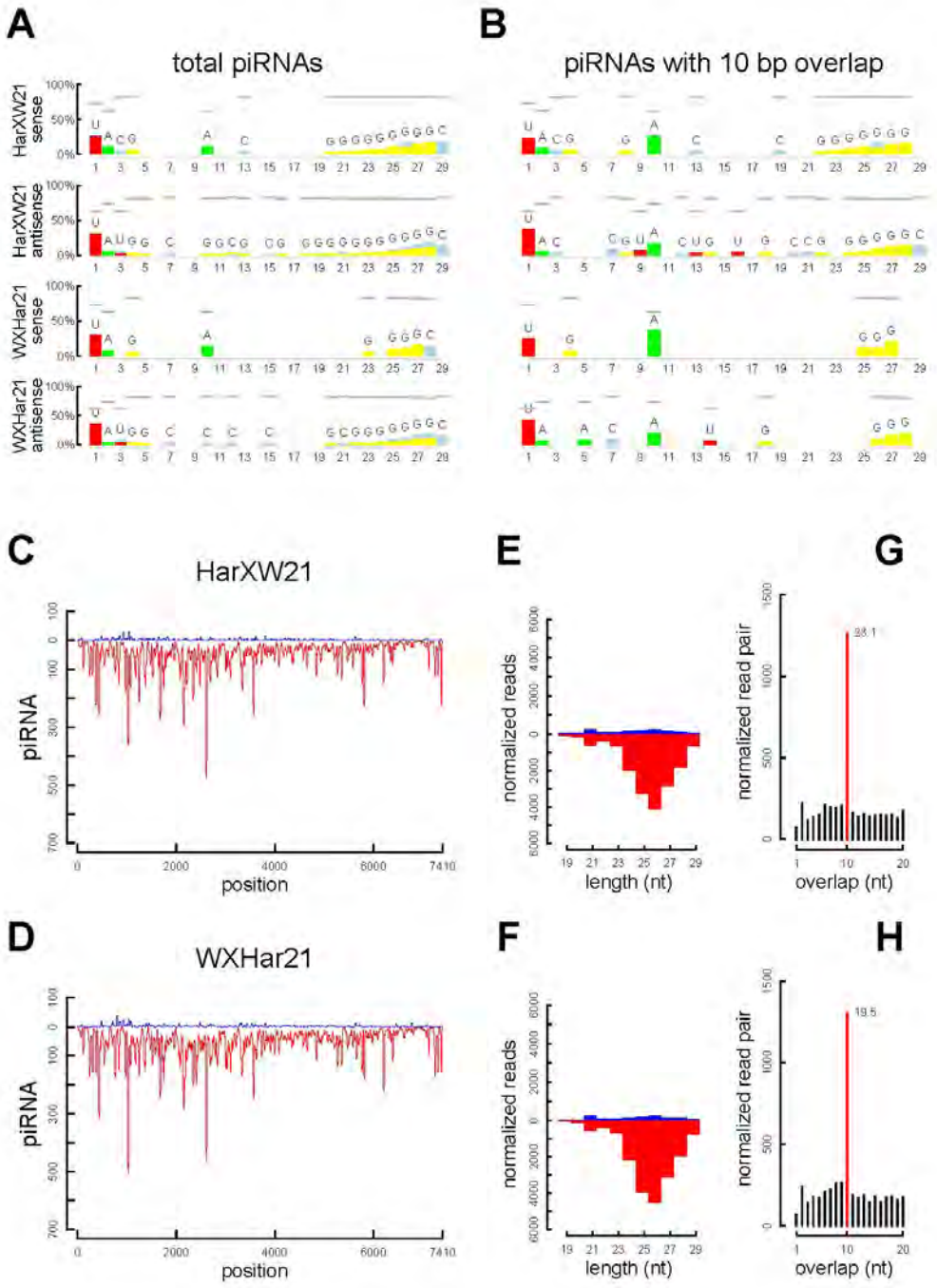
A
total piRNAs
B
piRNAs with 10 bp overlap
HarXW21 sense
HarXW21 antisense
WXHar21 sense
WXHar21 antisense
C
HarXW21
piRNA
position
D
WXHar21
piRNA
position
E
normalized reads
length (nt)
F
normalized reads
length (nt)
G
normalized read pair
overlap (nt)
H
normalized read pair
overlap (nt)

BS

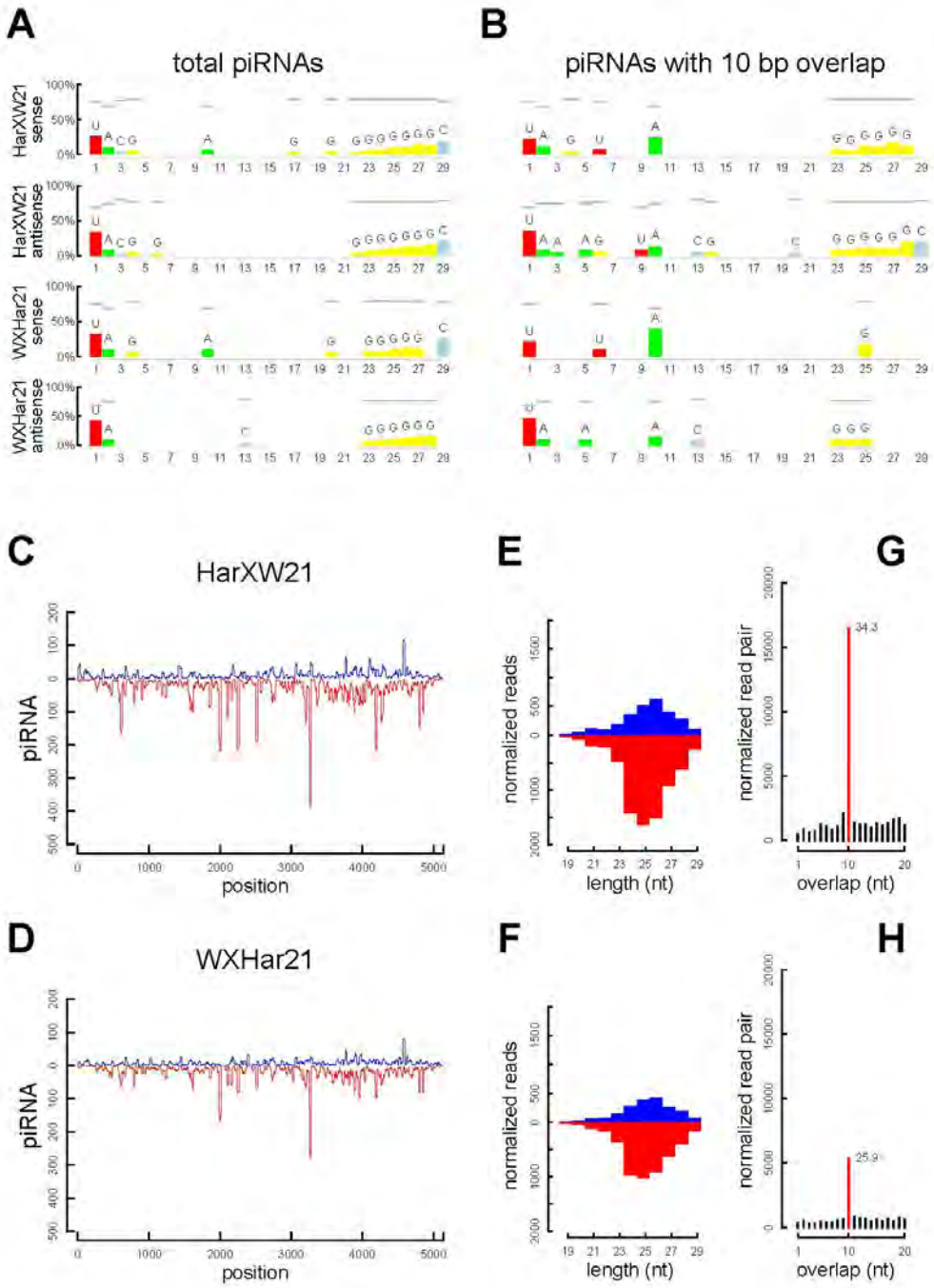
A
total piRNAs
B
piRNAs with 10 bp overlap
HarXW21 sense
HarXW21 antisense
WXHar21 sense
WXHar21 antisense
C
HarXW21
D
WXHar21
piRNA
position
E
F
normalized reads
length (nt)
G
H
normalized read pair
overlap (nt)
34.3
25.9

BS3

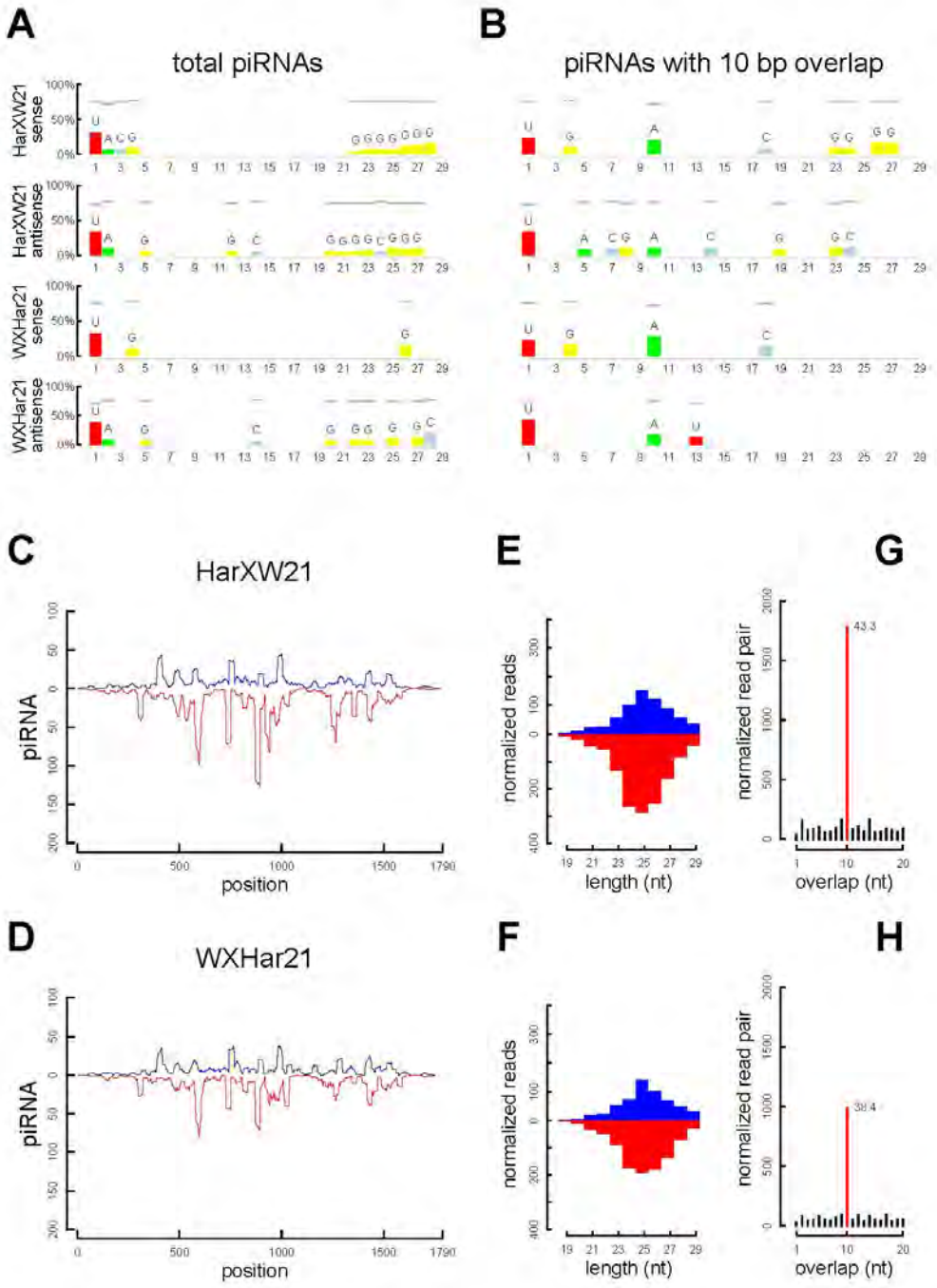
A
total piRNAs
B
piRNAs with 10 bp overlap
HarXW21 sense
HarXW21 antisense
WXHar21 sense
WXHar21 antisense
C
HarXW21
piRNA
position
D
WXHar21
piRNA
position
E
normalized reads
length (nt)
F
normalized reads
length (nt)
G
normalized read pair
overlap (nt)
43.3
H
normalized read pair
overlap (nt)
38.4

BS3#2

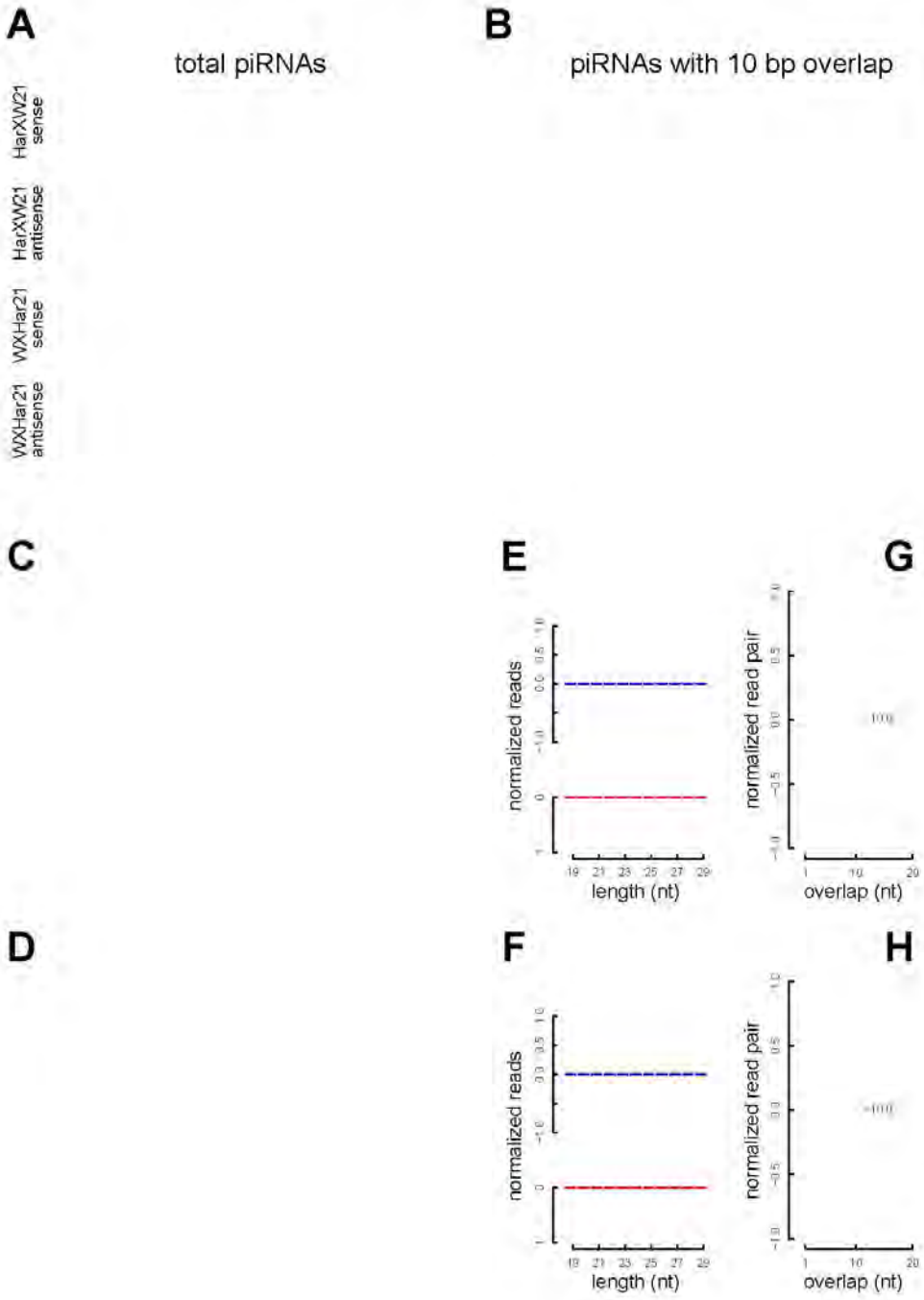
A
total piRNAs
HarXW21 sense
HarXW21 antisense
WXHar21 sense
WXHar21 antisense
B
piRNAs with 10 bp overlap
C
D
E
normalized reads
length (nt)
F
normalized reads
length (nt)
G
normalized read pair
overlap (nt)
H
normalized read pair
overlap (nt)

Burdock

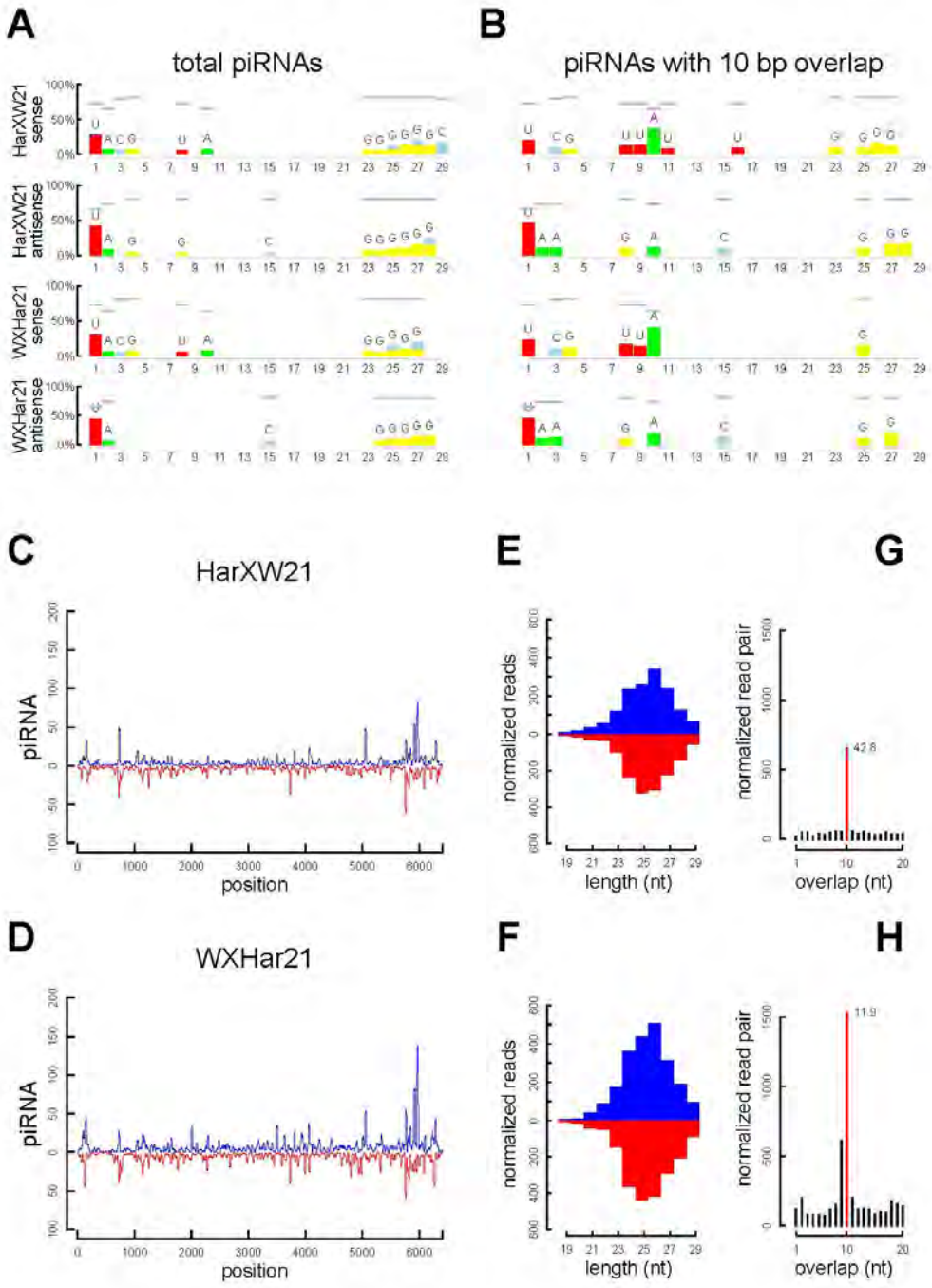
A
total piRNAs
B
piRNAs with 10 bp overlap
HarXW21 sense
HarXW21 antisense
WXHar21 sense
WXHar21 antisense
C
HarXW21
D
WXHar21
piRNA
position
E
F
normalized reads
length (nt)
G
H
normalized read pair
overlap (nt)
42.6
11.9

Circe

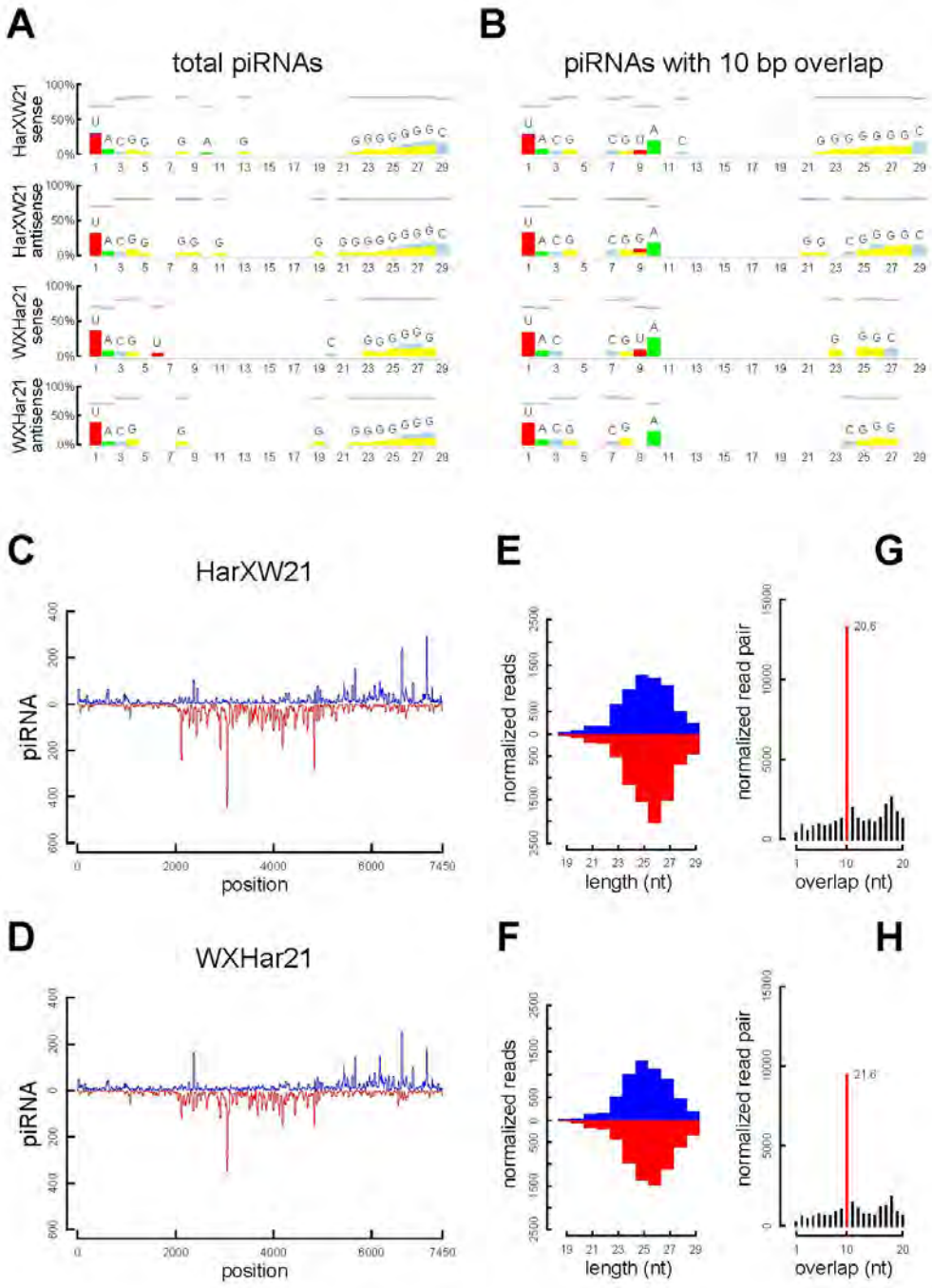
A
total piRNAs
B
piRNAs with 10 bp overlap
HarXW21 sense
HarXW21 antisense
WXHar21 sense
WXHar21 antisense
C
HarXW21
D
WXHar21
piRNA
position
E
F
normalized reads
length (nt)
G
H
normalized read pair
overlap (nt)
20.6
21.6

copia

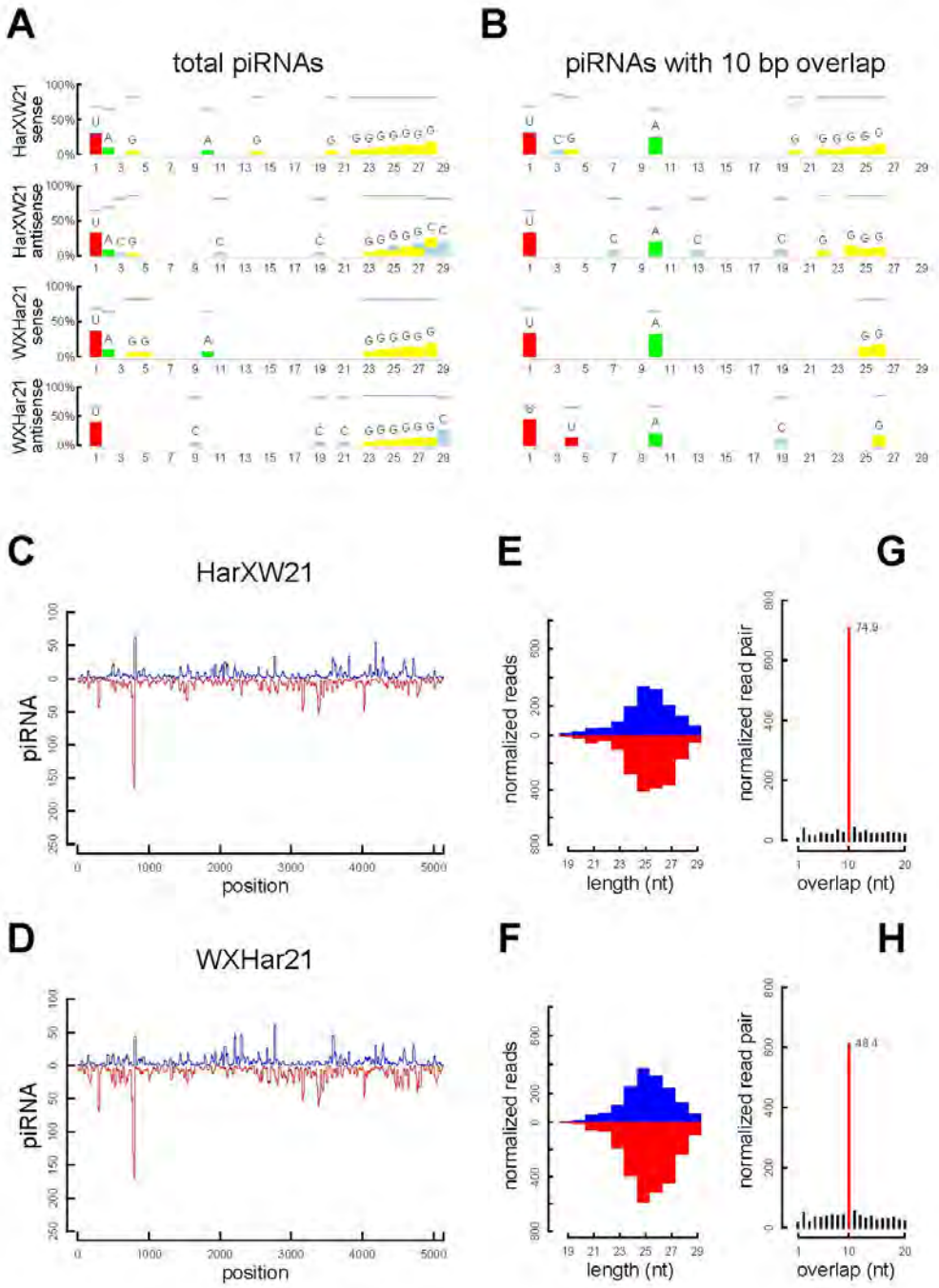
A
total piRNAs
B
piRNAs with 10 bp overlap
HarXW21 sense
HarXW21 antisense
WXHar21 sense
WXHar21 antisense
C
HarXW21
D
WXHar21
piRNA
position
E
F
normalized reads
length (nt)
G
H
normalized read pair
overlap (nt)
74.9
48.4

Cr1a

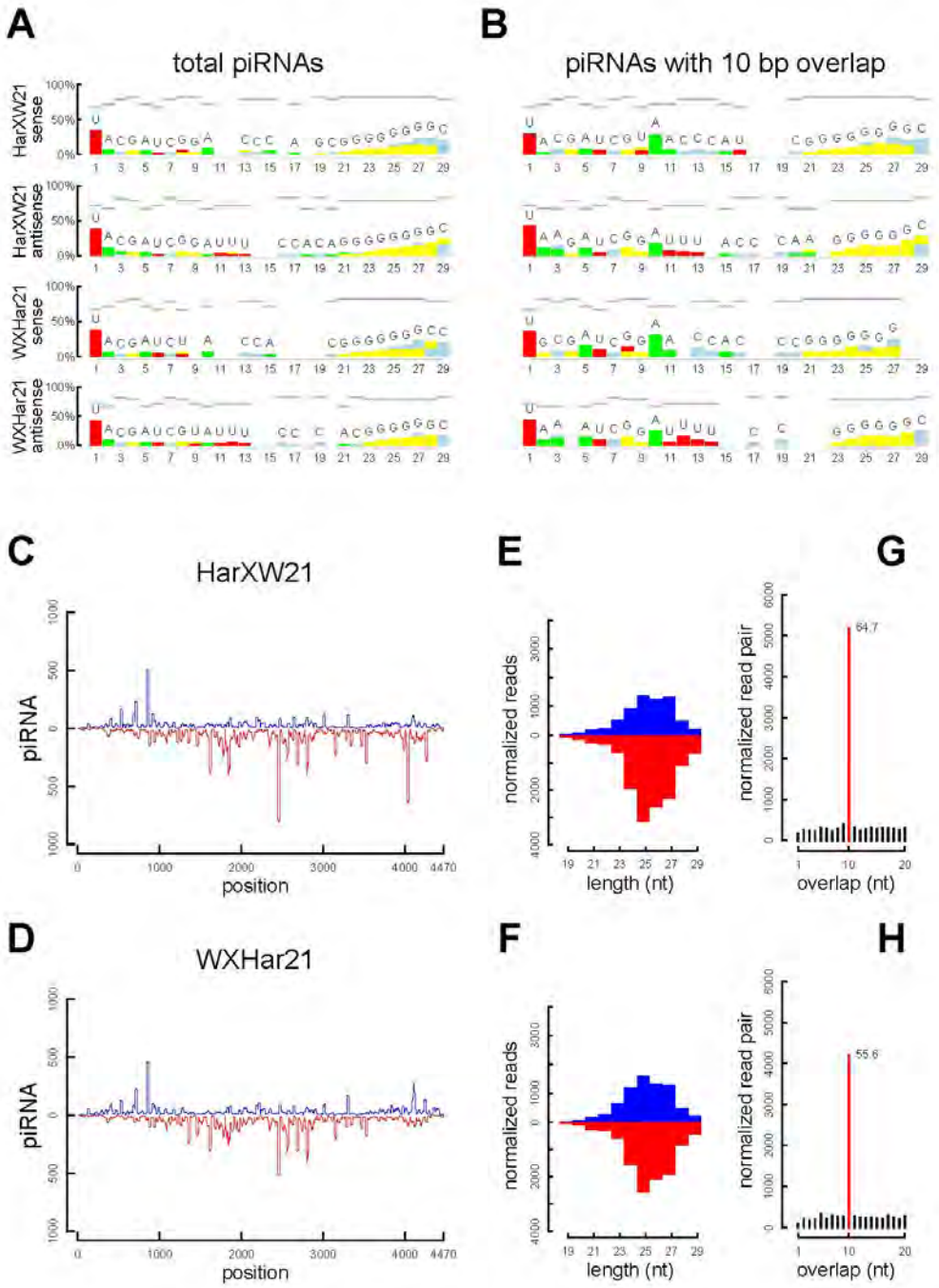
A
total piRNAs
B
piRNAs with 10 bp overlap
HarXW21 sense
HarXW21 antisense
WXHar21 sense
WXHar21 antisense
C
HarXW21
piRNA
position
D
WXHar21
piRNA
position
E
normalized reads
length (nt)
F
normalized reads
length (nt)
G
normalized read pair
64.7
overlap (nt)
H
normalized read pair
55.6
overlap (nt)

diver

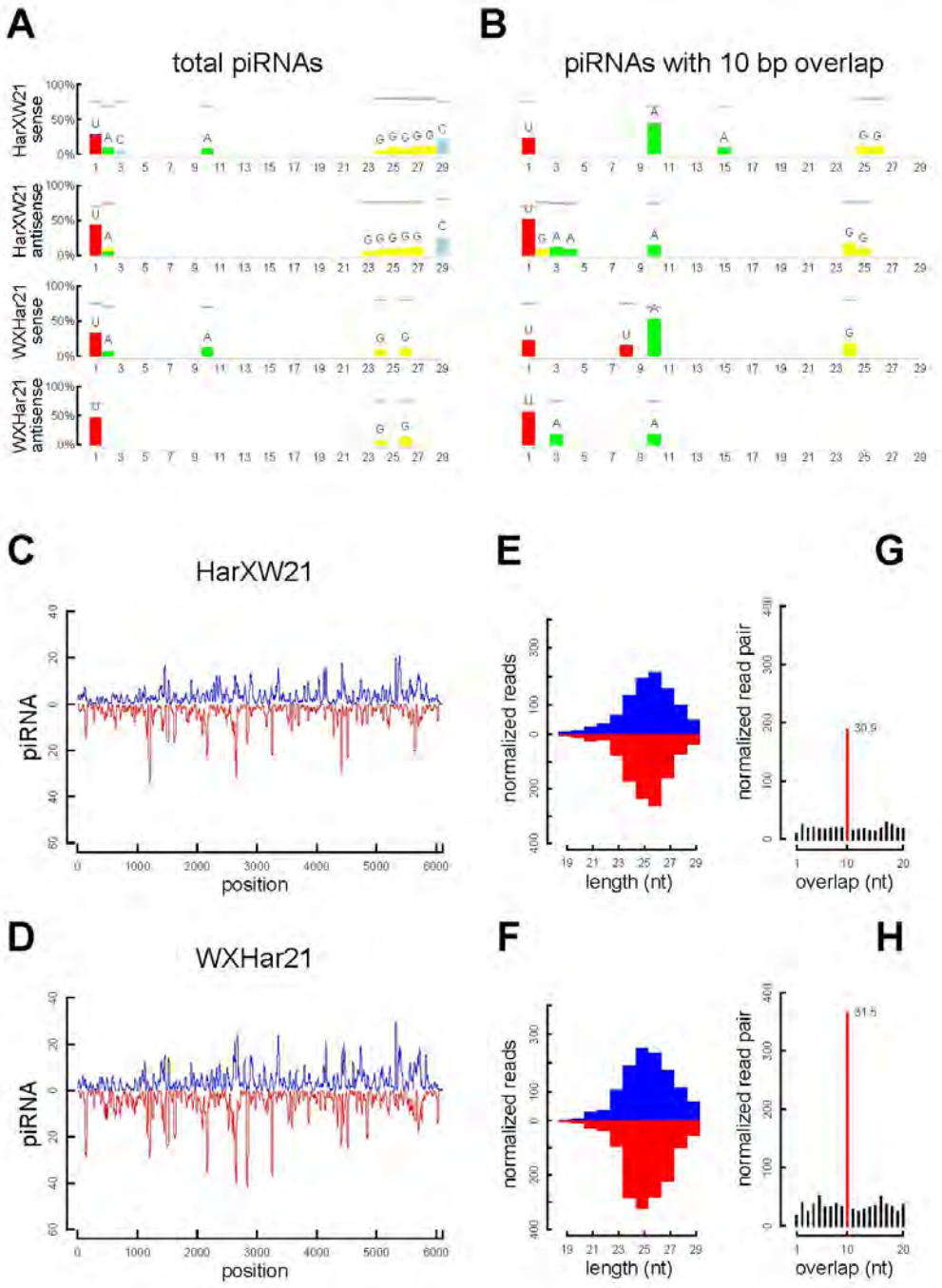
A
total piRNAs
B
piRNAs with 10 bp overlap
HarXW21 sense
HarXW21 antisense
WXHar21 sense
WXHar21 antisense
C
HarXW21
D
WXHar21
piRNA
position
E
F
normalized reads
length (nt)
G
H
normalized read pair
overlap (nt)
30.9
61.5

diver2

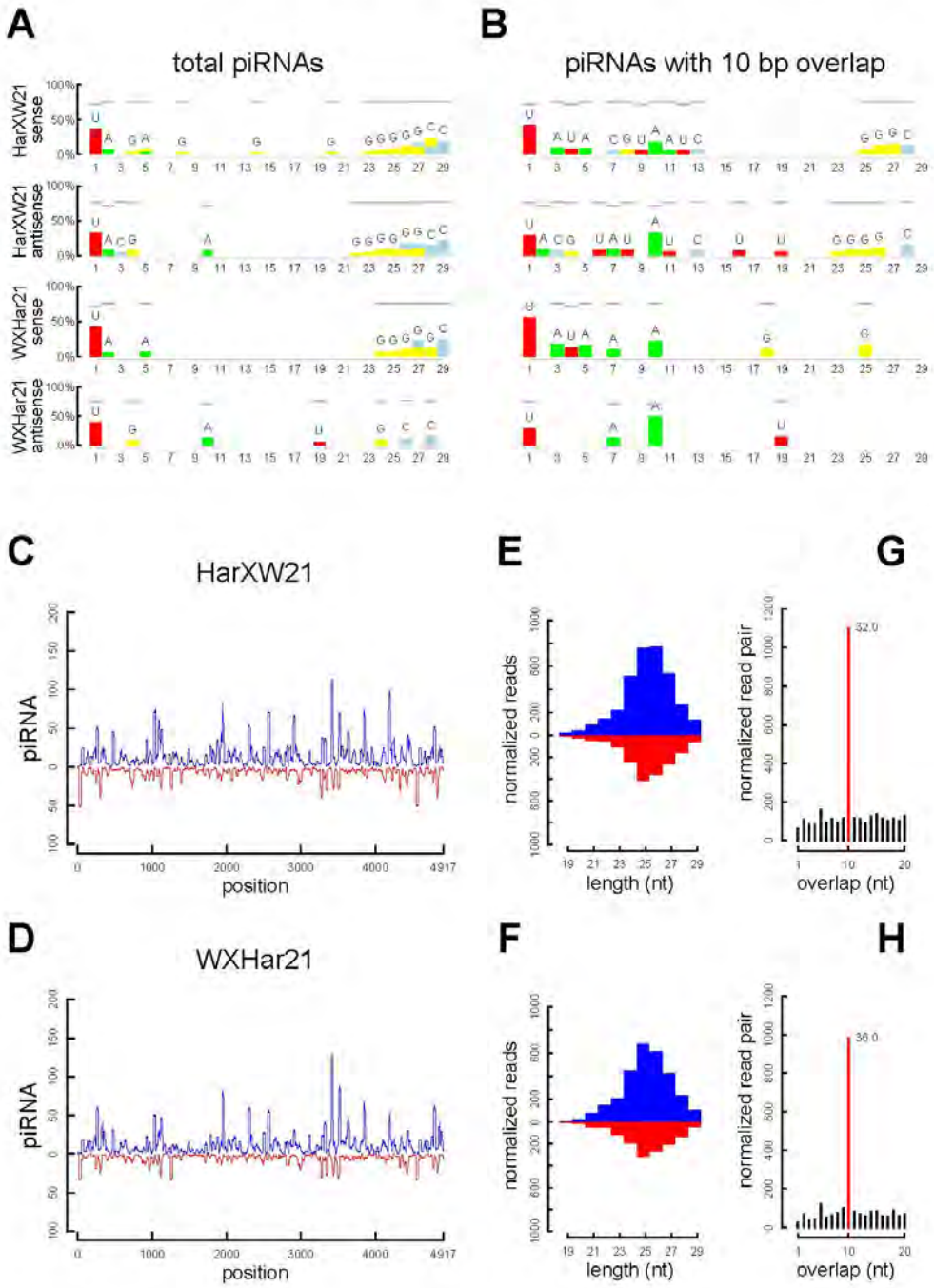
A
total piRNAs
B
piRNAs with 10 bp overlap
HarXW21 sense
HarXW21 antisense
WXHar21 sense
WXHar21 antisense
C
HarXW21
piRNA
position
D
WXHar21
piRNA
position
E
normalized reads
length (nt)
F
normalized reads
length (nt)
G
normalized read pair
32.0
overlap (nt)
H
normalized read pair
36.0
overlap (nt)

Dm88

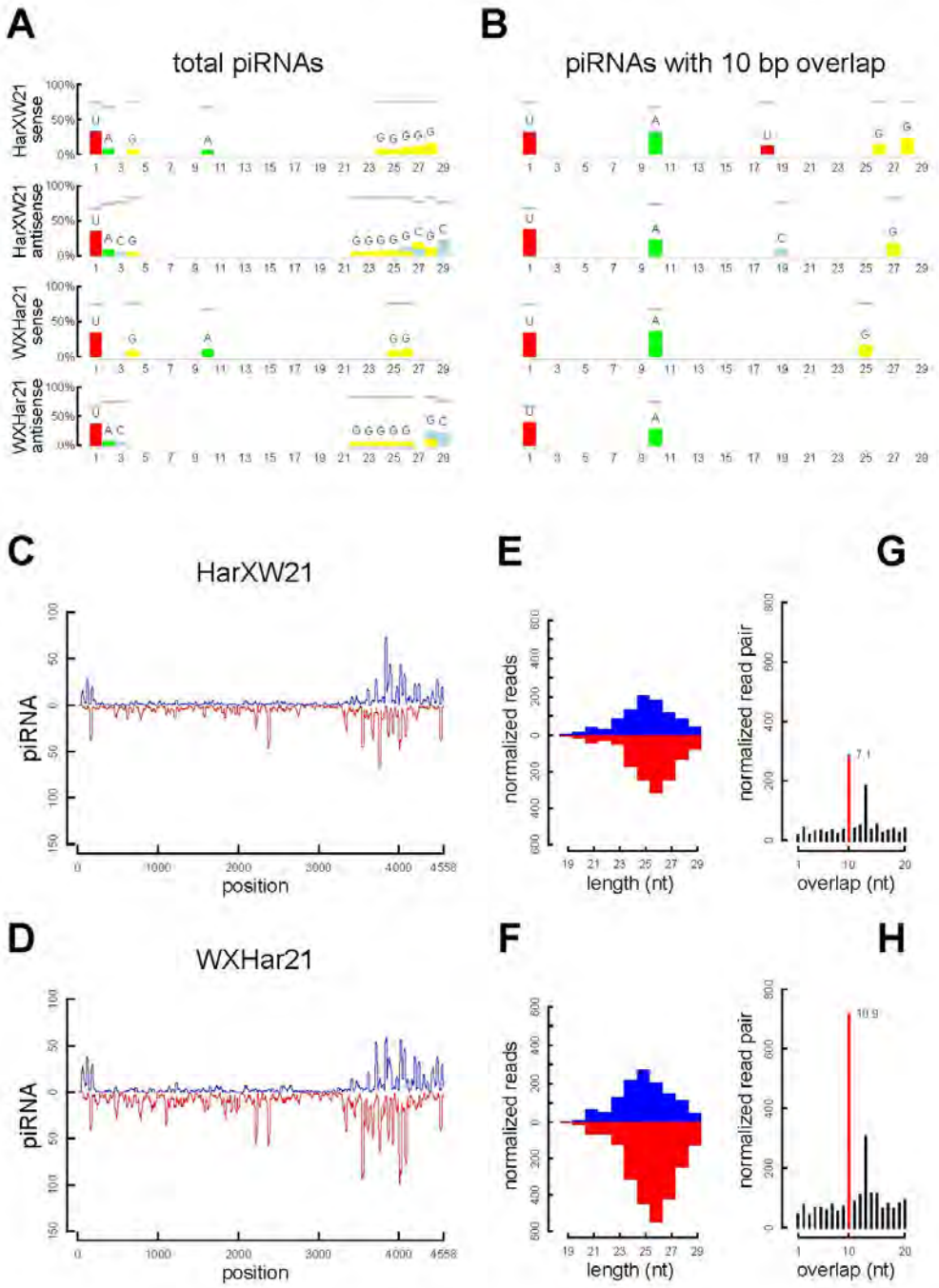
A
total piRNAs
B
piRNAs with 10 bp overlap
HarXW21 sense
HarXW21 antisense
WXHar21 sense
WXHar21 antisense
C
HarXW21
piRNA
position
D
WXHar21
piRNA
position
E
normalized reads
length (nt)
F
normalized reads
length (nt)
G
normalized read pair
overlap (nt)
7.1
H
normalized read pair
overlap (nt)
10.9

Doc

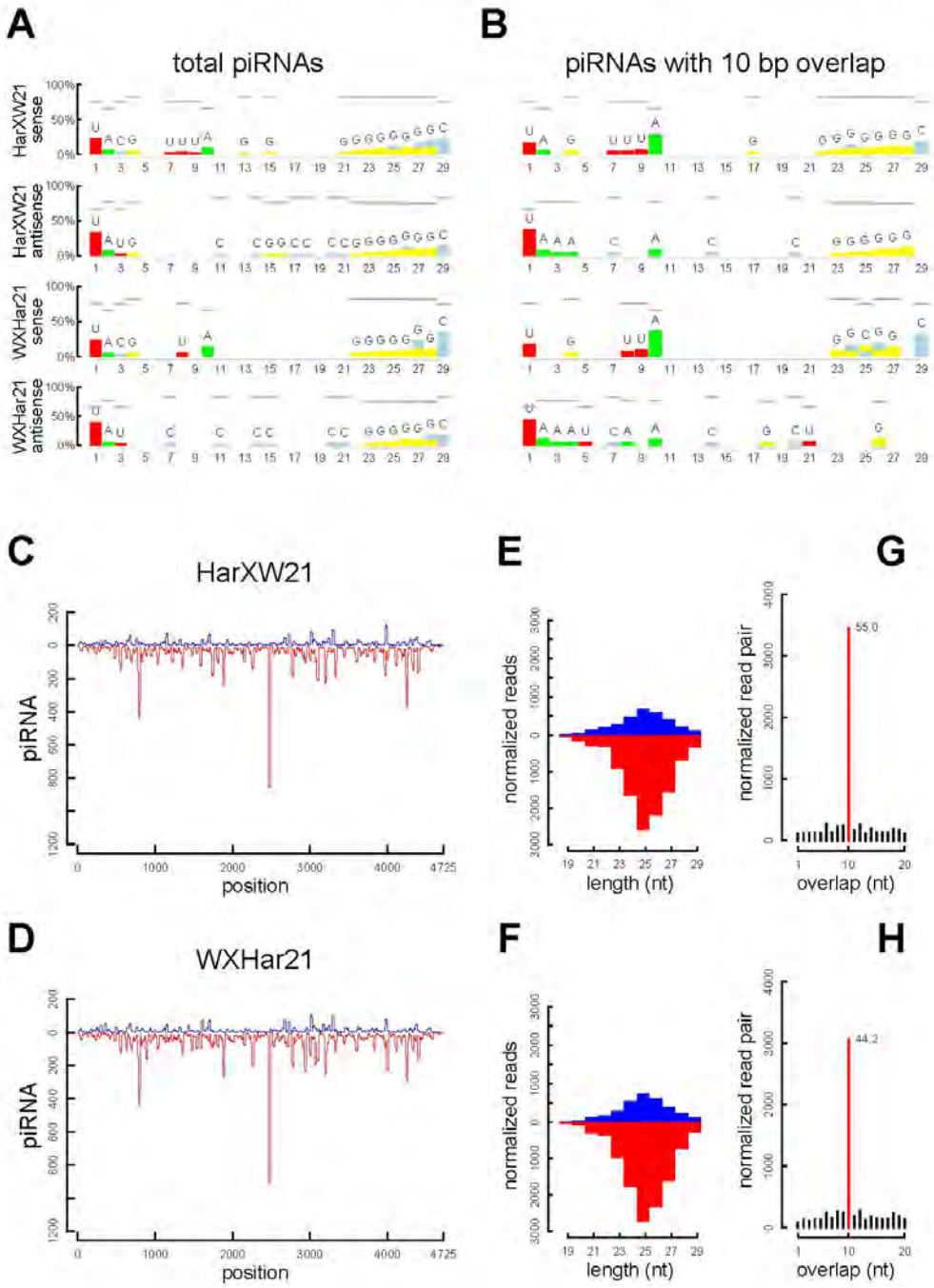
A
total piRNAs
B
piRNAs with 10 bp overlap
HarXW21 sense
HarXW21 antisense
WXHar21 sense
WXHar21 antisense
C
HarXW21
piRNA
position
D
WXHar21
piRNA
position
E
normalized reads
length (nt)
F
normalized reads
length (nt)
G
normalized read pair
55.0
overlap (nt)
H
normalized read pair
44.2
overlap (nt)

Doc2 element

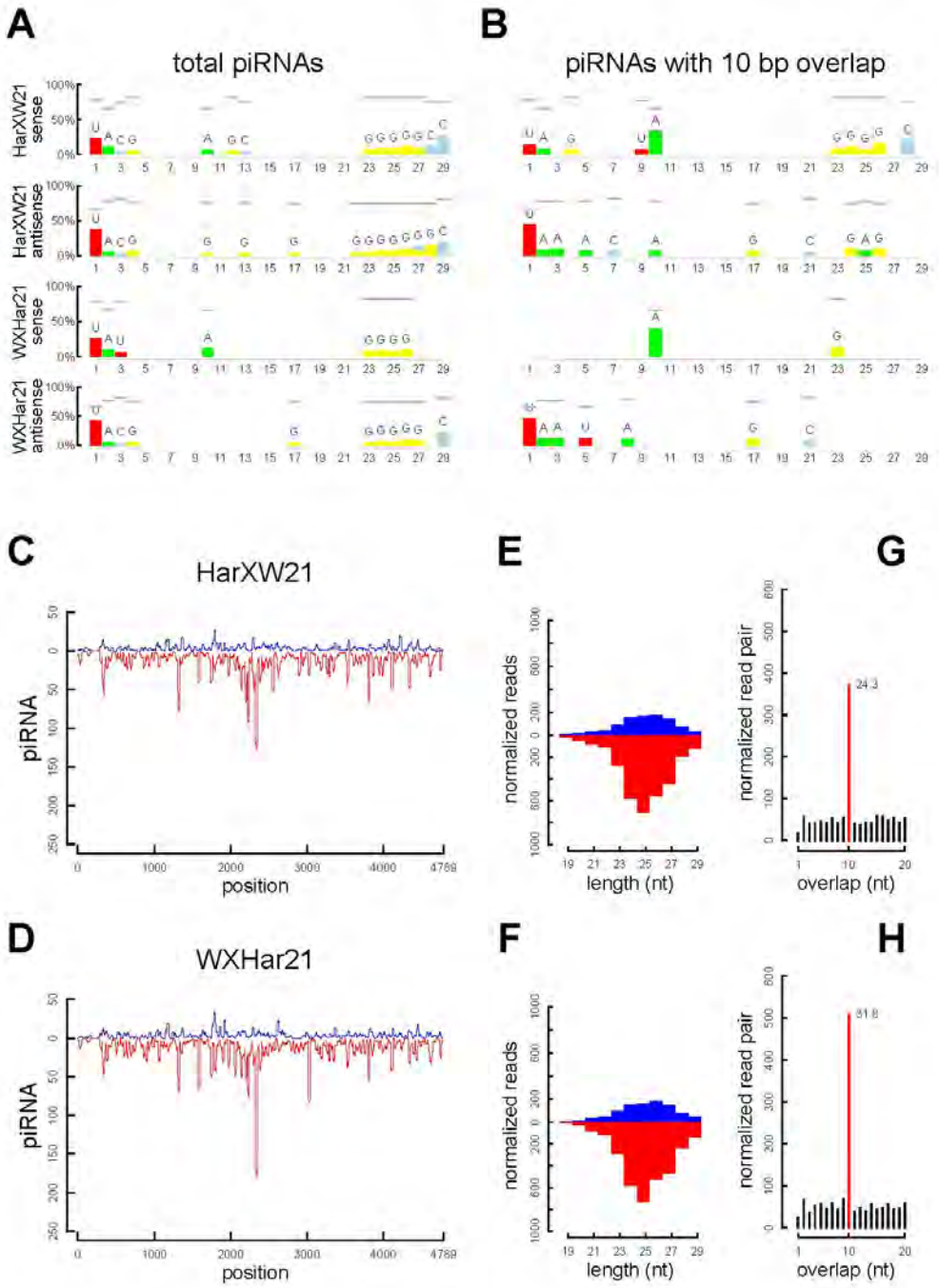

Doc3 element

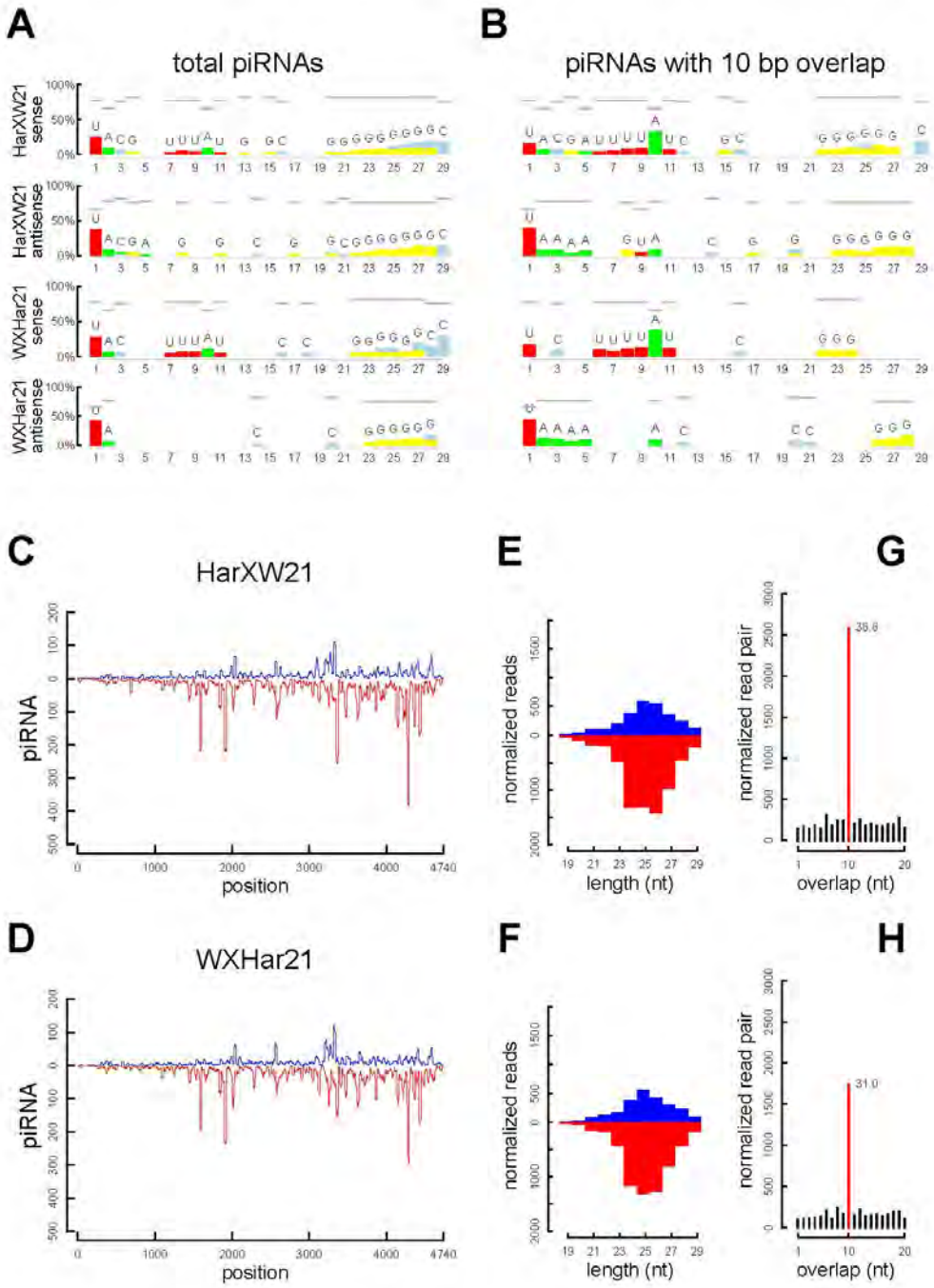

Doc4 element

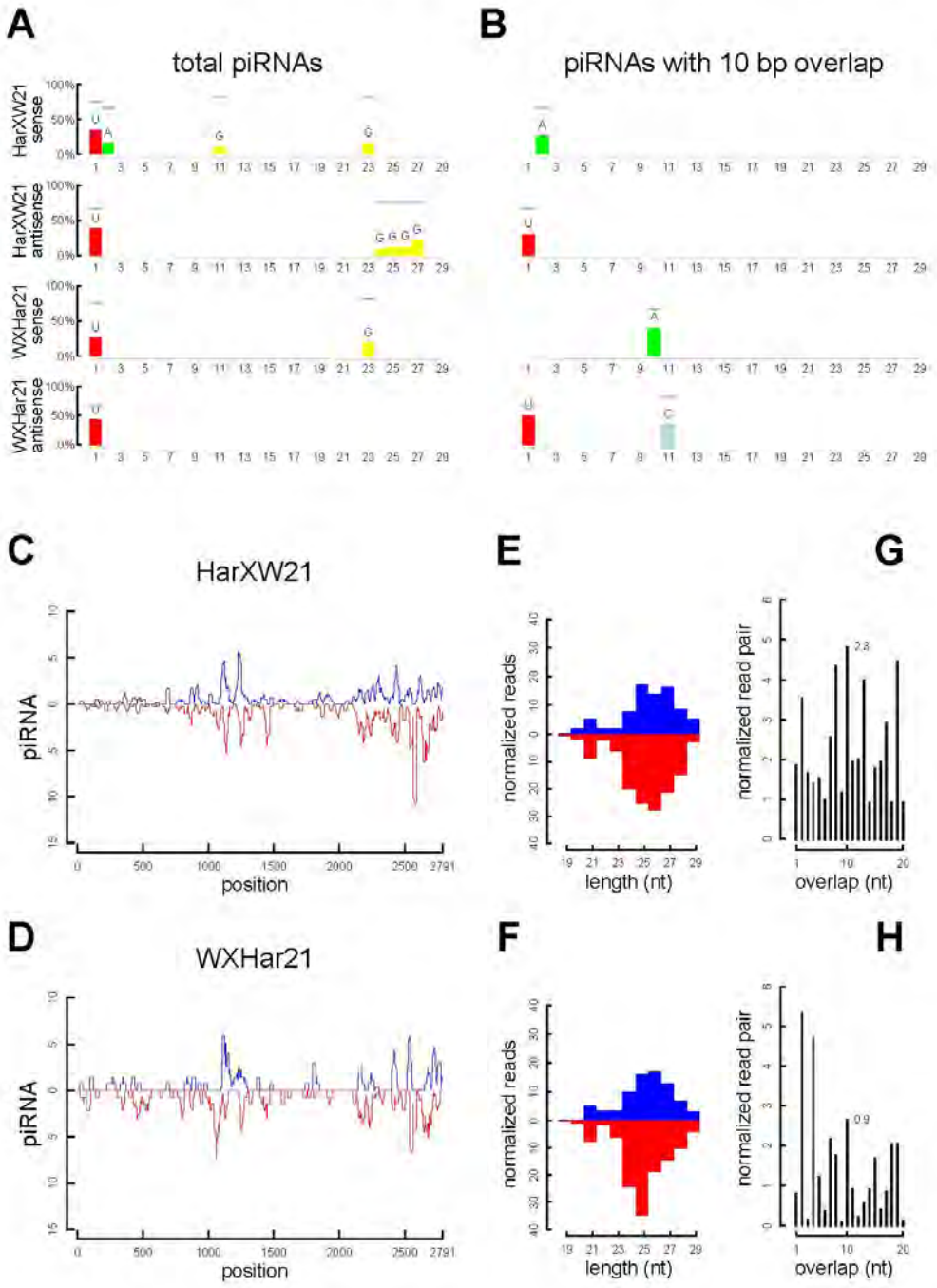

FB

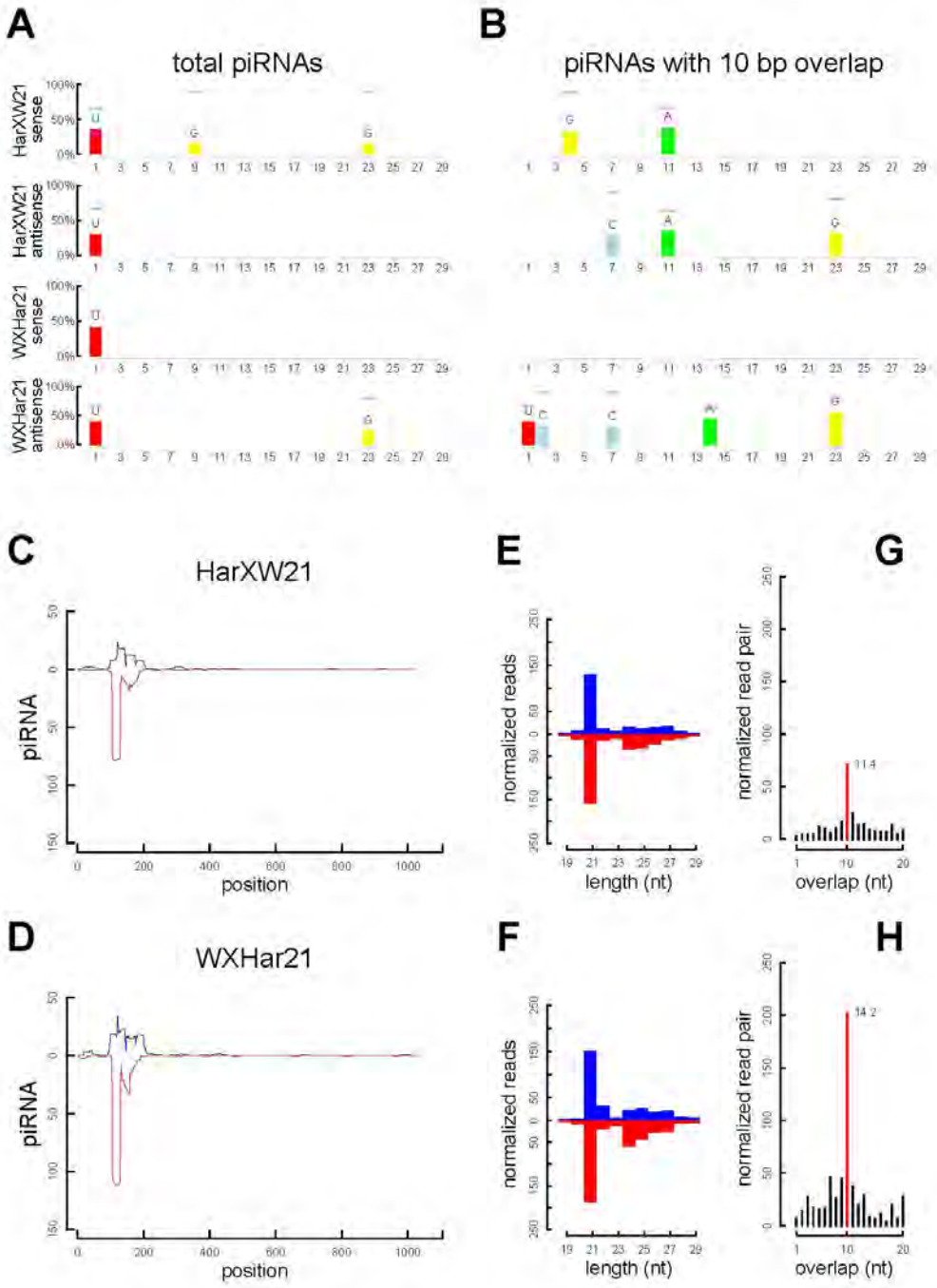
A
total piRNAs
B
piRNAs with 10 bp overlap
HarXW21 sense
HarXW21 antisense
WXHar21 sense
WXHar21 antisense
C
HarXW21
piRNA
position
D
WXHar21
piRNA
position
E
normalized reads
length (nt)
F
normalized reads
length (nt)
G
normalized read pair
overlap (nt)
11.4
H
normalized read pair
overlap (nt)
14.2

FBgn0063571

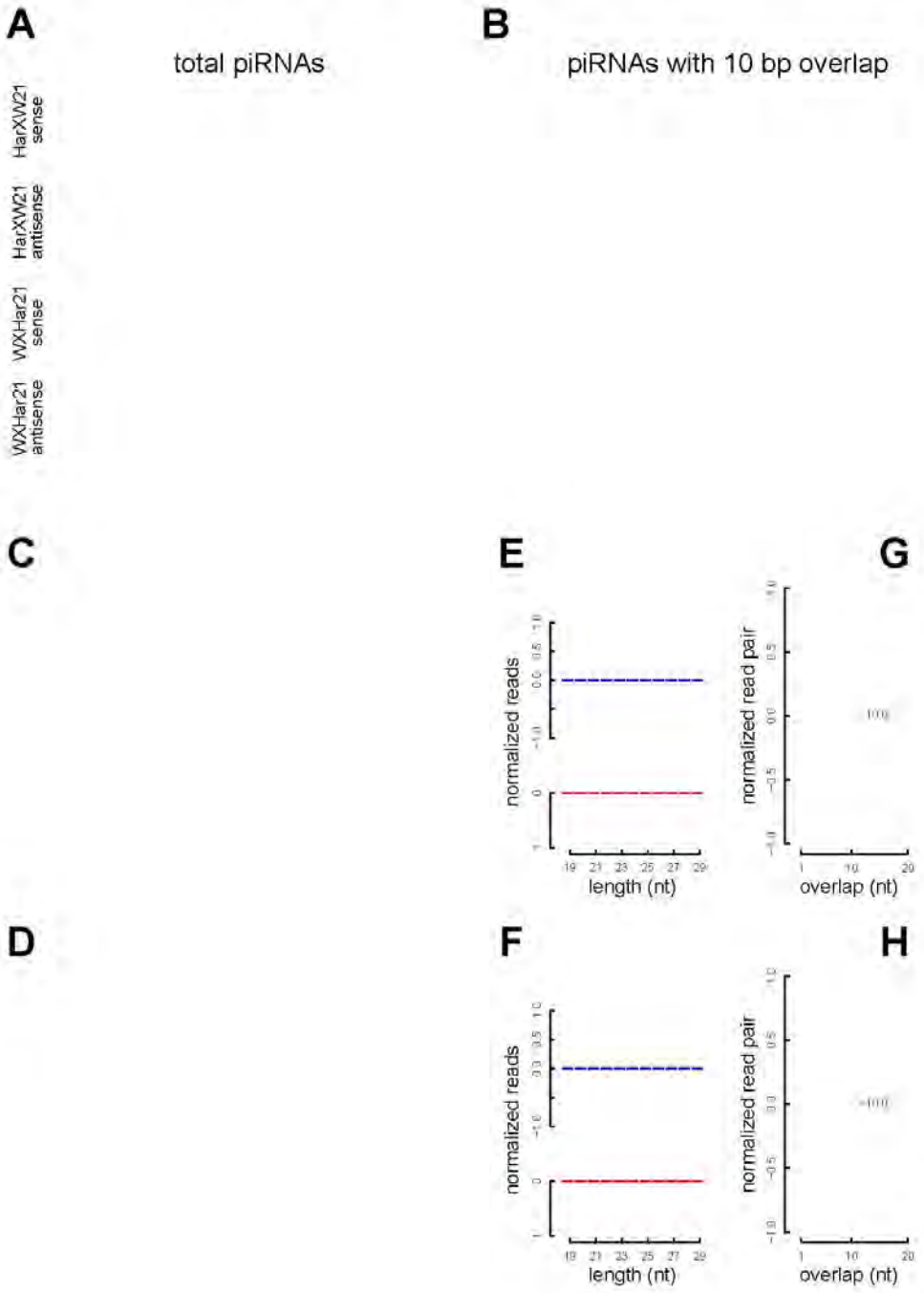

F element

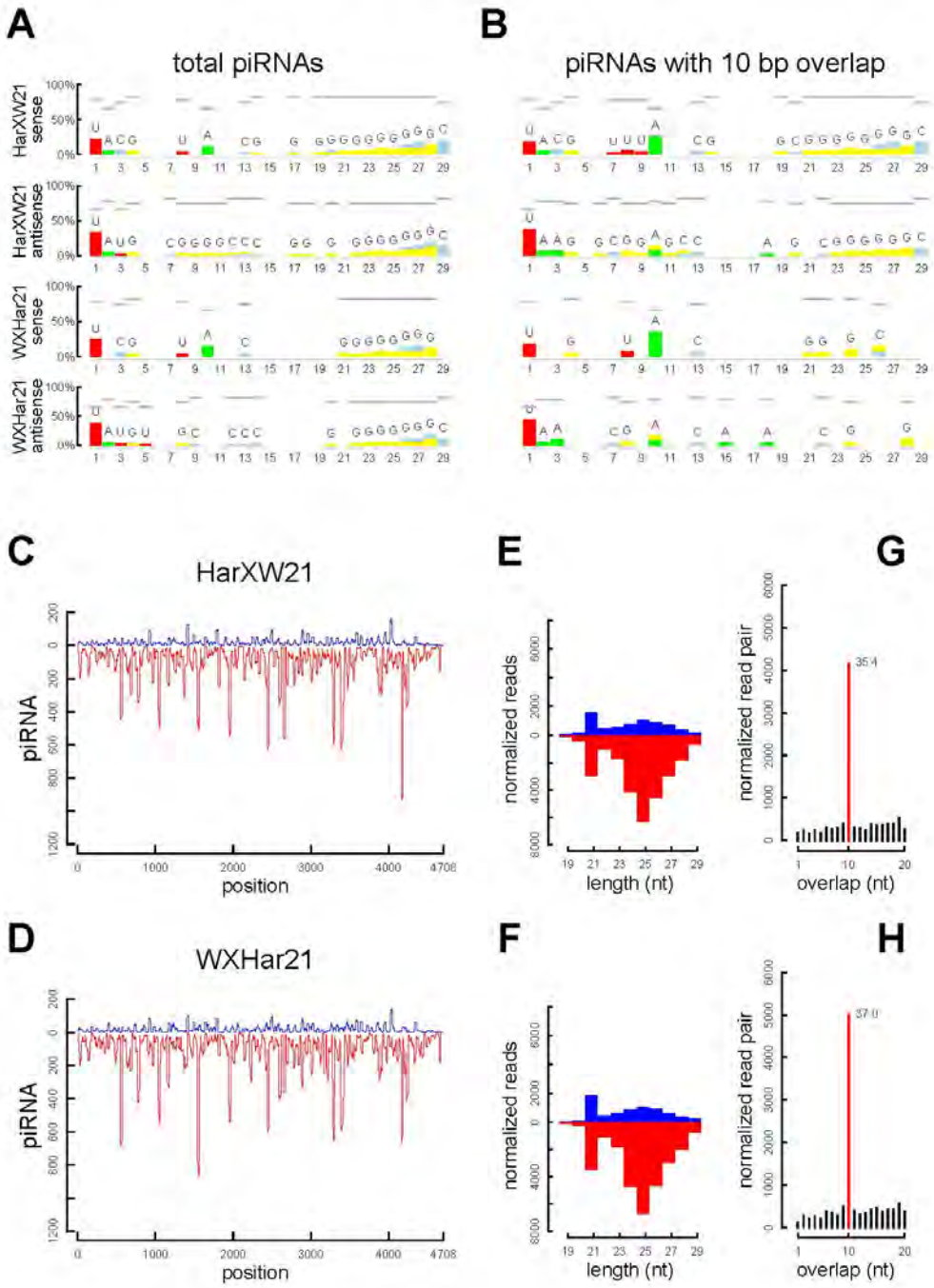
A
total piRNAs
B
piRNAs with 10 bp overlap
HarXW21 sense
HarXW21 antisense
WXHar21 sense
WXHar21 antisense
C
HarXW21
piRNA
position
D
WXHar21
piRNA
position
E
normalized reads
length (nt)
F
normalized reads
length (nt)
G
normalized read pair
overlap (nt)
354
H
normalized read pair
overlap (nt)
370

flea

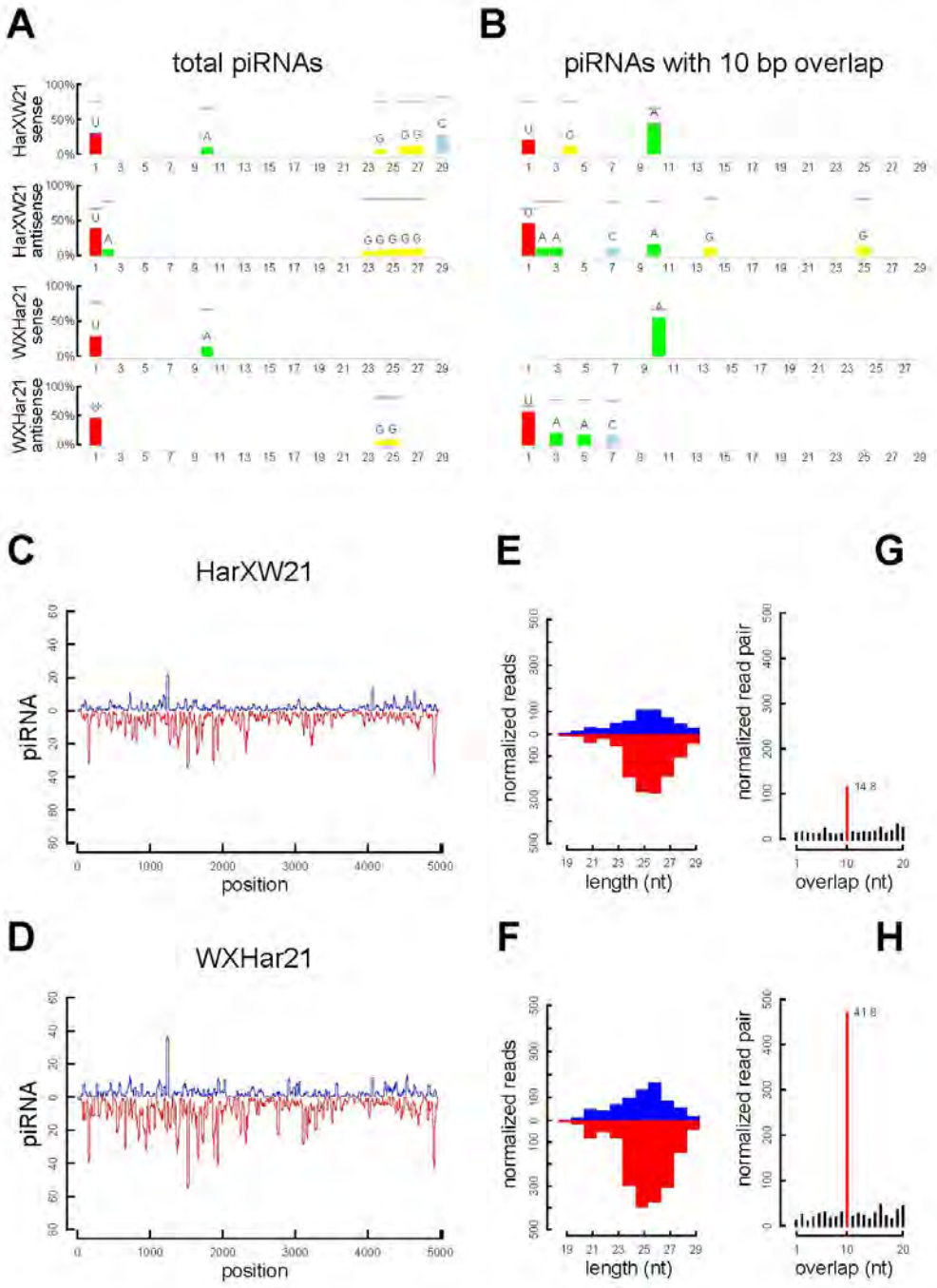
A
total piRNAs
B
piRNAs with 10 bp overlap
HarXW21 sense
HarXW21 antisense
WXHar21 sense
WXHar21 antisense
C
HarXW21
D
WXHar21
piRNA
position
E
F
normalized reads
length (nt)
G
H
normalized read pair
overlap (nt)
14.8
41.8

frogger

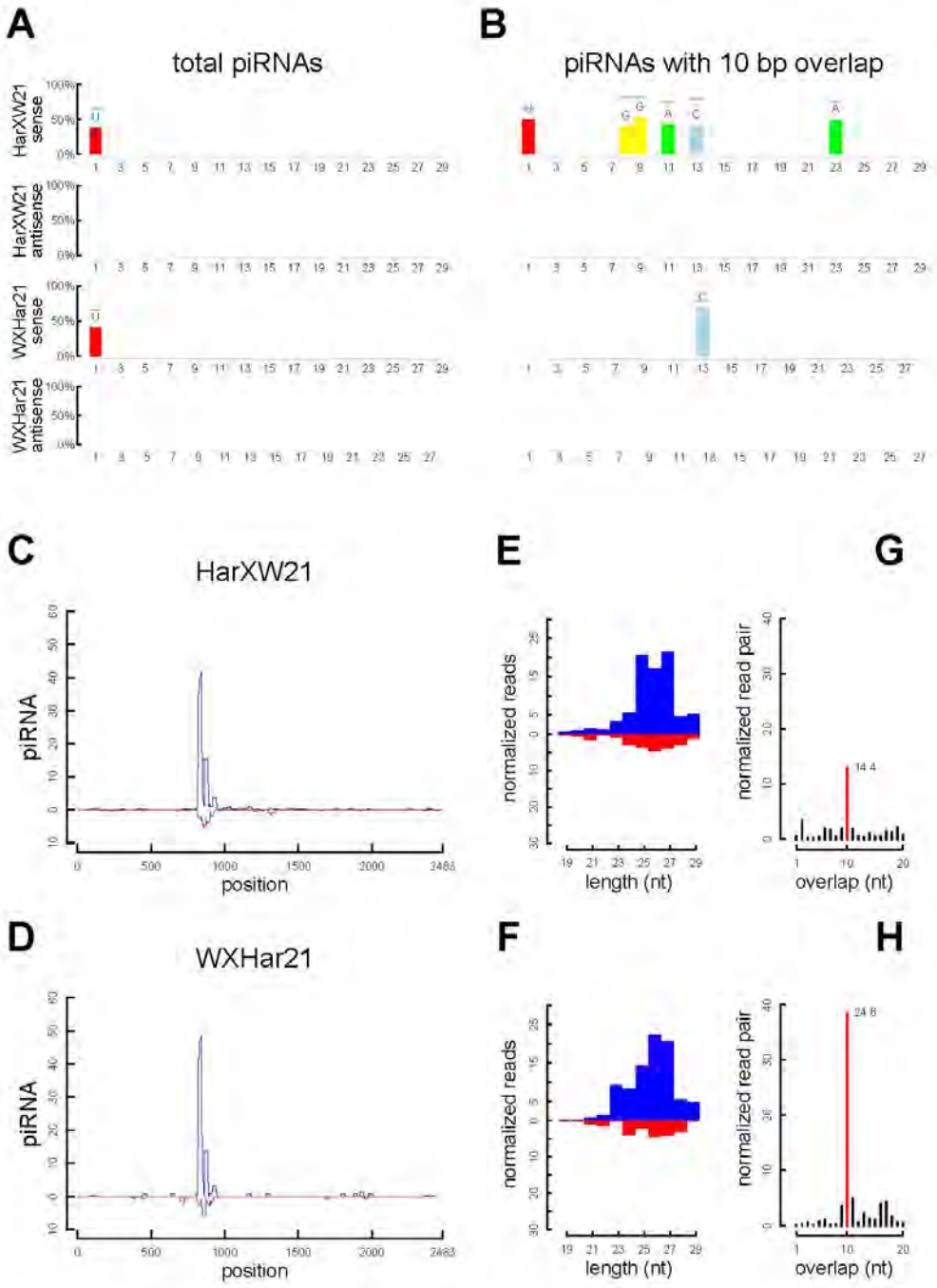
A
total piRNAs
B
piRNAs with 10 bp overlap
HarXW21 sense
HarXW21 antisense
WXHar21 sense
WXHar21 antisense
C
HarXW21
D
WXHar21
piRNA
position
E
F
normalized reads
length (nt)
G
H
normalized read pair
overlap (nt)
14.4
24.8

Fw2

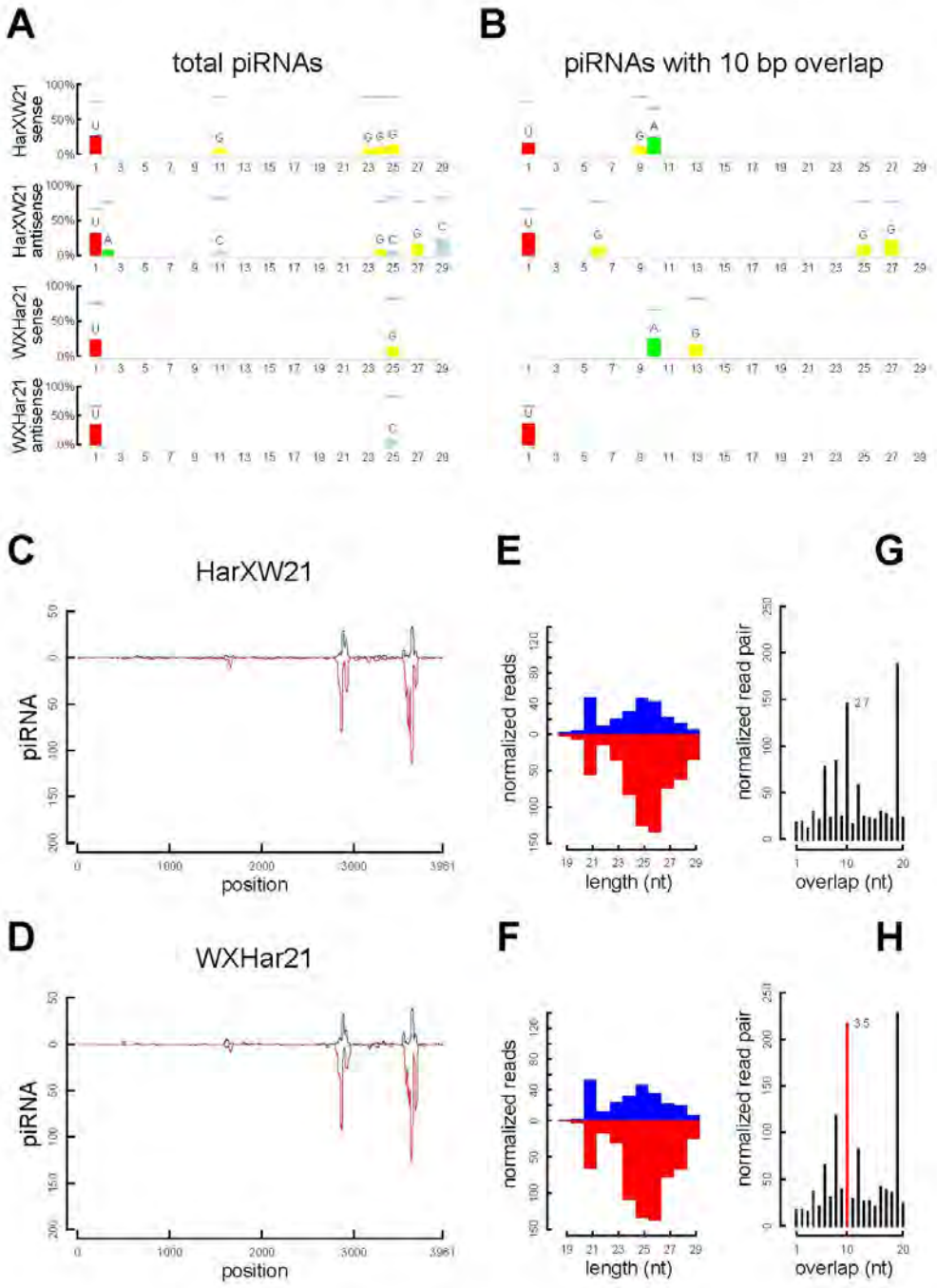
A
total piRNAs
B
piRNAs with 10 bp overlap
HarXW21 sense
HarXW21 antisense
WXHar21 sense
WXHar21 antisense
C
HarXW21
D
WXHar21
piRNA
position
E
F
normalized reads
length (nt)
G
H
normalized read pair
overlap (nt)
2.7
3.5

Fw3

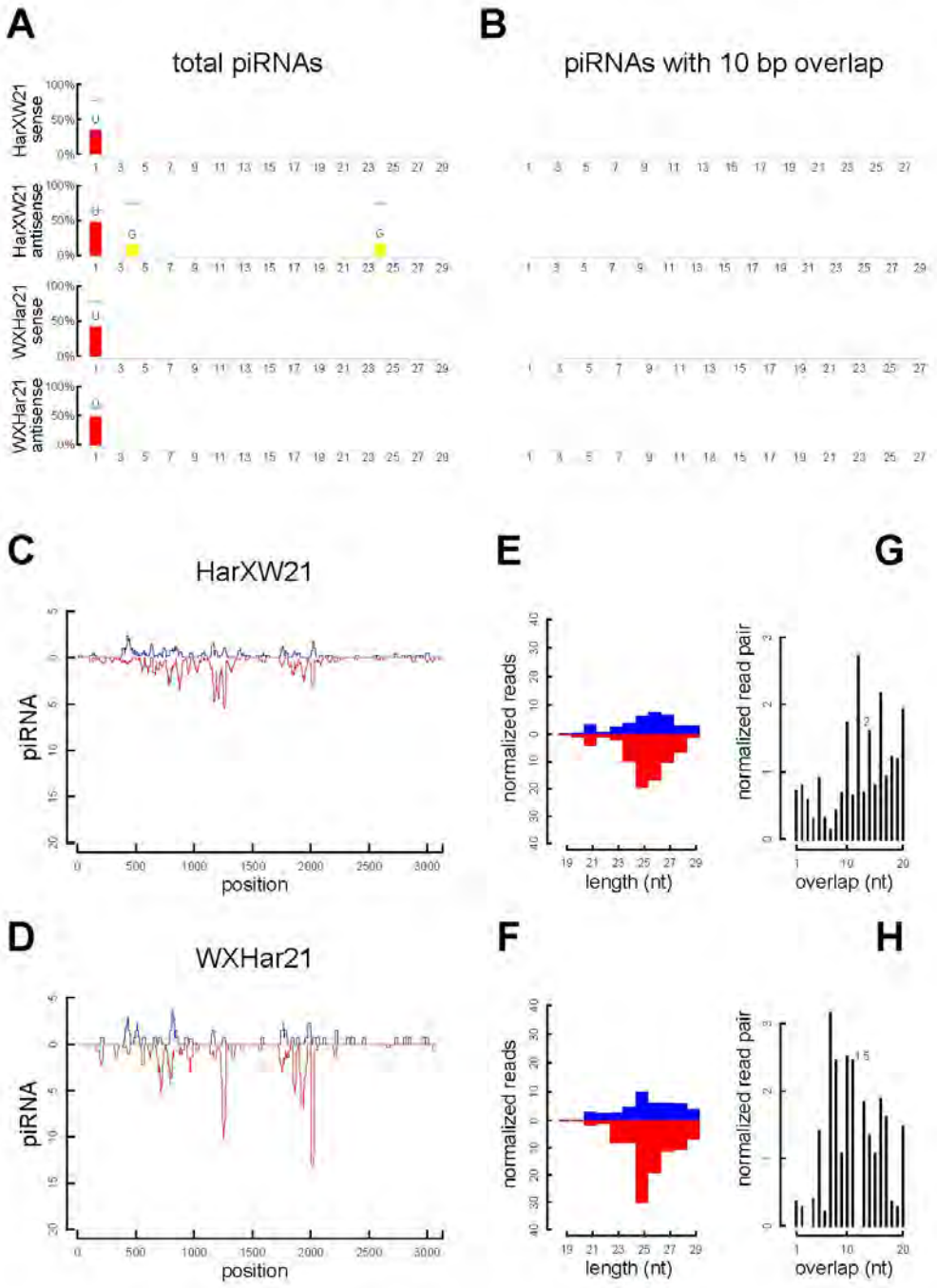
A
total piRNAs
B
piRNAs with 10 bp overlap
HarXW21 sense
HarXW21 antisense
WXHar21 sense
WXHar21 antisense
C
HarXW21
D
WXHar21
piRNA
position
E
F
normalized reads
length (nt)
G
H
normalized read pair
overlap (nt)

G2

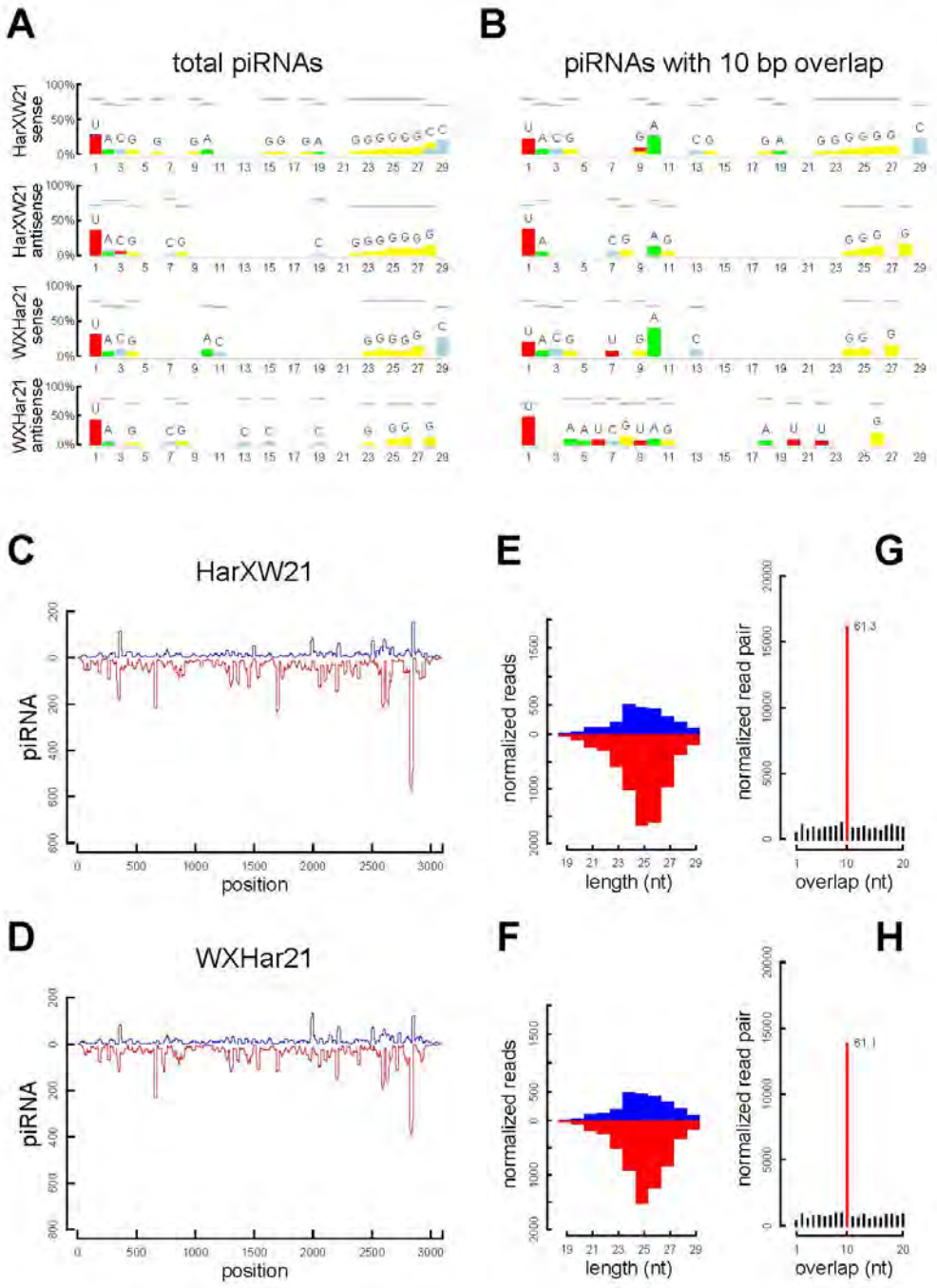
A
total piRNAs
B
piRNAs with 10 bp overlap
HarXW21 sense
HarXW21 antisense
WXHar21 sense
WXHar21 antisense
C
HarXW21
piRNA
position
D
WXHar21
piRNA
position
E
normalized reads
length (nt)
F
normalized reads
length (nt)
G
normalized read pair
overlap (nt)
61.3
H
normalized read pair
overlap (nt)
61.1

G3

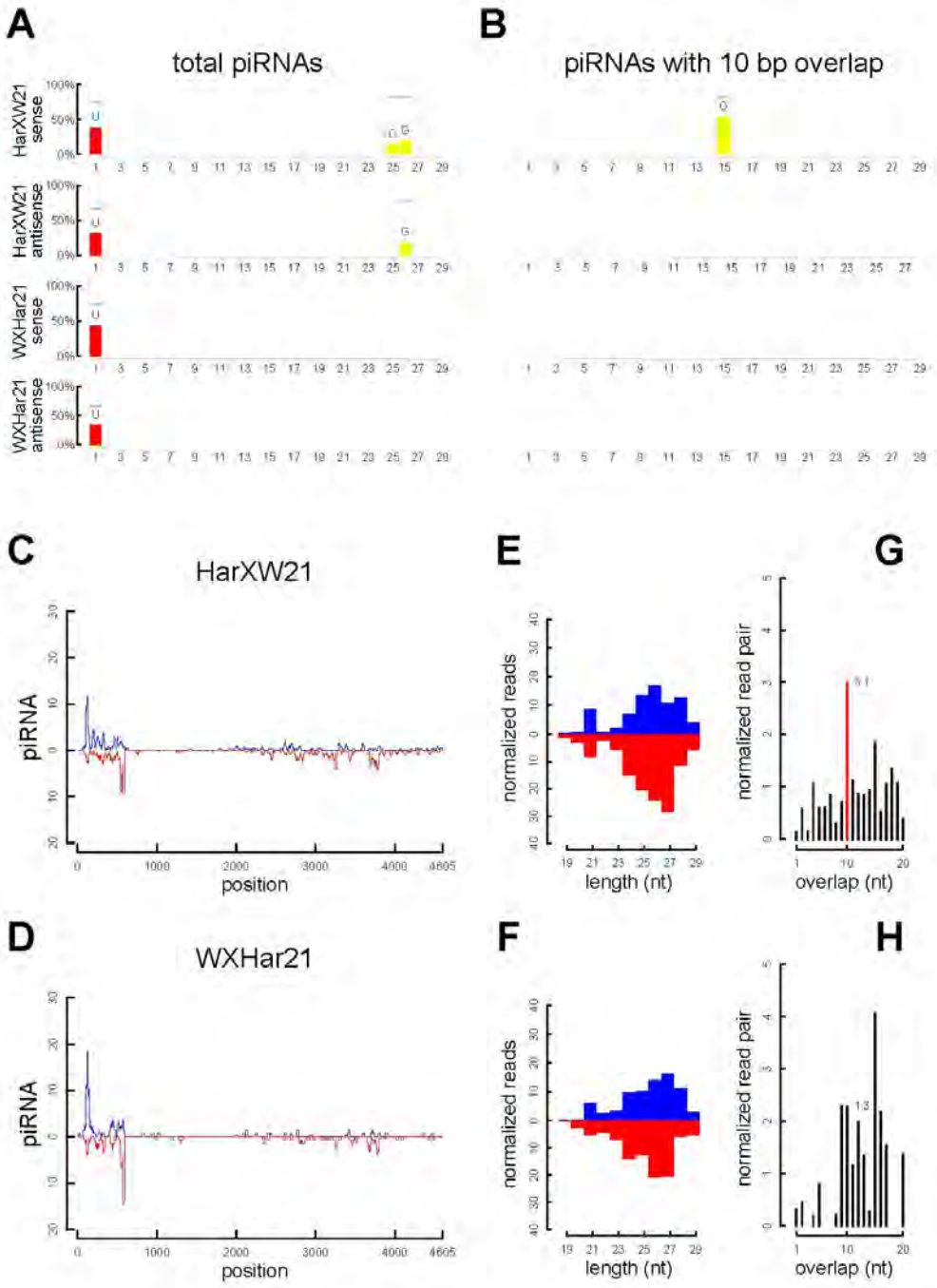
A
total piRNAs
B
piRNAs with 10 bp overlap
HarXW21 sense
HarXW21 antisense
WXHar21 sense
WXHar21 antisense
C
HarXW21
D
WXHar21
piRNA
position
E
F
normalized reads
length (nt)
G
H
normalized read pair
overlap (nt)

G4

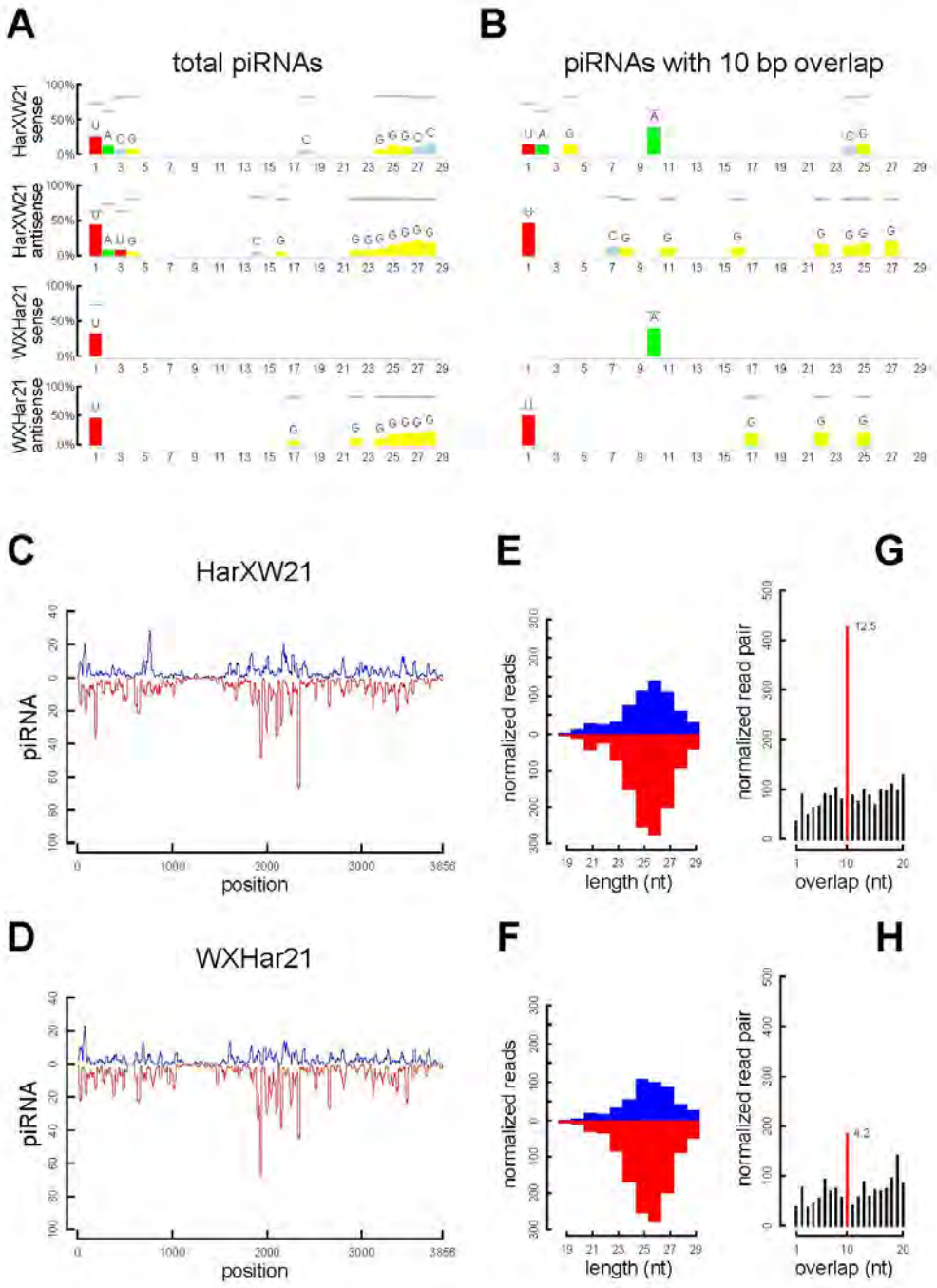
A
total piRNAs
B
piRNAs with 10 bp overlap
HarXW21 sense
HarXW21 antisense
WXHar21 sense
WXHar21 antisense
C
HarXW21
piRNA
position
D
WXHar21
piRNA
position
E
normalized reads
length (nt)
F
normalized reads
length (nt)
G
normalized read pair
overlap (nt)
12.5
H
normalized read pair
overlap (nt)
4.2

G5

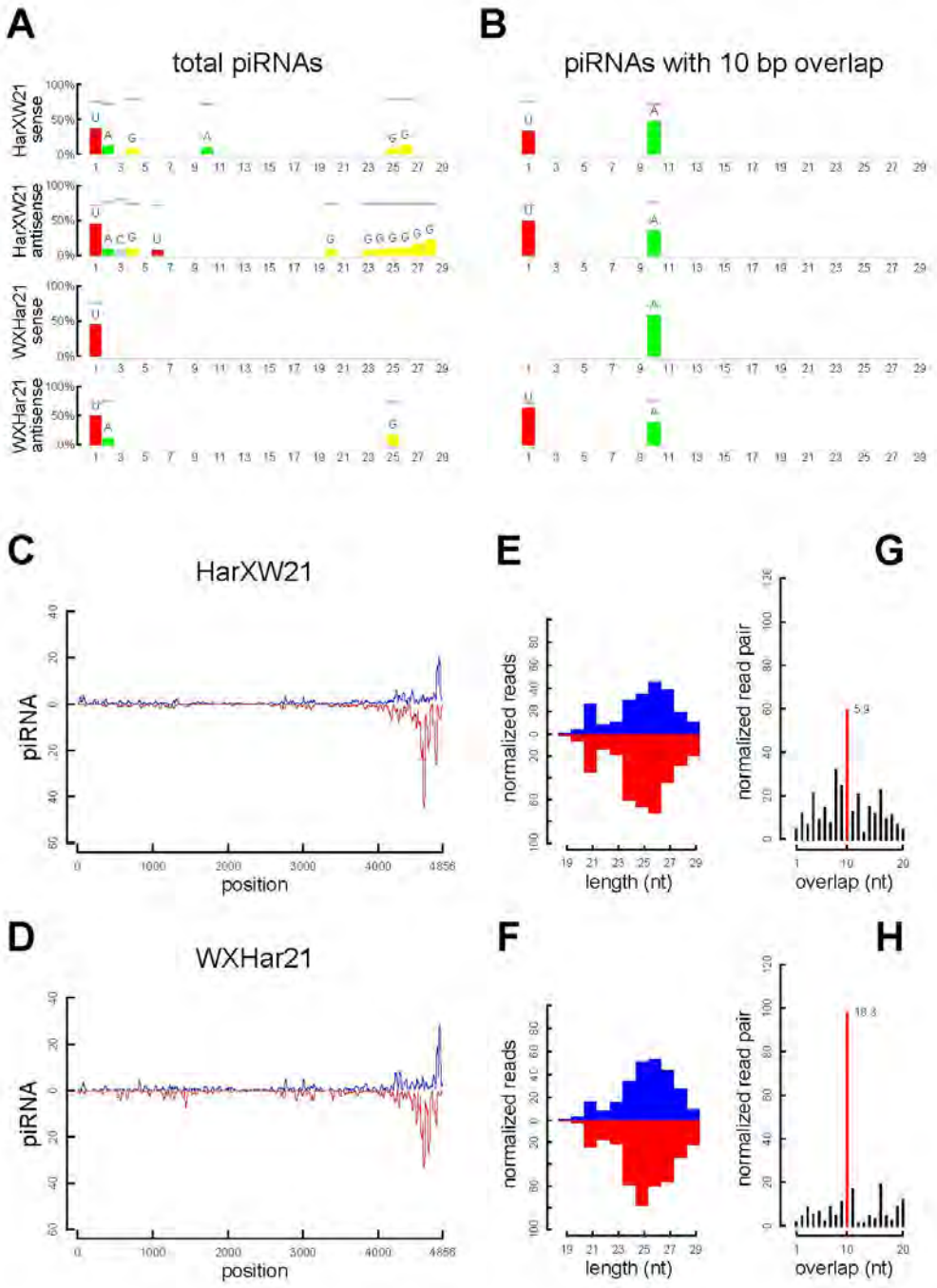
A
total piRNAs
B
piRNAs with 10 bp overlap
HarXW21 sense
HarXW21 antisense
WXHar21 sense
WXHar21 antisense
C
HarXW21
D
WXHar21
piRNA
position
E
F
normalized reads
length (nt)
G
H
normalized read pair
overlap (nt)
5.9
18.8

G5A

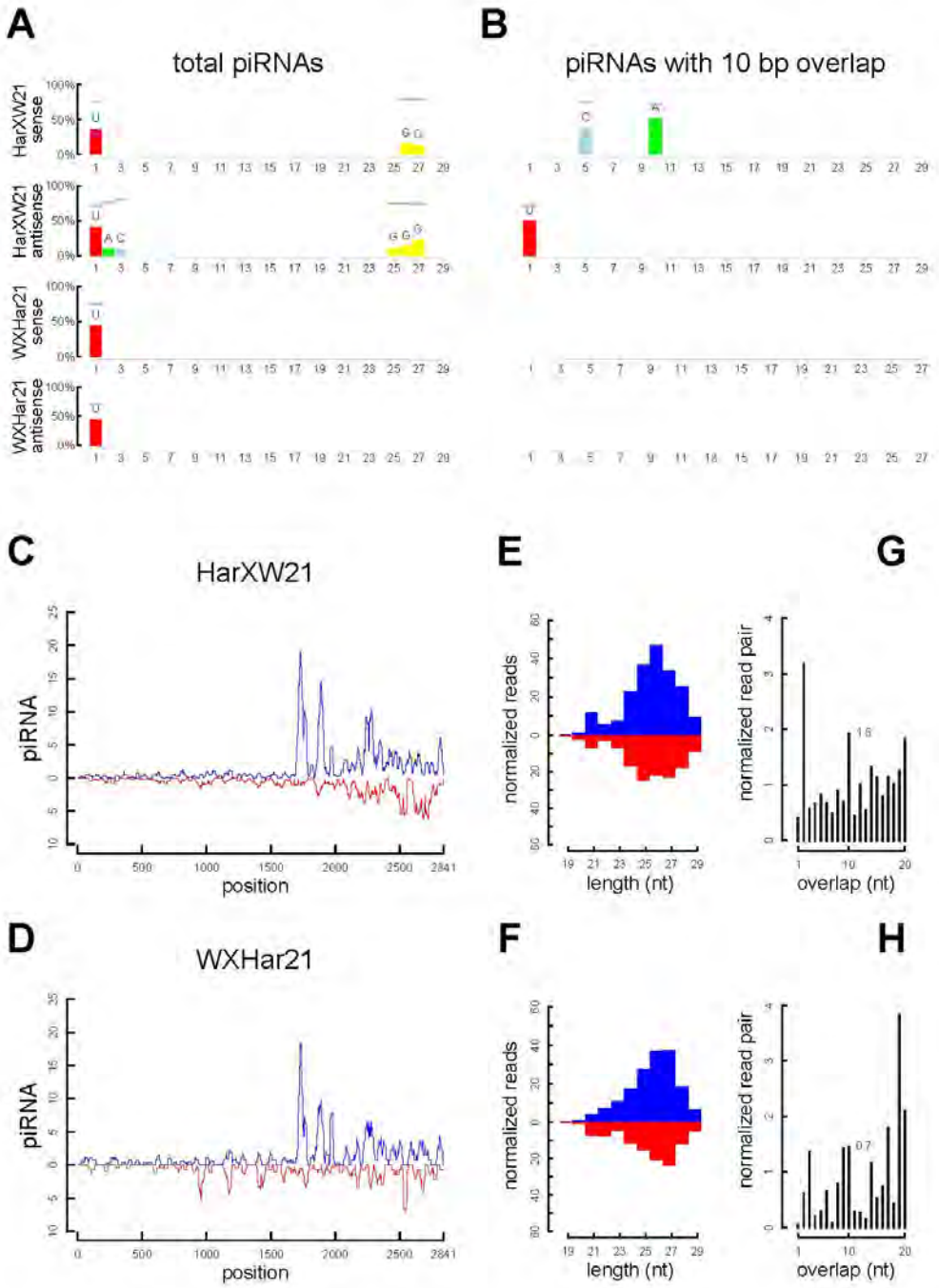
A
total piRNAs
B
piRNAs with 10 bp overlap
HarXW21 sense
HarXW21 antisense
WXHar21 sense
WXHar21 antisense
C
HarXW21
D
WXHar21
piRNA
position
E
F
normalized reads
length (nt)
G
H
normalized read pair
overlap (nt)

G6

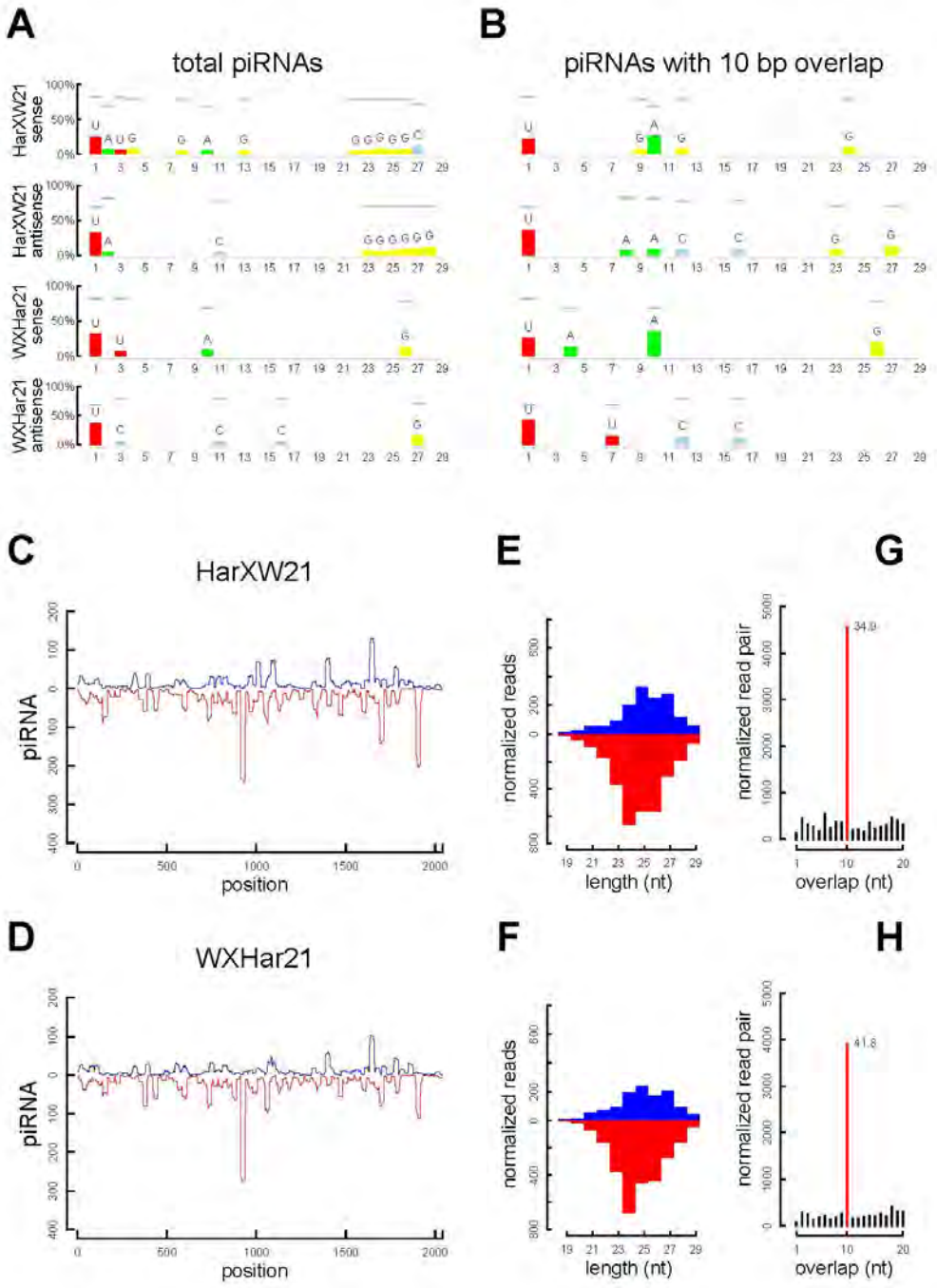
A
total piRNAs
B
piRNAs with 10 bp overlap
HarXW21 sense
HarXW21 antisense
WXHar21 sense
WXHar21 antisense
C
HarXW21
D
WXHar21
piRNA
position
E
F
normalized reads
length (nt)
G
H
normalized read pair
overlap (nt)
34.8
41.8

G7

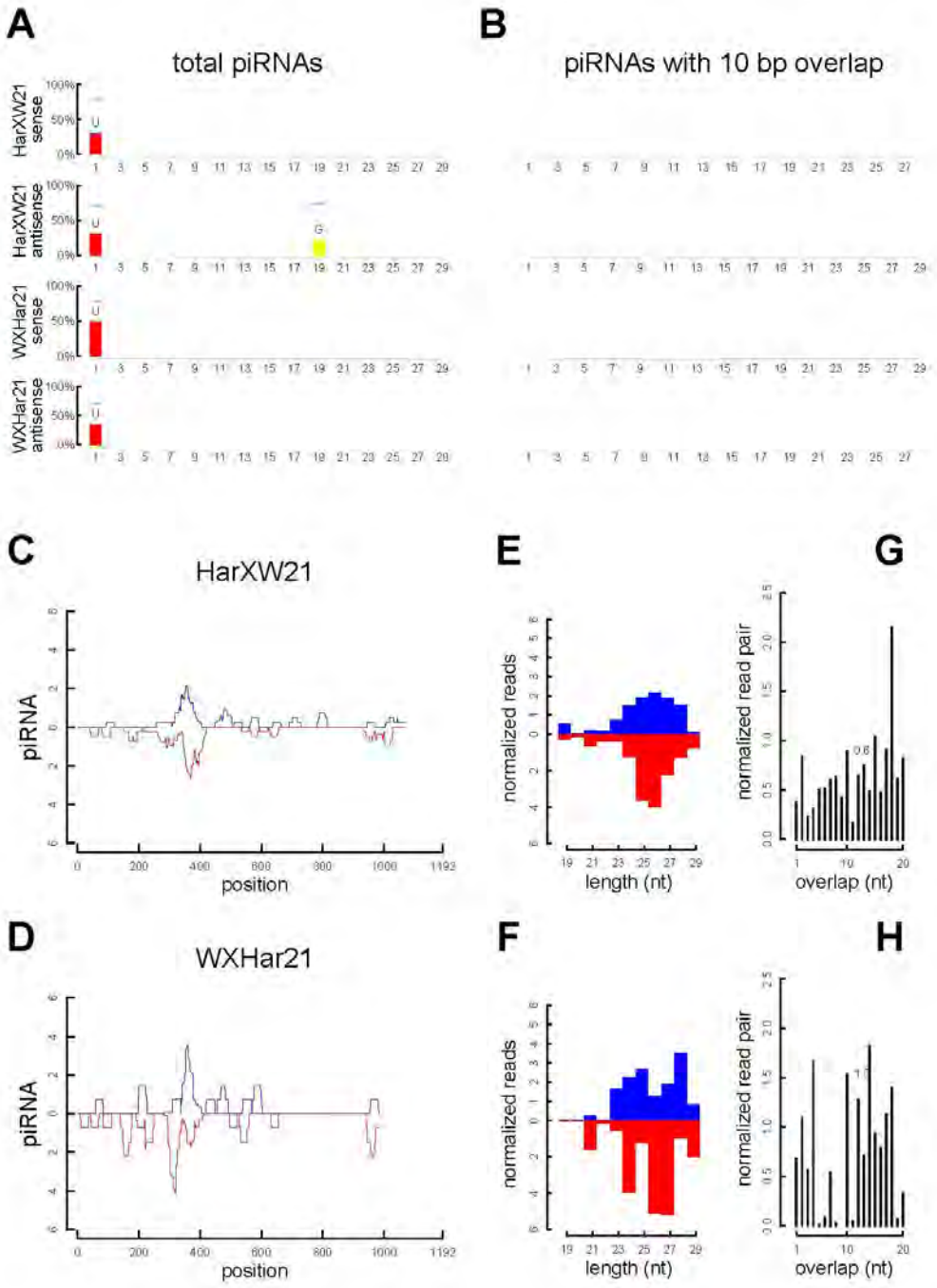
A
total piRNAs
B
piRNAs with 10 bp overlap
HarXW21 sense
HarXW21 antisense
WXHar21 sense
WXHar21 antisense
C
HarXW21
D
WXHar21
piRNA
position
E
F
normalized reads
length (nt)
G
H
normalized read pair
overlap (nt)

GATE

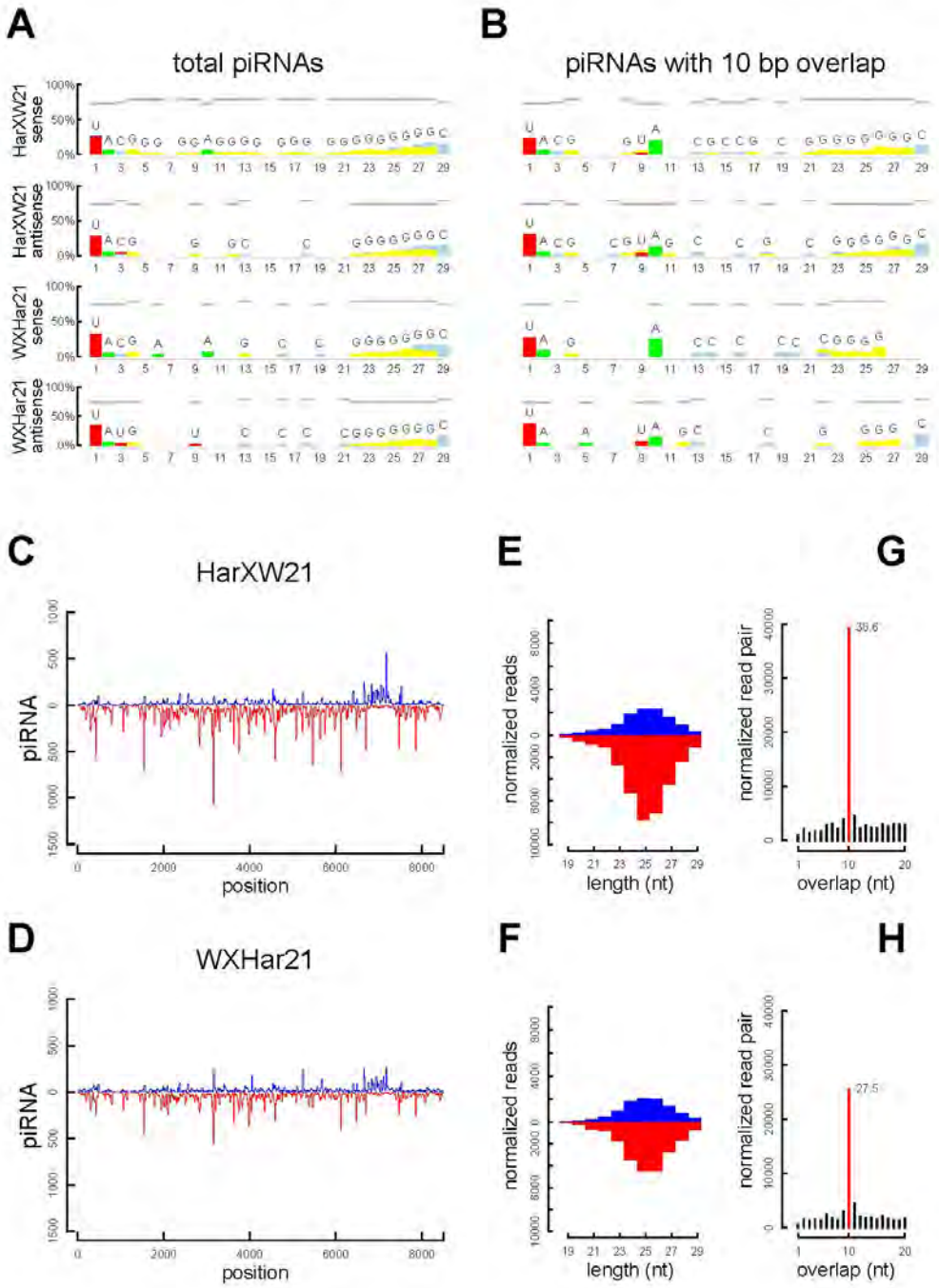
A
total piRNAs
HarXW21 sense
HarXW21 antisense
WXHar21 sense
WXHar21 antisense
B
piRNAs with 10 bp overlap
C
HarXW21
piRNA
position
D
WXHar21
piRNA
position
E
normalized reads
length (nt)
F
normalized reads
length (nt)
G
normalized read pair
35.6
overlap (nt)
H
normalized read pair
27.5
overlap (nt)

G element

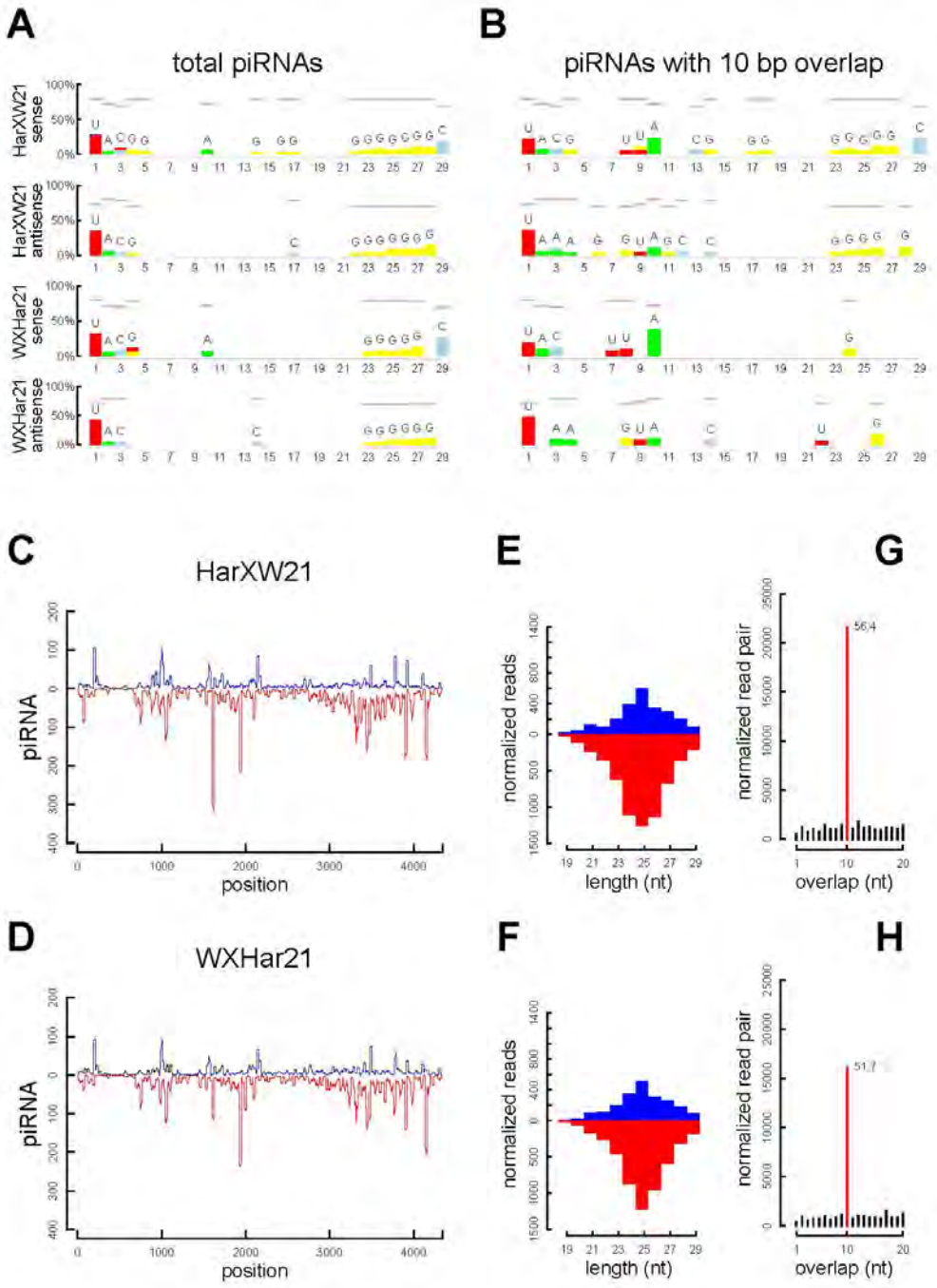
A
total piRNAs
B
piRNAs with 10 bp overlap
HarXW21 sense
HarXW21 antisense
WXHar21 sense
WXHar21 antisense
C
HarXW21
piRNA
position
D
WXHar21
piRNA
position
E
normalized reads
length (nt)
F
normalized reads
length (nt)
G
normalized read pair
overlap (nt)
56.4
H
normalized read pair
overlap (nt)
51.7

gtwin

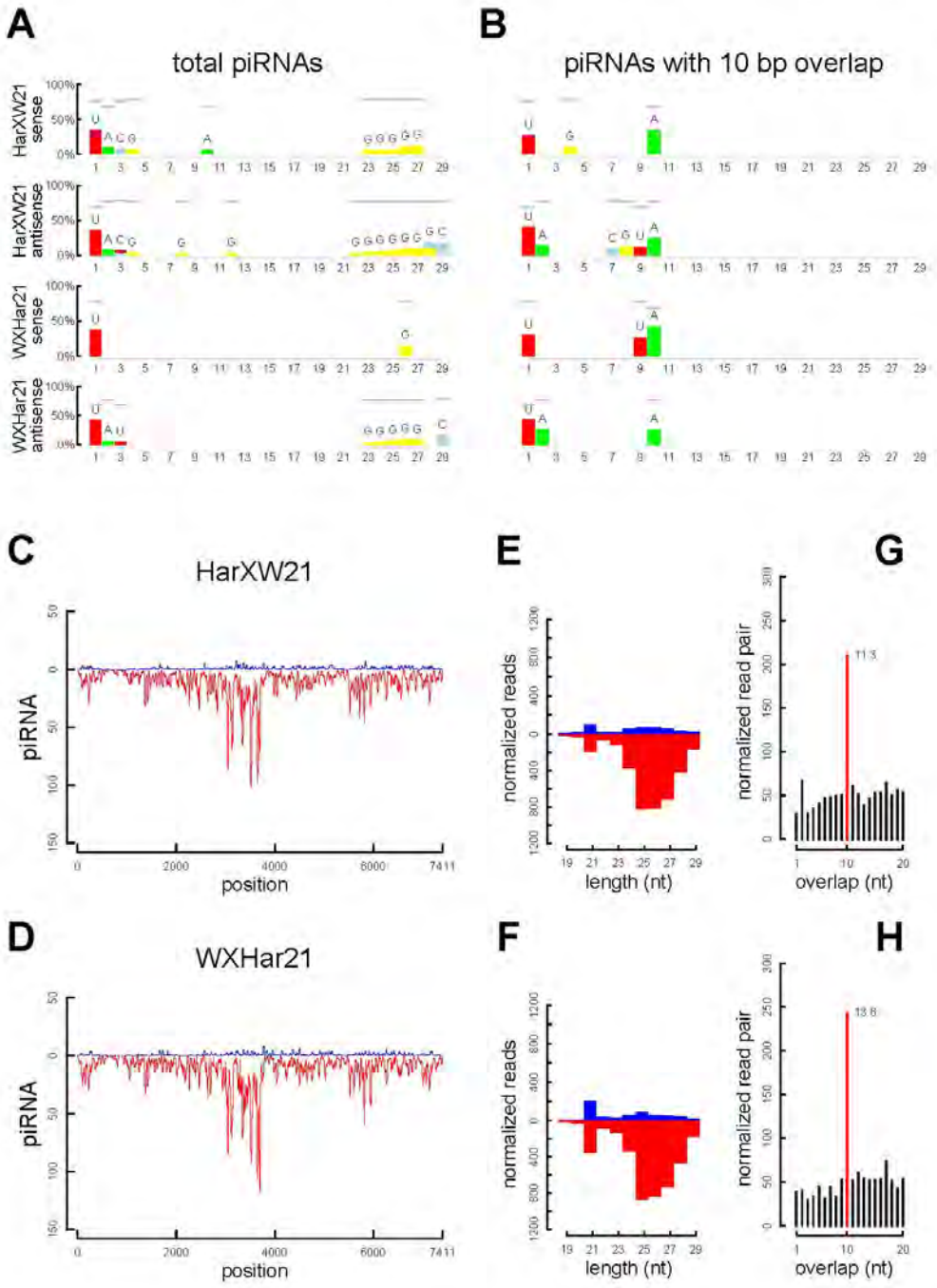
A
total piRNAs
B
piRNAs with 10 bp overlap
HarXW21 sense
HarXW21 antisense
WXHar21 sense
WXHar21 antisense
C
HarXW21
piRNA
position
D
WXHar21
piRNA
position
E
normalized reads
length (nt)
F
normalized reads
length (nt)
G
normalized read pair
overlap (nt)
H
normalized read pair
overlap (nt)

gypsy

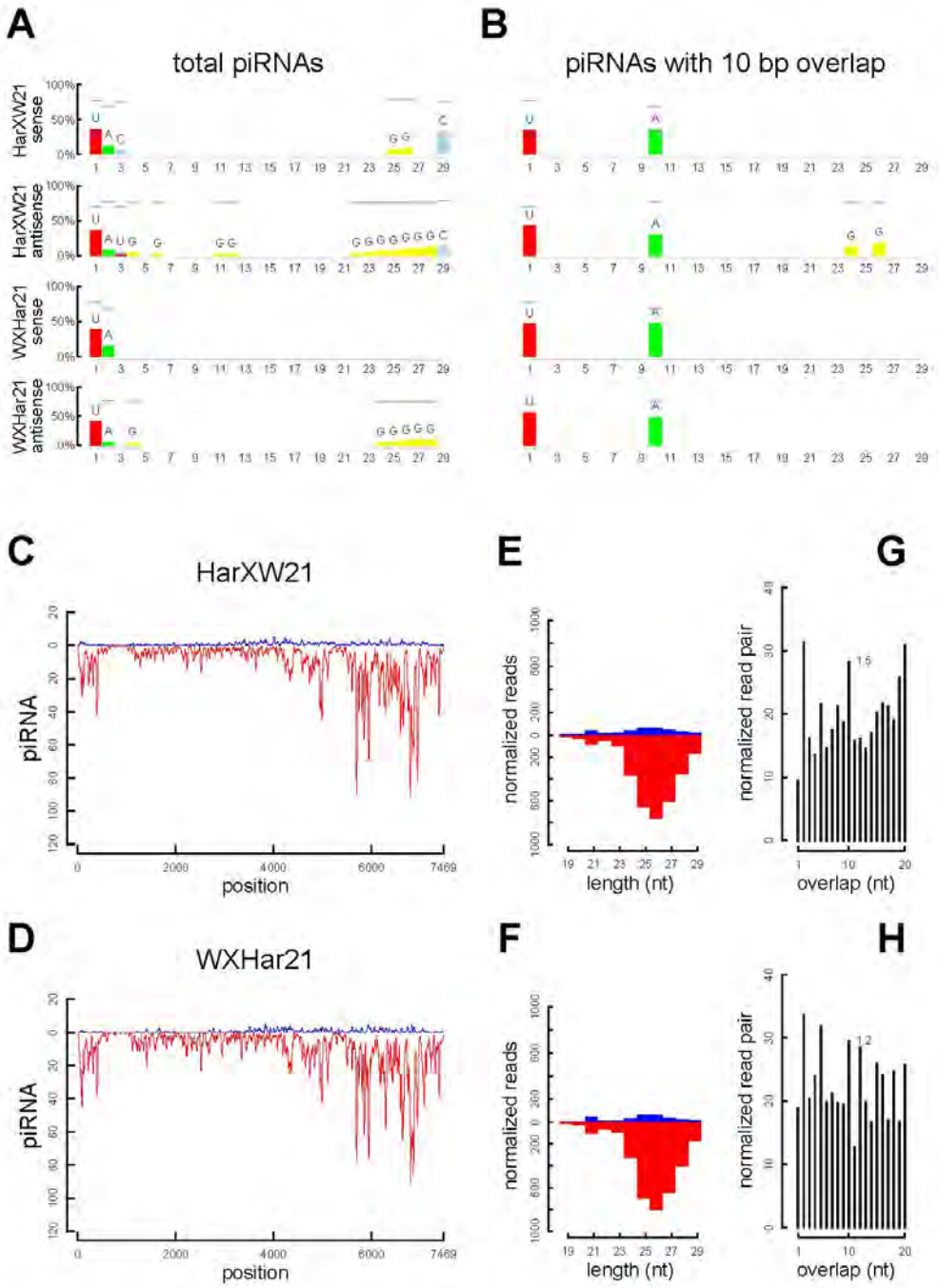
A
total piRNAs
B
piRNAs with 10 bp overlap
HarXW21 sense
HarXW21 antisense
WXHar21 sense
WXHar21 antisense
C
HarXW21
D
WXHar21
piRNA
position
E
F
normalized reads
length (nt)
G
H
normalized read pair
overlap (nt)

gypsy10

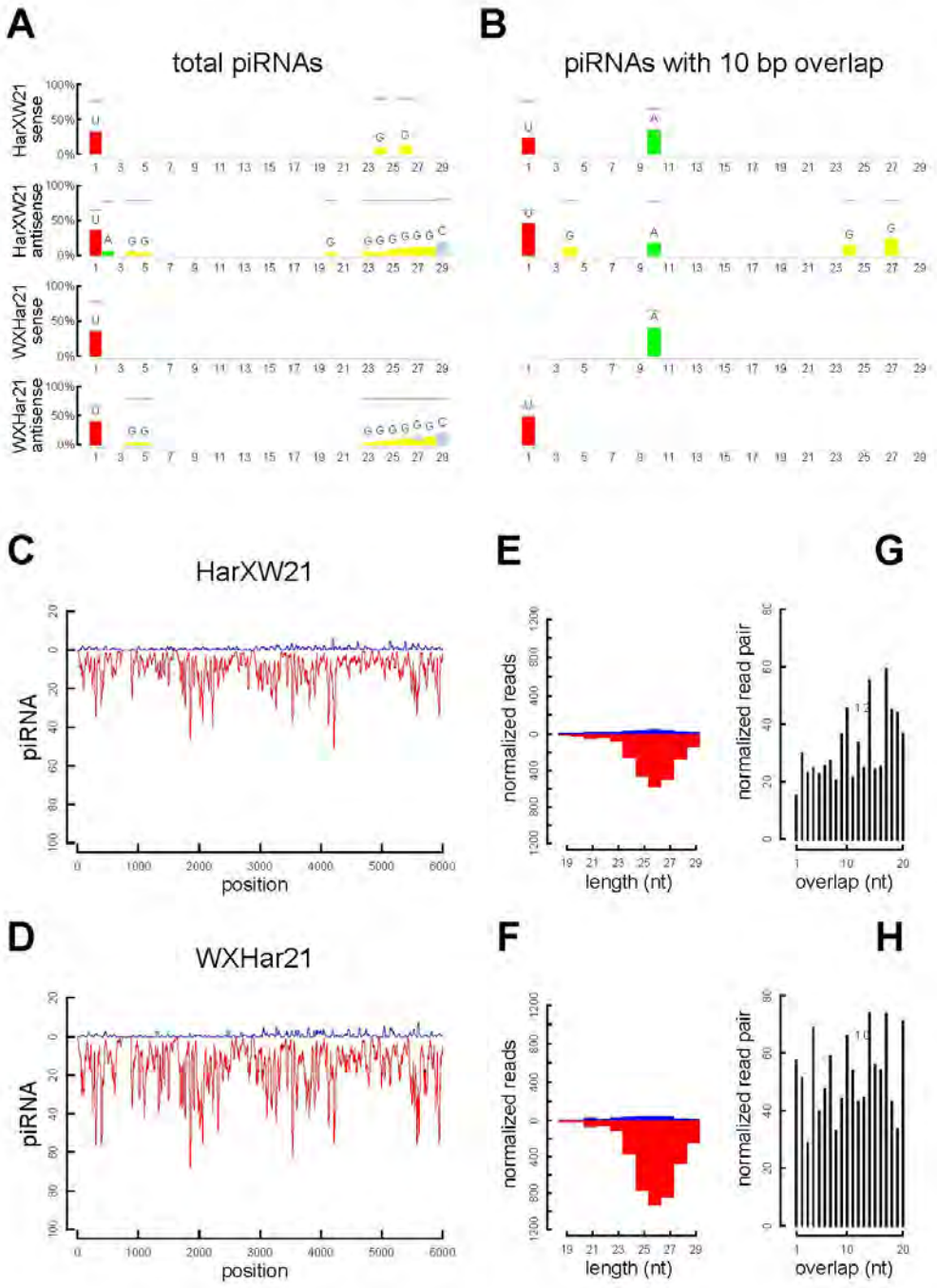
A
total piRNAs
B
piRNAs with 10 bp overlap
HarXW21 sense
HarXW21 antisense
WXHar21 sense
WXHar21 antisense
C
HarXW21
D
WXHar21
piRNA
position
E
F
normalized reads
length (nt)
G
H
normalized read pair
overlap (nt)

gypsy11

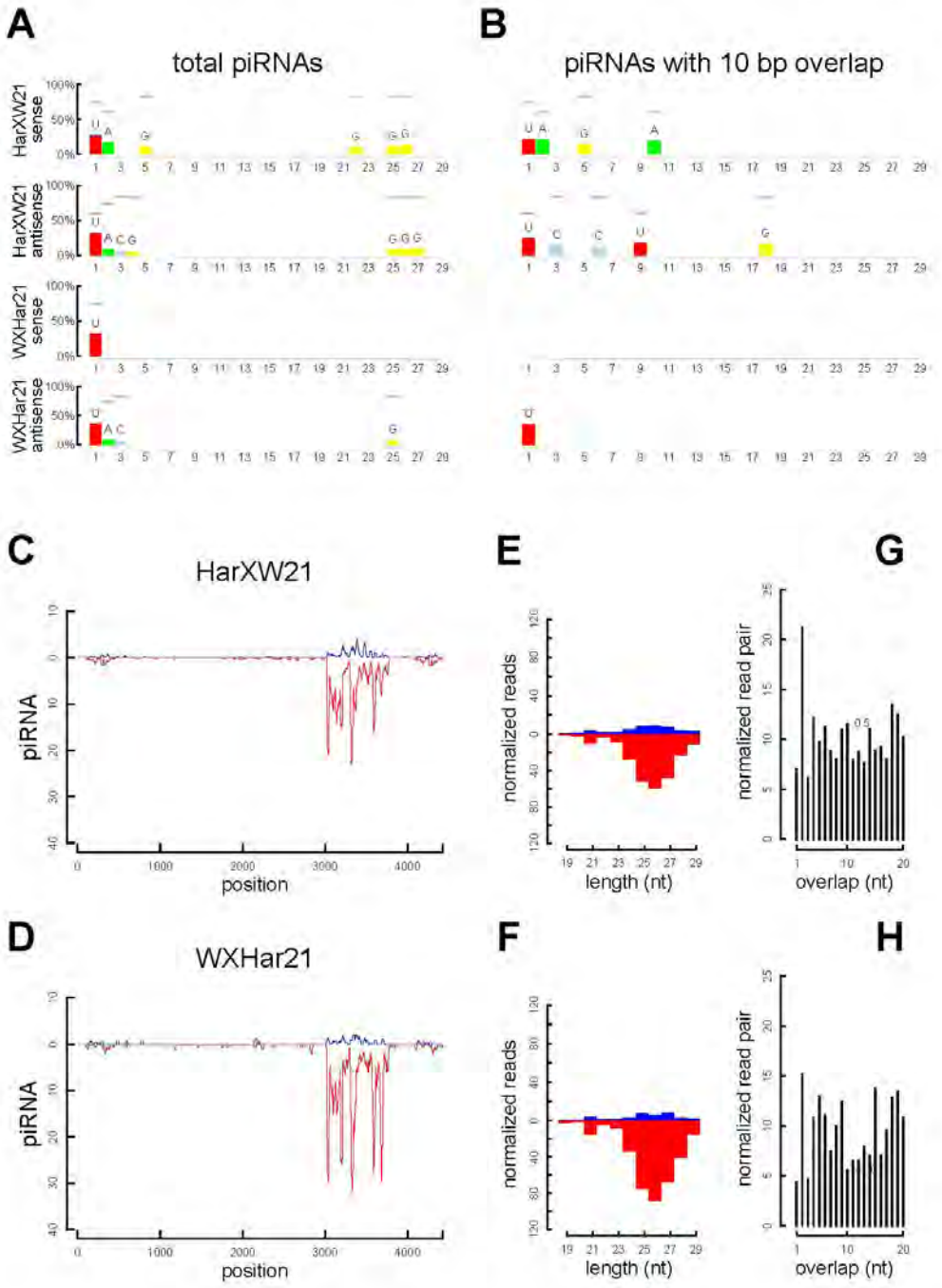
A
total piRNAs
B
piRNAs with 10 bp overlap
HarXW21 sense
HarXW21 antisense
WXHar21 sense
WXHar21 antisense
C
HarXW21
D
WXHar21
piRNA
position
E
F
normalized reads
length (nt)
G
H
normalized read pair
overlap (nt)

gypsy12

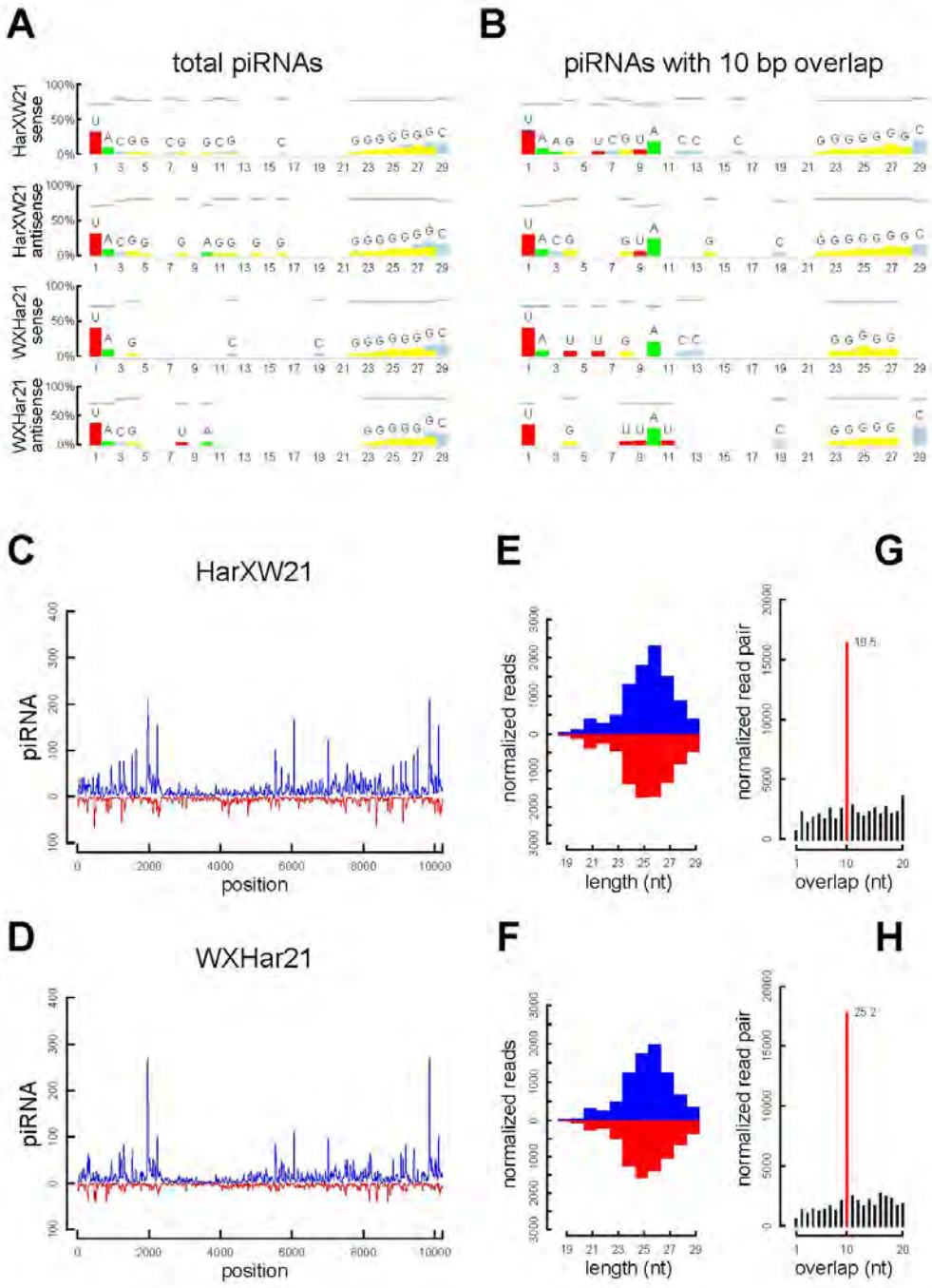
A
total piRNAs
B
piRNAs with 10 bp overlap
HarXW21 sense
HarXW21 antisense
WXHar21 sense
WXHar21 antisense
C
HarXW21
D
WXHar21
piRNA
position
E
F
normalized reads
length (nt)
G
H
normalized read pair
overlap (nt)
19.5
25.2

gypsy12#2

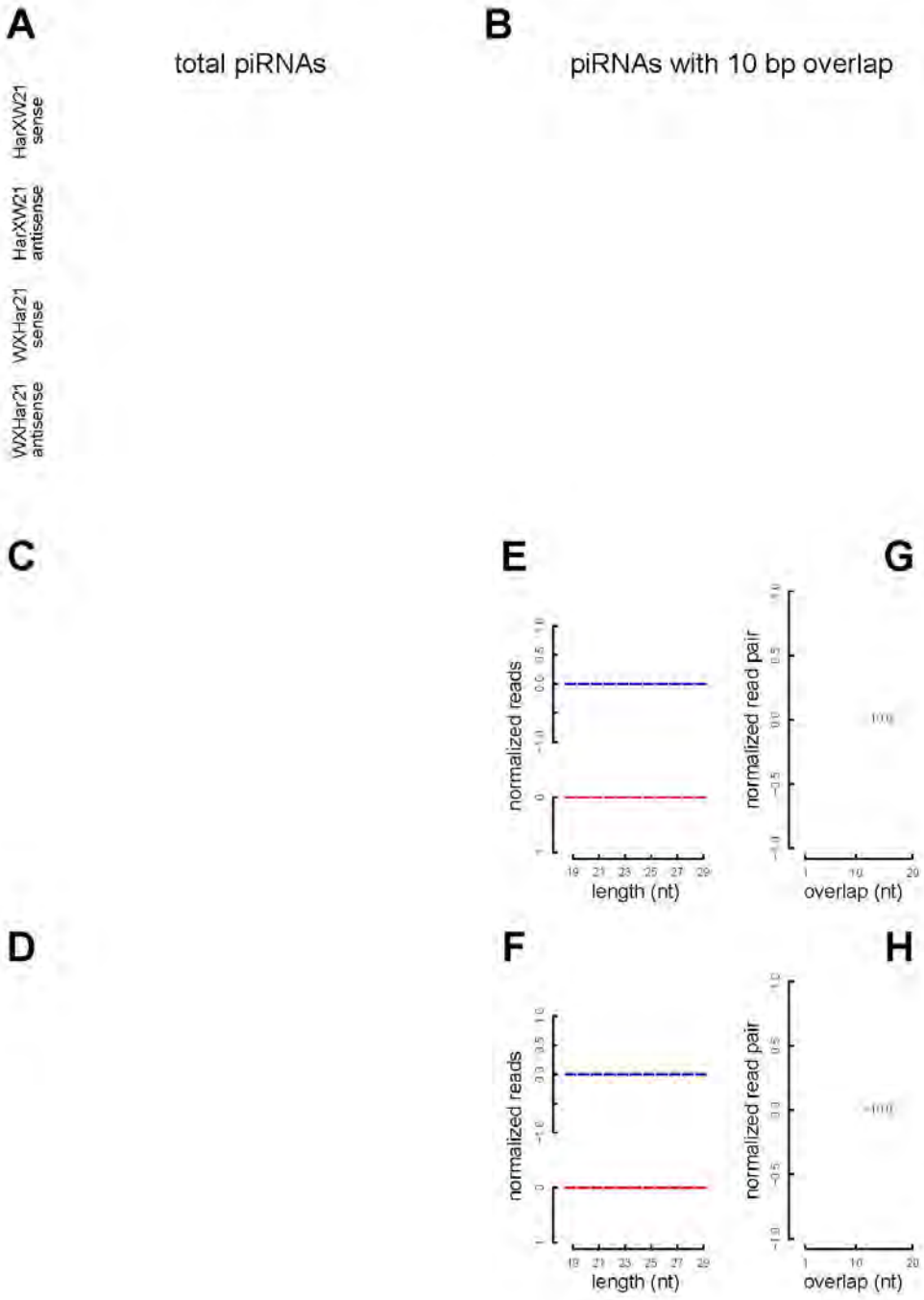
A
total piRNAs
B
piRNAs with 10 bp overlap
HarXW21 sense
HarXW21 antisense
WXHar21 sense
WXHar21 antisense
C
D
E
F
G
H
normalized reads
length (nt)
normalized read pair
overlap (nt)

gypsy2

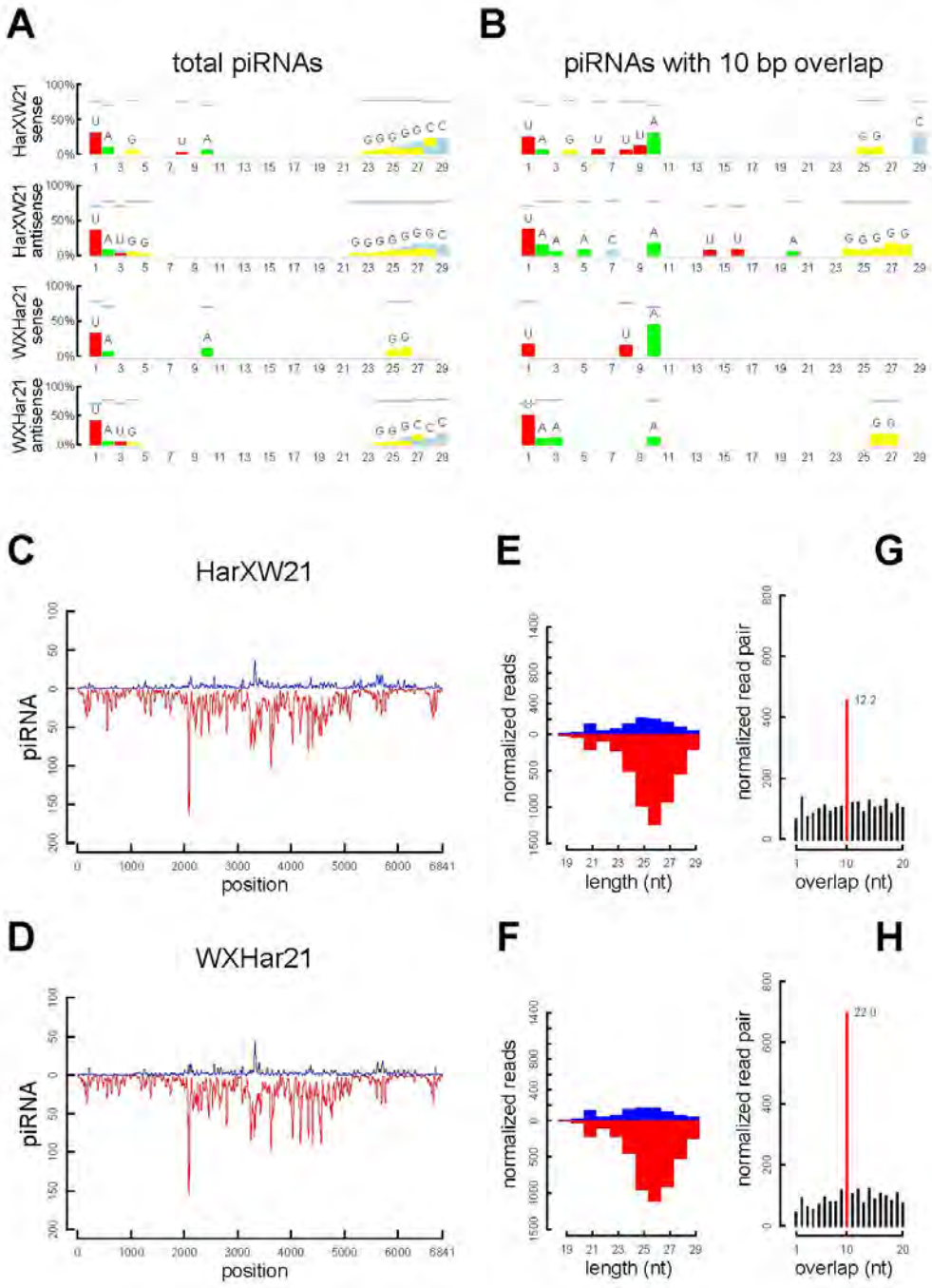
A
total piRNAs
B
piRNAs with 10 bp overlap
HarXW21 sense
HarXW21 antisense
WXHar21 sense
WXHar21 antisense
C
HarXW21
D
WXHar21
piRNA
position
E
F
normalized reads
length (nt)
G
H
normalized read pair
overlap (nt)
12.2
22.0

gypsy3

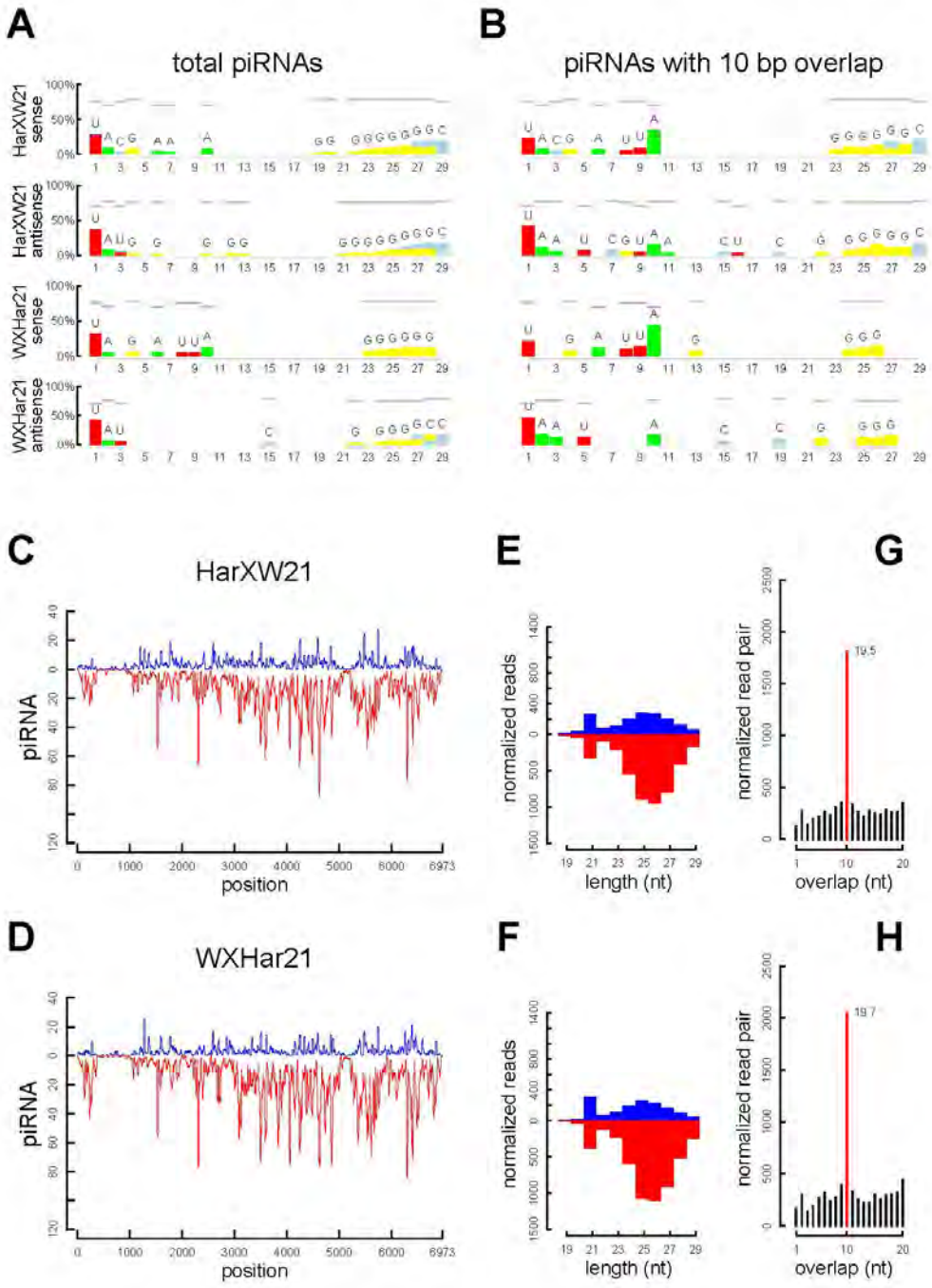
A
total piRNAs
B
piRNAs with 10 bp overlap
HarXW21 sense
HarXW21 antisense
WXHar21 sense
WXHar21 antisense
C
HarXW21
D
WXHar21
piRNA
position
E
F
normalized reads
length (nt)
G
H
normalized read pair
overlap (nt)
19.5
19.7

gypsy4

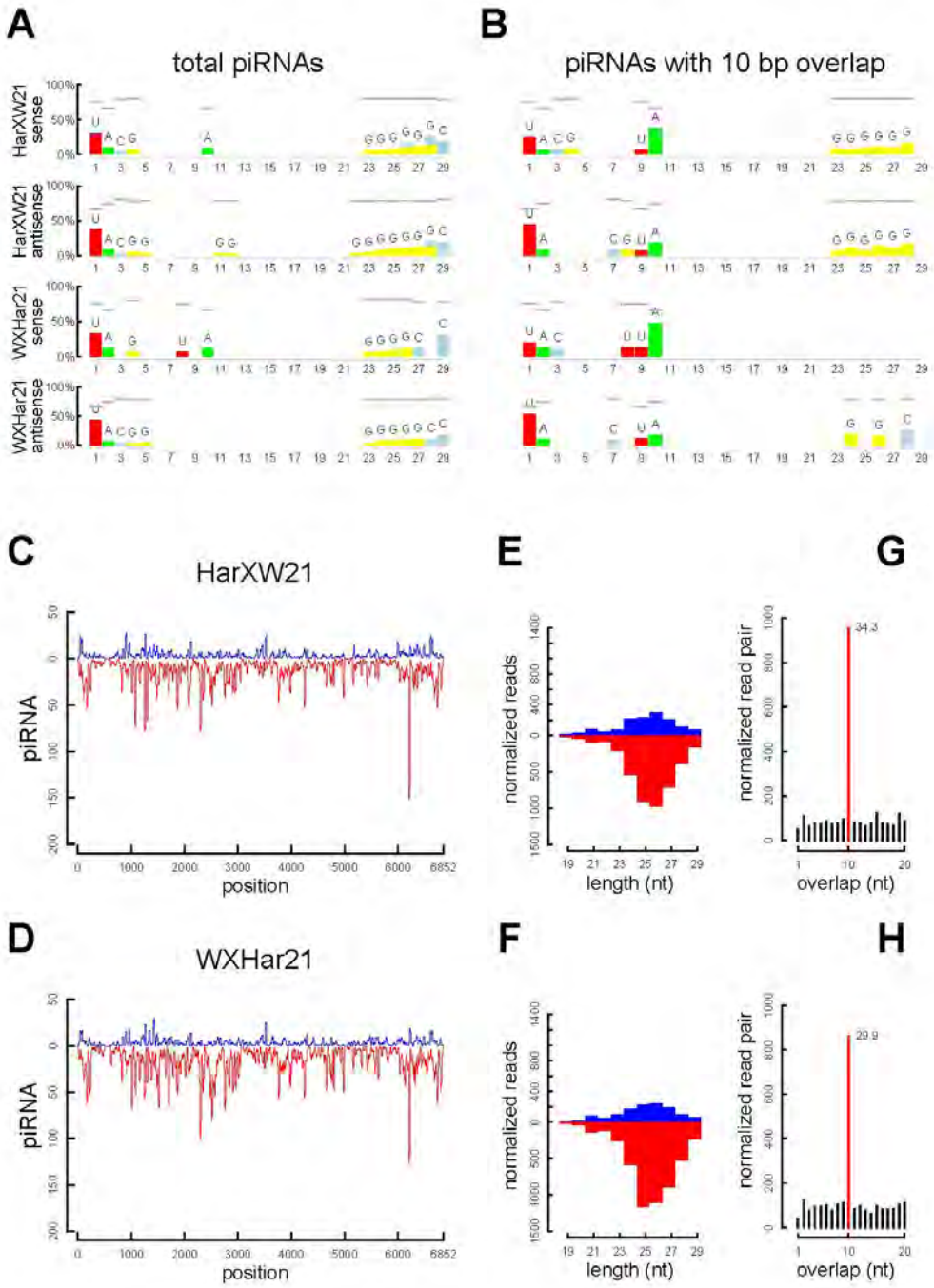
A
total piRNAs
B
piRNAs with 10 bp overlap
HarXW21 sense
HarXW21 antisense
WXHar21 sense
WXHar21 antisense
C
HarXW21
D
WXHar21
piRNA
position
E
F
normalized reads
length (nt)
G
H
normalized read pair
overlap (nt)
34.3
29.9

gypsy5

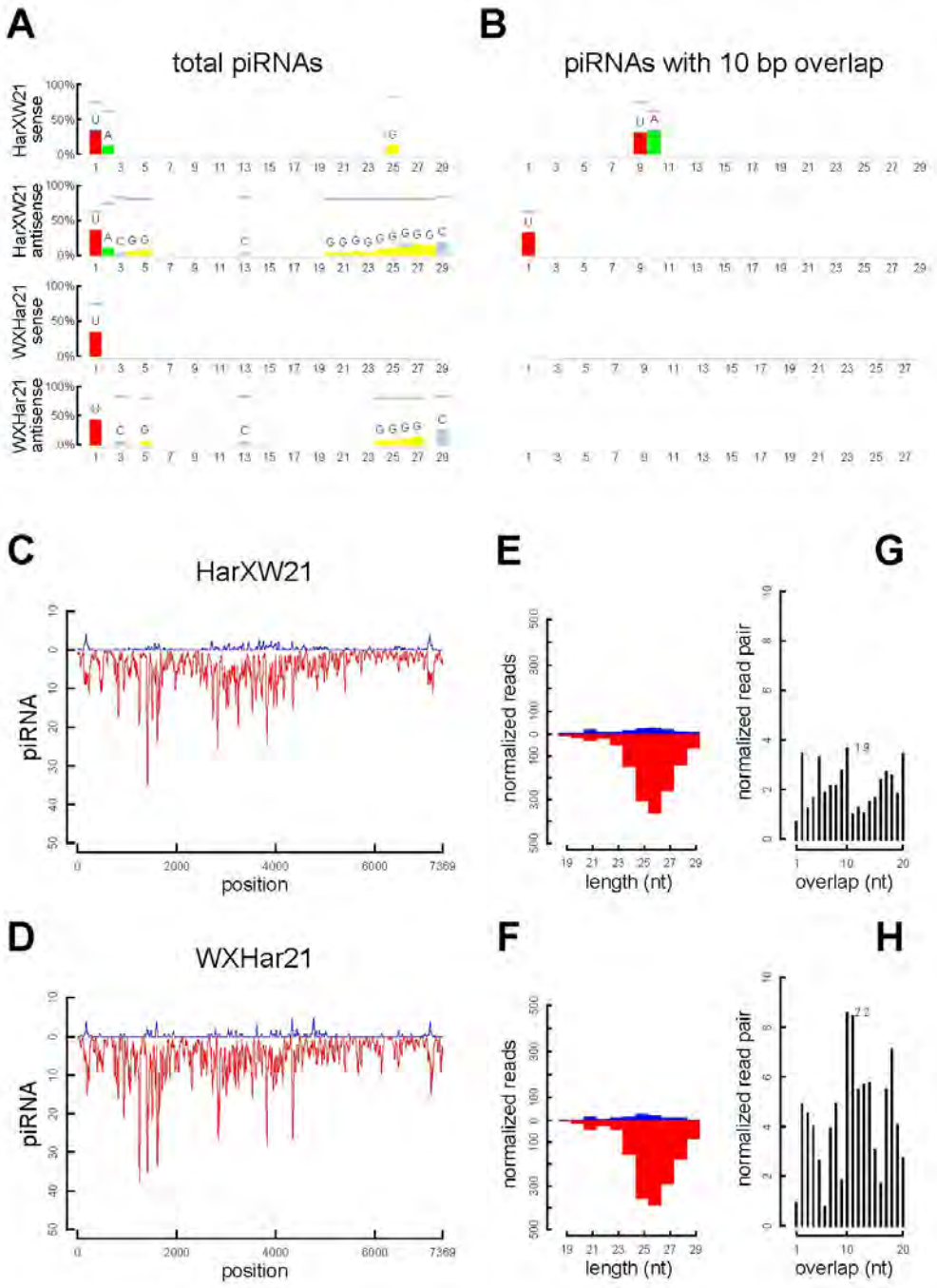
A
total piRNAs
B
piRNAs with 10 bp overlap
HarXW21 sense
HarXW21 antisense
WXHar21 sense
WXHar21 antisense
C
HarXW21
D
WXHar21
piRNA
position
E
F
normalized reads
length (nt)
G
H
normalized read pair
overlap (nt)

gypsy6

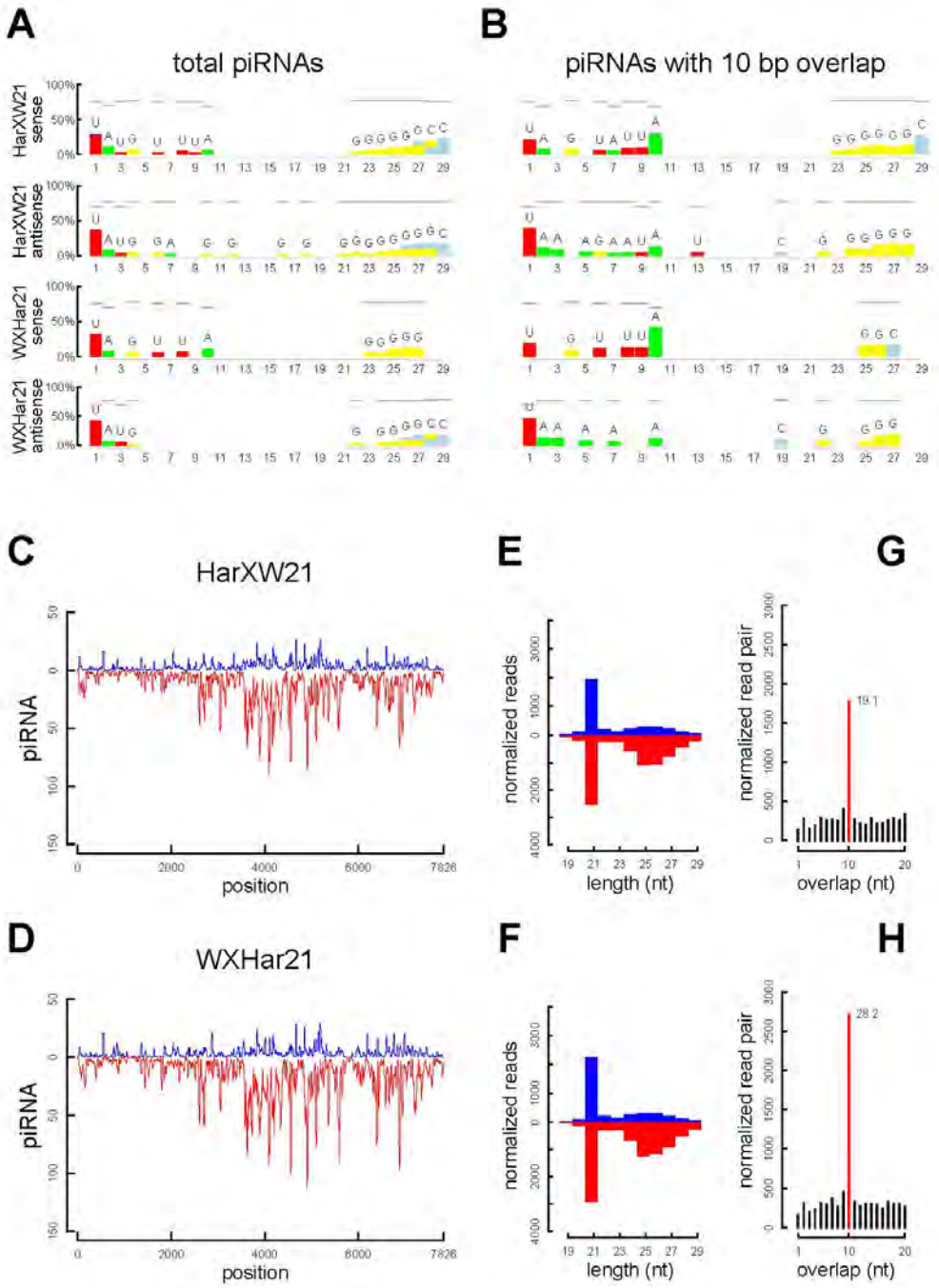
A
total piRNAs
B
piRNAs with 10 bp overlap
HarXW21 sense
HarXW21 antisense
WXHar21 sense
WXHar21 antisense
C
HarXW21
D
WXHar21
piRNA
position
E
F
normalized reads
length (nt)
G
H
normalized read pair
overlap (nt)
19.1
28.2

gypsy7

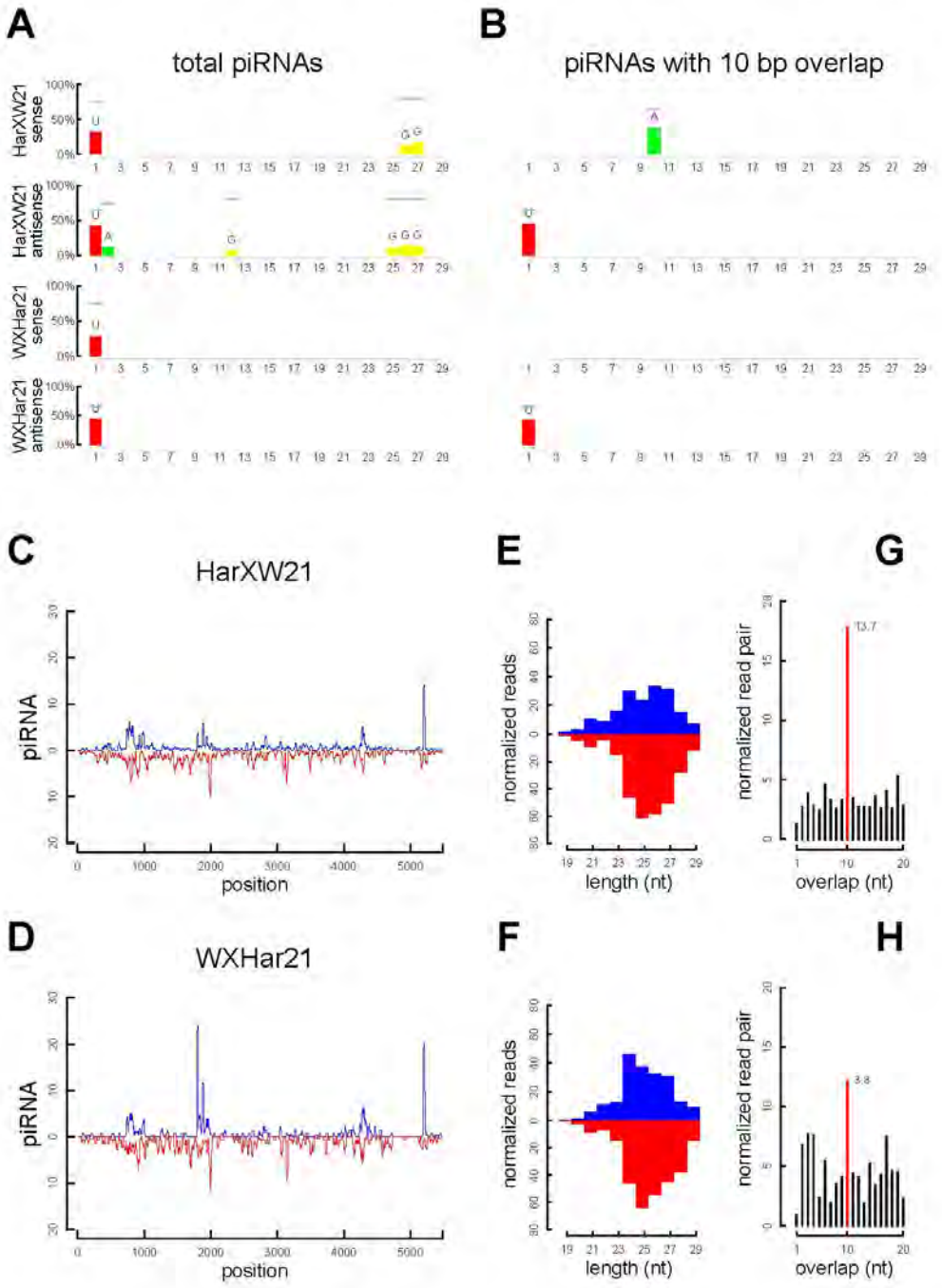
A
total piRNAs
B
piRNAs with 10 bp overlap
HarXW21 sense
HarXW21 antisense
WXHar21 sense
WXHar21 antisense
C
HarXW21
D
WXHar21
piRNA
position
E
F
normalized reads
length (nt)
G
H
normalized read pair
overlap (nt)
13.7
3.8

gypsy8

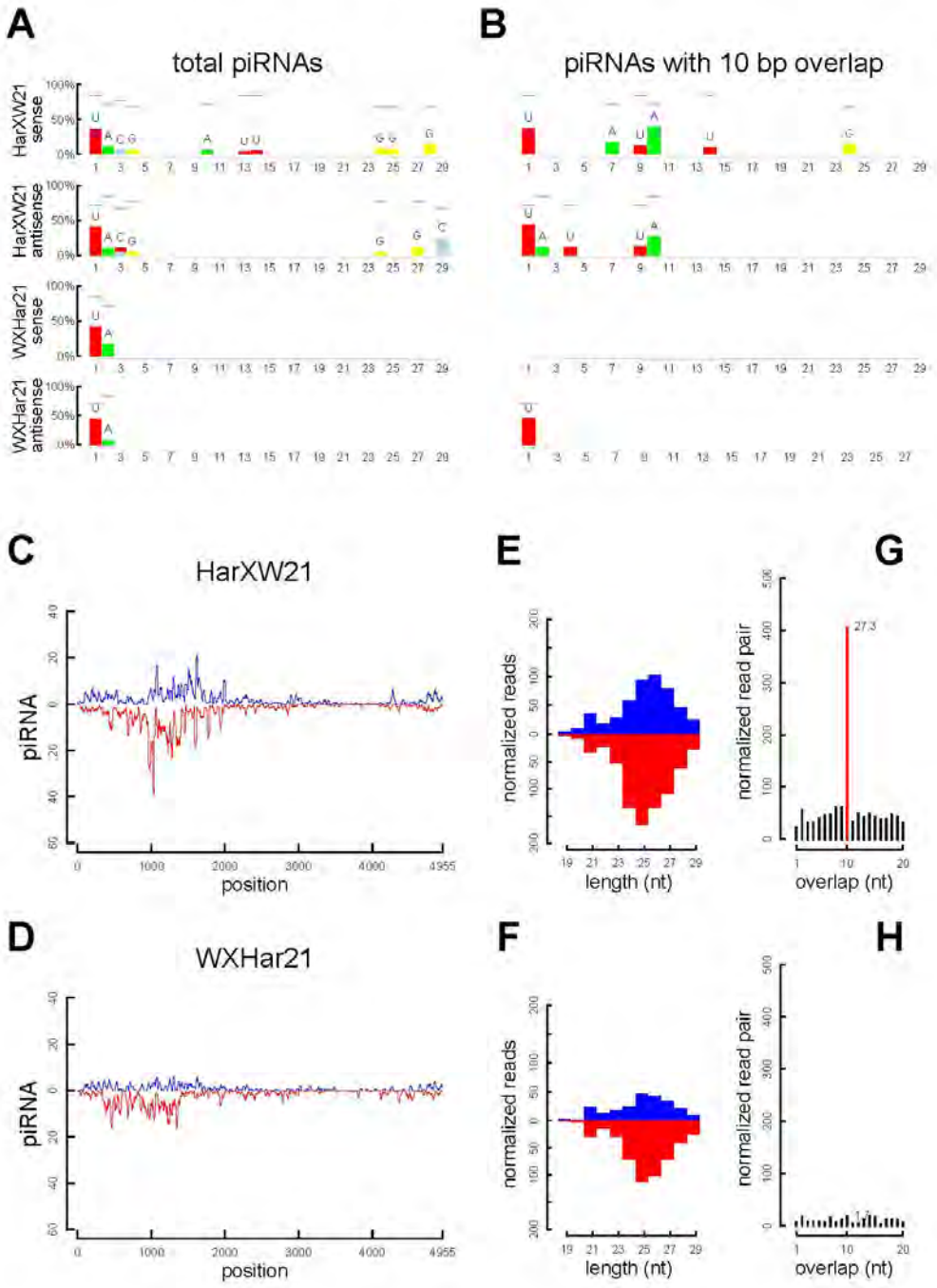
A
total piRNAs
B
piRNAs with 10 bp overlap
HarXW21 sense
HarXW21 antisense
WXHar21 sense
WXHar21 antisense
C
HarXW21
D
WXHar21
piRNA
position
E
F
normalized reads
length (nt)
G
H
normalized read pair
overlap (nt)
27.3

gypsy9

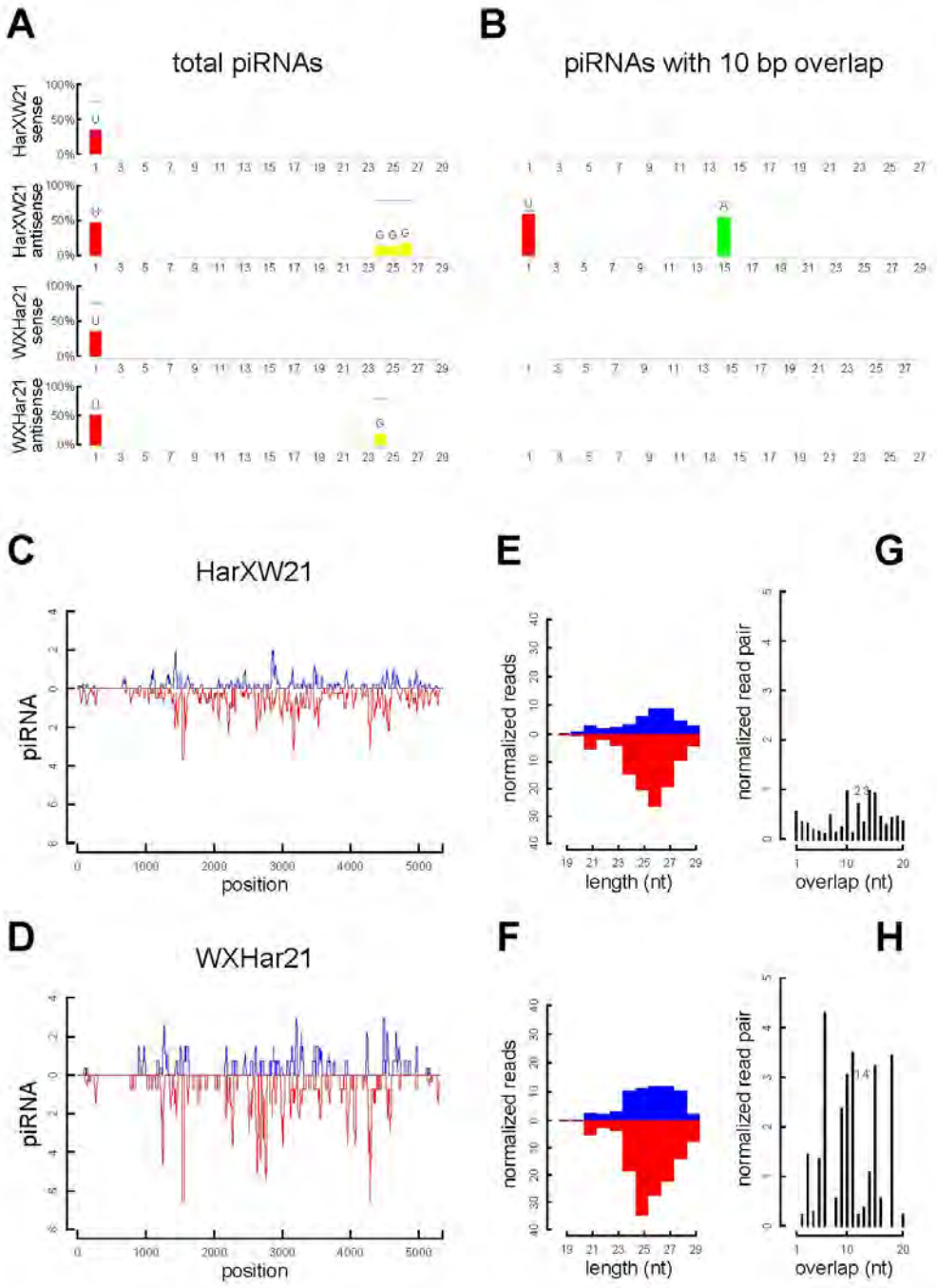
A
total piRNAs
B
piRNAs with 10 bp overlap
HarXW21 sense
HarXW21 antisense
WXHar21 sense
WXHar21 antisense
C
HarXW21
D
WXHar21
piRNA
position
E
F
normalized reads
length (nt)
G
H
normalized read pair
overlap (nt)

HB

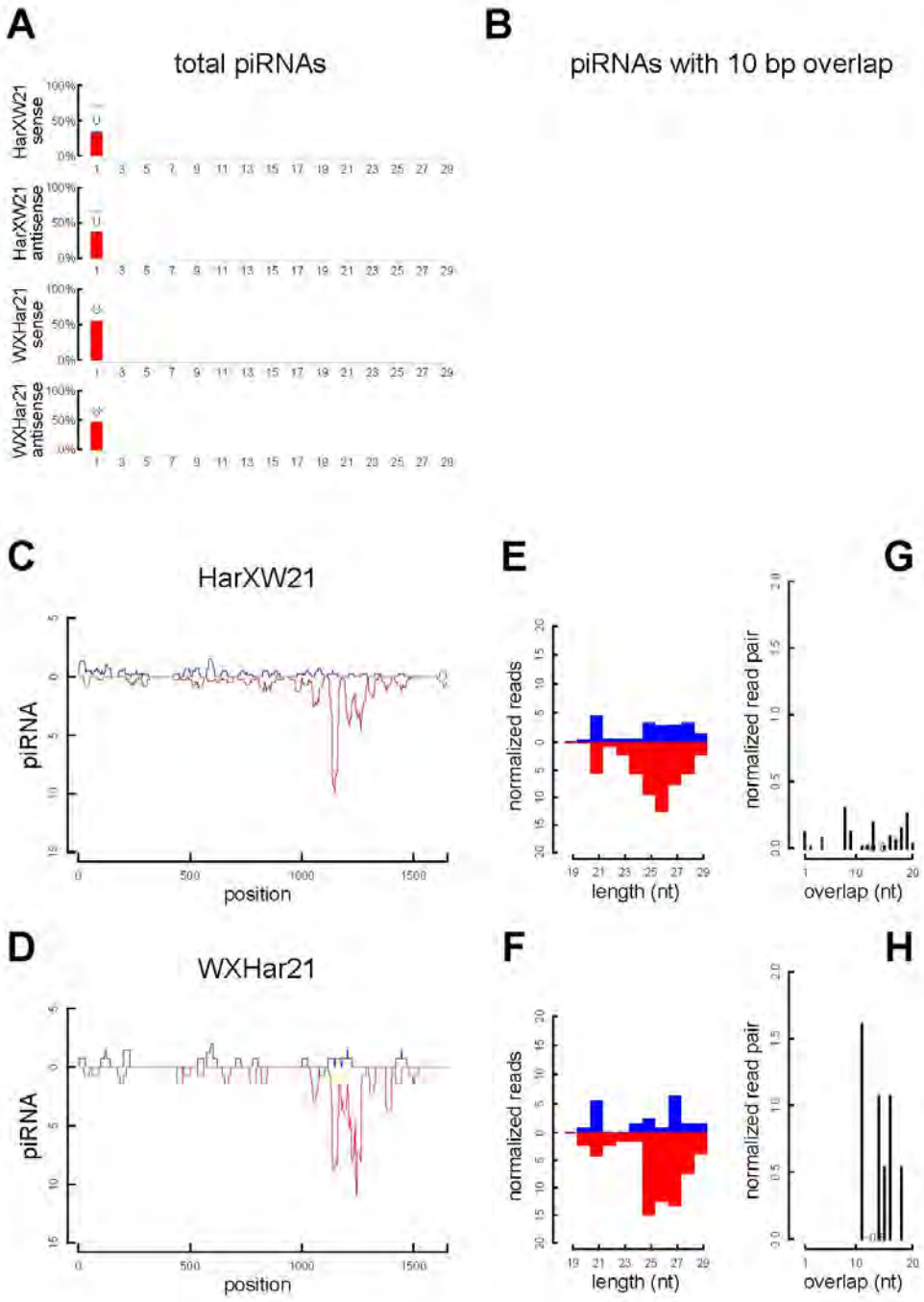
A
total piRNAs
B
piRNAs with 10 bp overlap
HarXW21 sense
HarXW21 antisense
WXHar21 sense
WXHar21 antisense
C
HarXW21
piRNA
position
D
WXHar21
piRNA
position
E
normalized reads
length (nt)
F
normalized reads
length (nt)
G
normalized read pair
overlap (nt)
H
normalized read pair
overlap (nt)

Helena

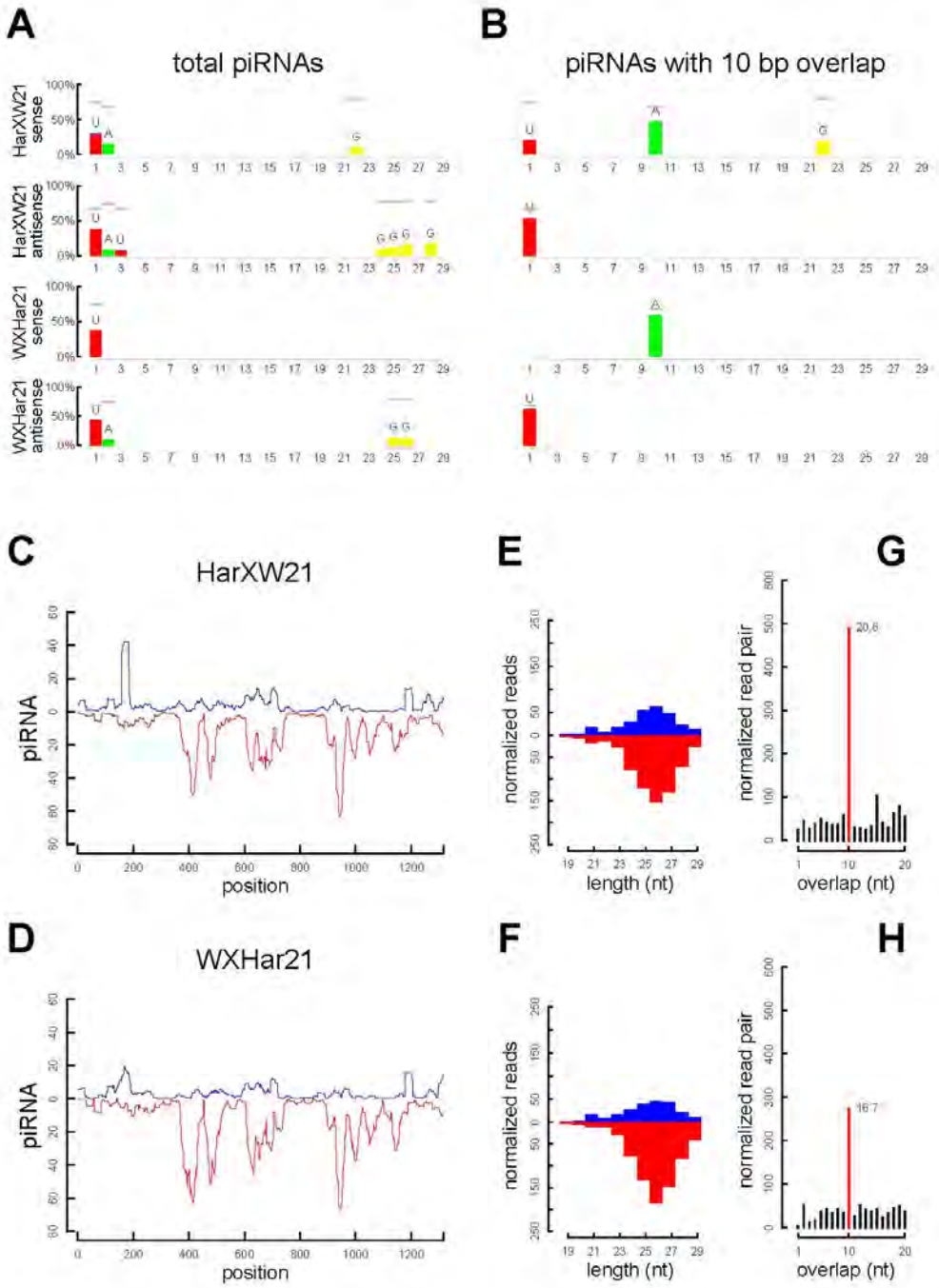
A
total piRNAs
B
piRNAs with 10 bp overlap
HarXW21 sense
HarXW21 antisense
WXHar21 sense
WXHar21 antisense
C
HarXW21
piRNA
position
D
WXHar21
piRNA
position
E
normalized reads
length (nt)
F
normalized reads
length (nt)
G
normalized read pair
20.8
overlap (nt)
H
normalized read pair
16.7
overlap (nt)

Helitron

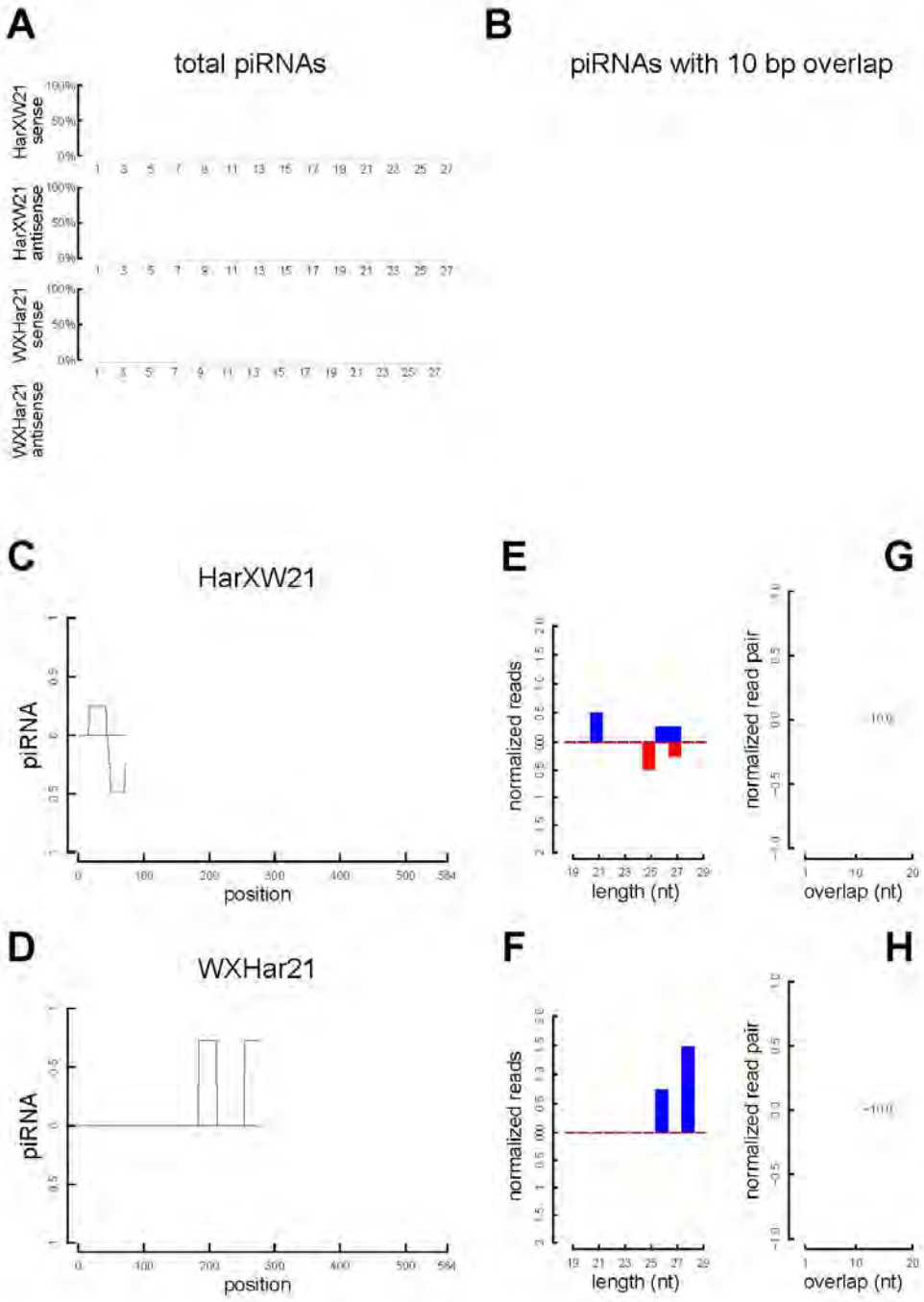
A
total piRNAs
HarXW21 sense
HarXW21 antisense
WXHar21 sense
WXHar21 antisense
B
piRNAs with 10 bp overlap
C
HarXW21
piRNA
position
D
WXHar21
piRNA
position
E
normalized reads
length (nt)
F
normalized reads
length (nt)
G
normalized read pair
overlap (nt)
H
normalized read pair
overlap (nt)

HeT A

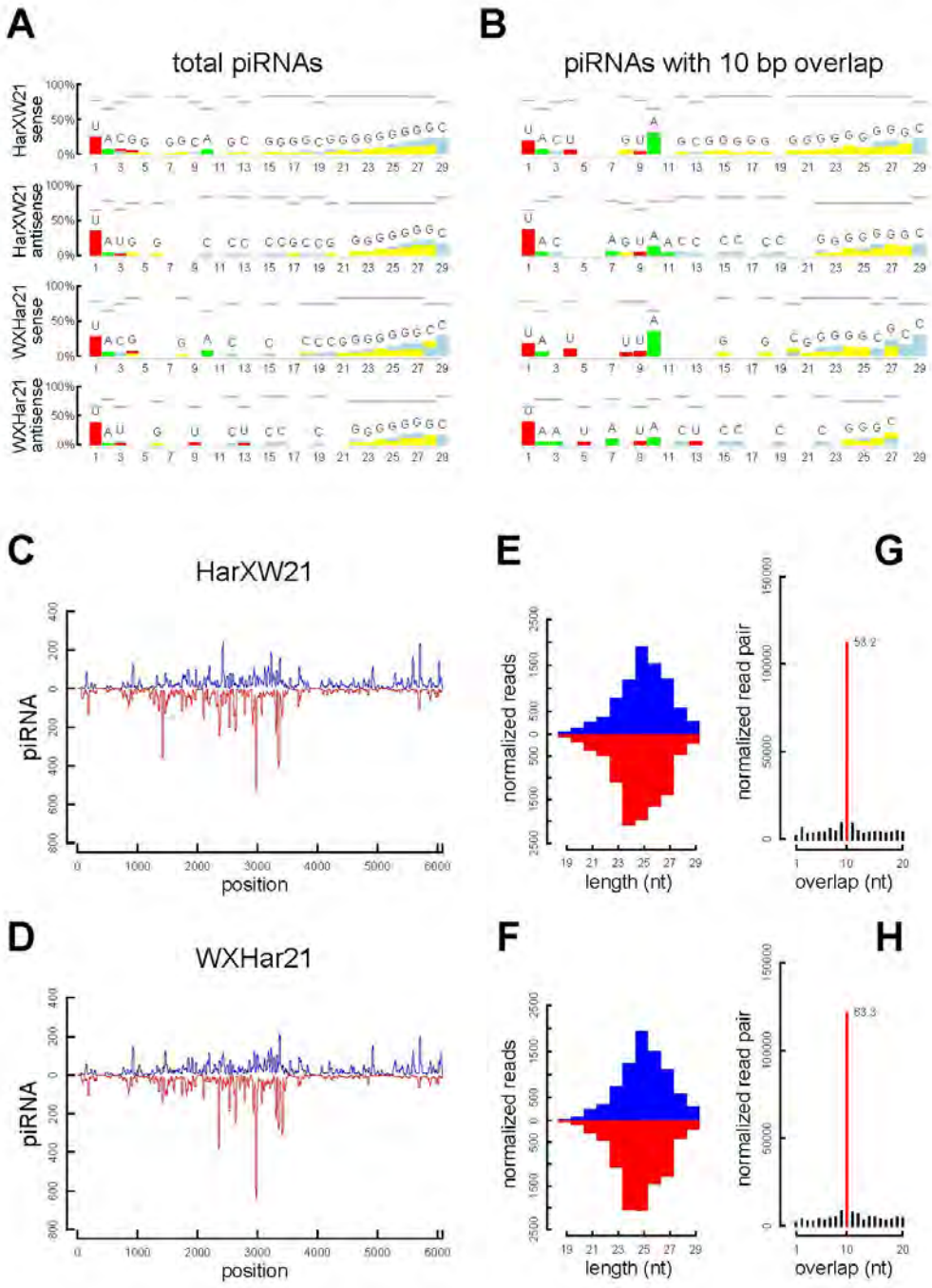
A
total piRNAs
B
piRNAs with 10 bp overlap
HarXW21 sense
HarXW21 antisense
WXHar21 sense
WXHar21 antisense
C
HarXW21
piRNA
position
D
WXHar21
piRNA
position
E
normalized reads
length (nt)
F
normalized reads
length (nt)
G
normalized read pair
58.2
overlap (nt)
H
normalized read pair
83.3
overlap (nt)

HMS Beagle

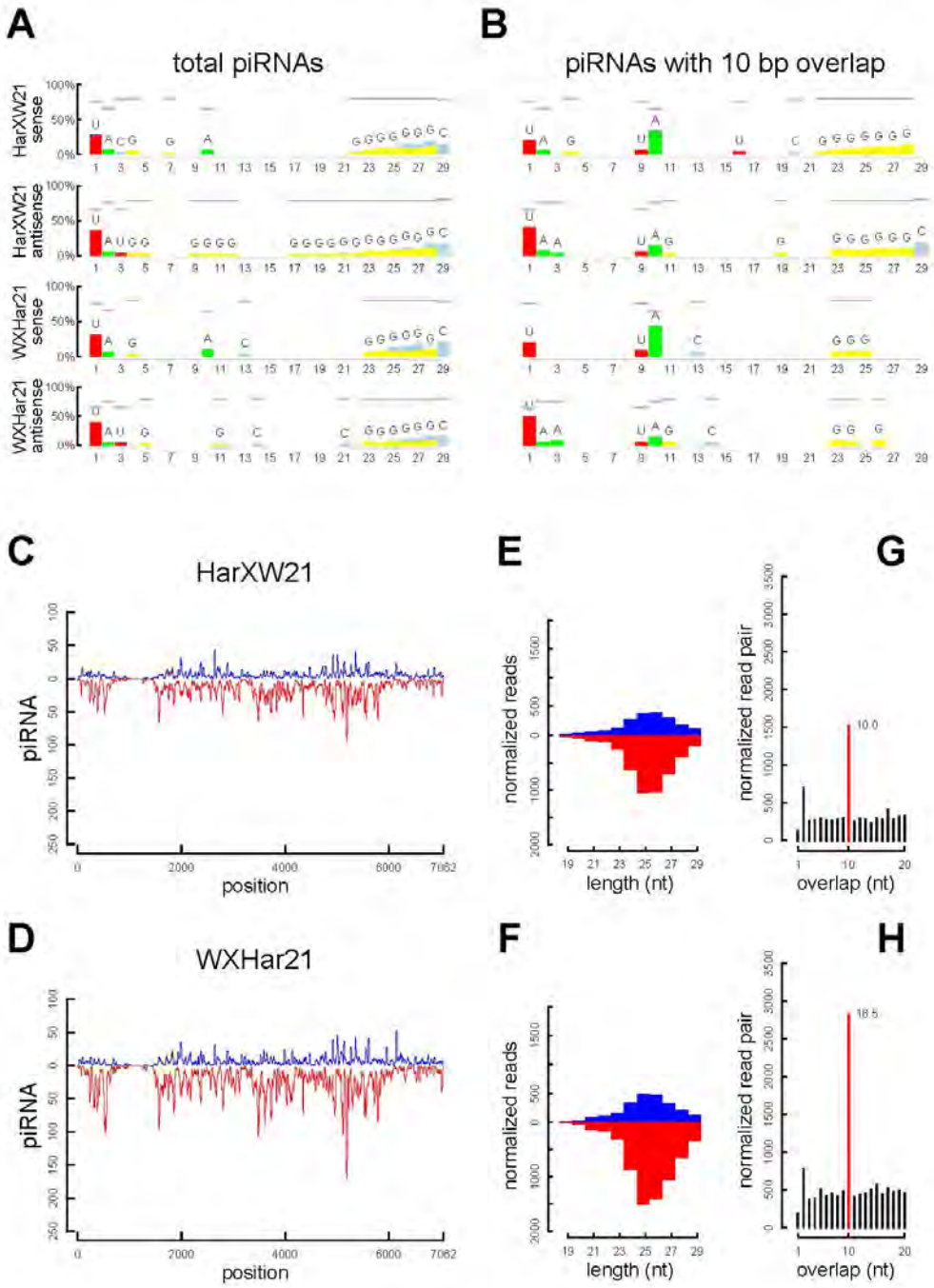
A
total piRNAs
B
piRNAs with 10 bp overlap
HarXW21 sense
HarXW21 antisense
WXHar21 sense
WXHar21 antisense
C
HarXW21
piRNA
position
D
WXHar21
E
normalized reads
length (nt)
F
G
normalized read pair
overlap (nt)
10.0
H
18.5

HMS Beagle2

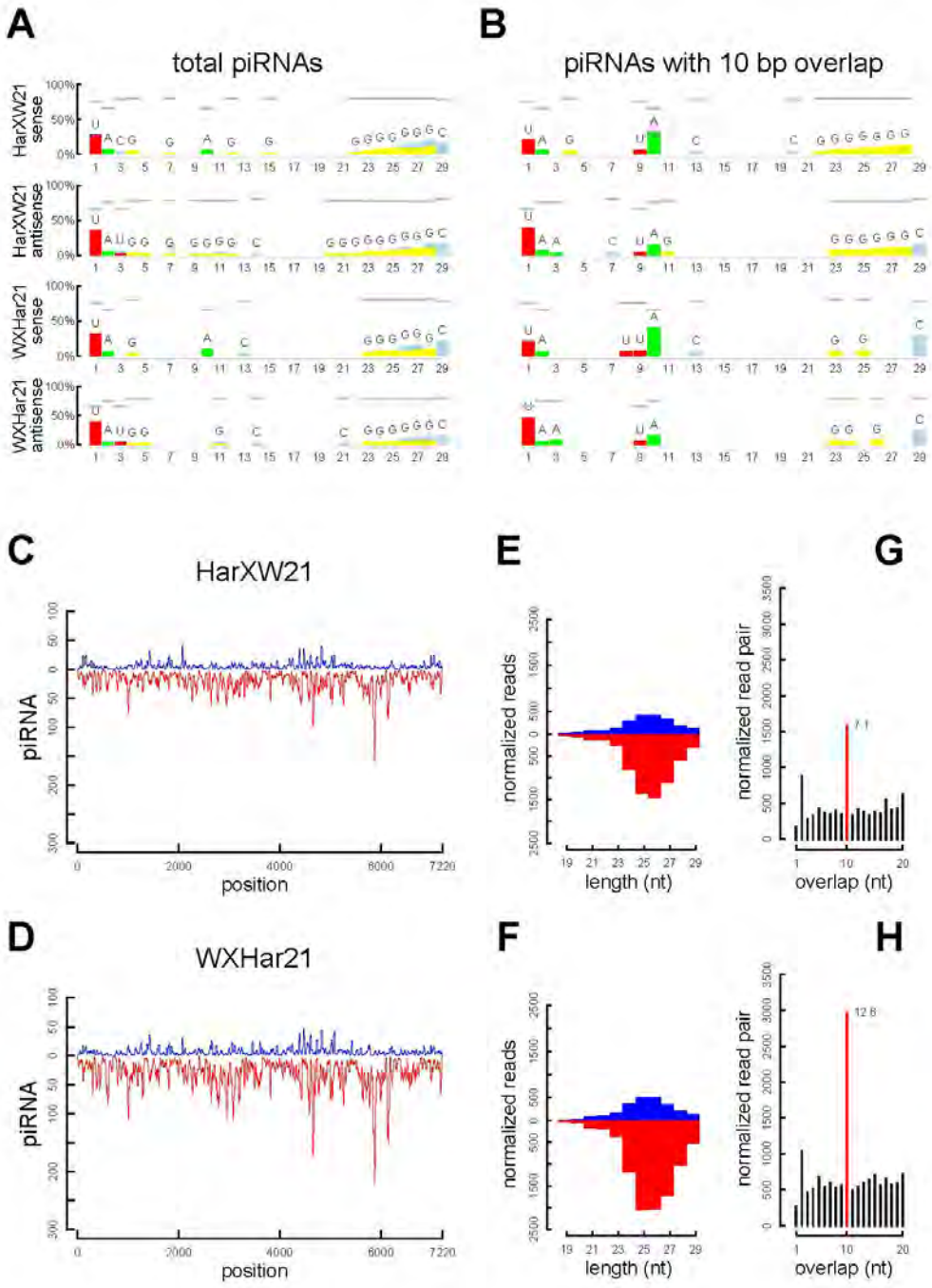
A
total piRNAs
B
piRNAs with 10 bp overlap
HarXW21 sense
HarXW21 antisense
WXHar21 sense
WXHar21 antisense
C
HarXW21
piRNA
position
D
WXHar21
E
F
normalized reads
length (nt)
G
H
normalized read pair
overlap (nt)
7.1
12.8

hobo

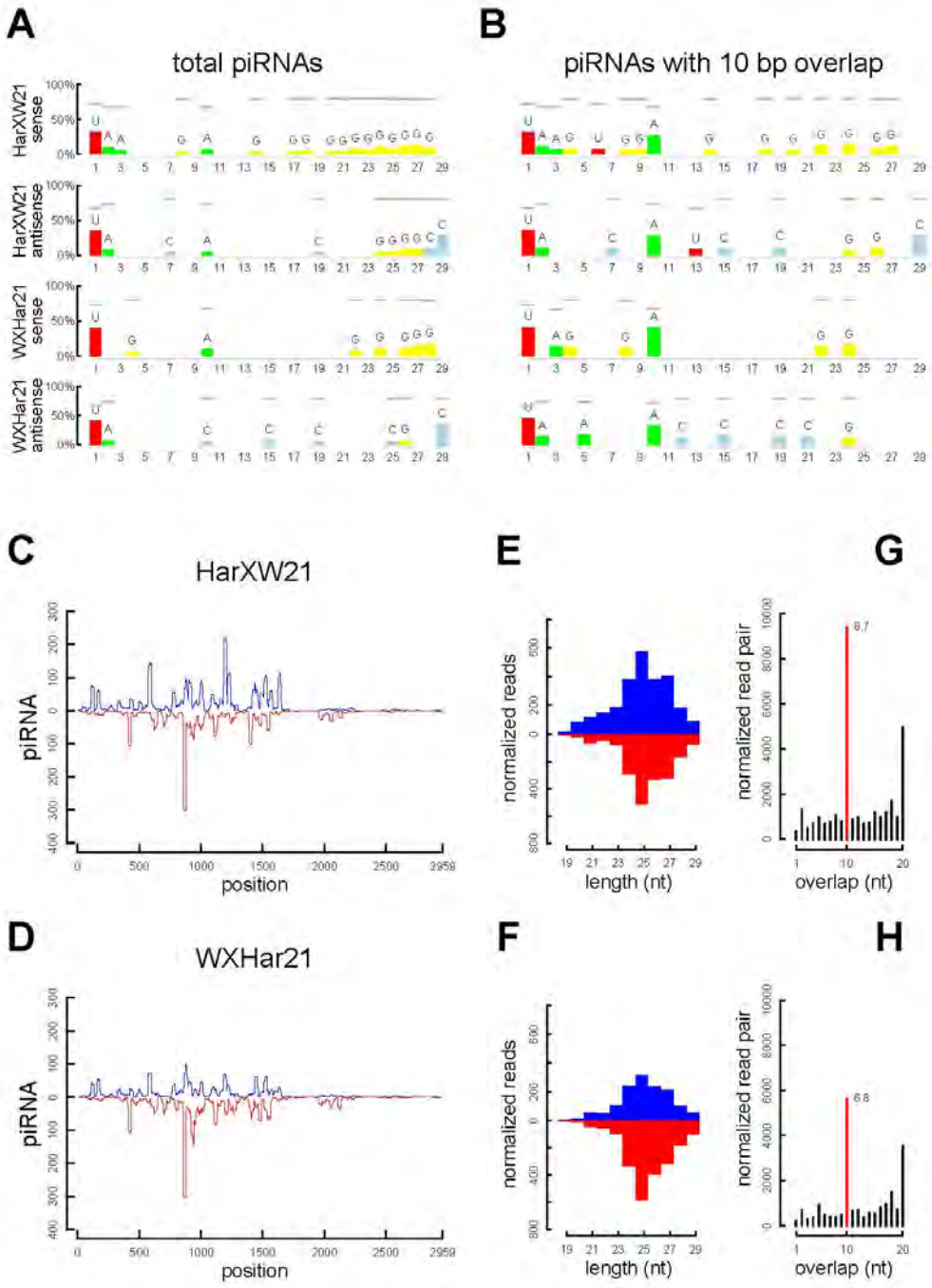
A
total piRNAs
B
piRNAs with 10 bp overlap
HarXW21 sense
HarXW21 antisense
WXHar21 sense
WXHar21 antisense
C
HarXW21
piRNA
position
D
WXHar21
piRNA
position
E
normalized reads
length (nt)
F
normalized reads
length (nt)
G
normalized read pair
overlap (nt)
8.7
H
normalized read pair
overlap (nt)
6.8

hopper

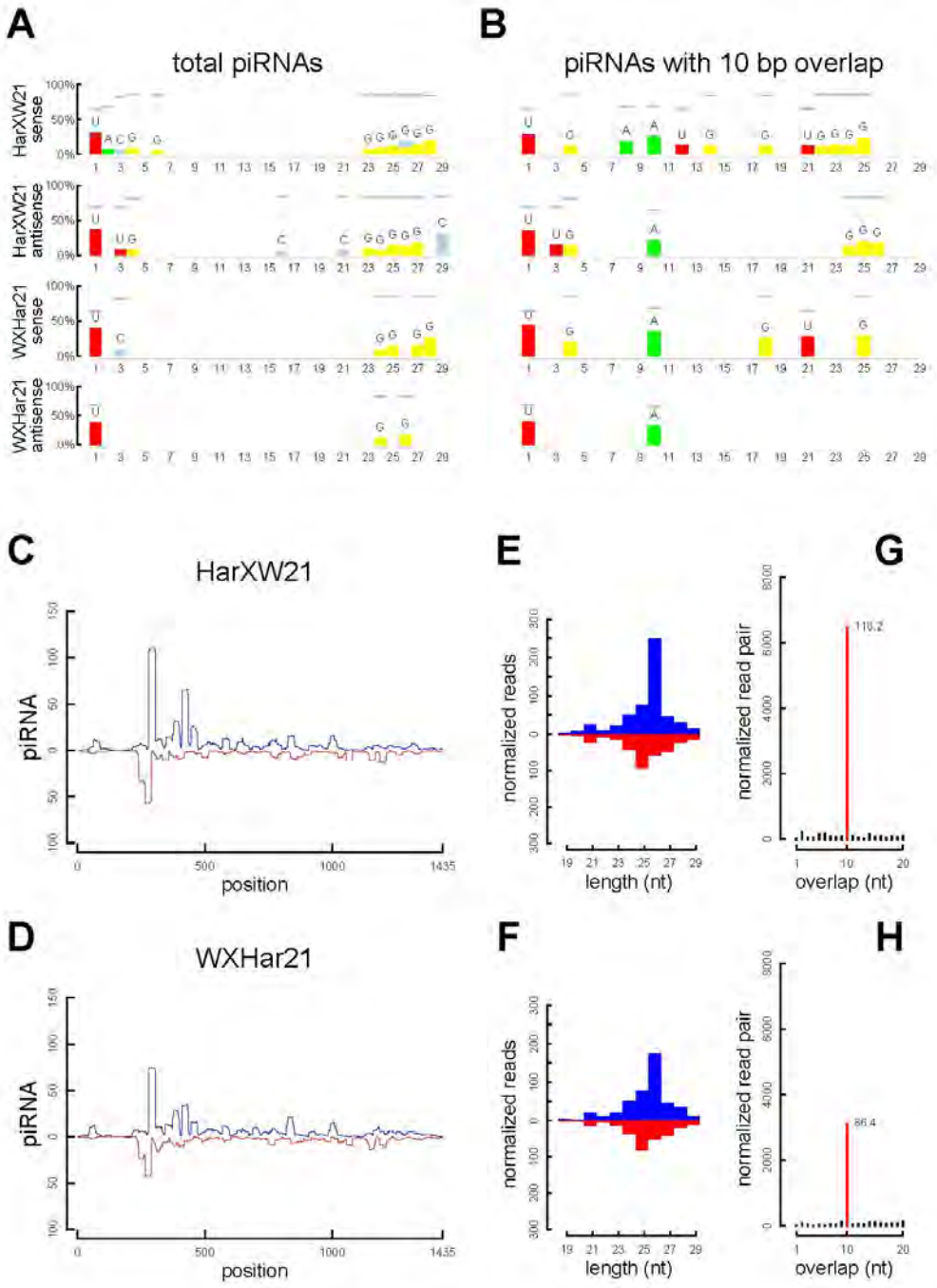
A
total piRNAs
B
piRNAs with 10 bp overlap
HarXW21 sense
HarXW21 antisense
WXHar21 sense
WXHar21 antisense
C
HarXW21
piRNA
position
D
WXHar21
E
F
normalized reads
length (nt)
G
H
normalized read pair
overlap (nt)
110.2
86.4

hopper2

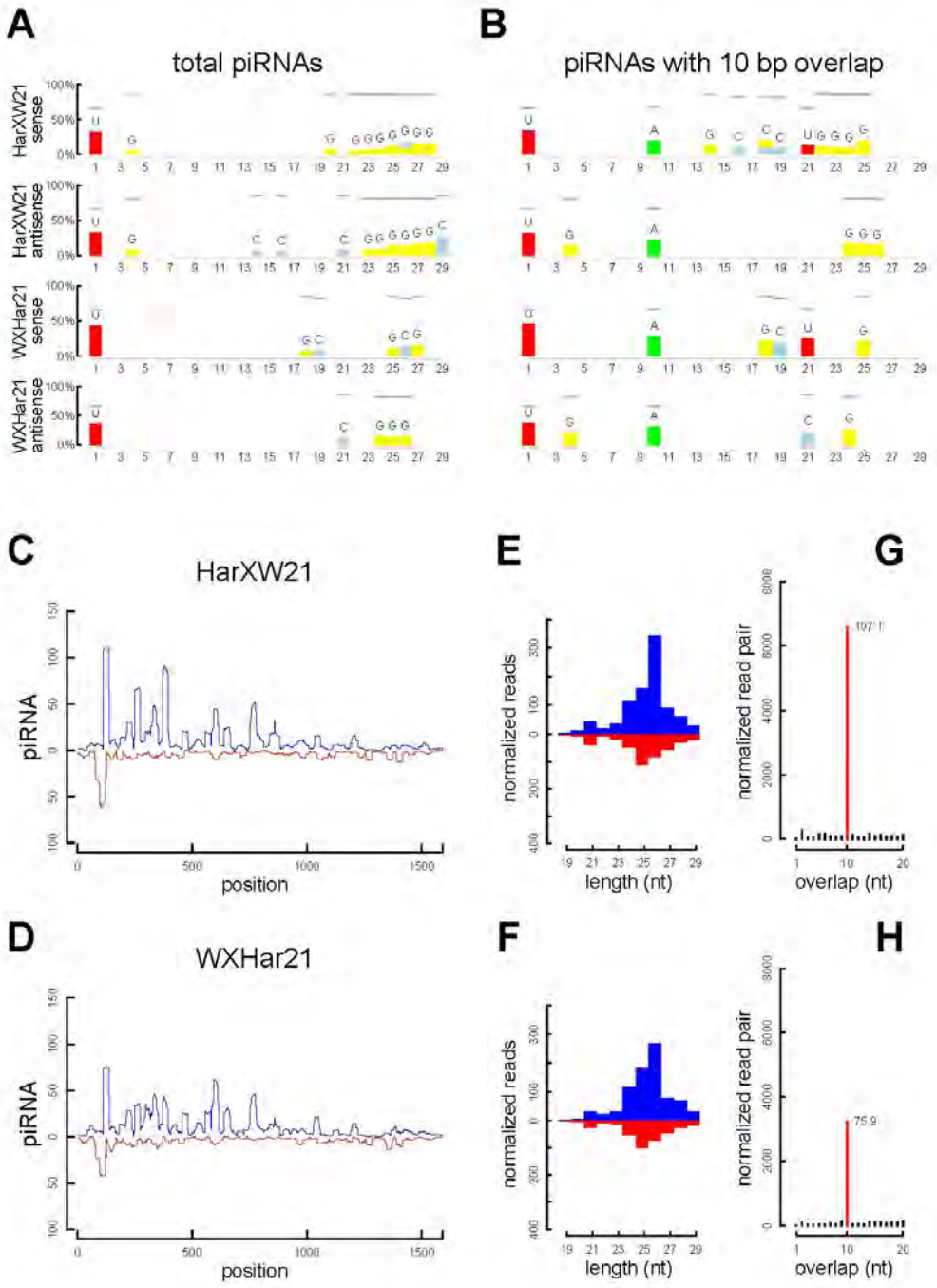
A
total piRNAs
B
piRNAs with 10 bp overlap
HarXW21 sense
HarXW21 antisense
WXHar21 sense
WXHar21 antisense
C
HarXW21
D
WXHar21
piRNA
position
E
F
normalized reads
length (nt)
G
H
normalized read pair
overlap (nt)
107.1
75.9

Idefix

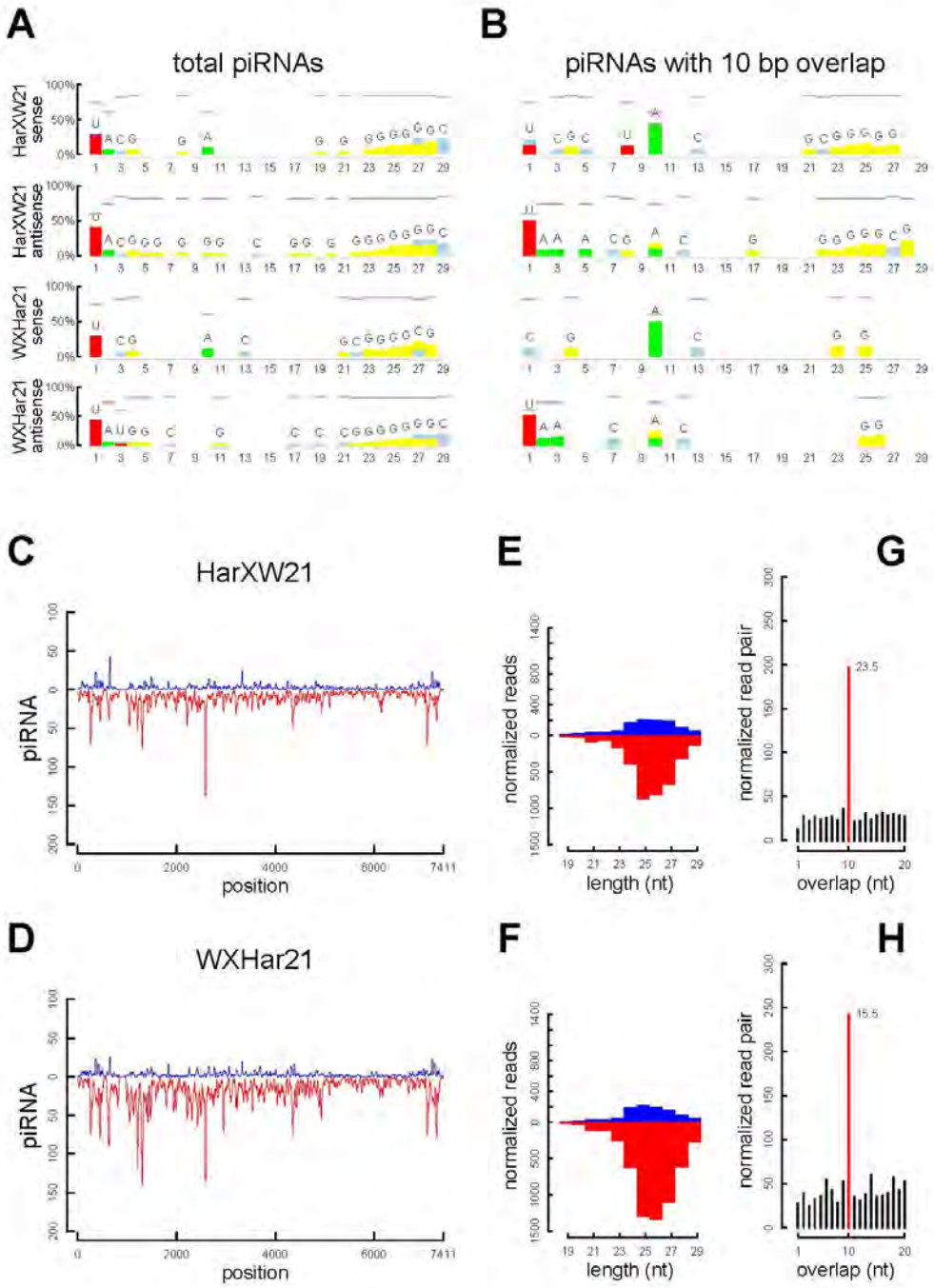
A
total piRNAs
B
piRNAs with 10 bp overlap
HarXW21 sense
HarXW21 antisense
WXHar21 sense
WXHar21 antisense
C
HarXW21
D
WXHar21
piRNA
position
E
F
normalized reads
length (nt)
G
H
normalized read pair
overlap (nt)
23.5
15.5

I element

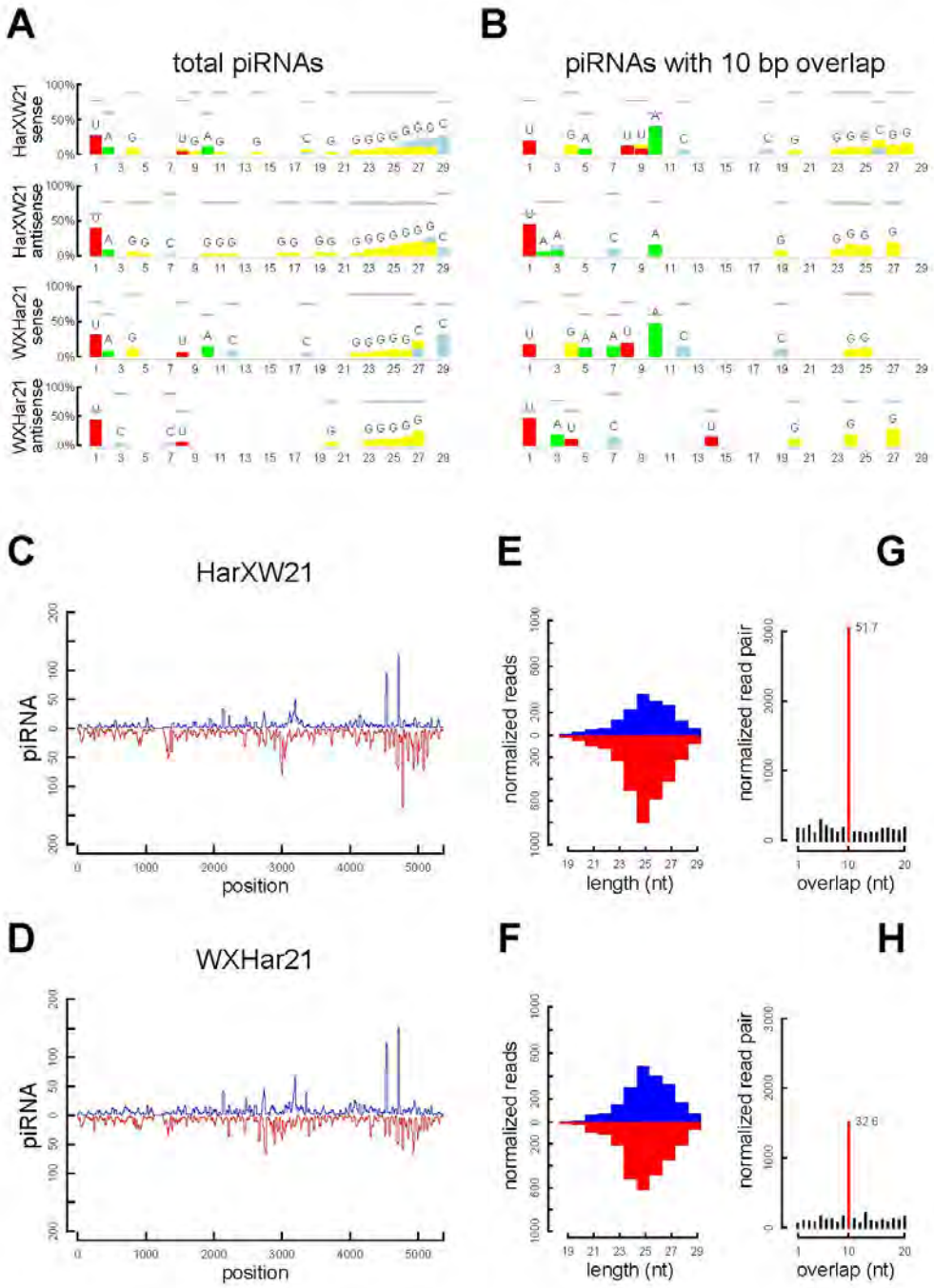
A
total piRNAs
B
piRNAs with 10 bp overlap
HarXW21 sense
HarXW21 antisense
WXHar21 sense
WXHar21 antisense
C
HarXW21
D
WXHar21
piRNA
position
E
F
normalized reads
length (nt)
G
H
normalized read pair
overlap (nt)
51.7
32.6

INE 1

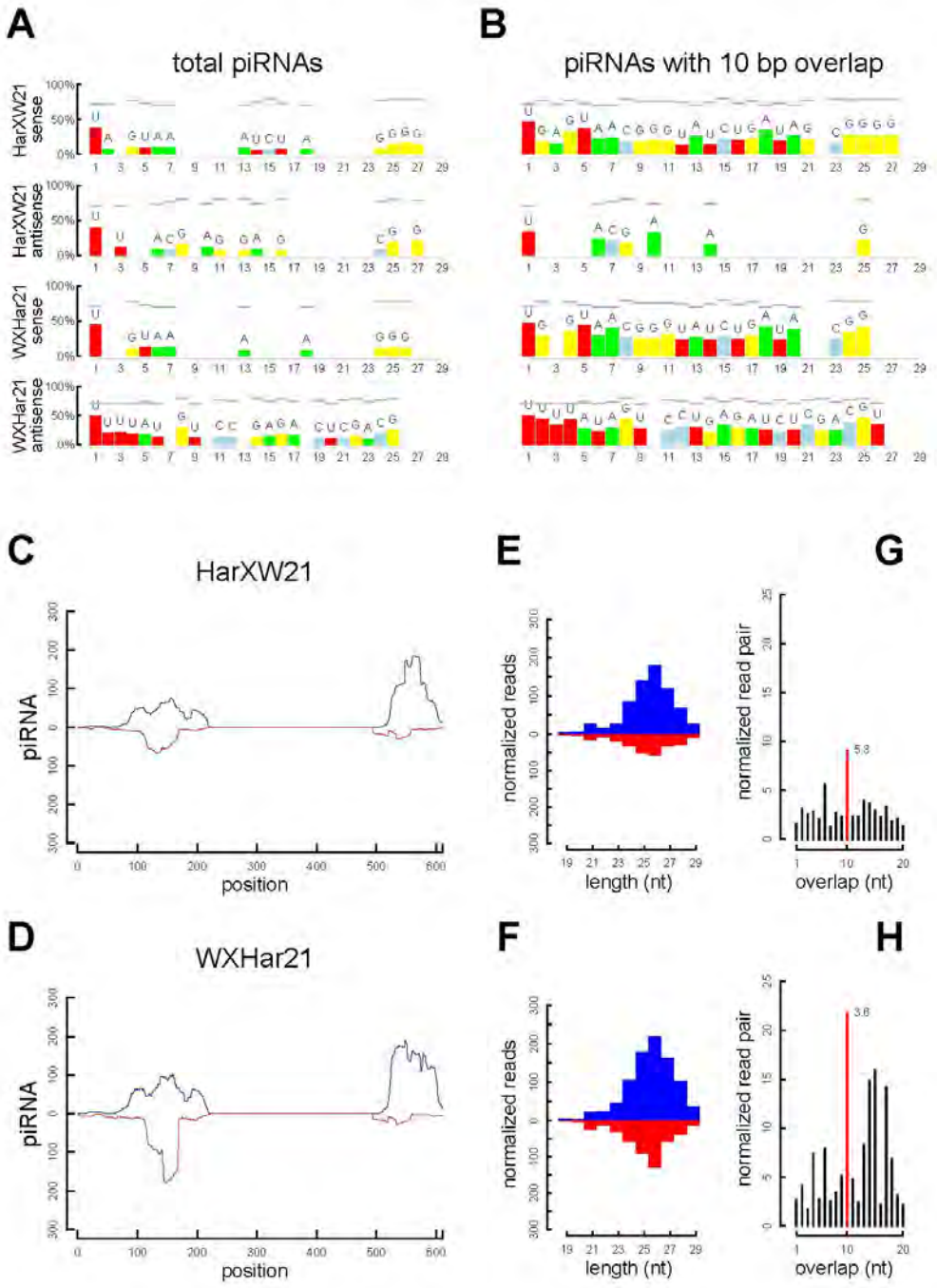
A
total piRNAs
B
piRNAs with 10 bp overlap
HarXW21 sense
HarXW21 antisense
WXHar21 sense
WXHar21 antisense
C
HarXW21
D
WXHar21
piRNA
position
E
F
normalized reads
length (nt)
G
H
normalized read pair
overlap (nt)
5.8
3.8

invader1

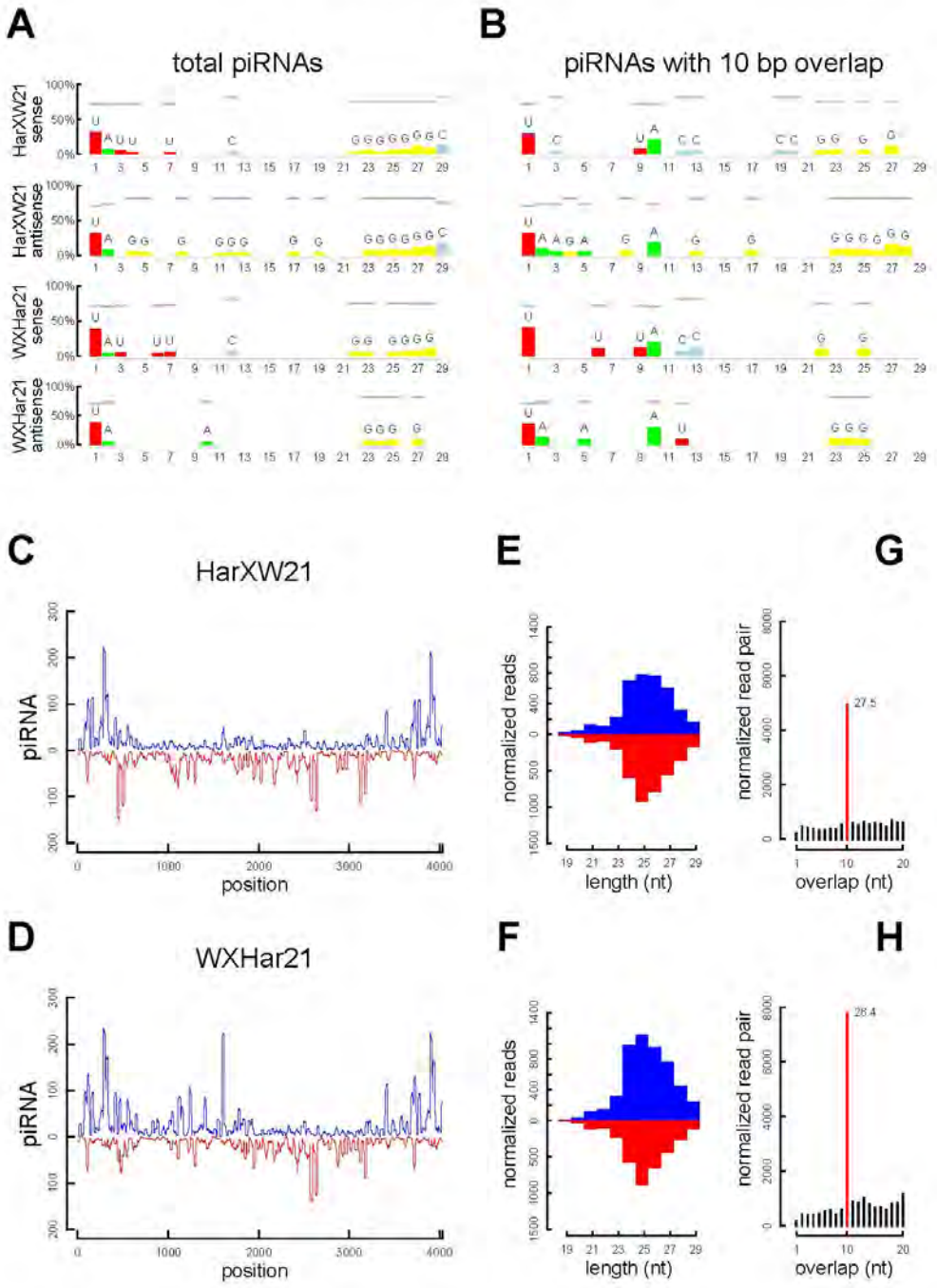
A
total piRNAs
B
piRNAs with 10 bp overlap
HarXW21 sense
HarXW21 antisense
WXHar21 sense
WXHar21 antisense
C
HarXW21
piRNA
position
D
WXHar21
piRNA
position
E
normalized reads
length (nt)
F
normalized reads
length (nt)
G
normalized read pair
27.5
overlap (nt)
H
normalized read pair
28.4
overlap (nt)

invader2

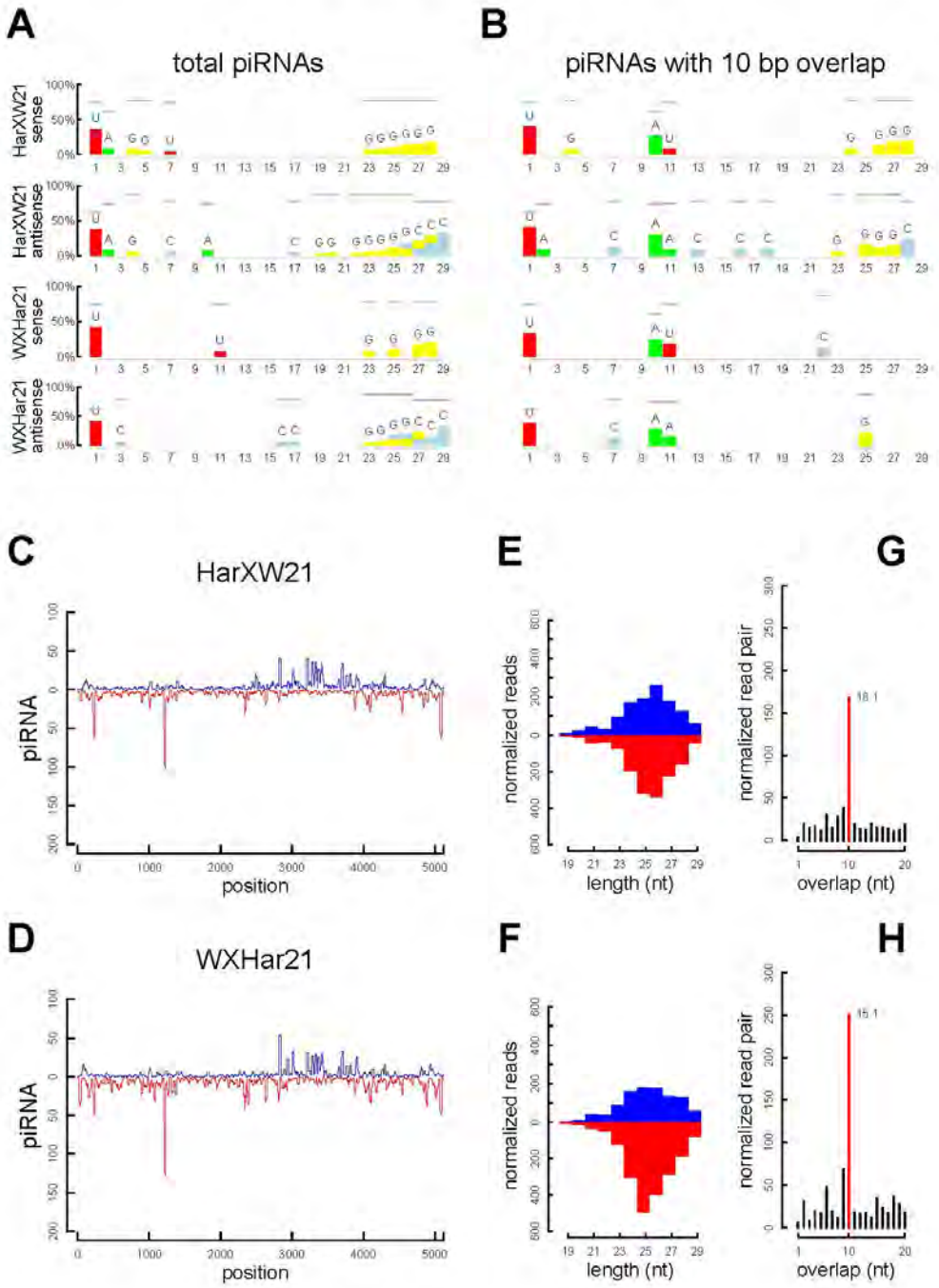
A
total piRNAs
B
piRNAs with 10 bp overlap
HarXW21 sense
HarXW21 antisense
WXHar21 sense
WXHar21 antisense
C
HarXW21
piRNA
position
D
WXHar21
piRNA
position
E
normalized reads
length (nt)
F
normalized reads
length (nt)
G
normalized read pair
overlap (nt)
18.1
H
normalized read pair
overlap (nt)
15.1

invader3

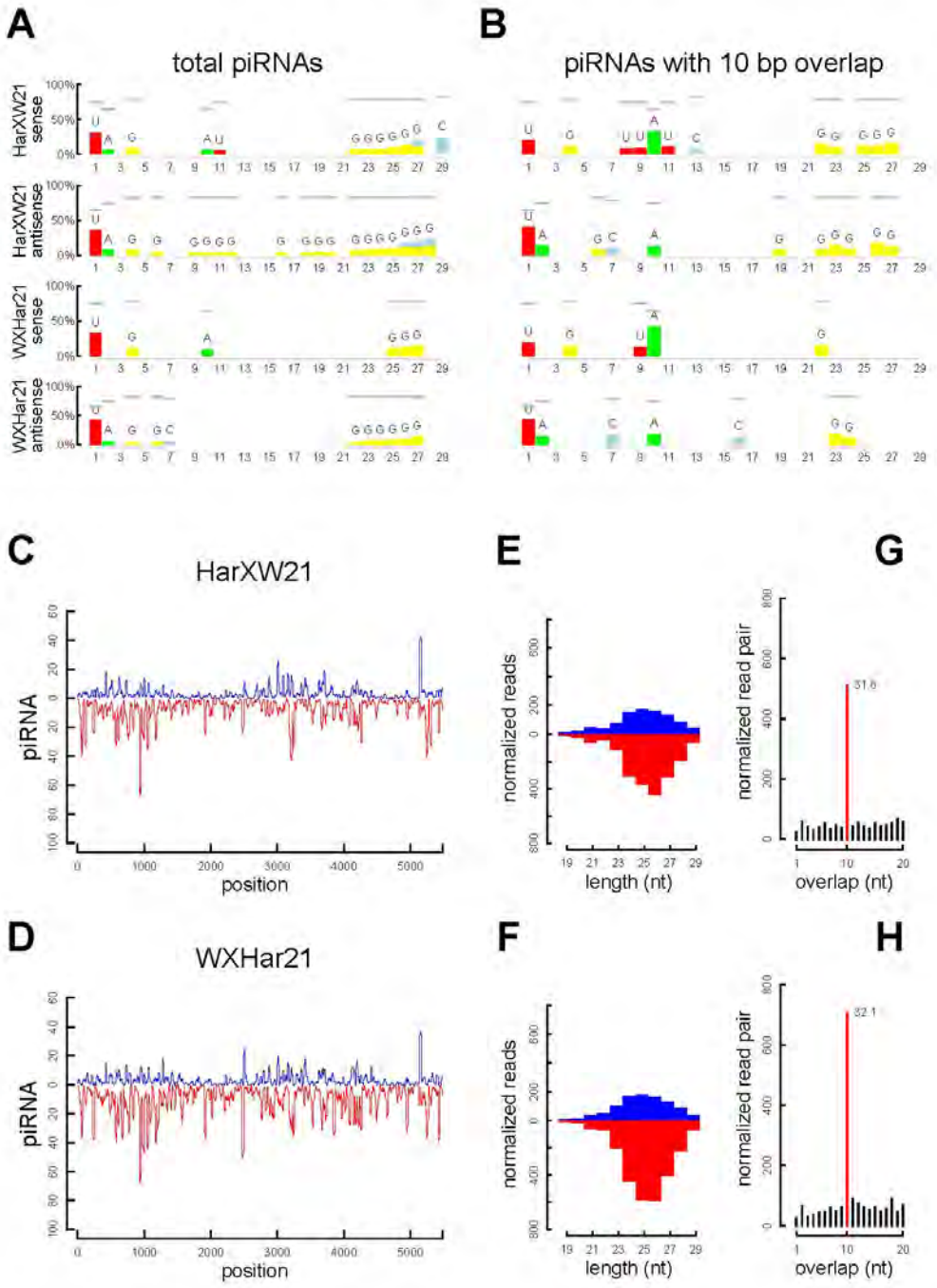
A
total piRNAs
B
piRNAs with 10 bp overlap
HarXW21 sense
HarXW21 antisense
WXHar21 sense
WXHar21 antisense
C
HarXW21
piRNA
position
D
WXHar21
piRNA
position
E
normalized reads
length (nt)
F
normalized reads
length (nt)
G
normalized read pair
31.6
overlap (nt)
H
normalized read pair
32.1
overlap (nt)

invader4

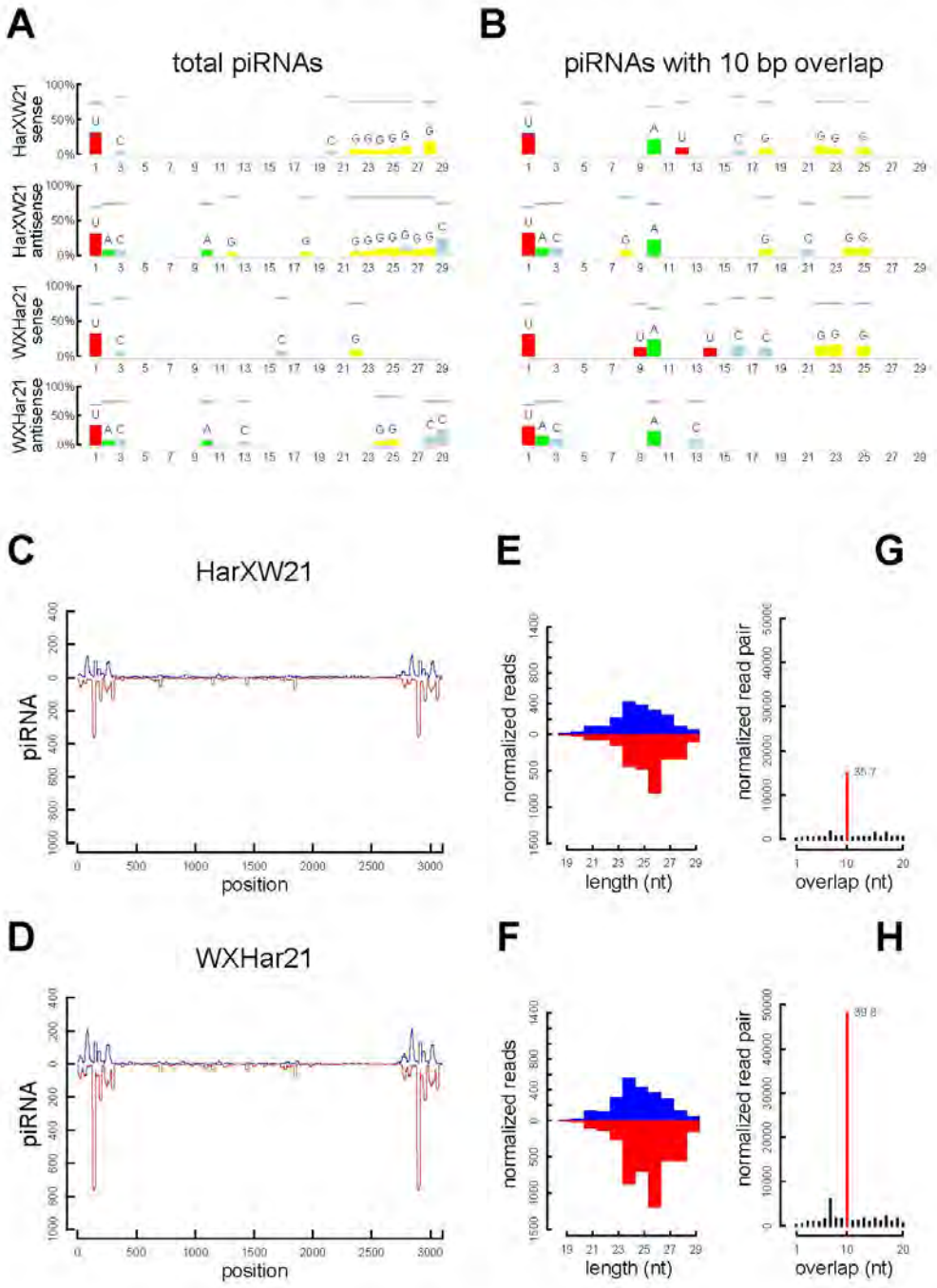
A
total piRNAs
B
piRNAs with 10 bp overlap
HarXW21 sense
HarXW21 antisense
WXHar21 sense
WXHar21 antisense
C
HarXW21
piRNA
position
D
WXHar21
E
normalized reads
length (nt)
F
G
normalized read pair
overlap (nt)
35.7
H
39.8

invader5

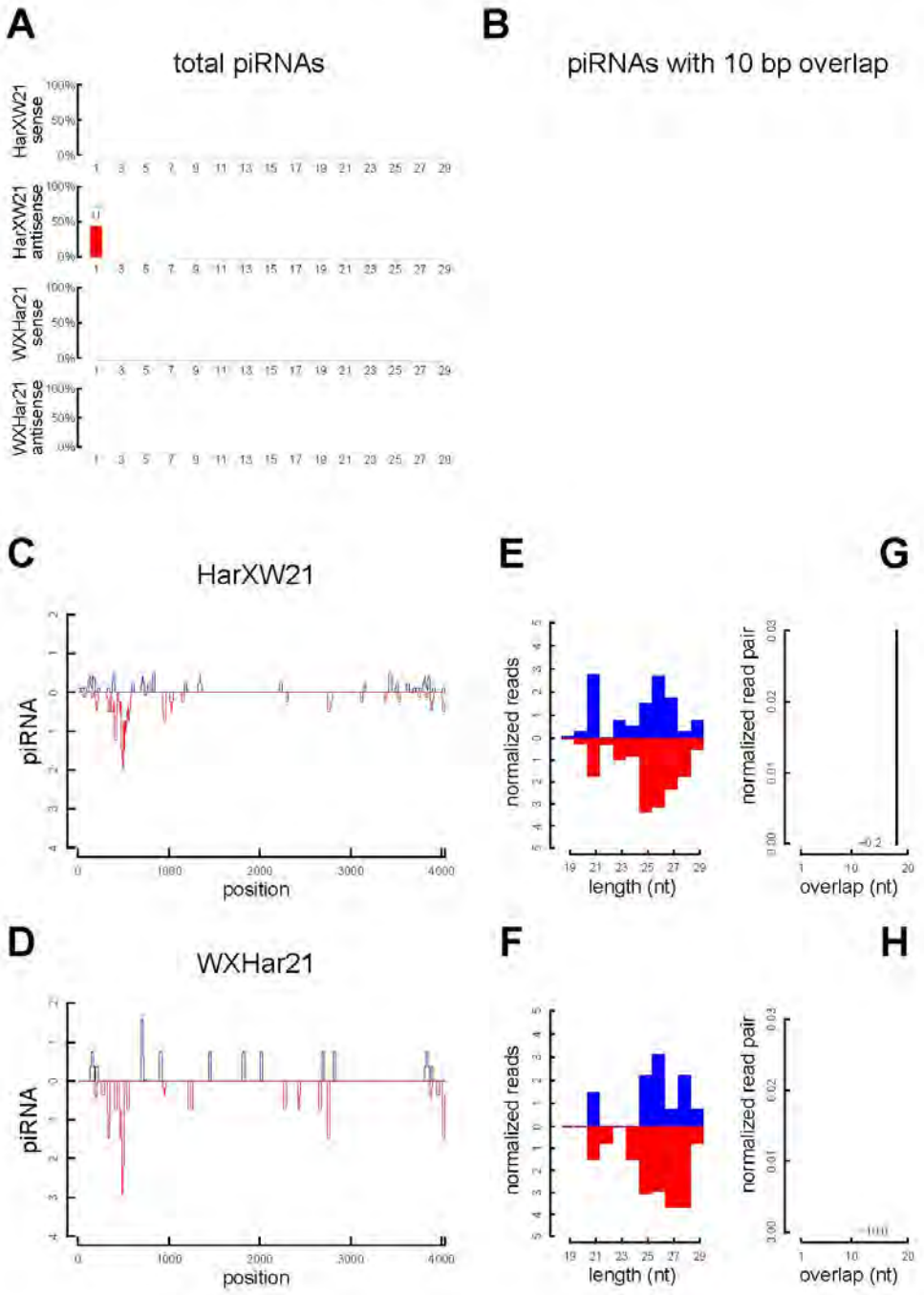
A
total piRNAs
HarXW21 sense
HarXW21 antisense
WXHar21 sense
WXHar21 antisense
B
piRNAs with 10 bp overlap
C
HarXW21
piRNA
position
D
WXHar21
piRNA
position
E
normalized reads
length (nt)
F
normalized reads
length (nt)
G
normalized read pair
overlap (nt)
H
normalized read pair
overlap (nt)

lvk

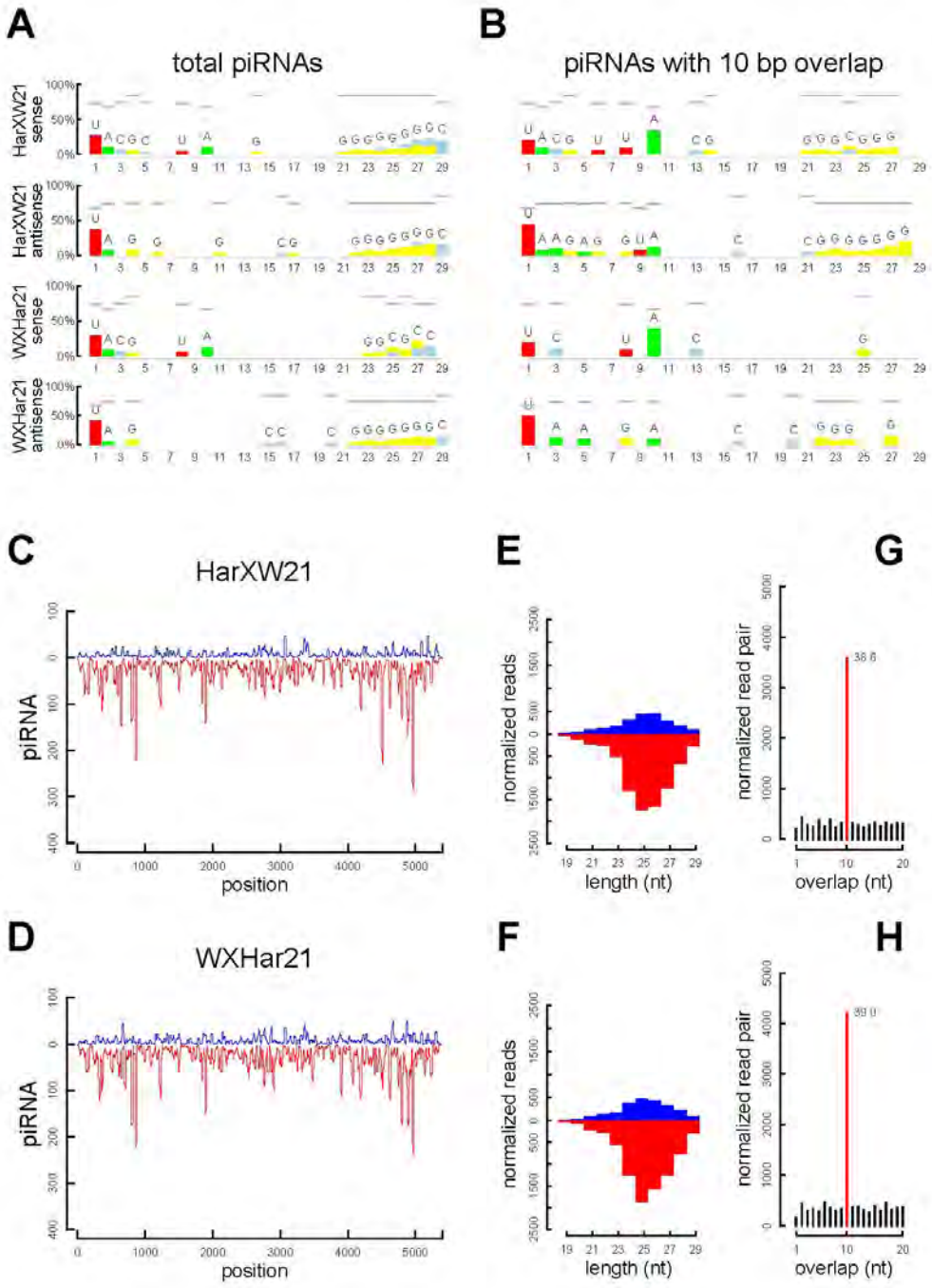
A
total piRNAs
B
piRNAs with 10 bp overlap
HarXW21 sense
HarXW21 antisense
WXHar21 sense
WXHar21 antisense
C
HarXW21
piRNA
position
D
WXHar21
piRNA
position
E
normalized reads
length (nt)
F
normalized reads
length (nt)
G
normalized read pair
overlap (nt)
H
normalized read pair
overlap (nt)

jockey

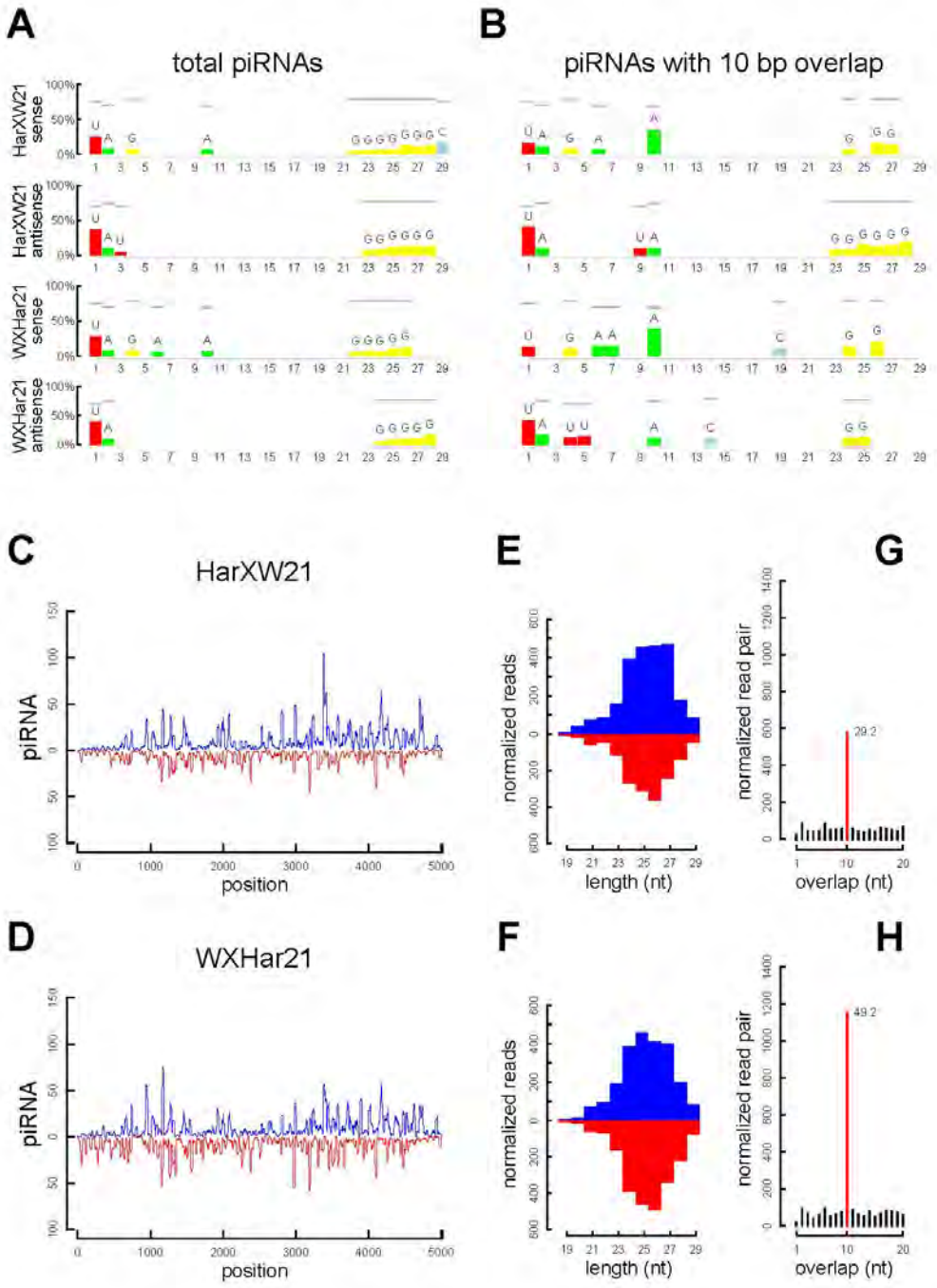
A
total piRNAs
B
piRNAs with 10 bp overlap
HarXW21 sense
HarXW21 antisense
WXHar21 sense
WXHar21 antisense
C
HarXW21
piRNA
position
D
WXHar21
piRNA
position
E
normalized reads
length (nt)
F
normalized reads
length (nt)
G
normalized read pair
29.2
overlap (nt)
H
normalized read pair
49.2
overlap (nt)

jockey2

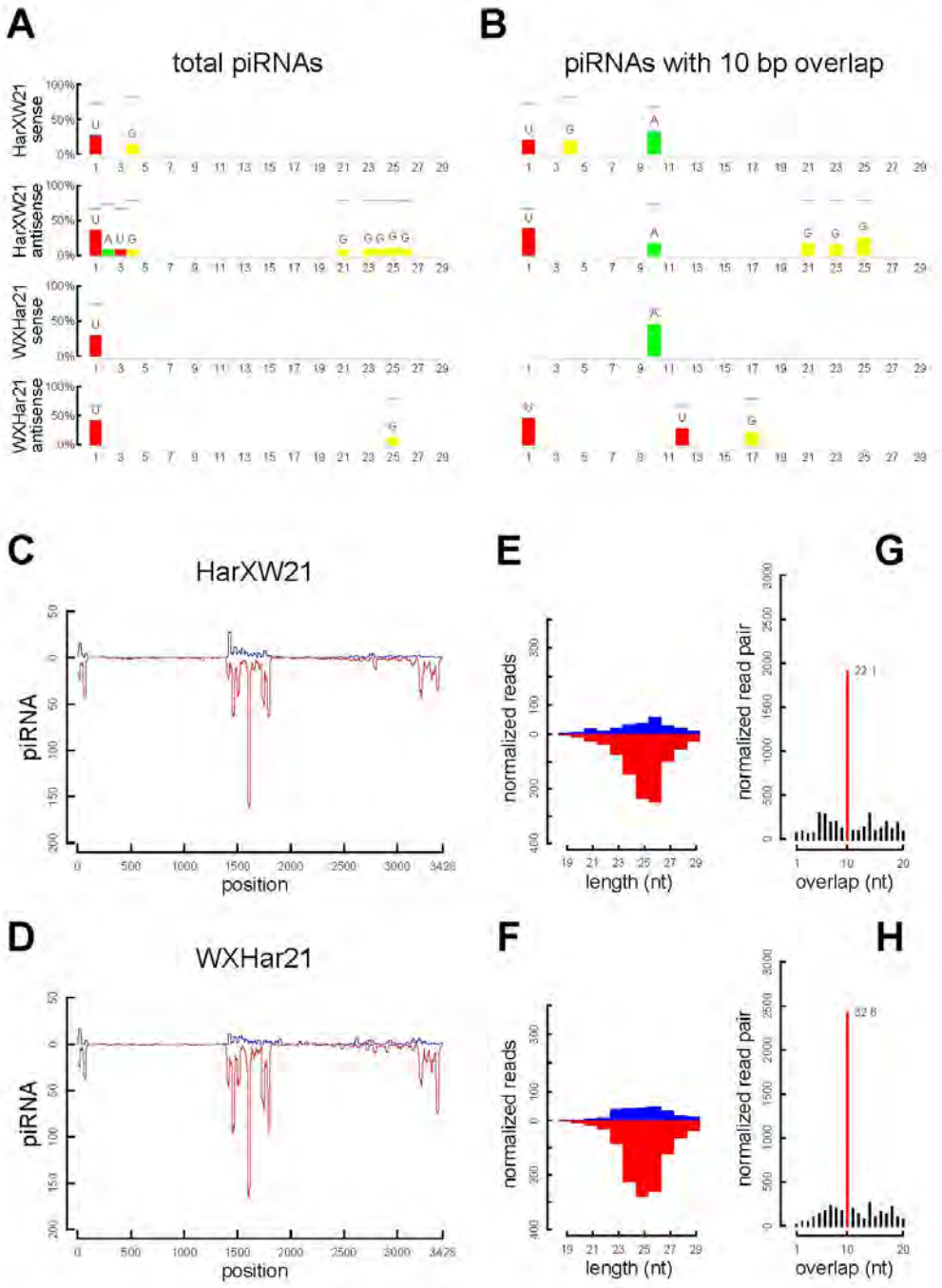
A
total piRNAs
B
piRNAs with 10 bp overlap
HarXW21 sense
HarXW21 antisense
WXHar21 sense
WXHar21 antisense
C
HarXW21
D
WXHar21
piRNA
position
E
F
normalized reads
length (nt)
G
H
normalized read pair
overlap (nt)

Juan

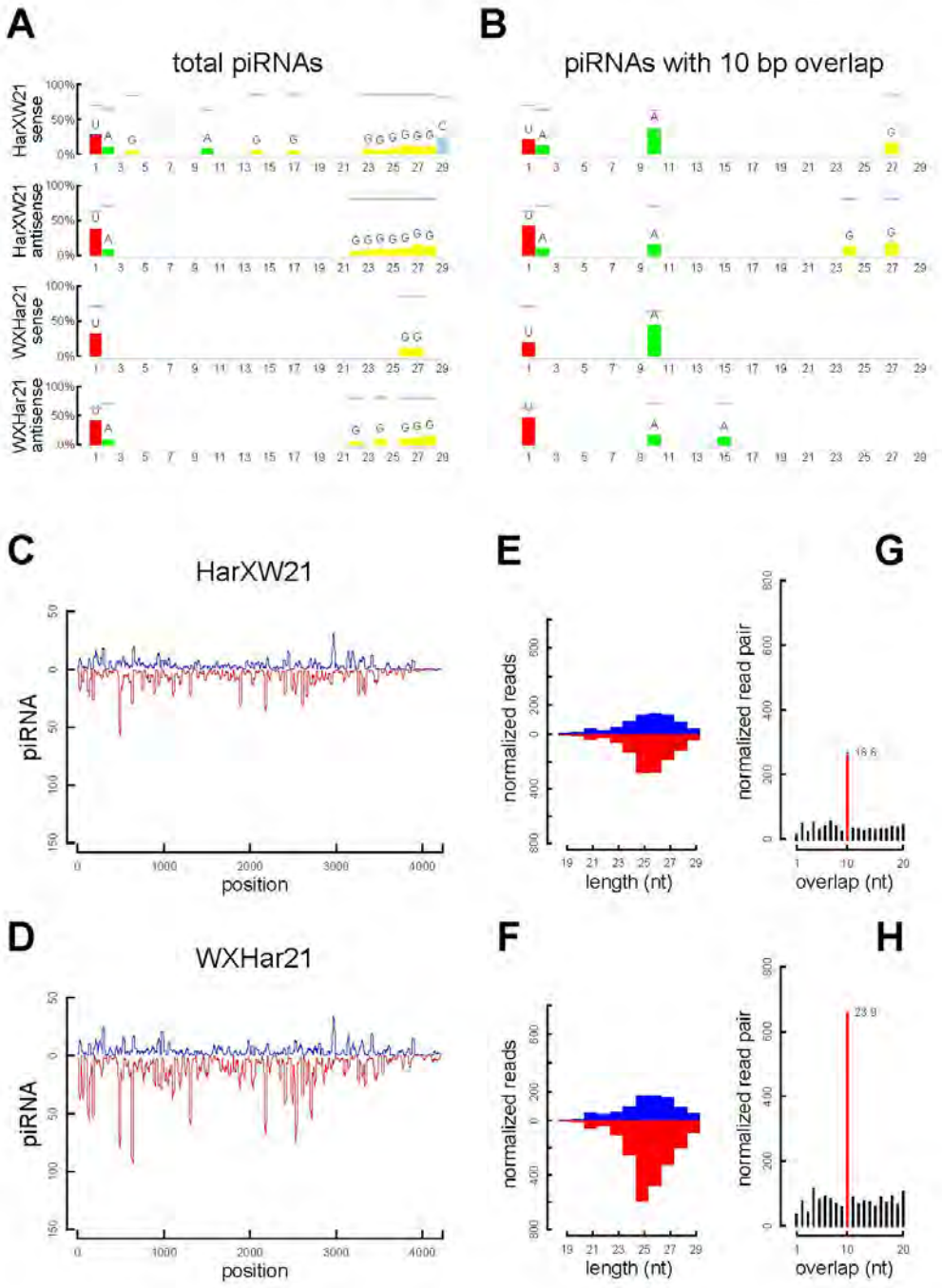
A
total piRNAs
B
piRNAs with 10 bp overlap
HarXW21 sense
HarXW21 antisense
WXHar21 sense
WXHar21 antisense
C
HarXW21
D
WXHar21
piRNA
position
E
F
normalized reads
length (nt)
G
H
normalized read pair
overlap (nt)

looper1

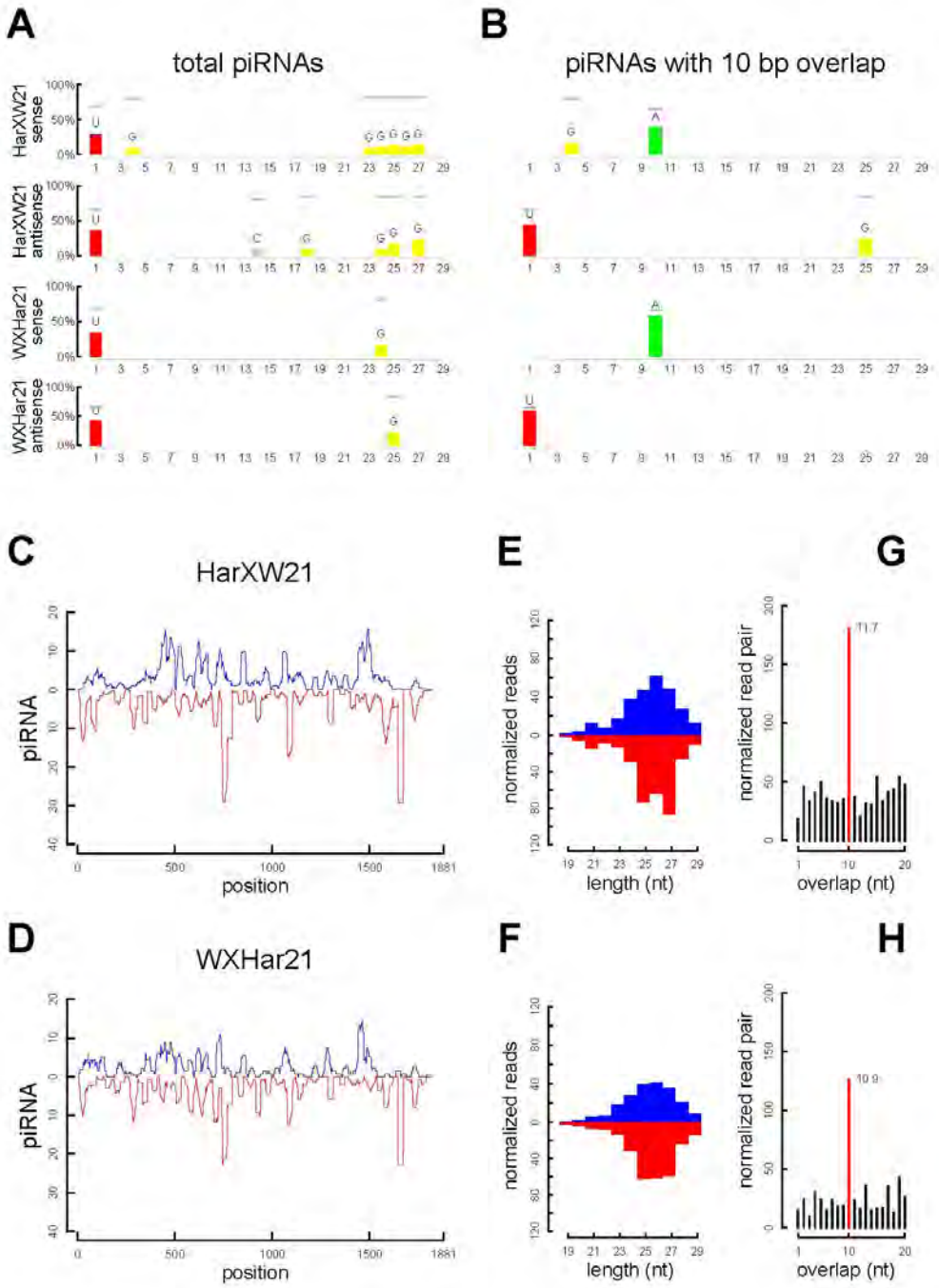
A
total piRNAs
B
piRNAs with 10 bp overlap
HarXW21 sense
HarXW21 antisense
WXHar21 sense
WXHar21 antisense
C
HarXW21
D
WXHar21
piRNA
position
E
F
normalized reads
length (nt)
G
H
normalized read pair
overlap (nt)
11.7
10.9

mariner2

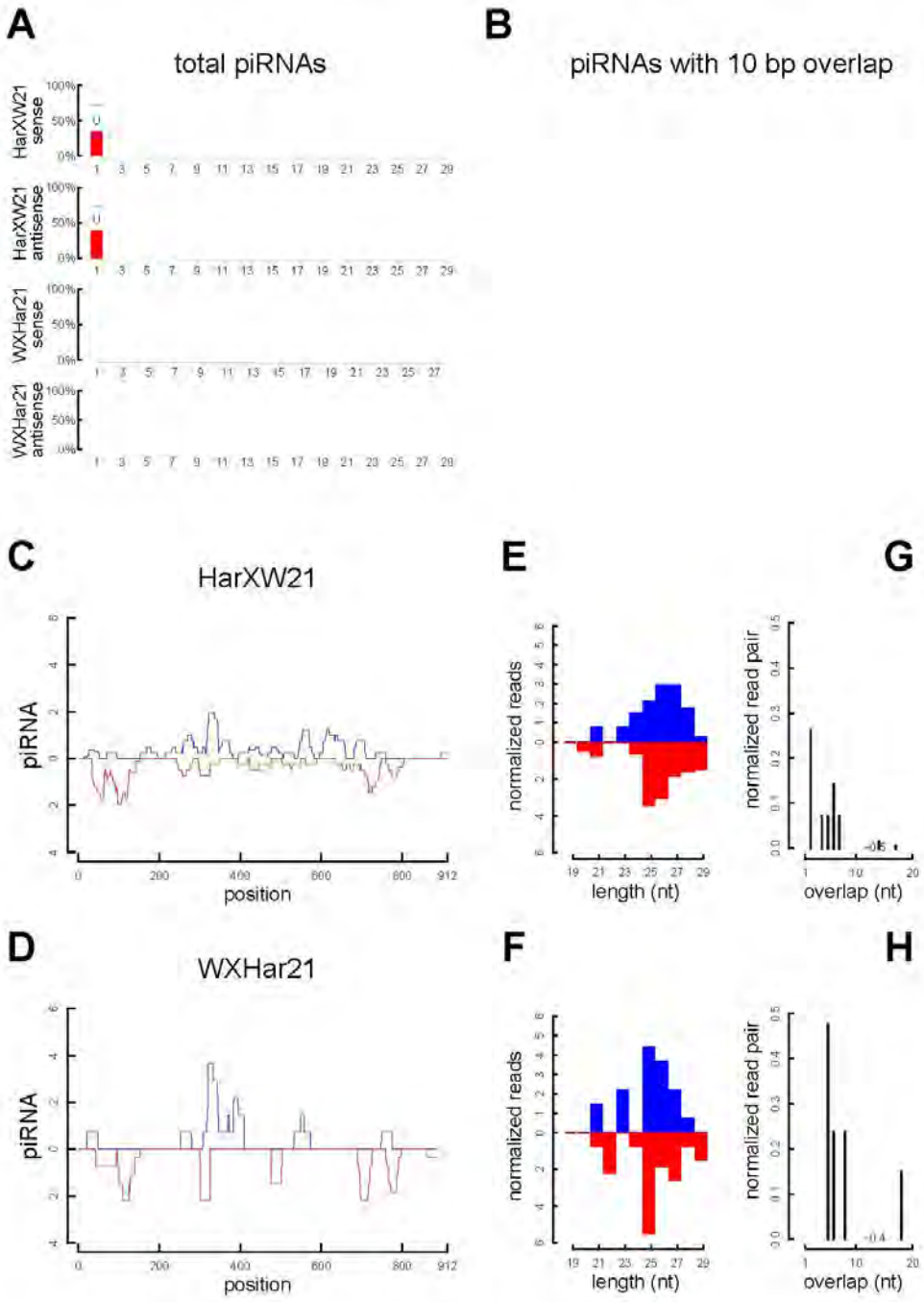
A
total piRNAs
B
piRNAs with 10 bp overlap
HarXW21 sense
HarXW21 antisense
WXHar21 sense
WXHar21 antisense
C
HarXW21
D
WXHar21
piRNA
position
E
F
normalized reads
length (nt)
G
H
normalized read pair
overlap (nt)

Max element

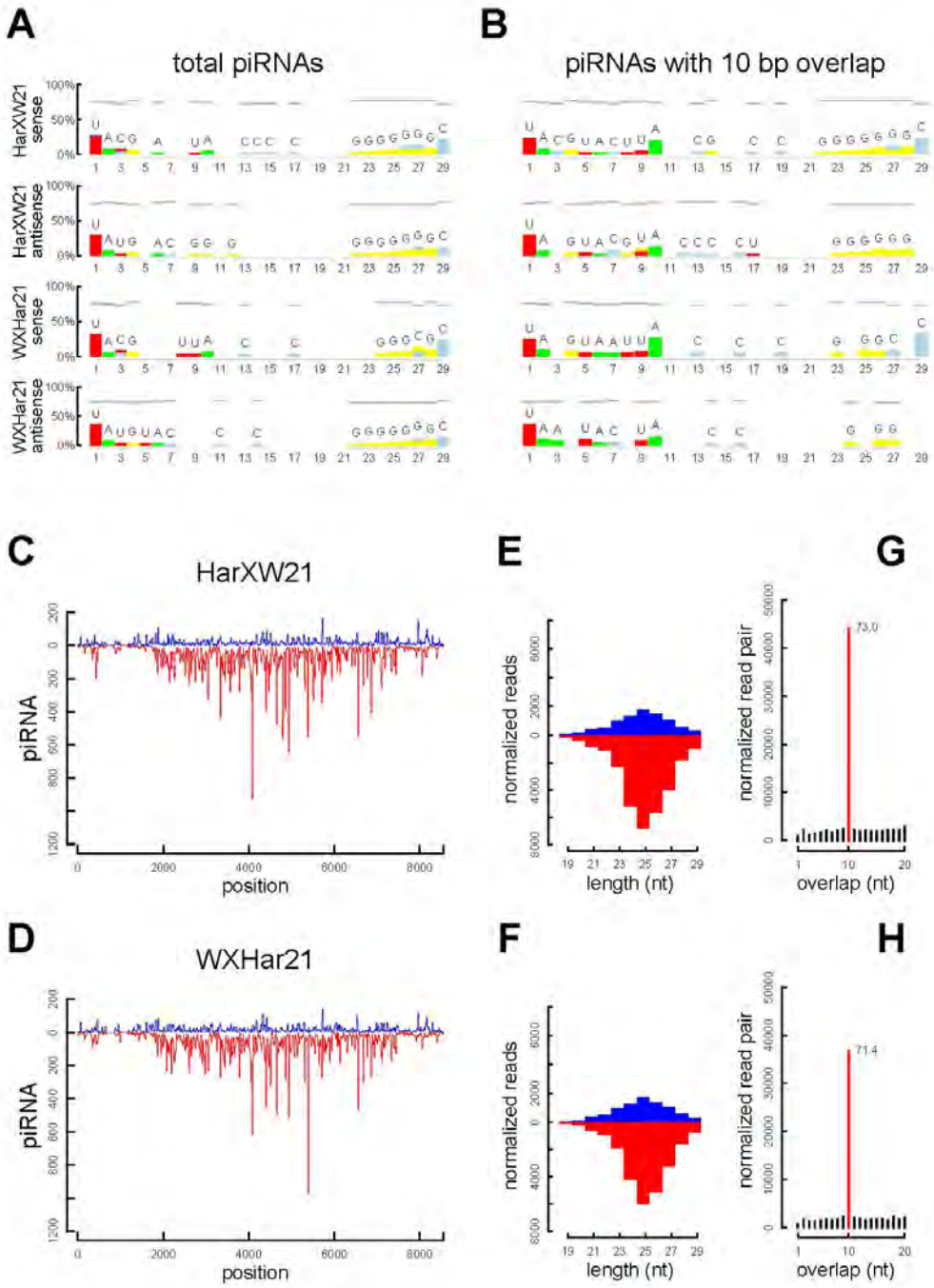
A
total piRNAs
B
piRNAs with 10 bp overlap
HarXW21 sense
HarXW21 antisense
WXHar21 sense
WXHar21 antisense
C
HarXW21
piRNA
position
D
WXHar21
piRNA
position
E
normalized reads
length (nt)
F
normalized reads
length (nt)
G
normalized read pair
73.0
overlap (nt)
H
normalized read pair
71.4
overlap (nt)

McClintock

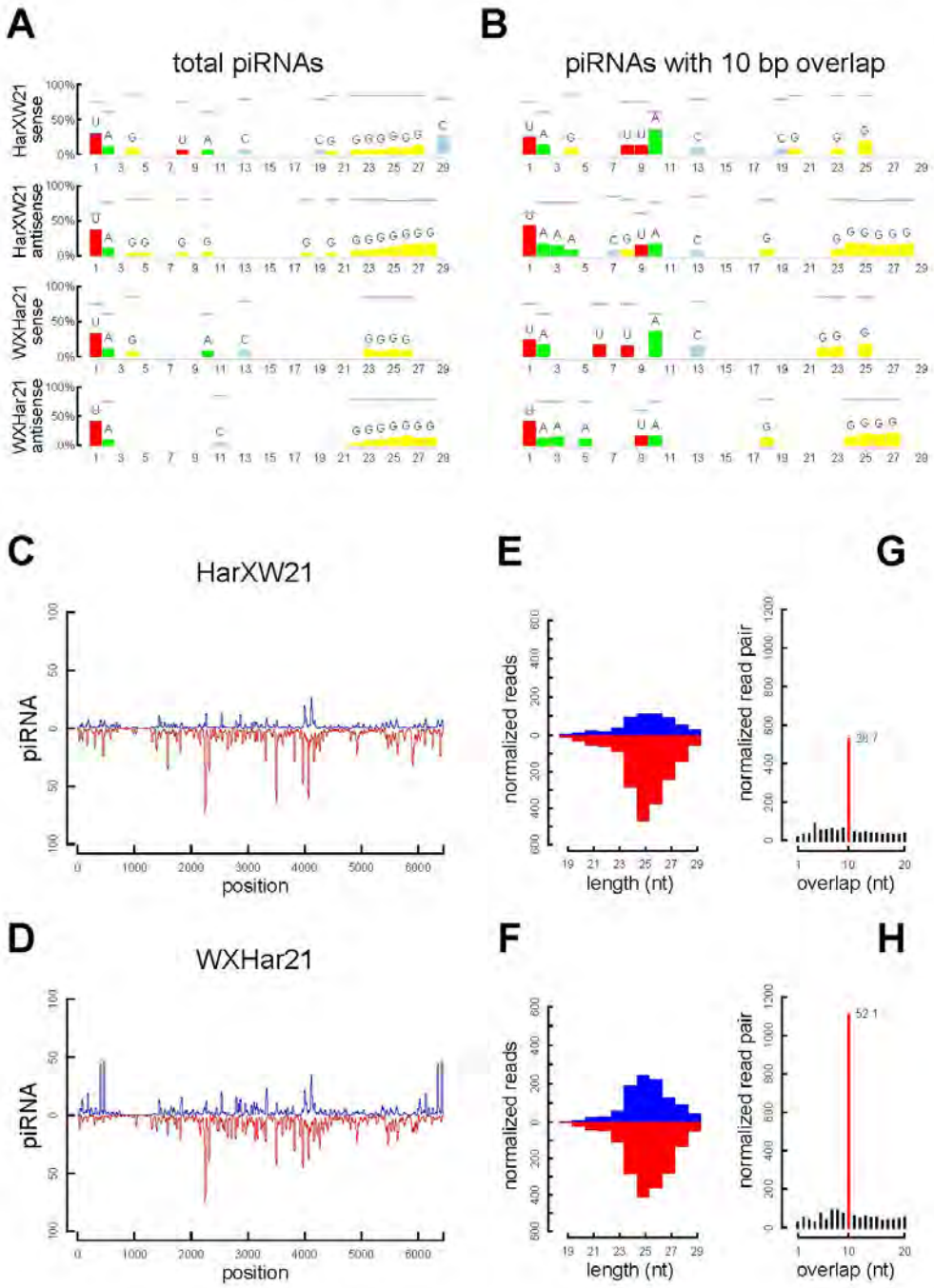
A
total piRNAs
B
piRNAs with 10 bp overlap
HarXW21 sense
HarXW21 antisense
WXHar21 sense
WXHar21 antisense
C
HarXW21
D
WXHar21
piRNA
position
E
F
normalized reads
length (nt)
G
H
normalized read pair
overlap (nt)

mdg1

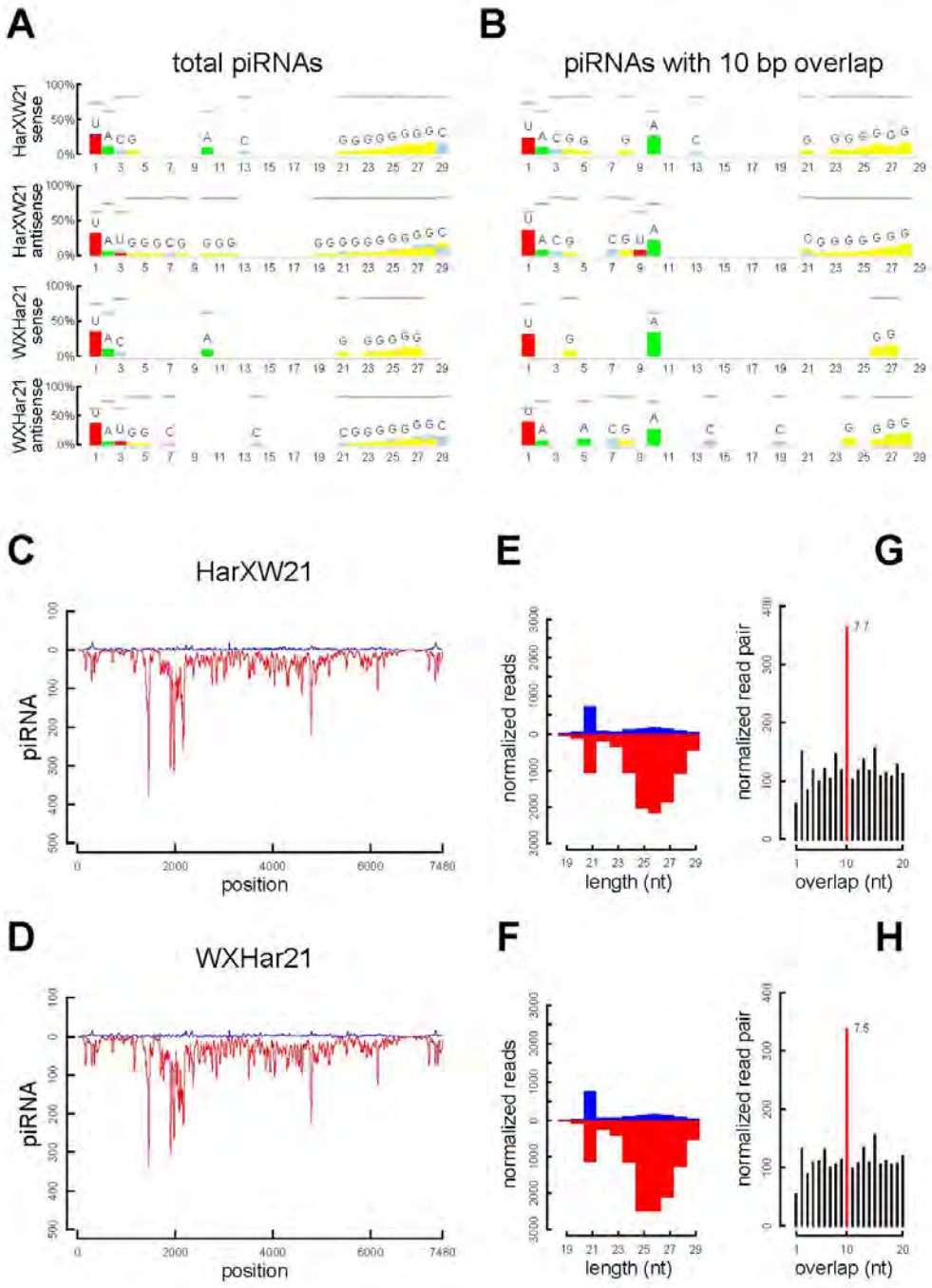
A
total piRNAs
B
piRNAs with 10 bp overlap
HarXW21 sense
HarXW21 antisense
WXHar21 sense
WXHar21 antisense
C
HarXW21
piRNA
position
D
WXHar21
piRNA
position
E
normalized reads
length (nt)
F
normalized reads
length (nt)
G
normalized read pair
overlap (nt)
7.7
H
normalized read pair
overlap (nt)
7.5

mdg3

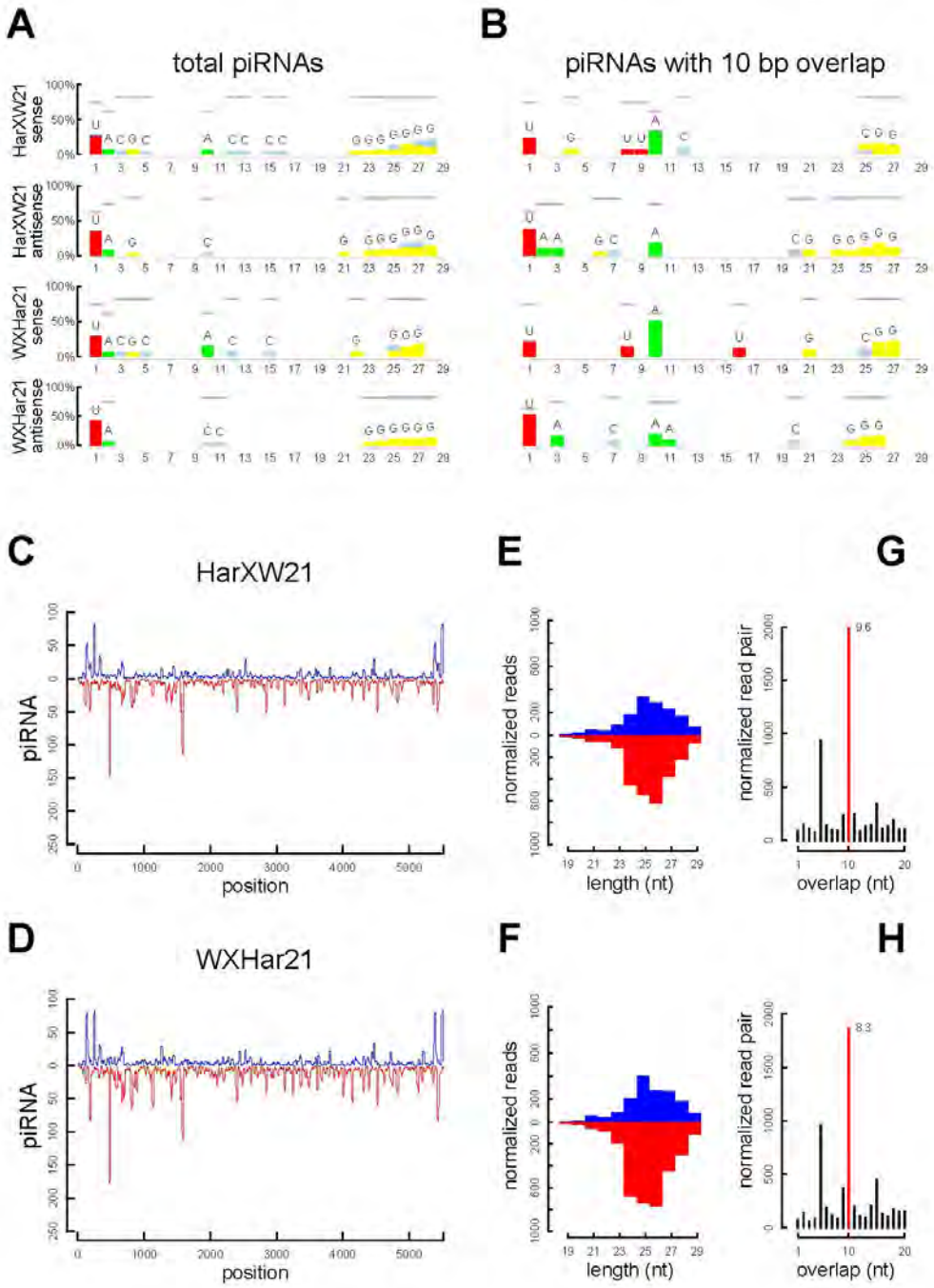
A
total piRNAs
B
piRNAs with 10 bp overlap
HarXW21 sense
HarXW21 antisense
WXHar21 sense
WXHar21 antisense
C
HarXW21
D
WXHar21
piRNA
position
E
F
normalized reads
length (nt)
G
H
normalized read pair
overlap (nt)
9.6
8.3

micropia

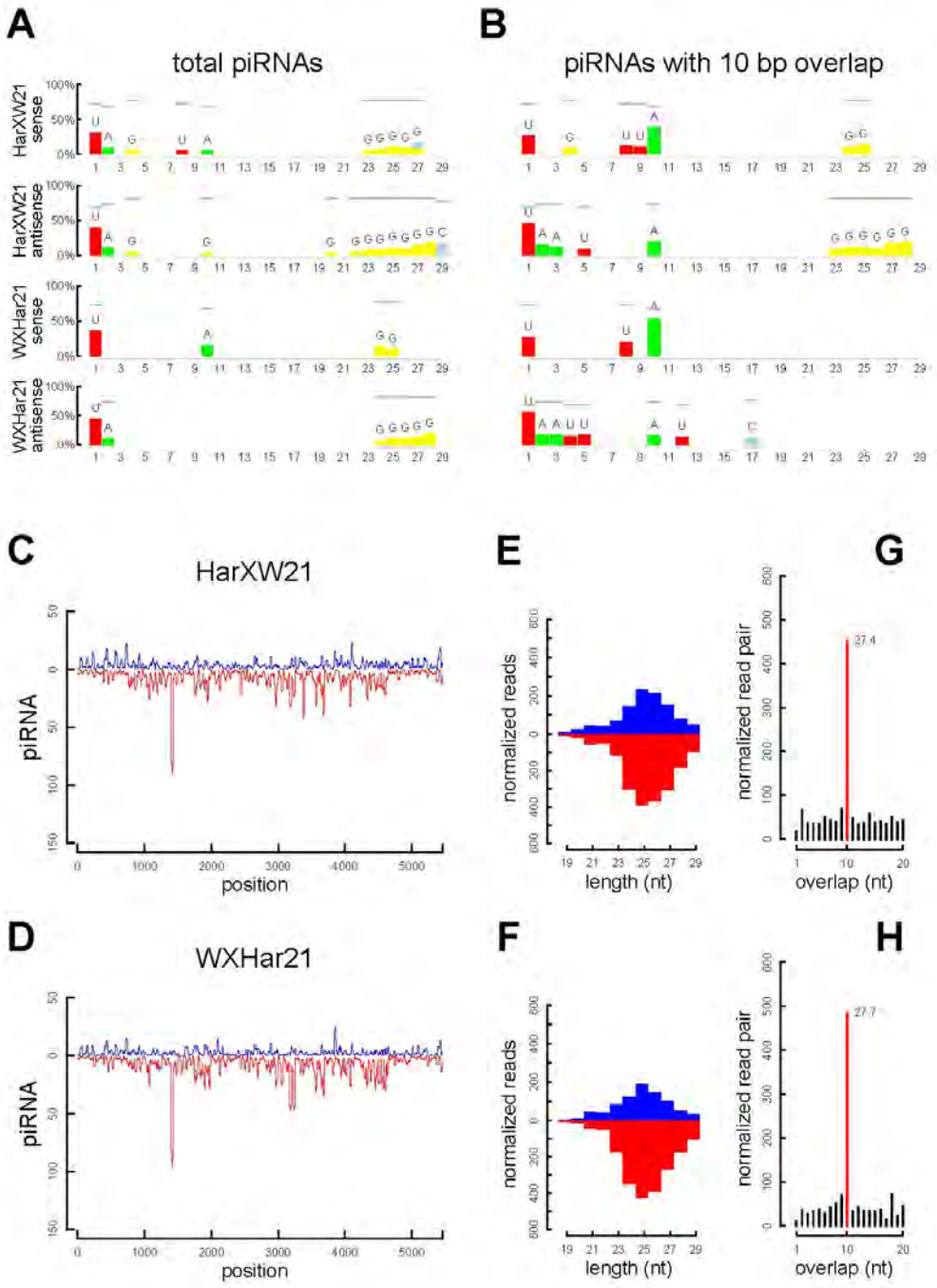
A
total piRNAs
B
piRNAs with 10 bp overlap
HarXW21 sense
HarXW21 antisense
WXHar21 sense
WXHar21 antisense
C
HarXW21
D
WXHar21
piRNA
position
E
F
normalized reads
length (nt)
G
H
normalized read pair
overlap (nt)
27.4
27.7

NOF

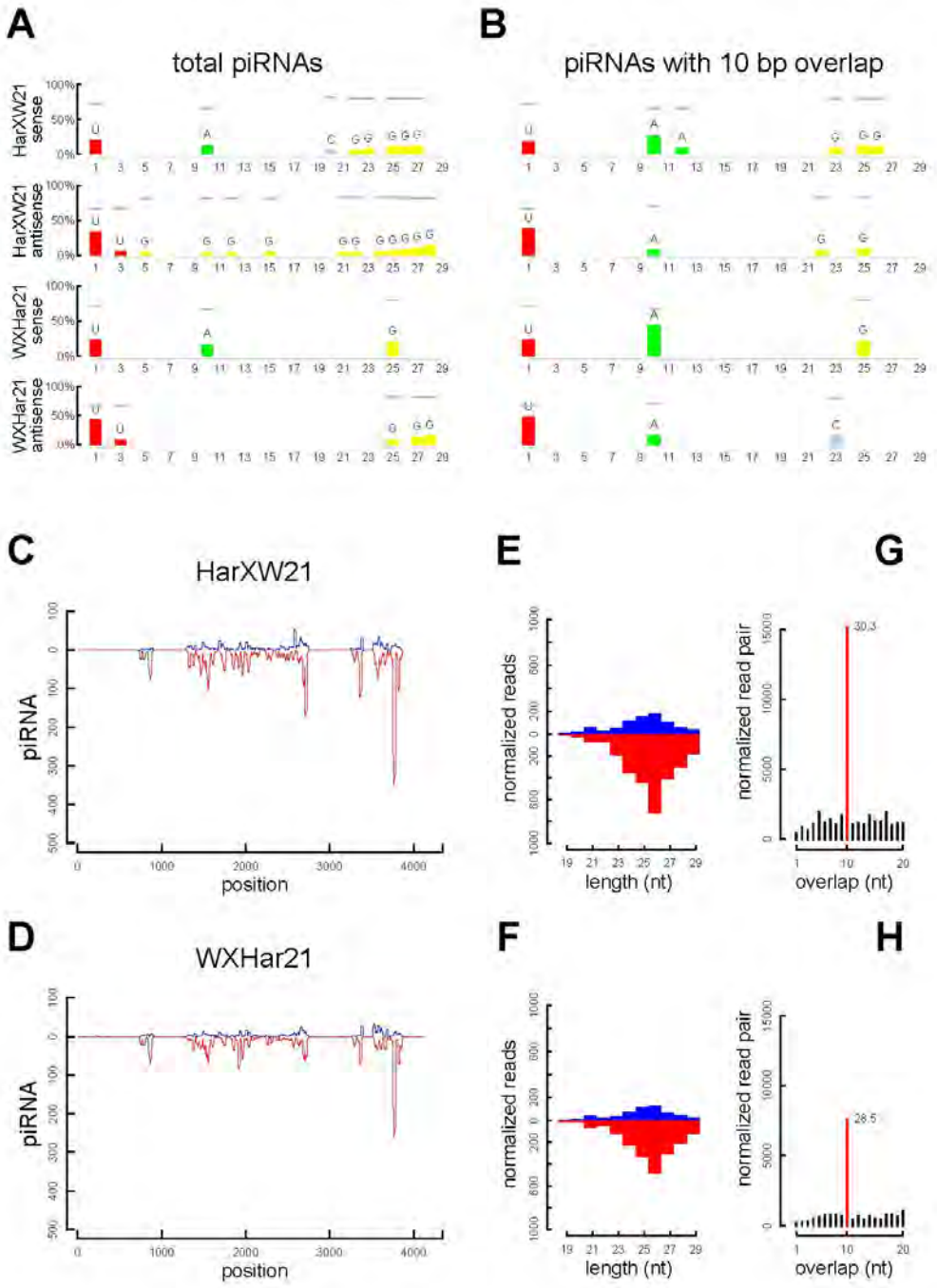
A
total piRNAs
B
piRNAs with 10 bp overlap
HarXW21 sense
HarXW21 antisense
WXHar21 sense
WXHar21 antisense
C
HarXW21
piRNA
position
D
WXHar21
piRNA
position
E
normalized reads
length (nt)
F
normalized reads
length (nt)
G
normalized read pair
overlap (nt)
30.3
H
normalized read pair
overlap (nt)
28.5

opus

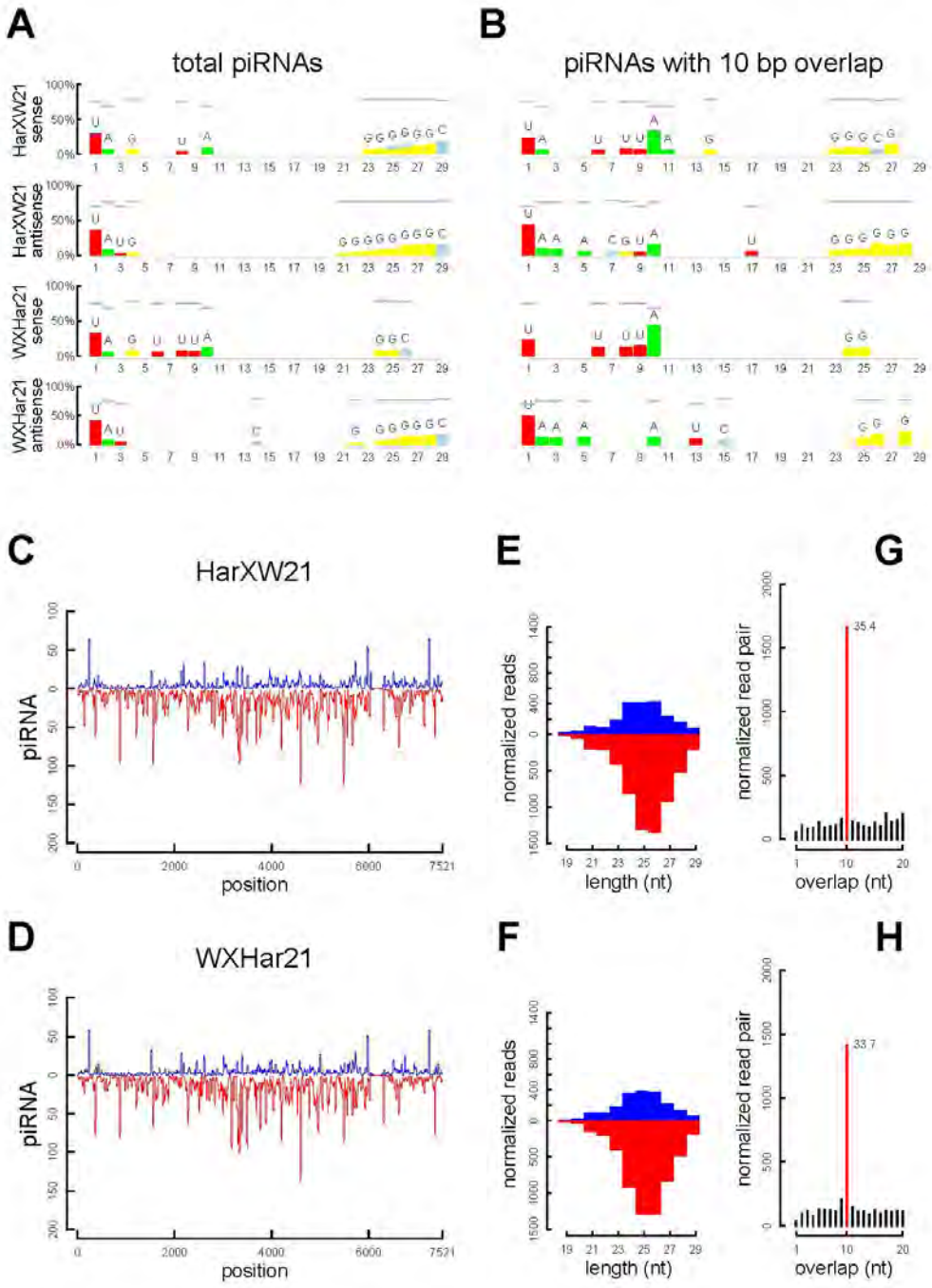
A
total piRNAs
B
piRNAs with 10 bp overlap
HarXW21 sense
HarXW21 antisense
WXHar21 sense
WXHar21 antisense
C
HarXW21
piRNA
position
D
WXHar21
piRNA
position
E
normalized reads
length (nt)
F
normalized reads
length (nt)
G
normalized read pair
35.4
overlap (nt)
H
normalized read pair
33.7
overlap (nt)

Osvaldo

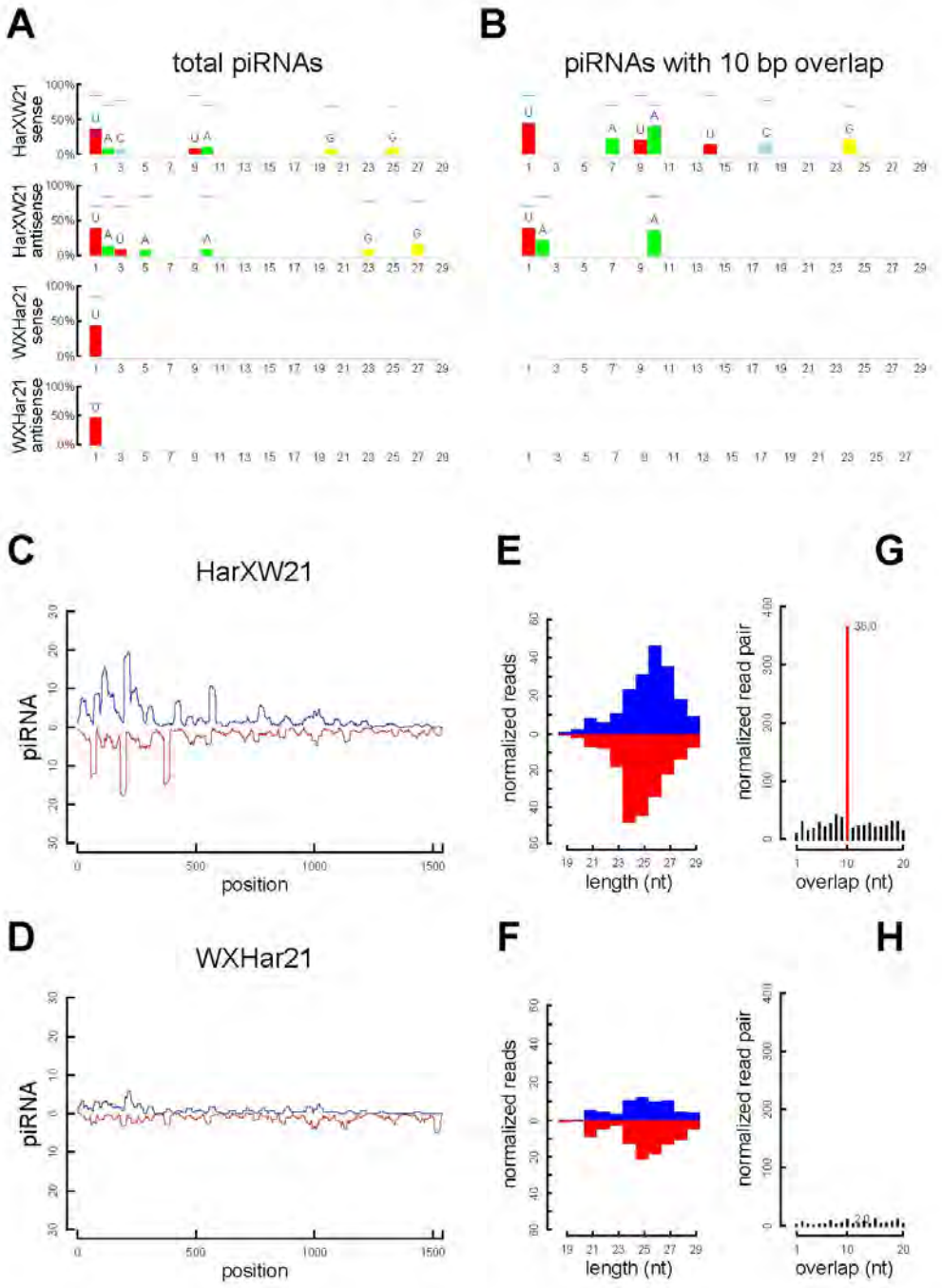
A
total piRNAs
HarXW21 sense
HarXW21 antisense
WXHar21 sense
WXHar21 antisense
B
piRNAs with 10 bp overlap
C
HarXW21
piRNA
position
D
WXHar21
piRNA
position
E
normalized reads
length (nt)
F
normalized reads
length (nt)
G
normalized read pair
overlap (nt)
H
normalized read pair
overlap (nt)

P element

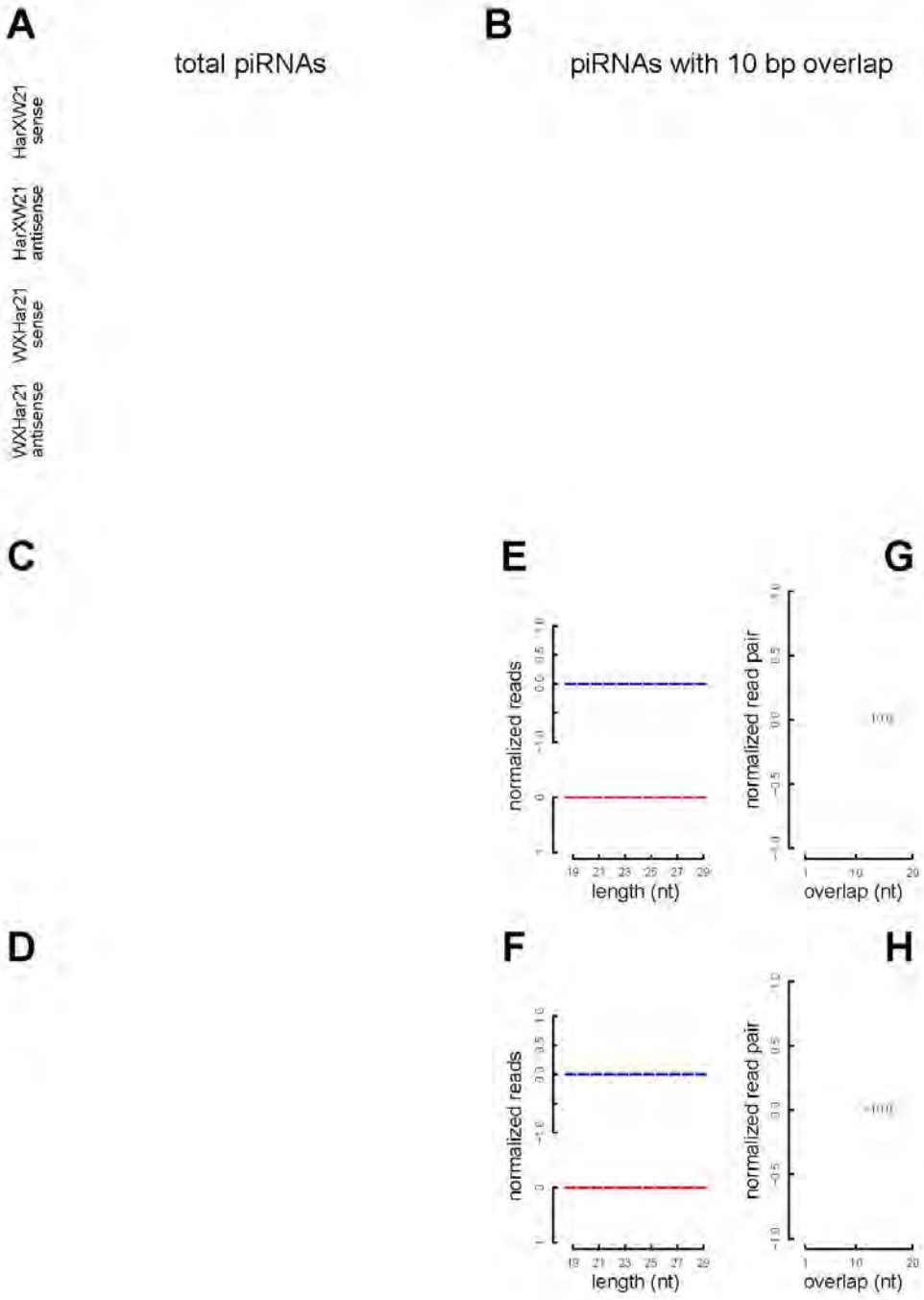
A
total piRNAs
B
piRNAs with 10 bp overlap
HarXW21 sense
HarXW21 antisense
WXHar21 sense
WXHar21 antisense
C
D
E
F
G
H
normalized reads
length (nt)
normalized read pair
overlap (nt)

Penelope

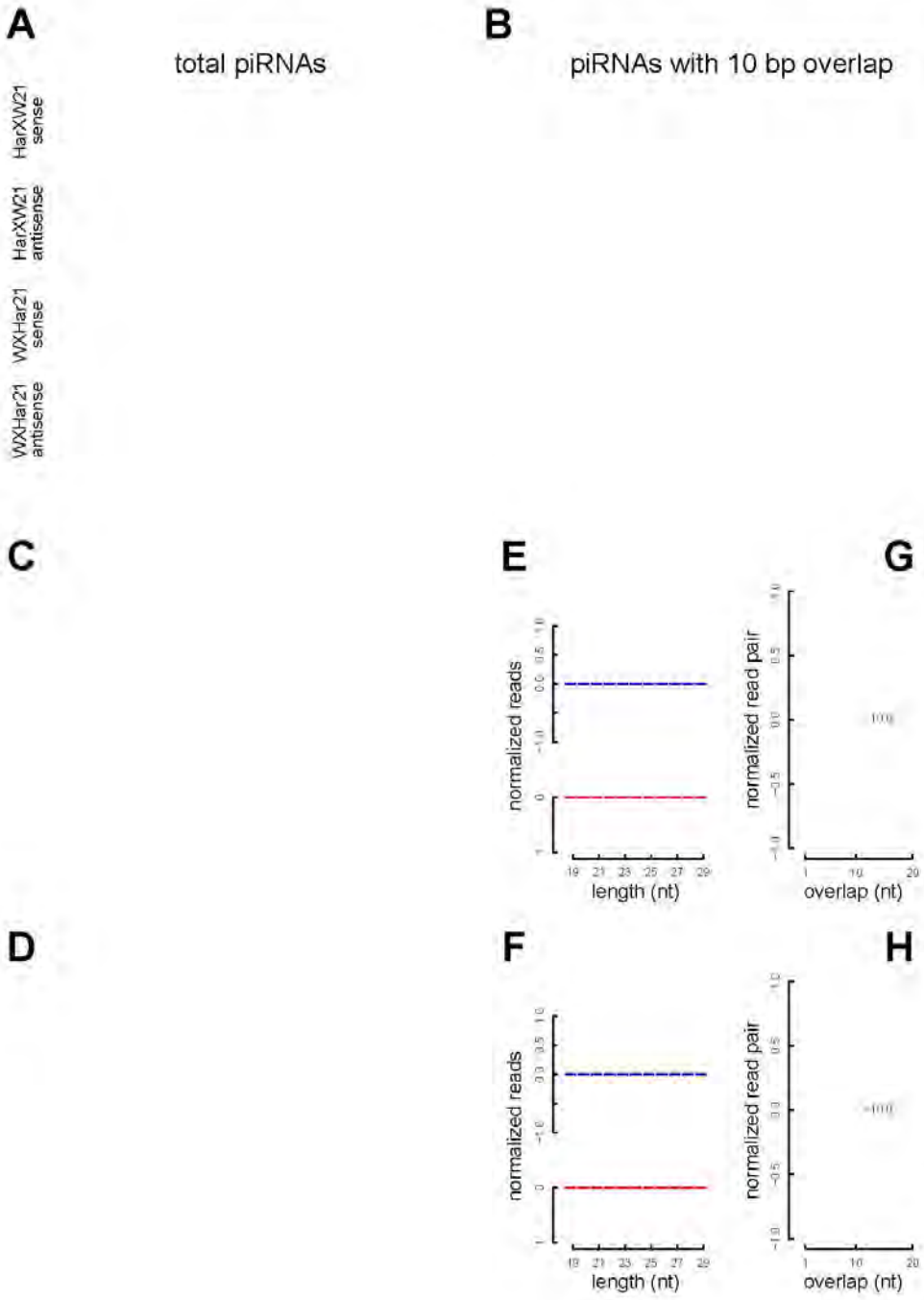
A
total piRNAs
HarXW21 sense
HarXW21 antisense
WXHar21 sense
WXHar21 antisense
B
piRNAs with 10 bp overlap
C
D
E
normalized reads
length (nt)
F
normalized reads
length (nt)
G
normalized read pair
overlap (nt)
H
normalized read pair
overlap (nt)

pogo

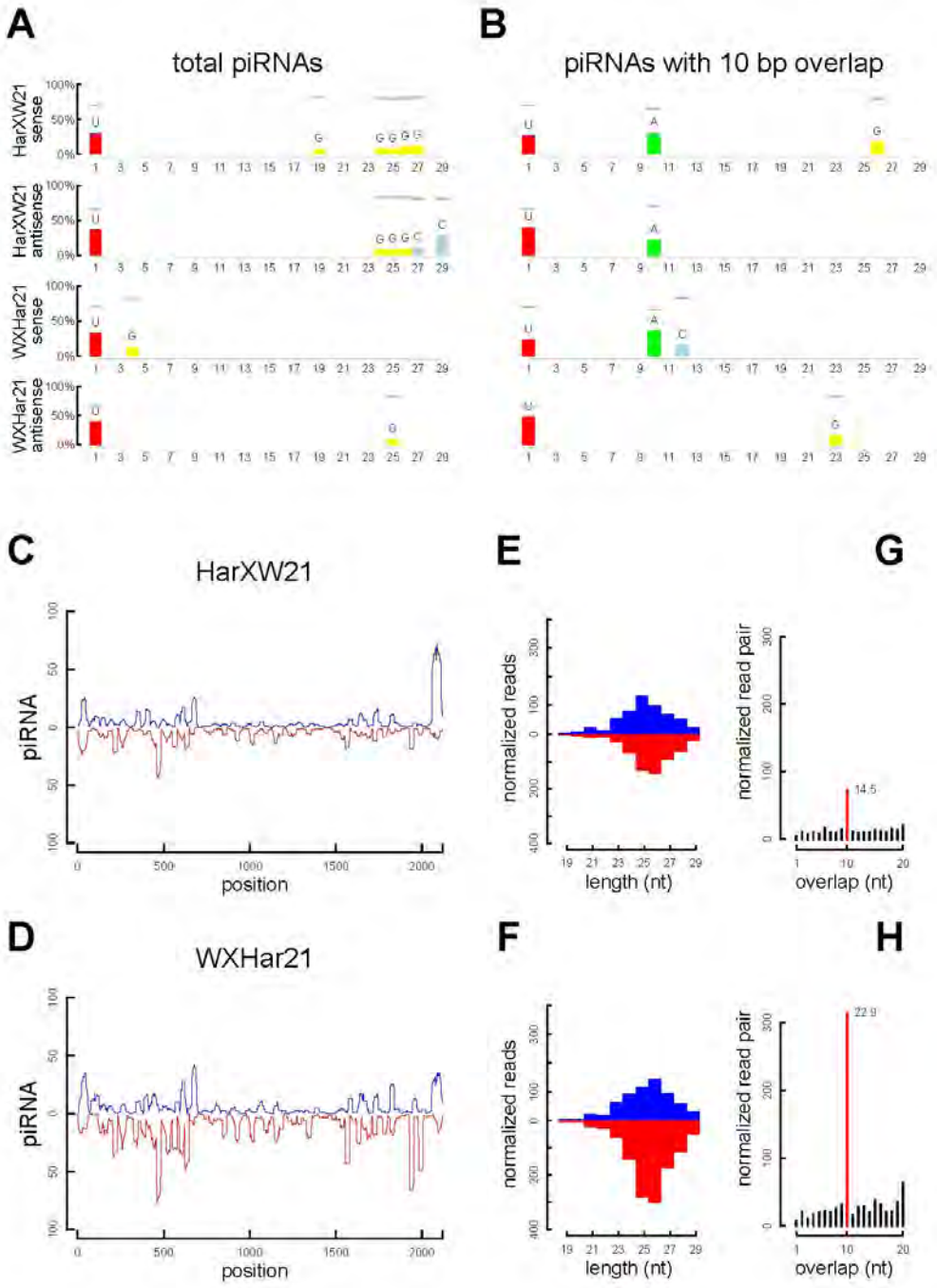
A
total piRNAs
B
piRNAs with 10 bp overlap
HarXW21 sense
HarXW21 antisense
WXHar21 sense
WXHar21 antisense
C
HarXW21
D
WXHar21
piRNA
position
E
F
normalized reads
length (nt)
G
H
normalized read pair
overlap (nt)
14.5
22.9

Porto1

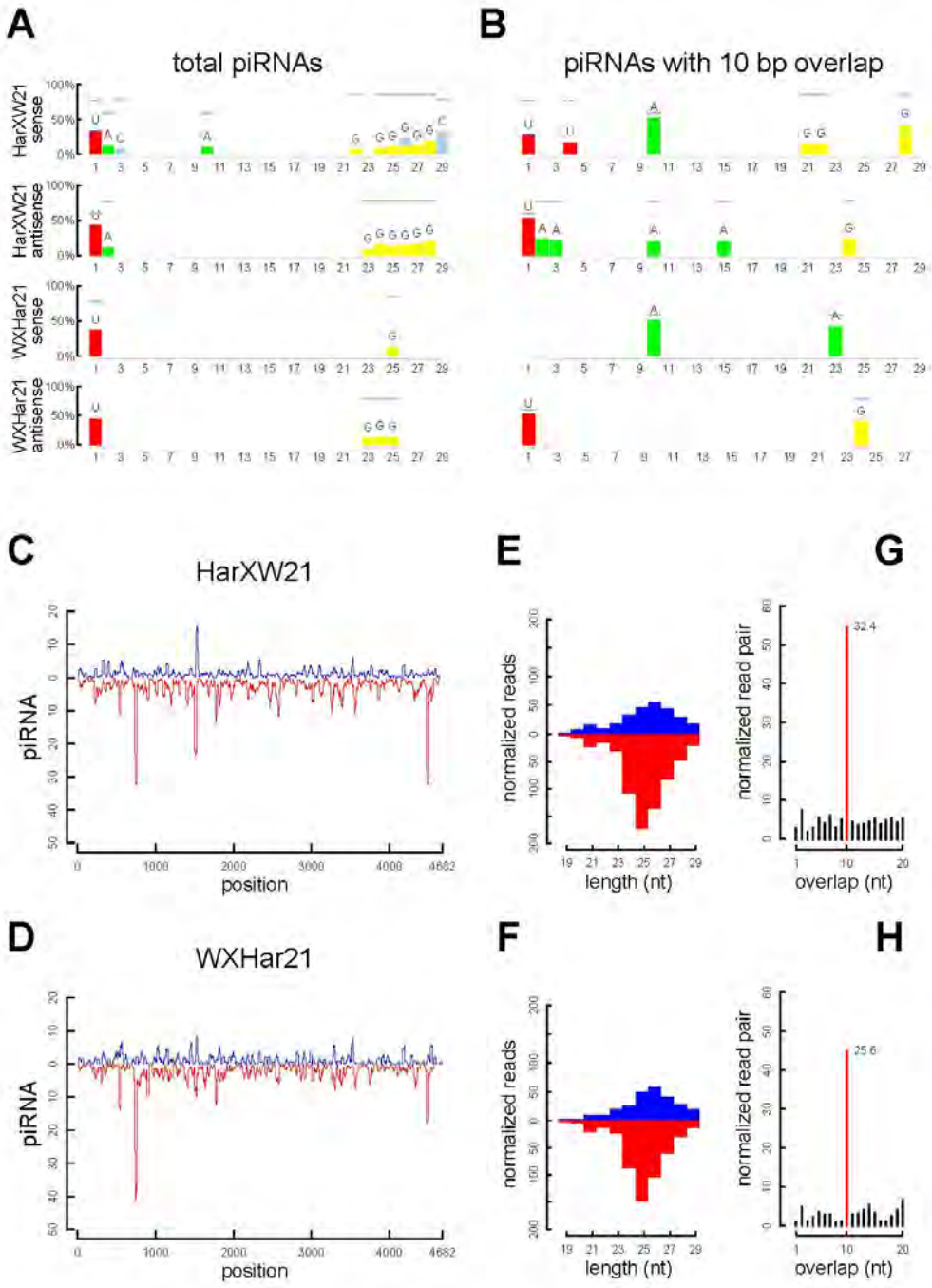
A
total piRNAs
B
piRNAs with 10 bp overlap
HarXW21 sense
HarXW21 antisense
WXHar21 sense
WXHar21 antisense
C
HarXW21
D
WXHar21
piRNA
position
E
F
normalized reads
length (nt)
G
H
normalized read pair
overlap (nt)
32.4
25.6

Q element

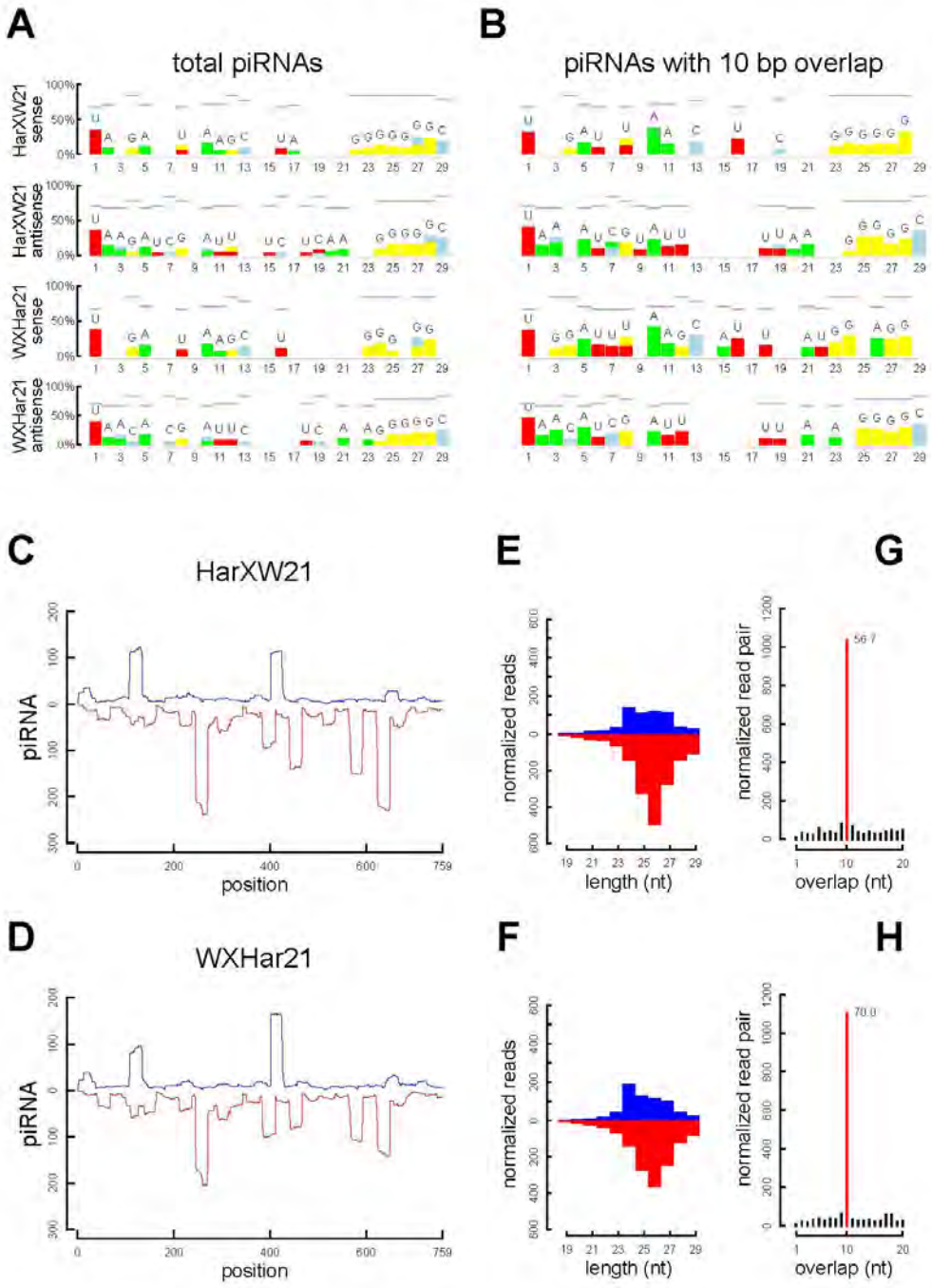
A
total piRNAs
B
piRNAs with 10 bp overlap
HarXW21 sense
HarXW21 antisense
WXHar21 sense
WXHar21 antisense
C
HarXW21
piRNA
position
D
WXHar21
piRNA
position
E
normalized reads
length (nt)
F
normalized reads
length (nt)
G
normalized read pair
overlap (nt)
56.7
H
normalized read pair
overlap (nt)
70.0

Quasimodo

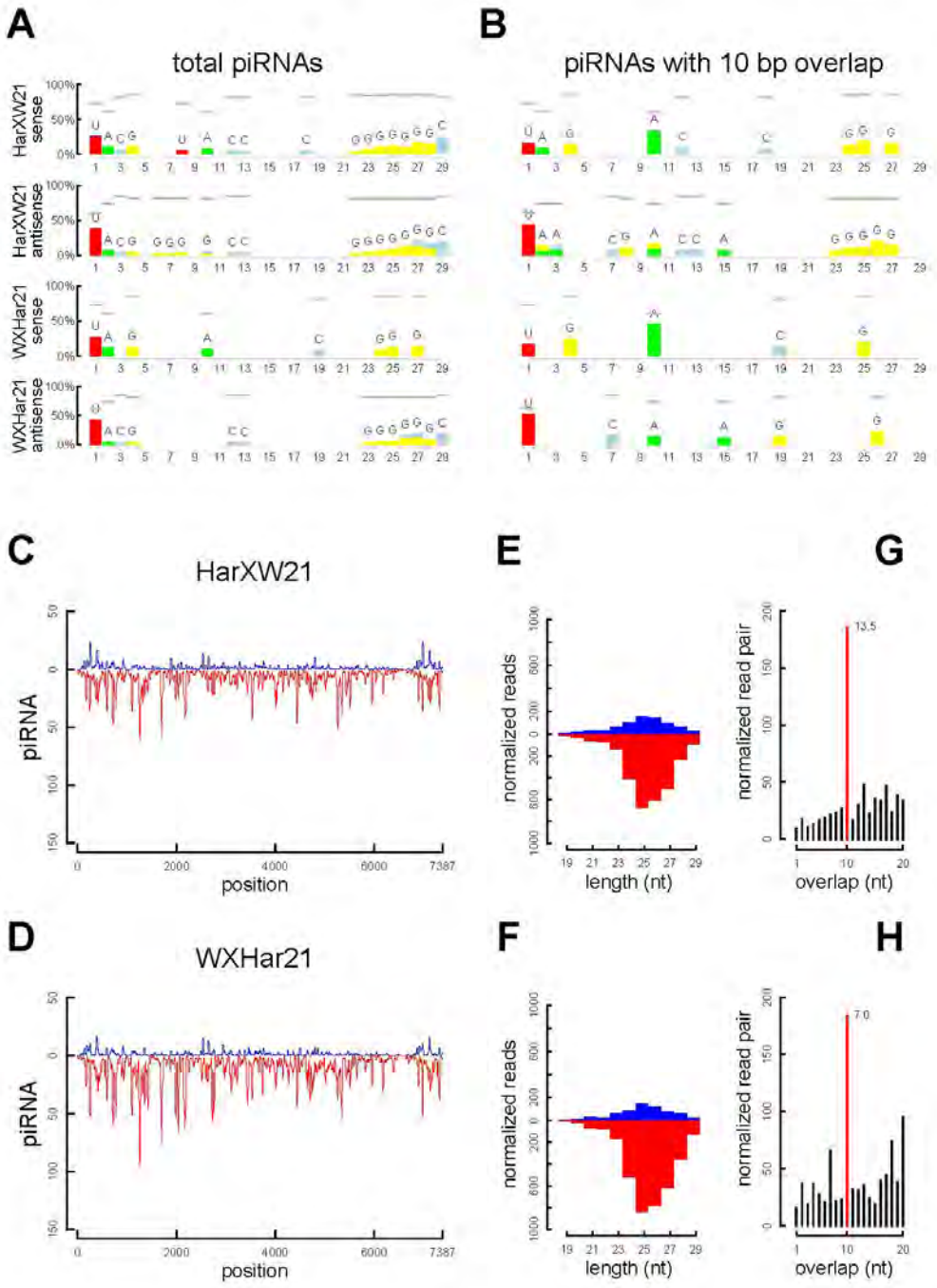
A
total piRNAs
B
piRNAs with 10 bp overlap
HarXW21 sense
HarXW21 antisense
WXHar21 sense
WXHar21 antisense
C
HarXW21
D
WXHar21
piRNA
position
E
F
normalized reads
length (nt)
G
H
normalized read pair
overlap (nt)
13.5
7.0

R1 2

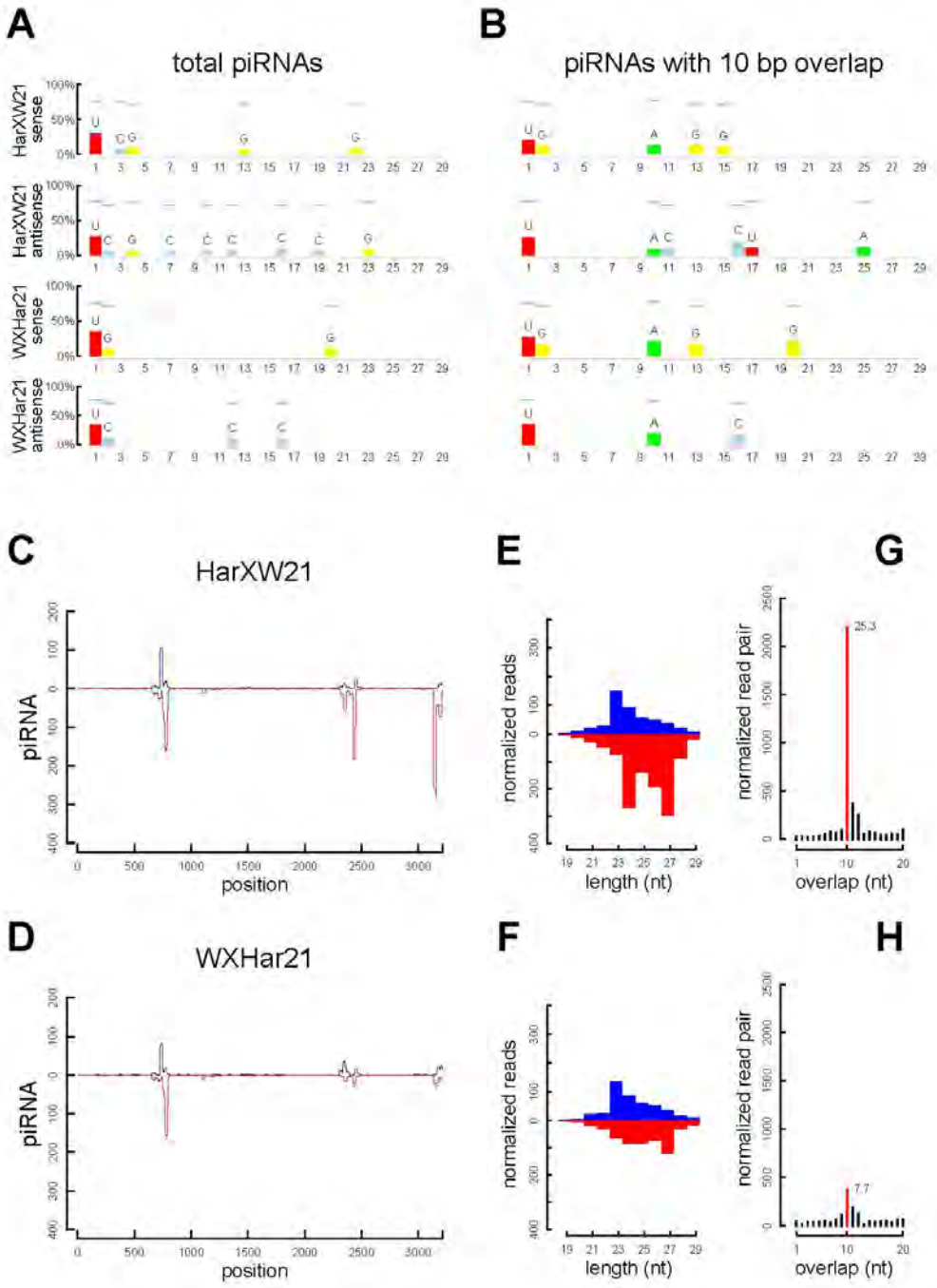
A
total piRNAs
B
piRNAs with 10 bp overlap
HarXW21 sense
HarXW21 antisense
WXHar21 sense
WXHar21 antisense
C
HarXW21
D
WXHar21
piRNA
position
E
F
normalized reads
length (nt)
G
H
normalized read pair
overlap (nt)
25.3
7.7

R1A1 element

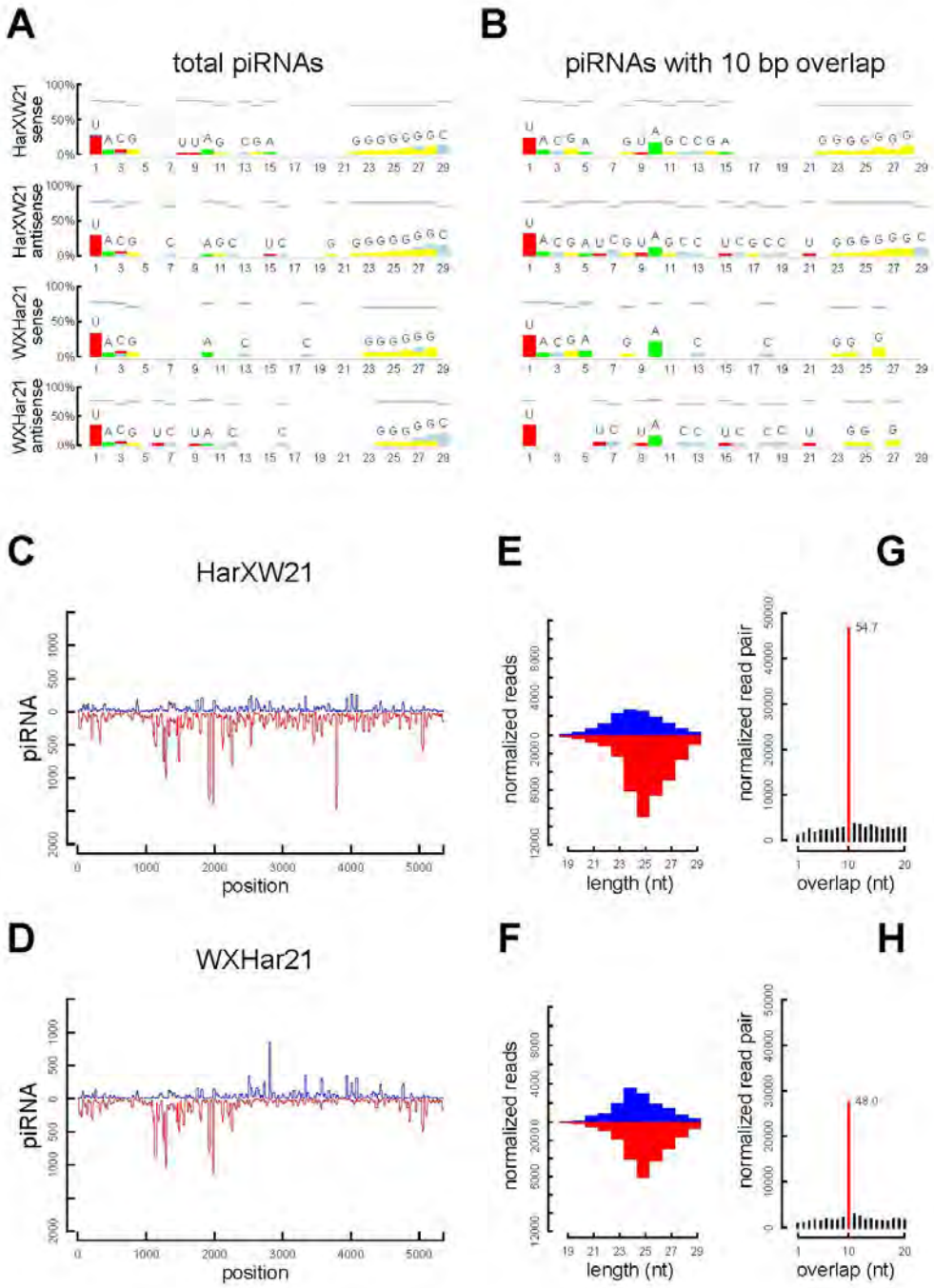

R2 element

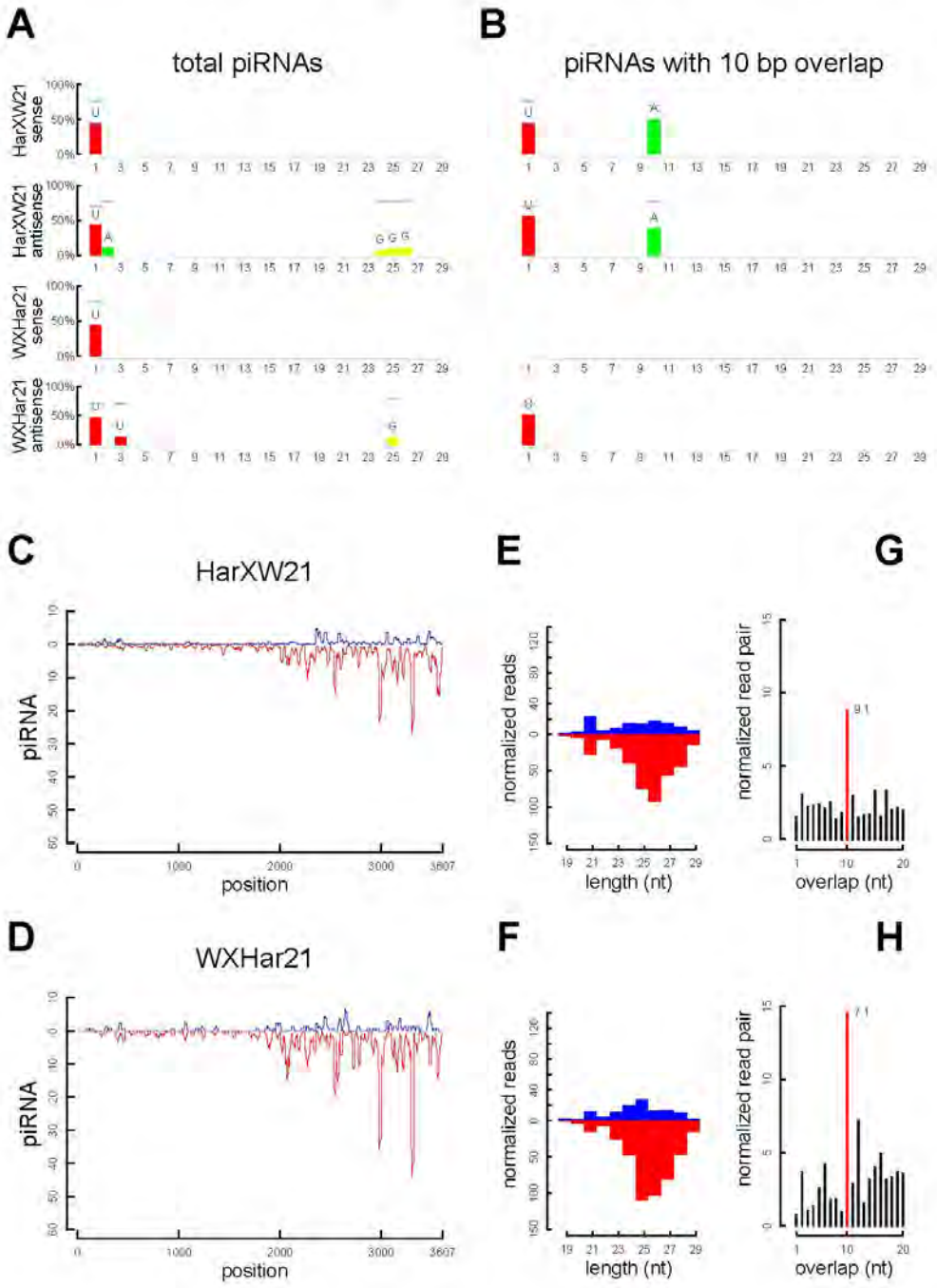
A
total piRNAs
B
piRNAs with 10 bp overlap
HarXW21 sense
HarXW21 antisense
WXHar21 sense
WXHar21 antisense
C
HarXW21
piRNA
position
D
WXHar21
piRNA
position
E
normalized reads
length (nt)
F
normalized reads
length (nt)
G
normalized read pair
overlap (nt)
9.1
H
normalized read pair
overlap (nt)
7.1

roo

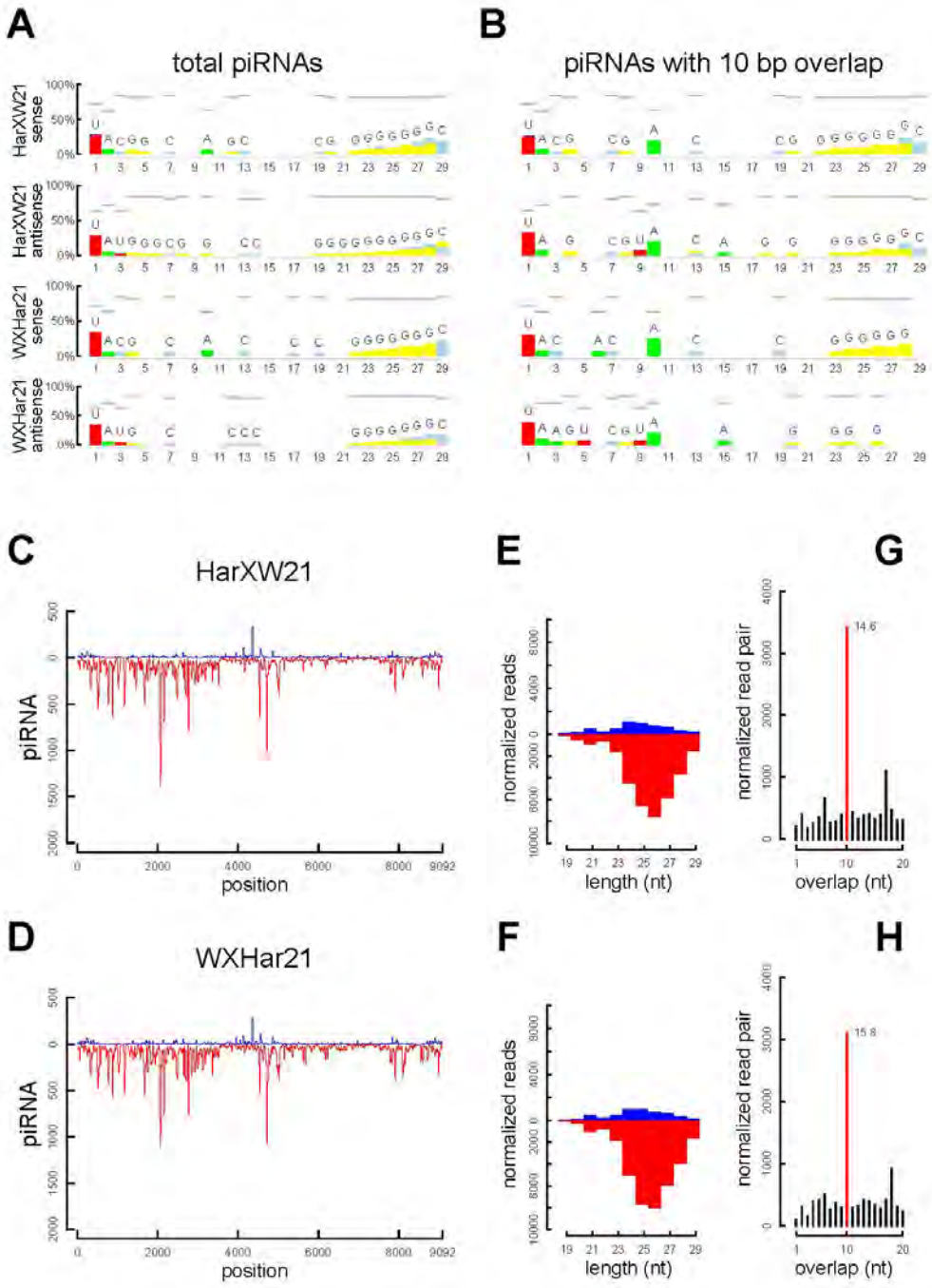
A
total piRNAs
B
piRNAs with 10 bp overlap
HarXW21 sense
HarXW21 antisense
WXHar21 sense
WXHar21 antisense
C
HarXW21
D
WXHar21
piRNA
position
E
F
normalized reads
length (nt)
G
H
normalized read pair
overlap (nt)
14.6
15.8

rooA

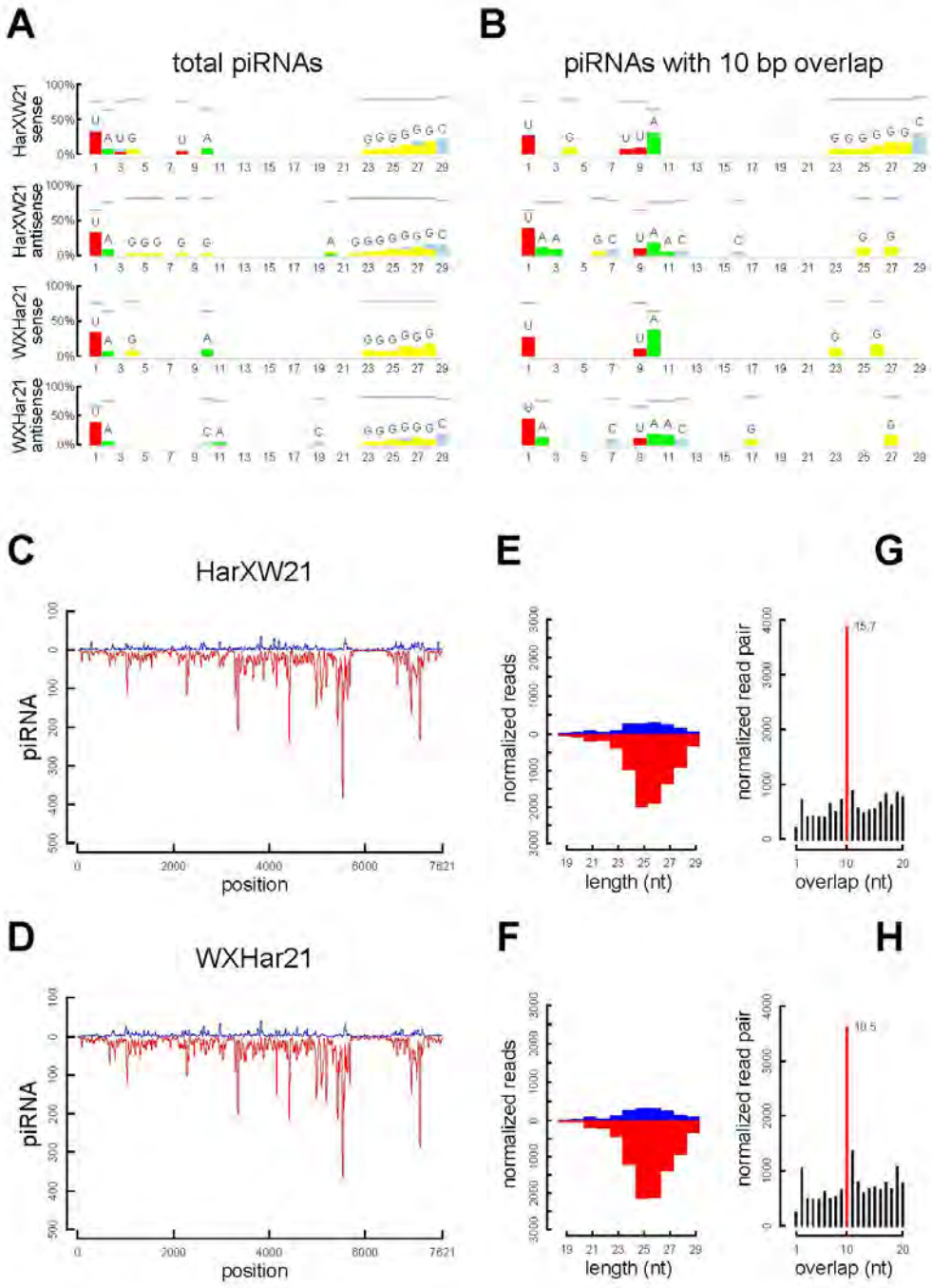
A
total piRNAs
B
piRNAs with 10 bp overlap
HarXW21 sense
HarXW21 antisense
WXHar21 sense
WXHar21 antisense
C
HarXW21
D
WXHar21
piRNA
position
E
F
normalized reads
length (nt)
G
H
normalized read pair
overlap (nt)
15.7
10.5

rover

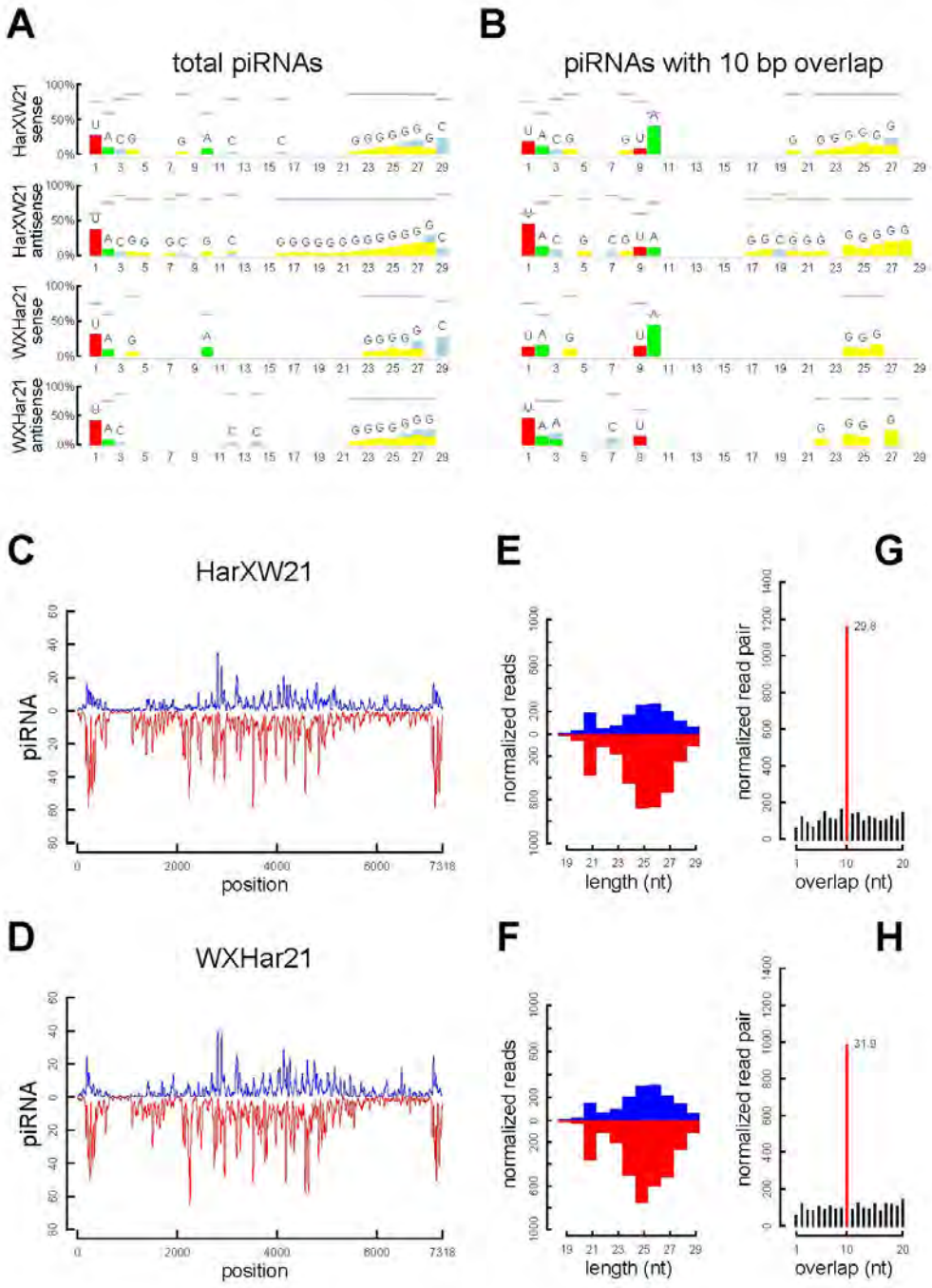
A
total piRNAs
B
piRNAs with 10 bp overlap
HarXW21 sense
HarXW21 antisense
WXHar21 sense
WXHar21 antisense
C
HarXW21
piRNA
position
D
WXHar21
piRNA
position
E
normalized reads
length (nt)
F
normalized reads
length (nt)
G
normalized read pair
overlap (nt)
29.8
H
normalized read pair
overlap (nt)
31.9

Rt1a

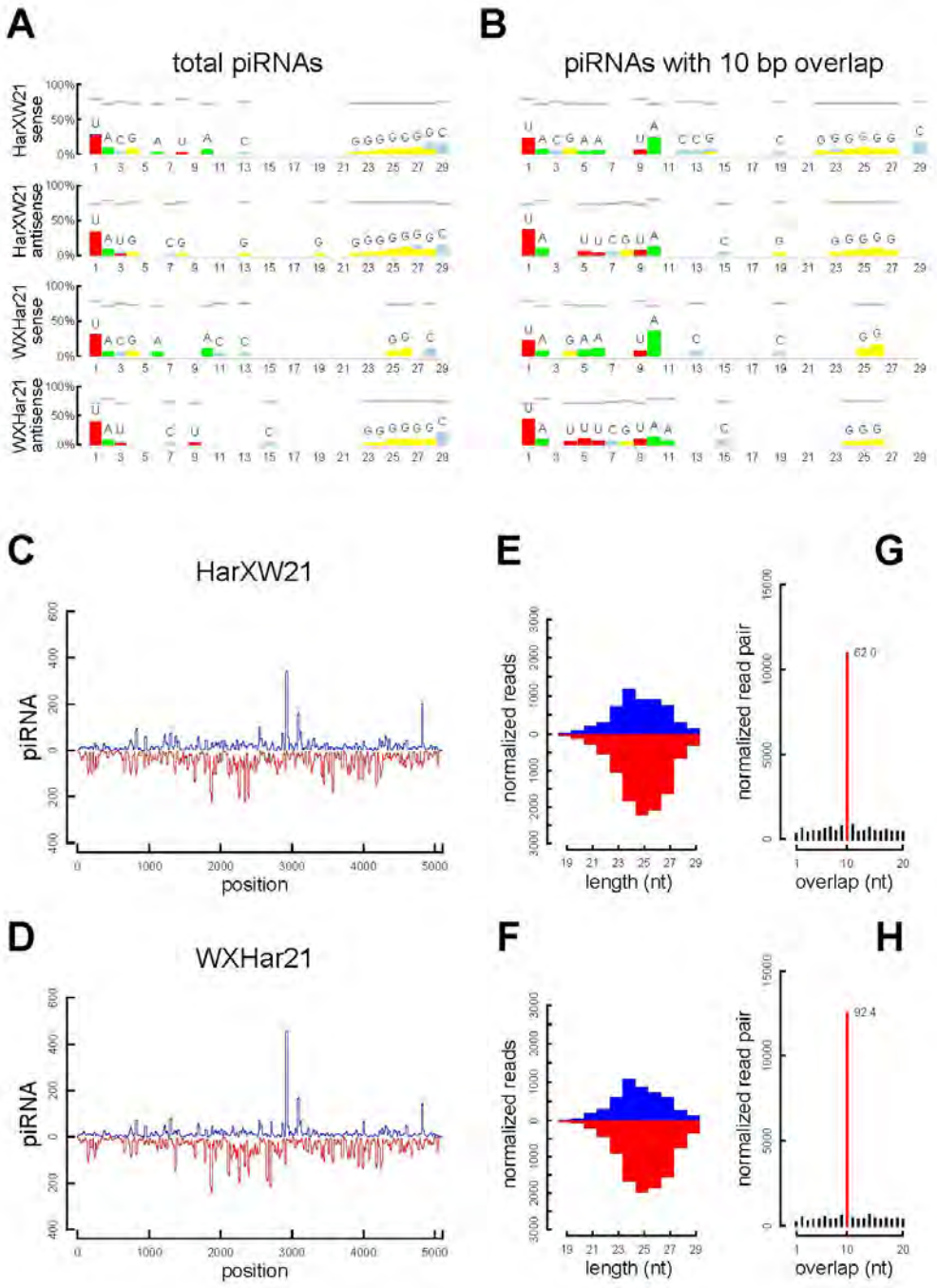
A
total piRNAs
B
piRNAs with 10 bp overlap
HarXW21 sense
HarXW21 antisense
WXHar21 sense
WXHar21 antisense
C
HarXW21
piRNA
position
D
WXHar21
piRNA
position
E
normalized reads
length (nt)
F
normalized reads
length (nt)
G
normalized read pair
62.0
overlap (nt)
H
normalized read pair
92.4
overlap (nt)

Rt1b

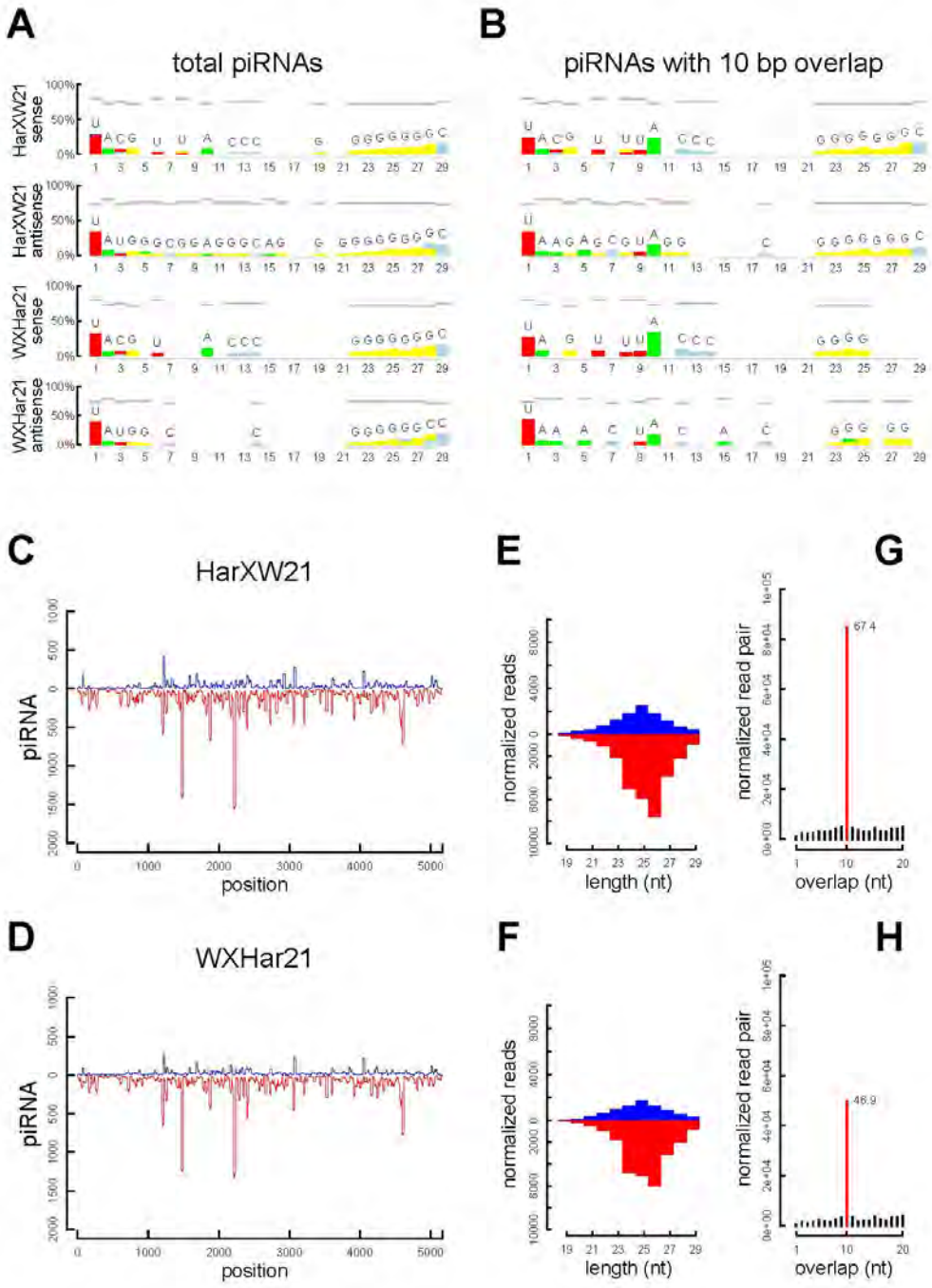
A
total piRNAs
B
piRNAs with 10 bp overlap
HarXW21 sense
HarXW21 antisense
WXHar21 sense
WXHar21 antisense
C
HarXW21
piRNA
position
D
WXHar21
piRNA
position
E
normalized reads
length (nt)
F
normalized reads
length (nt)
G
normalized read pair
overlap (nt)
67.4
H
normalized read pair
overlap (nt)
46.9

Rt1c

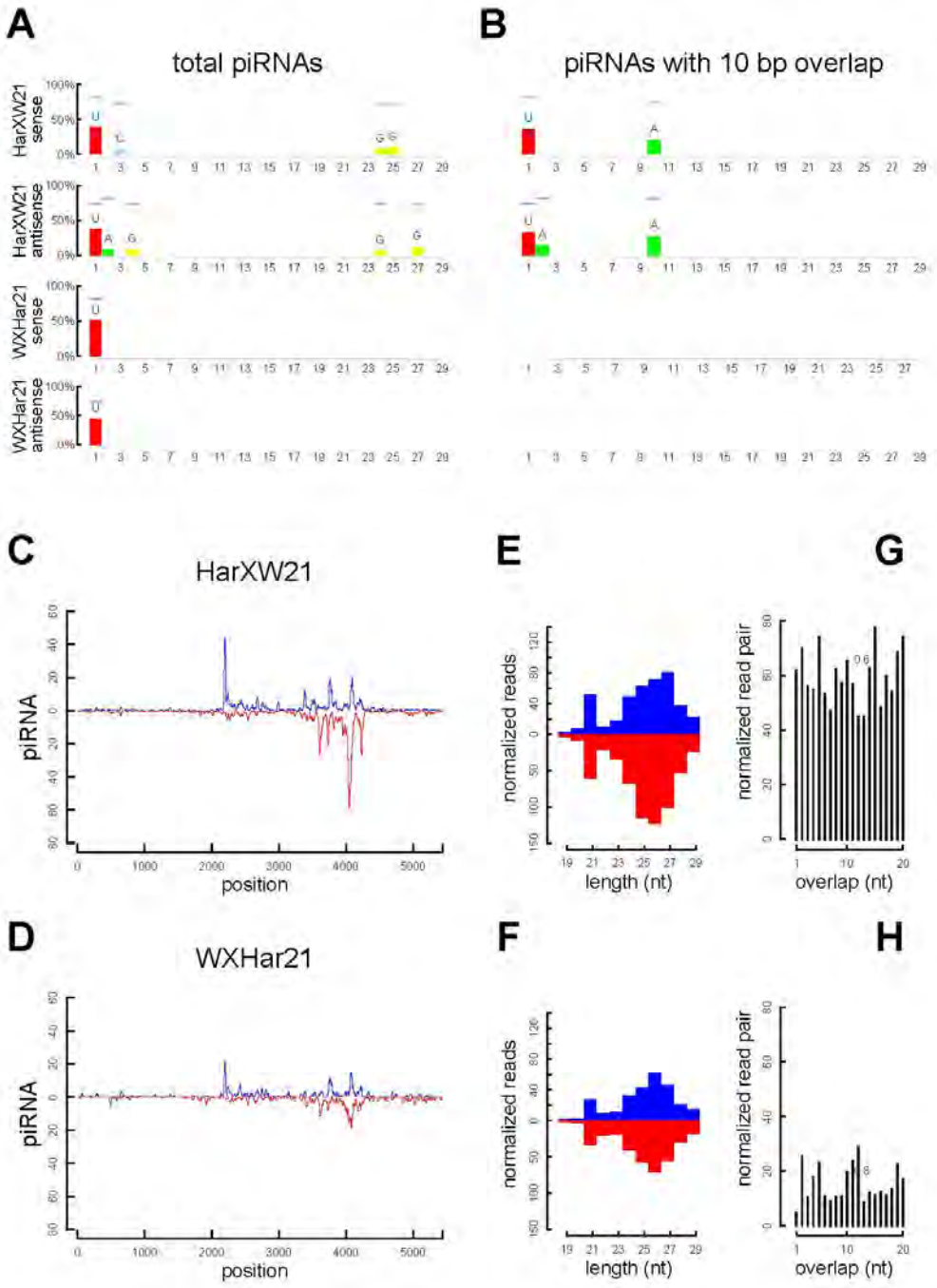
A
total piRNAs
B
piRNAs with 10 bp overlap
HarXW21 sense
HarXW21 antisense
WXHar21 sense
WXHar21 antisense
C
HarXW21
D
WXHar21
piRNA
position
E
F
normalized reads
length (nt)
G
H
normalized read pair
overlap (nt)

S2

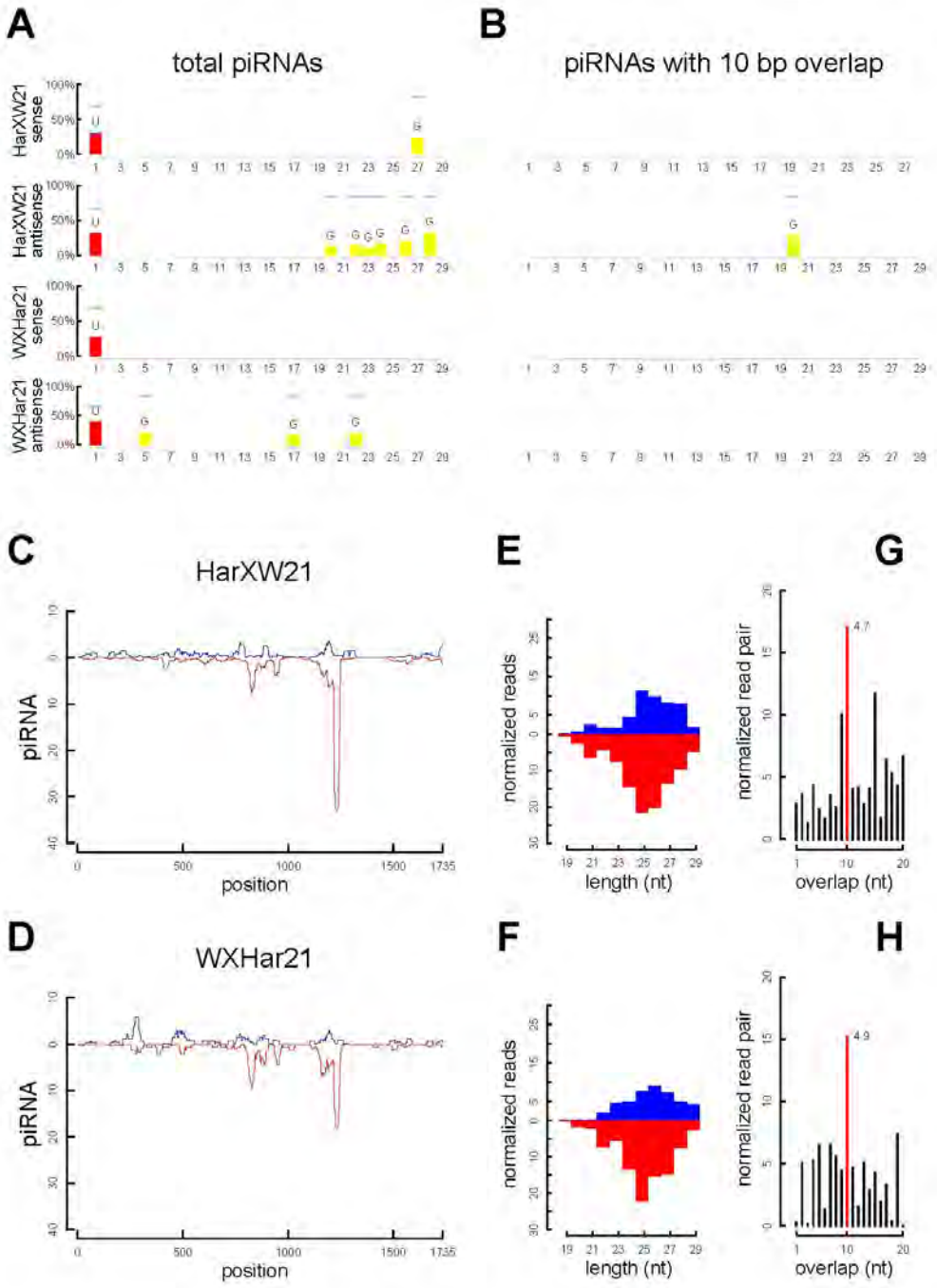
A
total piRNAs
B
piRNAs with 10 bp overlap
HarXW21 sense
HarXW21 antisense
WXHar21 sense
WXHar21 antisense
C
HarXW21
D
WXHar21
piRNA
position
E
F
normalized reads
length (nt)
G
H
normalized read pair
overlap (nt)
4.7
4.9

S element

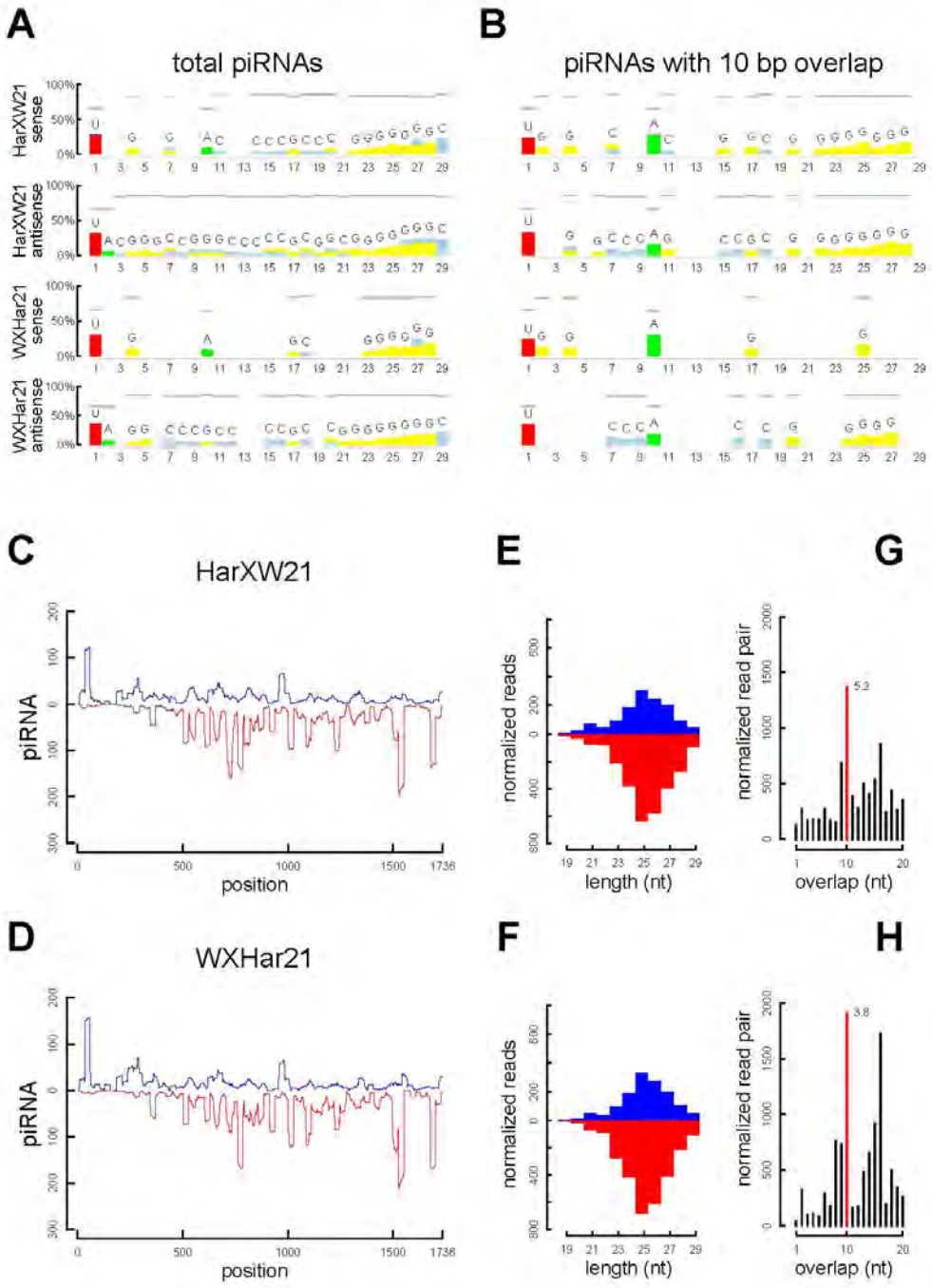
A
total piRNAs
B
piRNAs with 10 bp overlap
HarXW21 sense
HarXW21 antisense
WXHar21 sense
WXHar21 antisense
C
HarXW21
piRNA
position
D
WXHar21
piRNA
position
E
normalized reads
length (nt)
F
normalized reads
length (nt)
G
normalized read pair
overlap (nt)
5.2
H
normalized read pair
overlap (nt)
3.8

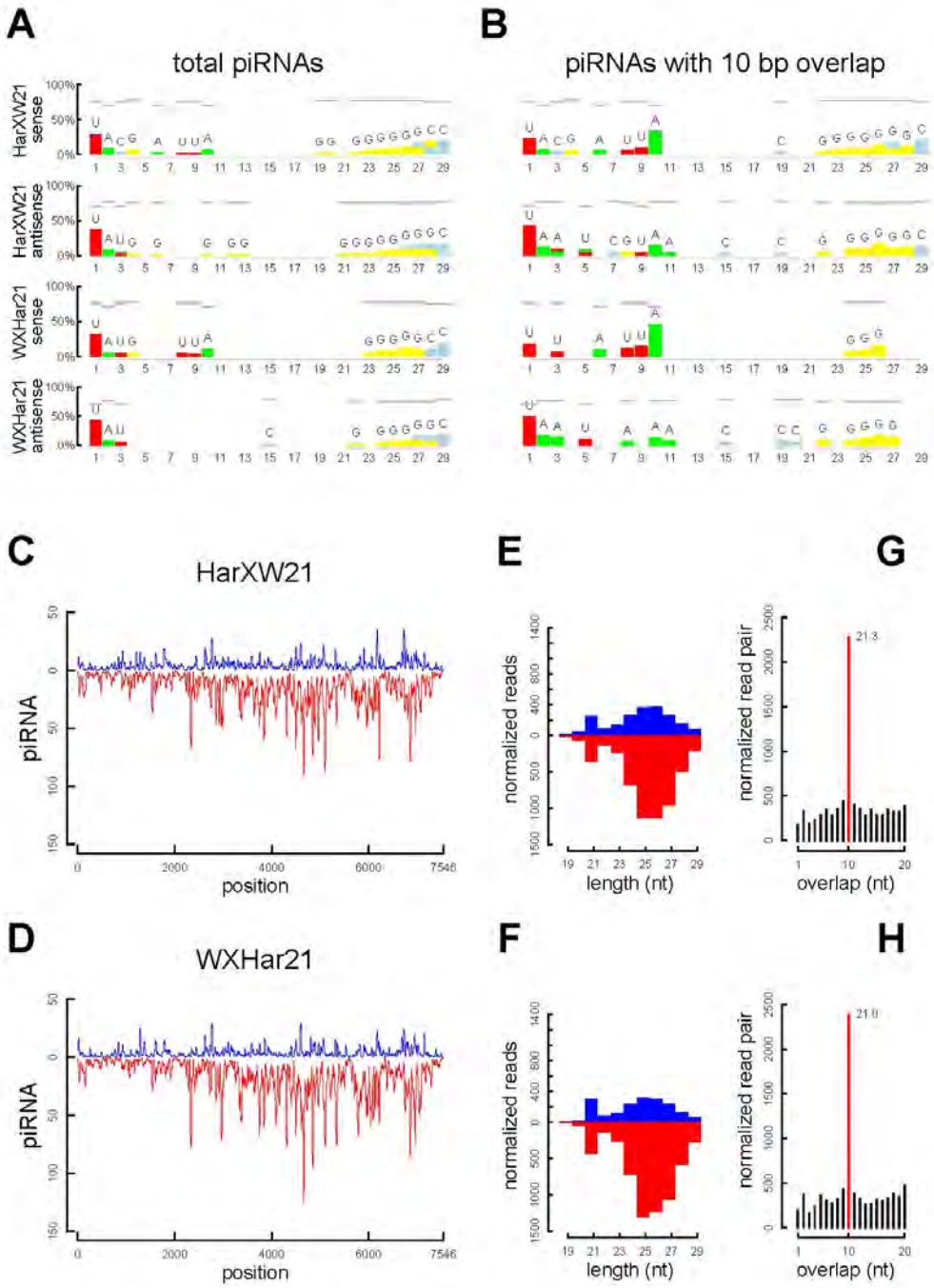
A
total piRNAs
B
piRNAs with 10 bp overlap
HarXW21 sense
HarXW21 antisense
WXHar21 sense
WXHar21 antisense
C
HarXW21
piRNA
position
D
WXHar21
E
F
G
H
normalized reads
length (nt)
normalized read pair
overlap (nt)
21.3
21.0

Stalker

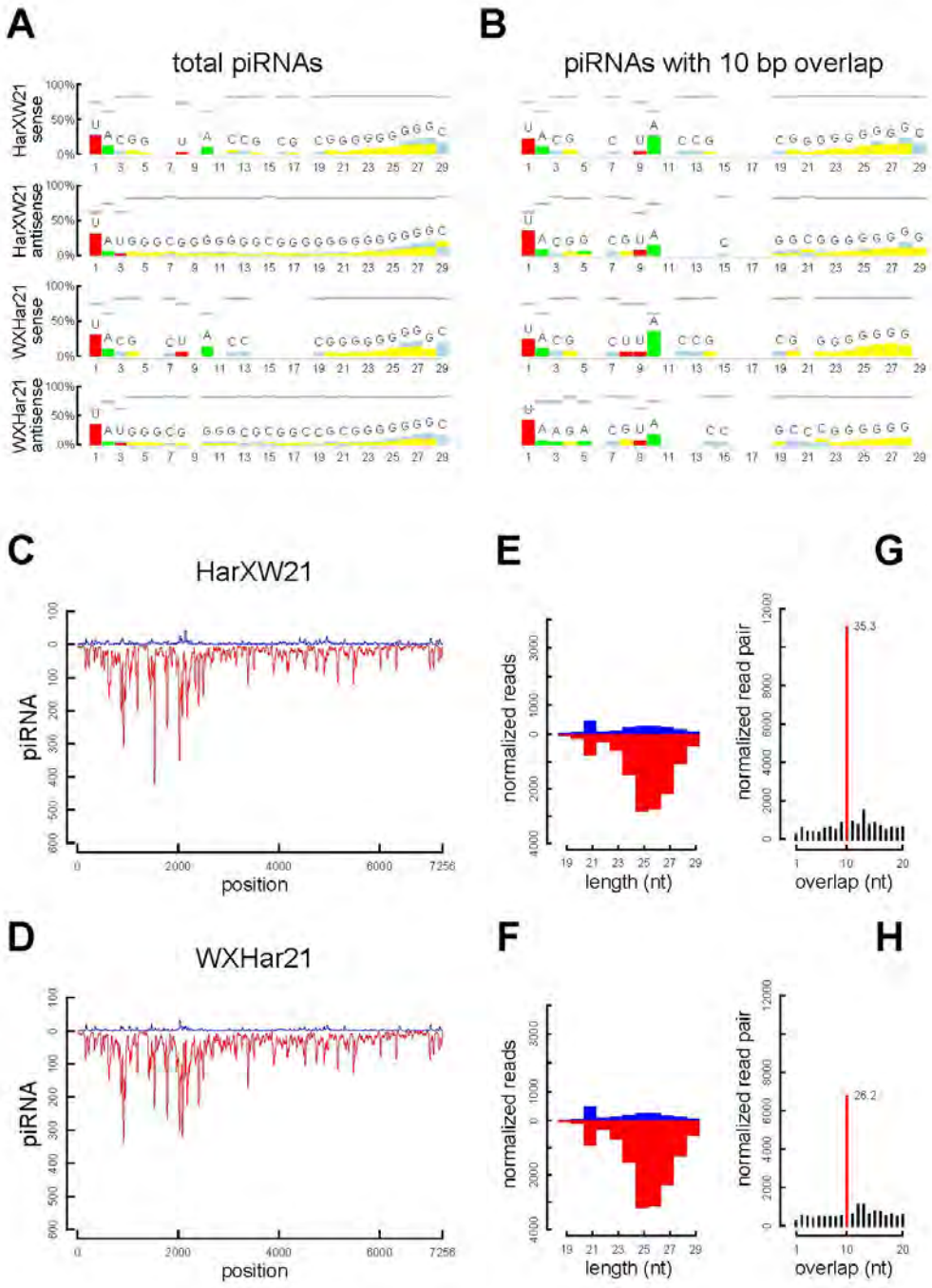
A
total piRNAs
B
piRNAs with 10 bp overlap
HarXW21 sense
HarXW21 antisense
WXHar21 sense
WXHar21 antisense
C
HarXW21
piRNA
position
D
WXHar21
E
F
normalized reads
length (nt)
G
H
normalized read pair
overlap (nt)
35.3
26.2

Stalker2

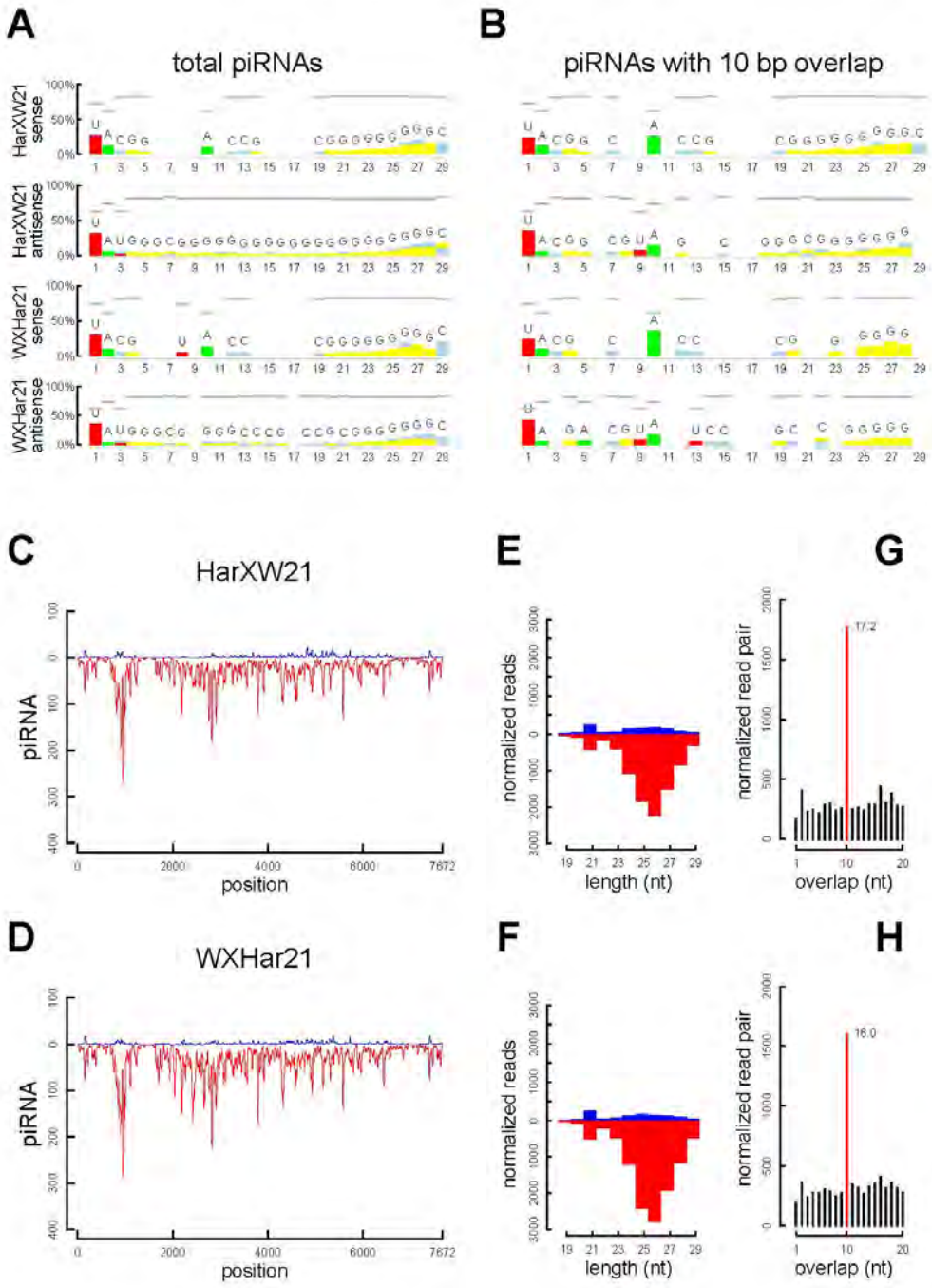
A
total piRNAs
B
piRNAs with 10 bp overlap
HarXW21 sense
HarXW21 antisense
WXHar21 sense
WXHar21 antisense
C
HarXW21
piRNA
position
D
WXHar21
piRNA
position
E
normalized reads
length (nt)
F
normalized reads
length (nt)
G
normalized read pair
overlap (nt)
17.2
H
normalized read pair
overlap (nt)
16.0

Stalker3

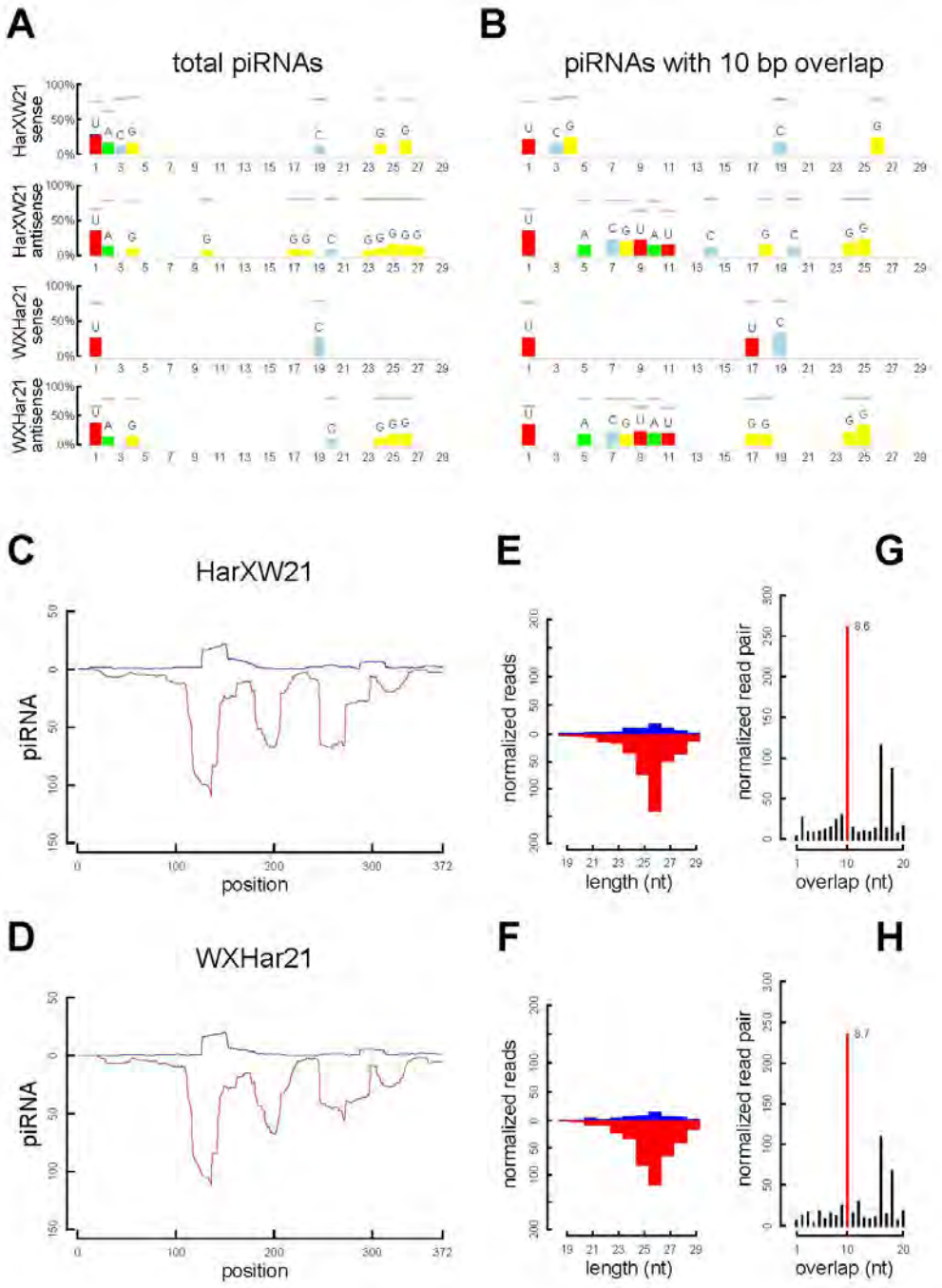
A
total piRNAs
B
piRNAs with 10 bp overlap
HarXW21 sense
HarXW21 antisense
WXHar21 sense
WXHar21 antisense
C
HarXW21
piRNA
position
D
WXHar21
piRNA
position
E
normalized reads
length (nt)
F
normalized reads
length (nt)
G
normalized read pair
overlap (nt)
8.6
H
normalized read pair
overlap (nt)
8.7

Stalker4

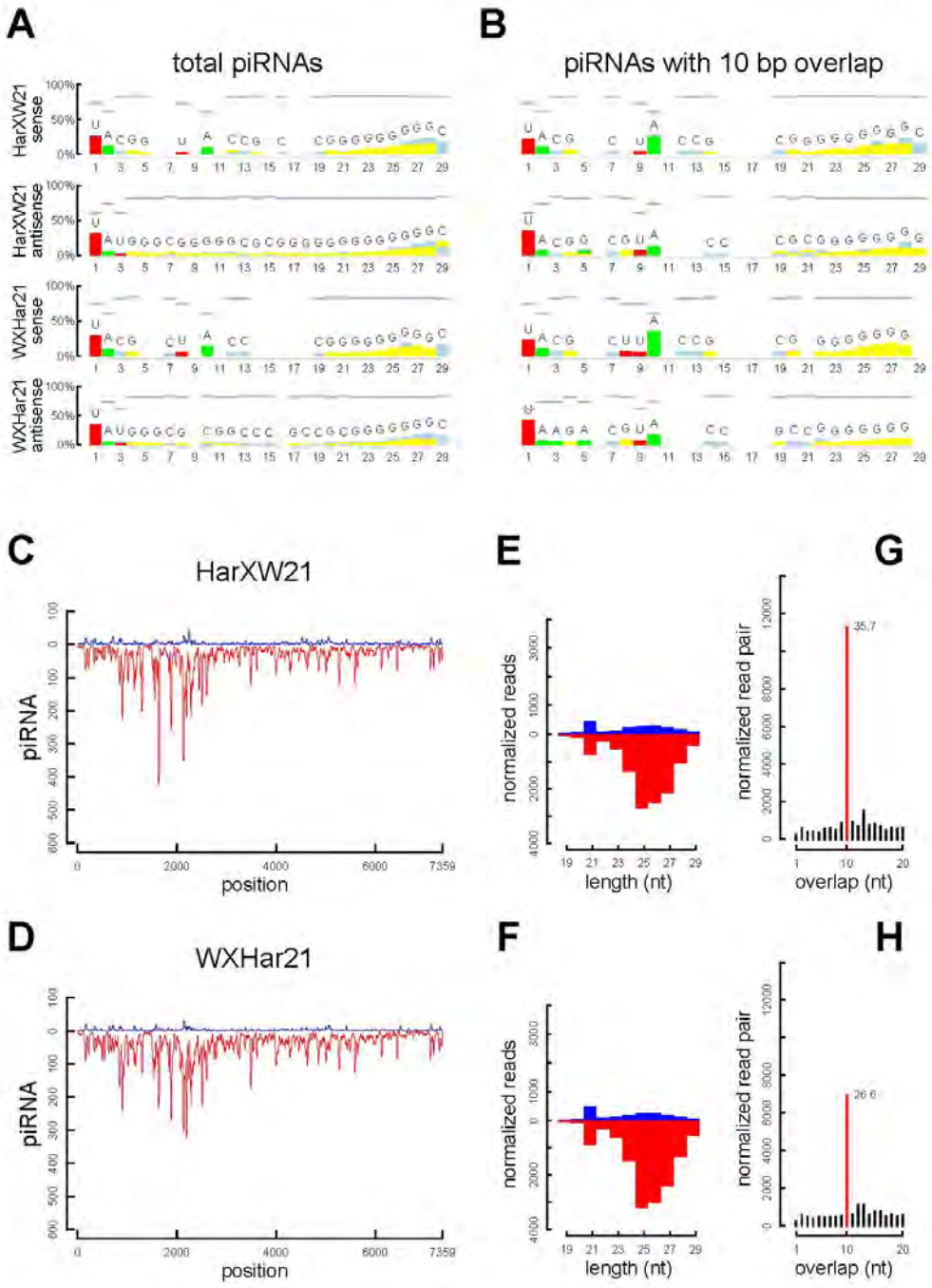
A
total piRNAs
B
piRNAs with 10 bp overlap
HarXW21 sense
HarXW21 antisense
WXHar21 sense
WXHar21 antisense
C
HarXW21
piRNA
position
D
WXHar21
piRNA
position
E
normalized reads
length (nt)
F
normalized reads
length (nt)
G
normalized read pair
35.7
overlap (nt)
H
normalized read pair
26.6
overlap (nt)

Tabor

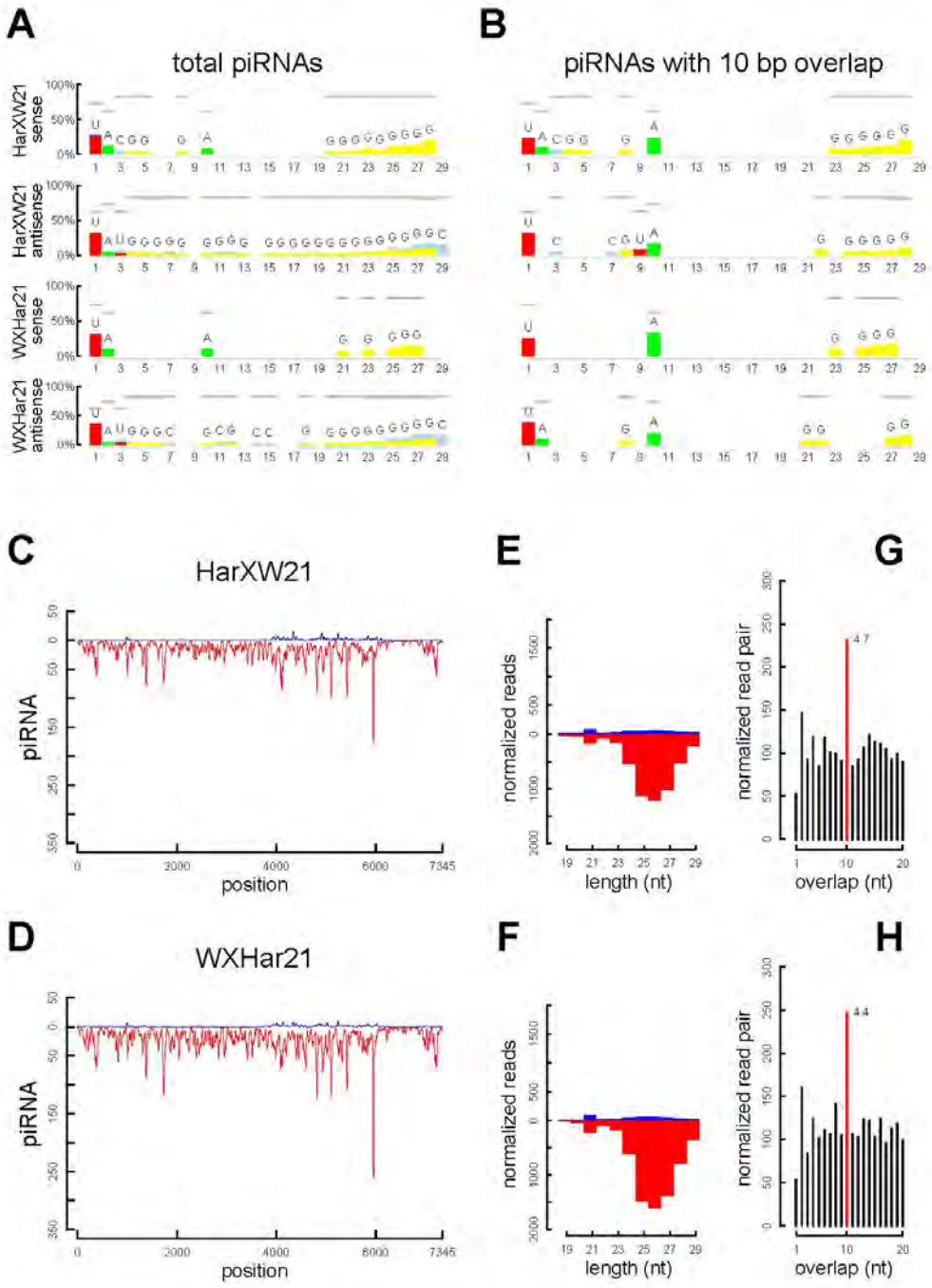
A
total piRNAs
B
piRNAs with 10 bp overlap
HarXW21 sense
HarXW21 antisense
WXHar21 sense
WXHar21 antisense
C
HarXW21
piRNA
position
D
WXHar21
piRNA
position
E
normalized reads
length (nt)
F
normalized reads
length (nt)
G
normalized read pair
overlap (nt)
4.7
H
normalized read pair
overlap (nt)
4.4

TAHRE

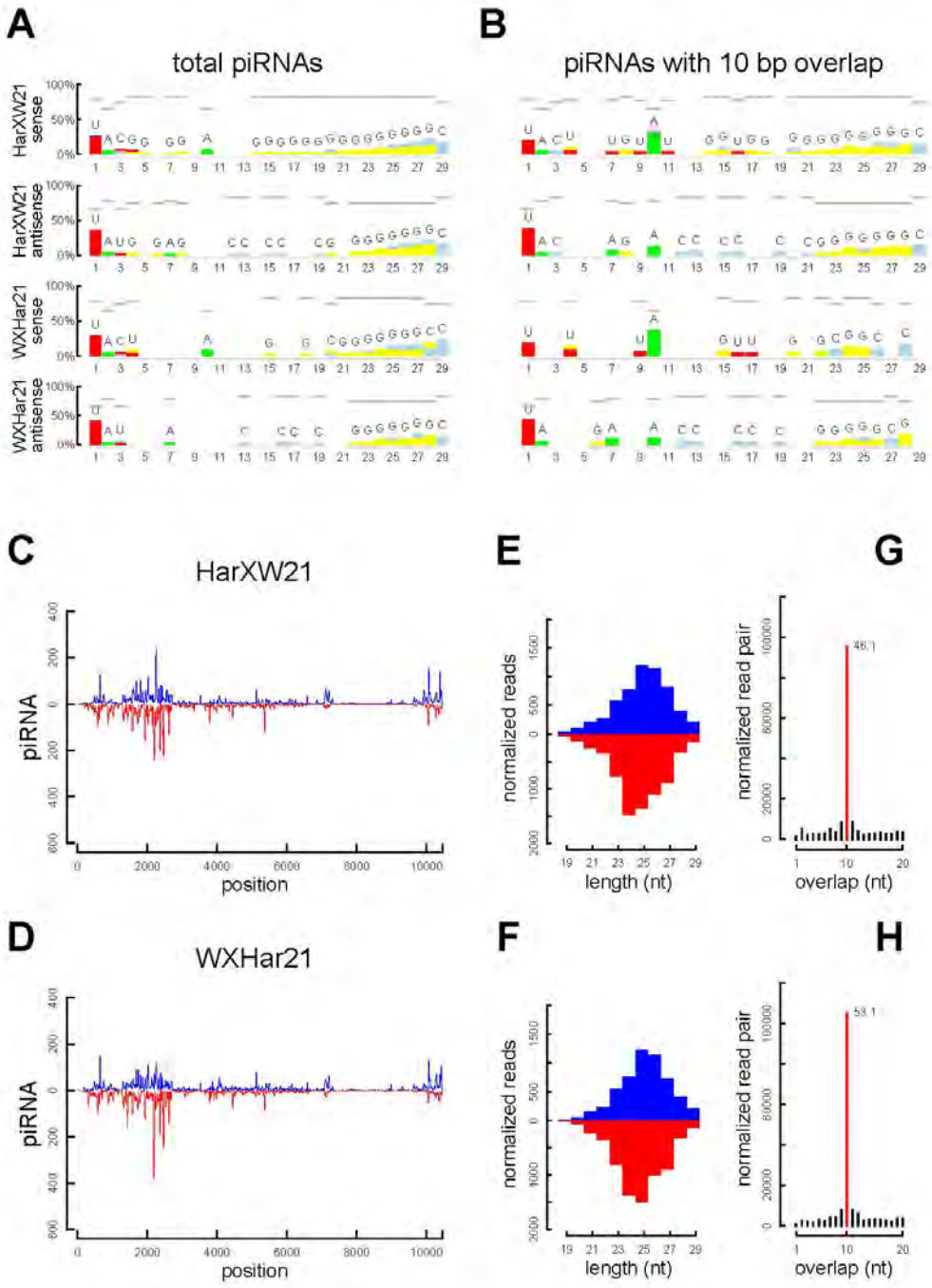
A
total piRNAs
B
piRNAs with 10 bp overlap
HarXW21 sense
HarXW21 antisense
WXHar21 sense
WXHar21 antisense
C
HarXW21
piRNA
position
D
WXHar21
piRNA
position
E
normalized reads
length (nt)
F
normalized reads
length (nt)
G
normalized read pair
overlap (nt)
46.1
H
normalized read pair
overlap (nt)
58.1

TART C TART B TART A

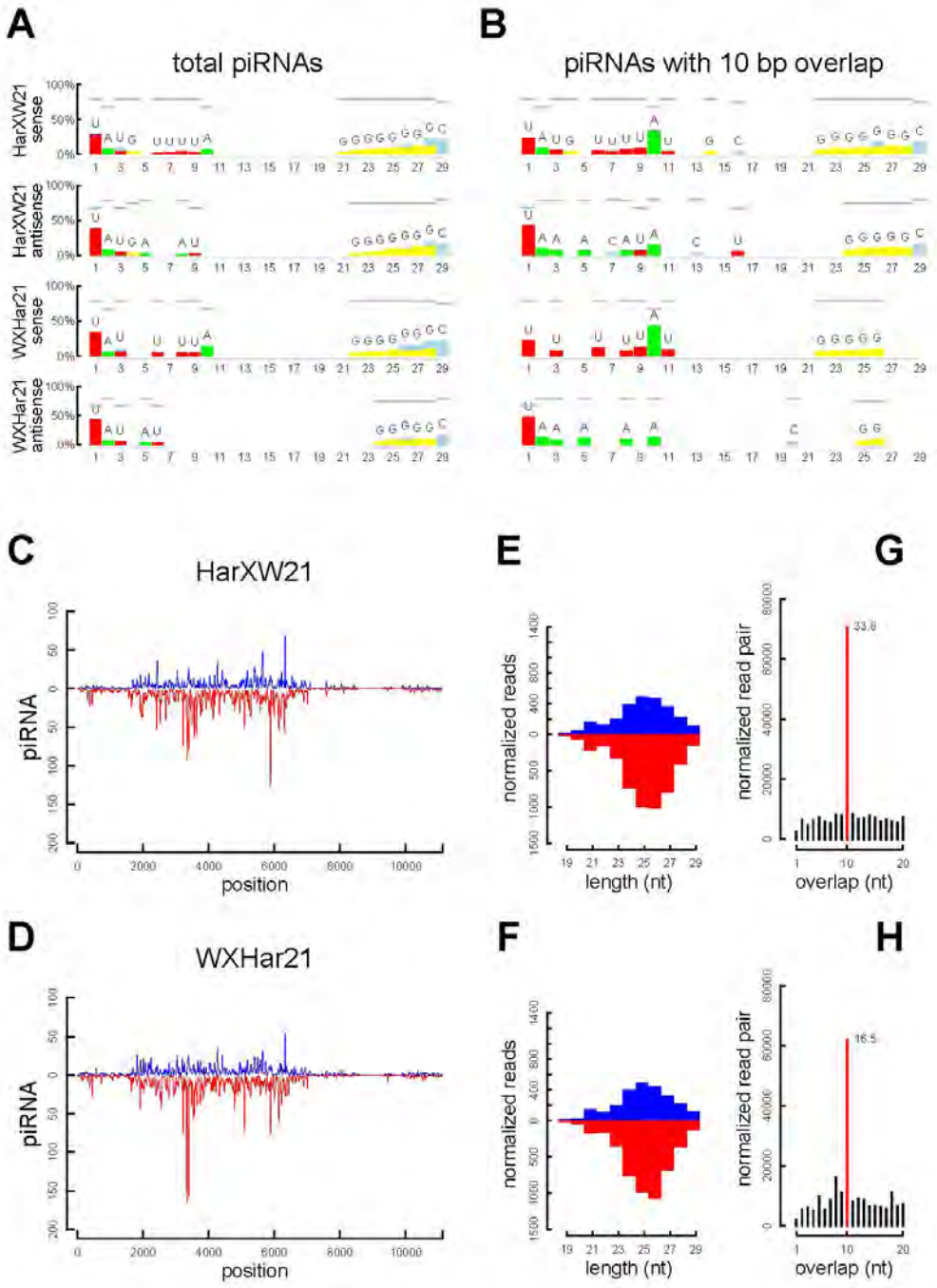

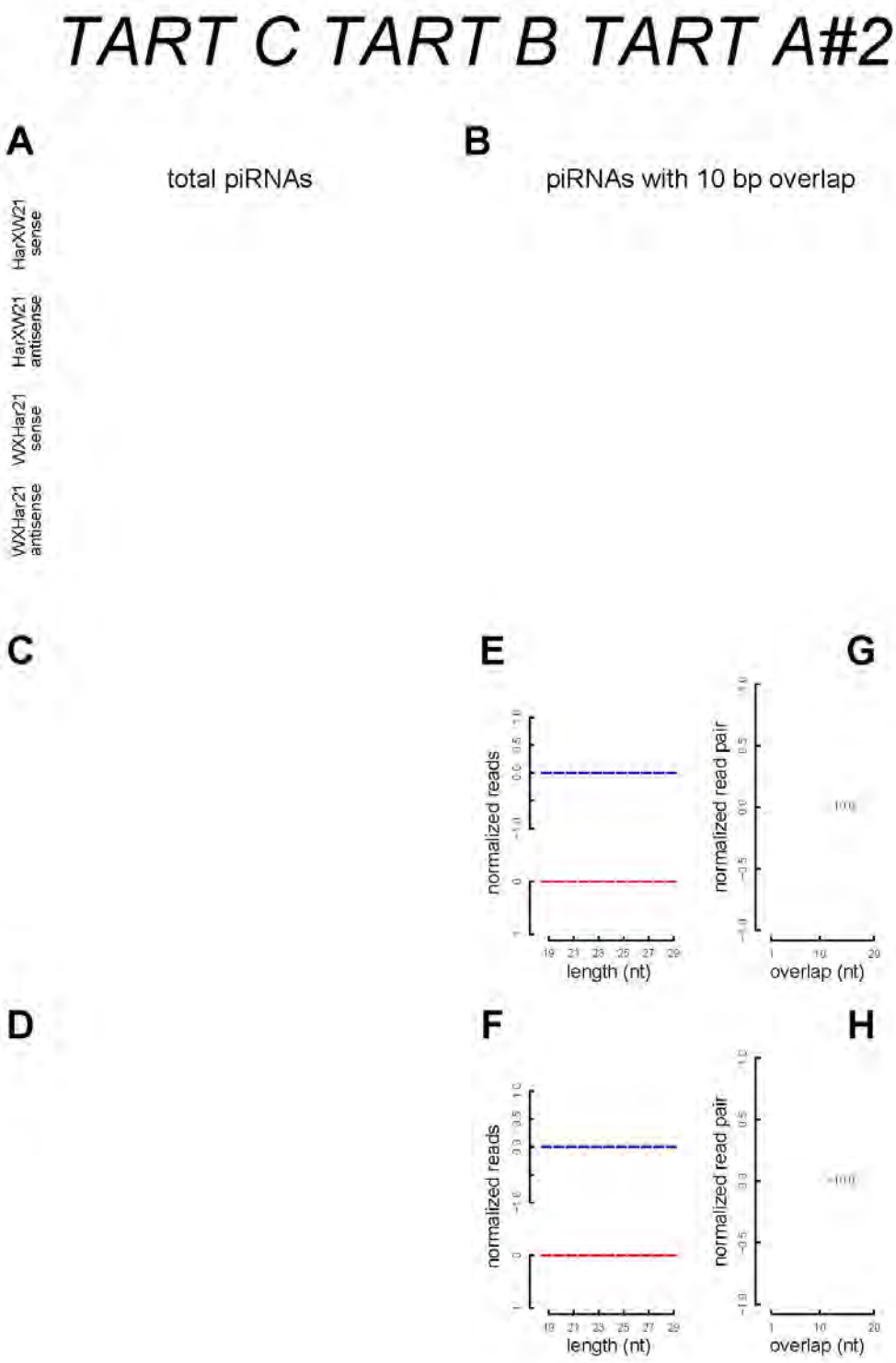
TART C TART B TART A#2
A
total piRNAs
B
piRNAs with 10 bp overlap
HarXW21 sense
HarXW21 antisense
WXHar21 sense
WXHar21 antisense
C
D
E
F
G
H
normalized reads
length (nt)
normalized read pair
overlap (nt)

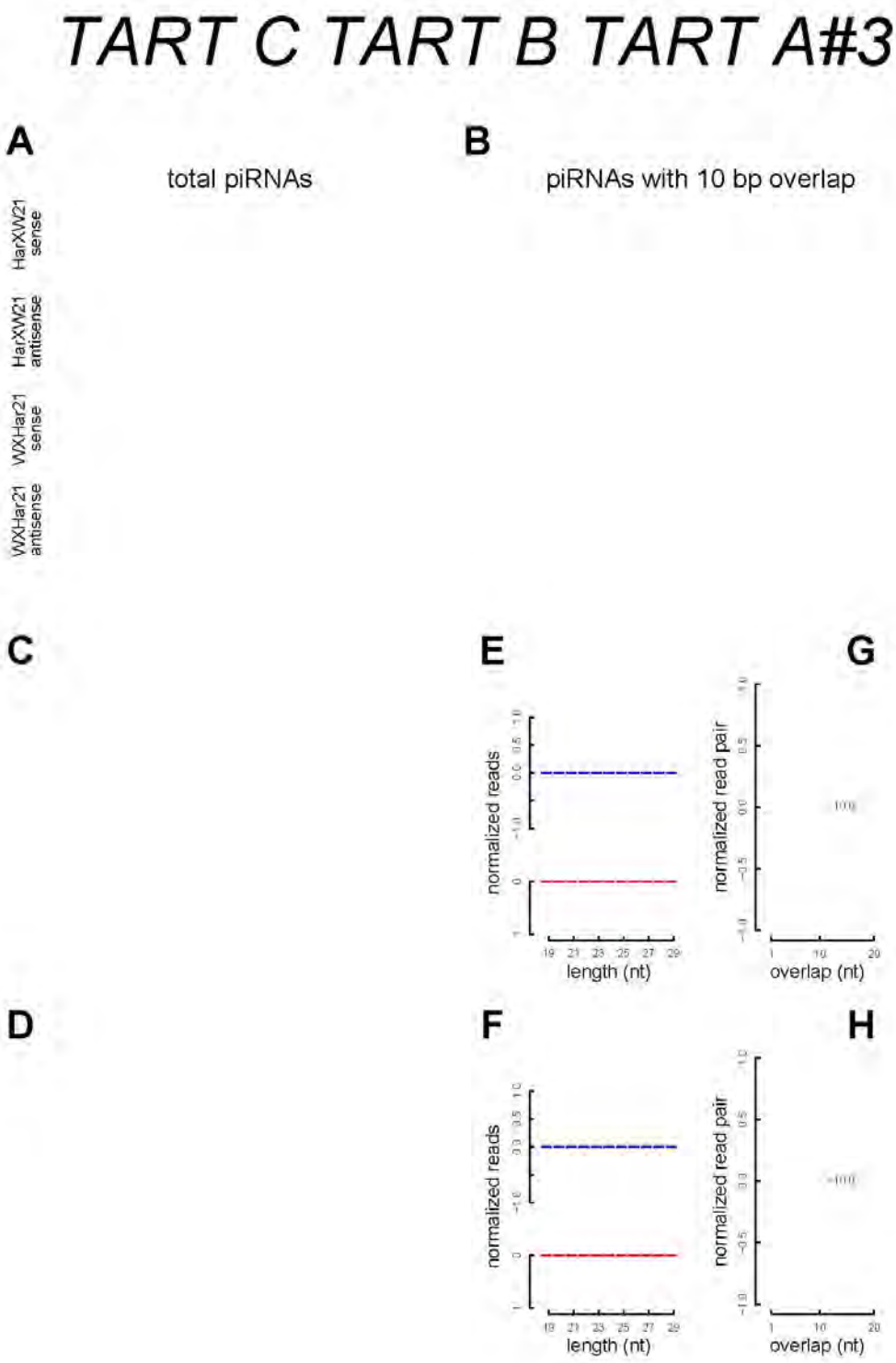
TART C TART B TART A#3
A
total piRNAs
B
piRNAs with 10 bp overlap
HarXW21 sense
HarXW21 antisense
WXHar21 sense
WXHar21 antisense
C
D
E
F
G
H
normalized reads
length (nt)
normalized read pair
overlap (nt)

Tc1

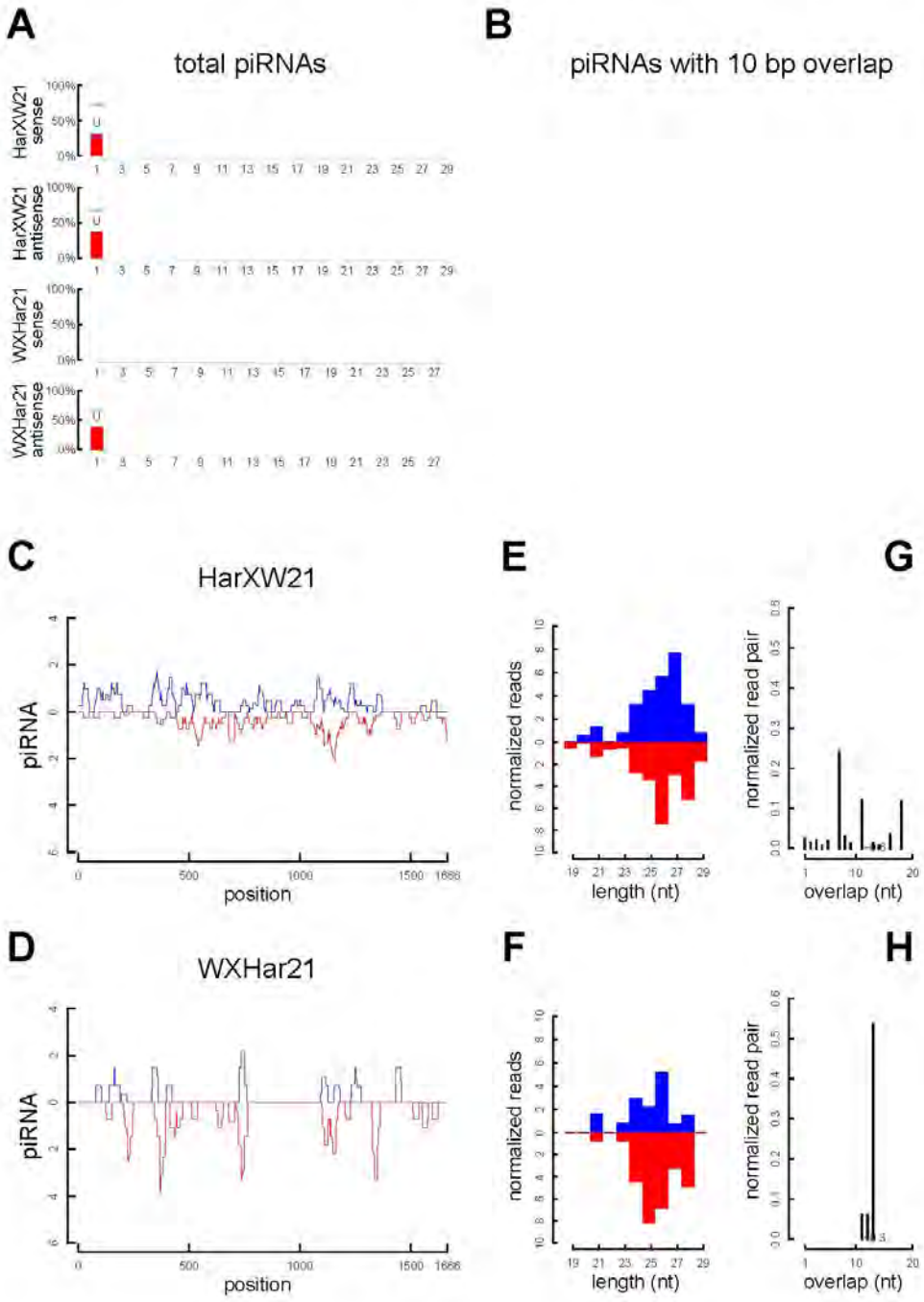
A
total piRNAs
B
piRNAs with 10 bp overlap
HarXW21 sense
HarXW21 antisense
WXHar21 sense
WXHar21 antisense
C
HarXW21
piRNA
position
D
WXHar21
piRNA
position
E
normalized reads
length (nt)
F
normalized reads
length (nt)
G
normalized read pair
overlap (nt)
H
normalized read pair
overlap (nt)

Tc1 2

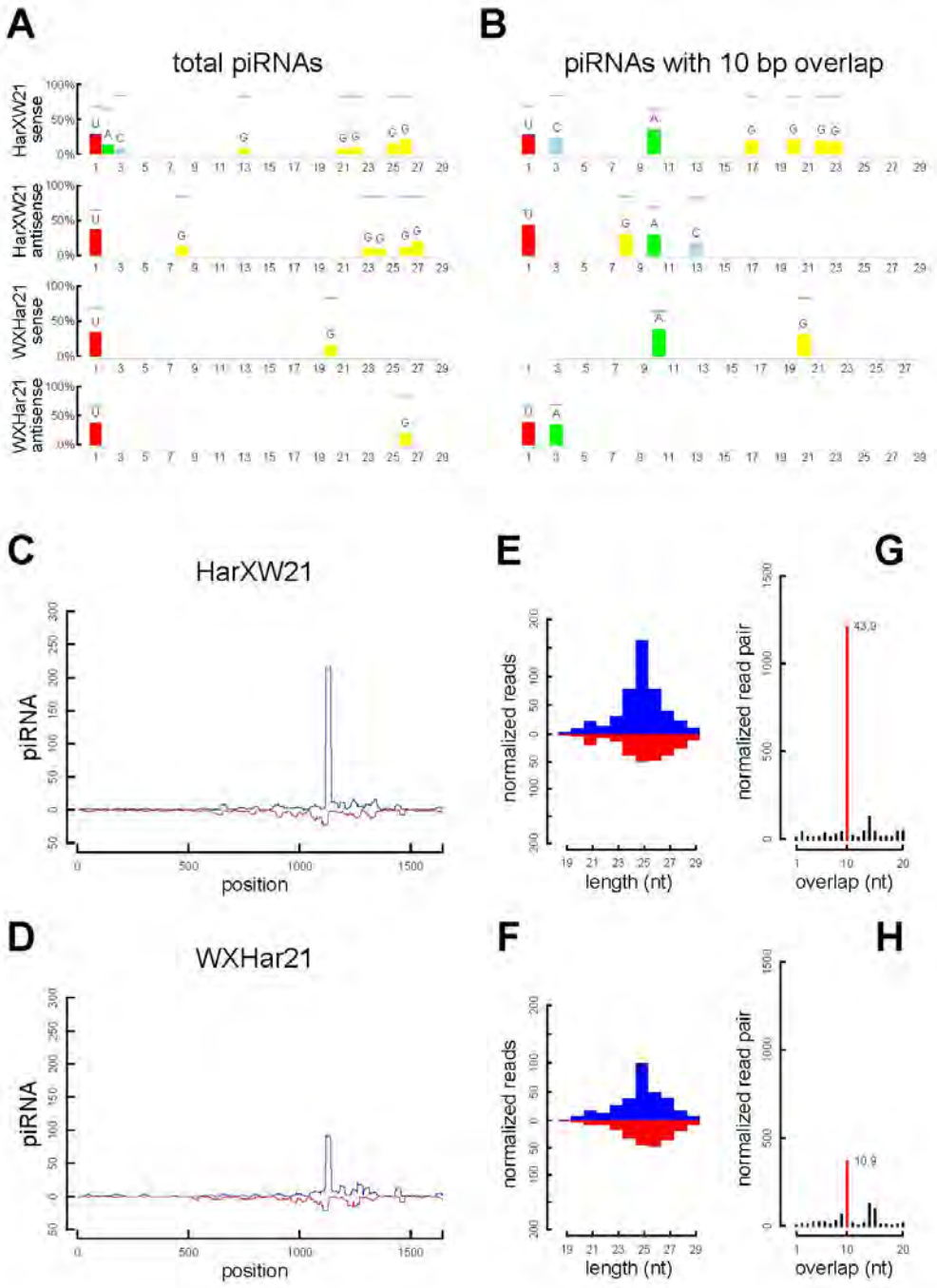
A
total piRNAs
B
piRNAs with 10 bp overlap
HarXW21 sense
HarXW21 antisense
WXHar21 sense
WXHar21 antisense
C
HarXW21
piRNA
position
D
WXHar21
piRNA
position
E
normalized reads
length (nt)
F
normalized reads
length (nt)
G
normalized read pair
43.9
overlap (nt)
H
normalized read pair
10.9
overlap (nt)

Tc3

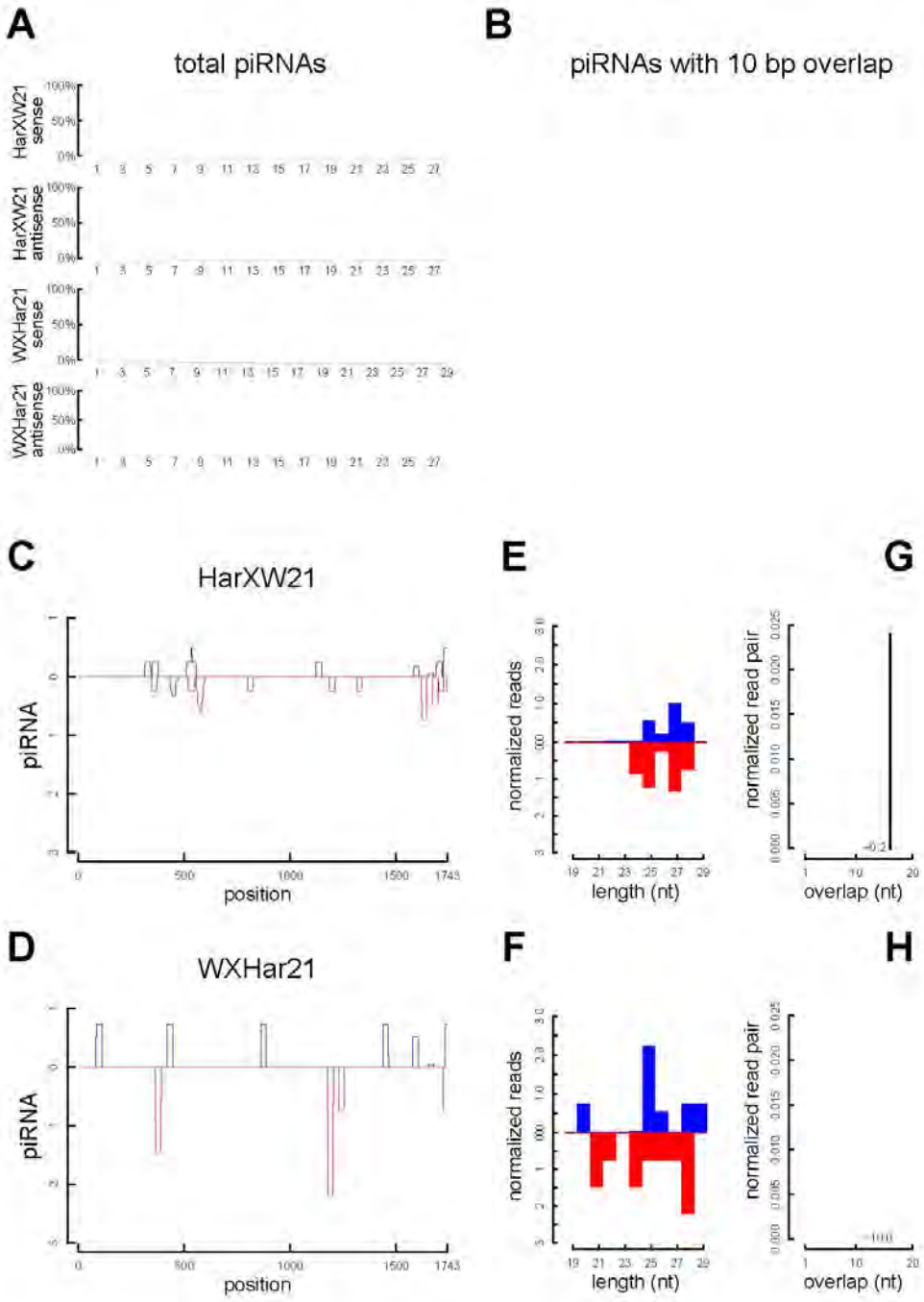
A
total piRNAs
B
piRNAs with 10 bp overlap
HarXW21 sense
HarXW21 antisense
WXHar21 sense
WXHar21 antisense
C
HarXW21
piRNA
position
D
WXHar21
piRNA
position
E
normalized reads
length (nt)
F
normalized reads
length (nt)
G
normalized read pair
overlap (nt)
H
normalized read pair
overlap (nt)

Tirant

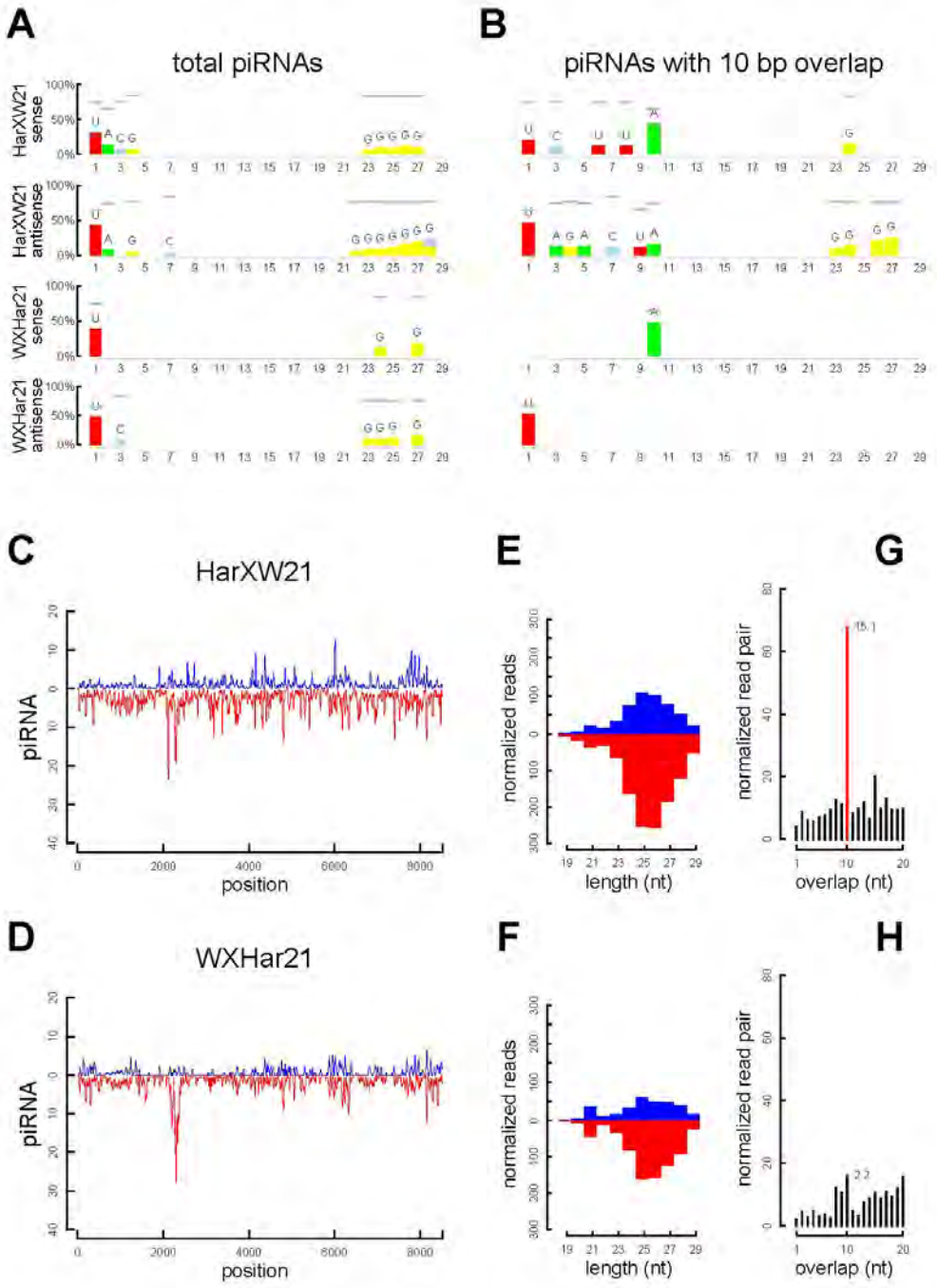
A
total piRNAs
B
piRNAs with 10 bp overlap
HarXW21 sense
HarXW21 antisense
WXHar21 sense
WXHar21 antisense
C
HarXW21
piRNA
position
D
WXHar21
piRNA
position
E
normalized reads
length (nt)
F
normalized reads
length (nt)
G
normalized read pair
overlap (nt)
H
normalized read pair
overlap (nt)

Tom1

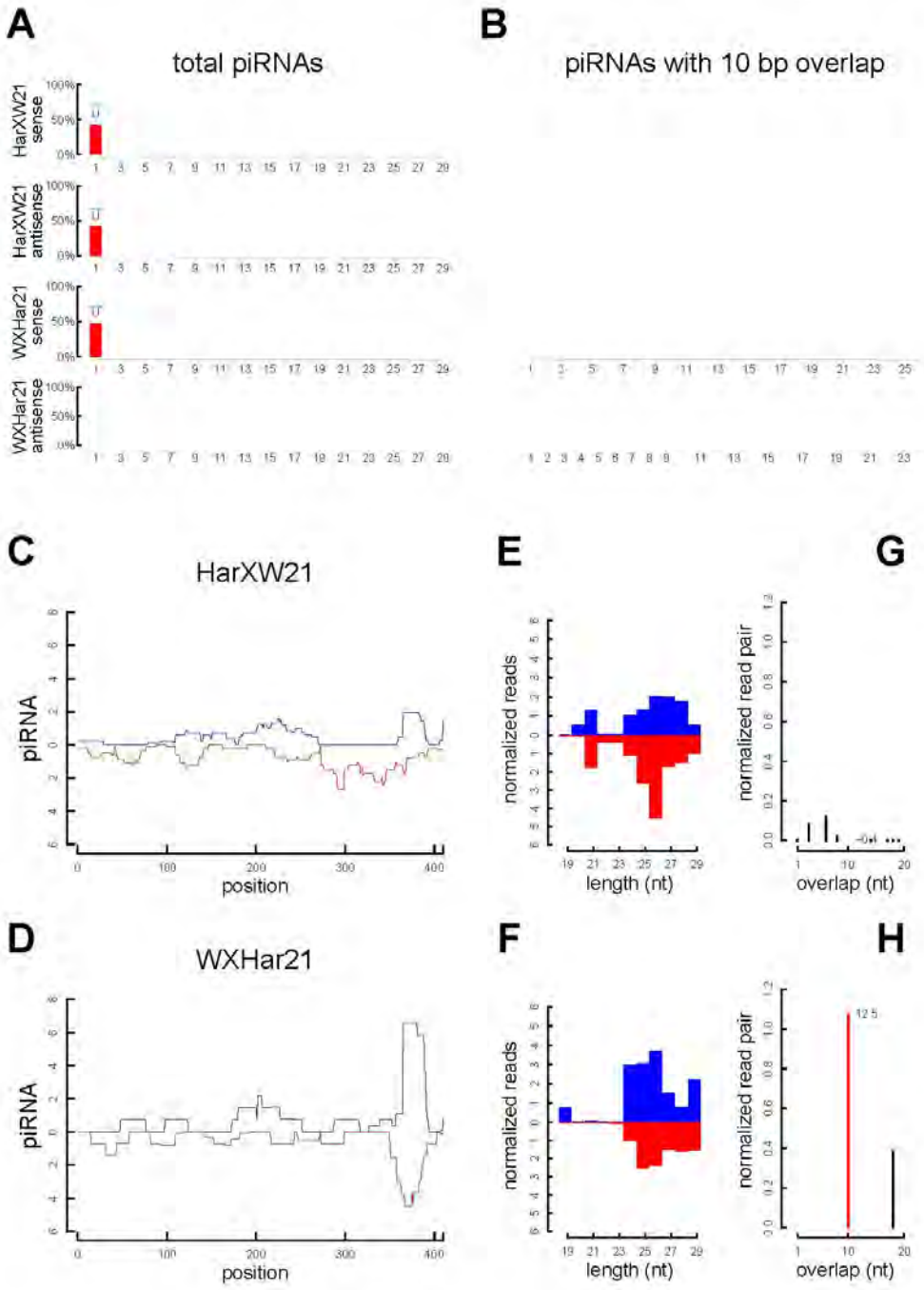
A
total piRNAs
HarXW21 sense
HarXW21 antisense
WXHar21 sense
WXHar21 antisense
B
piRNAs with 10 bp overlap
C
HarXW21
piRNA
position
D
WXHar21
piRNA
position
E
normalized reads
length (nt)
F
normalized reads
length (nt)
G
normalized read pair
overlap (nt)
H
normalized read pair
overlap (nt)

transib1

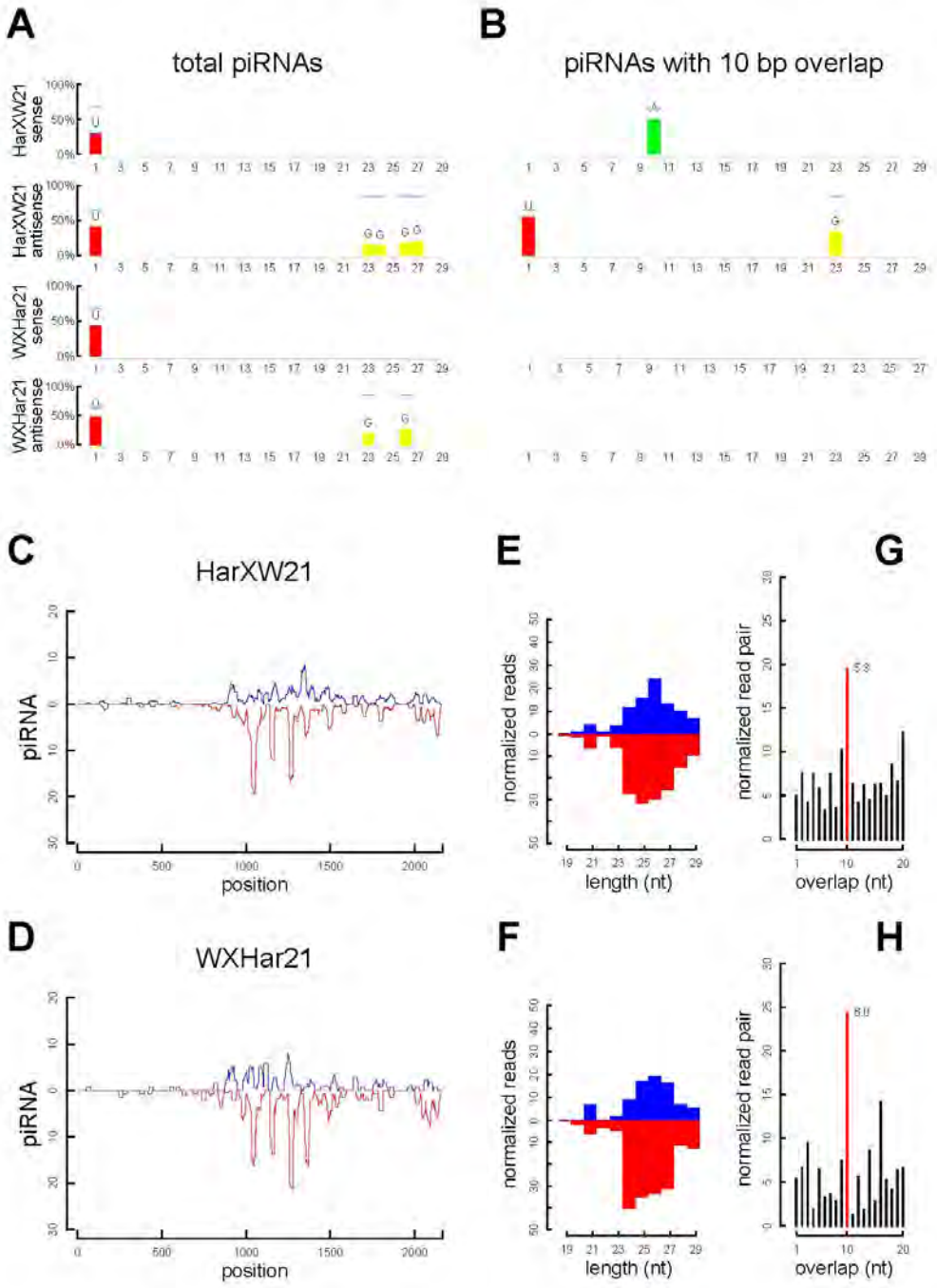
A
total piRNAs
HarXW21 sense
HarXW21 antisense
WXHar21 sense
WXHar21 antisense
B
piRNAs with 10 bp overlap
C
HarXW21
piRNA
position
D
WXHar21
piRNA
position
E
normalized reads
length (nt)
F
normalized reads
length (nt)
G
normalized read pair
overlap (nt)
H
normalized read pair
overlap (nt)

transib2

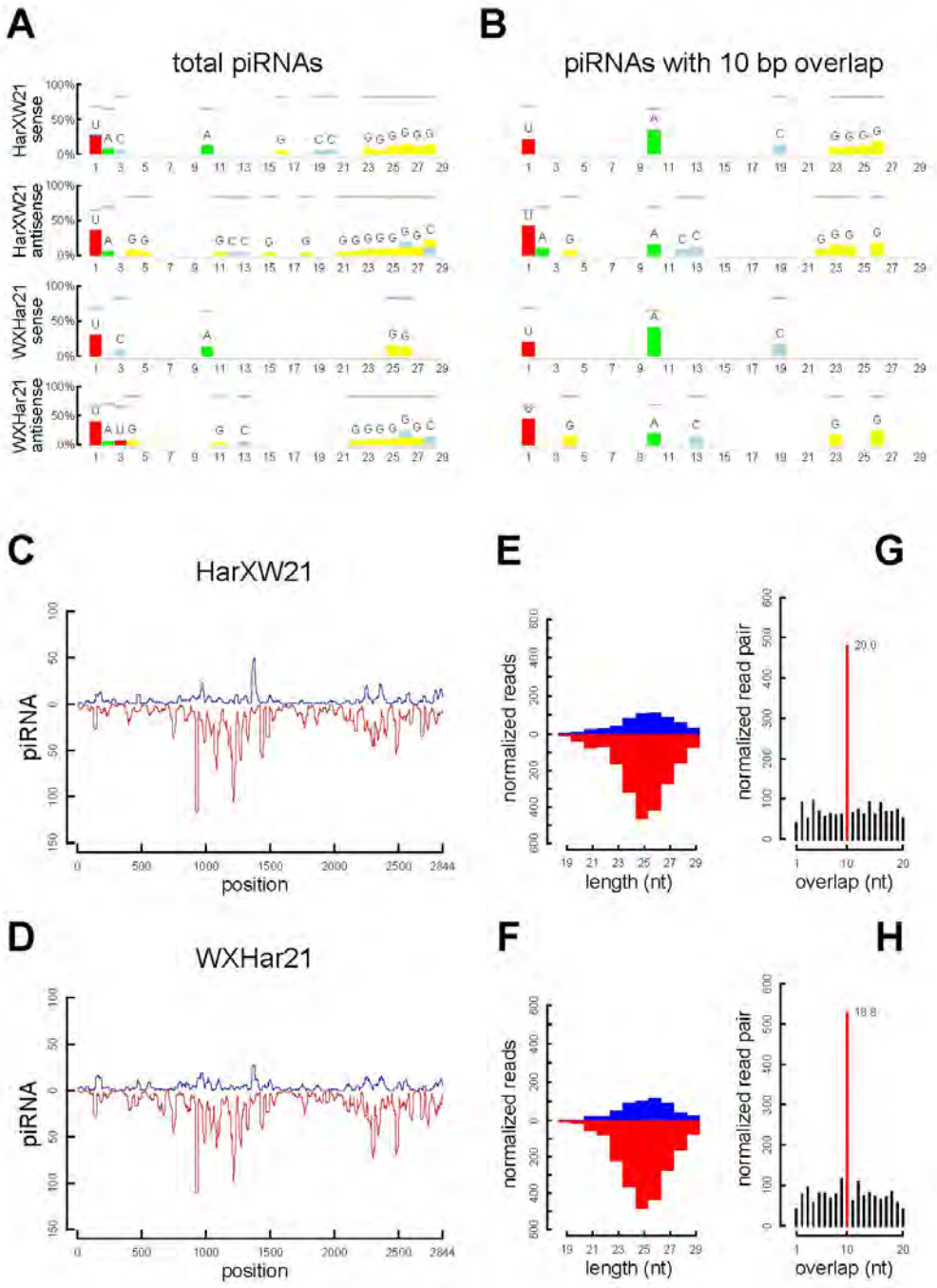
A
total piRNAs
B
piRNAs with 10 bp overlap
HarXW21 sense
HarXW21 antisense
WXHar21 sense
WXHar21 antisense
C
HarXW21
D
WXHar21
piRNA
position
E
F
normalized reads
length (nt)
G
H
normalized read pair
overlap (nt)
20.0
18.8

transib3

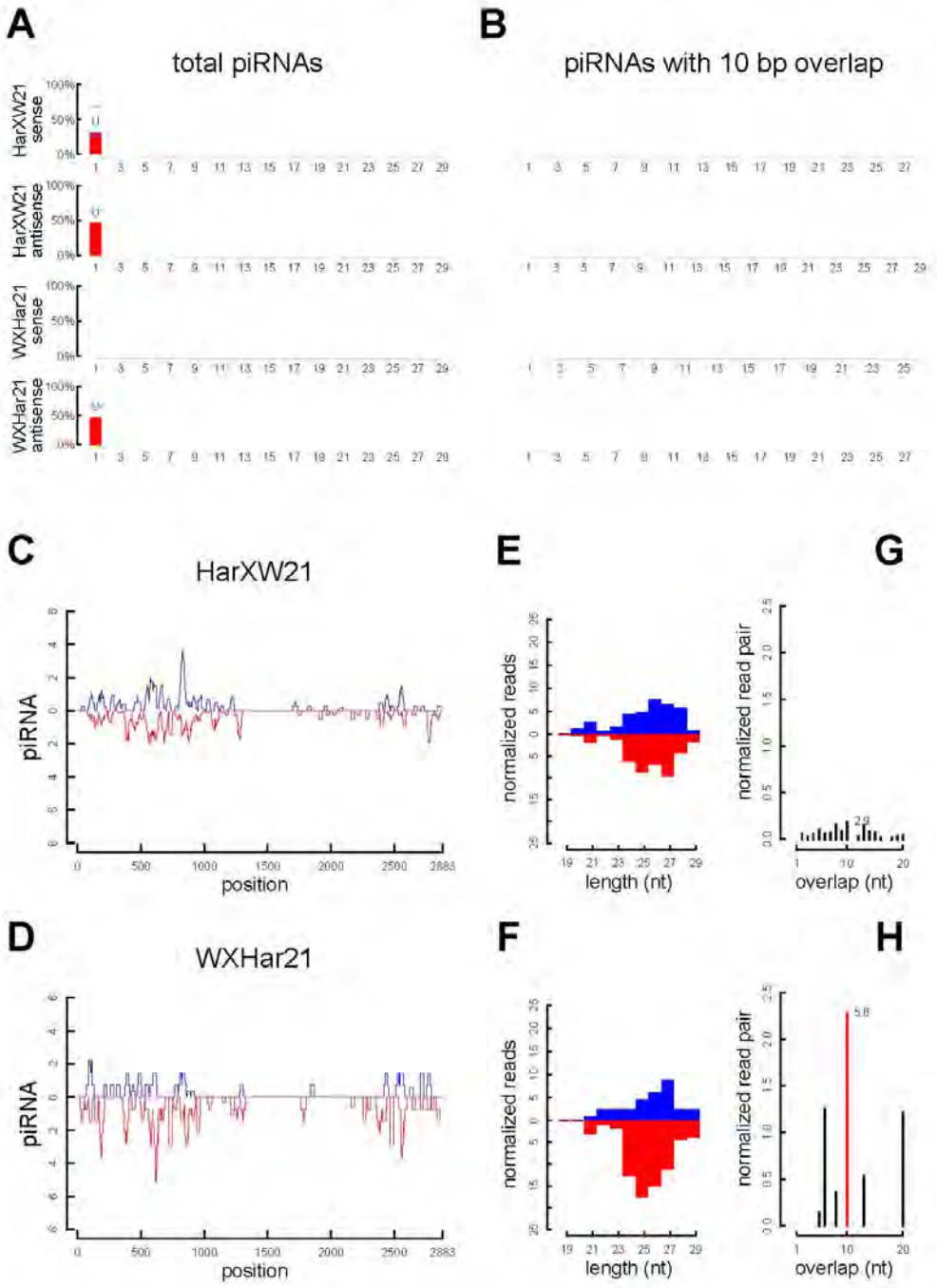
A
total piRNAs
B
piRNAs with 10 bp overlap
HarXW21 sense
HarXW21 antisense
WXHar21 sense
WXHar21 antisense
C
HarXW21
piRNA
position
D
WXHar21
piRNA
position
E
normalized reads
length (nt)
F
normalized reads
length (nt)
G
normalized read pair
overlap (nt)
H
normalized read pair
overlap (nt)

transib4

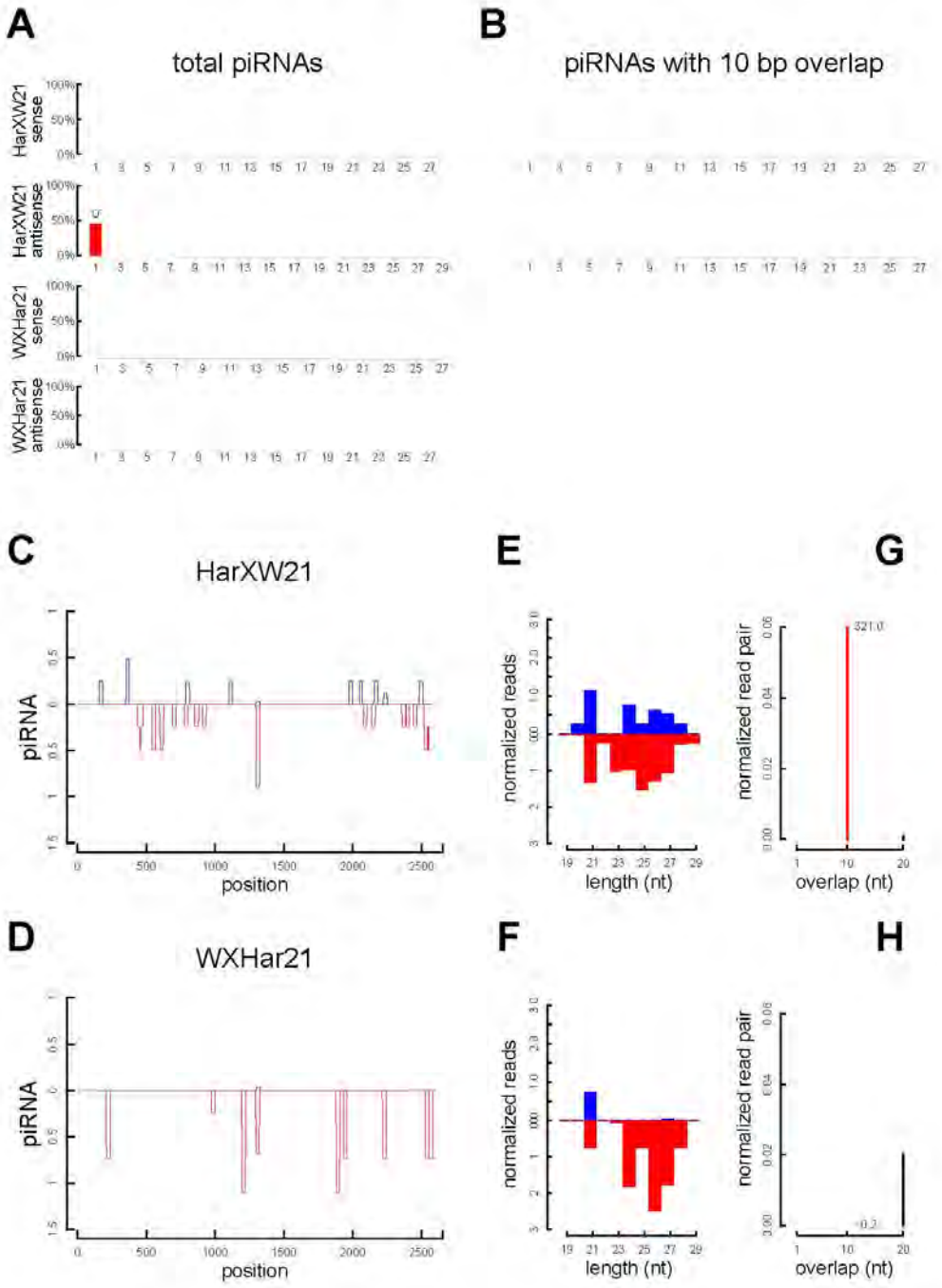
A
total piRNAs
HarXW21 sense
HarXW21 antisense
WXHar21 sense
WXHar21 antisense
B
piRNAs with 10 bp overlap
C
HarXW21
piRNA
position
D
WXHar21
piRNA
position
E
normalized reads
length (nt)
F
normalized reads
length (nt)
G
normalized read pair
321.0
overlap (nt)
H
normalized read pair
overlap (nt)

Transpac

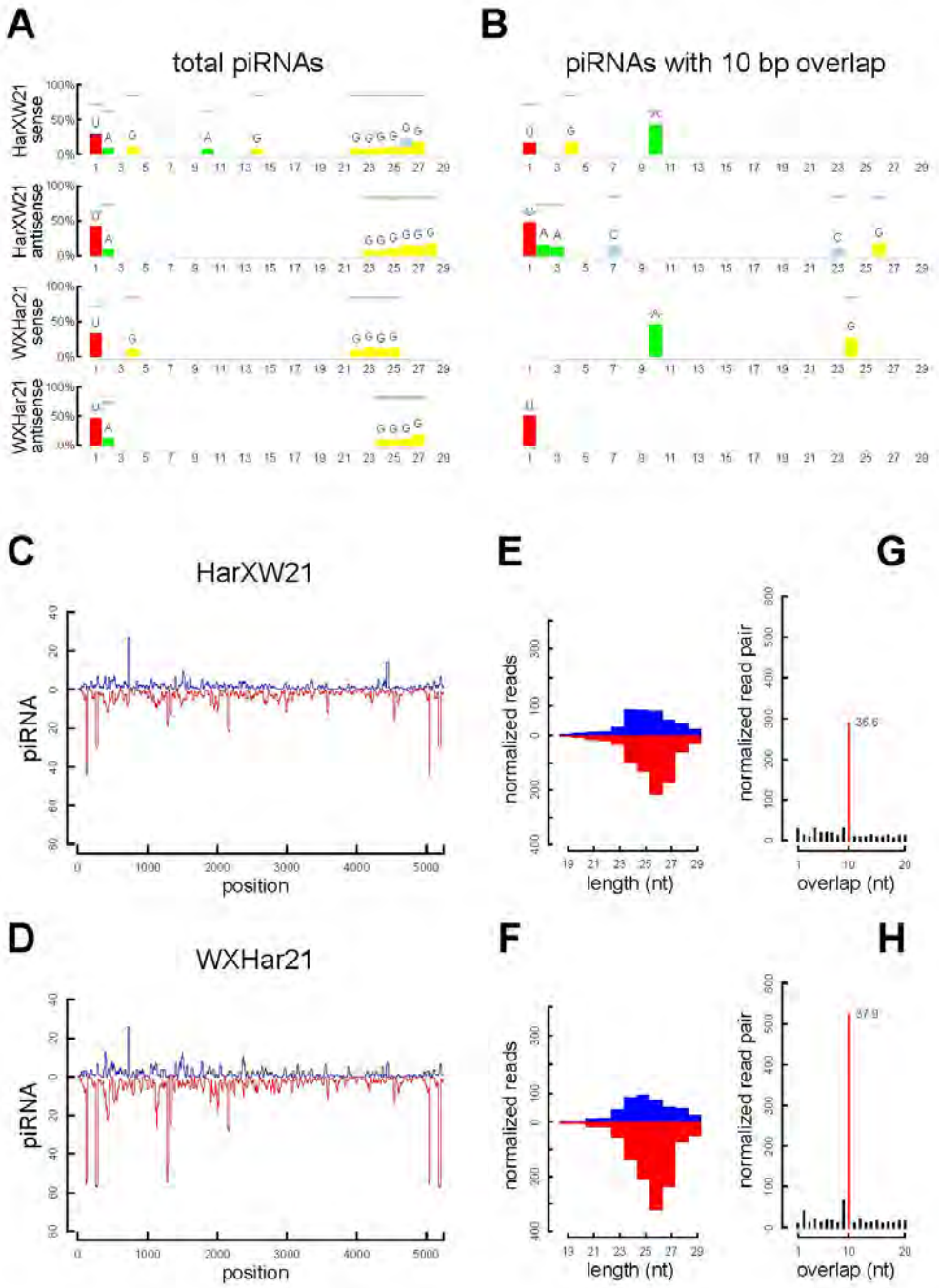
A
total piRNAs
B
piRNAs with 10 bp overlap
HarXW21 sense
HarXW21 antisense
WXHar21 sense
WXHar21 antisense
C
HarXW21
D
WXHar21
piRNA
position
E
F
normalized reads
length (nt)
G
H
normalized read pair
overlap (nt)
36.6
57.9

X element

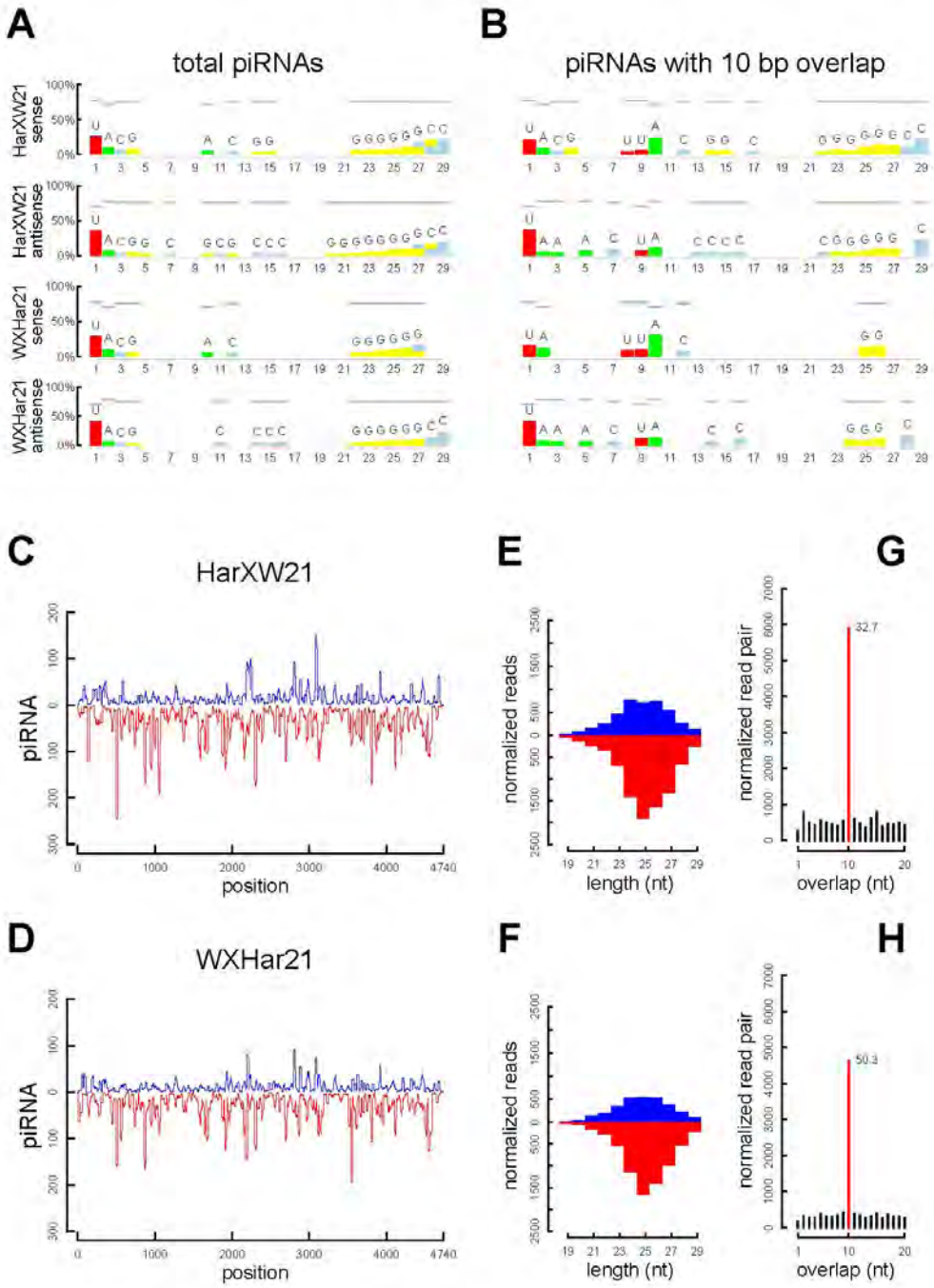
A
total piRNAs
B
piRNAs with 10 bp overlap
HarXW21 sense
HarXW21 antisense
WXHar21 sense
WXHar21 antisense
C
HarXW21
piRNA
position
D
WXHar21
E
normalized reads
length (nt)
F
G
normalized read pair
overlap (nt)
32.7
H
50.3

ZAM

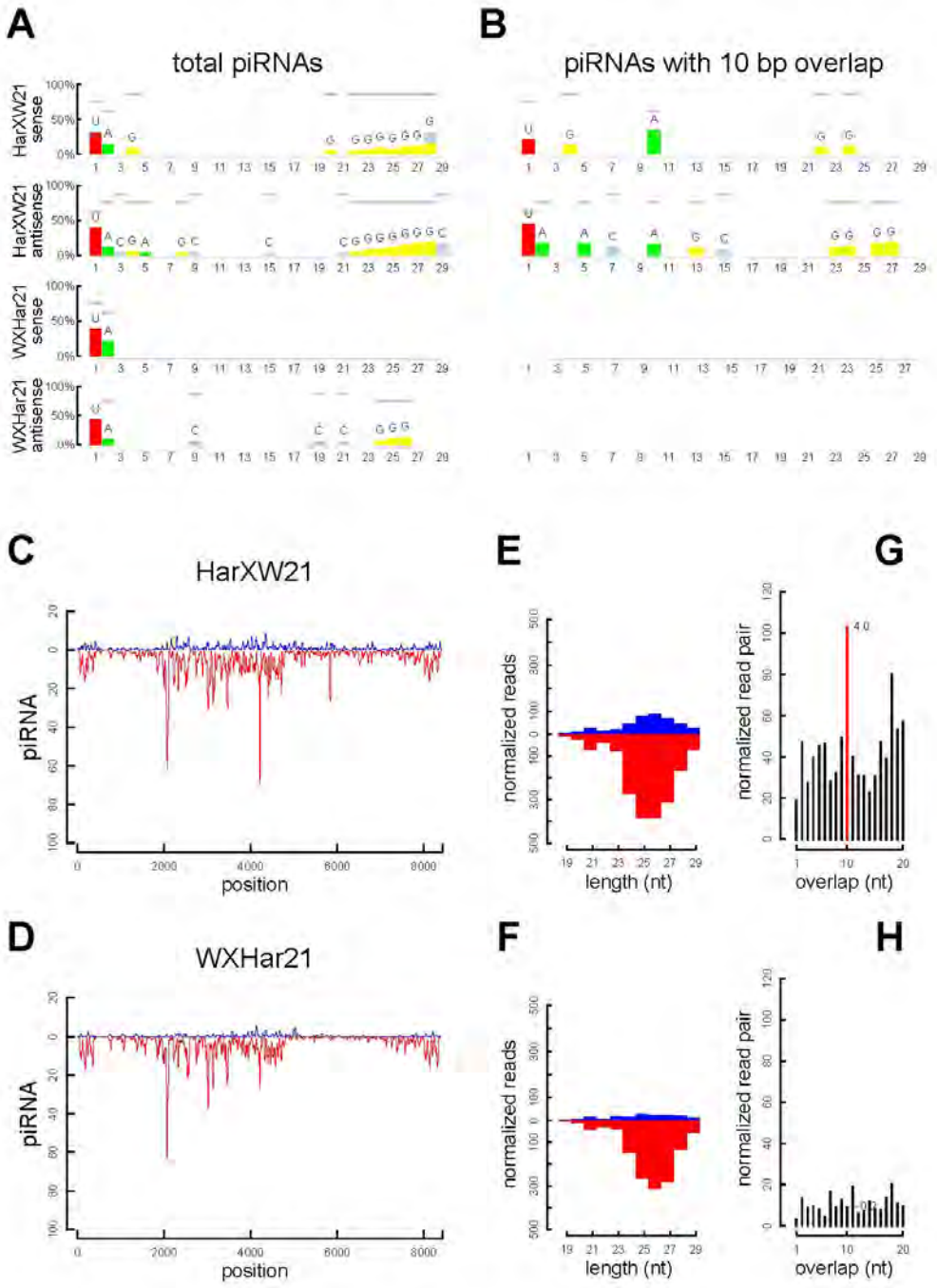
A
total piRNAs
B
piRNAs with 10 bp overlap
HarXW21 sense
HarXW21 antisense
WXHar21 sense
WXHar21 antisense
C
HarXW21
piRNA
position
D
WXHar21
piRNA
position
E
normalized reads
length (nt)
F
normalized reads
length (nt)
G
normalized read pair
overlap (nt)
H
normalized read pair
overlap (nt)

mst40

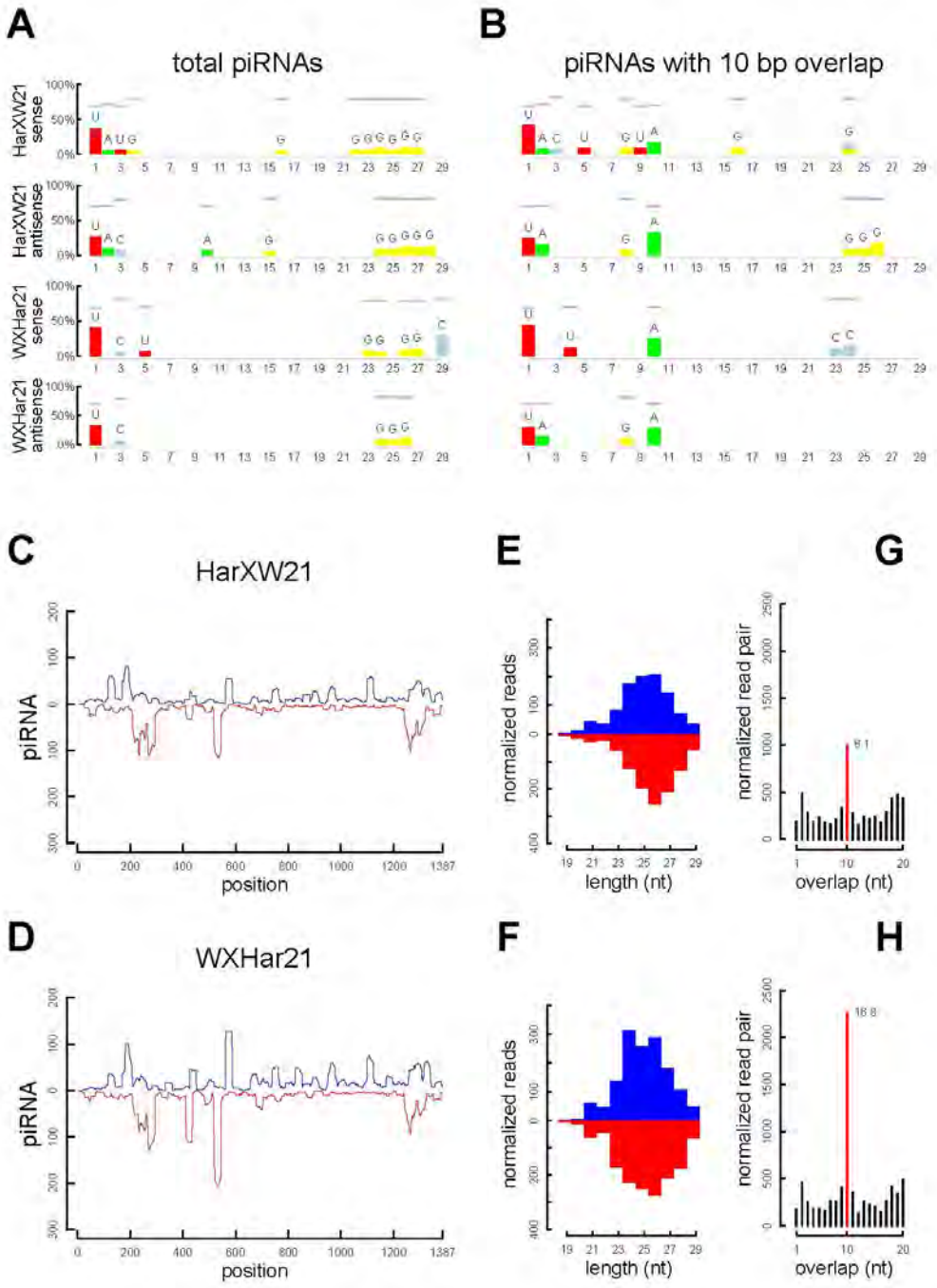
A
total piRNAs
B
piRNAs with 10 bp overlap
HarXW21 sense
HarXW21 antisense
WXHar21 sense
WXHar21 antisense
C
HarXW21
D
WXHar21
piRNA
position
E
F
normalized reads
length (nt)
G
H
normalized read pair
overlap (nt)

suffix

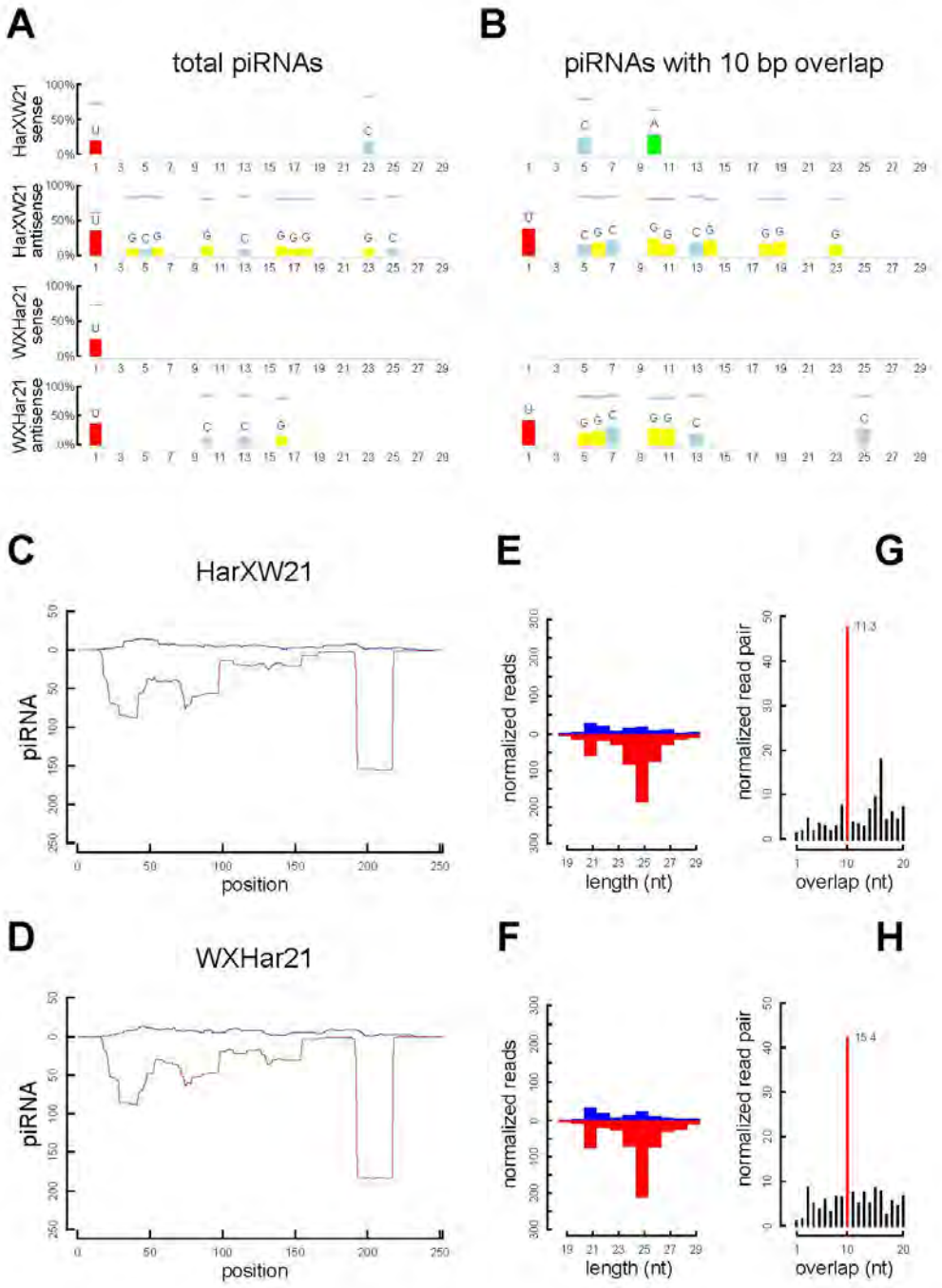
A
total piRNAs
B
piRNAs with 10 bp overlap
HarXW21 sense
HarXW21 antisense
WXHar21 sense
WXHar21 antisense
C
HarXW21
D
WXHar21
piRNA
position
E
F
normalized reads
length (nt)
G
H
normalized read pair
overlap (nt)
11.3
15.4

satellite

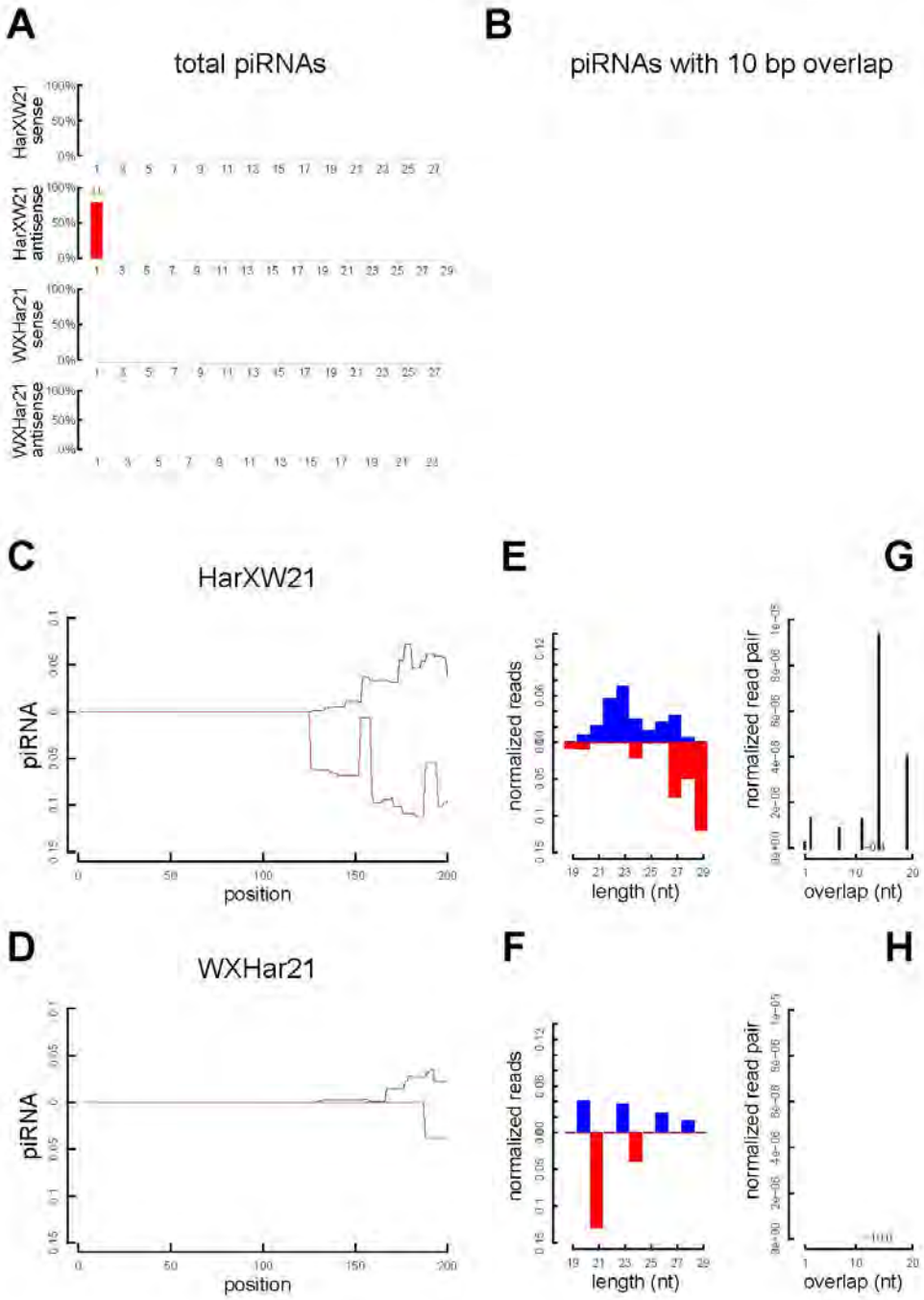
A
total piRNAs
B
piRNAs with 10 bp overlap
HarXW21 sense
HarXW21 antisense
WXHar21 sense
WXHar21 antisense
C
HarXW21
D
WXHar21
piRNA
position
E
F
normalized reads
length (nt)
G
H
normalized read pair
overlap (nt)

stellate

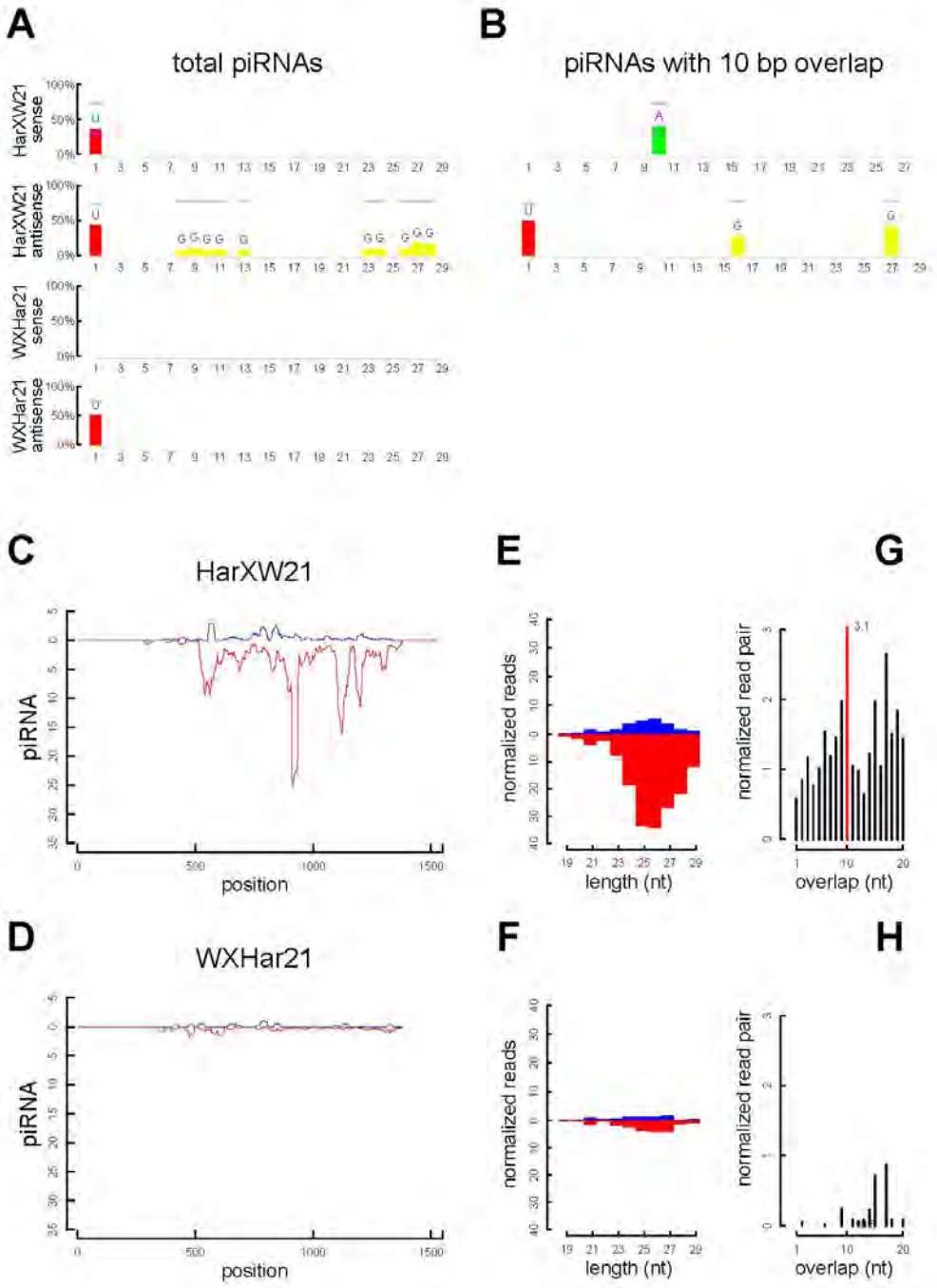
A
total piRNAs
HarXW21 sense
HarXW21 antisense
WXHar21 sense
WXHar21 antisense
B
piRNAs with 10 bp overlap
C
HarXW21
piRNA
position
D
WXHar21
piRNA
position
E
normalized reads
length (nt)
F
normalized reads
length (nt)
G
normalized read pair
overlap (nt)
H
normalized read pair
overlap (nt)

stellateHet

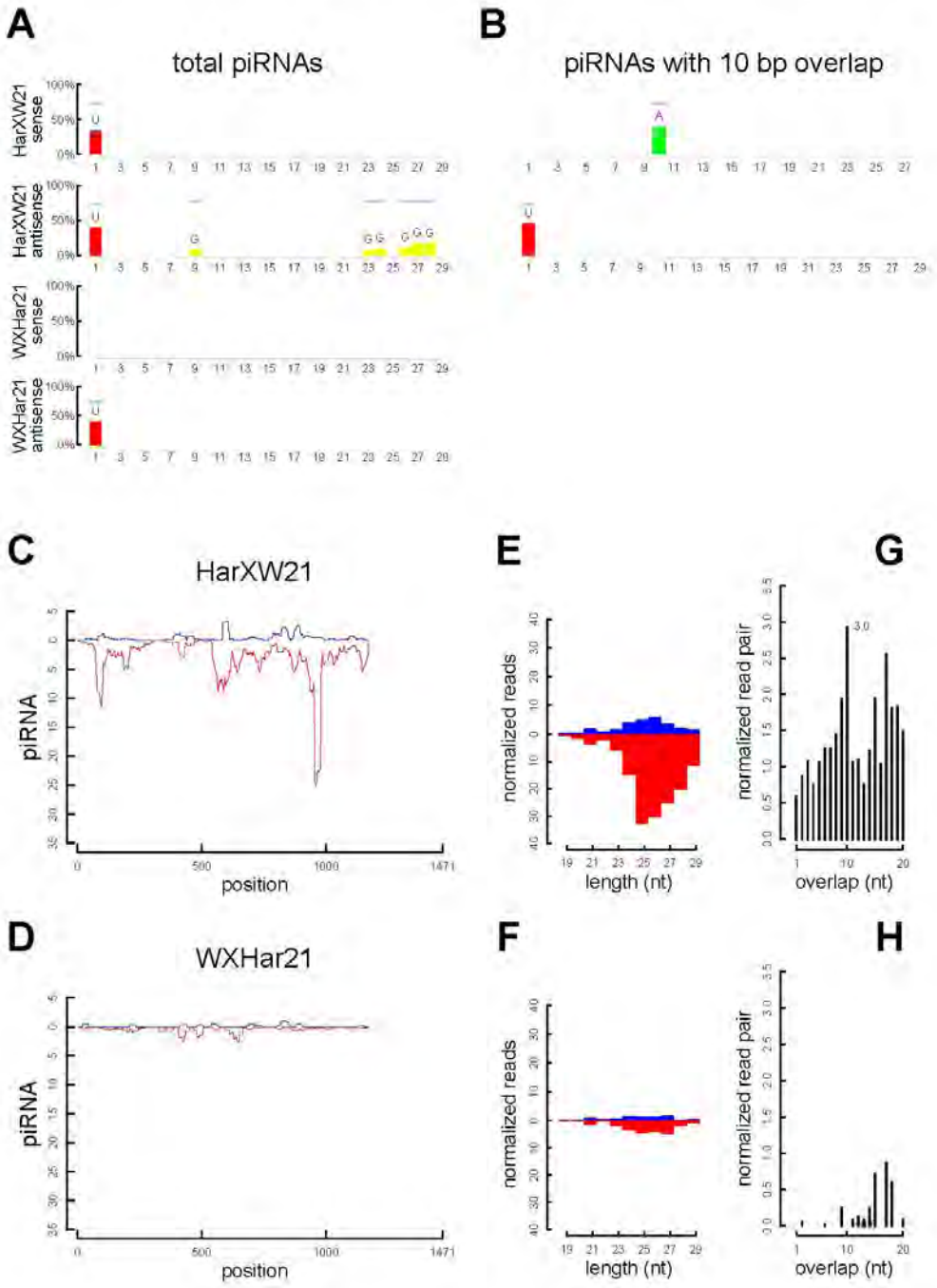

suste

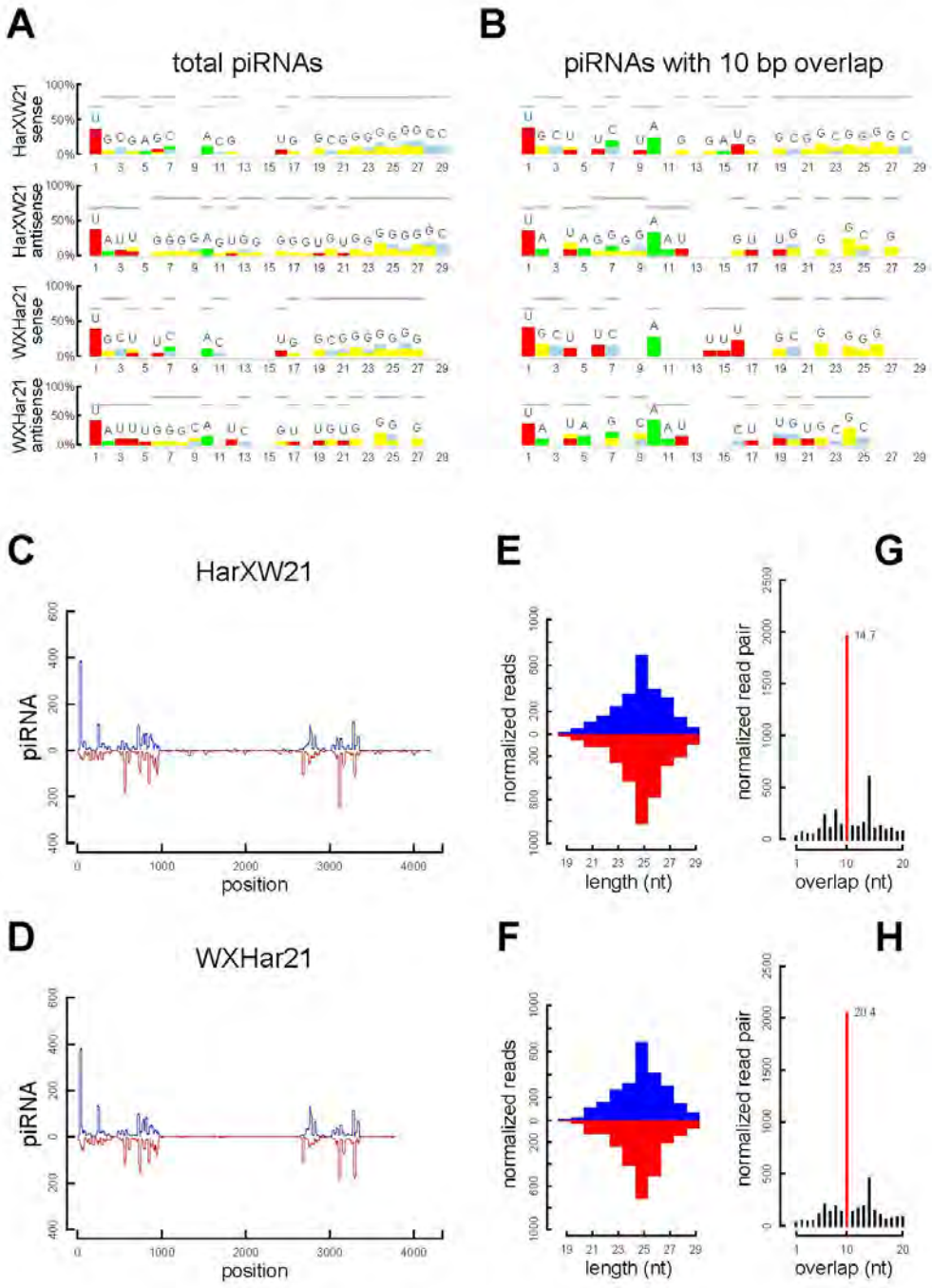
A
total piRNAs
B
piRNAs with 10 bp overlap
HarXW21 sense
HarXW21 antisense
WXHar21 sense
WXHar21 antisense
C
HarXW21
D
WXHar21
piRNA
position
E
F
normalized reads
length (nt)
G
H
normalized read pair
overlap (nt)
14.7
20.4

TARTA

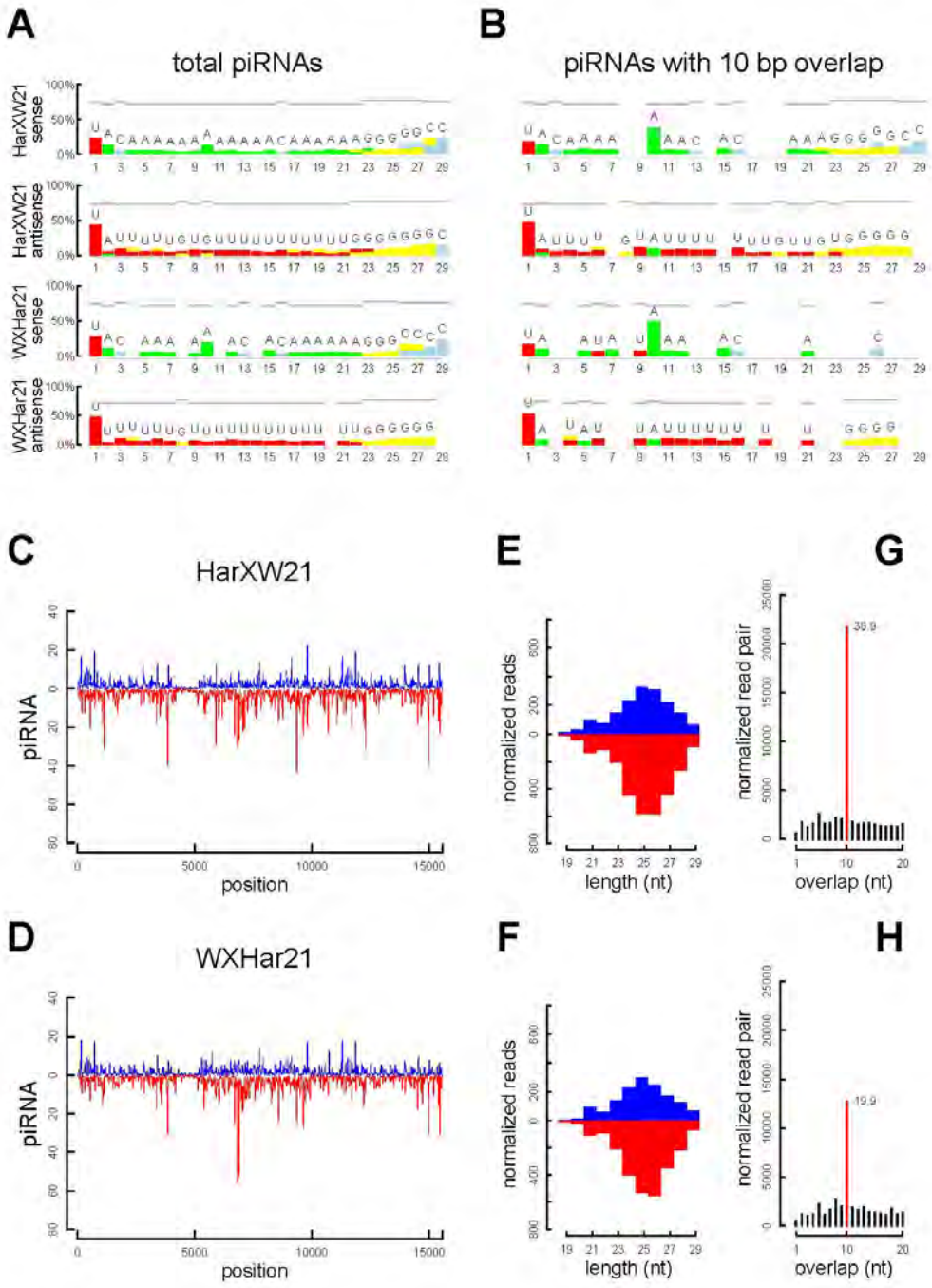
A
total piRNAs
B
piRNAs with 10 bp overlap
HarXW21 sense
HarXW21 antisense
WXHar21 sense
WXHar21 antisense
C
HarXW21
D
WXHar21
piRNA
position
E
F
normalized reads
length (nt)
G
H
normalized read pair
overlap (nt)
36.9
19.9

P-element

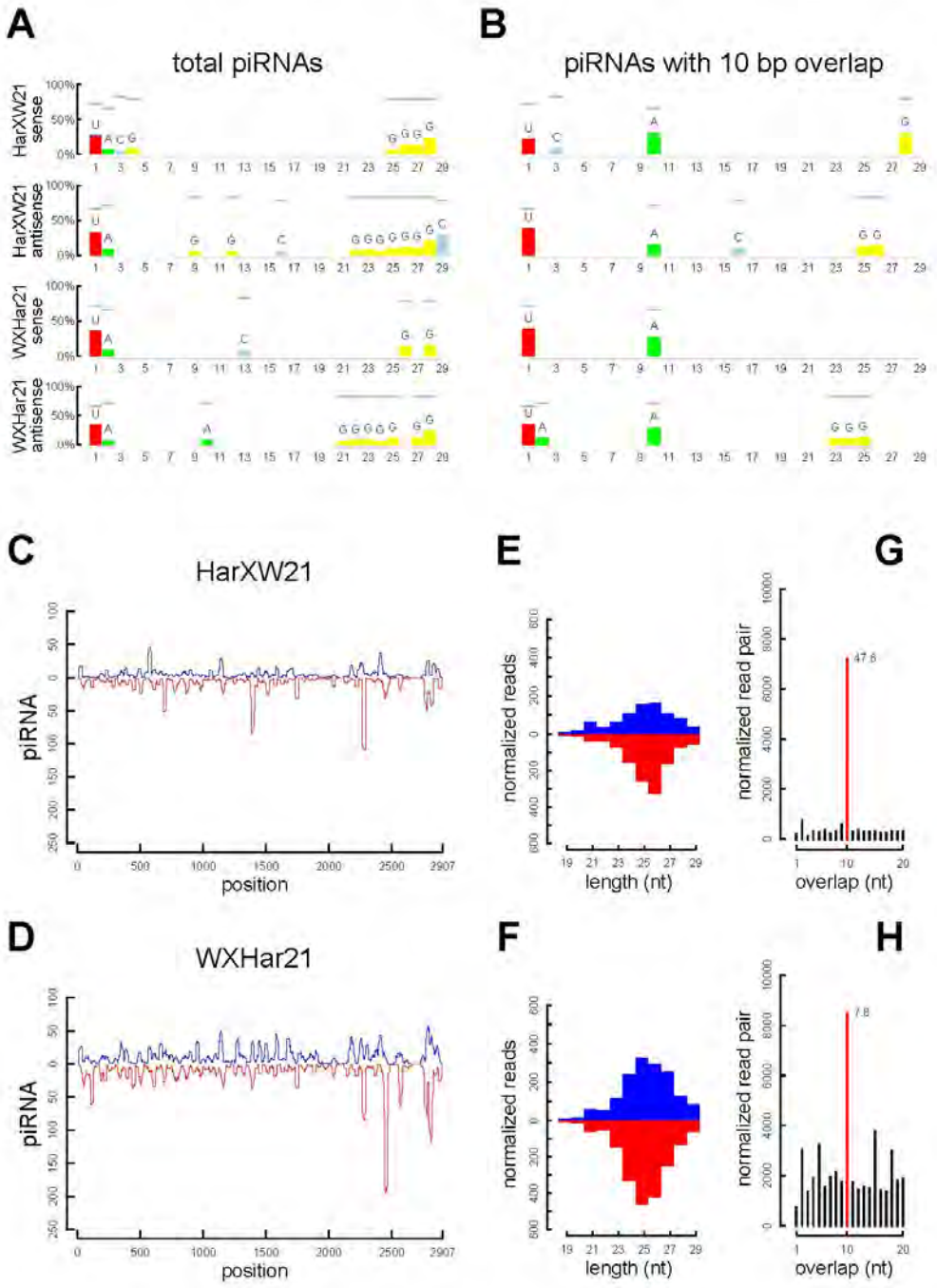
A
total piRNAs
B
piRNAs with 10 bp overlap
HarXW21 sense
HarXW21 antisense
WXHar21 sense
WXHar21 antisense
C
HarXW21
D
WXHar21
piRNA
position
E
F
normalized reads
length (nt)
G
H
normalized read pair
overlap (nt)
47.6
7.8

Materials and Methods

Fly husbandry

All the stocks and crosses were maintained at 25°C on cornmeal medium using standard conditions. *Harwich* stock was obtained from Stephane Ronsseray. w^1 was obtained from Bloomington Stock Center. For the dysgenic cross, w^1 females were mated to *Harwich* males and in the reciprocal cross, *Harwich* females were mated to w^1 males.

Immunohistochemistry

Immunostaining in the ovaries was performed as described earlier using the Buffer A staining protocol (Liu et al., 2002). Briefly, ovaries were dissected in 1X Robb's Medium and fixed in 4% formaldehyde. The staining procedure was followed as per published protocols (Liu et al., 2002). DNA DSBs were labeled using rabbit polyclonal antibody against γ-H2Av at 1:500 (Rockland). Vas protein was visualized using rat monoclonal anti-vasa antibody at 1:10 (Developmental Studies Hybridoma Bank, University of Iowa). TOTO-3 dye (Molecular Probes) was used at 1:500 to stain DNA.

Small RNA extraction and cloning

Total RNA was extracted from 2-4 day old and 21 day old ovaries from dysgenic and reciprocal control hybrids using MirVana kit (Ambion). 18-29 nt small RNAs were gel purified following 2S rRNA depletion and treated using previously published protocol(Li et al., 2009). Small RNA libraries were prepared for sequencing with a Solexa Genome Analyzer (Illumina, San Diego, CA).

RNA extraction and tiling array hybridization

Total RNA was extracted from manually dissected ovaries from 2-4 day old Harwich flies, 2-4 day old and 21-day old *w* x *Har* flies, using RNeasy Kit (Qiagen) using manufacturer's

instructions. Three independent RNA samples from each genotype was assayed as described before (Klattenhoff et al., 2009a).

Strand-specific Reverse Transcriptase PCR

Strand-specific RT-PCR was performed as described before (Klattenhoff et al., 2009a). Total RNA isolated from the ovaries was quantified and equal amounts were used to prepare cDNA using gene-specific primers to amplify specific regions of interest. Signal from a no-primer control was subtracted from the signal from the test primers to get strand-specific result. All the results were normalized against a primer which amplifies piRNA precursors coming from 42AB (Klattenhoff et al., 2009a).

CHAPTER 4

Conclusions and open questions

Introduction

Organisms are constantly exposed to internal and external challenges. At the intracellular level, one major threat to existence comes from genomic parasites or transposons that can move from one site to another in the genome and thus cause mutations and changes in gene expression. These genetic entities were discovered in maize and classified as 'controlling units' by Barbara McClintock in 1950's (McCLINTOCK, 1950), and are now known to be ubiquitous feature of all phyla. With their mobilization potential, transposons can have major effects on genome structure leading to disease causing mutations or contribute to speciation (Chen et al., 2005; Deininger and Batzer, 1999; Iskow et al., 2010; Vidal et al., 2002). Many other cases are known where the host has domesticated the parasite for its own purposes (Lynch and Tristem, 2003; Nowacki et al., 2009; Volff, 2006). Clearly, these symbionts share a whole continuum of relationships with their host ranging from mutualism to parasitism. Nonetheless, their activity in the germline has to be kept under control, to avoid transmission of harmful mutations to the next generation. Given the near universal existence of transposons in genomes, it is not hard to imagine a similar evolutionarily conserved host response against them. In recent years, small RNAs bound to their partner Argonaute proteins have been recognized as a potent immune response targeting transposons. RNAs bound to the PIWI-clade of Argonautes, the piRNAs, contain sequence information which could potentially target transposons and other repetitive elements in the genome. Owing to their role in transposon silencing, the PIWI-piRNA pathway is crucial to germline development in *Drosophila* (reviewed in Chapter 1, this dissertation). Given the

evolutionary conservation of this pathway in diverse animal groups, it is not far-fetched to propose its role in germ cell development in other systems.

piRNA function in zygote genome maintenance

In *Drosophila*, piRNAs are maternally deposited, and mutations that disrupt piRNA pathway function cause germline DNA damage and lead to embryonic lethality. This lethality is independent of the activation of ATR/Chk2 DNA damage signaling, as double mutants between Chk2 and piRNA pathway components are still embryonic lethal (Chen et al., 2007; Klattenhoff et al., 2007; Klattenhoff et al., 2009b; Pane et al., 2007). To define the genesis of the embryonic lethal phenotype, I cytologically analyzed embryos mutant for *aubergine* (*aub*), which encodes a PIWI Argonaute, and *armitage* (*armi*), encoding a putative RNA helicase. Both proteins are essential for piRNA biogenesis and function (Klattenhoff et al., 2009b; Li et al., 2009). Mutations in both these genes cause chromatin fragmentation during early embryonic development. It is possible that DNA breaks, formed earlier in the female germline, are inherited and amplified in mutant embryos. However, I showed that wild-type chromosomes, introduced into piRNA mutant embryos, are fragmented. This experiment shows that the DNA breaks are made *de novo*, indicating that genome maintenance is a key function for this pathway during early zygote development. However, it is possible that transposon RNA and proteins from the female are accumulating in the piRNA mutant embryos, thus compromising genome integrity. So, a true function for piRNA pathway in maintenance of zygotic genome integrity can be assigned if transposon activity is specifically induced in wild-type embryos following fertilization. Such experiments are possible by introducing a new transposon in the zygote through the male and follow early steps in embryogenesis. I have studied female germline

development in progenies from such inter-strain hybrid crosses. Studying earlier events in embryonic development in such cases would be highly informative.

Telomere protection

I found that the subset of embryos mutant for *aub* and *armi* that proceed through mitosis show high rates of telomere fusion, which are suppressed by *ligase IV* mutations that disrupt non-homologous end joining. The telomere protection complex (TPC) prevents recognition of chromosome ends as DNA breaks, and I also found that *aub* and *armi* mutations block recruitment of the TCP proteins HP1a and HOAP to telomeres. These observations suggested that the piRNA pathway is required for assembly of the TPC. The HP1a paralog, Rhino and PIWI Argonaute, Ago3 are required for piRNA biogenesis (Klattenhoff et al., 2009b; Li et al., 2009). I extended my analysis of embryonic lethality in piRNA mutants, *rhi* and *ago3*. Both these mutations lead to chromatin fragmentation with a very high penetrance, consistent with a role for the piRNA pathway in genome maintenance. However, normal mitotic figures were not present and chromosome segregation/telomere fusion could not be cytologically evaluated. I therefore analyzed TPC recruitment in those mutants using ChIP. In contrast to *aub* and *armi* mutants, *ago3* and *rhi* didn't disrupt TPC association with telomeric DNA. These observations raised the possibility that *aub* and *armi* define a branch of the piRNA pathway required for telomere protection.

Telomeres in *Drosophila* are composed of transposon repeats that are silenced by the piRNA pathway. A major cluster on the fourth chromosome encodes up to 80% of the primary piRNAs matching the telomeric transposons *HeT-A, TART* and *TAHRE*. Analysis of the size distribution of small RNAs from this cluster identified a population of 19-22 nt sense strand

species (excluding 21, since they most likely represent endo-siRNAs) that are significantly reduced in *aub* and *armi* mutants, but expressed at near wild type levels in *rhi* and *ago3*. Thus, there is a correlation between loss of 19-22 nt telomere-specific small RNAs and telomere deprotection. In the future, it would be useful to assay both telomere protection and the abundance of these RNAs in other piRNA pathway mutants. Interestingly, this subpopulation of small RNAs associates with Piwi, the only nuclear PIWI clade Argonaute. Piwi also binds HP1a in cytoplasmic extracts from ovarian tissues. Furthermore, embryos from *piwi* germline clones have been reported to display mitotic defects (Cox et al., 2000). Cytological and biochemical analysis of telomere protection in *piwi* mutants is therefore of particular interest.

piRNA function in genome evolution

Most of the resident transposons in the human genome are inactive. But, occasionally incompatibilities can arise in certain situations, e.g. a genetic conflict bet ween maternal and paternal genomes in mammalian embryos can lead to parent-of-origin specific gene expression, also known as gene imprinting. An incompatibility between cytoplasmic and nuclear genomes is an example of an inter-genomic conflict within the same cell which can change gene expression patterns in the daughter cells. Similarly, the potentially disruptive transposable elements often have conflicting interests with the rest of the genome, leading to an irreconcilable evolutionary tug of war between the host genome and the parasite, thus disrupting transmission ratios. It is known that introduction of a new transposon in the zygote in absence of the matching maternal piRNAs can lead to sterility in the progeny (Blumenstiel and Hartl, 2005; Brennecke et al., 2008; Chambeyron et al., 2008). This process, known as hybrid dysgenesis, gets its name because of the severe genetic defects in the F1 progeny from a cross between geographically isolated

populations of *D. melanogaster*, and has baffled many fly genetic researchers since early 1960's. The non-reciprocality of this phenomenon points to the epigenetic factors provided by the mother, which we now know, are piRNAs against the transposon in question. I was curious to understand the basis of such transposon-induced dysgenesis in the hybrid progeny. Using P-M system of dysgenesis, I studied the germline developmental defects in the F1 female hybrids. The females show massive amounts of DNA breaks, thus leading to a severe oogenesis arrest. Most of the ovaries from these hybrid females were rudimentary. Surprisingly though, the females progressively get fertile with age. This correlates with *P-element* transcript silencing, germline DNA repair and *P-element* piRNA production. This is remarkable since the hybrid progeny did not inherit any *P-element* piRNAs from the mother, and thus it shows that piRNA production can be triggered *de novo* in the adult germline. This observation begs the most obvious question a developmental biologist would ask- where in the germline does the silencing occur? Dissecting female ovaries from 2-4 days and 21-day old F1 hybrids revealed that the oogenesis restoration in older females is a stochastic event. The percentage of ovaries with vitellogenic stages increases remarkably by 21-days. However, a whole continuum of phenotypes is still visible in individual females. They range from fully populated ovarioles to single or a few ovarioles with strings of egg chambers to completely rudimentary. This random 'learning' process is possible if the events leading to adaptation are clonal in nature. Each embryo laid by the female is a result of a single germline stem cell division. Therefore, it is possible that the 'learning' event is a switch which occurs stochastically in the germline stem cells and their percentage increases with age. However, a detailed molecular analysis is required to fully support that claim. One way to approach this question would be by cytological visualization of *P-element* expression within the germline. If *P-element* transcripts can be detected in the germline stem cell niche of young

dysgenic hybrids, and its absence is correlated with the age, it would suggest that adaptation events occur in or near the stem cell environment.

The sterility associated with F1 hybrids is far greater than that manifested by many of the piRNA mutations studied to date. This is surprising since most piRNA mutants affect multiple transposon families, while the P-M dysgenic hybrids should only upregulate P-elements. While, it is possible that many piRNA mutations are not completely loss-of-function alleles, and the 'milder' effects are possible due to maternal perdurance, genome sequencing and tiling array expression analysis from dysgenic hybrid progenies tells a different tale. Surprisingly, more than 7 unrelated transposon families were found to be upregulated along with the *P-element* in the P-M dysgenic cross. This partly explains the severe developmental defects in the hybrids and also seems to be the explanation for nuage disruption around the nurse cells. Since nuage structure is restored along with the transposon silencing at 21-days, we propose that nuage in *Drosophila* acts as the center for transposon silencing.

A striking observation from genome sequencing was the strong selection for a handful of TE insertions in major piRNA clusters. We identified a number of stably inherited new TE insertions in known piRNA clusters in the hybrid progeny. Assuming equally random segregation probability of both alleles, the chromosome containing TE insertions should be present in a quarter of F2 progeny. However, these alleles containing TE insertions seem to have become isogenic in our sequenced population. This suggests that either these genomic regions are hot-spots for transposon insertions or that there is selection and survival of only those progeny which harbor these insertions. Either case be true, these TE insertions seem to have a functional impact on the organism. Not only is there an increase in piRNA abundance or improvement in ping-pong bias against some of these elements, there is also an increase in the

number of piRNAs matching the junction between the transposon and the genome region, signifying the relevance of these TE insertions in these piRNA clusters. Stably inherited TE insertions in regions other than piRNA clusters are a mystery at this moment. It remains to be seen whether these TE insertions are silenced by the heterochromatin machinery or they confer some selective advantage to the host owing to their genomic locations. The faithful inheritance of a number of TE insertions in the progeny is a remarkable observation, due in part to the high fidelity of their inheritance. These insertions defy Mendelian inheritance laws, and are seemingly homozygous in our sequenced population, suggesting TE-induced local homologous recombination. Recombination events in heterochromatin are rare, thus understanding the mechanism of inheritance of such TE insertions will be key to our knowledge of this adaptation process.

Our motivation to sequence genomic DNA from F1 and F2 hybrid progeny was to follow the fate of the P-elements in the genome following their activation. We were expecting to identify new *P-element* insertions in existing piRNA clusters as a means of adaptation of the older hybrids to its infection. However, there was no evidence of any new stably inherited *P-element* insertions in clusters in the progeny relative to the male parent. Thus, *P-element* silencing in the 21-day old progeny is not likely due to a genetic change involving *P-element*. The F1 progenies inherit the paternal *P-element* containing piRNA clusters. To analyze primary transcripts from *P-element* containing paternal clusters, I analyzed levels of longer transcripts from P-elements arising specifically from a major paternal piRNA cluster at chromosome 4^{th}. There is about 18-19-fold higher steady-state transcript levels from P-elements in that cluster in 2-4 day old hybrid progeny in comparison to 21-day old or their respective reciprocal controls. Since longer transcripts from piRNA clusters are potentially the precursors for mature piRNAs

following processing into primary piRNAs, we conclude that the processing of *P-element* piRNA precursors is the rate-limiting step to this adaptation. Thus, adaptation to *P-element* infection is linked to a progressive processing of paternal piRNA precursors into mature piRNAs.

Why would different transposons show such different behaviors? piRNA clusters are silencing loci, and landing of active transposons in such places could potentially lead to piRNA production against those transposons and hence their silencing. This seems like a host-mediated reaction in response to transposon activity. It is possible that host proteins interact with transposon-expressed proteins and actively drag them into piRNA clusters. Indeed, Rhino, a germline-enriched HP1 paralog required for piRNA production is encoded by a fast evolving gene which is under positive selection. It has been suggested that Rhino is involved in a germline genomic conflict which is why it is co-evolving with the rapidly evolving transposons in the genome (Vermaak et al., 2005). We have conjectured that Rhino might physically interact with the transposon encoded proteins and thus mediate transposon integration in piRNA clusters (Klattenhoff et al., 2009b). In the future, it will be important to identify Rhino binding proteins to test this hypothesis. However, while Rhino seems to be enriched at many piRNA clusters (Klattenhoff et al., 2009b), it does not bind *P-element* sequences present in piRNA clusters in *Harwich* strain. This might help explain the lack of new *P-element* insertions in existing piRNA clusters. P-elements have invaded *D.melanogaster* only in the last century and are thus a relatively new transposon family for the species. On the other hand, the stably inherited TE insertions we obtained in the piRNA clusters are in the order of 5-7 million years old. Thus, the host has had sufficient time during evolution to tame those species in contrast to the *P-element*.

Given all this data together, we have studied a system in which a single transposon is mobilized in the progeny and the early steps in piRNA biogenesis can be studied. Using this

system, we can now use mutant alleles of some candidate genes, to study their involvement in this adaptation process. I have used HP1 [*Su(var)205*] mutants in a cross with *Harwich* males and studied fertility assays in the progenies. The daughters carrying only one dose of *Su(var)205* gene take much longer to adapt to the dysgenesis, in comparison to their siblings. This suggests that proper heterochromatin assembly or function is required for this adaptation. In Chapter 1, we proposed that Zucchini and Squash, putative nucleases involved in piRNA biogenesis, can cleave and process longer piRNA precursors into mature piRNAs. In the future, we can use *zuc* or *squ* alleles and study the kinetics of adaptation.

The bigger picture

Transposons and other repetitive sequences make up a substantial portion of genomes in large eukaryotes. Due to their potent mutagenic ability which can cause deleterious effects on host fitness, these selfish genetic elements are under a strong selective pressure to diverge. In order to tackle this, the host's transposon targeting immune response has to co-evolve along with the genome invaders. Thus, the piRNA pathway, which seems to be the answer to the mighty transposon challenge in many eukaryotes, is readily responsive to change and is thus adaptable. Through a combination of genetic, cytological and molecular techniques, we have shown that the piRNA pathway has various functions in animal development. While the core function is that of genome maintenance, some components have additional roles in telomere protection. We also studied the effects of a new transposon infection in the resulting progeny and how they respond to and ultimately survive this challenge. This, in my opinion, is the first true representation of the adaptive nature of this pathway in tackling a transposon attack. Additionally, we also show how transposons can have a major impact by genome restructuring, and the surviving progeny are

fitter than their parents. Charles Darwin said, “It is not the strongest of the species that survives… nor the most intelligent that survives. It is the one that is the most adaptable to change.” The piRNA pathway in an evolutionary battle against the transposons, thus seems to be a major contributor to this responsiveness to change in the genomic environment, and thus is responsible for the natural selection of the fittest individuals.

Appendix I: Role of chromatin proteins and histone modifications in Aub/Armi mediated telomere protection

Telomeres in the cell are normally protected by a complex of proteins to avoid recognition by the DNA repair pathway (Smogorzewska et al., 2002). In our efforts to identify the potential role of piRNA pathway during early embryogenesis, we unraveled a new role for Aub and Armi, two piRNA pathway components, in telomere resolution. As described in Chapter 2 of this dissertation, we found that *aub* and *armi* mutants show defects in recruitment of HOAP and HP1 (TPC components) at telomeres. To shed some light onto the mechanism of Aub/Armi-mediated TPC recruitment, I wanted to characterize the role of some chromatin proteins and their responsible histone modifications at the telomeres.

Piwi: Out of the three PIWI proteins in *Drosophila*, Piwi is the only nuclear Argonaute protein, which localizes to the nurse cell nuclei in the female germline and the surrounding somatic tissue. Besides its role in the piRNA pathway, Piwi has been shown to bind HP1, suggesting that it functions in heterochromatin assembly/formation in somatic tissues (Brower-Toland et al., 2007b). Additionally, Piwi has been shown to be highly enriched at a sub-telomeric site on the right arm of chromosome 3, named 3R-TAS (Telomere-Associated Sequence) (Yin and Lin, 2007). Given this information, it is reasonable to conjecture a direct role for Piwi in telomere protection. To this, I isolated chromatin from wild-type ovaries and pulled down Piwi using standard protocol. However, no enrichment was found at the previously published 3R-TAS, telomeric transposons or even piRNA clusters. This negative result was confirmed using 3 different antibodies- one produced in our lab, another from Dr. H. Siomi (Keio University, Japan) and a commercial myc-antibody to pull down myc-Piwi protein from myc-Piwi expressing flies. I used a standard working protocol that I have used routinely in the lab for

dozens of other antibodies. Finally, I also tried the published protocol for Piwi ChIP, which was different in that it requires purification of nuclei from whole fly extracts, followed by standard immunoprecipitation (IP) (Brower-Toland et al., 2007b; Yin and Lin, 2007). Unfortunately, I was unable to get enrichment for Piwi at chromatin any higher than IgG control (Figure I-1A). Also shown in the same figure is a positive control using HP1 binding at the same chromatin regions using the same fly extracts. That the Piwi antibody is capable of pulling down Piwi protein was confirmed using standard IP protocol (Figure I-1B). Thus, it seems unlikely that the Piwi functions via a direct stable interaction with the chromatin. Nonetheless, Piwi's interaction with HP1 was confirmed from whole ovarian extracts (Figure I-1B). It is thus possible that Piwi programmed with telomeric piRNAs in the cytoplasm interacts with, and recruits HP1 which helps bring HOAP at the telomeres. A detailed analysis on embryos from *piwi* germline clones is needed to help justify this hypothesis.

Figure I-1: Role of Piwi in chromatin binding

(A) Chromatin-IP-qPCR analysis using whole adult flies for Piwi and HP1. The nuclear extract was divided into two and immunoprecipitated using Piwi or HP1 antibodies. The purified DNA was subjected to PCR using primers for sub-telomeric region (3R-TAS), telomeric transposons (*Het-A, TART*) and Rp49 as an unrelated locus.

(B) Immunoprecipitation (IP) for HP1, HOAP and Piwi from cytoplasmic ovarian extracts. The extract before IP (Input) was run along with the supernatant (sup.) and following extraction from beads (α-HP1, α-HOAP or α-Piwi) on a PAGE gel and immune-blotted for Piwi antibody. The results confirm the capability of Piwi antibody to pull down Piwi protein from extracts. Also shown is the presence of Piwi in HP1 pull down, suggesting binding of HP1 and Piwi in ovarian tissues.

Figure I

A

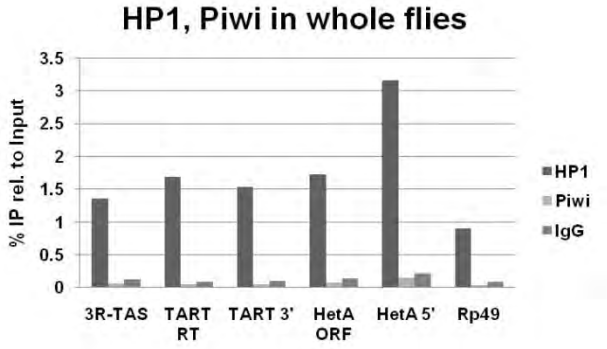
HP1, Piwi in whole flies
% IP rel. to Input
3.5
3
2.5
2
1.5
1
0.5
0
3R-TAS
TART RT
TART 3'
HetA ORF
HetA 5'
Rp49
HP1
Piwi
IgG

B


Input
Sup.
α-HP1
Input
Sup.
α-HOAP
Input
Sup.
α-Piwi
Piwi
IgG

Polycomb proteins: Polycomb group proteins (PcG) are a complex of chromatin modifying enzymes which mediate transcriptional silencing of their target genes. They are involved in silencing various genes encoding key developmental regulators in higher eukaryotes (Simon and Kingston, 2009). Recent studies suggest that the target regions produce long-non coding RNAs and accumulate H3K27me3, a repressive chromatin mark. This epigenetic mode of regulating gene expression profiles makes PcG proteins as important regulators of cancer, X-inactivation, stem cells, gene imprinting and eukaryotic development (Simon and Kingston, 2009).

In an effort to better understand piRNA biology, we performed a candidate gene-based pilot genetic screen to identify genes with dominant genetic interactions with piRNA mutations. Among the genes which displayed the most dramatic dominant interactions with *aub* or *armi*, was *Trithorax-like* (*trl*) (Figure I-2A). Trl protein, also known as GAGA factor, is a member of Trithorax group proteins (TrxG), which are chromatin activating factors that antagonize PcG-mediated silencing. Since some small RNA silencing components have been shown to affect PcG protein localization, a link between piRNA pathway and PcG/TrxG was probable (Grimaud et al., 2006; Simon and Kingston, 2009). In flies, mutations in genes affecting PcG/TrxG function, including GAGA factor, were shown to have chromatin mis-segregation and chromatin fragmentation during early embryogenesis (Bhat et al., 1996; O'Dor et al., 2006). Since, the sub-telomeric DNA (TAS) in flies are known to be binding sites for PcG proteins, I conjectured if *aub* and *armi* gene function is upstream of Polycomb binding at the TAS, and that PcG/TrxG mediated chromatin modifications at the TAS regulate HOAP/HP1 binding at the telomeric ends. To this, I checked if *aub* and *armi* mutants affect GAGA factor localization to the TAS. GAGA factor binds strongly to two different mini-satellite repeat elements located in the TAS of chromosome 2L (Figure I-2B). *aub* or *armi* mutants did not affect GAGA binding at any of those

satellite repeats (Figure I-2B). To confirm these results, I performed a ChIP for H3K27me3, the Polycomb effector histone modification, at the TAS or telomeric transposons. This histone modification can be detected at the TAS, but is absent from telomeric transposons in the wild-type (Figure I-2C). There was no significant difference between H3K27me3 levels between the mutants and control flies at the TAS mini-satellite sequences (Figure I-2C). In conclusion, Aub and Armi-mediated telomere protection is independent of Polycomb/Trithorax function at the sub-telomeric DNA.

Figure I-2: Interaction of Trithorax-like with piRNA pathway components.

A: Dominant genetic interactions between *trl* and *aub* or *armi* mutants. Egg production and % of wt appendages are presented for single and double mutant combinations. Absence of one copy of *trl* gene dramatically affects *aub* and *armi* phenotype.

B and C. ChIP for GAGA factor (B) and H3K27me3 (C) in wt, *armi* and *aub* mutant ovaries followed by qPCR analysis for sub-telomeric regions at chromosome 2L (2L-TAS1 and 2) and 3R (3R-TAS).

Figure I-2

A

Genotype	% wt appendages	Average number of females per day
OreR	100	84.2
aub^{HN}/aub^{QC}	44.9	29.9
$trl^{KG}/TM3$	100	65.9
$aub^{HN}/aub^{QC};Trl^{KG}/TM3$	0	1.4
$armi^{1}/armi^{72.1}$	3.5	8.3
$armi^{1}\ trl^{KG}/armi^{74.1}$	0	3.6

B

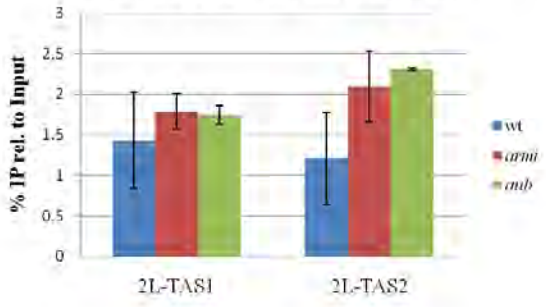

C

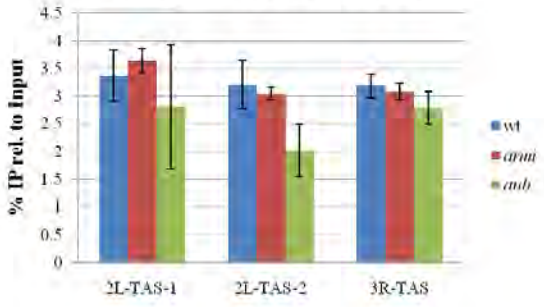

Appendix II: Role of maternally deposited piRNAs in providing immunity against transposons

piRNAs provide immunity against transposons in a sequence-dependent manner. Following production in the female germline, they are deposited in the mature egg which, after fertilization, protects the zygote against transposon challenge. There are strains of *Drosophila melanogaster* with differences in their transposon content, and thus an inter-strain cross between males carrying a particular transposon and naïve females are sterile. The non-reciprocal nature of such sterility points to the maternal inheritance of immunity factors against the transposon. It has been shown that there is a correlation between absence of maternally transmitted piRNAs against a specific transposon and sterility resulting due to its activation in the zygote (Blumenstiel and Hartl, 2005; Brennecke et al., 2008; Chambeyron et al., 2008). However, this available data is quite indirect. I have shown that piRNA production can also be induced in the adult germline in absence of maternal contribution (Chapter 3). Thus, it is important to ask whether it is crucial for the zygote to inherit the genetic source of piRNAs against a specific element in providing necessary resistance in such inter-strain hybrid crosses. I decided to test this using a simple genetic experiment. I used a strain [known as *LkP(1A)*] containing a single *P-element* insertion in a sub-telomeric region on the X-chromosome, which is a major piRNA generating cluster (X-TAS). Cross between *LkP(1A)* females and Harwich males produces fertile progeny owing to the maternal transmission of *P-element* piRNAs in the resulting zygote. I balanced the X-chromosome containing *P-element* X-TAS fly stocks and used those females in a cross with Harwich males (Figure II-A). All the resulting progeny inherit the *P-element* piRNAs from the maternal cytoplasm, however, only half of them acquire the genetic locus required for production of *P-element* piRNAs. The phenotypically distinct progeny (owing to the presence of a visible

eye marker on the balancer chromosome) were tested for fertility by counting the number of eggs produced and percentage of embryos hatched. The dorsal patterning of the embryos was scored by counting the percentage of embryos with wild-type number of appendages (2). It seems that both types of progeny were equally fertile, suggesting that the pre-existing piRNAs from the mother are important in providing the resistance against P-element infection (Figure II-B). My analysis with *w* x *Har* crosses suggested that a progressive processing of transcripts from paternal P-element containing piRNA clusters is linked to mature piRNA production in the older hybrid progeny (Chapter 3 in this dissertation). The results shown in Figure II-B suggest and confirm our hypothesis that the pre-existing piRNAs in the progeny are sufficient to readily drive piRNA biogenesis from paternal clusters and thus protect their genome against the deleterious effects of the transposon. A deep sequencing of small RNA population from the F1 progenies from this cross should further confirm our hypothesis. For it to hold true, both the F1 genotypes should have *P-element* piRNA populations arising from the paternal P-element piRNA clusters.

Figure II: Maternal inheritance of *P-element* piRNAs is sufficient for suppressing dysgenesis in hybrid progeny.

(A) Genetic scheme showing the cross between *Lk-P(1A)*/FM7 females and *Harwich* males. All the progeny inherit the same egg cytoplasmic components from the mother, however half of them [*Lk-P(1A)*/+] carry the source of *P-element* piRNAs and the other half do not (+/FM7). (B) The F2 progeny arising from selfing the genetically distinct F1 males and females were scored for the number of eggs, hatch rates and wild-type dorsal appendages. The data in (B) summarizes the result from 4 independent experiments.

Figure II

A

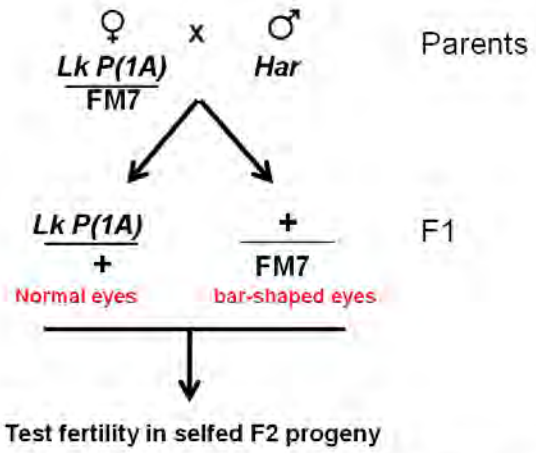

B

	Lk P(1A)/+	+/FM7
Average Eggs per female	9.1	6.9
	13.3	6.8
	26	19.6
	13.2	19.2
Hatch rates (%)	93.9	81.4
	81	44.8
	88.8	74.8
	85.8	72.3
Wt appendages (%)	100	96.9
	97.9	100
	100	99.6
	100	100

Bibliography

Abad, J.P., M. Carmena, S. Baars, R.D. Saunders, D.M. Glover, P. Ludeña, C. Sentis, C. Tyler-Smith, and A. Villasante. 1992. Dodeca satellite: a conserved G+C-rich satellite from the centromeric heterochromatin of Drosophila melanogaster. *Proceedings of the National Academy of Sciences of the United States of America*. 89:4663-4667.

Abdu, U., M. Brodsky, and T. Schupbach. 2002. Activation of a meiotic checkpoint during Drosophila oogenesis regulates the translation of Gurken through Chk2/Mnk. *Curr Biol*. 12:1645-51.

Aravin , Gaidatzis D, Pfeffer S, Lagos-Quintana M, Landgraf P, Iovino N, Morris P, Brownstein MJ, Kuramochi-Miyagawa S, Nakano T, Chien M, Russo JJ, Ju J, Sheridan R, Sander C, Zavolan M, and T. T. 2006. A novel class of small RNAs bind to MILI protein in mouse testes. *Nature.* 442:203-207.

Aravin, A., D. Gaidatzis, and T. Tuschl. 2006. A novel class of small RNAs bind to MILI protein in mouse testes. *Nature.* advanced online publication:203-207.

Aravin, A.A., M. Lagos-Quintana, A. Yalcin, M. Zavolan, D. Marks, B. Snyder, T. Gaasterland, J. Meyer, and T. Tuschl. 2003. The small RNA profile during Drosophila melanogaster development. *Dev Cell*. 5:337-50.

Aravin, A.A., N.M. Naumova, A.V. Tulin, V.V. Vagin, Y.M. Rozovsky, and V.A. Gvozdev. 2001. Double-stranded RNA-mediated silencing of genomic tandem repeats and transposable elements in the D. melanogaster germline. *Curr Biol*. 11:1017-27.

Aravin, A.A., R. Sachidanandam, A. Girard, K. Fejes-Toth, and G.J. Hannon. 2007. Developmentally regulated piRNA clusters implicate MILI in transposon control. *Science (New York, N.Y.)*. 316:744-747.

Ashraf, S.I., A.L. McLoon, S.M. Sclarsic, and S. Kunes. 2006. Synaptic protein synthesis associated with memory is regulated by the RISC pathway in Drosophila. *Cell*. 124:191-205.

Assis, R., and A.S. Kondrashov. 2009. Rapid repetitive element-mediated expansion of piRNA clusters in mammalian evolution. *Proc Natl Acad Sci U S A*. 106:7079-82.

Bannister, A., P. Zegerman, J. Partridge, E. Miska, J. Thomas, and R. Allshire. 2001. Selective recognition of methylated lysine 9 on histone H3 by the HP1 chromo domain. *Nature*. 410:120-124.

Batista, P.J., J.G. Ruby, J.M. Claycomb, R. Chiang, N. Fahlgren, K.D. Kasschau, D.A. Chaves, W. Gu, J.J. Vasale, S. Duan, J.D. Conte, S. Luo, G.P. Schroth, J.C. Carrington, D.P. Bartel, and C.C. Mello. 2008. PRG-1 and 21U-RNAs interact to form the piRNA complex required for fertility in C. elegans. *Molecular cell*. 31:67-78.

Belgnaoui, S.M., R.G. Gosden, O.J. Semmes, and A. Haoudi. 2006. Human LINE-1 retrotransposon induces DNA damage and apoptosis in cancer cells. *Cancer cell international*. 6:13.

Benton, R., I.M. Palacios, and D. St Johnston. 2002. Drosophila 14-3-3/PAR-5 is an essential mediator of PAR-1 function in axis formation. *Dev Cell*. 3:659-71.

Bhat, K.M., G. Farkas, F. Karch, H. Gyurkovics, J. Gausz, and P. Schedl. 1996. The GAGA factor is required in the early Drosophila embryo not only for transcriptional regulation but also for nuclear division. *Development (Cambridge, England)*. 122:1113-1124.

Bi, X., D. Srikanta, L. Fanti, S. Pimpinelli, R. Badugu, R. Kellum, and Y.S. Rong. 2005. Drosophila ATM and ATR checkpoint kinases control partially redundant pathways for telomere maintenance. *Proceedings of the National Academy of Sciences of the United States of America*. 102:15167-15172.

Bi, X., S.-C.D. Wei, and Y.S. Rong. 2004. Telomere protection without a telomerase; the role of ATM and Mre11 in Drosophila telomere maintenance. *Current biology : CB*. 14:1348-1353.

Biessmann, H., J.M. Mason, K. Ferry, M. d'Hulst, K. Valgeirsdottir, K.L. Traverse, and M.L. Pardue. 1990. Addition of telomere-associated HeT DNA sequences "heals" broken chromosome ends in Drosophila. *Cell*. 61:663-673.

Blumenstiel, J.P., R. Fu, W.E. Theurkauf, and R.S. Hawley. 2008. Components of the RNAi machinery that mediate long-distance chromosomal associations are dispensable for meiotic and early somatic homolog pairing in Drosophila melanogaster. *Genetics*. 180:1355-1365.

Blumenstiel, J.P., and D.L. Hartl. 2005. Evidence for maternally transmitted small interfering RNA in the repression of transposition in Drosophila virilis. *Proceedings of the National Academy of Sciences of the United States of America*. 102:15965-15970.

Boswell, R.E., and A.P. Mahowald. 1985. tudor, a gene required for assembly of the germ plasm in Drosophila melanogaster. *Cell*. 43:97-104.

Bratu, D.P., B.J. Cha, M.M. Mhlanga, F.R. Kramer, and S. Tyagi. 2003. Visualizing the distribution and transport of mRNAs in living cells. *Proc Natl Acad Sci U S A*. 100:13308-13.

Brendza, R.P., L.R. Serbus, J.B. Duffy, and W.M. Saxton. 2000. A function for kinesin I in the posterior transport of oskar mRNA and Staufen protein. *Science*. 289:2120-2.

Brennecke, J., A.A. Aravin, A. Stark, M. Dus, M. Kellis, R. Sachidanandam, and G.J. Hannon. 2007. Discrete small RNA-generating loci as master regulators of transposon activity in Drosophila. *Cell*. 128:1089-1103.

Brennecke, J., C. Malone, A. Aravin, R. Sachidanandam, A. Stark, and G. Hannon. 2008. An epigenetic role for maternally inherited piRNAs in transposon silencing. *Science (New York, N.Y.)*. 322:1387-1392.

Brower-Toland, B., S.D. Findley, L. Jiang, L. Liu, H. Yin, M. Dus, P. Zhou, S.C. Elgin, and H. Lin. 2007a. Drosophila PIWI associates with chromatin and interacts directly with HP1a. *Genes Dev*. 21:2300-11.

Brower-Toland, B., S.D. Findley, L. Jiang, L. Liu, H. Yin, M. Dus, P. Zhou, S.C.R. Elgin, and H. Lin. 2007b. Drosophila PIWI associates with chromatin and interacts directly with HP1a. *Genes & development*. 21:2300-2311.

Bucheton, A. 1973. [Study of non Mendelian female sterility in Drosophila melanogaster. Hereditary transmission of the degree of efficacy of the reactor factor]. *Comptes rendus hebdomadaires des séances de l'Académie des sciences. Série D: Sciences naturelles*. 276:641-644.

Bucheton, A. 1979. Non-Mendelian female sterility in Drosophila melanogaster: influence of aging and thermic treatments. III. Cumulative effects induced by these factors. *Genetics*. 93:131-142.

Bucheton, A., J.M. Lavige, G. Picard, and P. L'Heritier. 1976. Non-mendelian female sterility in Drosophila melanogaster: quantitative variations in the efficiency of inducer and reactive strains. *Heredity*. 36:305-314.

Carmell, M.A., A. Girard, H.J.G. van de Kant, D. Bourc'his, T.H. Bestor, D.G. de Rooij, and G.J. Hannon. 2007. MIWI2 is essential for spermatogenesis and repression of transposons in the mouse male germline. *Developmental cell*. 12:503-514.

Carpenter, A.T. 1975. Electron microscopy of meiosis in Drosophila melanogaster females. I. Structure, arrangement, and temporal change of the synaptonemal complex in wild-type. *Chromosoma*. 51:157-182.

Carpenter, A.T. 1979. Synaptonemal complex and recombination nodules in wild-type Drosophila melanogaster females. *Genetics*. 92:511-541.

Cenci, G., G. Siriaco, G. Raffa, R. Kellum, and M. Gatti. 2003. The Drosophila HOAP protein is required for telomere capping. *Nature cell biology*. 5:82-84.

Cha, B.J., L.R. Serbus, B.S. Koppetsch, and W.E. Theurkauf. 2002. Kinesin I-dependent cortical exclusion restricts pole plasm to the oocyte posterior. *Nat Cell Biol*. 4:592-8.

Chambeyron, S., A. Popkova, G. Payen-Groschêne, C. Brun, D. Laouini, A. Pelisson, and A. Bucheton. 2008. piRNA-mediated nuclear accumulation of retrotransposon transcripts in the Drosophila female germline. *Proceedings of the National Academy of Sciences of the United States of America*. 105:14964-14969.

Chen, J.M., N. Chuzhanova, P.D. Stenson, C. Férec, and D.N. Cooper. 2005. Meta-Analysis of gross insertions causing human genetic disease: Novel mutational mechanisms and the role of replication slippage. *Human Mutation*. 25:207-221.

Chen, Y., A. Pane, and T. Schüpbach. 2007. Cutoff and aubergine mutations result in retrotransposon upregulation and checkpoint activation in Drosophila. *Current biology : CB*. 17:637-642.

Cook, H., B. Koppetsch, J. Wu, and W. Theurkauf. 2004. The Drosophila SDE3 Homolog armitage Is Required for oskar mRNA Silencing and Embryonic Axis Specification. *Cell*. 116:817-829.

Cox, D.N., A. Chao, J. Baker, L. Chang, D. Qiao, and H. Lin. 1998. A novel class of evolutionarily conserved genes defined by piwi are essential for stem cell self-renewal. *Genes Dev*. 12:3715-27.

Cox, D.N., A. Chao, and H. Lin. 2000. piwi encodes a nucleoplasmic factor whose activity modulates the number and division rate of germline stem cells. *Development*. 127:503-14.

Cox, D.N., B. Lu, T.Q. Sun, L.T. Williams, and Y.N. Jan. 2001. Drosophila par-1 is required for oocyte differentiation and microtubule organization. *Curr Biol*. 11:75-87.

Czech, B., C. Malone, R. Zhou, A. Stark, C. Schlingeheyde, M. Dus, N. Perrimon, M. Kellis, J. Wohlschlegel, R. Sachidanandam, G. Hannon, and J. Brennecke. 2008. An endogenous small interfering RNA pathway in Drosophila. *Nature*.

de Rooij, D.G., and J.A. Grootegoed. 1998. Spermatogonial stem cells. *Current opinion in cell biology*. 10:694-701.

Deininger, P.L., and M.A. Batzer. 1999. Alu repeats and human disease. *Molecular genetics and metabolism*. 67:183-193.

Deng, W., and H. Lin. 1997. Spectrosomes and fusomes anchor mitotic spindles during asymmetric germ cell divisions and facilitate the formation of a polarized microtubule array for oocyte specification in Drosophila. *Dev Biol*. 189:79-94.

Deng, W., and H. Lin. 2002. miwi, a murine homolog of piwi, encodes a cytoplasmic protein essential for spermatogenesis. *Dev Cell*. 2:819-30.

Deshpande, G., G. Calhoun, and P. Schedl. 2005. Drosophila argonaute-2 is required early in embryogenesis for the assembly of centric/centromeric heterochromatin, nuclear division, nuclear migration, and germ-cell formation. *Genes & development*. 19:1680-1685.

Eddy, E.M. 1974. Fine structural observations on the form and distribution of nuage in germ cells of the rat. *The Anatomical record*. 178:731-757.

Feschotte, C. 2008. Transposable elements and the evolution of regulatory networks. *Nature reviews. Genetics*. advanced online publication:397-405.

Filipowicz, W., L. Jaskiewicz, F.A. Kolb, and R.S. Pillai. 2005. Post-transcriptional gene silencing by siRNAs and miRNAs. *Current opinion in structural biology*. 15:331-341.

Foe, V.E.O., G.M.; Edgar, B. 1993. Mitosis and morphogenesis in the Drosophila embryo: point and counterpoint. *In* The Development of Drosophila melanogaster. A.M.A. Michael Bate, editor. CSHL Press. 149-300.

Frost, R.J., F.K. Hamra, J.A. Richardson, X. Qi, R. Bassel-Duby, and E.N. Olson. 2010. MOV10L1 is necessary for protection of spermatocytes against retrotransposons by Piwi-interacting RNAs. *Proc Natl Acad Sci U S A*. 107:11847-52.

Gasior, S.L., T.P. Wakeman, B. Xu, and P.L. Deininger. 2006. The human LINE-1 retrotransposon creates DNA double-strand breaks. *Journal of molecular biology*. 357:1383-1393.

Ghabrial, A., R.P. Ray, and T. Schupbach. 1998. okra and spindle-B encode components of the RAD52 DNA repair pathway and affect meiosis and patterning in Drosophila oogenesis. *Genes Dev*. 12:2711-23.

Ghabrial, A., and T. Schupbach. 1999. Activation of a meiotic checkpoint regulates translation of Gurken during Drosophila oogenesis. *Nat Cell Biol*. 1:354-7. java/Propub/cellbio/ncb1099_354.fulltext java/Propub/cellbio/ncb1099_354.abstract.

Ghildiyal, M., H. Seitz, M.D. Horwich, C. Li, T. Du, S. Lee, J. Xu, E.L.W. Kittler, M.L. Zapp, Z. Weng, and P.D. Zamore. 2008. Endogenous siRNAs derived from transposons and mRNAs in Drosophila somatic cells. *Science (New York, N.Y.)*. 320:1157396-1081.

Ghildiyal, M., and P. Zamore. 2009. Small silencing RNAs: an expanding universe. *Nature reviews. Genetics*. 10:94-108.

Gilliland, W.D., S.F. Hughes, D.R. Vietti, and R.S. Hawley. 2009. Congression of achiasmate chromosomes to the metaphase plate in Drosophila melanogaster oocytes. *Developmental biology*. 325:122-128.

Girard, A.l., R. Sachidanandam, G. Hannon, and M. Carmell. 2006a. A germline-specific class of small RNAs binds mammalian Piwi proteins. *Nature*. advanced online publication:199-202.

Girard, A.l., R. Sachidanandam, G. Hannon, and M. Carmell. 2006b. A germline-specific class of small RNAs binds mammalian Piwi proteins. *Nature*. 442:199-202.

Grimaud, C., F. Bantignies, M. Pal-Bhadra, P. Ghana, U. Bhadra, and G. Cavalli. 2006. RNAi components are required for nuclear clustering of Polycomb group response elements. *Cell*. 124:957-971.

Grimson, A., M. Srivastava, B. Fahey, B. Woodcroft, H.R. Chiang, N. King, B. Degnan, D. Rokhsar, and D. Bartel. 2008. Early origins and evolution of microRNAs and Piwi-interacting RNAs in animals. *Nature*. 455:1193-1197.

Grivna, S.T., E. Beyret, Z. Wang, and H. Lin. 2006a. A novel class of small RNAs in mouse spermatogenic cells. *Genes and Development*. 20:1709-1714.

Grivna, S.T., B. Pyhtila, and H. Lin. 2006b. MIWI associates with translational machinery and PIWI-interacting RNAs (piRNAs) in regulating spermatogenesis. *Proceedings of the National Academy of Sciences of the United States of America*. 103:13415-13420.

Gunawardane, L.S., K. Saito, K.M. Nishida, K. Miyoshi, Y. Kawamura, T. Nagami, H. Siomi, and M.C. Siomi. 2007. A slicer-mediated mechanism for repeat-associated siRNA 5' end formation in Drosophila. *Science (New York, N.Y.)*. 315:1587-1590.

Hall, I.M., K. Noma, and S.I. Grewal. 2003. RNA interference machinery regulates chromosome dynamics during mitosis and meiosis in fission yeast. *Proc Natl Acad Sci U S A*. 100:193-8.

Harris, A.N., and P.M. Macdonald. 2001. Aubergine encodes a Drosophila polar granule component required for pole cell formation and related to eIF2C. *Development*. 128:2823-32.

Hartig, J.V., S. Esslinger, R. Böttcher, K. Saito, and K. Förstemann. 2009. Endo-siRNAs depend on a new isoform of loquacious and target artificially introduced, high-copy sequences. *The EMBO journal*. 28:2932-2944.

Hiraizumi, Y. 1971. Spontaneous recombination in Drosophila melanogaster males. *Proceedings of the National Academy of Sciences of the United States of America*. 68:268-270.

Horwich, M.D., C. Li, C. Matranga, V. Vagin, G. Farley, P. Wang, and P.D. Zamore. 2007. The Drosophila RNA methyltransferase, DmHen1, modifies germline piRNAs and single-stranded siRNAs in RISC. *Current biology : CB*. 17:1265-1272.

Houwing, S., L.M. Kamminga, E. Berezikov, D. Cronembold, A. Girard, H. van den Elst, D.V. Filippov, H. Blaser, E. Raz, C.B. Moens, R.H.A. Plasterk, G.J. Hannon, B.W. Draper, and R.F. Ketting. 2007. A role for Piwi and piRNAs in germ cell maintenance and transposon silencing in Zebrafish. *Cell*. 129:69-82.

Ikenishi, K. 1998. Germ plasm in Caenorhabditis elegans, Drosophila and Xenopus. *Dev Growth Differ*. 40:1-10.

Iskow, R.C., M.T. McCabe, R.E. Mills, S. Torene, W.S. Pittard, A.F. Neuwald, E.G. Van Meir, P.M. Vertino, and S.E. Devine. 2010. Natural mutagenesis of human genomes by endogenous retrotransposons. *Cell*. 141:1253-1261.

Jang, J.K., D.E. Sherizen, R. Bhagat, E.A. Manheim, and K.S. McKim. 2003. Relationship of DNA double-strand breaks to synapsis in Drosophila. *Journal of cell science*. 116:3069-3077.

Kawamura, Y., K. Saito, T. Kin, Y. Ono, K. Asai, T. Sunohara, T. Okada, M. Siomi, and H. Siomi. 2008. Drosophila endogenous small RNAs bind to Argonaute[thinsp]2 in somatic cells. *Nature*.

Kennerdell, J.R., S. Yamaguchi, and R.W. Carthew. 2002. RNAi is activated during Drosophila oocyte maturation in a manner dependent on aubergine and spindle-E. *Genes Dev*. 16:1884-9.

Kidwell, M.G., and J.F. Kidwell. 1975. Spontaneous male recombination and mutation in isogenic-derived chromosomes of Drosophila melanogaster. *J Hered*. 66:367-75.

Kidwell, M.G., and J.F. Kidwell. 1976. Selection for male recombination in Drosophila melanogaster. *Genetics*. 84:333-351.

Kidwell, M.G., J.F. Kidwell, and J.A. Sved. 1977. Hybrid Dysgenesis in DROSOPHILA MELANOGASTER: A Syndrome of Aberrant Traits Including Mutation, Sterility and Male Recombination. *Genetics*. 86:813-833.

Kim-Ha, J., J.L. Smith, and P.M. Macdonald. 1991. oskar mRNA is localized to the posterior pole of the Drosophila oocyte. *Cell*. 66:23-35.

Kirino, Y., N. Kim, M. de Planell-Saguer, E. Khandros, S. Chiorean, P.S. Klein, I. Rigoutsos, T.A. Jongens, and Z. Mourelatos. 2009. Arginine methylation of Piwi proteins catalysed by dPRMT5 is required for Ago3 and Aub stability. *Nature cell biology*. 11:652-658.

Klattenhoff, C., D.P. Bratu, N. McGinnis-Schultz, B.S. Koppetsch, H.A. Cook, and W.E. Theurkauf. 2007. Drosophila rasiRNA pathway mutations disrupt embryonic axis specification through activation of an ATR/Chk2 DNA damage response. *Developmental cell*. 12:45-55.

Klattenhoff, C., and W. Theurkauf. 2007. Biogenesis and germline functions of piRNAs. *Development*. 135:dev-006486.

Klattenhoff, C., H. Xi, C. Li, S. Lee, J. Xu, J.S. Khurana, F. Zhang, N. Schultz, B.S. Koppetsch, A. Nowosielska, H. Seitz, P.D. Zamore, Z. Weng, and W.E. Theurkauf. 2009a. The Drosophila HP1 Homolog Rhino Is Required for Transposon Silencing and piRNA Production by Dual-Strand Clusters. *Cell*. 138:1137.

Klattenhoff, C., H. Xi, C. Li, S. Lee, J. Xu, J.S. Khurana, F. Zhang, N. Schultz, B.S. Koppetsch, A. Nowosielska, H. Seitz, P.D. Zamore, Z. Weng, and W.E. Theurkauf. 2009b. The Drosophila HP1 Homolog Rhino Is Required for Transposon Silencing and piRNA Production by Dual-Strand Clusters. *Cell*. 138:1137-1149.

Klenov, M.S., S.A. Lavrov, A.D. Stolyarenko, S.S. Ryazansky, A.A. Aravin, T. Tuschl, and V.A. Gvozdev. 2007. Repeat-associated siRNAs cause chromatin silencing of retrotransposons in the Drosophila melanogaster germline. *Nucleic acids research*. 35:5430-5438.

Kotaja, N., H. Lin, M. Parvinen, and P. Sassone-Corsi. 2006. Interplay of PIWI/Argonaute protein MIWI and kinesin KIF17b in chromatoid bodies of male germ cells. *Journal of cell science*. 119:2819-2825.

Kuramochi-Miyagawa, S., T. Kimura, T.W. Ijiri, T. Isobe, N. Asada, Y. Fujita, M. Ikawa, N. Iwai, M. Okabe, W. Deng, H. Lin, Y. Matsuda, and T. Nakano. 2004. Mili, a mammalian member of piwi family gene, is essential for spermatogenesis. *Development (Cambridge, England)*. 131:839-849.

Kuramochi-Miyagawa, S., T. Watanabe, K. Gotoh, K. Takamatsu, S. Chuma, K. Kojima-Kita, Y. Shiromoto, N. Asada, A. Toyoda, A. Fujiyama, Y. Totoki, T. Shibata, T. Kimura, N. Nakatsuji, T. Noce, H. Sasaki, and T. Nakano. 2010. MVH in piRNA processing and gene silencing of retrotransposons. *Genes Dev*. 24:887-92.

Lachner, M., D. O'Carroll, S. Rea, and K. Mechtler. 2001. Methylation of histone H3 lysine 9 creates a binding site for HP1 proteins. *Nature*. 410:116-120.

Lane, M.E., and D. Kalderon. 1993. Genetic investigation of cAMP-dependent protein kinase function in Drosophila development. *Genes Dev*. 7:1229-43.

Lau, N., T. Ohsumi, M. Borowsky, R. Kingston, and M. Blower. 2009a. Systematic and single cell analysis of Xenopus Piwi-interacting RNAs and Xiwi. *The EMBO journal*. advance online publication:2945-2958.

Lau, N.C., N. Robine, R. Martin, W.-J. Chung, Y. Niki, E. Berezikov, and E.C. Lai. 2009b. Abundant primary piRNAs, endo-siRNAs, and microRNAs in a Drosophila ovary cell line. *Genome research*.

Lau, N.C., A.G. Seto, J. Kim, S. Kuramochi-Miyagawa, T. Nakano, D.P. Bartel, and R.E. Kingston. 2006. Characterization of the piRNA complex from rat testes. *Science*. 313:363-367.

Lee, Y.S., K. Nakahara, J.W. Pham, K. Kim, Z. He, E.J. Sontheimer, and R.W. Carthew. 2004. Distinct roles for Drosophila Dicer-1 and Dicer-2 in the siRNA/miRNA silencing pathways. *Cell*. 117:69-81.

Li, C., V.V. Vagin, S. Lee, J. Xu, S. Ma, H. Xi, H. Seitz, M.D. Horwich, M. Syrzycka, B.M. Honda, E.L.W. Kittler, M.L. Zapp, C. Klattenhoff, N. Schulz, W.E. Theurkauf, Z. Weng, and P.D. Zamore. 2009. Collapse of germline piRNAs in the absence of Argonaute3 reveals somatic piRNAs in flies. *Cell*. 137:509-521.

Li, L., J.M. Olvera, K.E. Yoder, R.S. Mitchell, S.L. Butler, M. Lieber, S.L. Martin, and F.D. Bushman. 2001. Role of the non-homologous DNA end joining pathway in the early steps of retroviral infection. *The EMBO journal*. 20:3272-3281.

Liang, L., W. Diehl-Jones, and P. Lasko. 1994. Localization of vasa protein to the Drosophila pole plasm is independent of its RNA-binding and helicase activities. *Development*. 120:1201-11.

Lim, A., and T. Kai. 2007. Unique germ-line organelle, nuage, functions to repress selfish genetic elements in Drosophila melanogaster. *Proceedings of the National Academy of Sciences of the United States of America*. 104:6714-6719.

Lin, H., and A.C. Spradling. 1997. A novel group of pumilio mutations affects the asymmetric division of germline stem cells in the Drosophila ovary. *Development*. 124:2463-76.

Liu, H., J.K. Jang, N. Kato, and K.S. McKim. 2002. mei-P22 encodes a chromosome-associated protein required for the initiation of meiotic recombination in Drosophila melanogaster. *Genetics*. 162:245-258.

Livak, K.J. 1990. Detailed structure of the Drosophila melanogaster stellate genes and their transcripts. *Genetics*. 124:303-16.

Lynch, C., and M. Tristem. 2003. A co-opted gypsy-type LTR-retrotransposon is conserved in the genomes of humans, sheep, mice, and rats. *Current biology : CB*. 13:1518-1523.

Madigan, J.P., H.L. Chotkowski, and R.L. Glaser. 2002. DNA double-strand break-induced phosphorylation of Drosophila histone variant H2Av helps prevent radiation-induced apoptosis. *Nucleic acids research*. 30:3698-3705.

Malone, C.D., J. Brennecke, M. Dus, A. Stark, W.R. McCombie, R. Sachidanandam, and G.J. Hannon. 2009. Specialized piRNA pathways act in germline and somatic tissues of the Drosophila ovary. *Cell*. 137:522-535.

Malone, C.D., and G.J. Hannon. 2009. Small RNAs as guardians of the genome. *Cell*. 136:656-668.

Marcon, E., T. Babak, G. Chua, T. Hughes, and P.B. Moens. 2008. miRNA and piRNA localization in the male mammalian meiotic nucleus. *Chromosome research : an international journal on the molecular, supramolecular and evolutionary aspects of chromosome biology*. 16:243-260.

McCLINTOCK, B. 1950. The origin and behavior of mutable loci in maize. *Proceedings of the National Academy of Sciences of the United States of America*. 36:344-355.

McClintock, B. 1953. Induction of Instability at Selected Loci in Maize. *Genetics*. 38:579-599.

McKim, K.S., J.K. Jang, and E.A. Manheim. 2002. Meiotic recombination and chromosome segregation in Drosophila females. *Annu Rev Genet*. 36:205-32.

Megosh, H.B., D.N. Cox, C. Campbell, and H. Lin. 2006. The role of PIWI and the miRNA machinery in Drosophila germline determination. *Current biology : CB*. 16:1884-1894.

Mével-Ninio, M., A. Pelisson, J. Kinder, A.R. Campos, and A. Bucheton. 2007. The flamenco locus controls the gypsy and ZAM retroviruses and is required for Drosophila oogenesis. *Genetics*. 175:1615-1624.

Mills, R.E., E.A. Bennett, R.C. Iskow, and S.E. Devine. 2007. Which transposable elements are active in the human genome? *Trends in genetics : TIG*. 23:183-191.

Nakayama, J., J.C. Rice, B.D. Strahl, C.D. Allis, and S.I. Grewal. 2001. Role of histone H3 lysine 9 methylation in epigenetic control of heterochromatin assembly. *Science (New York, N.Y.)*. 292:110-113.

Neuman-Silberberg, F.S., and T. Schupbach. 1993. The Drosophila dorsoventral patterning gene gurken produces a dorsally localized RNA and encodes a TGF alpha-like protein. *Cell*. 75:165-74.

Niki, Y., T. Yamaguchi, and A.P. Mahowald. 2006. Establishment of stable cell lines of Drosophila germ-line stem cells. *Proceedings of the National Academy of Sciences of the United States of America*. 103:16325-16330.

Nishida, K.M., T.N. Okada, T. Kawamura, T. Mituyama, Y. Kawamura, S. Inagaki, H. Huang, D. Chen, T. Kodama, H. Siomi, and M.C. Siomi. 2009. Functional involvement of Tudor and dPRMT5 in the piRNA processing pathway in Drosophila germlines. *The EMBO journal*. 28:3820-3831.

Nishida, K.M., K. Saito, T. Mori, Y. Kawamura, T. Nagami-Okada, S. Inagaki, H. Siomi, and M.C. Siomi. 2007. Gene silencing mechanisms mediated by Aubergine piRNA complexes in Drosophila male gonad. *RNA (New York, N.Y.)*. 13:1911-1922.

Nowacki, M., B.P. Higgins, G.M. Maquilan, E.C. Swart, T.G. Doak, and L.F. Landweber. 2009. A functional role for transposases in a large eukaryotic genome. *Science (New York, N.Y.)*. 324:935-938.

O'Dor, E., S.A. Beck, and H.W. Brock. 2006. Polycomb group mutants exhibit mitotic defects in syncytial cell cycles of Drosophila embryos. *Developmental biology*. 290:312-322.

Okamura, K., W.-J. Chung, J.G. Ruby, H. Guo, D. Bartel, and E. Lai. 2008. The Drosophila hairpin RNA pathway generates endogenous short interfering RNAs. *Nature*. 453:803-806.

Pal-Bhadra, M., B.A. Leibovitch, S.G. Gandhi, M. Rao, U. Bhadra, J.A. Birchler, and S.C. Elgin. 2004a. Heterochromatic silencing and HP1 localization in Drosophila are dependent on the RNAi machinery. *Science*. 303:669-72.

Pal-Bhadra, M., B.A. Leibovitch, S.G. Gandhi, M. Rao, U. Bhadra, J.A. Birchler, and S.C.R. Elgin. 2004b. Heterochromatic silencing and HP1 localization in Drosophila are dependent on the RNAi machinery. *Science (New York, N.Y.)*. 303:669-672.

Palakodeti, D., M. Smielewska, Y.-C. Lu, G. Yeo, and B. Graveley. 2008. The PIWI proteins SMEDWI-2 and SMEDWI-3 are required for stem cell function and piRNA expression in planarians. *RNA*. 14.

Pane, A., K. Wehr, and T. Schüpbach. 2007. zucchini and squash encode two putative nucleases required for rasiRNA production in the Drosophila germline. *Developmental cell*. 12:851-862.

Park, J.K., X. Liu, T.J. Strauss, D.M. McKearin, and Q. Liu. 2007. The miRNA pathway intrinsically controls self-renewal of Drosophila germline stem cells. *Current biology : CB*. 17:533-538.

Patil, V.S., and T. Kai. 2010. Repression of Retroelements in Drosophila Germline via piRNA Pathway by the Tudor Domain Protein Tejas. *Current biology : CB*.

Perrini, B., L. Piacentini, L. Fanti, F. Altieri, S. Chichiarelli, M. Berloco, C. Turano, A. Ferraro, and S. Pimpinelli. 2004. HP1 controls telomere capping, telomere elongation, and telomere silencing by two different mechanisms in Drosophila. *Molecular cell*. 15:467-476.

Picard, G. 1976. Non-mendelian female sterility in Drosophila melanogaster: hereditary transmission of I factor. *Genetics*. 83:107-23.

Picard, G., A. Bucheton, J.M. Lavige, and A. Fleuriet. 1972. [A sterility phenomenon of nonmendelian determinism in Drosophila melanogaster]. *Comptes rendus hebdomadaires des séances de l'Académie des sciences. Série D: Sciences naturelles*. 275:933-936.

Raffa, G.D., G. Siriaco, S. Cugusi, L. Ciapponi, G. Cenci, E. Wojcik, and M. Gatti. 2009. The Drosophila modigliani (moi) gene encodes a HOAP-interacting protein required for telomere protection. *Proceedings of the National Academy of Sciences of the United States of America*. 106:2271-2276.

Robine, N., N.C. Lau, S. Balla, Z. Jin, K. Okamura, S. Kuramochi-Miyagawa, M.D. Blower, and E.C. Lai. 2009. A broadly conserved pathway generates 3'UTR-directed primary piRNAs. *Current biology : CB*. 19:2066-2076.

Roth, S., F.S. Neuman-Silberberg, G. Barcelo, and T. Schupbach. 1995. cornichon and the EGF receptor signaling process are necessary for both anterior-posterior and dorsal-ventral pattern formation in Drosophila. *Cell*. 81:967-78.

Rouget, C., C. Papin, A. Boureux, A. Meunier, B. Franco, N. Robine, E. Lai, A. Pelisson, and M. Simonelig. 2010. Maternal mRNA deadenylation and decay by the piRNA pathway in the early Drosophila embryo. *Nature*. 467:1128-1132.

Rozhkov, N.V., A.A. Aravin, E.S. Zelentsova, N.G. Schostak, R. Sachidanandam, W.R. McCombie, G.J. Hannon, and M.B. Evgen'ev. 2010. Small RNA-based silencing strategies for transposons in the process of invading Drosophila species. *RNA*. 16:1634-45.

Rubin, G.M., M.G. Kidwell, and P.M. Bingham. 1982. The molecular basis of P-M hybrid dysgenesis: the nature of induced mutations. *Cell*. 29:987-994.

Ruby, J.G., C. Jan, C. Player, M.J. Axtell, W. Lee, C. Nusbaum, H. Ge, and D.P. Bartel. 2006. Large-scale sequencing reveals 21U-RNAs and additional microRNAs and endogenous siRNAs in C. elegans. *Cell*. 127:1193-1207.

Saito, K., S. Inagaki, T. Mituyama, Y. Kawamura, Y. Ono, E. Sakota, H. Kotani, K. Asai, H. Siomi, and M. Siomi. 2009. A regulatory circuit for piwi by the large Maf gene traffic jam in Drosophila. *Nature*. 461:1296-1299.

Saito, K., H. Ishizu, M. Komai, H. Kotani, Y. Kawamura, K.M. Nishida, H. Siomi, and M.C. Siomi. 2010. Roles for the Yb body components Armitage and Yb in primary piRNA biogenesis in Drosophila. *Genes Dev*.

Saito, K., K. Nishida, T. Mori, Y. Kawamura, K. Miyoshi, T. Nagami, H. Siomi, and M. Siomi. 2006. Specific association of Piwi with rasiRNAs derived from retrotransposon and heterochromatic regions in the Drosophila genome. *Genes & development*. 20:2214-2222.

Saito, K., Y. Sakaguchi, T. Suzuki, T. Suzuki, H. Siomi, and M.C. Siomi. 2007. Pimet, the Drosophila homolog of HEN1, mediates 2′-O-methylation of Piwi- interacting RNAs at their 3′ ends. *Genes & development*. 21:1603-1608.

Sarot, E., G. Payen-Groschene, A. Bucheton, and A. Pelisson. 2004. Evidence for a piwi-Dependent RNA Silencing of the gypsy Endogenous Retrovirus by the Drosophila melanogaster flamenco Gene. *Genetics*. 166:1313-1321.

Savitsky, M., D. Kwon, P. Georgiev, A. Kalmykova, and V. Gvozdev. 2006. Telomere elongation is under the control of the RNAi-based mechanism in the Drosophila germline. *Genes & development*. 20:345-354.

Schupbach, T. 1987. Germ line and soma cooperate during oogenesis to establish the dorsoventral pattern of egg shell and embryo in Drosophila melanogaster. *Cell*. 49:699-707.

Schupbach, T., and E. Wieschaus. 1991. Female sterile mutations on the second chromosome of Drosophila melanogaster. II. Mutations blocking oogenesis or altering egg morphology. *Genetics*. 129:1119-36.

Serbus, L.R., B.J. Cha, W.E. Theurkauf, and W.M. Saxton. 2005. Dynein and the actin cytoskeleton control kinesin-driven cytoplasmic streaming in Drosophila oocytes. *Development*. 132:3743-52.

Simon, J., and R. Kingston. 2009. Mechanisms of polycomb gene silencing: knowns and unknowns. *Nature reviews. Molecular cell biology*. 10:697-708.

Siomi, M.C., T. Miyoshi, and H. Siomi. 2010. piRNA-mediated silencing in Drosophila germlines. *Seminars in cell & developmental biology*.

Siriaco, G.M., G. Cenci, A. Haoudi, L.E. Champion, C. Zhou, M. Gatti, and J.M. Mason. 2002. Telomere elongation (Tel), a new mutation in Drosophila melanogaster that produces long telomeres. *Genetics*. 160:235-245.

Slanchev, K., J. Stebler, G. de la Cueva-Méndez, and E. Raz. 2005. Development without germ cells: the role of the germ line in zebrafish sex differentiation. *Proceedings of the National Academy of Sciences of the United States of America*. 102:4074-4079.

Smogorzewska, A., J. Karlseder, H. Holtgreve-Grez, A. Jauch, and T. de Lange. 2002. DNA ligase IV-dependent NHEJ of deprotected mammalian telomeres in G1 and G2. *Current biology : CB*. 12:1635-1644.

Spradling, A.C. 1993. Developmental Genetics of Oogenesis. *In* The Development of *Drosophila Melanogaster*. Vol. I. M. Bate and A.M. Arias, editors. 1-70.

Spradling, A.C., M. de Cuevas, D. Drummond-Barbosa, L. Keyes, M. Lilly, M. Pepling, and T. Xie. 1997. The Drosophila germarium: stem cells, germ line cysts, and oocytes. *Cold Spring Harb Symp Quant Biol*. 62:25-34.

Takada, S., A. Kelkar, and W.E. Theurkauf. 2003. Drosophila checkpoint kinase 2 couples centrosome function and spindle assembly to genomic integrity. *Cell*. 113:87-99.

Tan, C.-H., T.-C. Lee, S.D. Weeraratne, V. Korzh, T.-M. Lim, and Z. Gong. 2002. Ziwi, the zebrafish homologue of the Drosophila piwi: co-localization with vasa at the embryonic genital ridge and gonad-specific expression in the adults. *Mechanisms of development*. 119 Suppl 1:S221-4.

Theurkauf, W.E. 1994. Immunofluorescence analysis of the cytoskeleton during oogenesis and early embryogenesis. *Methods Cell Biol*. 44:489-505.

Theurkauf, W.E., and R.S. Hawley. 1992. Meiotic spindle assembly in Drosophila females: behavior of nonexchange chromosomes and the effects of mutations in the nod kinesin-like protein. *J Cell Biol*. 116:1167-80.

Tomari, Y., T. Du, B. Haley, D. Schwarz, R. Bennett, H. Cook, B. Koppetsch, W. Theurkauf, and P.D. Zamore. 2004. RISC Assembly Defects in the Drosophila RNAi Mutant armitage. *Cell*. 116:831-841.

Unhavaithaya, Y., Y. Hao, E. Beyret, H. Yin, S. Kuramochi-Miyagawa, T. Nakano, and H. Lin. 2009. MILI, a PIWI-interacting RNA-binding protein, is required for germ line stem cell self-renewal and appears to positively regulate translation. *The Journal of biological chemistry*. 284:6507-6519.

Vagin, V.V., M.S. Klenov, A.I. Kalmykova, A.D. Stolyarenko, R.N. Kotelnikov, and V.A. Gvozdev. 2004. The RNA interference proteins and vasa locus are involved in the silencing of retrotransposons in the female germline of Drosophila melanogaster. *RNA biology*. 1:54-58.

Vagin, V.V., A. Sigova, C. Li, H. Seitz, V. Gvozdev, and P.D. Zamore. 2006. A distinct small RNA pathway silences selfish genetic elements in the germline. *Science*. 313:320-324.

Verdel, A., S. Jia, S. Gerber, T. Sugiyama, S. Gygi, S.I. Grewal, and D. Moazed. 2004. RNAi-mediated targeting of heterochromatin by the RITS complex. *Science*. 303:672-6.

Verdel, A., A. Vavasseur, M. Le Gorrec, and L. Touat-Todeschini. 2009. Common themes in siRNA-mediated epigenetic silencing pathways. *The International journal of developmental biology*. 53:245-257.

Vermaak, D., S. Henikoff, and H.S. Malik. 2005. Positive selection drives the evolution of rhino, a member of the heterochromatin protein 1 family in Drosophila. *PLoS Genetics*. 1:96-108.

Vidal, F., E. Farssac, J. Tusell, L. Puig, and D. Gallardo. 2002. First molecular characterization of an unequal homologous alu-mediated recombination event responsible for hemophilia. *Thrombosis and haemostasis*. 88:12-16.

Volff, J.-N. 2006. Turning junk into gold: domestication of transposable elements and the creation of new genes in eukaryotes. *BioEssays*. 28:913-922.

Volpe, A.M., H. Horowitz, C.M. Grafer, S.M. Jackson, and C.A. Berg. 2001. Drosophila rhino encodes a female-specific chromo-domain protein that affects chromosome structure and egg polarity. *Genetics*. 159:1117-34.

Volpe, T.A., C. Kidner, I.M. Hall, G. Teng, S.I. Grewal, and R.A. Martienssen. 2002. Regulation of heterochromatic silencing and histone H3 lysine-9 methylation by RNAi. *Science*. 297:1833-7.

Watanabe, T., A. Takeda, T. Tsukiyama, K. Mise, T. Okuno, H. Sasaki, N. Minami, and H. Imai. 2006. Identification and characterization of two novel classes of small RNAs in the mouse germline: retrotransposon-derived siRNAs in oocytes and germline small RNAs in testes. *Genes & development*. 20:1732-1743.

Wicker, T., F. Sabot, A. Hua-Van, J. Bennetzen, P. Capy, B. Chalhoub, A. Flavell, P. Leroy, M. Morgante, O. Panaud, E. Paux, P. SanMiguel, and A. Schulman. 2007. A unified classification system for eukaryotic transposable elements. *Nature reviews. Genetics*. 8:973-982.

Yin, H., and H. Lin. 2007. An epigenetic activation role of Piwi and a Piwi-associated piRNA in Drosophila melanogaster. *Nature*. advanced online publication:304-308.

Zheng, K., J. Xiol, M. Reuter, S. Eckardt, N.A. Leu, K.J. McLaughlin, A. Stark, R. Sachidanandam, R.S. Pillai, and P.J. Wang. 2010. Mouse MOV10L1 associates with Piwi proteins and is an essential

component of the Piwi-interacting RNA (piRNA) pathway. *Proc Natl Acad Sci U S A.* 107:11841-6.

Zimyanin, V.L., K. Belaya, J. Pecreaux, M.J. Gilchrist, A. Clark, I. Davis, and D. St Johnston. 2008. In vivo imaging of oskar mRNA transport reveals the mechanism of posterior localization. *Cell*. 134:843-53.